Final Report 1998-11

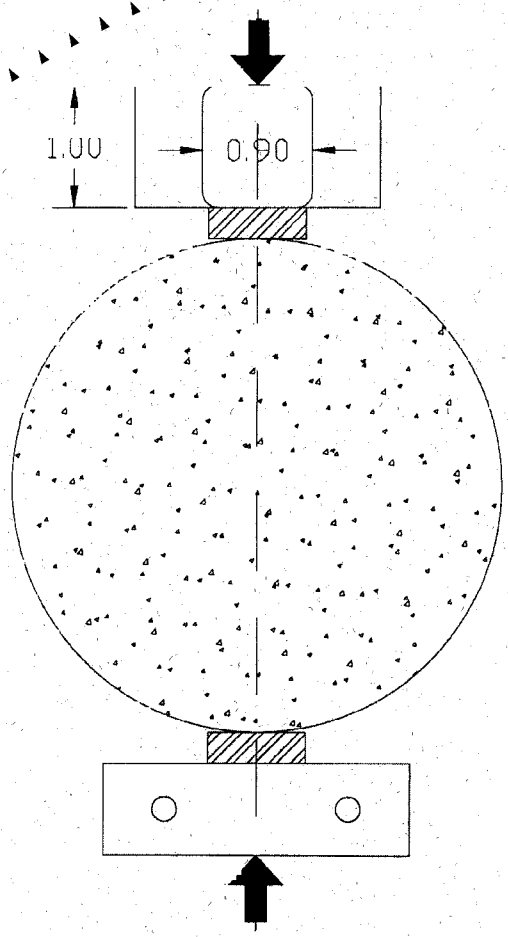

Mechanical Properties of High-Strength Concrete

UNIVERSITY OF MINNESOTA
CENTER FOR TRANSPORTATION STUDIES

This research was made possible with the support and contributions from the Minnesota Prestress Association. Many of its members took a role in the fabrication and testing of the girder specimens.

Technical Report Documentation Page

1. Report No.	2.	3. Recipient's Accession No.
1998-11		

4. Title and Subtitle	5. Report Date
MECHANICAL PROPERTIES OF HIGH STRENGTH CONCRETE	January 1998
	6.

7. Author(s)	8. Performing Organization Report No.
Alireza Mokhtarzadeh Catherine E. French	

9. Performing Organization Name and Address	10. Project/Task/Work Unit No.
Department of Civil Engineering University of Minnesota 500 Pillsbury Dr. S.E. Minneapolis, MN 55455-0220	11. Contract (C) or Grant (G) No. (C) 69098 TOC # 83

12. Sponsoring Organization Name and Address	13. Type of Report and Period Covered
Minnesota Department of Transportation 395 John Ireland Boulevard Mail Stop 330 St. Paul, Minnesota 55155	Final Report 1993-1998
	14. Sponsoring Agency Code

15. Supplementary Notes

16. Abstract (Limit: 200 words)

Researchers conducted an experimental program to investigate production techniques and mechanical properties of high-strength concrete and to provide recommendations for using these concretes in manufacturing precast/prestressed bridge girders.

High-strength concretes with 28-day compressive strengths in the range of 8,000 to 18,600 psi (55.2 to 128 MPa) were produced. Test variables included total amount and composition of cementitious material, portland cement, fly ash, and silica fume; type and brand of cement; type of silica fume, dry densified and slurry; type and brand of high-range water-reducing admixture; type of aggregate; aggregate gradation; maximum aggregate size; and curing.

Testing determined the effects of these variables on changes in compressive strength and modulus of elasticity over time, on splitting tensile strength, on modulus of rupture, on creep, on shrinkage, and on adsorption potential as an indirect indicator of permeability. The study also investigated the effects of test parameters such as mold size, mold material, and end condition. More than 6,300 specimens were cast from approximately 140 mixes over a period of three years.

17. Document Analysis/Descriptors	18. Availability Statement
compressive strength Creep mechanical properties high performance concrete modulus of elasticity permeability tensile strength Shrinkage	No restrictions. Document available from: National Technical Information Services, Springfield, Virginia 22161

19. Security Class (this report)	20. Security Class (this page)	21. No. of Pages	22. Price
Unclassified	Unclassified	595	

MECHANICAL PROPERTIES OF HIGH-STRENGTH CONCRETE

Final Report

Prepared by

Alireza Mokhtarzadeh
Catherine E. French

Department of Civil Engineering
University of Minnesota

January 1998

Published by

Minnesota Department of Transportation
Office of Research Administration
200 Ford Building Mail Stop 330
117 University Avenue
St. Paul, Minnesota 55117

ACKNOWLEDGMENTS

This project was collectively sponsored by the Minnesota Department of Transportation, Minnesota Prestress Association, University of Minnesota Center for Transportation Studies, Prestressed/Precast Concrete Institute, and NSF Grant No. NSF/GER-9023496-02. The authors acknowledge the generous donations of materials and equipment from Holnam Inc., Lehigh Portland Cement Company; National Minerals Corporation; J. L. Shiely Company; Edward Kraemer & Sons, Inc.; Meridian Aggregates; W. R. Grace & Co.; and Elk River Concrete Products. The views expressed herein are those of the authors and do not necessarily reflect the views of the sponsors.

TABLE OF CONTENTS

CHAPTER 8 - TEST RESULTS: TENSILE STRENGTH

CHAPTER 9 - TEST RESULTS: EFFECT OF COARSE AGGREGATE ON MECHANICAL PROPERTIES OF HIGH STRENGTH CONCRETE

CHAPTER 10 - SHRINKAGE AND CREEP

LIST OF TABLES

LIST OF FIGURES

NOTATION

The following notation is used throughout the text, tables and figures.

AASHTO	American Association of State Highway and Transportation Officials
ACI	American Concrete Institute
AIJ	Architectural Institute of Japan
ASTM	American Society for Testing and Materials
CANMET	Canada Center for Mineral and Energy Technology
CEB	Comité Euro - International du Béton
CERF	Civil Engineering Research Foundation
d	total deformation of the specimen throughout the effective gage length, in. (mm)
d	time to one-half ultimate creep, days
E_c	static modulus of elasticity of concrete, psi (MPa)
e_g	eccentricity of the compressometer-extensometer gage from the axis of the specimen, in. (mm)
e_r	eccentricity of the compressometer-extensometer pivot from the axis of the specimen, in. (mm)
FA	fly ash
FIP	Fédération Internationale de la Précontrainte
f_c	compressive strength of concrete, psi (MPa)
f_{cc}	compressive strength of concrete measured on cylinders with height-to-diameter ratio = 2, psi (MPa)
f_{ck}	characteristic compressive strength of 6 x 12 in. (150 x 300 mm) cylinders, psi (MPa)
f_{cm}	actual compressive strength of 6 x 12 in. (150 x 300 mm) cylinders, psi (MPa)
f_{sp}	splitting tensile strength of concrete, psi (MPa)

NOTATION

f_r	flexural tensile strength of concrete (modulus of rupture), psi (MPa)
g	gage reading, in. (mm)
gal	gallons (3.785 l)
G1	granite from source 1
G2	granite from source 2
HSC	high strength concrete
hp	horse power (746 watt)
in.	inches (25.4 mm)
k_1	correction factor with regard to coarse aggregate
k_2	correction factor with regard to mineral additions
kg	kilograms (2.203 lb.)
kN	kilonewtons (224.719 lbf.)
l	liters (0.264 gal)
lb.	pounds (0.454 kg)
L1	high absorption limestone
L2	low absorption limestone
m	meters (39.370 in.)
ml	milliliters (0.034 fl. oz.)
mm	millimeters (0.039 in.)
MPa	megapascals (145.138 psi)
New RC	National Research and Development Project (Japan)
oz./cwt	fluid ounce of admixture per 100 pounds of cement weight (0.652 ml/kg)
pcf	pounds per cubic foot (16.016 kg/m^3)
PCI	Precast/Prestressed Concrete Institute
pcy	pounds per cubic yard (0.593 kg/m^3)

NOTATION

psi	pounds per square inch (6.895×10^{-3} MPa)
R^2	coefficient of determination (square of the ordinary correlation coefficient)
R1	round river gravel
R2	partially crushed river gravel
SF	silica fume
SHRP	Strategic Highway Research Program
SI	metric International System of units
t	time in days after loading
USC	U.S. Customary units (inch-pound)
v_t	creep coefficient at time t
v_u	ultimate creep coefficient
w	unit weight of concrete at the time of testing, pcf (kg/m^3)
w/c	water-to-cement ratio
w/cm	water-to-cementitious material ratio: $w/(c+f+s)$; where w, c, f, and s are weights of water, portland cement, fly ash and silica fume respectively
$(\varepsilon_{sh})_t$	shrinkage strain at any time t
$(\varepsilon_{sh})_u$	ultimate shrinkage strain, in/in, (m/m)
ψ	time-ratio

EXECUTIVE SUMMARY

The objective of the research was to investigate the effects of various test and material variables on the mechanical properties of high strength concrete. The main test variables included: mold material; mold size; specimen end condition; curing condition; heat-curing temperature; and age. The material variables investigated were: total cementitious material content of the mix; percent replacement of cement by weight with fly ash, silica fume or their combination; type and gradation of coarse aggregate; type of superplasticizer; and type and brand of cement. Efforts were made to use materials and procedures considered typical of those used by the precast/prestressed industry. In addition, standard tests were conducted on companion specimens to correlate the results of this study with results reported elsewhere in the literature. High strength concretes with 28-day compressive strengths in the range of 8,000 to 18,600 psi (55.2 to 128 MPa) were produced.

In all, more than 6,300 concrete specimens from 142 high strength concrete mixes were tested for compressive and tensile strength, strength gain with time, modulus of rupture, static modulus of elasticity, shrinkage, creep, and absorption potential (indirect permeability). The following is a brief summary of the conclusions:

Compressive strength - The influence of the coarse aggregate type on the compressive strength varied in magnitude and depended on the curing condition and cementitious material of the mix.

Reference concrete mixes made with limestone had higher compressive strengths than those made with round gravel due to the superior bond characteristics of the limestone with the cement paste. The plane of fracture in the limestone concrete crossed most of the coarse aggregate particles. In contrast, the plane of fracture in the round gravel mixes passed around most of the coarse aggregate particles. The addition of silica fume had the greatest effect on mixes made with round gravels (attributed to the improved bond between the aggregate and the paste). In the case where the strength of the aggregate controlled the strength of the mix (limestone), the addition of silica fume had little effect on the mix.

Moist-curing proved to be essential for getting full advantage of using fly ash and/or silica fume in the mix. In the absence of adequate moisture, any benefit from inclusion of fly ash and/or silica fume was limited to grain refinement of the cement matrix.

When the strength of concrete is controlled by failure of the aggregate, further reduction in the water-to-cementitious materials ratio will not increase strength and may cause problems due to decreased workability.

Modulus of elasticity - One day modulus of elasticity values of heat-cured specimens were, on average, 98 percent of the 28-day values. At one year, the modulus of elasticity of the heat-cured specimens dropped to 96 percent of the 28-day stiffness. In the case of the moist-cured specimens, the stiffness at one year represented an average

increase of 108 percent over the 28-day value.
The aggregate type appeared to have a dominant effect on the concrete stiffness; however, because of the variation in aggregate properties from different sources, it is not possible to generalize coefficients to account for the aggregate type.

For the quantities of fly ash and/or silica fume used in this study, there was no noticeable effect on the modulus of elasticity.

At equivalent compressive strengths, the measured modulus of elasticity values for moist-cured specimens tested in the wet condition were somewhat higher than those of the heat-cured specimens or specimens moist-cured for a limited period of time and tested in a dry condition. The presence of moisture at the time of testing causes a relative decrease in the concrete compressive strength and a relative increase in the modulus of elasticity values compared with those of specimens tested in the dry condition.

Current design equations may overpredict the modulus of elasticity based on compressive strength and should be used with caution. The equations proposed by ACI 363 and CEB-FIP resulted in the most reasonable predictions for this study. For construction with high-strength concrete, it is recommended that mix samples be cast and tested to determine modulus of elasticity values to be used for design.

Tensile strength – The type of curing significantly affected the modulus of rupture test results. Drying shrinkage strains in heat-cured beams (maximum on the surfaces of the beam) are added to the flexural tensile strains (maximum on the outermost fibers) during two point loading of the beams causing the heat-cured beams to break at a lower load. The moist-cured samples (moist up to the time of test) did not suffer from shrinkage strain; therefore a higher load was needed to break the moist-cured beams. The flexural tensile strengths of heat-cured specimens ranged between the ACI 318-95 and ACI High Strength Committee 363 predicted values.

The type of curing did not affect the splitting tensile strength of high strength concrete samples. Elements along the diagonal plane, inside the concrete (with the least amount of shrinkage strain), are under tension and therefore pre-existing shrinkage strain (mostly on the surface) does not interfere with the test result. The splitting tensile strength of both heat- and moist-cured specimens was adequately predicted by the ACI 318 equation. The proposed ACI 363 equation overestimated the results.

Shrinkage – Drying shrinkage strains ranged between 63 to 83 percent of the values predicted by ACI 209 equations. The lower water-to-cementitious material ratio and denser matrix of the high strength concrete were believed to be the main reasons for the observed smaller ultimate shrinkage relative to normal strength concrete.

Creep – The range of ultimate creep coefficients (V_u) varied between 0.92 and 2.46 as compared to the 1.30 to 4.15 range reported by ACI 209 for normal strength concrete.

Absorption Potential (Indirect Permeability) – For the coarse aggregates included in the study and for both curing conditions, the weight gain of submerged specimens was highest for mixes containing 20 percent fly ash, followed by reference mixes and mixes

containing a combination of 20 percent fly ash and 7.5 percent silica fume. The lowest water weight gain was observed for the mixes containing 7.5 percent silica fume.

CHAPTER 1
INTRODUCTION

1.1 General

The development and use of high performance materials is important to the construction and maintenance of our civil infrastructure system. High performance materials have the potential of increasing the economy and durability of structural systems and are the topic of much current research throughout the world. Major recent research efforts include the "New RC Program" in Japan, the Network of Centers for Excellence "High Performance Concrete Program" in Canada, and the Strategic Highway Research Program (SHRP) in the United States.

A comprehensive technical report has been published by the Civil Engineering Research Foundation (CERF), in April of 1993 which addresses "High Performance Construction Materials and Systems: An Essential Program for America and Its Infrastructure". The report identifies the need for a national program focused on these issues *[CERF 1993]*. Concrete and steel are the particular building materials addressed in this first report. The report defines high performance concrete as "concrete meeting special performance requirements which cannot always be achieved routinely using only conventional constituents and normal mixing, placing and curing practices." The definition not only encompasses strength enhancement, it also describes a wide range of properties such as ease of placement and consolidation without segregation, toughness and durability. The primary issue described in this report is the strength enhancement property of high performance concrete. This issue in itself is not well defined.

Given the variability in physical properties and availability of concrete-making materials in different regions, the definition of high strength concrete varies with location. The meaning of high strength concrete also changes with time. A few years ago a concrete strength of 7,500 psi (51.7 MPa) was considered a very high strength. Concrete strengths of 14,000 psi (96.5 MPa) and more, which can now be reached without difficulty, were certainly beyond the

scope of most existing standards and design recommendations. In general, high strength concrete is defined as concrete with a uniaxial compressive strength greater than what is ordinarily obtained in a region. Despite all the complications which may arise from defining high strength concrete, concrete made with normal-weight aggregates with 28-day uniaxial compressive strength as determined by a standard 6 x 12 in. (150 x 300 mm) test specimen in excess of 6,000 psi (41.4 MPa) is generally referred to as high strength concrete. The following arguments may justify the above definition:

1. More rigid quality control and more care in the selection and proportioning of materials are needed to produce concrete with uniaxial compressive strengths in excess of 6,000 psi (41.4 MPa).
2. Experimental studies show that this class of specially formulated concrete has microstructure and properties which are in many respects different from conventional moderate- and low strength concrete.

High strength concrete with compressive strength in excess of 10,000 psi (69.0 MPa) can be made with carefully selected but commonly available cement, sand and stone, by using a very low water-to-cement ratio and careful quality control in production. Furthermore, by inclusion of some newly developed (but not exotic) supplementary cementing materials and chemical admixtures in concrete, compressive strengths ranging to about 20,000 psi (138 MPa) are no longer unusual in practice.

1.2 History

"Imagine, for example, concrete with an available strength of 10,000 pounds per square inch (69.0 MPa). Smaller columns, thinner and lighter beams and slabs would at once result. Precast units, easy to handle, would be available. The present limiting heights of buildings, of spans of bridges would be at least double. A new basis of design, new codes and specifications would be required," said Professor S.C. Hollister, former Dean of Engineering at Cornell University during the ACI's 30th Annual Dinner in 1934.

The dreams of Professor Hollister have now been accomplished. High strength concrete have been used throughout the world in construction of high-rise buildings, large span bridges, prefabricated elements, offshore structures and pavements during the past three decades. Concrete compressive strength is improving continuously due to availability and adoption of cements of higher quality, more efficient chemical admixtures and effective supplementary cementing materials. However, the evolution of high strength concrete has been a gradual development.

In 1940, using ordinary portland cement and pressed consolidation technique, high strength concrete with compressive strength in excess of 14,500 psi (100 MPa) was obtained in the laboratory of the University of Tokyo. The concrete had a water-to-cement ratio of 0.31 at the time of casting and had a final water-to-cement ratio of 0.22 after being subjected to a 1,450 psi (10.0 MPa) consolidating pressure for one day. The concrete was then subjected to a standard curing condition until testing. This concrete was intended to be used in fabrication of precast shield segments for undersea tunnels *[Ikeda 1993]*. In the 1960's, using quality aggregates together with low water-to-cement ratio and cement contents as large as 1,100 lb/yd^3 (650 kg/m^3), high strength concretes with compressive strengths in the range of 8,500 to 11,000 psi (58.6 to 75.9 MPa) were developed in the United States mostly for military applications. These concretes contained no chemical admixtures or supplementary cementing materials and posed significant constructibility and thermal gradient problems *[Hoff 1993]*. The first American applications of high strength concrete in construction of high-rise buildings also occurred in the 1960's which led the way to widespread use of high strength concrete in the years that followed. High strength concrete in Europe had been developed and used both as high strength and high performance concrete. The discovery of silica fume as an additive to concrete, in combination with the development of high-range water reducers (superplasticizers) led to significant increases in concrete strength and durability in a period of only a few years. Since the 1970's high strength concrete, incorporating newly developed chemical admixtures and supplementary cementing materials, has been used in Norway in the construction of

offshore concrete platforms. These structures are both subjected to large environmental loading and aggressive environments.

Today, high strength concrete is commonly available in almost all metropolitan areas. This breakthrough has been made possible by the recent advances in quality control, materials, development of techniques by which mixes of special characteristics can be made, transported, placed, or compacted and through the use of very low water-to-cement ratios due to availability of very efficient high-range water reducing admixtures. It is possible to obtain even higher strengths through the use of other additives such as silica fume.

1.2.1 High Strength Concrete in Tall Buildings

The main reason to use high strength concrete in the construction of tall buildings is the desire to build high and at the same time to increase the amount of useable space in buildings. High strength concrete allows construction of columns of smaller cross section and with less reinforcement and thus increased effective floor area and substantial cost savings. As an example, some of the columns in Place Victoria building in Montreal (once the tallest concrete building in North America built in 1964) were built with 6,000 psi (41.4 MPa) concrete. These columns were 7 x 7 ft. (2.1 x 2.1 m) and 4.5 x 8 ft. (1.4 x 2.4 m) in cross section and contain 6.5 percent reinforcement. If the technology was available in 1964 to produce 8,700 psi (60.0 MPa) concrete, the column size could have been reduced to 4.5 x 4.5 ft. (1.4 x 1.4 m) or the reinforcement quantities reduced to only 1 percent for the original column size. Both changes would have provided substantial savings *[Hoff 1993]*.

1.2.2 High Strength Concrete in Bridges

High strength concrete has been used in bridge structures as early as 1960 when the Washington State Highway Department specified 6,000 psi (41.4 MPa) concrete for prestressed bridge girders. The main advantage of high strength concrete in bridge construction is smaller cross sections which leads to reduced dead load for the same carrying capacity, reduced number of girders, longer spans and therefore substantial savings in construction

costs. The result of a study performed at the University of Texas at Austin shows that for a span length of 115 ft. (35 m) and a bridge width of 36 ft. (11 m), the required number of AASHTO-PCI Type IV girders can be reduced from nine using 6,000 psi (41.4 MPa) concrete to four when 10,000 psi (69.0 MPa) concrete is used. Additional savings result from the reduction in the total number of strands required for the bridge, which is due to the reduced dead load *[Castrodale et al. 1988]*.

1.2.3 Other Applications of High Strength Concrete

Besides high strength, high strength concrete has much more to offer. Other benefits of high strength concrete are being discovered and new applications are found. Higher stiffness, high-early strength; high plasticity of concrete mixture; resistance against abrasion, wear and tear and large resistance against penetration of chemicals has led to its use in a variety of applications.

1.3 Problem Statement

The availability of high strength concrete has made it necessary to review our codes and design specifications. Empirical equations used to predict properties of concrete or to design structural members have been based on tests of concrete made with traditional materials having compressive strengths less than about 6,000 psi (41.4 MPa). Extrapolation of these empirical equations to materials of higher strength and different microstructure is unjustified and may be dangerous. In a 1987 report produced by American Concrete Institute (ACI) Committee 363-High Strength Concrete *[ACI-363 1987]*, numerous research needs were identified for high strength concrete, many of which emphasized the need for information on mechanical properties of high strength concrete with which to modify codes and specifications to accommodate the new material characteristics. In 1992, American Concrete Institute Committee 363 presented a revised summary of current high strength concrete research *[ACI-363R 1992]*. Other recent state-of-the-art reports on high strength concrete include ones published by an FIP-CEB working group on high strength concrete and the British Cement Association *[FIP/CEB 1990; Parrott 1988]*. Production, utilization and performance of high

strength concrete has been a topic of discussion in many national and international symposiums in recent years *[Holand 1987; Hester 1990; Holand 1993; de Larrard et al. 1996]*. Although there has been much recent research conducted regarding high strength concrete, several issues still remain unanswered. In addition, much of the research has been directed toward cast-in-place use of high strength concrete. Very little information is available regarding the production and behavior of high strength concrete for precast/prestressed applications.

1.4 Research Objective

The objective of this research was to document the effects of mix materials, proportions, curing, age, and test procedures on the mechanical properties of high strength concrete. Variables included: total amount and composition of cementitious material (portland cement, fly ash and silica fume), type and brand of cement, type of silica fume (dry-densified and slurry), type and brand of superplasticizer, type of aggregate, aggregate gradation, maximum aggregate size, and curing conditions. Mechanical properties investigated included: compressive strength and modulus of elasticity change with time, modulus of rupture, splitting tensile strength, creep, shrinkage, weight loss and absorption potential of high strength concrete. Also investigated were effects of testing parameters such as: mold size, mold material, and end condition on test results.

1.5 Format

This report includes 13 chapters, a bibliography on mechanical properties and applications of high strength concrete, a list of references and 6 appendices. Chapter 2 contains a review of concrete-making materials. The experimental program is described in Chapter 3. Chapter 4 contains a review of the literature and research on the effect of some of the test parameters relevant to this study. The compressive strength test results are presented in Chapter 5. Review of the literature and test results on static modulus of elasticity of high strength concrete are presented in Chapters 6 and 7. Chapter 8 presents tensile strength test results. Chapter 9 discusses the effect of coarse aggregate on mechanical properties of high strength concrete. Chapter 10 contains a review of the literature relevant to the shrinkage and

creep study and describes the shrinkage and creep experimental program, and test results. Results of the indirect absorption potential tests are presented in Chapter 11. A discussion of selected test results is presented in Chapter 12. Chapter 13 contains a summary of the project and a statement of general conclusions. The bibliography is included to provide researchers and practitioners with an up to date list of references on high strength concrete pertaining particularly to precast/prestressed concrete. Appendices A through F contain all the experimental data collected during the course of this study.

CHAPTER 2
CONCRETE-MAKING MATERIALS

2.1 General

Modern concrete is a mixture of hydraulic cement, aggregates, water and in many cases admixtures. The following definitions have been given for the principal concrete-making materials *[ASTM C-125, ACI-116]*:

"*Cement* is a finely pulverized material which by itself is not a binder, but develops the binding property as a result of hydration. A cement is called *hydraulic* when the hydration products are stable in an aqueous environment. The most commonly used hydraulic cement for making concrete is *portland cement*, which consists essentially of hydraulic calcium silicates. The calcium silicate hydrates formed on the hydration of portland cement are primarily responsible for its adhesive characteristic, and are stable in aqueous environments."

"*Aggregate* is the granular material, such as sand, gravel, or crushed stone used with a cementing medium to form hydraulic-cement concrete or mortar. The term *coarse aggregate* refers to aggregate particles larger than No. 4 sieve (4.75 mm), and the term *fine aggregate* refers to aggregate particles smaller than No. 4 sieve (4.75 mm) but larger than No. 200 sieve (75 μm). *Gravel* is the coarse aggregate resulting from natural disintegration and abrasion of rock or processing of weakly bound conglomerate. The term *sand* is commonly used for fine aggregate resulting from natural disintegration and abrasion of rock or processing of friable sandstone. *Crushed stone* is the product resulting from industrial crushing of rocks, boulders, or large cobblestones."

"*Admixtures* are defined as materials other than water, aggregates, cement, and fiber reinforcement, which are added to the concrete batch immediately before or during

mixing. Important classes of concrete admixtures are: *accelerating admixtures* that accelerates the setting and early strength development of concrete, *retarding admixture* which retards the setting of concrete, *water-reducing admixtures* which plasticizes fresh concrete mixtures by reducing the surface tension of water, and *air-entraining admixtures* which improve durability of concrete exposed to cold weather."

The above definition of concrete does not include a fifth component, *pozzolans* (supplementary cementing materials such as fly ash and silica fume), which are frequently used in production of high strength concrete. Pozzolans can improve the resistance of concrete to thermal cracking, alkali-aggregate expansion, and sulfate attack.

"*Pozzolan* is defined as a siliceous or siliceous and aluminous material which in itself possesses little or no cementitious value but will, in finely divided form and in the presence of moisture, chemically react with calcium hydroxide at ordinary temperatures to form compounds possessing cementitious properties," *[ASTM C-125]*.

Concrete can also be considered as a three-phase composite material consisting of cement matrix (binding medium), aggregate and the transition zone between cement matrix and aggregate. Properties and characteristics of concrete depend on the properties and characteristics of its constituent materials and its individual components (phases). The following is a literature review on characteristics of principal concrete-making materials and their effects on some properties of concrete.

2.2 Portland Cement

Selection of portland cement for production of high strength concrete has been shown to be very important *[Chicago Committee on High-Rise Buildings 1977; Hester 1977]*. Within a given cement type, different brands may exhibit different strength development characteristics mainly due to the variations in chemical composition and fineness that are permitted by ASTM C-150, Specification for Portland Cement, shown in Table 2.1. Portland cement is made

primarily from a calcareous material, such as limestone, or chalk, alumina and silica found in clay or shale, and iron bearing materials such as iron ore and pyrites. The raw materials also contain small amounts of other compounds such as magnesia, alkalis, phosphates, fluorine compounds, zinc oxide, lead oxide, and sulfides. Selection and sources of raw materials for the production of cement are the main causes for the variations in chemical composition of the final product.

The reaction of portland cement powder with water is referred to as *hydration* of cement. During hydration, cement paste changes from a fluid mixture of cement powder and water to a rigid solid. This reaction is exothermic and is driven by the tendency of the anhydrous oxides present in portland cement to achieve their lowest energy state. In doing so, anhydrous solids and water are consumed and hydrated solids are formed. A shorthand notation, which describes each oxide by one letter is used by cement chemists to write hydration reaction equations or products. In this notation $Cao=C$; $SiO_2=S$; $Al_2O_3=A$; $Fe_2O_3=F$; $SO_3=\underline{S}$; and likewise H_2O is denoted by H. This notation will be used frequently throughout this report.

Four minerals are usually regarded as the major compounds of cement. These are: *alite*: impure tricalcium silicate C_3S ($3CaO.SiO_2$); *belite*: impure dicalcium silicate C_2S ($2CaO.SiO_2$); *tricalcium aluminate* C_3A ($3CaO.Al_2O_3$); and *tetracalcium aluminoferrite* C_4AF ($4CaO.Al_2O_3.Fe_2O_3$). In addition there exist small amounts of other oxides in the cement, such as MgO, TiO_2, Mn_2O_3, K_2O, and Na_2O, that are usually referred to as minor compounds and amount to not more than a few percent of the weight of the cement. However, it should be born in mind that the term minor only refers to their quantity and not necessarily to their importance.

As cement is made up of several compounds, its hydration involves a number of chemical reactions which take place simultaneously. The alite and belite (C_3S and C_2S) make up approximately 70% of the cement, so the properties of the hardened cement paste are significantly influenced by their hydration products. Therefore, a more detailed discussion of the

hydration of the silicates [alite (tricalcium silicate) and belite (dicalcium silicate)] are presented here followed by a brief discussion on the hydration of aluminates.

2.2.1 Hydration of Silicates in Portland Cement

The calcium silicates react with water to give calcium hydroxide ($CH = Ca(OH)_2$) and calcium silicate hydrate ($C_3S_2H_3 = 3Cao.2SiO_2.3H_2O$):

- for tricalcium silicate: $2C_3S + 6H \rightarrow C_3S_2H_3 + 3CH$ *(2.1)*
- for dicalcium silicate: $2C_2S + 4H \rightarrow C_3S_2H_3 + CH$ *(2.2)*

The cementitious calcium silicate hydrate phase ($C_3S_2H_3$ *usually denoted as C-S-H*) makes up 50 to 60 percent of the volume of solids in a completely hydrated cement paste and is, therefore, the most important in determining the properties of the paste *[Mehta 1986]*. Because the chemical composition of calcium silicate hydrate is uncertain and depends on time, hydration temperature, type of cement and water-to-cement ratio, it is common to refer to it as *C-S-H* without being specific about its fixed composition. However, on complete hydration the composition of *C-S-H* corresponds to $C_3S_2H_3$.

The calcium hydroxide (*CH*) phase constitutes 20 to 25 percent of the volume of solids in the hydrated cement paste and has no cementitious value *[Mehta 1986]*. While the presence of considerable amount of calcium hydroxide makes cement paste highly alkaline and provides good protection to embedded steel against corrosion, it has the adverse effect on its chemical durability to acidic solutions *[Soroka 1980]*. It follows from the hydration equations *(2.1)* and *(2.2)* that the hydration products of C_3S are richer in *CH* than those of C_2S. In fact, as is shown below, the *CH* produced amounts to 40% and 18% of the total hydration products of the C_3S and C_2S respectively:

Using the atomic weights of basic elements, the molecular weights of different compounds involved in the hydration equations are:

- $C_3S = 3CaO.SiO_2$: (2.3)

$3[(40)_{Ca}+(16)_O]+[(28)_{Si}+2(16)_O] = 228$ units

- $C_2S = 2CaO.SiO_2$: (2.4)

$2[(40)_{Ca}+(16)_O]+[(28)_{Si}+2(16)_O] = 172$ units

- $H = H_2O$: (2.5)

$[2(1)_H+(16)_O] = 18$ units

- $C_3S_2H_3 = 3CaO.2SiO_2.3H_2O$: (2.6)

$3[(40)_{Ca}+(16)_O]+2[(28)_{Si}+2(16)_O]+3[2(1)_H+(16)_O] = 342$ units

- $CH = Ca(OH)_2$: (2.7)

$\{(40)_{Ca}+2[(16)_O+(1)_H]\} = 74$ units

hence,

- for hydration of C_3S, equation *(2.1)*, the percent *CH* produced is:
  $\{3(74)/[2(228)+6(18)]\}100 = 40\%$ (2.8)

- and for hydration of C_2S, equation *(2.2)*, the percent *CH* produced is:
  $\{(74)/[2(172)+4(18)]\}100 = 18\%$ (2.9)

Similar calculations based on atomic weights show that C_3S and C_2S react with approximately the same amount of water (24% and 21% of water, respectively) for their hydration.

The presence of impurities in the alite and the belite (impure C_3S and impure C_2S) affects the composition and properties of their hydration products *[Neville 1975]*. Nevertheless, it is generally assumed that their hydration products are *C-S-H* gel of average composition of $C_3S_2H_3$ and $Ca(OH)_2$.

2.2.2 Hydration of Aluminates in Portland Cement

Gypsum is added during grinding of the cement clinker in order to regulate the setting time of cement. The aluminates react with water and the added gypsum ($C\underline{S} = CaSO_4$ calcium sulfate) to give hydration products which are isostructural with calcium aluminum trisulfate ($C_3A.3C\underline{S}.32H = 3CaO.Al_2O_3.3CaSO_4.32H_2O$ ettringite) and calcium aluminum monosulfate ($C_3A.C\underline{S}.12H = 3CaO.Al_2O_3.CaSO_4.12H_2O$ monosulphate) usually referred to as AF_t (Al-Fe-tri) and AF_m (Al-Fe-mono) with *F* indicating the possible substitution of iron for aluminum in the structure (-tri and -mono show number of moles of $C\underline{S}$ in the compound).

2.2.3 Hydration of Portland Cement

The hydration process starts at the surface of cement particles. Therefore the rate of hydration depends on the total surface area of cement particles (fineness of cement) available for the hydration process. At the start of hydration, a dense *C-S-H* gel coating is formed on the cement grains. This coating together with the ettringite coating on the C_3A particles retards further hydration and explains presence of a period of relative inactivity lasting 1-2 hours, during which the paste remains plastic and workable (dormant period). At the end of the dormant period the breakup of the gel coatings exposes the cement particles and hydration is resumed. For a rapid development of strength (as is needed in precast/prestressed industry), a high fineness is required. However, the workability requirement of fresh concrete sets a limit on the maximum fineness of the cement. Maximum cement fineness of 400 m^2/kg (281,000 in^2/lb) (Blaine) has been suggested *[Blick et al. 1985; Chicago Committee on High-Rise Buildings 1977]*.

Several types of portland cement are available commercially and special cements can be produced for specific uses. ACI Committee 363 recommends use of ordinary portland cement

(ASTM C-150 Type I) in production of high strength concrete except when high initial strength is the objective, such as in prestressed concrete *[ACI-363R 1992]*. Ordinary portland cement is the most common cement in use. It is suitable for use in general construction when there is no exposure to sulphates in the soil or in the groundwater. High early strength portland cement (ASTM C-150 Type III) is very similar to ordinary portland cement. The increased rate of strength gain of Type III cement is achieved by a higher C_3S content and by finer grinding of the cement clinker. It should be noted that cement manufacturers invariably produce Type I cements that are much finer than 280 m^2/kg (197,000 in^2/lb) prescribed by ASTM C-150. Also many plants produce Type I cements with a high C_3S content. Therefore sometimes in practice there is little difference between high early strength and some ordinary cements. Table 2.1 summarizes the ASTM C-150 requirements for all types of cements.

Except for the dormant period, the rate of hydration is maximum at early ages and decreases with time. Formation of a dense layer of *C-S-H* gel around the cement particles may be the reason for the decrease in the rate of hydration. Even for immersed paste, hydration stops after a time while still an appreciable amount of unhydrated cement is left in the paste which can amount to more than 50% of the original weight of the cement *[Soroka 1980]*. However, it is reported that the presence of unhydrated cement, in a properly consolidated mix, is not detrimental to the strength of the paste and that the quality of concrete depends primarily on the gel/space ratio of the paste *[Neville 1975]*. The lower the water-to-cement ratio, the lower the average rate of hydration and the sooner the hydration comes to a halt. This effect is attributed to the decrease in the available space for formation of hydration products *[Soroka 1980, Neville 1975]*.

When drying of the paste is prevented, the rate of hydration increases with temperature at early ages. Drying slows down hydration and may stop it completely. Klieger compared 1-, 3-, 7- and 28-day compressive strengths of two concretes made with Type I and Type III portland cements, cured at 73, 90, 105 and 120 °F *[Klieger 1958]*. He reported that while higher temperature led to an increase in strength of concrete at early ages, the strength at later ages

started to decrease beyond a certain temperature which was lower for early strength portland cement than for ordinary portland cement.

2.3 Water

The requirements for water quality for high strength concrete are no more stringent than those for conventional concrete *[ACI-363R 1992]*. Blick et al. did not find a detrimental effect on the high strength concrete mixtures when various sources of water were used *[Blick et al. 1985]*. It was concluded that the limitations listed in ASTM C 94 were adequate for use in high strength concrete.

2.3.1 Water-to-Cementitious Material Ratio

Most researchers agree that the single most important variable in achieving higher strength concrete is low water-to-cement ratio (*w/c*). To compute *w/c* the weight of mix water, except that absorbed in the aggregates, is divided by the weight of cement in the mix. Other things being equal, strength and durability of concrete increases with decrease in *w/c*.

Many high strength concrete mixes include supplementary cementing materials in addition to the portland cement. For this reason a relatively new term, water-to-cementitious material ratio (*w/cm*) is being used. To compute *w/cm* weight of mix water is divided by the total weight of cementitious materials present in the mix. As is the case for *w/c* it is believed that strength and durability of concrete increases with a decrease in *w/cm*. Achieving higher strengths is conditional, of course, on the selection of the optimum strength producing materials *[Blick 1985]*.

As defined in ACI-318-89R92, cementitious materials include portland cement and blended hydraulic cements, fly ash and other pozzolans, and ground granulated blast furnace slag. Each of these components have ASTM standard specifications. There was no ASTM standard for silica fume when ACI-318-89R92 was issued, and it is not counted as a cementitious material in this code. However, silica fume is frequently used as part of cementitious material composition, typically as 5% to 10% replacement by weight of portland cement.

The initial porosity of the cement paste is a function of the water-to-cementitious material ratio. Because the volume of the hydration products is greater than that of the reacting cement, at later ages the porosity of the paste decreases as hydration proceeds. However, at the same degree of hydration, the porosity of the paste and the transition zone is determined by its initial porosity and therefore by its water-cementitious materials ratio. Some important properties of the paste, such as strength, stiffness, creep, drying shrinkage, paste-aggregate bond, permeability, and durability, are highly dependent on porosity and thus on water-to-cementitious material ratio. Increase in porosity of the paste and porosity of the transition zone with increase in water-to-cementitious material ratio can explain *w/cm* - strength relationship.

The total volume of voids in concrete also depends on the degree of compaction of concrete. With the decreasing water content, mixing, placing, compacting and finishing fresh concrete become more and more difficult. In practice for any concrete mix there is a limit for water-to-cementitious material ratio below which full compaction of concrete is no longer possible. At this point, a lower water-to-cementitious material ratio will not lead to a higher strength. The actual value for this limit depends on the means of compaction.

2.4 Aggregates

In most cases natural mineral aggregates such as natural sand, gravel, and crushed stones are used for the production of high strength concrete. Physical characteristics, impurities and contaminants, mechanical properties, and chemical stability of aggregate particles can have significant effects on the workability of the fresh concrete and the strength and durability of the hardened concrete.

Sands and gravel are rock fragments of more resistant minerals which have been able to withstand the destructive effects of weathering and transport for a long period of time. Most sands and gravels are obtained from rivers and glacial deposits. Deposits of coarse-grained soil are also good sources of natural sand and gravel. Soil deposits must be removed from the

surfaces of sand and gravel particles by washing or dry screening. The choice of the process between washing and dry screening will influence the amount of deleterious substances in the aggregate that will adversely affect the properties of both fresh and hardened concrete.

Crushed limestone rocks constitute about two-thirds of all the crushed aggregate used in production of concrete while other crushed rocks such as granite, sandstone, and basalt make up the rest *[Mehta 1986]*. Since the conditions under which limestones are formed and consolidated vary significantly, characteristics of limestones, such as shape, texture, porosity, strength, and soundness can vary widely from one source to another source or from one elevation to another elevation within the same quarry. Limestones tend to be porous if formed under relatively low pressure and dense if formed under high pressure. The choice of crushing equipment affects the shape of particles. Laminated limestones tend to produce elongated and flaky fragments, especially when jaw crushers are used for processing.

In regard to mineral composition, limestones belong to the group of carbonated rocks. They range from pure limestone, consisting of mineral calcite (calcium carbonate, $CaCO_3$), to pure dolomite, consisting of the mineral dolomite (equimolecular proportions of calcium carbonate and magnesium carbonate, 54.28 and 45.72 mass percentages of $CaCO_3$ and $MgCO_3$, respectively). In general, limestones contain both carbonate minerals in various proportions and significant amounts of noncarbonate impurities, such as clay and sand.

Shape and surface texture of coarse aggregate affect the total mixing water requirement of concrete. Rough-textured, angular, elongated particles require more water to produce workable concrete than do smooth, round, compact aggregates. These characteristics also control the cement matrix-aggregate bond characteristics and therefore play a significant role in strength producing qualities in high strength concrete *[Blick 1985, Albinger 1988, ACI 363R-92 1992]*. Bond is partly due to the interlocking effect between aggregate and the cement matrix. A rougher surface, such as that of crushed particles, results in better bond. Better bond is also usually obtained with softer, porous, and mineralogically heterogeneous particles *[Neville 1975]*.

Mineralogy of aggregate may also affect the cement matrix-aggregate bond characteristics. Observed better bond between limestone aggregate particles and portland cement paste has been attributed to possible chemical interaction between limestone and cement paste *[Xie Ping et al. 1991; Aïtcin and Mehta 1990; Neville 1975]*. The ideal aggregate for production of high strength concrete has been described as a clean, cubical, angular, 100 percent crushed aggregate with a minimum of flat and elongated particles *[ACI-363R 1992]*.

It is well known that in general the compressive strength of concrete increases as the maximum size of aggregate decreases *[Bloem and Gaynor 1964, Blick 1985]*. While using small size and angular shaped coarse aggregate increases total mixing water requirement, the associated strength loss is overcome by improved bond developed between the paste and the aggregate. The thickness of water layer at the aggregate particle-portland cement paste interface in fresh concrete as well as the thickness of the transition zone in hardened concrete decreases with decreasing particle size *[Xie Ping et al. 1991]*. Keeping the maximum size of the coarse aggregate to a minimum is also advantageous in that less severe concentrations of stress around aggregate particles occur when smaller aggregate sizes are used.

High strength concrete contains such high amounts of fine cementitious materials that the gradation of the aggregates used is not as important as for the case of less rich concretes *[ACI-363R 1992]*. Both fine and coarse aggregates used for production of high strength concrete should at least meet the requirements of ASTM C-33 *[ACI-363R 1992]*. The division between fine and coarse aggregates is an arbitrary one based on size. For concrete that portion of material which passes a No. 4 sieve (4.75 mm) is usually classified as fine (sand), and larger materials are classified as coarse *[ASTM C-125]*. Tables 2.2 and 2.3 summarize ASTM C-33 grading requirements for coarse and fine aggregates.

Selection of fine aggregate for high strength concrete should be based more on its effect on water requirement than on gradation. In one study the use of sands with fineness modulus around 3.0 (which are considered coarse for use in normal strength concrete) provided the best

workability and highest compressive strengths *[Blick et al. 1985]*. It was also reported that natural sand produces higher strengths than manufactured sand made from either limestone or traprock. This observation was attributed to the reduced mixing water demand for the natural sand (less angular material) *[Smith et al. 1964]*.

The previous sections discussed indirect influence of aggregate properties on the strength of concrete through their effects on the aggregate-paste bond strength. However it is reported that other properties of aggregate, such as strength and stiffness, affect concrete strength. When strength of aggregate becomes the dominant factor, further increase in the strength of the paste does not significantly affect concrete strength. This effect is visible in testing some high strength concretes, in which cracks propagate through the aggregate *[French and Mokhtarzadeh 1993]*. Aggregate stiffness affects the stress distribution in the concrete during external loading. Assuming equal strains, a stiffer aggregate takes a higher fraction of the load and consequently the fraction of the load taken by the paste decreases. When the strength of the paste is the limiting factor, a decrease in the loading on the paste delays fracture and therefore increases the concrete strength.

2.5 High-Range Water Reducers (HRWR) or Superplasticizers

Admixtures are ingredients that are added to the concrete batch immediately before or during mixing. They offer beneficial effects to concrete, including enhanced frost and sulfate resistance, controlled setting and hardening, improved workability, increased strength, etc. In this research program only high-range water reducers (also more commonly called superplasticizers) were used for production of high strength concrete mixtures. The following is a brief review of the characteristics and the use of superplasticizers in high strength concrete.

Water requirements of a given concrete mixture can be reduced by approximately 10 to 15% with the use of a normal water reducer. Further reduction of water requirement may be obtained by using higher dosages but this may lead to undesirable effects on setting, air content, bleeding, segregation, and hardening of concrete *[Ramachandran and Malhotra 1984]*.

Superplasticizers, also called superfluidizers, superfluidifiers, super water reducers or high-range water reducers *(HRWR)*, are a more recent and more effective type of water reducer. They consist of long chain, high molecular weight anionic surfactants with a large number of polar groups in the hydrocarbon chain. When adsorbed on the surface of cement particles, the surfactant negatively charges the cement particles, makes them mutually repulsive and results in a better dispersion of cement particles. It is also said that the adsorbed superplasticizer forms a thin film membrane around the anhydrous cement particle preventing early hydration and as a consequence more water remains available to fluidify the system. Many other mechanisms have been suggested to explain the fluidifying effect of water reducers *[Collepardi 1984]*. Whatever the mechanism of action, superplasticizers are capable of reducing the water requirement of a given concrete mixture by about 30 percent *[Ramachandran and Malhotra 1984]*.

Superplasticizers permit production of high strength concrete by allowing less water to be used (low *w/c* or *w/cm*) while maintaining workability. The opposing effect of *w/c* (or *w/cm*) on consistency and strength of concrete makes superplasticizers a vital ingredient of high strength concrete mixtures *[Lambotte and Taerwe 1989]*. Superplasticizers can also reduce quantities of both cement and water to obtain a given strength and workability. Easy and quick placement characteristics of superplasticized concrete makes it suitable, among many other applications, for placement in precast/prestressed bridge girder forms. Better dispersion of the cement particles in superplasticized concrete accelerates the rate of hydration resulting in higher compressive strengths at early ages *[Whiting 1979]*. This is of special interest in the precast concrete industry, where high early strengths are required for faster turnover of the formwork.

There are limitations associated with the use of superplasticizers. The improved workability produced by superplasticizers is of a short duration and a high rate of slump loss is observed in superplasticized concretes *[Whiting 1979; Gebler 1982; Aïtcin et al. 1991]*. Aïtcin et al. associated the slump loss of superplasticized concrete with the amount and reactivity of C_3A, the fineness of cement, and its soluble alkali content *[Aïtcin et al. 1991]*. The ideal concrete mix

should have moderate slump loss over a period of 1 hour to ensure easy delivery and placing. In precast plants this poses a lesser problem because casting of concrete is usually done within 15 minutes of batching. Matching the admixture to the cement, both in type and dosage rate, is reported to be important. Some cements appear to be more reactive than others at very low *w/c* *[Aïtcin et al. 1991; ACI 363R92 1992]*. The ability of the superplasticizer to increase the slump of concrete depends on the type, dosage and time of addition of the superplasticizer, water-to-cementitious material ratio, nature and amount of cement and aggregate, temperature, etc. In some cases, plasticity is not recoverable, even by redosing the superplasticizer *[Aïtcin et al. 1991]*. To avoid problems associated with potential cement-superplasticizer incompatibility, it is recommended to test selected superplasticizers in combination with job cements under conditions to be expected on the jobsite prior to their actual incorporation into any full-scale field project *[Whiting 1979]*.

In general, superplasticizers are classified into four groups:

1. sulfonated melamine-formaldehyde condensate (SMF);
2. sulfonated naphthalene-formaldehyde condensate (SNF);
3. modified lignosulfonates (MLS);
4. Others including sulfonic-acid esters, carbohydrate esters, etc.

Variations exist in each of these groups and some formulations may contain a second ingredient. ASTM C 494, Specifications for Chemical Admixtures for Concrete, defines the characteristics of superplasticizers. ACI Committee 212-Chemical Admixtures, provides updated guidelines for use of superplasticizers in concrete *[ACI 212.4R 1993]*. Most of the available data on superplasticized concrete are obtained using SMF- and SNF-based superplasticizers *[Ramachandran and Malhotra 1984]*.

2.6 Pozzolans (Supplementary Cementing Materials)

According to ASTM C 618, Specifications for Fly Ash and Raw or Calcined Natural Pozzolan for Use as a Mineral Admixture in Portland Cement Concrete, a Pozzolan is defined as:

> "A siliceous or siliceous and aluminous material which in itself possesses little or no cementitious value but will, in finely divided form and in the presence of moisture, chemically react with calcium hydroxide ($Ca(OH)_2$) at ordinary temperature to form compounds possessing cementitious properties."

When pozzolans are incorporated into concrete, the portland cement component becomes the source of calcium hydroxide (product of hydration of portland cement) which reacts with aluminosilicates present in the pozzolan to produce more cementitious hydrates.

Although natural pozzolans are still being used in some parts of the world, many industrial byproducts such as fly ash and silica fume are rapidly becoming the primary source of pozzolans in use today. Although silica fume and several other byproducts such as granulated slags and rice husk ash had been in use as pozzolans for many years they are not covered by the ASTM C 618 Classification. It was just recently in 1993, that the new ASTM C 1240 specification addressed the use of silica fume in concrete.

Three basic mix proportioning approaches have been suggested for use of fly ash in concrete *[Helmuth 1987; Berry and Malhotra 1980]*:

1. Replacement by weight of a portion of the portland cement with fly ash on a 1 to 1 basis.
2. Inclusion of fly ash in concrete mixture as fine aggregate without reduction of portland cement content.

3. Optimizing the proportions of concrete for both strength development and economy by partial replacement of the portland cement with fly ash and making adjustments in water and fine aggregate content.

Silica fume can practically be used in concrete in the same manner as is described above for fly ash *[FIP 1988]*.

Two factors adversely affect strength of concrete: the presence of large voids in the hydrated cement paste; and the microcracks at the aggregate-cement paste transition zone. Inclusion of pozzolans in concrete can transform large pores into fine pores and reduce microcracking in the transition zone *[Mehta 1984]*.

2.6.1 Fly Ash

Fly ash is a byproduct of the burning of pulverized coal in power plants. On entry into the furnace, where the temperatures are usually around 2700° F, the volatile matter and carbon are burned off, whereas most of mineral impurities present in the coal, such as shales and clays (basically consisting of silica, alumina, and iron oxide), melt at high temperature. On rapid cooling some of the mineral matter agglomerates and forms bottom ash, but most of it forms into spherical particles and flies out with the combustion gases and is called *fly ash*. This ash is removed by mechanical collectors or electrostatic precipitators before combustion gases are discharged into the atmosphere *[Swamy 1986]*.

For use in concrete, ASTM C 618 divides fly ashes into three distinct categories:

1. *Class N*: Raw or calcined natural pozzolans such as diatomaceous earths, opaline cherts, clays and shales, tuffs and volcanic ashes or pumicites.
2. *Class F* or low-lime (low-calcium) fly ash: Fly ash produced from burning anthracite or bituminous coal.

3. *Class C* or High-lime (high-calcium) fly ash: Fly ash normally produced from lignite or sub-bituminous coal which may contain analytical *CaO* contents higher than 10%.

A summary of the chemical and physical requirements for fly ashes given in ASTM C 618 is presented in Table 2.4.

In general low-lime fly ash is the product of combustion of anthracite and bituminous coals. Low-lime fly ash usually contains less than 5 percent *CaO*. This category possesses only pozzolanic properties and needs the calcium hydroxide ($Ca(OH)_2$) produced during hydration of portland cement as an activator to undergo reaction and produce more of the cementitious material *C-S-H*. This reaction can be represented by the following simplified equation:

- $xCH + yS + zH \quad C_xS_yH_{x+z}$ **(2.10)**

High-lime fly ash is generally the product of combustion of lignite and subbituminous coals and contains 15 to 35 percent *CaO*. Because of the high *CaO* content, high-lime fly ash does not need an external source of calcium to activate pozzolanic reaction. Therefore high-lime fly ash, in the presence of water, can exhibit some cementitious properties on its own.

Fly ash suitable for use in concrete consists mostly of glassy, hollow, spherical particles with specific gravity between 1.9 to 2.4. The loose bulk density of dry fly ash is about 50 pcf (800 kg/m^3). Depending on the method of collection, fly ash may be finer or coarser than ordinary portland cement. The color of fly ash ranges from almost cream to dark gray, basically depending on the amount of its unburned carbon and iron content.

Despite extensive research on the effect of fly ash on properties of concrete there have been persistent problems in its application due to the variability of fly ash (even from a single source) and the difficulty of characterizing it for predictable performance in concrete *[Helmuth 1987]*. Much of the research concerns bituminous coal fly ash and does not necessarily apply to

the subbituminous coal and lignite fly ash found and used in the Western United States *[Helmuth 1987]*.

Inclusion of fly ash influences concrete mix proportions, rheological behavior of plastic concrete, degree of hydration of portland cement, strength and permeability of hardened concrete, resistance to thermal cracking, alkali-silica expansion, and sulfate attack *[Berry and Malhotra 1980; Mehta 1984]*. It acts in part as fine aggregate and in part as a cementitious component. In general, concretes containing fly ash show reduced bleeding and segregation. Unlike other pozzolans, fly ash reduces the water requirement for a given degree of workability when used as a partial replacement for portland cement in concrete. Water reductions of 7% or more have been reported *[Berry and Malhotra 1980; Helmuth 1987]*. The reduction of the water requirement for fly ash concrete is usually attributed to the fact that most of the fly ash is composed of spherical particles with smooth surfaces leading to improved workability. It has been suggested that this explanation is too simplistic and that the deflocculation effects appear to be more important *[Helmuth 1987]*. Some Australian, Indian, and Korean fly ashes (generally of higher carbon content) have increased water requirement of the mix *[Shin 1990]*.

The contribution of fly ash to concrete strength was studied by Slanicka and Smith. Slanicka proposed modified forms of Abrams and Bolomey formulas *[Slanicka 1990]*. Smith *(1967)* introduced the following formula for computing the equivalent water-to-cement ratio for mixes containing fly ash:

- $(w/c)_e = w/(c+Kf) = (w/c)\{1/[1+K(f/c)]\}$ **(2.11)**

where

$(w/c)_e$ = equivalent water-to-cement ratio

w = weight of water

c = weight of cement

f = weight of fly ash

K = cementing efficiency of fly ash (i.e. for a given strength, a given weight f of fly ash is equivalent to a weight Kf of cement)

For the fly ashes that Smith used, K had a value of about 0.25. It was also reported that inclusion of fly ash increases the setting time of concrete. This is consistent with Smith's equation since equivalent water-cement ratio of the mix increases.

It is reported that hydration of cement is usually accelerated by fly ash after some initial retardation *[Helmuth 1987]*. When a control mix and a mix containing fly ash was compared, it was at 91 days or more that the fly ash concrete showed higher strengths than control mixes *[Mehta 1984]*. However, the low early strength of a fly-ash concrete can be increased by simultaneous use of silica fume *[Sarkar et al. 1991]*. For concretes made with Chicago fly ash, Washa and Withey (*1953*) recommended replacement with a greater amount of fly ash than the amount of portland cement removed to obtain 28-day strengths equal to those of concretes without Chicago fly ash.

Reactivity of fly ash is significantly influenced by its fineness, glass content, and silica-plus-alumina contents *[Helmuth 1987]*. Sarkar et al. (*1991*) reported that it is the composition of the individual particles not the particle size that affects the fly ash reactivity.

2.6.2 Condensed Silica Fume

Condensed silica fume is a byproduct from electric arc furnaces used in the smelting process to produce silicon metal and ferrosilicon alloys. In general, it contains more than 90 percent silicon dioxide (SiO_2), most of which is amorphous *[ACI 226]*. In the literature, condensed silica fume has been called various names, such as microsilica, ferrosilicon dust, arc furnace silica, silica flue dust, amorphous silica, volatized silica, silica dust, silica flour, pyrogenic silica, and silica fume. "Condensed silica fume" or simply "silica fume", as used throughout this report, seems to be the most appropriate name since the production process involves oxidation of SiO vapor followed by condensation of the SiO_2 fume.

Silica fume for use in concrete is either in the natural state, densified, or in slurry form mixed with an equal mass of water. Silica fume in the natural state has a bulk density between 12.5 to 15.5 pcf (200 to 250 kg/m^3). This low bulk density causes serious difficulties in handling the material. Densification of silica fume into a powder that is somewhat coarser than portland cement results in a bulk density of 31 to 45 pcf (500 to 720 kg/m^3) depending on the extent of densification. Densified silica fume is relatively easy to bag and transport.

As will be discussed later, the performance of silica fume is a function of its chemical composition as well as its very fine particle size. When using the densified form of silica fume, higher duration and energy of mixing is required to breakdown densified agglomerates into the individual fine particles. Incomplete breakdown of densified silica fume in concrete leaves some unreacted silica fume particles in the mix which not only adversely affect the strength and permeability of concrete but may become potential sites for formation of expansive alkali silica gel in case of exposure to alkali ions at a later time.

A practical approach in using silica fume in concrete production is to make a slurry of silica fume by mixing it with an equal weight of water. The slurry form of silica fume has a specific gravity of 1.3 to 1.4. When using the slurry form of silica fume, settlement of solids from the suspension should be prevented by frequent agitation. A study by Cohen and Olek showed no significant differences in the engineering properties of concretes containing either of the three forms of silica fume *[Cohen and Olek 1989]*. Table 2.5 shows a summary of the ASTM C 1240 chemical and physical requirements of silica fume for use in concrete.

In concrete applications, part of the cement may be replaced by a much smaller quantity of silica fume without loss of strength. As an example, ACI Committee 226 report states that, on a weight basis, 1 part of silica fume may replace 3 to 4 parts of portland cement with no significant effect on strength of concrete *[ACI 226]*. Very high strength concretes have been produced when up to 25 percent of the weight of the cement had been replaced by an equal

weight of silica fume *[ACI 226]*. Addition of silica fume is usually accompanied by reduced bleeding and an increase in the water demand of concrete. Full strength-producing potential of silica fume is utilized when it is used with a compatible water-reducing agent *[Mehta 1986, Albinger 1988]*.

Addition of silica fume to concrete densifies the paste through two primary mechanisms: filler effect and the basic pozzolanic reaction. The particle size distribution of typical silica fume shows most particles to be smaller than 1 μm with an average diameter of about 0.1 μm, which is approximately 100 times smaller than the average cement particle *[ACI 226]*. The extreme fineness of silica fume particles allows it to fill the microscopic voids between cement particles (filler effect). These effects lead to pore refinement of the cement paste which improves the strength and durability of the silica fume cement system. It is reported that, when concrete is cured at normal temperatures, at very early ages silica fume merely acts as a filler material *[Detwiler and Mehta 1989; Sarkar 1991]*. At later ages, high reactivity of silica fume with calcium hydroxide, released by the hydration of cement produces additional cementitious C-S-H gel (pozzolanic reaction). However, high reactivity of silica fume can be somewhat dampened in low *w/cm* concrete due to the lack of calcium hydroxide, one of the essential ingredients of pozzolanic reaction *[Sarkar and Aïtcin 1987; Sarkar et al. 1991]*.

Recent studies have shown that the use of silica fume densifies the transition zone between the aggregate and the cement paste *[Goldman and Bentur 1989; Detwiler and Mehta 1989]*. The relative higher concentration of calcium hydroxide at the transition zone favors production of extra C-S-H gel in the available pores thereby reducing the thickness of the transition zone and densifying and homogenizing the paste in the near vicinity of the aggregate *[Larbi and Bijen 1991]*. This zone is thought to be the weakest link in concrete with respect to permeability. The strength of the transition zone also limits the overall concrete strength.

The long-term compressive strength of silica fume concrete has been recently questioned by some researchers *[Carette et al. 1987]*. However, Aïtcin and Laplante reported no sign of

strength loss in cores taken from seven field silica fume concretes, exposed for 4-6 years to severe environmental conditions *[Aïtcin and Laplante 1990]*.

2.7 Concluding Remarks

High strength concrete is gaining widespread acceptance in both cast-in-place and precast/prestressed applications. In general, concrete can be considered as a three-phase composite material consisting of the cement matrix, aggregate, and the transition zone between the cement matrix and the aggregate. Therefore, it is clear that production of high strength concrete involves strength improvement of the cement matrix and the transition zone between the cement matrix and the aggregate together with the selection of a type of aggregate which is stiff, strong and promotes good bond with the cement matrix.

The problem of selection of the materials and mix proportions for high strength concrete becomes complicated by the fact that production of high strength concrete requires a low water-to-cementitious material ratio and simultaneous incorporation of various chemical admixtures and supplementary cementing materials such as normal water-reducing and set retarding admixtures, superplasticizers, air entraining agents, fly ash and silica fume. In addition, performance of many of these constituents may be adversely affected in a low water-to-cementitious material concrete environment.

Table 2.1. Summary of the ASTM C 150 specifications for portland cement

Cement Type	I	IA	II	IIA	III	IIIA	IV	V
A. Standard Chemical Requirements								
SiO_2, min, %	-	-	20.0	20.0	-	-	-	-
Al_2O_3, max, %	-	-	6.0	6.0	-	-	-	-
Fe_2O_3, max, %	-	-	6.0	6.0	-	-	6.5	-
MgO, max, %	6.0	6.0	6.0	6.0	6.0	6.0	6.0	6.0
SO_3, max, % when C_3A <or= 8%	3.0	3.0	3.0	3.0	3.5	3.5	2.3	2.3
SO_3, max, % when C_3A> 8%	3.5	3.5	NA	NA	4.5	4.5	NA	NA
Loss on Ignition, max, %	3.0	3.0	3.0	3.0	3.0	3.0	2.5	3.0
Insoluble residue, max, %	0.75	0.75	0.75	0.75	0.75	0.75	0.75	0.75
C_3S, max, %	-	-	-	-	-	-	35	-
C_2S, min, %	-	-	-	-	-	-	40	-
C_3A, max, %	-	-	8	8	15	15	7	5
$(C_4AF+2(C_3A))$ or (C_4AF+C_2F), max, %	-	-	-	-	-	-	-	25
B. Optional Chemical Requirements								
C_3A, max , % (for moderate sulfate resistance)	-	-	-	-	8	8	-	-
C_3A, max , % (for high sulfate resistance)	-	-	-	-	5	5	-	-
(C_3S+C_3A), max, % (for moderate heat of hydration)	-	-	58	58	-	-	-	-
Alkalies $(Na_2O+0.658K_2O)$, max, %	0.60	0.60	0.60	0.60	0.60	0.60	0.60	0.60
C. Standard Physical Requirements								
Air content of mortar, volume %: max min	12 -	22 16	12 -	22 16	12 -	22 16	12 -	12 -
Fineness, specific surface, m^2/kg:								
Turbidimeter test, min	160	160	160	160	-	-	160	160
Air permeability test, min	280	280	280	280	-	-	280	280
Autoclave expansion, max, %	0.80	0.80	0.80	0.80	0.80	0.80	0.80	0.80
Compressive strength, min, psi								
1-day	-	-	-	-	1800	1450	-	-
3-days	1800	1450	1500	1200	3500	2800	-	1200
7-days	2800	2250	2500	2000	-	-	1000	2200
28-days	-	-	-	-	-	-	2500	3000
Time of setting:								
*Gillmore test:								
initial set, min, not less than	60	60	60	60	60	60	60	60
final set, min, not more than	600	600	600	600	600	600	600	600
*Vicat test:								
time of setting, min, not less than	45	45	45	45	45	45	45	45
time of setting, min, not more than	375	375	375	375	375	375	375	375
D. Optional Physical Requirements								
False Set, final penetration, min, %	50	50	50	50	50	50	50	50
Heat of hydration:								
7 days, max, cal/g	-	-	70	70	-	-	60	-
28 days, max, cal/g	-	-	-	-	-	-	70	-
Compressive strength, min, psi								
28-days	4000	3200	4000	3200	-	-	-	-
Sulfate expansion, 14 days, max, %	-	-	-	-	-	-	-	0.040

NA: Not Applicable

Table 2.2. Summary of the ASTM C 33 grading requirements for coarse aggregates

Size No.	Nominal size	Amounts finer than each laboratory sieve (square opening), weight percent passing												
		4 in. *100 mm*	3½ in. *90 mm*	3 in. *75 mm*	2½ in. *63 mm*	2 in. *50 mm*	1½ in. *37.5 mm*	1 in. *25.0 mm*	¾ in. *19.0 mm*	½ in. *12.5 mm*	3/8 in. *9.5 mm*	No. 4 *4.75 mm*	No. 8 *2.36 mm*	No. 16 *1.18 mm*
1	3½ - 1½ in.	100	90-100	-	25-60	-	0-15	-	0-5	-	-	-	-	-
2	2½ - 1½ in.	-	-	100	90-100	35-70	0-15	-	0-5	-	-	-	-	-
3	2 - 1 in.	-	-	-	100	90-100	35-70	0-15	-	0-5	-	-	-	-
357	2 in. - No. 4	-	-	-	100	95-100	-	35-70	-	10-30	-	0-5	-	-
4	1½ - ¾ in.	-	-	-	-	100	90-100	20-55	0-15	-	0-5	-	-	-
467	1½ in. - No. 4	-	-	-	-	100	95-100	-	35-70	-	10-30	0-5	-	-
5	1 - ½ in.	-	-	-	-	-	100	90-100	20-55	0-10	0-5	-	-	-
56	1 - 3/8 in.	-	-	-	-	-	100	90-100	40-85	10-40	0-15	0-5	-	-
57	1 in. - No. 4	-	-	-	-	-	100	95-100	-	25-60	-	0-10	0-5	-
6	¾ - 3/8 in.	-	-	-	-	-	-	100	90-100	20-55	0-15	0-5	-	-
67	¾ in. - No. 4	-	-	-	-	-	-	100	90-100	-	25-55	0-10	0-5	-
7	½ in. - No. 4	-	-	-	-	-	-	-	100	90-100	40-70	0-15	0-5	-
8	3/8 in. - No. 4	-	-	-	-	-	-	-	-	100	85-100	10-30	0-10	0-5

Table 2.3. Summary of the ASTM C 33 grading requirements for fine aggregates

Sieve size	Percent passing by weight
3/8 in. (*9.5 mm*)	100
No. 4 (*4.75 mm*)	95-100
No. 8 (*2.36 mm*)	80-100
No. 16 (*1.18 mm*)	50-85
No. 30 (*600 μm*)	25-60
No. 50 (*300 μm*)	10-30
No. 100 (150 *μm*)	2-10

Table 2.4. Summary of the ASTM C 618 specifications for fly ash

Fly ash Class	Class N	Class F	Class C
A. Standard Chemical Requirements			
(SiO_2+Al_2O_3+Fe_2O_3), min, %	70.0	70.0	50.0
SO_3, max, %	4.0	5.0	5.0
Moisture content, max, %	3.0	3.0	3.0
Loss on ignition, max, %	10.0	6.0	6.0
B. Optional Chemical Requirements			
Available alkalies, as Na_2O, max , %	1.50	1.50	1.50
C. Standard Physical Requirements			
Fineness:			
Amount retained when wet-sieved on No. 325 (45 μm) sieve, max, %	34	34	34
Strength activity index:			
With portland cement, at 7-days, min, % of control	75	75	75
With portland cement, at 28-days, min, % of control	75	75	75
Water requirement, max, % of control	115	105	105
Soundness:			
Autoclave expansion or contraction, max, %	0.8	0.8	0.8
Uniformity:			
The density and oversize of individual samples shall not vary from the average of previous 10 or by all preceding tests if the number is less than ten, by more than:			
Density, max variation from average, %	5	5	5
Oversize, percent retained on No. 325 (45 μm) sieve, max variation, percentage points from average	5	5	5
D. Optional Physical Requirements			
Multiple factor, product of LOI, max, %, and fineness, max, %	-	255	-
Increase of drying shrinkage of mortar bars at 28-days, max, %	0.03	0.03	0.03
Uniformity requirements:			
When air-entraining concrete is specified, quantity of AE agent required to produce air content of 18.0 vol % shall not vary from the average of previous 10 or by all preceding tests if the number is less than ten by more than, %	20	20	20
Reactivity with cement alkalies:			
Reduction of mortar expansion at 14-days, min, %	75	-	-
Mortar expansion at 14-days, max, %	0.020	0.020	0.020

Table 2.5. Summary of the ASTM C 1240 specifications for silica fume

A. Standard Chemical Requirements	
SiO_2, min, %	85.0
Moisture content, max, %	3.0
Loss on Ignition, max, %	6.0
B. Optional Chemical Requirements	
Available alkalies as NaO_2, max , %	1.50
C. Standard Physical Requirements	
Oversize: Percent retained on No. 325 (45 μm) sieve, max, %	10
Accelerated pozzolanic activity index: With portland cement at 7-days, min percent of control	85
Uniformity requirements: The density and oversize of individual samples shall not vary from the average of previous 10 or by all preceding tests if the number is less than ten, by more than: Density, max variation from average, %	5
Oversize, percent retained on No. 325 (45 μm) sieve, max variation, percentage points from average	5
D. Optional Physical Requirements	
Increase of drying shrinkage of mortar bars at 28-days, max, %	0.10
Specific surface area, m^2/g	15-30
Uniformity requirements: When air-entraining concrete is specified, quantity of AE agent required to produce air content of 18.0 vol % shall not vary from the average of previous 10 or by all preceding tests if the number is less than ten, by more than, %	20
Reactivity with cement alkalies: Reduction of mortar expansion at 14-days, min, %	80
Sulfate resistance expansion: (moderate resistance) 6 months, max, % (high resistance) 6 months, max, % (very high resistance) 1 year, max, %	0.10 0.05 0.05

CHAPTER 3
EXPERIMENTAL PROGRAM:
MIXES, MATERIALS, FABRICATION AND CURING

3.1 Introduction

During the course of this research program, over 6,300 specimens from 142 high strength concrete mixes with 28-day compressive strengths in the range of 8,000 to 18,600 psi (55.2 to 128 MPa) were cast, prepared and tested. These concrete mixtures had water-to-cementitious material ratios (*w/cm*) between 0.28 to 0.32 and contained the following combinations of supplementary cementing materials: none, fly ash only, silica fume only, or both fly ash and silica fume, replacement by weight of cement.

Each high strength concrete mix was assigned a mix number and an identification code (ID code), such as: ***Mix No. 28; 131-MBL1-F30M15-130***. The mix number simply designates the order in which the mix was batched. For example, the above mix was the twenty-eighth high strength concrete mix batched for the purpose of this study. Figure 3.1 gives a detailed explanation of the notation used in the mix ID codes. Each mix ID code was divided into four parts separated by dashed lines. A typical mix ID code provided the following information about the high strength concrete mix:

- cementitious material content (*131-MBL1-F30M15-130*);
- type of portland cement (*131-MBL1-F30M15-130*);
- brand of portland cement (*131-MBL1-F30M15-130*);
- gradation of coarse aggregate (*131-MBL1-F30M15-130*);
- coarse/fine aggregate ratio (*131-MBL1-F30M15-130*);
- type of coarse aggregate (*131-MBL1-F30M15-130*);
- source of coarse aggregate (*131-MBL1-F30M15-130*);
- type and amount of supplementary cementing materials (*131-MBL1-F30M15-130*);
- type of superplasticizer (*131-MBL1-F30M15-130*);

- water-to-cementitious material ratio (*131-MBL1-F30M15-130*).

All of the mixes considered in this research program together with their mix ID codes are presented in Table 3.1.

3.2 High Strength Concrete Mixes

High strength concrete mixes considered in this study were designed to:

- study the effect of test variables on the mechanical properties of high strength concrete; and
- study the effect of mix variables on the mechanical properties of high strength concrete.

Throughout this study, efforts were made to use materials and procedures which were considered to be representative of typical practice used in the precast/prestressed industry. A survey of five local manufacturers of precast/prestressed elements, conducted at the beginning of this research program, provided information about materials and procedures used by the industry. In addition, standard tests were conducted on companion specimens, to correlate the results of this study with the results reported elsewhere in the literature.

Test variables included parameters which had an effect on strength test results (e.g. mold material, mold size, specimen end condition). The curing process of typical precast bridge girders was simulated by heat-curing specimens according to the manufacturing procedure described in Section 3.4.4. Results of the heat-cured specimen tests were compared with companion tests on specimens cured in standard lime-saturated water and other curing conditions. Details of curing procedures used are given in Sections 3.4.3-5 of this report. Tests were conducted at various specimen ages. One day compressive strengths gave an indication of the achievable girder strengths at the time of prestress transfer, 28-day compressive strengths

were used to correlate with code equations, and older age specimen compressive strengths corresponded with strength of girders in service. The test variables investigated were:

1.	Mold type:	reusable steel, single-use plastic
2.	Mold size:	4 x 8 in., 6 x 12 in. (100 x 200 mm, 150 x 300 mm)
3.	End condition:	high strength sulfur cap, ground ends, unbonded neoprene caps
4.	Curing conditions:	heat-curing at 120 or 150 °F (50 or 65 °C), heat-curing followed by 1 or 3 days of moist-curing, 7, 14, or 28 days of moist-curing, continuous moist-curing
5.	Age at testing:	1 through 365 days

The following is the list of the material variables investigated:

1.	Total cementitious material content:	750, 850, 950 lb/yd^3 (445, 505, 565 kg/m^3)
2.	Type of cement:	Type I, Type III
3.	Brand of cement:	2
4.	Percent of fly ash:	0%, 10%, 20%, 30%, replacement by weight of portland cement
5.	Percent of silica fume:	0%, 7.5%, 10%, 15%, replacement by weight of portland cement
6.	Type of silica fume:	dry densified, slurry
7.	Type and brand of superplasticizer:	5
8.	Type and source of coarse aggregate:	2 limestones (high- and low-absorption), 2 granites, river gravel (round and crushed)

9. Aggregate gradation:	as received, recombined
10. Maximum aggregate size:	1/2 in. and 3/4 in. (12.5 mm and 19.0 mm)

There were several combinations and permutations of variables listed. For example, for each total cementitious material content, mixes containing fourteen combinations of the listed fly ash and silica fume percentages were investigated.

Based on the stated objectives, different sets of high strength concrete mixes were batched and appropriate specimens were cast and tested to study the effects of some of the test and mix variables at a time. More detailed information about mixes, their ingredients and their specific objectives follows.

Mixes 1, 2 and 3: Concrete balls were formed during production of mixes 1, 2, and 3. Production of high strength concrete with a very low water-to-cementitious material ratio needs an efficient mixer. In general, prior to the addition of superplasticizers, high strength concrete mixes are very dry, stiff and unworkable. Therefore the type and efficiency of the mixer to break up agglomerates in a stiff mix can play an important role in the successful production of high strength concrete. For the production of Mix Nos. 1-3 a fixed-blade rotating-drum mixer was used. The low amount of free water in the mix together with the inefficiency of this type of mixer resulted in the concrete forming balls during mixing. Generally when this happened, so much water had to be added to the mix to break up the concrete balls that the resulting mix was unacceptable. As a result, concrete Mix Nos. 1-3 were discarded. The remainder of the mixes were produced with the fixed-drum mixer described later in Section 3.4.2 of this report.

Mixes 4 and 5: Except for the coarse aggregate used, these two mixes had identical mix designs. Mix Nos. 4 and 5 were designed to study the effect of the source of limestone aggregates on concrete compressive strength and to narrow down to one source of limestone for future experiments. Limestone aggregates considered had different absorption rates. The high-absorption limestone is designated as "*L1*" and the low-absorption limestone is referred to

as "*L2*" throughout this report. Detailed information on the properties of all aggregates used is given in Section 3.3.2 of this report. Tests were also conducted to investigate the effects of mold material, mold size, specimen end condition (capped vs. ground), and age on compressive strength test results.

In order to minimize the effect of cleanness and gradation of the coarse aggregate on the test results, coarse aggregates were washed, separated into individual size fractions and then recombined to produce a "*standard*" gradation (gradation "S" in ID codes), conforming to the grading requirements of ASTM C 33 for size No. 7. The grain size distribution curve for this gradation together with the limits specified by ASTM C 33 for size No. 7 is shown in Figure 3.2. As can be seen from this figure the standard gradation selected is closer to the coarser limit specified by ASTM C 33.

Mixes 6 to 14: These mixes, with the exception of Mix No. 8 which was discarded, were used to compare the compressive strengths of high strength concrete mixes made with the limestone aggregate from Source #1, *L1* (selected from results of the previous mixes) with those made with round river gravel aggregate, referred to as "*R1*" throughout this report. Aggregates used for these mixes were also washed, separated into individual size fractions and then recombined to produce the "*standard*" gradation, Figure 3.2. Tests were also conducted to study the effects of specimen end condition (capped vs. ground), age and curing methods (heat-curing, air-curing, moist-curing) on compressive strength test results.

Of the eight mixes studied, two had no supplementary cementing materials (reference mixes), two contained 10% fly ash, two contained 7.5% silica fume, and two contained the combination of 10% fly ash and 7.5% silica fume as part of their cementitious material content. In all cases, the total amount of cementitious materials was held constant at 750 lb/yd^3 (445 kg/m^3).

Mixes 15 to 21: These mixes were made with limestone aggregate from Source #1 (*L1*) and were designed to study the effect of the gradation of coarse aggregate on the workability and compressive strength of high strength concrete. Tests were also conducted to investigate the effects of mold size, specimen end condition (capped vs. unbonded neoprene caps), and age on compressive strength test results.

Mixes considered had various cementitious material compositions. Mix Nos. 15 and 17 were replicas and contained no supplementary cementing materials (reference mixes). Mix Nos. 16 and 18 were also replicas and were made with combination of 10% fly ash with 7.5% silica fume. Mix Nos. 19-21 had 10% of silica fume as part of their cementitious material. In all cases, the total amount of cementitious materials was held constant at 750 lb/yd^3 (445 kg/m^3).

Four coarse aggregate gradations were considered. Mix Nos. 15 through 18 used "as received gradation" (gradation "X" in the ID codes), shown in Figure 3.3. The coarse aggregates for Mix Nos. 19 and 20 were separated into individual size fractions and then recombined to produce two different gradations: Gradation "A", and "B". Gradation "A" and "B" were the upper and lower limits specified by ASTM C 33 for size No. 7.

Gradation "M" was obtained by combining the "as received" ASTM C 33 size No. 7 coarse aggregate with an "as received" ASTM C 33 size No. 8 coarse aggregate from the same source. The result was a gradation with less fines (particles smaller than No. 4 sieve) and smaller particles, conforming to the grading requirements of ASTM C 33 for size No. 7. The grain size distribution curve for gradation "M" together with the limits specified by ASTM C 33 for size No. 7 are shown in Figure 3.4.

Mixes 22 to 29 and 50 to 83: Total amount of cementitious material as well as the binder material composition were varied in Mix Nos. 22-29 and 50-83 to determine their

effects on cylinder compressive strength, static modulus of elasticity, modulus of rupture, and splitting tensile strength of high strength concrete. These mixes were all made with limestone from Source #1 (*L1*) and with gradation "M", Figure 3.4. Total cementitious material contents of 750, 850, and 950 lb/yd^3 (445, 505, 565 kg/m^3) were investigated with several combinations and permutations of 0, 10, 20, and 30% fly ash and 0, 7.5, 10, and 15% silica fume all as replacement by weight of portland cement. Also tests were conducted to collect additional data on the effect of mold size, end condition (capped vs. unbonded neoprene caps), age, and curing condition (heat-curing, continuous moist-curing) on compressive strength test results.

Mixes 30 to 49: Mix Nos. 30 to 49 were designed to investigate the effect of the type and brand of five superplasticizers on the compressive strength and strength gain with age of high strength concrete. Table 3.2 provides detailed information about the superplasticizers used. Additional variables in this part of the study included the amount of silica fume (0, 7.5%), type of coarse aggregate (limestone from Source #1: *L1*, and partially crushed river gravel: *R2*), and curing condition (heat-curing, continuous moist-curing).

Mix Nos. 30 to 33 and 44 to 49 used "as received", washed limestone coarse aggregate from source #1 (*L1*), Figure 3.3. Other mixes, 34 to 43, used an "as received", washed partially crushed river gravel (*R2*) as coarse aggregate, Figure 3.5. It should be noted that the "as received" gradation (gradation "X") for the two types of aggregates were different and as can be seen from Figure 3.5, the partially crushed river gravel had more fine particles and its grading curve fell outside the limits specified by ASTM C 33 for size No. 7 coarse aggregate.

Mixes 84 to 91: Mix Nos. 84 to 91 were an expansion to the investigation of the effect of varying the binder material composition on the mechanical properties of high strength concrete (see description for Mix Nos. 22 to 29 and 50 to 83). The coarse aggregate used was the partially crushed river gravel with "as received" gradation, Figure 3.5.

Mixes 92 to 99: These mixes contained granite from Source #1 (G1) as their coarse aggregate. For Mix Nos. 92 to 95, the granite was washed, separated into individual size fractions and then recombined to produce the "*standard*" gradation shown in Figure 3.2. For Mix Nos. 96 to 99 the "as received" gradation of granite was washed and used, Figure 3.6. As can be seen from Figure 3.6, the aggregate *G1* contained more large particles and its grading curve fell outside the limits specified by ASTM C 33 for size No. 7 coarse aggregate. Gradation of the coarse aggregate, as well as the cementitious material composition were the mix variables studied in this portion of the investigation. In addition tests were also conducted to investigate the effects of age and curing condition (heat-curing, continuos moist-curing) on compressive strength test results.

Of the eight mixes studied, Mix Nos. 92 and 96 had no supplementary cementing materials (reference mixes), Mix Nos. 93 and 97 contained 10% fly ash, Mix Nos. 94 and 98 contained 7.5% silica fume, and Mix Nos. 95 and 99 contained the combination of 10% fly ash and 7.5% silica fume as part of their cementitious material content. In all cases, the total amount of cementitious materials was held constant at 750 lb/yd^3 (445 kg/m^3).

Mixes 100 to 139: Based on the results from the previous mixes (Mix Nos. 1 to 99) this set of mixes was designed to provide additional information on the effect of test and mix variables on mechanical properties of high strength concrete. In this portion of the study, the total cementitious material content, water-to-cementitious material ratio, and coarse to fine aggregate ratio were held constant at 750 lb/yd^3 (445 kg/m^3), 0.30, and 1.5, respectively. Four cementitious material compositions were investigated: reference mix (portland cement only) and three comparison mixes containing 20% fly ash, 7.5% silica fume, and the combination of 20% fly ash with 7.5% silica fume.

Several new test variables were introduced and studied in this part of the study. Effect of heat-curing temperature, as well as the effect of the duration of moist-curing on test results

were investigated. Also investigated was the effect of limited period of moist-curing after the initial heat-curing period on test results.

Five different types of coarse aggregates were used in this phase of the investigation: round river gravel (*R1*), partially crushed river gravel (*R2*), two crushed limestones (high- and low-absorption: *L1* and *L2*), and a new granite from a different source (*G2*). All coarse aggregates were washed in the laboratory prior to mixing and were used with their "as received" gradations (Figures 3.3, 3.5, 3.7, 3.8, and 3.9).

Effects of type and brand of portland cement together with the effects of heat-curing temperature on mechanical properties of high strength concrete were studied with Mix Nos. 100 to 123. Two different types of portland cement from two manufacturers were studied: Type III of Brand #1 and Type I and Type III of Brand #2. Specimens cast from each batch were subjected to heat-curing at 120 and 150 °F (50 and 65 °C). Standard lime-saturated water moist-curing was used on companion specimens.

In addition to testing for compressive strength, static modulus of elasticity, modulus of rupture, and splitting tensile strength, high strength concrete specimens from this series of mixes were tested for creep and shrinkage properties. Weight loss of shrinkage specimens and weight gain in water of high strength concrete specimens were also investigated.

3.3 Materials

3.3.1 Cementitious Material

The cementitious material comprised ASTM C 150 Type I or Type III portland cements, ASTM C 618 Class C fly ash, and dry densified or slurry forms of silica fume. High strength concrete mixes studied contained a total of 750, 850 or 950 lb/yd^3 (445, 505, or 565 kg/m^3) of cementitious material.

Two brands of ASTM C 150 portland cements were chosen. These two brands were the most frequently used commercial cements by local precast plants. To eliminate the effects of shipment variations in chemical and physical properties of portland cement, inherent in the production of portland cement, all of the cements required for the purpose of this study were delivered in single shipments on 40-bag pallets shrink-wrapped by plastic and were stored in the laboratory until used. Table 3.3 shows the manufacturers' lab report on the chemical and physical properties of the portland cements used in making the high strength concrete investigated. As can be seen within each brand of portland cement, the main difference between Type I and Type III cements was the fineness of the cement particles.

ASTM C 618 Class C fly ash was used in making high strength concrete specimens. Bulk fly ash was obtained from the supplier in a single shipment and was stored in air tight 55 gallon (210 l) steel drums in the laboratory. Table 3.4 shows the chemical and physical properties of the fly ash used. Depending on the mix, fly ash constituted 0, 10, 20 or 30 percent of the total weight of the cementitious materials of the mix.

Both dry densified and slurry forms of silica fume, from a single manufacturer, were used in this study. Dry densified silica fume was delivered in a single shipment in 50 lb. (22.7 kg) bags. Silica fume bags were stored on wooden pallets in the laboratory until time of use. Silica fume slurry was delivered in 55 gallon (210 l) steel drums in a single shipment and was stored in the laboratory until used. The slurry contained 5.5 pounds of silica fume per gallon of slurry (0.66 kilogram of silica fume per liter of slurry). When the slurry form of the silica fume was used, the mix water was adjusted to account for the water in the slurry. Prior to its use in concrete, while inside the drum, the silica fume slurry was mixed for at least 4 hours by a powerful full-height electric mixer mounted over the drum. Mixing the slurry was essential because silica fume particles settle as a sediment and get separated from the liquid phase over time.

Depending on the mix, silica fume constituted 0, 7.5, 10 or 15% of the total weight of the cementitious materials of the mix. A typical composition of the silica fume, provided by the manufacturer, is given in Table 3.5.

A 50 lb. (22,700 g) maximum capacity electronic balance with 0.1 lb. (45.4 g) resolution (OHAUS Model D5-00) was used to measure the portland cement, fly ash and silica fume used in all mixes.

3.3.2 Aggregates

All of the aggregates were obtained from local sources. In order to minimize the effect of cleanness of coarse aggregates on properties of concrete in both fresh and hardened states, all coarse aggregates were washed in the laboratory prior to their use in high strength concrete mixtures. Type, source, and gradation of coarse aggregates used in different mixes is shown in Table 3.1 (as part of the Mix ID Code) and was described in detail in Section 3.2 of this chapter. Absorption capacities of the coarse aggregates used in this study were 1.11 percent for the round river gravel (R1), 1.39 percent for the partially crushed river gravel (R2), 1.00 percent for the granites from Source #1 and Source #2 (G1 and G2), 2.97 percent for the high-absorption limestone (L1) (except for Mix Nos. 124 and 125) and 2.05 percent for the L1 used in Mix Nos. 124 and 125, and 1.50 percent for the low-absorption limestone (L2). The reason for listing two absorption capacities for the high-absorption limestone is that the aggregate was obtained at two different times from the same source.

A single natural coarse sand with a fineness modulus and absorption capacity of 2.80 and 0.50%, respectively and a gradation within the limits of ASTM C 33 was used for all fine aggregate. Gradation of the fine aggregate used is shown with the gradation of all coarse aggregates in Figures 3.2 to 3.9.

A 1000 lb. (454 kg) maximum capacity mechanical balance with 1 lb. (0.454 kg) graduations (TOLEDO) was used to measure both fine and coarse aggregates used in all mixes.

3.3.3 Chemical Admixtures

High-range water reducers (superplasticizers) were added to all mixes to bring the concrete slump in the range of 4 to 6 in. (100 to 150 mm). In some cases (highly dependent on the cementitious materials composition), increased dosages of high-range water reducer up to 35 oz./cwt (23 ml/kg), more than the maximum dosage recommended by the admixture manufacturer, were found to be necessary to bring the slump in the desired range. It should be noted that the use of high dosages of high-range water reducers in production of high strength concrete is not unusual *[Aïtcin et al. 1994]*. In all cases, the mix water was adjusted to account for the water in the high-range water reducer. To study the effect and compatibility of different high-range water reducers with other materials selected for production of high strength concrete in this research program, five different high-range water reducers were investigated. Detailed information about the type of high-range water reducers used is given in Table 3.2.

An 8 lb. (4,000 g) maximum capacity high precision electronic balance with 0.0035 oz. (0.1 g) resolution (OHAUS Model GT 4800) was used to measure high-range water reducers used in all mixes.

3.4 Fabrication and Curing: Equipment and Techniques

For each mix investigated, all specimens were cast from a single batch. All high strength concrete mixes were mixed, cured, and tested in the Structural Engineering Laboratory of the Civil Engineering Department at the University of Minnesota. The following equipment and techniques were used for mixing, fabricating, and curing of the concrete specimens:

3.4.1 Mixer and Mixing Procedure

A 10 ft^3 (0.3 m^3), fixed-drum mixer powered by a 5 hp (3,730 watt) electric motor was used to mix all the concrete used in this study. The moving shaft inside the fixed drum was equipped with two open web spiral shape blades which shoveled concrete from one side of the

drum to the other resulting in a uniform mix. Rubber scrapers were mounted at the edges of the blades to minimize the amount of cement paste sticking to the sides of the drum.

Following the evaluation of a few trial batches, the standard laboratory mixing and batching procedures recommended by ASTM C 192 were slightly modified to allow an easy and uniform production technique. The mixing procedure used throughout this research program consisted of the following steps:

1. Immediately before loading the mixer, spray interior of the mixer with water. Completely drain the mixer.
2. Load the mixer with all coarse aggregate and half of the mixing water. Mix for ½ minute.
3. Stop the mixer and allow the coarse aggregate to absorb water for 10 minutes. This procedure helped to avoid early loss of slump.
4. Dissolve high-range water reducer in the remaining water.
5. Turn on the mixer and add sand, cementitious material, remaining water with high-range water reducer. Mix for 5 minutes.
6. Stop the mixer for 1 minute. Conduct a slump test. Evaluate mix workability. Measure additional amount of high-range water reducer, up to total of 35 oz/cwt (23 ml/kg of cement) if needed.
7. Turn on the mixer for 3 more minutes and if needed, add the additional high-range water reducer (from step 6).
8. Do a final slump test and discharge the concrete into clean, moist metal bins and cast the specimens.

For each of the mixes, slump and air contents were measured according to ASTM C 143 and C 173 (volumetric method) procedures, respectively.

3.4.2 Molds and Making Specimens

Plastic molds were used to cast cylindrical specimens throughout this study. However, to study the effect of mold material on compressive strength test results, companion 6 x 12 in. (150 x 300 mm) cylindrical specimens, from selected mixes, were cast in heavy-gauge reusable steel molds. Modulus of rupture specimens, 6 x 6 x 24 in. (150 x 150 x 600 mm) beams, were cast in heavy-gauge reusable steel molds.

One day prior to mixing, the inside of all molds was lightly oiled with a commercially available form coating oil (nox-crete). Molds were filled and manually rodded in accordance with the provisions of ASTM C 192. With the exception of tamping rod, identical tools were used in filling and consolidating the molds. For 4 in. (100 mm) diameter cylinders, the tamping rod was a 3/8 in. (10 mm) diameter rod with both ends rounded to a hemispherical tip of the same diameter. A similar 5/8 in. (16 mm) diameter rod was used for consolidating the 6 x 12 in. (150 x 300 mm) cylindrical and 6 x 6 x 24 in. (150 x 150 x 600 mm) beam molds. The surface of the concrete was stricken off with the tamping rod and the specimens were placed immediately into the lime-saturated water bath or heat-curing chamber. To prevent evaporation of water from the unhardened concrete, the exposed surfaces of those specimens which were moved to the heat-curing chamber were covered immediately with a piece of plastic wrap. A rubber band kept the plastic wrap in place.

3.4.3 Curing Conditions

The following curing conditions were studied during the course of this research program:

1. H Condition: Specimens were heat-cured @ 120 or 150 °F (50 or 65 °C). Specimens were then tested dry at predetermined ages.
2. HW1 and HW3 Conditions: Initial heat-curing of specimens was followed by an additional 1- or 3-day moist-curing in lime-saturated bath. Specimens were then tested dry at 28-days of age.

3. W7 and W14 Conditions: Specimens were moist-cured in lime-saturated bath for either 7- or 14-days. Specimens were then tested dry at 28-days of age.
4. W28 Condition: Specimens were moist-cured in lime-saturated bath for 28-days. Specimens were then tested wet at 28-, and dry at 182- and 365-days of age.
5. W182, and W365 Conditions: Specimens were moist-cured in lime-saturated bath for their entire life. Specimens were then tested wet at 182-, or 365-days respectively.

The following sections describe heat- and moist-curing methods used throughout this study.

3.4.3.1 Heat-Curing @ 120 or 150 °F (50 or 65 °C)

In order to simulate the accelerated heat-curing process typical of that used by precast-prestressed bridge girder manufacturers, the walk-in environmental chamber at the Structural Engineering Laboratory of the Department of Civil Engineering, University of Minnesota, was used as the heat-curing room. The temperature inside the chamber was electronically controlled and was varied according to the following procedure:

- 3 hours at room temperature (preset period after casting);
- temperature increased to 120 or 150 °F (50 or 65 °C) over the next 2.5 hours;
- temperature held constant for 12 hours;
- specimens returned to room temperature over the next 2 hours.

The heat-cured specimen molds were stripped after 24 ± 4 hours. These specimens were then stored in laboratory ambient humidity and temperature until the time of test.

3.4.3.2 Moist-Curing in Lime-Saturated Water

A 2 ft. (610 mm) deep, 385 gal. (1460 l), galvanized steel tank was used for curing concrete specimens immersed in lime-saturated water. A clamp-on heater/circulator was used

to maintain the curing temperature at 73.4±3 °F (23±1.7 °C) throughout the tank. The heater/circulator had a 1,000 watt capacity electric heater, a dial-type thermostat with a range of 35-100 °F (2-38 °C), and a single speed submersion pump circulator. An independent thermometer was installed to verify the accuracy of the thermostat setting. The specimens to be moist-cured were placed into the lime-saturated water bath immediately after casting. To avoid damage to the young specimens, molds were stripped after 48 hours (instead of 24±8 hours, as specified by ASTM C 192). The exception was when 1-day compressive strength of moist-cured specimens were required, where molds were stripped off after 20±4 hours. The specimens were immediately returned to the lime-saturated water bath where they completed their planned curing duration.

Table 3.1. Mixes considered in this research program

No.	Mix ID Code *	No.	Mix ID Code *	No.	Mix ID Code *
1	DISCARDED	26	131-MBL1-F00M15-130	51	231-MBL1-F30M00-130
2	DISCARDED	27	331-MBL1-F00M15-130	52	231-MBL1-F00M15-130
3	DISCARDED	28	131-MBL1-F30M15-130	53	231-MBL1-F30M15-130
4	131-SAL2-F00M00-132	29	331-MBL1-F30M15-130	54	131-MBL1-F00M75-130
5	131-SAL1-F00M00-132	30	131-XAL1-F00M00-130	55	131-MBL1-F00M10-130
6	131-SAR1-F00M00-130	31	131-XAL1-F00M00-230	56	231-MBL1-F00M75-130
7	131-SAR1-F10M00-130	32	131-XAL1-F00M75-130	57	231-MBL1-F00M10-130
8	DISCARDED	33	131-XAL1-F00M75-230	58	331-MBL1-F00M10-130
9	131-SAR1-F00M75-130	34	131-XAR2-F00M00-130	59	331-MBL1-FOOM75-130
10	131-SAL1-F00M00-130	35	131-XAR2-F00M00-230	60	131-MBL1-F10M00-130
11	131-SAL1-F10M00-130	36	131-XAR2-F00M75-130	61	131-MBL1-F10M75-130
12	131-SAR1-F10M75-130	37	131-XAR2-F00M75-230	62	131-MBL1-F10M10-130
13	131-SAL1-F00M75-130	38	131-XAR2-F00M00-330	63	231-MBL1-F10M00-130
14	131-SAL1-F10M75-130	39	131-XAR2-F00M00-430	64	231-MBL1-F10M75-130
15	131-XAL1-F00M00-130	40	131-XAR2-F00M00-530	65	231-MBL1-F10M10-130
16	131-XAL1-F10M75-130	41	131-XAR2-F00M75-330	66	331-MBL1-F10M00-130
17	131-XAL1-F00-M00-130	42	131-XAR2-F00M75-430	67	331-MBL1-F10M75-130
18	131-XAL1-F10M75-130	43	131-XAR2-F00M75-530	68	331-MBL1-F10M10-130
19	111-AAL1-F00M10-128	44	131-XAL1-F00M00-330	69	131-MBL1-F20M00-130
20	111-BAL1-F00M10-128	45	131-XAL1-F00M00-430	70	131-MBL1-F20M75-130
21	111-MAL1-F00M10-128	46	131-XAL1-F00M00-530	71	131-MBL1-F20M10-130
22	131-MBL1-F00M00-130	47	131-XAL1-F00M75-330	72	231-MBL1-F20M00-130
23	331-MBL1-F00M00-130	48	131-XAL1-F00M75-430	73	231-MBL1-F20M75-130
24	131-MBL1-F30M00-130	49	131-XAL1-F00M75-530	74	231-MBL1-F20M10-130
25	331-MBL1-F30M00-130	50	231-MBL1-F00M00-130	75	331-MBL1-F20M00-130

* See Figure 1

Table 3.1. Mixes considered in this research program (continued ...)

No.	Mix ID Code *	No.	Mix ID Code *	No.	Mix ID Code *
76	231-MBL1-F20M75-130	101	112-XAR1-F00M00-130	126	131-XAL1-F20M00-130
77	331-MBL1-F20M10-130	102 #	112-XAR1-F20M00-130	127	131-XAL1-F20M75-130
78	131-MBL1-F30M75-130	103	112-XAR1-F20M00-130	128	131-XAR2-F00M00-130
79	131-MBL1-F30M10-130	104 #	112-XAR1-F00M75-130	129	131-XAR2-F00M75-130
80	231-MBL1-F30M75-130	105	112-XAR1-FOOM75-130	130	131-XAR2-F20M00-130
81	231-MBL1-F30M10-130	106 #	112-XAR1-F20M75-130	131	131-XAR2-F20M75-130
82	331-MBL1-F30M75-130	107	112-XAR1-F20M75-130	132	131-XAL2-F00M00-130
83	331-MBL1-F30M10-130	108	131-XAR1-F00M00-130	133	131-XAL2-F00M75-130
84	131-XBR2-F00M00-130	109	132-XAR1-F00M00-130	134	131-XAL2-F20M00-130
85	131-XBR2-F00M15.130	110	131-XAR1-F20M00-130	135	131-XAL2-F20M75-130
86	131-XBR2-F30M00-130	111	132-XAR1-F20M00-130	136	131-XAG2-F00M00-130
87	131-XBR2-F30M15-130	112	131-XAR1-F00M75-130	137	131-XAG2-F00M75-130
88	331-XBR2-F00M00-130	113	132-XAR1-F00M75-130	138	131-XAG2-F20M00-130
89	331-XBR2-F00M15-130	114	131-XAR1-F20M75-130	139	131-XAG2-F20M75-130
90	331-XBR2-F30M00-130	115	132-XAR1-F20M75-130	140	131-MBL1-F00M15-130
91	331-XBR2-F30M15-130	116 #	131-XAR1-F00M00-130	141	131-MBL1-F00M00-130
92	131-SAG1-F00M00-130	117 #	132-XAR1-F00M00-130	142	131-MBL1-F00M15-130
93	131-SAG1-F10M00-130	118 #	131-XAR1-F20M00-130		
94	131-SAG1-F00M75-130	119 #	132-XAR1-F20M00-130		
95	131-SAG1-F10M75-130	120 #	131-XAR1-F00M75-130		
96	131-XAG1-F00M00-130	121 #	132-XAR1-F00M75-130		
97	131-XAG1-F10M00-130	122 #	131-XAR1-F20M75-130		
98	131-XAG1-F00M75-130	123 #	132-XAR1-F20M75-130		
99	131-XAG1-F10M75-130	124	131-XAL1-F00M00-130		
100 #	112-XAR1-F00M00-130	125	131-XAL1-F00M75-130		

* See Figure 1

Heat-cured at 120 °F (50 °C)

Table 3.2. High-range water reducers (HRWR) used

Type & Brand of HRWR	Properties
HRWR #1	ASTM C 494 Type A and F; HRWR Aqueous solution of a modified naphthalene sulfonate. % Solids: 40% Specific Gravity: 1.20 Manufacturer's Recommended Dosage: 6-20 oz/cwt (4-13 ml/kg)
HRWR #2	ASTM C 494 Type A and F; HRWR Melamine formaldehyde-based water soluble polymer. % Solids: 33% Specific Gravity: 1.20 Manufacturer's Recommended Dosage: 6-30 oz/cwt (4-20 ml/kg)
HRWR #3	ASTM C 494 Type F; HRWR Water-soluble sulphonated naphthalene condensate. % Solids: 42% Specific Gravity: 1.20 Manufacturer's Recommended Dosage: 6-18 oz/cwt (4-12 ml/kg)
HRWR #4	ASTM C 494 Type D and G; HRWR Based on sodium salts of an unsaturated carboxylic acid and the hydroxyalkyl ester of such acids. % Solids: 22% Specific Gravity: 1.11 Manufacturer's Recommended Dosage: 6-18 oz/cwt (4-12 ml/kg)
HRWR #5	ASTM C 494 Type A and F; HRWR Combination of a water-soluble anionic melamine polycondensate and a naphthalene condensate. % Solids: 39% Specific Gravity: 1.23 Manufacturer's Recommended Dosage: 6-25 oz/cwt (4-16 ml/kg)

Table 3.3. Chemical and physical properties of portland cements used in this study based on the cement manufacturer's laboratory reports.

	Brand #1		Brand #2	
	Type I	Type III	Type I	Type III
SiO_2 %	21.4	21.6	20.52	20.47
Al_2O_3 %	5.0	5.5	4.56	4.54
Fe_2O_3 %	2.2	2.3	2.22	2.28
CaO %	64.2	64.1	63.95	63.98
MgO %	2.2	2.0	2.47	2.62
SO_3 %	3.3	3.4	2.99	3.33
Loss on Ignition %	0.73	0.75	1.01	0.88
Na_2O Equivalent %	0.45	0.51	0.40	0.37
C_3S %	52	47	62.1	61.6
C_3A %	10	11	8.3	8.2
Fineness (Blaine) m^2/kg	362	513	366	581
Set (Gillmore):				
* Initial (hr:min)	3:00	2:20	2:30	2:10
* Final (hr:min)	4:55	4:10	4:50	3:50
Autoclave expansion %	0.010	0.03	0.011	0.012
Air content %	6.8	7.3	5.1	7.7
Insoluble Residue	0.13	0.14	0.32	0.30
Compressive strength				
* 1-day, psi	-	4,110	2,210	3,705
* 3-day, psi	3,720	5,180	3,960	4,810
* 7-day, psi	4,870	-	5,100	5,675
* 28-day, psi	-	-	6,630	-

Table 3.4. Chemical and physical properties of the ASTM C 618 Class C fly ash used in this study based on the fly ash supplier laboratory report.

Chemical and Physical Analysis	Fly ash used	ASTM C 618 Class C
1. Chemical Analysis		
SiO_2 %	33.74	
Al_2O_3 %	22.44	
Fe_2O_3 %	6.04	
$(SiO_2+Al_2O_3+Fe_2O_3)$ %	62.22	50.0 Min
SO_3 %	1.57	5.0 Max
CaO %	28.47	
Moisture content %	0.13	3.0 Max
Loss on ignition %	0.37	6.0 Max
Available alkalies, as Na_2O %	1.46	1.5 Max
2. Physical Analysis		
Fineness: Amount retained when wet-sieved on No. 325 (45 μm) sieve %	16.93	34 Max
Specific gravity	2.70	
Soundness: Autoclave expansion or contraction, %	-0.033	0.8 Max
Strength activity index: With portland cement, at 7-days, % of control	100.87	75 Min
With portland cement, at 28-days, % of control	102.87	75 Min
Water requirement, % of control	94.6	105 Max

Table 3.5. Chemical and physical properties of the dry densified and slurry silica fume used in this study based on the silica fume supplier laboratory reports.

	Silica Fume Used		
	Dry Densified	Slurry	ASTM C 1240
SiO_2 %	94.5 to 96.5	95.26	85.0, min
CaO %	0.36	0.40	-
Al_2O_3 %	0.35	0.32	-
Fe_2O_3	0.144	0.14	-
MgO %	0.120	0.27	-
Loss on Ignition %	2.5 to 4.00	2.94	6.0, max
Moisture Content %	0.20 to 0.50	NA	3.0, max
Total Alkali Metal %	0.50	0.57	1.50, max
+45 Micron	-	1.59	10, max
PH	-	6.34	-
Solids %	-	53.98	-

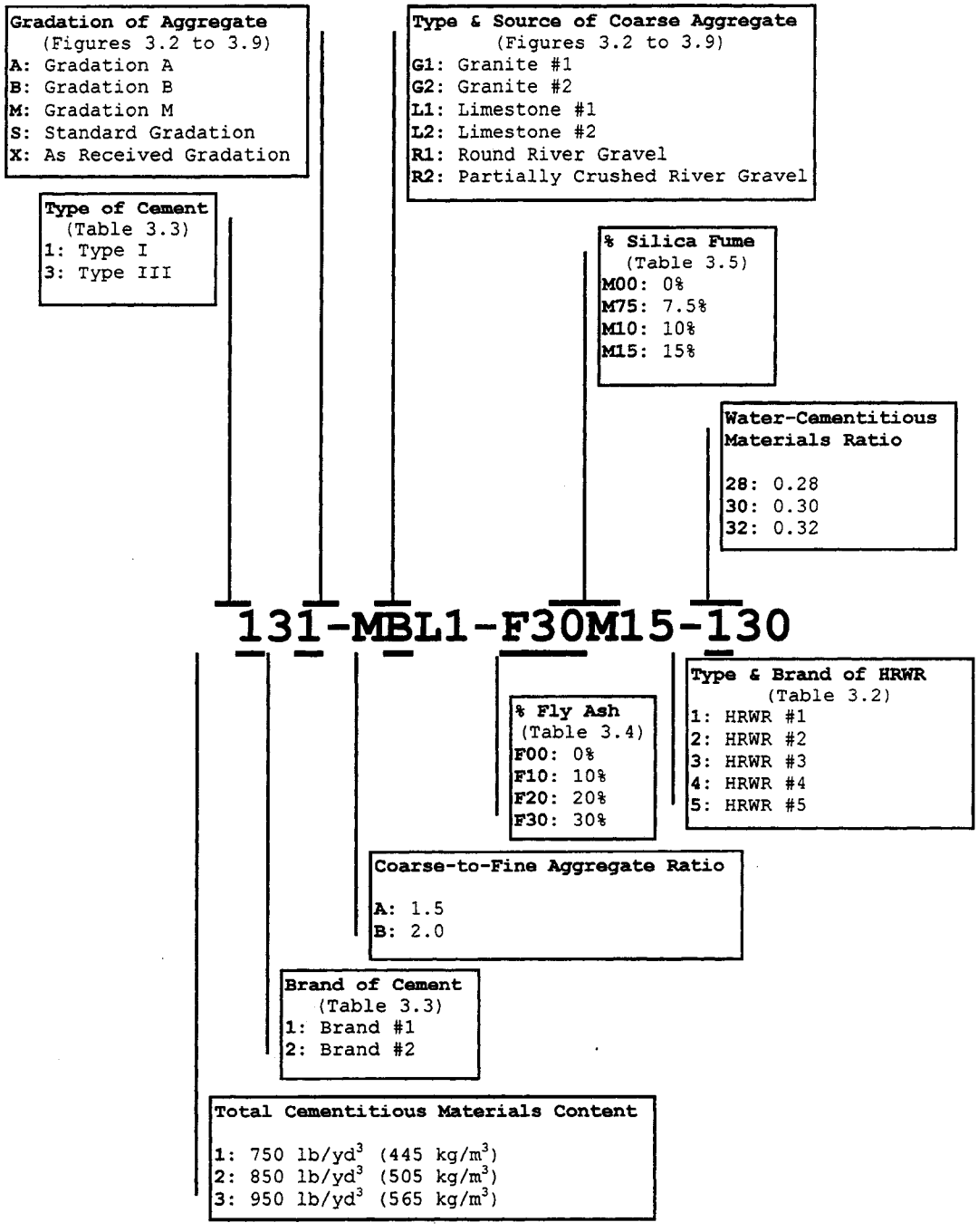

Figure 3.1. Notation used in the mix identification codes.

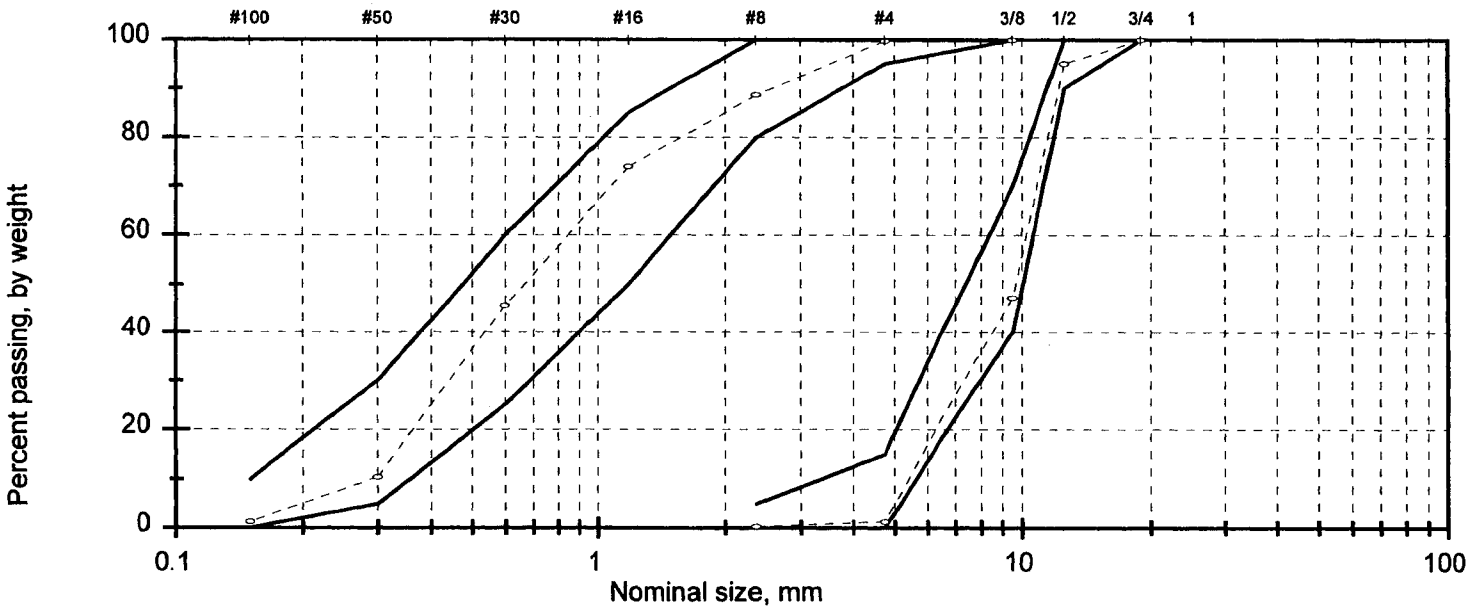

Figure 3.2. Grading curve for the **"standard"** gradation of coarse aggregates (gradation **"S"**). Also shown is the grading curve for the fine aggregate used. Solid lines indicate the limits specified in ASTM C 33 for coarse (size no. 7) and fine aggregates.
[GRADE_S.WMF]

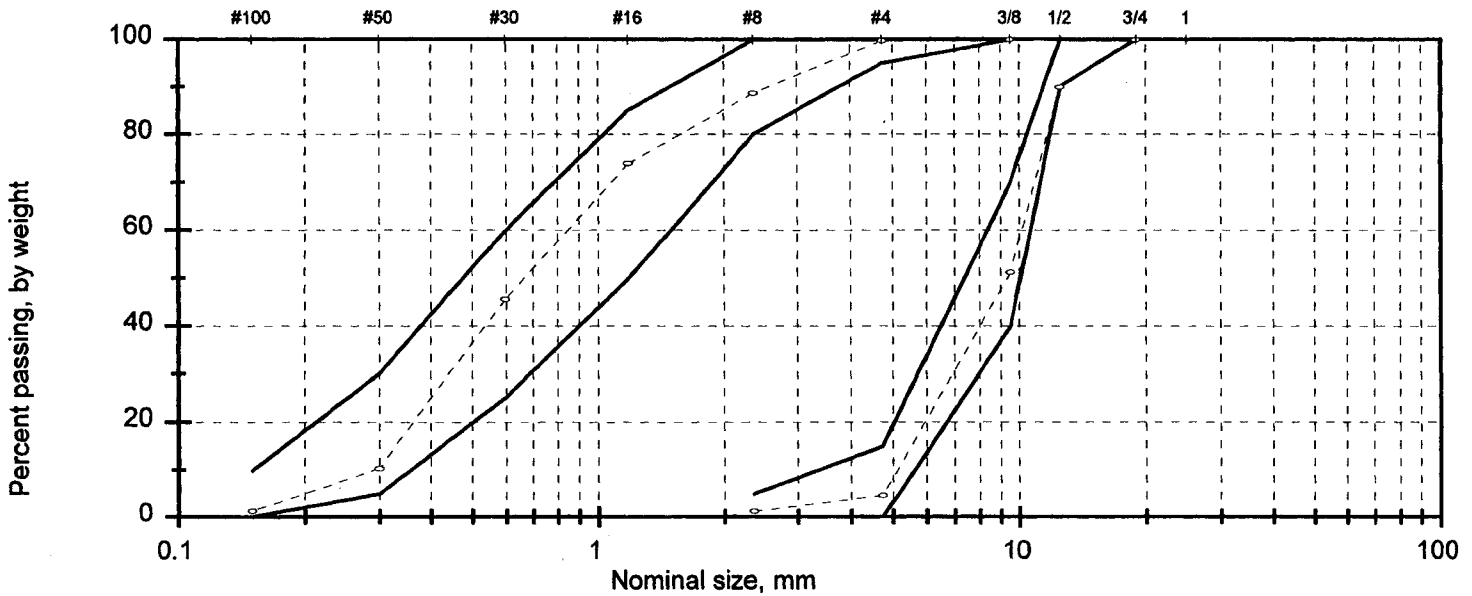

Figure 3.3. Grading curve for the **"as received"** gradation of **limestone coarse aggregate from Source #1** (Gradation **"X"**). Also shown is the grading curve for the fine aggregate used. Solid lines indicate the limits specified in ASTM C 33 for coarse (size no. 7) and fine aggregates.
[GRAD_L1X.WMF]

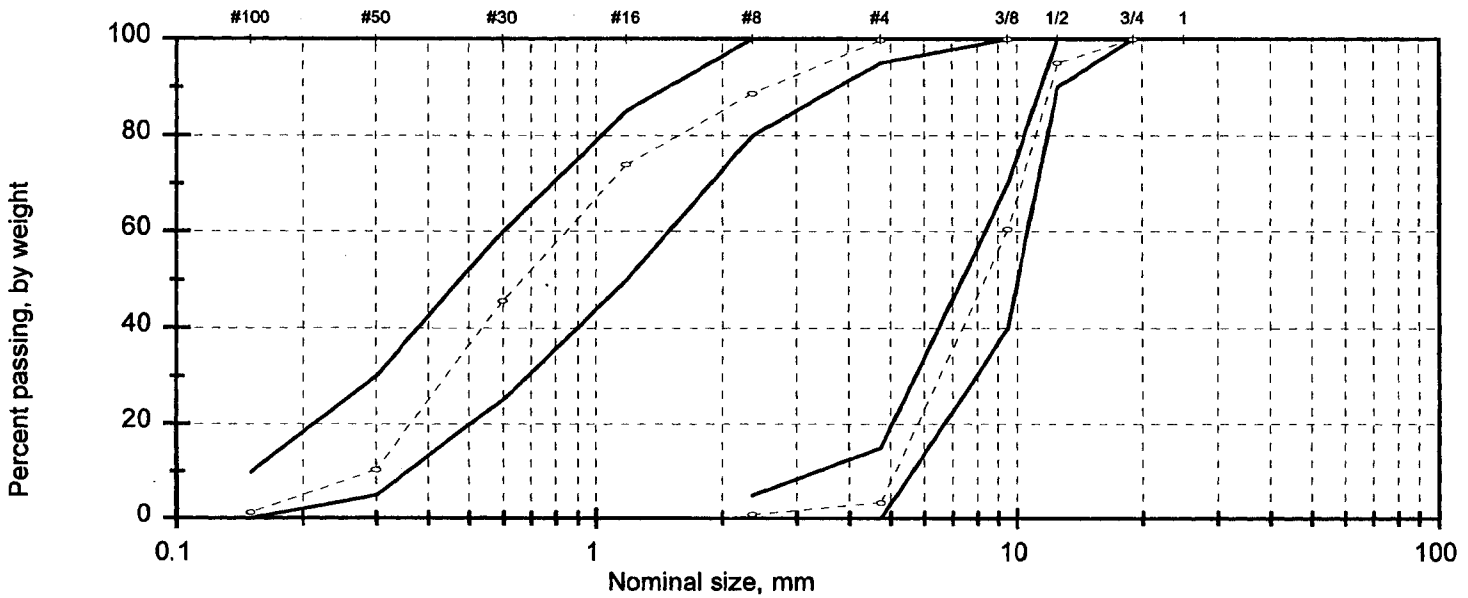

Figure 3.4. Grading curve for Gradation "M" of coarse aggregates. Also shown is the grading curve for the fine aggregate used. Solid lines indicate the limits specified in ASTM C 33 for coarse (size no. 7) and fine aggregates. [GRADE_M.WMF]

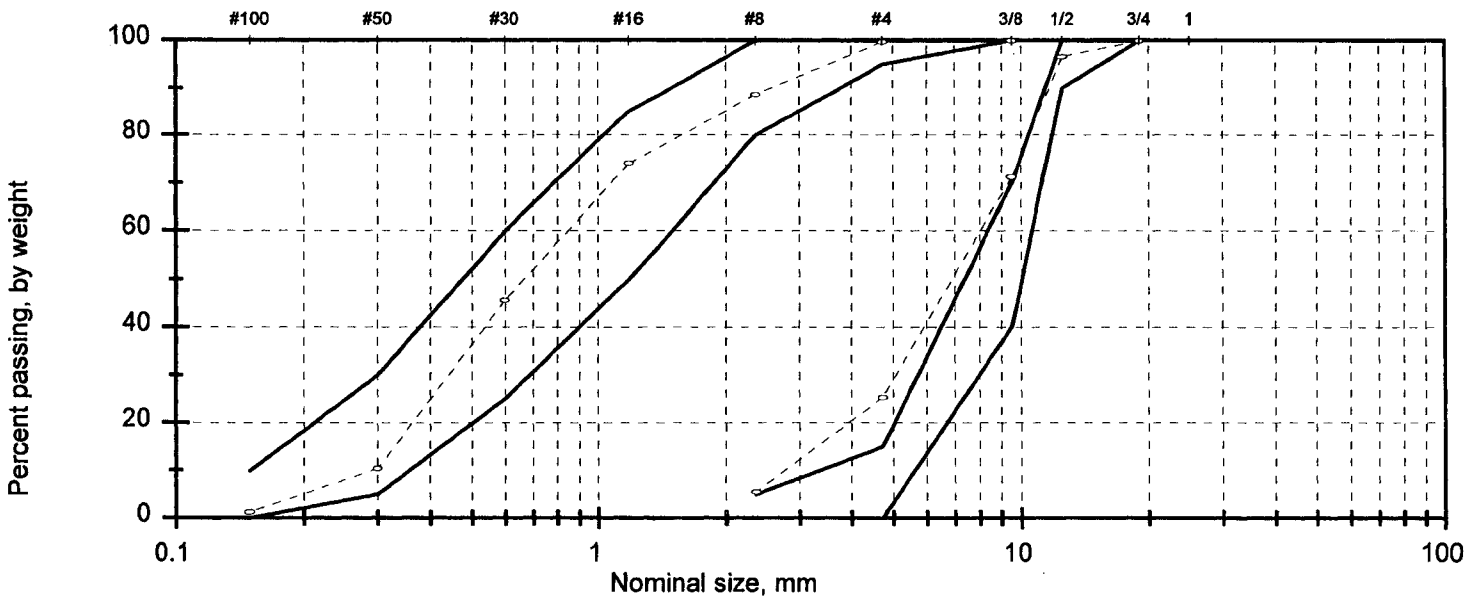

Figure 3.5. Grading curve for the **"as received"** gradation of **partially crushed river gravel** coarse aggregate (Gradation **"X"**). Also shown is the grading curve for the fine aggregate used. Solid lines indicate the limits specified in ASTM C 33 for coarse (size no. 7) and fine aggregates.
[GRAD_PCX.WMF]

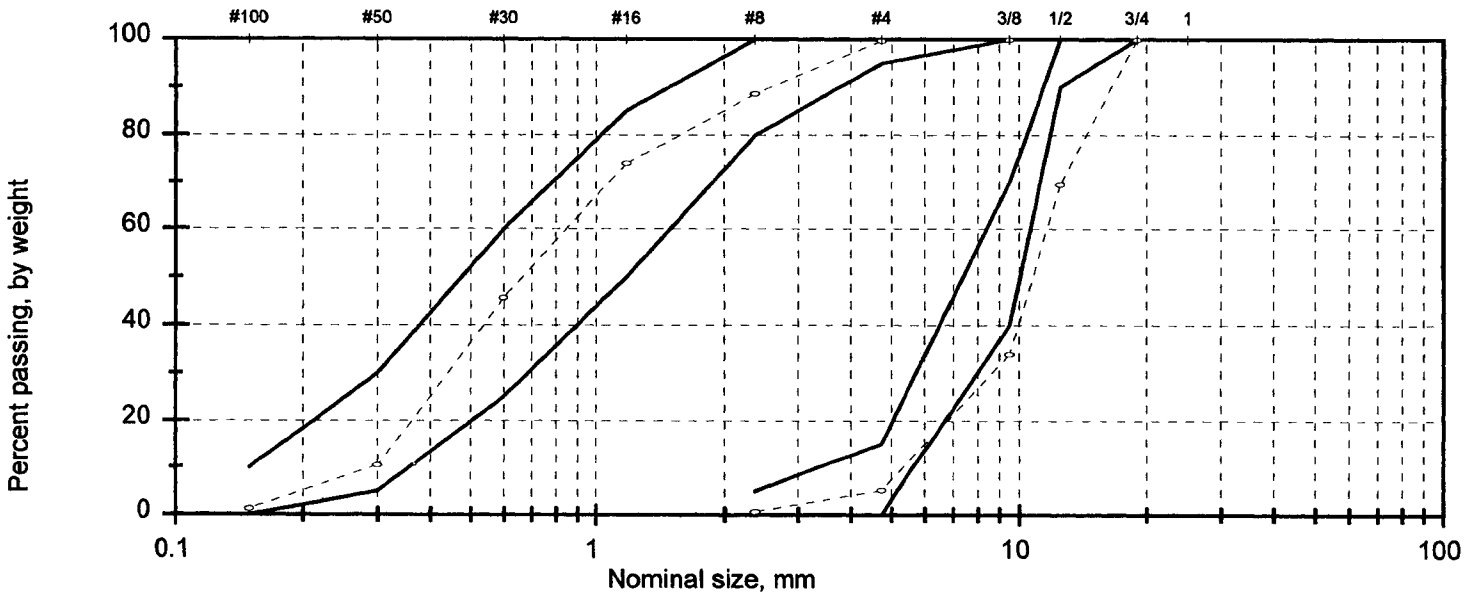

Figure 3.6. Grading curve for the **"as received"** gradation of **granite #1** coarse aggregate (Gradation **"X"**). Also shown is the grading curve for the fine aggregate used. Solid lines indicate the limits specified in ASTM C 33 for coarse (size no. 7) and fine aggregates. [GRAD_G1X.WMF]

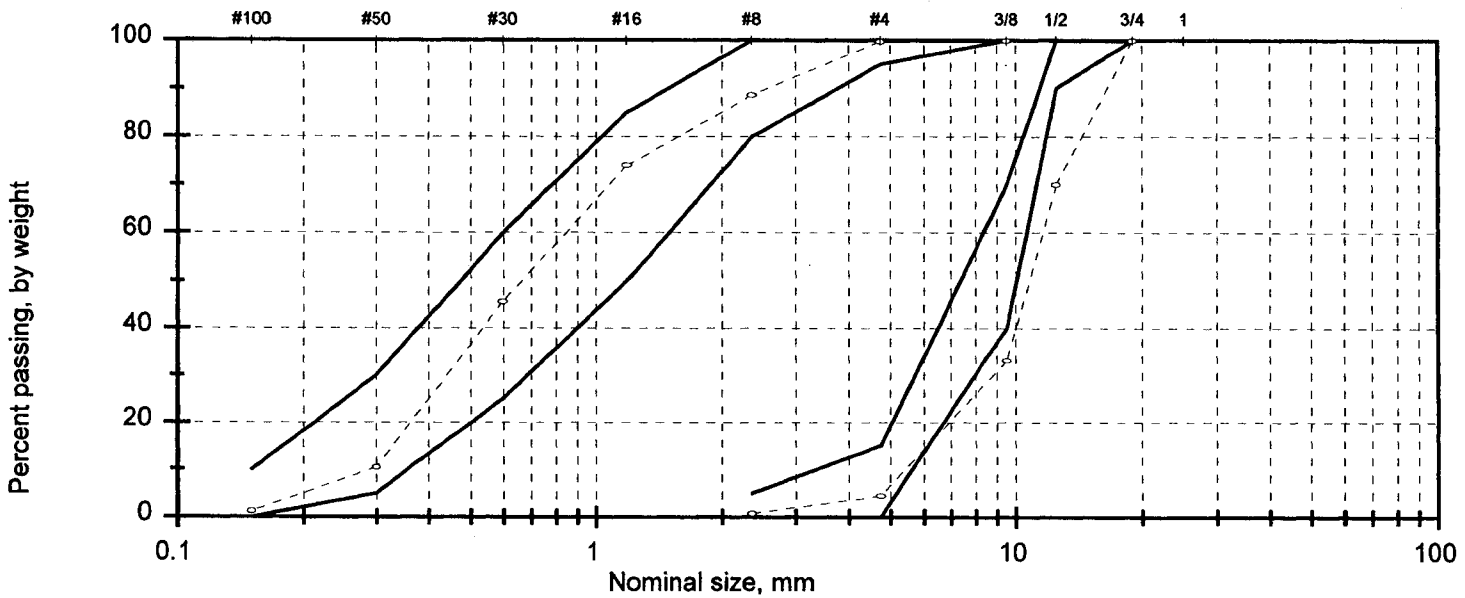

Figure 3.7. Grading curve for the **"as received"** gradation of **granite #2** coarse aggregate (Gradation **"X"**). Also shown is the grading curve for the fine aggregate used. Solid lines indicate the limits specified in ASTM C 33 for coarse (size no. 7) and fine aggregates. [GRAD_G2X.WMF]

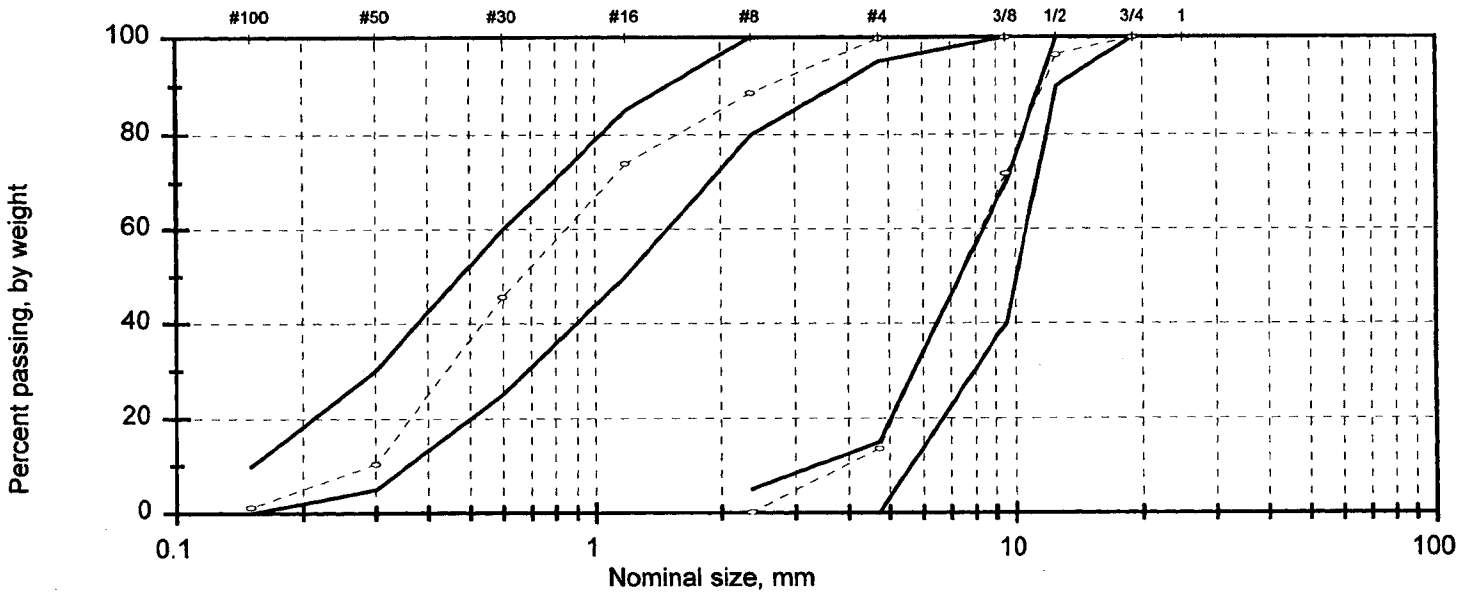

Figure 3.8. Grading curve for the **"as received"** gradation of **round river gravel** coarse aggregate (Gradation **"X"**). Also shown is the grading curve for the fine aggregate used. Solid lines indicate the limits specified in ASTM C 33 for coarse (size no. 7) and fine aggregates.
[GRAD_R1X.WMF]

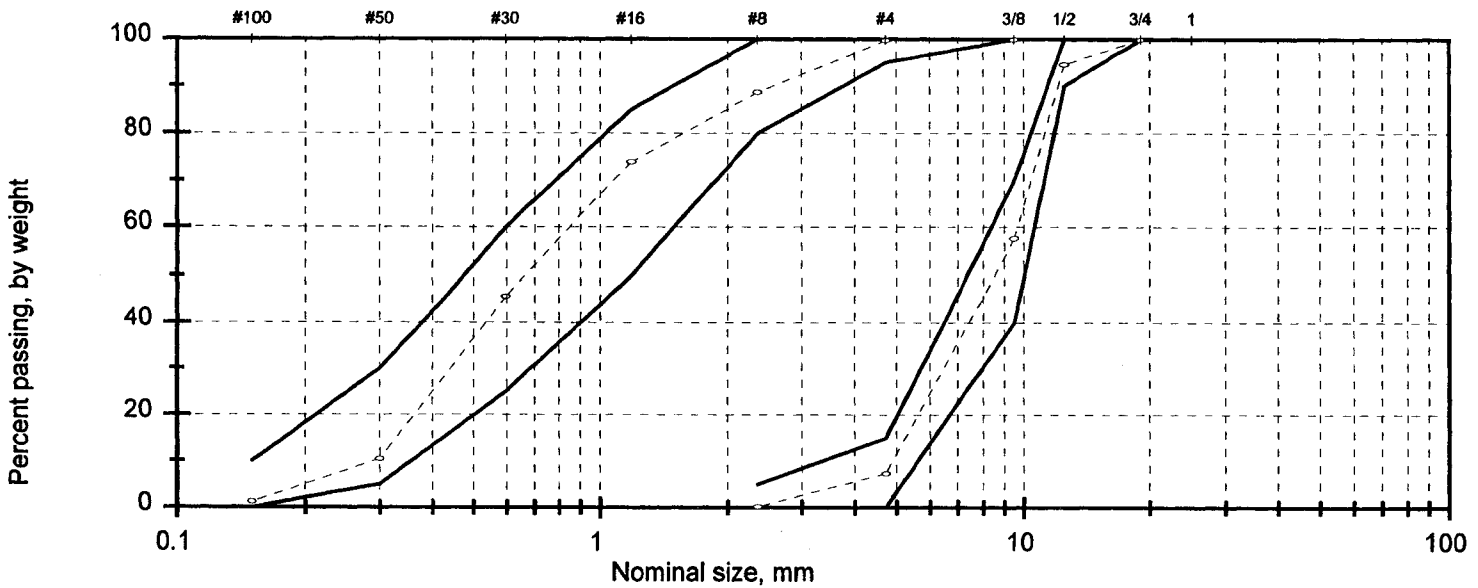

Figure 3.9. Grading curve for the **"as received"** gradation of **limestone coarse aggregate from Source #2** (Gradation **"X"**). Also shown is the grading curve for the fine aggregate used. Solid lines indicate the limits specified in ASTM C 33 for coarse (size no. 7) and fine aggregates.
[GRAD_L2X.WMF]

CHAPTER 4
LITERATURE REVIEW:
EFFECTS OF SOME OF THE TEST PARAMETERS ON THE COMPRESSIVE STRENGTH TEST RESULTS

4.1 General

Although in many practical cases characteristics other than strength of concrete may be of more importance (e.g. durability, impermeability, etc.), strength test results usually provide an overall picture of the concrete quality. While strength test results are directly related to the structure of the hardened cement paste, they are also significantly affected by other factors involving the test specimen.

Part of this research program was devoted to the study of some of the factors that may have an effect on strength test results. These parameters included mold size, mold material, and specimen end condition. The results from this part of the study were used by the author to narrow the parameters used in other parts of the study, and also to correlate the results from this study with published results from other studies with different test setups.

4.2 Effect of Specimen Size

In the United States, 6 x 12 in. (150 x 300 mm.) cylinders have been used as standard specimen for testing concrete since 1921 when ASTM adopted a tentative standard test method for measuring compressive strength of concrete (ASTM C 39-21T). Today most concrete suppliers and precast/prestressed plants have testing machines with a nominal compressive capacity of approximately 250,000 lb. (1,100 kN). This correlates with maximum compressive strengths of 8,800 psi for 6 x 12 in. (60.7 MPa for 150 x 300 mm) cylinders and 19,900 psi for 4 x 8 in. (137 MPa for 100 x 200 mm) cylinders. The limitation on the capacity of existing testing machines has led companies to use 4 x 8 in. (100 x 200 mm) cylinders. Smaller size cylinders have the added advantage of easier fabrication, handling and transportation, smaller required storage space, and less concrete and capping compound required to fabricate test

specimens *[Janak 1985]*. However, in general, smaller size cylinders are more susceptible to damage due to mishandling and can only be used when the nominal maximum size of the coarse aggregate does not exceed 1 inch *[Malhotra 1976, Janak 1985]*.

A general tendency that compressive strengths of standard 6 x 12 in. (150 x 300 mm) cylinders are lower than those of 4 x 8 in. (100 x 200 mm) cylinders has been pointed out by several researchers, (see Table 4.1). However, the results are not consistent. At least two studies reported that 6 x 12 in. (150 x 300 mm.) high strength concrete specimens resulted in higher compressive strength values than companion 4 x 8 in. (100 x 200 mm) specimens *[Carrasquillo and Carrasquillo 1986; Radain et al. 1993]*. Many studies have attributed the differences in strength between the two sizes of cylinders to the influence of specimen dimension and shape. However, particularly with high strength concrete, there are studies suggesting measured strengths are also affected by the manner in which the specimens are fabricated, cured, and loaded *[Hester 1980]* as well as the type of coarse aggregate used in concrete *[SHRP 1993]*.

Some studies have suggested that when 4 x 8 in. (100 x 200 mm) cylinders are used in measuring compressive strength of concrete, an increased number of smaller specimens should be used in order to provide comparable precision *[Tucker 1941, 1945; Malhotra 1976, Hester 1980]*. This is contrary to the view expressed by others that no significant dispersion of results are observed when testing smaller specimens *[Moreno 1990; Lessard et al. 1993]*. It has also been suggested that the difference in the strength of two sizes of specimens increases with increase in the strength level of concrete *[Malhotra 1976; Janak 1985]*. Researchers have been urged to clearly indicate the size, shape, methods of fabrication and testing of specimens considered in any reported results *[Lessard et al. 1993]*. The following represent some of the studies that have been conducted on the effect of specimen size on compressive strength test results. Table 4.1 summarizes compressive strength conversion factors reported by different sources.

[Gonnerman 1925]: Harrison F. Gonnerman of the Lewis Institute was among the earliest researchers who investigated the relative compressive strength of different forms of test specimens (cylinders, cubes and prisms of different sizes) when compared with the compressive strength of standard 6 x 12 in. (150 x 300 mm) cylinders from the same concrete. His investigation comprised compressive strength tests on 1,755 concrete specimens with 28-day compressive strengths of 6 x 12 in. (150 x 300 mm) cylinders ranging from 1,200 to 4,680 psi (8.3 to 32.3 MPa). He concluded that for cylinders with length equal to 2 diameters, lower strengths were generally observed with the larger cylinders, however, the decrease in strength with increasing size of cylinder was not significant for diameters under 6 in. (150 mm). For example, for the case of 4 x 8 in. (100 x 200 mm) specimens he found that the f_{4x8}/f_{6x12} ratio was 1.01. He also recommended that the ratio of the cylinder diameter to the maximum size of aggregate should not be less than 3.0.

[Tucker 1941, 1945]: John Tucker Jr. attempted to explain the effect of specimen size on compressive strength test results theoretically. Based on the assumption that each test specimen is made up of smaller elements with an inherent strength distribution, he studied two models: a series model (*the weakest-link theory*) and a parallel model (*the strength-summation theory*). In the weakest-link theory a specimen fails when the stress in any one of the component elements is just sufficient to cause at least one element to fail. As Tucker stated in this model it is not assumed that failure will necessarily occur in the element subjected to the maximum stress but it may occur in a weaker element subjected to a lower stress level. In the strength-summation theory the strength of the specimen is equal to the sum of the strengths of all the elements.

Using test data, Tucker concluded that the strength-summation theory better predicted the effect of specimen size on compressive strength results. According to this theory: (i) the compressive strength of geometrically similar concrete cylinders (i.e. specimens having constant length-diameter ratio) is independent of the diameter of the specimen; and (ii) the standard deviation of the compressive strength test results increases with decrease in cylinder

diameter; however, equal information is obtained if the summation of the cross-sectional area of the cylinders of the two sizes are equal. Therefore to measure average compressive strength of concrete using 4 x 8 in. (100 x 200 mm) specimens with the same precision as that obtained when standard 6 x 12 in. (150 x 300 mm) specimens are used, 2.25 times more 4 x 8 in. (100 x 200 mm) cylinders are needed:

- USC, in^2: ***(4.1-a)***

$$A_{6x12} = 9\pi;$$

$$A_{4x8} = 4\pi;$$

$$A_{6x12}/A_{4x8} = 9\pi/4\pi = 2.25$$

- SI, mm^2: ***(4.1-b)***

$$A_{150x300} = 5625\pi;$$

$$A_{100x200} = 2500\pi;$$

$$A_{150x300}/A_{100x200} = 5625\pi/2500\pi = 2.25$$

where

A_{6x12} ($A_{150x300}$) = cross-sectional area of a 6 x 12 in. cylinder in^2, (150 x 300 mm) mm^2

A_{4x8} ($A_{100x200}$) = cross-sectional area of a 4 x 8 in. cylinder in^2, (100 x 200 mm) mm^2

[Price, 1951]: Walter H. Price of the United States Bureau of Reclamation has published data regarding the influence of the specimen diameter on the 28-day compressive strength for the same concrete tested in cylinders with diameters ranging between 2 and 36 in. (51 and 914 mm) and with length/diameter ratios remaining constant at 2, Figure 4.1. According to his results (Figure 4.1), the average 28-day compressive strength of 4 x 8 in. (100 x 200 mm) cylindrical specimens is about 104 percent of the standard 6 x 12 in. (150 x 300 mm) cylinders. In another part of his study he reported practically the same compressive

strength values for 10 and 22 in. (254 and 560 mm) diameter cores drilled from five year old concrete test blocks. Based on these observations Price concluded that smaller diameter cylinders may have a faster strength gain and that age may equalize the difference in compressive strengths of geometrically similar specimens (specimens having constant length-diameter ratio) of different diameters.

[Neville 1966]: Adam N. Neville suggested that the three most important variables affecting compressive strength of a test specimen were its volume, its maximum lateral dimension, and its ratio of height to lateral dimension. Based on this assumption Neville suggested the following empirical equation to relate the strength of a specimen of any size and shape to the strength of a standard 6 in. (150 mm) cube specimen:

- USC, psi: ***(4.2-a)***

$$P/P_6 = [0.56 + (0.697d)/(h + V/6h)]$$

- SI, MPa: ***(4.2-b)***

$$P/P_{150} = [0.56 + (0.697d)/(h + V/150h)]$$

where

P = strength of a specimen of any dimension, psi (MPa)

P_6 (P_{150}) = strength the standard 6 in. cube specimen psi, (150 mm) MPa

d = specimen maximum lateral dimension, in. (mm)

V = volume of the specimen, in^3 (mm^3)

h = specimen height, in. (mm)

Based on the above equation 4 x 8 in. (100 x 200 mm) cylinders test three percent

higher than companion 6 x 12 in. (150 x 300 mm) cylinders:

$$P_{4x8} / P_6 = P_{100x200} / P_{150} = 0.836 \quad \text{and}$$
$$P_{6x12} / P_6 = P_{150x300} / P_{150} = 0.810 \quad \text{hence}$$
$$P_{4x8} / P_{6x12} = P_{100x200} / P_{150x300} = 0.836/0.810 = 1.03 \qquad (4.3)$$

[Malhotra 1976]: V. M. Malhotra compared the relative strength of 4 x 8 in. (100 x 200 mm) concrete cylinders with the strength of companion 6 x 12 in. (150 x 300 mm) cylinders from a variety of mixes available to CANMET (Canada Center for Mineral and Energy Technology) during a period of several years. A comparative study was conducted on parallel sets of specimens at ages of 3 to 218 days. The 28-day compressive strengths of concretes investigated were in the range of 1,000 to 6,000 psi (6.9 to 41.4 MPa). Malhotra concluded that: (i) the compressive strengths of 4 x 8 in. (100 x 200 mm) cylinders were higher than those of 6 x 12 in. (150 x 300 mm) cylinders; however, at low strength levels the reverse may be true; (ii) the difference in the strength of two sizes of cylinders increases with increase in the strength level of concrete; (iii) considerably more than twice the number of 4 x 8 in. (100 x 200 mm) cylinders (as suggested by Tucker's strength-summation theory *[Tucker 1941, 1945]*) must be tested for each 6 x 12 in. (150 x 300 mm) cylinder to gain the same degree of precision.

Malhotra reported values between 0.84 to 1.32 for the ratio of the strengths of 4 x 8 in. (100 x 200 mm) concrete cylinders to those of 6 x 12 in. (150 x 300 mm) cylinders at 28 days. He suggested that the use of 4 x 8 in. (100 x 200 mm) cylinders will not result in any technical advantages or savings in testing costs. He stated that due to their smaller size and weight, 4 x 8 in. (100 x 200 mm) cylinders are more open to abuse at the construction sites, and the cost of testing will increase if more specimens are to be tested to gain equal precision. However, he stated that on projects staffed with competent quality control personnel, the 4 x 8 in. (100 x 200 mm) cylinder can be satisfactorily used for overall production control.

[Hester 1980]: Weston T. Hester reported the results of a critical review of the contemporary testing procedures for high-strength concrete. In his report he concluded that the observed differences between the measured strengths of nonstandard (i.e., other than 6 x 12 in. (150 x 300 mm) cylinders) and standard specimens are not only influenced by specimen shape and dimensions but, particularly with high-strength concrete, are affected by the manner in which the specimen is fabricated, cured, and loaded in compression. Hester recommended exclusive use of vertically cast 6 x 12 in. (150 x 300 mm) cylinders. He pointed to the interaction of test specimen with the testing machine at the platen-specimen interface and argued that "short" specimens (i.e., less than 6 in. (150 mm) high in the loading axis) will develop a non-uniform distribution of stress throughout their height, but the "long" specimens (e.g., 6 x 12 in. (150 x 300 mm) cylinder) will develop a more uniform compressive stress distribution and rupture at the specimen mid-height. Hester urged meticulous attention to the proper functioning of the test equipment, compliance of the test specimen with appropriate specifications, and increased number of specimens to gain comparable levels of precision if nonstandard specimens are used for testing.

[Carrasquillo, Nilson, and Slate 1981]: Carrasquillo et al. have stated that the average ratio of compressive strengths of 4 x 8 in. (100 x 200 mm) concrete cylinders to 6 x 12 in. (150 x 300 mm) concrete cylinders is about 1.11 regardless of compressive strength level or age at testing. Compressive strengths of concretes investigated ranged from about 3,000 to 11,000 psi (20.7 to 75.9 MPa). In a separate study later on 6,000 to 14,500 psi (41 to 100 MPa) high-strength concrete *[Carrasquillo and Carrasquillo 1988]*, Carrasquillo made a different conclusion and reported that strength of 4 x 8 in. (100 x 200 mm) cylinders are approximately 93 percent of companion 6 x 12 in. (150 x 300 mm) cylinders.

[Janak 1985]: Karl J. Janak conducted a comparative study of compressive strengths of 4 x 8 in. (100 x 200 mm) versus 6 x 12 in. (150 x 300 mm) concrete cylinders for the Materials and Tests Division of Texas SDHPT (Texas State Department of Highways and Public Transportation). In this study, concrete cylinders from 22 different mix designs, made

with a variety of cement, aggregate and admixture types and brands, with 28-day, 6 x 12 in. (150 x 300 mm) cylinder compressive strengths in the range of 6,000 to 10,000 psi (41.4 to 69.0 MPa) were investigated. Comparisons were conducted at ages of 7, 14, 28 and 56 days. For the entire data, the relationship between compressive strengths of 4 x 8 in. (100 x 200 mm) and 6 x 12 in. (150 x 300 mm) cylindrical specimens was plotted. Based on that plot the compressive strengths of 4 x 8 in. (100 x 200 mm) cylinders and 6 x 12 in. (150 x 300 mm) cylinders were related according to the following equation:

- USC, psi: $f_{4x8} = 1.09 f_{6x12} - 456$ ***(4.4-a)***
- SI, MPa: $f_{100x200} = 1.09 f_{150x300} - 3.14$ ***(4.4-b)***

Janak concluded that (i) 4 x 8 in. (100 x 200 mm) cylinders tested slightly higher than 6 x 12 in. (150 x 300 mm) cylinders; (ii) the difference in the compressive strength of the two sizes of cylinders increased with an increase in the strength level of concrete; and (iii) the difference in the compressive strength of the two sizes of cylinders was not significant for compressive strength levels of up to 10,000 psi (69.0 MPa). Janak found the 4 x 8 in. (100 x 200 mm) cylinders were satisfactory for compressive strength determination of concretes up to 10,000 psi (69.0 MPa), the maximum concrete compressive strength investigated in this study.

Janak suggested that the replacement of the 6 x 12 in. (150 x 300 mm) cylinders by smaller 4 x 8 in. (100 x 200 mm) cylinders may be advantageous in that : (1) smaller cylinders are easier to fabricate, handle and transport; (2) smaller storage space is required by smaller cylinders; and (3) less concrete and capping compound is needed to make and test concrete specimens. However, he noted the susceptibility to mishandling due to its smaller size and the 1 inch (25.4 mm) limit on maximum size of aggregate in concrete as disadvantages of the use of 4 x 8 in. (100 x 200 mm) cylinders.

[Peterman and Carrasquillo 1986]: Peterman et al. reported the results from their study of the effects of specimen size on compressive strength. The range in compressive

strengths of the concretes investigated was 7,000 to 11,000 psi (48.3 to 75.9 MPa). In this study, 4 x 8 in. (100 x 200 mm) cylinders always yielded higher compressive strength results than companion 6 x 12 in. (150 x 300 mm) specimens when cast in molds made of the same material. They concluded that, for specimens cast in steel molds, 4 x 8 in. (100 x 200 mm) cylinders can result in compressive strength values of between 10 to 15 percent higher than 6 x 12 in. (150 x 300 mm) concrete cylinders of the same batch.

[Carrasquillo and Carrasquillo 1988]: Carrasquillo et al. reported the results of a research program for the study of the various quality control procedures as applied to high-strength concrete. Among the variables studied was the effect of test specimen size on compressive strength of concrete having compressive strengths ranging from 6,000 to 14,500 psi (41.4 to 100 MPa). Their results indicated that on average, compressive strength test results from 4 x 8 in. (100 x 200 mm) cylinders were approximately 93 percent of those from 6 x 12 (150 x 300 mm) concrete cylinders. This conclusion differs from conclusions of two earlier investigations conducted by one of the authors *[Carrasquillo et al. 1981, Peterman et al. 1986].*

[Howard and Leatham 1989]: Howard et al. have reported the results of comparative tests between 4 x 8 in. (100 x 200 mm) and 6 x 12 in. (150 x 300 mm) cylinders on mock-ups of the Two Union Square Building in Seattle, Washington. The range of compressive strengths of the concretes investigated was approximately 10,000 to 17,000 psi (69.0 to 121 MPa) measured on 6 x 12 in. (150 x 300 mm) standard cylinders. Concrete specimens were cast in both plastic and steel molds and were either rodded, vibrated, or filled without compaction. Concrete cylinders received three different curing conditions: ambient cure, moist room, or lime-saturated water bath. They reported that although more sensitive to abuse, the 4 x 8 in. (100 x 200 mm) cylinders cast in steel molds and rodded by hand yielded the highest and most consistent results. Based on a figure published in their paper, compressive strengths of 4 x 8 in. (100 x 200 mm) cylinders and 6 x 12 in. (150 x 300 mm) cylinders were related according to the following equation:

- USC, psi: $f_{4x8} = 1.09f_{6x12} - 150$ **(4.5-a)**
- SI, MPa: $f_{100x200} = 1.09f_{150x300} - 1.04$ **(4.5-b)**

[Moreno 1990]: Jaime Moreno reported the results from comparative tests between two parallel sets of 4 x 8 in. (100 x 200 mm) 12,000 and 14,000 psi (82.8 and 96.6 MPa) concrete cylinders to standard 6 x 12 in. (150 x 300 mm) cylinders from concrete delivered to 225 W. Wacker Drive Project, Chicago. Reported results indicate almost identical (3.4% and 3.8%) within-test coefficient of variations on 6 x 12 in. (150 x 300 mm) and 4 x 8 in. (100 x 200 mm) cylinders. In this study, 4 x 8 in. (100 x 200 mm) cylinders exhibited strengths which were 101 percent of those from 6 x 12 in. (150 x 300 mm) specimens.

[Burg and Ost 1992]: Burg et al. reported the results from the first 19 months of a three year study of engineering properties of high-strength concrete conducted at Construction Technology Laboratories (CTL), Skokie, Illinois. Compressive strengths of 6 x 12 in. (150 x 300 mm) cylinders from six concrete mixes with 28-day compressive strengths in the range of 11,400 to 17,250 psi (78.6 to 119 MPa) were compared to companion 4 x 8 in. (100 x 200 mm) cylinders. They reported good general agreement for the strength of the two specimen sizes with 4 x 8 in. (100 x 200 mm) cylinders yielding strength values within about one percent of those determined from 6 x 12 in. (150 x 300 mm) cylinders. They concluded that 4 x 8 in. (100 x 200 mm) cylinders are an acceptable substitute for 6 x 12 in. (150 x 300 mm) cylinders at least for developmental work.

[Lessard, Chaallal, and Aïtcin 1993]: Lessard et al. tested and compared compressive strength test results from 18 pairs of 6 x 12 in. (150 x 300 mm) and 4 x 8 in. (100 x 200 mm) specimens from 10 different high-strength concrete mixes. The 28- and 91-day compressive strengths of 6 x 12 in. (150 x 300 mm) cylinders considered ranged from 10,500 to 15,700 psi (72.4 to 108 MPa) and 14,000 to 17,000 psi (96.6 to 117 MPa) respectively. They concluded that the average conversion factor f_{4x8}/f_{6x12} ($f_{100x200}/f_{150x300}$) was 1.05. Contrary to the view that

the dispersion of results is larger for smaller specimens, results from this study showed almost identical within-test coefficient of variation when sets of three 6 x 12 in. (150 x 300 mm) and 4 x 8 in. (100 x 200 mm) specimens from the same concrete mix were tested. They urged researchers to clearly indicate the diameter of specimens considered in any reported results.

[Novokshchenov 1993]: Vladimir Novokshchenov reported the results of a study on the effects of various factors on the compressive strength of high-strength concrete. As a part of this study, Novokshchenov compared compressive strength test results from two sets of 4 x 8 in. (100 x 200 mm) and 6 x 12 in. (150 x 300 mm) concrete cylinders. One set of specimens was subjected to standard moist-curing condition and the specimens were tested at 7, 28 and 56 days. The second set was air-cured at 55 percent relative humidity and approximately 74 °F (23 °C) for 56 days and then tested. Compressive strength of the air-cured 6 x 12 in. (150 x 300 mm) cylinders at 56 days was reported to be 18,000 psi (124 MPa). According to this study, regardless of curing conditions, the average strength of 4 x 8 in. (100 x 200 mm) cylinders was higher than that of 6 x 12 in. (150 x 300 mm) cylinders. For moist-cured specimens, age at testing did not have any significant effect on difference in strength of the two sizes of specimens, and the difference in strength due to specimen size did not exceed 3 percent. The difference in compressive strengths for air-cured cylinders was reported to be about 7.2 percent.

[Radain, Samman, and Wafa 1993]: Radain et al. reported higher compressive strength test results (approximately 2 percent higher) for 6 x 12 in. (150 x 300 mm) cylinders when compared to values obtained by testing 4 x 8 in. (100 x 200 mm) cylinders. They tested specimens from twenty concrete mixes with 28-day compressive strengths between 5,770 to 13,000 psi (39.8 to 89.7 MPa) as measured on standard 6 x 12 in. (150 x 300 mm) cylinders.

[Tomosawa, Noguchi, and Onoyama 1993]: Tomosawa et al. reported results from an experimental investigation conducted in Japan by University of Tokyo and the Building Research Institute of the Ministry of Construction on the effects of various parameters on

compressive strength results of high-strength concrete. The range of compressive strengths of concretes investigated was 5,800 to 17,400 psi (40.0 to 120 MPa). The study covered many factors that may affect the test results. Among them was the specimen size effect. Tomosawa et al. reported increases of 2 to 9 percent in compressive strength of high-strength concrete when the size of specimens decreased from 6 x 12 in. (150 x 300 mm) to 4 x 8 in. (100 x 200 mm). In this study the coefficients of variation of compressive strength of high-strength concretes fell within the rage of approximately 5 percent regardless of the specimen size, and tended to decrease as the specimen size increased.

[Day and Haque 1993]: Day et al. published the results of a study on the influence of specimen size on the measured compressive strengths of concrete. Comparison was made between compressive strengths of 3 x 6 in. (75 x 150 mm) and 6 x 12 in. (150 x 300 mm) cylindrical specimens. In order to substantiate their findings, they also included the results of strength comparison between 3 x 6 in. (75 x 150 mm) and 4 x 8 in. (100 x 200 mm) cylinders with those of standard 6 x 12 in. (150 x 300 mm) specimens available in the literature from other sources (Date and Schnormeier). The conclusions indicated that for concretes with compressive strengths less than 7,250 psi (50.0 MPa) there was a statistical equivalence between strength measured on 6 in. (150 mm) diameter cylinders and that measured on 3 or 4 in. (75 or 100 mm) diameter cylinders. They also stated that the confidence interval for prediction of large-cylinder strengths from small-cylinder tests increased with increase in the strength level of concrete.

[Strategic Highway Research Program "SHRP" 1993]: Results from strength comparisons between 4 x 8 in. (100 x 200 mm) and 6 x 12 in. (150 x 300 mm) cylinders for HPC (high-performance concrete) have been published in a series of SHRP documents. SHRP classifies HPC into the following three categories: (1) very early strength concrete (VES); (2) high early strength concrete (HES); and (3) very high strength concrete (VHS). VES concrete is defined as concrete that will achieve a minimum compressive strength of 2,000 psi (13.8 MPa) in 6 hours or 2,500 psi (17.2 MPa) in 4 hours (VES concrete options A and B

respectively). HES concrete is defined as concrete that will achieve a minimum compressive strength of 5,000 psi (34.5 MPa) in 24 hours. VHS concrete is defined as concrete that will achieve a minimum compressive strength of 10,000 psi (69.0 MPa) in 28 days. All above categories shall meet the minimum durability factor of 80% after 300 cycles of freezing and thawing according to ASTM C666, Procedure A. It was concluded that the ratio of 4 x 8 in. (100 x 200 mm) cylinder strength to 6 x 12 in. (150 x 300 mm) cylinder strength varies with the type of coarse aggregate used. Values for f_{4x8}/f_{6x12} ($f_{100x200}/f_{150x300}$) were between 1.06-1.49 for VES (A), 1.18-1.35 for VES (B), 0.95-1.11 for HES, and 1.02-1.10 for VHS concretes. For the coarse aggregates studied, the ratio of f_{4x8}/f_{6x12} ($f_{100x200}/f_{150x300}$) was lowest for concrete made with a marine marl and highest for concrete made with crushed granite. Concretes made with round gravel produced lower ratios for f_{4x8}/f_{6x12} ($f_{100x200}/f_{150x300}$) than concretes made with dense limestone.

4.3 Effect of Mold Material

Availability, ease of use and other advantages offered by single-use molds (plastic, tin, or cardboard) have made them a practical mold option for the concrete construction industry. In addition ASTM C 470, "Standard Specification for Molds for Forming Concrete Test Cylinders Vertically", does not explicitly require that a consistent type of mold be used for a particular series of tests. In fact it is common practice to use reusable rigid steel molds for laboratory prepared concretes and single-use plastic molds for field specimens. As an example, Burgess et al., reporting on the use of high strength concrete for the Willows Bridge, indicated that while all specimens were made in tin molds, cast iron molds were used in the preparation of specimens for final acceptance testing *[Burgess et al. 1970]*. As a result, it is advantageous and of interest to compare and find a relation between the compressive strength test results obtained from concrete cylinders cast in single-use molds and those obtained from companion cylinders cast in heavy-gauge reusable steel molds.

The following section presents a brief review of the results from some of the published research conducted in this area.

[Hester 1980]: Hester reported the results of a critical review of the contemporary testing procedures for high-strength concrete. In his report he recommended use of rigid, reusable steel molds to maximize measured strengths and minimize variations.

Hester also presented results from a limited study on the comparison of the compressive strengths of concrete specimens cast in steel, tin molds, new plastic molds, and plastic molds after multiple (approximately 20) reuses. He showed that the specimens cast in steel molds achieved approximately 6 percent higher strengths than those cast in tin molds. Hester also reported that the specimens cast in steel molds produced about 13 percent higher compressive strengths than those cast in new single-use plastic molds. Strengths of specimens cast in plastic molds were further reduced with reuse of the mold as it became more flexible.

[Peterman and Carrasquillo 1986]: Peterman et al. reported the results from their study on the effects of mold type on 28-day compressive strength test results from four high strength concrete mixes. The 28-day compressive strengths of the concretes investigated ranged from 8,000 to 11,000 psi (55.2 to 75.9 MPa). Both 4 x 8 in. (100 x 200 mm) and 6 x 12 in. (150 x 300 mm) cylindrical specimens were investigated. Based on the results from 4 x 8 in. (100 x 200 mm) specimens, concrete cast in steel molds always had higher compressive strengths, than specimens made using cardboard.

For 6 x 12 in. (150 x 300 mm) specimens, concrete cast in steel molds were generally stronger than those made in cardboard molds. Comparison of the compressive strength test results between specimens made in plastic and steel molds was inconclusive. Table 4.2 summarizes their findings.

[Carrasquillo and Carrasquillo 1988]: Carrasquillo et al. reported the results of a research program for the study of the various quality control procedures as applied to high-strength concrete. Among the variables studied was the effect of mold material on compressive

strength of concrete having compressive strengths ranging from 6,000 to 14,500 psi (41.4 to 100 MPa). Their results indicated that compressive strengths of 4 x 8 in. (100 x 200 mm) cylinders were, on average, equal for specimens cast in steel, plastic, or cardboard molds. This conclusion differs from conclusions made in a study reported by one of the authors *[Peterman and Carrasquillo 1986]* where it was concluded that an increase in compressive strength of 10 percent can be expected when using same size cylinder molds made of steel rather than cardboard.

For 6 x 12 in. (150 x 300 mm) specimens, the compressive strength of cylinders cast in plastic molds was about 97 percent of cylinders cast in rigid steel molds. The more pronounced effect of the mold material on larger specimens was attributed to the greater flexibility of a 6 x 12 in. (150 x 300 mm) plastic cylinder mold as opposed to a 4 x 8 in. (100 x 200 mm) plastic or cardboard cylinder mold.

4.4 Effect of Specimen End Condition

When a concrete cylindrical specimen is tested for its compressive strength, expected modes of failure can be classified into three general modes:

- ***Mode 1*:** Under normal conditions of test (i.e. with friction acting), the testing machine platens restrain the lateral expansion of the concrete specimen and the specimen assumes a barrel-like shape and at some load fails at its mid-height.
- ***Mode 2***: When the friction is eliminated, the specimen exhibits a uniform lateral expansion along its entire height and eventually at some load splits vertically along its full height.
- ***Mode 3***: When the concrete is stronger than the cap, the cap fails first and the failure of the test specimen starts at the ends of the cylinder. This mode of failure leads to weak and scattered results in compression tests.

It is reported that for a given concrete, compression tests with Mode 2 or Mode 3 failures produce test results lower than those obtained from Mode 1 failure *[Neville 1975, Tomosawa et al. 1993].*

The limit on the compressive strength of commercially available sulfur-based capping mortars has made researchers look for other practical options for end preparation of high strength concrete specimens. A few alternative approaches for end preparation of high strength concrete cylinders have been proposed:

1. *Grinding the cylinder ends*. This technique eliminates the need for capping and the cylinders can be put in direct contact with the platens of the testing machine.
2. *Use of an unbonded capping system*. In this method the idea is to transfer the load from the testing machine platen to the concrete specimen through neoprene pads placed in rigid steel retainer frames, as shown in Figure 2. The pads between the concrete specimen and the retainer frames flow under compression to fill irregularities in cylinder ends. In this system the pads may be reused several times and the retainer frames are permanent. Pads with adequate hardness must be used to prevent the pad from flowing out of the retaining frame during application of load.
3. *Use of the sand-box system [Boulay and de Larrard 1993]*. In this method a fine siliceous clean dry sand is used in lieu of the neoprene pad in the unbonded capping system. The concrete specimen is placed in a steel retainer frame partially filled with sand and the space between the frame and the specimen is filled with molten paraffin. After the paraffin is hardened the other end of the specimen is capped in the same way.

Since capping the ends of cylindrical concrete specimens with sulfur mortars is an accepted standard, it is important to establish a relationship between the test results obtained from specimens with alternative end conditions to those obtained by using sulfur mortar. Once

this relationship is established, the end preparation technique to be used, at any strength level, shall be the one that economically provides the most consistent results.

In this research program, compressive strengths of specimens with ends ground or with ends capped with unbonded neoprene caps were compared with the test results from specimens capped with a high strength sulfur-based capping compound. In the following sections, results from some of the studies on the effect of specimen end condition on strength test results of high strength concrete are briefly presented.

[Ozyildirim 1985]: Celik Ozyildirim studied the feasibility of using unbonded neoprene caps instead of sulfur-mortar caps in compressive strength tests of 438 pairs of 6 x 12 in. (150 x 300 mm) cylinders. Cylinders were cast from commercial batches and were moist cured until tested at 14 days. The great majority of the 14-day compressive strength values ranged from 3,000 to 5,500 psi (20.7 to 37.9 MPa). The neoprene pads used were 1/2 in. (13 mm) thick and had a 50 durometer hardness.

Based on a statistical paired *t* test, the difference between the two procedures was determined to be statistically significant. However, Ozyildirim reported good correlation between the results from the two test methods and concluded that for practical purposes the differences in the values obtained by the two capping methods were negligible. In fact, the largest difference in compressive strength values between the two methods was found to be 108 psi (0.7 MPa). For the entire data, the average of all tests with the neoprene pads was only 55 psi (0.4 MPa) lower than the average for the cylinders capped with sulfur mortar.

[Carrasquillo and Carrasquillo 1988]: Carrasquillo et al. reported the results of a comparative study on the compressive strength values of 6 x 12 in. (150 x 300 mm) high strength concrete cylinders capped with a high strength sulfur mortar and those capped with unbonded neoprene caps. Based on their study, for concrete strengths between 6,000 and 10,000 psi (41.4 and 70.0 MPa), specimens tested with unbonded caps produced 97 percent of

the compressive strength values of companion specimens tested with high strength sulfur mortar. However, for concrete strengths between 10,000 and 17,000 psi (70.0 and 117 MPa) specimens tested with unbonded neoprene caps produced much higher compressive strength values than those capped with high strength sulfur mortar. Insufficient strength of the sulfur mortar at the time of the test and the reduction of the effective *L/d* ratio of the specimen due to the flow of the neoprene pad, under load, into the space between the steel retainer frame and the concrete specimen was presented by the authors as the probable causes for the observed differences in test values at high compressive strength levels of concrete.

For all concrete strength levels, the within-test variations for tests using the unbonded neoprene caps were lower than those using high strength sulfur mortar.

[Richardson 1990]: David N. Richardson studied the effects of both in-specification and out-of-specification deviations on compressive strength test results of specimens with unbonded neoprene caps versus those of specimens capped with the standard sulfur mortar. A total of 127 pairs of 6 x 12 in. (150 x 300 mm) specimens from ten batches with compressive strengths in the range of 3,500 to 6,000 psi (24.1 to 41.4 MPa) were investigated. Deviations considered were: roughness of the cylinder end (bad finishing), air gap under cap (bad capping), eccentric loading, inclined specimen ends, out-of-roundness of one end of the specimen, and rate of loading.

Based on the results of this study Richardson concluded that, for the range of compressive strengths considered, the unbonded neoprene cap system can be used as an alternative to sulfur mortar caps if ASTM tolerances are followed for the test variables included in the study.

[Pistilli and Willems 1993]: Pistilli et al. conducted a study on the effect of alternative end-preparation methods on the measured compressive strength of high strength concrete. Concrete with compressive strengths in the range of 3,000 to 18,000 psi (20.7 to 124 MPa)

were used to compare compressive strength test results of specimens tested with sulfur caps with those of specimens tested with an unbonded cap system. Both 6 x 12 in. (150 x 300 mm) and 4 x 8 in. (100 x 200 mm) cylindrical specimens were included in their study.

Pistilli et al. concluded that for 6 x 12 in. (150 x 300 mm) specimens and concrete strengths up to 8,000 psi (55.2 MPa) there was no significant difference between compressive strengths of specimens tested with unbonded caps and those of companion specimens tested with sulfur mortar. Likewise, there was no significant difference up to 13,000 psi (89.7 MPa) for 4 x 8 in. (100 x 200 mm) specimens. Above these levels, specimens tested with the unbonded cap system produced higher compressive strength values. The following two equations were proposed to correlate compressive strengths obtained with sulfur mortar and unbonded cap systems:

- USC, psi: ***(4.6-a)***

$$f_p = 0.76(f_s)^{1.033} \qquad \textit{for 6 x 12 in.}$$

$$f_p = 0.45(f_s)^{1.092} \qquad \textit{for 4 x 8 in.}$$

- SI, MPa: ***(4.6-b)***

$$f_p = 0.90(f_s)^{1.033} \qquad \textit{for 150 x 300 mm}$$

$$f_p = 0.71(f_s)^{1.092} \qquad \textit{for 100 x 200 mm}$$

where

f_p = compressive strength of specimen measured with unbonded cap system, psi (MPa)

f_s = compressive strength of specimen measured with sulfur mortar, psi (MPa)

[New RC Project: Tomosawa et al. 1993]: As part of a report on the method of compressive strength testing of high strength concrete, Tomosawa et al. reported results of a study on the effect of end preparation on compressive strengths of three 5,800, 11,600, and

17,400 psi (40, 80 and 120 MPa) high strength concretes. The following are some of their findings relevant to this section of the report:

1. Regardless of the strength level, all specimens with ground ends exhibited Mode 1 failure (cone). In the case of specimens capped with sulfur mortar, only specimens of the 5,800 psi (40 MPa) strength level exhibited Mode 1 failure (cone). Specimens from the two other strength levels exhibited Mode 2 failure (split).
2. Regardless of the strength level, all specimens with a 0.12 in. (3 mm) thick sulfur mortar cap exhibited Mode 1 failure (cone). When the thickness of the cap was increased to 0.39 in. (10 mm) only specimens from the 5,800 psi (40 MPa) concrete exhibited Mode 1 failure (cone). Specimens from the two other strength levels exhibited Mode 3 failure (failure started at ends).
3. Specimens with unbonded caps produced compressive strength test values equivalent to those of specimens tested with ground ends. Exceptions were some of the specimens from 5,800 psi (40 MPa) strength level, which showed a significant loss in the compressive strength test results for the unbonded cap end condition.
4. The failure mode of the specimens tested with unbonded caps was either a localized fracture at the ends of the specimen or a flexural fracture.

4.5 Concluding Remarks

High strength concretes are being more frequently utilized in structural applications and therefore, there exists an increasing need for in-situ quality control of high strength concretes. Availability, ease of use and other advantages offered by single-use plastic molds have made them a practical mold option for the concrete construction industry. Limitation on the capacity of the existing testing machines suggests the use of 4 x 8 in. (100 x 200 mm) concrete cylinders instead of the standard 6 x 12 in. (150 x 300 mm) specimens. Also, the limit on compressive strength of commercially available capping compounds makes it necessary to look for other practical options for end preparation of high strength concrete specimens.

Recently many researchers have focused on the effect of flexible single-use plastic molds, the use of smaller size specimens, and alternative end conditions on compressive strength test results of high strength concrete. Different relationships have been proposed to correlate the compressive strengths of "nonstandard" specimens with those of "standard" specimens. In some cases, these studies have reached different or conflicting conclusions about the effect of these test parameters on compressive strength test results.

These variables were included in the investigation described herein (Sections 5.4-5.6). In addition, the effect of specimen size on the modulus of elasticity and splitting tensile strength test results of high strength concrete was studied (Sections 7.6 and 8.3.1). Very little information is available in the literature on these latter effects.

Table 4.1. Compressive strength conversion factors according to different sources

Year	Source	Concrete Strength, psi	Conversion Factor
1925	Gonnerman	1,200 - 4,680	$f_{4x8} / f_{6x12} = 1.01$
1961	RILEM	1,450	$f_{4x8} / f_{6x12} = 1.03$
1951	Price (Bureau of Reclamation)	-	$f_{4x8} / f_{6x12} = 1.04$
1966	Neville	-	$f_{4x8} / f_{6x12} = 1.03$
1976	Malhotra	1,000 - 6,000	$f_{4x8} / f_{6x12} = 0.84$ to 1.32
1981	Carrasquillo, Nilson, Slate	3,000 - 11,000	$f_{4x8} / f_{6x12} = 1.11$
1981	Forstie and Schnormeier	<2,870 3,050 6,950	$f_{4x8} / f_{6x12} < 1.0$ $f_{4x8} / f_{6x12} > 1.0$ $f_{4x8} / f_{6x12} = 1.14$
1984	Date and Schnormeier	3,500 - 5,200	$f_{4x8} / f_{6x12} > 1.0$
1985	Janak	6,231 - 9,988	$f_{4x8} = 1.09 f_{6x12} - 456$
1986	Peterman and Carrasquillo	7,000 - 11,000	$f_{4x8} / f_{6x12} = 1.10$ to 1.15
1988	Carrasquillo and Carrasquillo	6,000 - 14,500	$f_{4x8} / f_{6x12} = 0.93$
1989	Howard and Leatham	10,000 - 17,500	$f_{4x8} = 1.09 f_{6x12} - 150$
1990	Moreno	12,000 & 14,000	$f_{4x8} / f_{6x12} = 1.01$
1992	Burg and Ost	11,400 - 17, 250	$f_{4x8} / f_{6x12} = 1.01$
1993	Lessard, Chaallal and Aïtcin	10,500 - 17,000	$f_{4x8} / f_{6x12} = 1.05$
1993	Novokshchenov	18,000	$f_{4x8} / f_{6x12} = 1.03$ moist-cured $f_{4x8} / f_{6x12} = 1.07$ air-cured
1993	Radain, Samman and Wafa	5,770 - 13,000	$f_{4x8} / f_{6x12} = 0.98$
1993	Tomosawa, Noguchi and Onoyama	5,800 - 17,400	$f_{4x8} / f_{6x12} = 1.02$ to 1.09
1993	Day and Haque	2,900 - 5,800	$f_{4x8} / f_{6x12} = 1.0$
1993	SHRP: Very Early Strength (VES): "A" Very Early Strength (VES): "B" High Early Strength (HES) Very High Strength (VHS)	 1,540 - 2,205 1,670 - 2,670 4,300 - 6,370 7,910 - 12,230	 $f_{4x8} / f_{6x12} = 1.06$ to 1.49 $f_{4x8} / f_{6x12} = 1.18$ to 1.35 $f_{4x8} / f_{6x12} = 0.95$ to 1.11 $f_{4x8} / f_{6x12} = 1.02$ to 1.10

Table 4.2. Comparison of the compressive strength test results of specimens made in plastic, cardboard and steel molds *[Peterman and Carrasquillo 1986]*.

Mold Size	Strength Ratio	Mix Q	Mix R	Mix S	Mix T
4 x 8 in. (100 x 200 mm)	Cardboard/Steel	0.88	0.95	0.98	0.93
6 x 12 in. (150 x 300 mm)	Cardboard/Steel	0.96	1.02	0.95	0.99
6 x 12 in. (150 x 300 mm)	Plastic/Steel	0.93	1.13	0.93	1.07

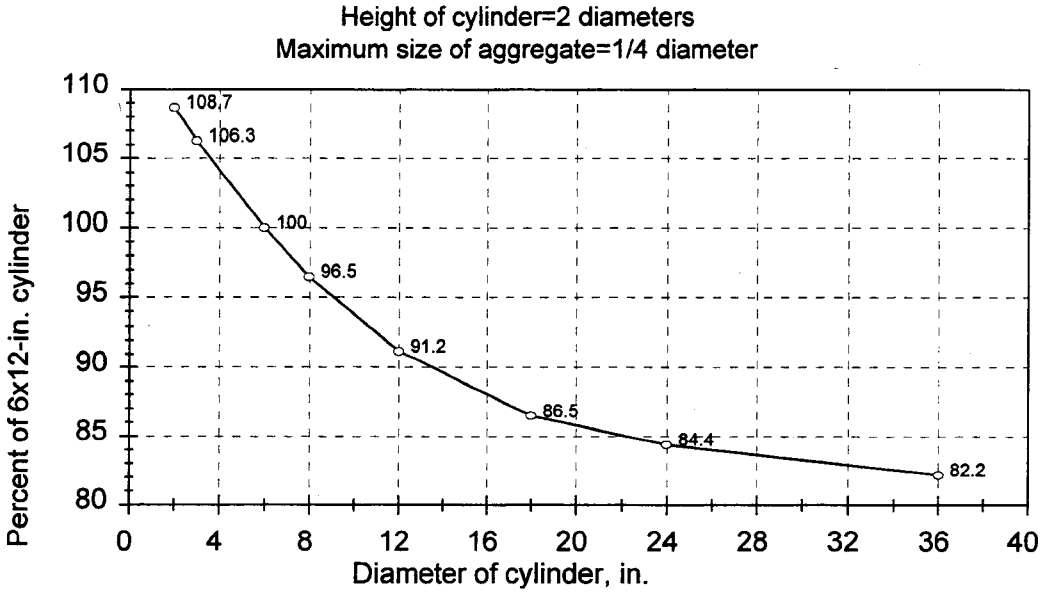

Figure 4.1. Effect of diameter of cylinder on compressive strength of concrete reported by Price *(1951)*. This shows the strength of a 4 in. (100 mm) diameter cylinder as being approximately 104% that of a 6 in. (150 mm) diameter cylinder. [SZ_PRICE.WMF]

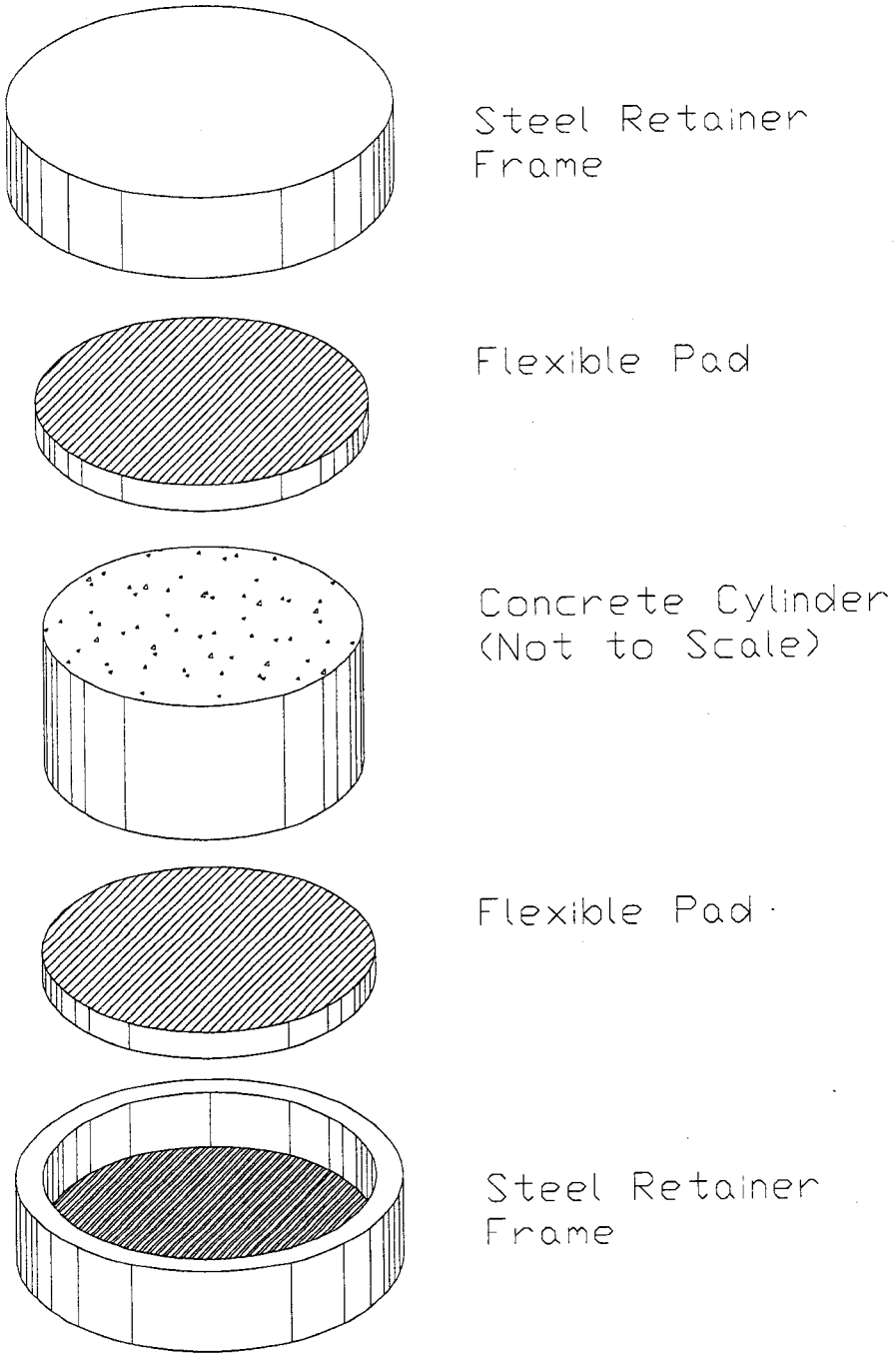

Figure 4.2. Unbonded capping system.
[2CAP.PLT]

CHAPTER 5
TEST RESULTS: COMPRESSIVE STRENGTH

5.1 Test Machine

All compression tests, splitting tensile strength tests and modulus of rupture tests were conducted using an MTS Model 810 Material Testing System. The system has a dual capacity of 120,000 or 600,000 lb. (534 or 2,670 kN), tension or compression, and can be programmed to operate in either load or displacement control modes. The spherical bearing block of the testing machine conformed to the requirements stated in ASTM C 39. The same bearing block was used in all tests regardless of the type of test or the size of the specimens. Figure 5.1 shows a schematic sketch of the spherical bearing block used.

For compression tests, the load was continuously applied to the specimens, in a displacement mode, by moving the top spherical bearing block at a rate of 0.05 in. (1.3 mm) per minute. The splitting tensile strength tests and modulus of rupture tests were conducted under the load control mode with the 120,000 lb. (534 kN) capacity of the testing machine selected. Splitting tensile strength of 4 x 8 in. (100 x 200 mm) cylinders and 6 x 12 in. (150 x 300 mm) cylinders were determined by loading the specimens at a rate of 7,540 lb. (33.5 kN) and 16,965 lb. (75.5 kN) per minute respectively. The modulus of rupture specimens were loaded at a rate of 1,800 lb. (8 kN) per minute. These loading rates corresponded to a stress increase of 150 psi (1.03 MPa) per minute. The ASTM C 496 (Standard Test Method for Splitting Tensile Strength of Cylindrical Concrete Specimens) and ASTM C 78 (Standard Test Method for Flexural Strength of Concrete Using Simple Beam with Third-Point Loading) specified ranges for loading rates were 100 to 200 psi (0.69 to 1.38 MPa) and 125 to 175 psi (0.86 to 1.21 MPa) per minute respectively.

Detailed descriptions of the apparatus and the test procedures specific to each test are provided in the chapters where the test results are discussed. Compressive strength test apparatus, procedures and results are the focus of the present chapter. Test apparatus and

procedures used to study modulus of elasticity and tensile strength of high strength concrete specimens together with the discussion of the test results are presented in Chapters 7 and 8 respectively. Apparatus, test procedures, and results from the study of shrinkage and creep of high strength concrete are described in Chapter 10. All of the experimental test data collected during the course of this study are presented in Appendices A through F at the end of this report.

5.2 Effect of Disturbance on Compressive Strength Test Results

Compressive strengths of undisturbed specimens were compared to those of disturbed specimens, remanence from modulus of elasticity tests. During the tests for modulus of elasticity, specimens were loaded to 50 percent of their ultimate strength, as determined by testing undisturbed (virgin) specimens. The study included both 4 x 8 in. (100 x 200 mm) and 6 x 12 in. (150 x 300 mm) cylindrical specimens from 98 high-strength concrete mixes cast during the course of this research program.

Each value of compressive strength of disturbed specimens was paired with and then plotted against the value of the compressive strength of companion undisturbed specimens. These scatter diagrams are shown in Figures 5.2-5.4. In the case of 4 x 8 in. (100 x 200 mm) specimens, data from total of 2,585 concrete cylinders (1,313 undisturbed and 1,272 disturbed) with compressive strengths in the range of 6,000 to 19,500 psi (41.4 to 135 MPa) were used to form a set of 711 pairs of data. Each element of the pairs was the average of between 1 to 4 replicas. Similarly a set of 260 paired data for 6 x 12 in. (150 x 300 mm) specimens were obtained by using data of compression tests on 744 concrete cylinders (376 undisturbed and 368 disturbed) with compressive strengths in the range of 5,500 to 16,000 psi (38.0 to 110 MPa). Each element of the pairs was average of between 1 to 3 replicas. Detailed information on the compressive strengths of specimens considered, together with their mix numbers, curing, age at testing and number of replicate specimens tested to obtain elements of each pair of data are shown in Table 5.1 for 4 x 8 in. (100 x 200 mm) cylinders and in Table 5.2 for 6 x 12 in. (150 x 300 mm) cylinders.

The pattern made by the test data on the scatter diagrams, shown in Figures 5.2-5.4, strongly suggests a linear relationship between the two measured compressive strengths. The points are scattered around the line of equality shown in the scatter diagrams. Regression analysis was done on the test data to link the compressive strength of undisturbed and disturbed specimens. The resulting equations for best-fit, zero-intercept, least-squares regression lines for each of the three cases were:

- 4 x 8 in.: *(5.1)*

$f_{disturbed} = 1.00 f_{undisturbed}$ $(R^2 = 0.96)$

- 6 x 12 in.: *(5.2)*

$f_{disturbed} = 0.99 f_{undisturbed}$ $(R^2 = 0.94)$

- All data: *(5.3)*

$f_{disturbed} = 1.00 f_{undisturbed}$ $(R^2 = 0.96)$

where R^2 is the coefficient of determination showing the strength of the relationship. It ranges from 0 to 1, where 1 indicates a perfect relationship.

Figure 5.5 shows the approximately normal (bell-shaped) spread of the compressive strength ratios of the undisturbed to disturbed specimens ($f_{undisturbed}/f_{disturbed}$) for the entire set of data. As a check on the normality of the strength ratio data, a normal probability plot for the compressive strength ratios was constructed and is shown in Figure 5.6. It is a plot of the compressive strength ratio data versus the values that would be obtained, on average, if the data came from a normal population. This plot resembles an approximately straight line if the data is from a normal population. The best-fit line through the points in the normal probability plot of Figure 5.6 shows that the spread of the strength ratios is very close to normal distribution. The best-fit line had a coefficient of determination (R^2) of 0.98. Descriptive statistics for the compressive strength ratios were computed and are shown in Table 5.3.

Figures 5.2 through 5.6 together with Table 5.3 indicate that, regardless of the specimen size, the compressive strengths of the high-strength concrete cylindrical specimens were not significantly affected when specimens were once loaded to 50 percent of their ultimate strength. The average value of the compressive strength ratios was approximately 1.00 (0.998) with a standard error of 0.0012.

When each element of a compressive strength data pair was the average of more than 2 replicate specimens the coefficient of variation of the compressive strength of both undisturbed and disturbed specimens were calculated. In all, 618 data pairs for coefficient of variation of compressive strength values were found and are compared in the scatter diagram of Figure 5.7. As can be seen there is no clear difference between the coefficients of variation of the two sets of specimens (undisturbed and disturbed), and the majority of the coefficient of variation values for both sets of the specimens fell within the range of approximately 0 to 5%. For the data shown in Figure 5.7, the means and the standard errors of the coefficients of variation were 2.434 and 0.0877 for undisturbed specimens and 2.413 and 0.0868 for disturbed specimens.

Based on this study, the specimens which were used once for determining modulus of elasticity of concrete were tested for compressive strength and the result of disturbed and undisturbed specimens, with no adjustment, were averaged, used, and reported.

5.3 Compressive Strength versus Time

American Concrete Institute Committee 209 *[ACI 209 1971]* has recommended the following general expression for the time dependent strength of concrete:

- $(f'_c)_t = [t/(a+bt)](f'_c)_{28d}$ **(5.4)**

where

$(f'_c)_t$ = compressive strength of concrete at any time t

t = time in days from placing concrete

$(f'_c)_{28d}$ = 28-day compressive strength of concrete

a = constant, $(0.50 < a < 9.25)$

b = constant, $(0.67 < b < 0.98)$

The following equations approximate time dependent strength of moist- and steam-cured normal strength concretes made with Type I and Type III portland cements *[ACI 209 1971]*:

- Moist-cured concrete, Type I cement: ***(5.5)***

  $(f'_c)_t = [t/(4.00+0.85t)](f'_c)_{28d}$

- Moist-cured concrete, Type III cement: ***(5.6)***

  $(f'_c)_t = [t/(2.30+0.92t)](f'_c)_{28d}$

- Steam-cured concrete, Type I cement: ***(5.7)***

  $(f'_c)_t = [t/(1.00+0.95t)](f'_c)_{28d}$

- Steam-cured concrete, Type III cement: ***(5.8)***

  $(f'_c)_t = [t/(0.70+0.98t)](f'_c)_{28d}$

A study of concrete strength versus time for all of the data collected during the course of this study, resulted in the following equations:

- **Moist-cured concrete, Type I cement:**

⇒ ***All Mixes:*** $(f'_c)_t=[t/(3.09+0.89t)](f'_c)_{28d}$ ***(5.9)***

⇒ Enough data was not available to compute reliable values for constants a and b for special cases of *Ref. mixes*, *FA mixes*, *SF mixes*, and *FA+SF mixes* individually.

- **Moist-cured concrete, Type III cement**:

⇒ ***All Mixes:*** $(f'_c)_t=[t/(1.00+0.96t)](f'_c)_{28d}$ ***(5.10-a)***

⇒ *Ref. mixes:* $(f'_c)_t=[t/(0.89+0.97t)](f'_c)_{28d}$ ***(5.10-b)***

⇒ *FA mixes:* $(f'_c)_t=[t/(3.76+0.86t)](f'_c)_{28d}$ ***(5.10-c)***

$\Rightarrow$ *SF mixes:* $(f'_c)_t=[t/(1.04+0.96t)](f'_c)_{28d}$ **(5.10-d)**

$\Rightarrow$ *FA+SF mixes:* $(f'_c)_t=[t/(1.10+0.96t)](f'_c)_{28d}$ **(5.10-e)**

- **Heat-cured concrete, Type I cement:**

$\Rightarrow$ *All Mixes:* $(f'_c)_t=[t/(0.15+0.99t)](f'_c)_{28d}$ **(5.11-a)**

$\Rightarrow$ *Ref. mixes:* $(f'_c)_t=[t/(0.24+0.98t)](f'_c)_{28d}$ **(5.11-b)**

$\Rightarrow$ *FA mixes:* $(f'_c)_t=[t/(0.24+0.98t)](f'_c)_{28d}$ **(5.11-c)**

$\Rightarrow$ *SF mixes:* $(f'_c)_t=[t/(0.09+0.99t)](f'_c)_{28d}$ **(5.11-d)**

$\Rightarrow$ *FA+SF mixes:* $(f'_c)_t=[t/(0.10+1.00t)](f'_c)_{28d}$ **(5.11-e)**

- **Heat-cured concrete, Type III cement:**

$\Rightarrow$ *All Mixes:* $(f'_c)_t=[t/(0.21+1.00t)](f'_c)_{28d}$ **(5.12-a)**

$\Rightarrow$ *Ref. mixes:* $(f'_c)_t=[t/(0.28+0.99t)](f'_c)_{28d}$ **(5.12-b)**

$\Rightarrow$ *FA mixes:* $(f'_c)_t=[t/(0.28+0.99t)](f'_c)_{28d}$ **(5.12-c)**

$\Rightarrow$ *SF mixes:* $(f'_c)_t=[t/(0.17+1.00t)](f'_c)_{28d}$ **(5.12-d)**

$\Rightarrow$ *FA+SF mixes:* $(f'_c)_t=[t/(0.16+1.00t)](f'_c)_{28d}$ **(5.12-e)**

These equations were derived by fitting a total of 865 observed values of $(f'_c)_t/(f'_c)_{28d}$ versus time in the general equation suggested by ACI Committee 209, using the method of nonlinear least-square regression analysis. Total numbers of data points used to derive each equation were 21 for moist-cured concrete Type I cement, 289 for moist-cured concrete Type III cement, 32 for heat-cured concrete Type I cement, and 523 for heat-cured concrete Type III cement respectively. All of the experimental data fell within about 20 percent of the predicted values given by the equations derived for "*All Mixes*" in each case. The same level of accuracy was reported for the equations suggested by ACI Committee 209 for normal strength concrete.

ACI 209 equations were compared with the derived equations from the experimental data. The results from this comparison are summarized in Tables 5.4-A and 5.4-B.

As expected the strength developed at early ages was higher for moist-cured concretes made with rapid hardening portland cement (Type III) than for ordinary portland cement (Type I). However, heat-cured high strength concrete specimens made with ordinary portland cement and rapid-hardening portland cement had basically the same strength development rate. High cement content and low water-to-cementitious material ratio used in the production of high strength concrete leaves considerable amount of unhydrated cement particles in the hardened concrete. When cement is not hydrated there is no difference between the use of ordinary and rapid hardening portland cement.

It is seen that high early strengths were obtained by high strength concretes considered. The portion of the 28-day compressive strength developed at early ages was significantly higher for high strength concretes than for normal strength concretes. The only exception was the case of moist-cured concretes containing fly ash where the strength development was slower than for normal strength concrete. This behavior was not unexpected because the pozzolanic reaction of fly ash takes place at a much slower rate than hydration of portland cement. High $(f'_c)_{ultimate}/(f'_c)_{28d}$ ratio, (1.16), of moist-cured fly ash concrete supports this argument. Inclusion of fly ash did not affect strength development of heat-cured high strength concrete because fly ash practically replaced unhydrated cement particles in the cement matrix.

Partial replacement of portland cement with silica fume, alone or in combination with fly ash, on a 1 to 1 basis slightly increased early age strength development of heat-cured specimens. Improved strength development of heat-cured silica fume concretes was attributed to silica fume high reactivity (high surface area). Silica fume had no apparent effect on the strength development of moist-cured high strength concretes at all ages.

As seen in Tables 5.4-A and 5.4-B, except for moist-cured fly ash concrete, the $(f'_c)_t/(f'_c)_{28d}$ ratios do not change significantly with time at later ages. In heat-cured specimens, the limit on $(f'_c)_t/(f'_c)_{28d}$ ratio is reached when the hydration process comes to a halt due to lack of moisture, and therefore, there is no further improvement in quality of the cement matrix

with time. In moist-cured specimens, the limited strength of the aggregate-cement matrix bond or the limited strength of the aggregate itself, set a limit on $(f'_c)_t/(f'_c)_{28d}$ ratio. Improvement in the quality of the cement matrix, in moist-cured fly ash concretes, is reflected in $(f'_c)_t/(f'_c)_{28d}$ ratios at later ages.

The reader is reminded of the difference between the steam-curing procedure (used by ACI Committee 209) and heat-curing used throughout this study. Steam-curing provides a favorable accelerated curing environment for concrete by providing both heat and moisture. However, heat-curing as used in this study is basically application of dry heat to a sealed specimen. This curing condition is less ideal and is assumed to be more realistic.

Based on the studied experimental data, the following empirical equations are proposed for predicting compressive strength at any time t for the reference, silica fume and combination fly ash/silica fume (FA+SF) mixes:

- Moist-cured concrete:

⇒ Type I cement:

$$(f'_c)_t=[t/(3.09+0.89t)](f'_c)_{28d} \qquad \textbf{(5.13-a)}$$

⇒ Type III cement:

$$(f'_c)_t=[t/(1.00+0.96t)](f'_c)_{28d} \qquad \textbf{(5.13-b)}$$

- Heat-cured concrete:

⇒ Type I cement:

$$(f'_c)_t=[t/(0.15+0.99t)](f'_c)_{28d} \qquad \textbf{(5.14-a)}$$

⇒ Type III cement:

$$(f'_c)_t=[t/(0.21+1.00t)](f'_c)_{28d} \qquad \textbf{(5.14-b)}$$

The empirical equation to predict the compressive strength at any time t for moist-cured fly ash mixes made with Type III cement is proposed as:

- Moist-cured concrete, Type III cement:

$\Rightarrow$ *FA mixes:*

$$(f'_c)_t=[t/(3.76+0.86t)](f'_c)_{28d} \qquad (5.15)$$

Note that these equations refer to average values only and are valid for high strength concretes made and cured similar to the concretes studied in this research program. Change in the water-to-cementitious material ratio of the mix, use of steam-curing, or replacement of portland cement with pozzolans in levels which differ significantly from those used in this study may affect substantially the strength-time relationships.

5.4 Effect of Specimen Size on Compressive Strength Test Results

Compressive strength of 4 x 8 in. (100 x 200 mm) cylinders: Compressive strength test results of both 4 x 8 in. (100 x 200 mm) and the standard 6 x 12 in. (150 x 300 mm) high strength concrete specimens were analyzed to determine the effect of the specimen size on the strength test results. A total of 1,833 specimens formed 278 data pairs some of which were compressive strengths of individual specimens while others were the average of replicate specimens. Tables 5.5-5.7 provide detailed information on the compressive strengths of specimens considered, together with their mix numbers, age at testing and number of replicate specimens tested to obtain elements of each data pair, for each of the moist-cured and heat-cured sets of specimens.

High strength concrete specimens considered were cast from 94 different batches, used in this research program, and were made with different cementitious material compositions and different aggregate types. All specimens were cast using plastic molds and were capped with a high strength sulfur-based capping mortar. Heat-cured specimens were tested for compressive strength at 1-, and 28-days. Moist-cured specimens were tested after 28-days of continuous moist-curing in a lime-saturated water bath.

Figure 5.8 shows the compressive strengths of 4 x 8 in. (100 x 200 mm) specimens plotted as a function of the compressive strengths of the companion standard 6 x 12 in. (150 x 300 mm) specimens. The data presented in Figure 5.8 include test results from both heat-cured and moist-cured high strength concrete specimens. Also shown in Figure 5.8 is the line of equality. It is clearly seen that the average compressive strengths of both heat-cured and moist-cured 6 x 12 in. (150 x 300 mm) cylinders were lower than those of companion 4 x 8 in. (100 x 200 mm) cylinders. The data also shows a linear relationship between the two measured strengths. The linear correlation coefficient (r) for the measured compressive strengths of 6 x 12 in. (150 x 300 mm) cylinders and the measured compressive strengths of companion 4 x 8 in. (100 x 200 mm) cylinders shown in Figure 5.8 was found to be 0.98 indicating a very strong positive correlation between the two measured compressive strengths (a value of $r = 1$ is a perfect positive correlation). The equation for a best-fit, zero-intercept, least-squares regression line for the data shown in Figure 5.8 was determined to be:

- USC, psi: $f_{4x8} = 1.07 f_{6x12}$ ***(5.16-a)***
- SI, MPa: $f_{100x200} = 1.07 f_{150x300}$ ***(5.16-b)***

To determine the effect of curing condition on the size effect, if any, the heat-cured and the moist-cured data were analyzed separately. For heat-cured specimens the linear correlation coefficient (r) for the data was found to be 0.98. The linear correlation coefficient (r) for moist-cured specimens was slightly lower and was found to be 0.93. However, the same best-fit zero-intercept least-squares regression line equation was obtained in both cases. Limited strength of the capping compound, and not the curing condition, is believed to be the possible cause for the less than perfect linear relationship between the two measured compressive strengths in the case of the moist-cured specimens. As can be seen from Figure 5.8, the compressive strengths of the 6 x 12 in. (150 x 300 mm) cylinders did not increase significantly when the compressive strength of the companion 4 x 8 in. (100 x 200 mm) specimen exceeded the 15,000 psi level. Results of this study, did not support the SHRP report *[Strategic Highway Research Program 1993]* conclusion that the ratio of the 4 x 8 in. (100 x 200 mm) cylinder

strength to 6 x 12 in. (150 x 300 mm) cylinder strength depends on the type of coarse aggregate.

The histogram of the f_{4x8}/f_{6x12} strength ratios ($f_{100x200}/f_{150x300}$), shown in Figure 5.9, resembles a normal distribution. Close agreement of the observed distribution of the strength ratio values with a normal distribution was checked and verified by constructing the normal probability plot, shown in Figure 5.10. The average value of the strength ratio for all data was computed as 1.07 with a standard error of 0.002. Thus it can be concluded that the compressive strength measured using 4 x 8 in. (100 x 200 mm) specimens will on average, be about 7% greater than that measured using 6 x 12 in. (150 x 300 mm) specimens.

When test results from two or more replicate specimens were used to generate each element of a data pair, the coefficient of variation values for the compressive strengths of both 4 x 8 in. (100 x 200 mm) cylinders and 6 x 12 in. (150 x 300 mm) cylinders were computed and compared. Figure 5.11 shows the coefficient of variation of compressive strength values obtained from testing 4 x 8 in. (100 x 200 mm) cylinders versus those obtained from testing 6 x 12 in. (150 x 300 mm) cylinders. No distinct relationship between the coefficients of variations of the two cylinder sizes is observed. Table 5.8 gives the descriptive statistics of the coefficient of variation of the compressive strength values for both sizes of cylinders for each curing condition. As seen in Figure 5.11 and Table 5.8 the majority of the coefficient of variation values for both sizes of specimens fell within the range of approximately 5% regardless of the specimen size and had a tendency to decrease with increase in the size of the specimen. These findings agree with earlier findings of Tomosawa et al. and Lessard et al. *[Tomosawa et al 1993, Lessard et al. 1993].*

Figures 5.12 and 5.13 show that the coefficient of variation of the compressive strength values of the two sizes of cylinders do not have a clear systematic relationship with the compressive strength of concrete.

Compressive strength of 4 x 11 in. (100 x 280 mm) cylinders: According to ASTM C31 or C192 compressive strength tests of hardened concrete must be performed on cylindrical specimens with a length as close to twice the diameter as possible. Correction factors are available in ASTM C42 for specimens with lengths 1 to 2 times the diameter. When the test specimens do not have these relative dimensions, a curve such as the one suggested by the U.S. Bureau of Reclamation, shown in Figure 5.14, or an equation such as the one suggested by Neville *[Neville 1966]*, described in Section 4.2 of this report, may be used to correct indicated strength so they will be comparable with those obtained from standard specimens. Both the curve suggested by the U.S. Bureau of Reclamation and the equation suggested by Neville were developed from tests on normal strength concretes. Cylindrical high strength concrete creep specimens used in this study had a 4 x 11 in. (100 x 280 mm) dimension with $L/D = 2.75$ (ratio of length of cylinder to its diameter). In order to apply the sustained loads during the creep tests with reasonable accuracy it was necessary to conduct a limited study on the effect of change in specimen geometry (length/diameter ratio) on compressive strength of high strength concrete specimens. The result was a relationship between compressive strengths of 4 x 11 in. (100 x 280 mm) creep specimens with those of standard 6 x 12 in. (150 x 300 mm) specimens, Figure 5.15. Each data point shown in this figure is the average of the 1-day compressive strengths of two replicate heat-cured high strength concrete specimens made from some of the mixes considered in this study. Figure 5.15 shows that the average compressive strengths of 4 x 11 in. (100 x 280 mm) specimens were only slightly lower than those of companion standard 6 x 12 in. (150 x 300 mm) cylinders. The least-squares regression line for the data shown in Figure 5.15 was determined to be:

- USC, psi: $f_{4x11} = 0.98 f_{6x12}$ ***(5.17-a)***
- SI, MPa: $f_{100x280} = 0.98 f_{150x300}$ ***(5.17-b)***

Figure 5.14 and Neville's equation suggest 0.97 and 0.96 values for the f_{4x11}/f_{6x12} ($f_{100x280}/f_{150x300}$) strength ratios respectively. Because the effect of the change in specimen geometry was observed to be small, it was decided to use the compressive strength of the

standard 6 x 12 in. (150 x 300 mm) specimens as the basis for computing the sustained loads for the creep tests.

5.5 Effect of End Condition of the Test Specimen on Compressive Strength Test Results

Compressive strength test results of 4 x 8 in. (100 x 200 mm) high strength concrete cylinders with three end conditions were compared. High strength concrete specimens considered were either capped with a commercially available high strength sulfur-based capping compound, capped with an unbonded capping system, or had ground ends. In all cases both ends of the specimens (top and bottom) had similar end conditions.

Sulfur based capping: When the high strength sulfur-based capping compound was used, the capping procedures specified by ASTM C 617, Standard Practice for Capping Cylindrical Concrete Specimens, were closely followed. An automatic temperature control capping compound melting pot was used to melt "Hi-Cap ™" high strength capping compound. This particular capping compound is distributed by Forney Inc., Wampum, PA, and according to its manufacturer is suitable for use with high strength concrete up to 16,000 psi (110 MPa). The ideal melting temperature for this capping compound was 265 °F (130 °C). Significant loss of strength was observed when melting temperatures exceeded approximately 280 °F (138 °C). To assure maximum cap strength, all the test specimens were capped at least 1-day in advance. Moist-cured specimens were returned to the curing tank after capping the specimen.

Unbonded capping (neoprene pad) system: Figure 5.16 shows a schematic sketch and dimensions of the unbonded cap system used in this study. Each cap consisted of a steel retainer frame and a flexible neoprene pad. The steel retainer frames had no seams or welds and were machined from one piece. The inside and outside bearing surfaces of the retainer frames were plane within 0.002 in. (0.05 mm). The pads had a durometer hardness of 70, were flat on both sides and fit snugly into the retainer frames. A schematic diagram of the concrete specimen with the unbonded capping system is shown in Figure 5.17. During a uniaxial

compressive test, the pads between the concrete specimen and the steel retainer frames flow under compression and provide uniform load by filling irregularities in specimen ends. After each test, the pads were blown with compressed air and wiped clean.

Ground ends: Before grinding the ends of the high strength concrete cylinders, a thin slice, approximately 1/8 in. (3 mm), was cut from the troweled end of the specimens. This reduced the grinding time significantly while the length to diameter ratio (L/d) ratio was still within ASTM C 39 specifications. A manually controlled industrial surface grinder was then used to grind both ends of the specimens. Saw cutting and grinding of the ends of the specimens were done with a "FELKER DI-MET" saw, made by Felker Mfg. Co., Torrance, CA, and a surface grinding machine made by K.O. Lee Company of Aberdeen, SD. The saw was equipped with a 14 in. (356 mm) diameter, 0.075 in. (1.9 mm) thick diamond saw blade. The blade and the sample were kept cool during the saw cutting process by a constant stream of water. The surface grinding machine had a precision of removing 0.001 in. (0.025 mm) per pass. The grinding wheel and the surface of the specimen were kept cool by a constant stream of a 2% solution of "Hi-D S973" (coolant and antirust solution). The ground specimens were washed with plain tap water upon completion of the grinding process.

Compressive strength test results from 360 4 x 8 in. (100 x 200 mm) specimens formed a total of 42 data pairs used in this part of the study. Concrete specimens were made from 21 high strength concrete batches mixed at the early stages of this research program and had compressive strengths in the range of 8,500 to 15,800 psi (58.6 to 109 MPa). Tables 5.9 and 5.10 provide detailed information on the compressive strengths of specimens considered, together with their mix numbers, curing condition, age at testing, and number of replicate specimens tested to obtain elements of each data pair.

The two scatter diagrams shown in Figures 5.18 and 5.19 give a graphical presentation of the compressive strength test results of the specimens tested with the unbonded cap system and ground ends versus those of specimens capped with the high strength sulfur-based capping

compound. Also shown in Figures 5.18 and 5.19 is the line of equality. The data in both scatter diagrams clearly are clustered around the line of equality. This observation was verified when the equations for zero-intercept best fitting lines through both sets of data were computed using the least-square regression method:

- Figure 5.18: $f_{neoprene} = 1.01 f_{cap}$ $(R^2 = 0.96)$ *(5.18)*
- Figure 5.19: $f_{ground} = 1.01 f_{cap}$ $(R^2 = 0.98)$ *(5.19)*

where R^2 is the coefficient of determination showing the strength of the relationship. Therefore, for the range of compressive strengths considered in this part of the study, the compressive strengths of ground cylinders and concrete cylinders tested with the unbonded cap system were only slightly higher than those of concrete cylinders capped with a high strength sulfur-based capping compound. However, the grinding process is costly and the advantage obtained by grinding both ends is insignificant (about 1%). Grinding should be used as the last resort when high strength concrete with compressive strengths up to 15,500 psi (107 MPa) are being tested.

The coefficient of variation of the compressive strengths of cylinders tested with the unbonded cap system and ground ends were also compared with the coefficient of variation of the compressive strengths of cylinders with capped ends using a high strength sulfur-based capping compound, Figures 5.20 and 5.21. Table 5.11 gives the descriptive statistics for the coefficients of variation of the compressive strength for both cases considered (unbonded cap versus sulfur cap and ground ends versus sulfur cap). It is seen that on average, the coefficients of variation of the compressive strength test results were lower for specimens with ground ends and the unbonded cap system than those of specimens tested with the high strength sulfur-based capping compound. Similar observations about variability of the compressive strength test data were also reported by Pistelli et al. *(1993)*.

In addition to the compressive strength values, the type of break of high strength concrete specimens of different end conditions were also recorded. In general, most of the breaks for specimens capped with the high strength sulfur-based capping compound and specimens with ground ends were shear or double-cone type failure. The failure of the specimens tested with the unbonded cap system, depending on the strength of the concrete, was either a localized fracture at the ends of the specimen or at the higher strength levels, complete shattering of the specimen upon failure. While shattering of specimens was also observed in some specimens tested with the high strength sulfur-based capping compound, shattering of the specimens tested with unbonded cap systems was more frequent and happened at lower concrete strength levels. The stored energy in the flexible pads developed during the compressive strength tests of high strength concrete is believed to be the cause of the more frequent cases of violent failure of specimens tested with unbonded cap systems.

5.6 Effect of Mold Material on Compressive Strength Test Results

Table 5.12 shows compressive strength data, that were collected during the course of the study, for 6 x 12 in. (150 x 300 mm) high strength concrete specimens cast in heavy-gauge reusable steel molds and single-use plastic molds. A total of 8 data pairs were formed by testing the compressive strengths of 42 high strength concrete specimens. Each element of a data pair, as is shown in Table 5.12, was the average of 2 to 4 replicate specimens. Figure 5.22 shows the compressive strengths of high strength concrete specimens cast in single-use plastic molds versus those of companion specimens cast in heavy-gauge reusable steel molds. As can be seen in the figure, the compressive strength of the high strength concrete decreased when specimens were cast in single-use plastic molds. For the data pairs considered, on average the change in compressive strength was -236 psi. The minus sign indicates that this change was negative, so compressive strength decreased on average when single-use plastic molds were used. The equation for a zero-intercept best fit line through the data was

determined to be:

- 6 x 12 in.: $f_{plastic} = 0.97 f_{steel}$ $(R^2 = 0.98)$ *(5.20)*

where

$f_{plastic}$ = compressive strength of specimens cast in single-use plastic molds, psi (MPa)

f_{steel} = compressive strength of specimens cast in heavy-gauge reusable steel molds, psi (MPa)

R^2 = coefficient of determination, showing the strength of the relationship.

Figure 5.23 shows a comparison of the coefficient of variation of the compressive strength values associated with the two mold materials. It is seen that, on average, the coefficient of variation of compressive strength increased when high strength concrete specimens were cast in single-use plastic molds. For the data considered, the average increase in the coefficient of variation of compressive strength test results, due to the use of single-use plastic molds, was 2.82% with a 95% confidence interval of -0.64% to 6.29%.

Flexibility of the plastic molds, in general, results in convexity of one end and out of roundness of the other end of the test specimen. The rigid steel molds will deform less during consolidation and result in more compacted specimens. Regular use of steel molds, however, is cumbersome and expensive and its benefit does not warrant its use in routine testing.

Other researchers have reported that the mold material has a more pronounced effect for the larger cylinder sizes. Carrasquillo et al. *(1988)* reported equal compressive strength values for 4 x 8 in. (100 x 200 mm) specimens cast in steel, plastic or cardboard molds. The results of their study on the effect of mold material on 6 x 12 in. (150 x 300 mm) specimens was quite consistent with the results reported in the present study.

5.7 Effect of Type of High-Range Water Reducers (HRWR or Superplasticizers) on Compressive Strength Test Results

The use of high-range water reducers in the production of concrete can either improve the strength of concrete at a given workability, by allowing less water to be used, or reduce quantities of both water and cement used to produce concrete of a given strength and workability. When high-range water reducers are used in high dosages, such as 1 to 4 gal./yd^3 (5 - 20 l/m^3) required in the production of high strength concrete with low water-to-cementitious material ratios, unexpected behaviors such as entrainment of excessive amount of large air bubbles, loss of entrained air, over retardation, rapid slump loss, severe segregation, etc. due to incompatibility between cement and high-range water reducer (usually referred to as "*cement-superplasticizer incompatibility*") may be experienced *[Aïtcin et al. 1994]*.

In order to avoid problems associated with the cement-superplasticizer combination, a study was made of five commercially available high-range water reducers used in high strength concrete mixes made with the selected cement for this project (ASTM C 150 Type III, Brand 1). The high-range water reducers selected were supplied in aqueous solution and represented those used by local precast manufacturers. Pertinent properties for the high-range water reducers considered are given in Table 5.13.

To investigate the effect of superplasticizers, a total of 360 4 x 8 in. (100 x 200 mm) cylinders from 20 high strength concrete mixes (Mix No. 30 to Mix No. 49) made with two different types of coarse aggregates (high absorption limestone "L1" and partially crushed river gravel "*R2*") were prepared and tested at 1, 14 and 28-days of age. The high strength concrete mixes were designed for a nominal cementitious material content of 750 lb/yd^3 (445 kg/m^3), and ASTM Type III (Brand 1) cement. In ten of the mixes considered, 7.5% of the total weight of the cementitious material content was replaced by silica fume. A sufficient amount of superplasticizer, up to a maximum of 35 oz./cwt (23 ml/kg), was added to obtain a target slump in the range of 4 to 6 in. (100 to 150 mm). Both heat-cured and moist-cured specimens were studied in this part of the research program.

Except for high strength concrete mixes made with high-range water reducer No. 4 which experienced almost immediate slump loss, all other high-range water reducers provided expected workability, minimal bleeding and performed satisfactorily as a fluidifying agent. Rapid slump loss of high strength concrete mixes made with high-range water reducer No. 4 was a clear case of a cement-superplasticizer incompatibility because it happened with all coarse aggregates and cementitious material compositions considered.

Compressive strength development of high strength concrete mixes made with all five of the high-range water reducers considered and for both curing conditions are shown in Figures 5.26 through 5.31. Data are presented in Table 5.14. Each point represents the average of three 4 x 8 in. (100 x 200 mm) cylinders capped with a high strength sulfur-based capping compound. Figures 5.24 through 5.27 show the test results for high strength concrete mixes made with the high absorption limestone while Figures 5.28 through 5.31 show the results of high strength concrete mixes made with the partially crushed river gravel.

Practically, for all combinations of cementitious material composition and curing condition, the high strength concretes made with high-range water reducer No. 1 resulted in the highest compressive strength at all ages. There were only a few exceptions for which the compressive strength of high strength concretes made with the high-range water reducer No. 1 was slightly lower than the maximum values obtained. Table 5.14 also shows the compressive strength development of all high strength concrete mixes expressed as a percentage of the compressive strength of the high strength concrete mixes made with the high-range water reducer No. 1 at equal ages and similar curing conditions.

In mixes with 7.5% silica fume, high-range water reducers No. 2 and No. 3 resulted in compressive strengths close to those of high strength concrete mixes containing high-range water reducer No. 1. On average, in mixes with 7.5% silica fume, compressive strengths of specimens made with high-range water reducers No. 2 and No. 3 were 96% and 98% of

compressive strengths of companion specimens made with high-range water reducer No. 1. For reference mixes, these percentages were calculated to be 91% for both high-range water reducers No. 2 and No. 3.

Extreme difficulty was experienced during consolidation of specimens cast from high strength concrete mixes made with high-range water reducer No. 4, due to their rapid slump loss. On average, compressive strengths of specimens cast from high strength concrete mixes made with high-range water reducer No. 4 were 78% of the compressive strength of companion specimens cast from high strength concrete mixes made with high-range water reducer No. 1.

High strength concrete mixes made with high-range water reducer No. 5 produced compressive strength test results lower than those of companion specimens from high strength concrete mixes made with high-range water reducer No. 3. It is interesting to note that the compressive strength gain of high strength concrete mixes made with this high-range water reducer depended on the type of coarse aggregate used in the mix. When high-range water reducer No. 5 was used in high strength concrete mixes with limestone as coarse aggregate, its 28-day compressive strength results were approximately 92% of companion specimens made with high-range water reducer No. 1. This percentage reduced to 83% when this high-range water reducer was used in high strength concrete mixes made with partially crushed river gravel.

Results from this part of the study suggest that in order to gain the most benefit and avoid serious problems from incorporation of high-range water reducers, prior to their actual use in any full-scale field project, the user should investigate compatibility of the candidate admixtures with all the cementitious materials, and other constituents under conditions to be expected on the job site. In addition, the selection of high-range water reducers not only should be based on their effect on the properties of the fresh concrete but also should include the effect of the high-range water reducer on the long term properties of concrete as well.

Based on the results of this part of the study high-range water reducer No. 1 was selected and used for all other high strength concrete mixes used in this research program.

5.8 Effect of Type of Coarse Aggregate on Compressive Strength Test Results

Table 5.15 shows the effect of aggregate type on compressive strength of high strength concrete mixes. In comparing the compressive strength of concrete made with crushed limestone (L1 and L2) versus round river gravel (R1), the concrete made with limestone aggregate achieved higher compressive strengths. Crushed limestone particles showed a very strong bond with cement paste, and the plane of fracture in the limestone concrete crossed through many coarse aggregate particles. In contrast, the smooth surface of round river gravel particles resulted in a relatively poor bond with cement paste, and the plane of fracture passed around all but the smaller coarse aggregate particles. Compressive strengths of the mixes using granite (G2) and partially crushed river gravel (R2) were between those of the limestone and the round river gravel mixes. The partially crushed river gravel mix failures were attributed to the flaky physical nature of the aggregate. Detailed discussion on the effect of the type of coarse aggregate on compressive strength of high strength concrete mixes made with different cementitious material compositions is presented in Sections 9.2 and 12.4 of this report.

5.9 Concluding Remarks

A number of parameters were studied in relation to the compressive strength of high strength concrete. To increase the database of specimens used to investigate compressive strength, an investigation was conducted to determine whether compressive strength data obtained from the modulus of elasticity test specimens (specimens loaded to 50% of ultimate compressive strength, unloaded, and subsequently loaded to ultimate compressive strength) could be included in the database. It was concluded that the compressive strength data from the modulus of elasticity test specimens could be included in the database with no modification to their results.

Empirical equations were developed to describe the compressive strength gain with time of the high strength concrete mixes. The results showed that the high strength concrete mixes investigated in this study achieved higher proportions of their respective 28-day compressive strengths at earlier ages relative to those predicted by American Concrete Institute Committee 209 *[ACI 209 1971]* relations. The reverse trend was observed at later ages with the exception of moist-cured fly ash specimens. That is, the high strength concrete mixes developed compressive strengths at later ages, relative to their respective 28-day compressive strengths, that were lower than those predicted by the ACI 209 *[ACI 209 1971]* relations.

A pilot investigation was conducted to investigate the effect of specimen size, end condition, and mold material on compressive strength. The compressive strengths of 4 x 8 in. (100 x 200 mm) specimens were seven percent greater than those of corresponding 6 x 12 in. (150 x 300 mm) specimens; whereas the compressive strengths of 4 x 11 in. (100 x 280 mm) specimens were comparable to their 6 x 12 in. (150 x 300 mm) counterparts. Relative to the specimens capped with a commercially available high strength sulfur-based capping compound, a one- percent increase in compressive strength was observed both for specimens capped with neoprene pads and for specimens with the ground end condition. Using the manual rodding technique for consolidation, specimens cast in plastic molds had compressive strengths, which were approximately three percent less than those observed for specimens cast in steel molds.

The effect of type and brand of high range water reducers (HRWRs) on compressive strength were also studied. A total of five different HRWRs were investigated using twenty mixes (reference and silica fume mixes) with two different curing conditions and tested at different ages (1-,14-,and 28-day). The HRWRs were found to have a significant impact on both the fresh and hardened concrete. Before producing high strength concrete, it is recommended that pilot tests be conducted to test the compatibility of the HRWR with other mix ingredients.

Table 5.1. Comparison of compressive strengths of undisturbed and disturbed specimens, 4 x 8 in. (100 x 200 mm) cylinders.

No.	Cure	Age	$f_{undisturbed}$ psi	n	STD psi	$f_{disturbed}$ psi	n	STD psi	Diff. psi	Ratio
22	H	1	10979	3	43	10533	2	392	446	1.04
22	H	28	13808	3	947	14121	2	105	-313	0.98
23	H	28	12930	3	247	13381	2	24	-451	0.97
24	H	28	10980	3	210	10967	2	277	13	1.00
25	H	1	8442	3	111	8174	2	135	267	1.03
25	H	28	10028	3	242	10046	2	20	-18	1.00
26	H	1	12073	3	711	12388	2	30	-314	0.97
26	H	28	13691	3	284	14140	2	172	-450	0.97
27	H	1	10297	2	43	10320	2	409	-23	1.00
27	H	28	11329	3	364	11738	2	327	-410	0.97
28	H	1	7298	3	259	7334	2	169	-36	1.00
28	H	28	8913	3	78	9201	1		-288	0.97
29	H	1	8682	3	189	8413	2	398	269	1.03
29	H	28	10417	3	185	10156	2	68	262	1.03
50	H	1	9870	4	135	10108	1		-238	0.98
50	H	28	12299	3	184	12197	2	395	103	1.01
51	H	1	7722	3	267	7947	2	300	-225	0.97
51	H	28	10147	2	154	9888	2	95	259	1.03
51	H	182	10519	1		10271	2	82	247	1.02
52	H	1	11244	3	62	11247	2	165	-2	1.00
52	H	28	13104	3	116	12994	2	78	110	1.01
52	H	182	11960	1		12631	2	368	-671	0.95
53	H	1	6083	3	232	6252	2	354	-170	0.97
53	H	28	8900	3	183	8819	2	223	81	1.01
53	H	182	8733	1		8513	2	196	220	1.03
54	H	1	11310	3	283	11359	2	41	-49	1.00
54	H	28	13416	2	487	14302	2	523	-886	0.94
54	H	182	13231	1		13562	2	98	-332	0.98
54	W28	182	14773	1		14868	1		-95	0.99
55	H	1	10471	3	149	10511	2	159	-41	1.00
55	H	28	11956	2	311	12818	2	10	-862	0.93
55	H	182	11029	1		11323	2	51	-294	0.97
55	W28	182	13135	1		12376	1		759	1.06
56	H	1	11098	3	183	11278	2	108	-180	0.98
56	H	28	13006	3	50	12987	2	439	19	1.00
56	H	182	11932	1		12259	2	17	-327	0.97
56	W28	182	14028	1		13718	1		310	1.02
57	H	1	11006	3	13	11065	2	287	-60	0.99
57	H	28	12497	3	404	12111	2	105	386	1.03
57	H	182	11284	1		11834	2	3	-550	0.95
58	H	1	11349	2	263	11416	2	236	-67	0.99
58	H	28	12680	3	140	12744	2	257	-64	1.00
58	H	182	12008	1		12225	2	186	-217	0.98
58	W28	182	14162	1		12997	1		1165	1.09
59	H	1	11136	3	82	10989	2	327	147	1.01
59	H	28	12589	3	115	12739	2	1006	-150	0.99
59	H	182	11860	1		11746	2	257	115	1.01
60	H	1	9198	3	210	9389	2	98	-192	0.98
60	H	28	11388	3	492	11810	2	37	-423	0.96
60	H	182	11512	1		11249	1		263	1.02
61	H	1	10024	3	131	10077	2	111	-53	0.99
61	H	28	12061	3	261	11879	2	1107	181	1.02
61	H	182	11416	1		11980	2	101	-563	0.95
62	H	1	10827	3	466	11034	2	257	-207	0.98
62	H	28	12483	3	225	12815	2	54	-333	0.97

n = number of replicate specimens tested
STD = sample standard deviation (n > 1)
Diff. = $f_{undisturbed} - f_{disturbed}$
Ratio = $f_{undisturbed} / f_{disturbed}$

Table 5.1. Comparison of compressive strengths of undisturbed and disturbed specimens, 4 x 8 in. (100 x 200 mm) cylinders. Continued ...

No.	Cure	Age	$f_{undisturbed}$ psi	n	STD psi	$f_{disturbed}$ psi	n	STD psi	Diff. psi	Ratio
62	H	182	12724	1		13266	2	64	-542	0.96
63	H	1	9893	3	274	10492	2	78	-599	0.94
63	H	28	11402	3	331	12116	2	145	-714	0.94
63	H	182	11335	1		11540	2	34	-205	0.98
64	H	1	10297	2	71	11710	2	10	-1413	0.88
64	H	28	13133	2	98	12985	2	341	148	1.01
64	H	182	12424	1		12533	2	61	-110	0.99
64	W28	182	15069	1		14505	1		563	1.04
65	H	1	10571	2	230	12419	2	317	-1848	0.85
65	H	28	13551	2	174	13804	2	527	-252	0.98
65	H	182	13522	1		13054	2	243	468	1.04
65	W28	182	15618	1		15317	1		301	1.02
66	H	1	9514	3	271	9393	2	9	120	1.01
66	H	28	12354	2	341	11805	2	685	549	1.05
66	H	182	11898	1		11481	2	199	418	1.04
66	W28	182	15061	1		15331	1		-271	0.98
67	H	1	10908	3	368	10480	2	378	428	1.04
67	H	28	11970	2	540	12414	2	27	-444	0.96
67	H	182	11855	1		11276	2	326	579	1.05
67	W28	182	13913	1		13947	1		-33	1.00
68	H	1	10366	3	153	11089	2	179	-723	0.93
68	H	28	12815	3	385	12868	2	68	-53	1.00
68	H	182	12285	1		11839	2	91	446	1.04
68	W28	182	14992	1		14405	2	14	587	1.04
69	H	1	8349	3	103	8984	2	564	-634	0.93
69	H	28	11710	2	118	11595	2	253	115	1.01
69	H	182	11034	1		10805	2	560	229	1.02
69	W28	182	13350	1		13374	2	290	-24	1.00
70	H	1	11244	3	67	11559	2	270	-315	0.97
70	H	28	12293	3	404	12175	2	34	118	1.01
70	H	182	12328	1		12794	2	246	-466	0.96
71	H	1	10487	3	218	10460	2	374	27	1.00
71	H	28	11944	3	406	12049	2	152	-105	0.99
71	H	182	12185	1		12020	2	294	165	1.01
71	W28	182	14004	1		14486	1		-482	0.97
72	H	1	9003	3	466	9478	2	290	-474	0.95
72	H	28	10924	3	215	10695	2	20	229	1.02
72	H	182	10657	1		10815	2	344	-158	0.99
72	W28	182	13675	1		14276	1		-602	0.96
73	H	1	9734	3	459	10528	2	128	-794	0.92
73	H	28	13028	3	526	13094	2	179	-66	0.99
73	H	182	13140	1		13159	2	47	-19	1.00
73	W28	182	16028	1		15370	1		659	1.04
74	H	1	9853	3	256	10098	2	371	-245	0.98
74	H	28	13265	3	170	12579	2	125	686	1.05
74	H	182	13030	1		12920	2	432	110	1.01
74	W28	182	15040	1		14916	1		124	1.01
75	H	1	9580	3	238	10034	2	17	-454	0.95
75	H	28	11266	3	17	11292	2	203	-26	1.00
75	H	182	11626	1		11189	2	436	437	1.04
75	W28	182	14844	1		14672	1		172	1.01
76	H	1	9868	3	363	10163	2	152	-295	0.97
76	H	28	11834	2	118	11559	2	162	275	1.02
76	H	182	11473	1		11755	2	88	-282	0.98
76	W28	182	13837	1		14663	2	108	-826	0.94

n = number of replicate specimens tested
STD = sample standard deviation (n > 1)
Diff. = $f_{undisturbed} - f_{disturbed}$
Ratio = $f_{undisturbed} / f_{disturbed}$

Table 5.1. Comparison of compressive strengths of undisturbed and disturbed specimens, 4 x 8 in. (100 x 200 mm) cylinders. Continued ...

No.	Cure	Age	$f_{undisturbed}$ psi	n	STD psi	$f_{disturbed}$ psi	n	STD psi	Diff. psi	Ratio
77	H	1	10757	3	101	10523	2	0	234	1.02
77	H	28	11796	2	98	11686	2	64	110	1.01
77	H	182	11547	2	294	11707	2	41	-160	0.99
77	W28	182	14329	1		15432	1		-1103	0.93
78	H	1	10215	3	74	9969	2	7	245	1.02
78	H	28	11400	3	106	11607	2	81	-207	0.98
78	H	182	12314	1		12066	1		248	1.02
79	H	1	10628	3	54	10573	2	233	55	1.01
79	H	28	11490	2	30	11574	2	95	-84	0.99
79	H	182	11879	1		12116	2	321	-236	0.98
79	W28	182	14926	1		14720	1		205	1.01
80	H	1	10324	3	191	10447	2	520	-123	0.99
80	H	28	11672	3	228	11600	2	192	72	1.01
80	H	182	12132	1		11996	2	246	136	1.01
80	W28	182	13698	1		12142	1		1557	1.13
81	H	1	10323	3	84	10325	2	105	-2	1.00
81	H	28	11450	3	78	11414	2	91	36	1.00
81	H	182	11397	1		11550	2	169	-153	0.99
81	W28	182	13436	1		13197	1		239	1.02
82	H	1	8658	3	117	8714	2	34	-56	0.99
82	H	28	9419	3	290	9471	2	91	-52	0.99
82	H	182	9397	1		9287	1		110	1.01
82	W28	182	12624	1		12724	1		-100	0.99
83	H	1	9740	3	174	9476	2	106	264	1.03
83	H	28	10514	3	146	10793	2	3	-279	0.97
83	H	182	10495	1		10373	2	118	122	1.01
83	W28	182	13297	1		13436	1		-138	0.99
84	H	1	10794	3	291	10492	2	3	302	1.03
84	H	28	12561	3	105	12538	2	27	22	1.00
84	H	182	13188	1		13159	2	81	29	1.00
85	H	1	11937	3	241	11965	2	101	-29	1.00
85	H	28	12365	3	311	12666	2	224	-302	0.98
85	H	182	12242	1		12331	2	91	-88	0.99
85	W28	182	15857	1		15842	1		14	1.00
86	H	1	7461	3	196	7871	2	118	-410	0.95
86	H	28	9644	3	217	9917	2	61	-273	0.97
86	H	182	10251	1		10502	2	37	-251	0.98
86	W28	182	13885	1		14391	1		-506	0.96
87	H	1	8588	3	320	8941	2	17	-353	0.96
87	H	28	9597	3	149	9725	2	1	-128	0.99
87	H	182	9330	1		9506	2	486	-177	0.98
87	W28	182	13675	1		13722	1		-48	1.00
88	H	1	9931	3	83	10017	1		-86	0.99
88	H	28	11604	3	41	11691	2	179	-87	0.99
88	H	182	12056	1		11877	2	125	179	1.02
88	W28	182	15484	1		15193	1		291	1.02
89	H	1	10439	3	179	10729	2	135	-290	0.97
89	H	28	11195	3	131	11039	2	27	156	1.01
89	H	182	10824	1		11201	2	425	-377	0.97
89	W28	182	15011	1		15002	1		10	1.00
90	H	1	6774	3	52	6785	2	47	-11	1.00
90	H	28	7918	3	282	8131	2	7	-213	0.97
90	H	182	8427	1		8217	2	270	210	1.03
90	W28	182	11817	1		12519	1		-702	0.94
91	H	1	8147	3	103	8009	2	30	138	1.02

n = number of replicate specimens tested
STD = sample standard deviation (n > 1)
Diff. = $f_{undisturbed} - f_{disturbed}$
Ratio = $f_{undisturbed} / f_{disturbed}$

Table 5.1. Comparison of compressive strengths of undisturbed and disturbed specimens, 4 x 8 in. (100 x 200 mm) cylinders. Continued ...

No.	Cure	Age	$f_{undisturbed}$ psi	n	STD psi	$f_{disturbed}$ psi	n	STD psi	Diff. psi	Ratio
91	H	28	8607	3	279	8563	2	3	44	1.01
91	H	182	8642	1		8673	2	226	-31	1.00
91	W28	182	12796	1		12696	1		100	1.01
92	H	28	11579	2	176	11605	2	415	-26	1.00
92	W28	28	12913	2	125	13016	2	769	-103	0.99
92	W28	182	14782	1		14295	2	263	487	1.03
93	H	28	9993	2	162	9607	2	196	387	1.04
93	W28	28	11889	2	311	11908	2	0	-19	1.00
93	W28	182	13622	1		13269	2	101	353	1.03
94	H	28	12197	2	465	11848	2	179	349	1.03
94	W28	28	14615	2	41	14455	2	78	160	1.01
94	W28	182	16277	1		15792	2	199	485	1.03
95	H	28	10883	2	182	10301	2	57	582	1.06
95	W28	28	13990	2	169	13913	2	560	76	1.01
95	W28	182	15981	1		15210	2	179	771	1.05
96	H	28	11600	2	354	12015	2	64	-415	0.97
96	W28	28	12946	2	51	13025	2	176	-79	0.99
96	W28	182	14945	1		15243	2	226	-298	0.98
97	H	28	9681	2	226	9910	2	192	-229	0.98
97	W28	28	11848	2	186	12128	2	54	-279	0.98
97	W28	182	13574	1		13601	2	111	-26	1.00
98	H	28	12513	2	308	12545	2	71	-33	1.00
98	W28	28	15284	2	338	15300	2	159	-17	1.00
98	W28	182	16759	1		16356	2	409	403	1.02
99	H	28	11698	2	108	11872	2	132	-174	0.99
99	W28	28	14684	2	456	14742	2	3	-57	1.00
99	W28	182	15623	1		16401	2	0	-778	0.95
100	H	1	8606	2	44	8489	2	162	117	1.01
100	H	28	10805	2	47	10416	2	449	389	1.04
100	H	182	11185	2	172	11075	2	78	110	1.01
100	H	365	11021	2	33	10552	2	142	469	1.04
100	HW1	28	11550	2	176	11268	2	230	282	1.03
100	HW3	28	11922	2	385	12292	2	807	-370	0.97
100	W7	28	12887	2	203	12662	2	27	224	1.02
100	W14	28	11712	2	601	12646	2	658	-933	0.93
100	W28	28	11022	2	726	11294	2	618	-272	0.98
100	W28	182	13577	2	409	13357	2	449	220	1.02
100	W28	365	13444	2	232	13658	2	294	-214	0.98
100	W182	182	12648	2	297	12521	2	356	127	1.01
100	W365	365	13254	2	378	13030	2	196	224	1.02
101	H	1	8578	2	30	8673	2	17	-95	0.99
101	H	28	10308	2	594	10285	2	770	24	1.00
101	H	182	10869	2	517	11118	2	260	-248	0.98
101	H	365	10946	2	172	11013	2	382	-67	0.99
101	HW1	28	10581	2	189	10894	2	529	-314	0.97
101	HW3	28	10733	2	284	10994	2	145	-260	0.98
101	W7	28	12887	2	203	12662	2	27	224	1.02
101	W14	28	11712	2	601	12646	2	658	-933	0.93
101	W28	28	11022	2	726	11294	2	618	-272	0.98
101	W28	182	13577	2	409	13357	2	449	220	1.02
101	W28	365	13443	2	233	13658	2	294	-215	0.98
101	W182	182	12648	2	297	12521	2	356	127	1.01
101	W365	365	13254	2	378	13030	2	196	224	1.02
102	H	1	6482	2	415	6844	2	517	-363	0.95
102	H	28	8358	2	111	8659	2	199	-301	0.97

n = number of replicate specimens tested
STD = sample standard deviation (n > 1)
Diff. = $f_{undisturbed} - f_{disturbed}$
Ratio = $f_{undisturbed} / f_{disturbed}$

Table 5.1. Comparison of compressive strengths of undisturbed and disturbed specimens, 4 x 8 in. (100 x 200 mm) cylinders. Continued ...

No.	Cure	Age	$f_{undisturbed}$ psi	n	STD psi	$f_{disturbed}$ psi	n	STD psi	Diff. psi	Ratio
102	H	182	9155	2	375	8683	2	246	473	1.05
102	H	365	8480	2	95	8671	2	162	-191	0.98
102	HW1	28	8859	2	591	9151	2	253	-291	0.97
102	HW3	28	8907	2	422	9611	2	81	-704	0.93
102	W7	28	11325	2	668	11130	2	277	196	1.02
102	W14	28	11175	2	955	11700	2	213	-525	0.96
102	W28	28	10117	2	432	10427	2	771	-310	0.97
102	W28	182	12901	2	405	13049	2	432	-148	0.99
102	W28	365	13023	2	591	12851	2	982	172	1.01
102	W182	182	12961	2	490	12638	2	864	322	1.03
102	W365	365	13142	2	37	14095	2	405	-953	0.93
103	H	1	7351	2	483	7606	1		-255	0.97
103	H	28	8761	2	142	8382	2	658	380	1.05
103	H	182	9549	2	34	9714	2	17	-165	0.98
103	H	365	10180	2	574	9313	2	618	867	1.09
103	HW1	28	9215	2	47	9148	2	270	67	1.01
103	HW3	28	9432	2	24	9375	2	186	57	1.01
103	W7	28	11325	2	668	11130	2	277	196	1.02
103	W14	28	11175	2	955	11700	2	213	-525	0.96
103	W28	28	10117	2	432	10427	2	771	-310	0.97
103	W28	182	12901	2	405	13049	2	432	-148	0.99
103	W28	365	13023	2	591	12851	2	982	172	1.01
103	W182	182	12961	2	490	12638	2	864	322	1.03
103	W365	365	13142	2	37	14095	2	405	-953	0.93
104	H	1	11108	2	17	10939	2	74	170	1.02
104	H	28	12285	2	162	11199	2	834	1086	1.10
104	H	182	12789	2	91	13059	2	250	-270	0.98
104	H	365	12559	2	88	12467	2	203	92	1.01
104	HW1	28	12042	2	547	12206	2	544	-165	0.99
104	HW3	28	11839	2	469	12271	2	257	-432	0.96
104	W7	28	14649	2	763	15193	2	344	-544	0.96
104	W14	28	14579	2	402	14966	2	51	-387	0.97
104	W28	28	13992	2	564	13802	2	990	190	1.01
104	W28	182	16279	2	422	15088	2	594	1191	1.08
104	W28	365	14839	2	937	15642	2	74	-803	0.95
104	W182	182	15157	2	78	14880	2	989	277	1.02
104	W365	365	14835	2	7	14895	2	341	-60	1.00
105	H	1	10134	2	598	10516	2	3	-382	0.96
105	H	28	11643	2	192	10542	2	452	1101	1.10
105	H	182	11877	2	213	11858	2	273	19	1.00
105	H	365	10865	2	1394	11703	2	506	-838	0.93
105	HW1	28	11707	2	8	11325	2	270	381	1.03
105	HW3	28	12075	2	101	11526	2	189	549	1.05
105	W7	28	14649	2	763	15193	2	344	-544	0.96
105	W14	28	14579	2	402	14966	2	51	-387	0.97
105	W28	28	13992	2	564	13802	2	990	190	1.01
105	W28	182	16279	2	422	15088	2	594	1191	1.08
105	W28	365	14839	2	937	15642	2	74	-803	0.95
105	W182	182	15157	2	78	14880	2	989	277	1.02
105	W365	365	14835	2	7	14895	2	341	-60	1.00
106	H	1	9652	2	111	9599	2	51	53	1.01
106	H	28	10464	2	760	10948	2	74	-485	0.96
106	H	182	10430	2	159	10566	2	216	-136	0.99
106	H	365	10113	2	263	9989	2	230	124	1.01
106	HW1	28	11132	2	44	11038	2	1	94	1.01

n = number of replicate specimens tested
STD = sample standard deviation (n > 1)
Diff. = $f_{undisturbed} - f_{disturbed}$
Ratio = $f_{undisturbed} / f_{disturbed}$

Table 5.1. Comparison of compressive strengths of undisturbed and disturbed specimens, 4 x 8 in. (100 x 200 mm) cylinders. Continued ...

No.	Cure	Age	$f_{undisturbed}$ psi	n	STD psi	$f_{disturbed}$ psi	n	STD psi	Diff. psi	Ratio
106	HW3	28	11111	2	162	11056	2	24	55	1.00
106	W7	28	13020	2	1290	13620	2	240	-599	0.96
106	W14	28	13295	2	989	14083	2	429	-788	0.94
106	W28	28	11571	2	37	12710	2	7	-1139	0.91
106	W28	182	15009	2	625	15319	2	307	-310	0.98
106	W28	365	14763	2	439	14601	2	790	162	1.01
106	W182	182	14466	2	447	14163	2	741	303	1.02
106	W365	365	14283	2	436	13961	2	952	322	1.02
107	H	1	8847	2	14	8707	2	523	141	1.02
107	H	28	9456	2	10	9599	2	753	-143	0.99
107	H	182	10032	2	709	9960	2	128	72	1.01
107	H	365	9559	2	189	9392	2	27	167	1.02
107	HW1	28	9163	2	34	9411	2	108	-248	0.97
107	HW3	28	9005	2	81	9502	2	155	-497	0.95
107	W7	28	13020	2	1290	13620	2	240	-599	0.96
107	W14	28	13295	2	989	14083	2	429	-788	0.94
107	W28	28	11571	2	37	12710	2	7	-1139	0.91
107	W28	182	15009	2	625	15319	2	307	-310	0.98
107	W28	365	14763	2	439	14601	2	790	162	1.01
107	W182	182	14466	2	447	14163	2	741	303	1.02
107	W365	365	14283	2	436	13961	2	952	322	1.02
108	H	1	8785	1		8900	1		-115	0.99
108	H	28	11101	1		11335	1		-234	0.98
108	H	182	11428	2	219	11402	2	311	26	1.00
108	H	365	11476	2	321	11271	2	476	205	1.02
108	HW1	28	11583	2	1040	12276	2	331	-692	0.94
108	HW3	28	12218	2	966	12223	2	176	-5	1.00
108	W7	28	14541	2	658	13854	2	712	688	1.05
108	W14	28	14721	2	458	14434	2	182	287	1.02
108	W28	28	12574	2	1286	13796	2	652	-1222	0.91
108	W28	182	15257	2	915	14631	2	700	626	1.04
108	W28	365	14964	2	506	15176	2	422	-212	0.99
108	W182	182	14462	2	149	14515	2	560	-53	1.00
108	W365	365	14713	2	327	14966	2	780	-253	0.98
109	H	1	8746	2	137	8520	2	557	225	1.03
109	H	28	11146	2	246	11118	2	172	29	1.00
109	H	182	11144	2	621	11120	2	14	24	1.00
109	H	365	10619	2	311	11220	2	304	-602	0.95
109	HW1	28	11538	2	503	11022	2	64	516	1.05
109	HW3	28	11750	2	7	11956	2	20	-205	0.98
109	W7	28	13603	2	878	13297	2	966	306	1.02
109	W14	28	13414	2	996	14088	2	1124	-673	0.95
109	W28	28	12416	2	382	12791	2	412	-375	0.97
109	W28	182	14405	2	1209	14196	2	1015	209	1.01
109	W28	365	13605	2	523	14718	2	1212	-1112	0.92
109	W182	182	13505	2	679	14040	2	678	-535	0.96
109	W365	365	14372	2	750	14114	2	675	258	1.02
110	H	1	8544	2	132	8406	2	267	138	1.02
110	H	28	11049	2	20	10767	2	567	282	1.03
110	H	182	11280	2	199	11321	2	311	-41	1.00
110	H	365	10924	2	189	10727	2	759	197	1.02
110	HW1	28	10569	2	294	11275	2	287	-707	0.94
110	HW3	28	11523	2	32	11686	2	354	-163	0.99
110	W7	28	13159	2	736	13288	2	500	-129	0.99
110	W14	28	13032	2	523	13094	2	246	-62	1.00

n = number of replicate specimens tested
STD = sample standard deviation (n > 1)
Diff. = $f_{undisturbed} - f_{disturbed}$
Ratio = $f_{undisturbed} / f_{disturbed}$

Table 5.1. Comparison of compressive strengths of undisturbed and disturbed specimens, 4 x 8 in. (100 x 200 mm) cylinders. Continued ...

No.	Cure	Age	$f_{undisturbed}$ psi	n	STD psi	$f_{disturbed}$ psi	n	STD psi	Diff. psi	Ratio
110	W28	28	11855	2	939	11909	2	156	-53	1.00
110	W28	182	14801	2	338	15045	2	392	-244	0.98
110	W28	365	14438	2	276	14861	2	523	-423	0.97
110	W182	182	14324	2	149	14357	2	101	-33	1.00
110	W365	365	14945	2	47	15052	2	118	-107	0.99
111	H	1	7501	2	527	8296	2	165	-795	0.90
111	H	28	10409	2	169	10106	2	219	303	1.03
111	H	182	10507	2	396	10705	2	236	-197	0.98
111	H	365	10466	2	358	10230	2	611	236	1.02
111	HW1	28	10270	2	338	10650	2	159	-380	0.96
111	HW3	28	10139	2	233	11197	2	385	-1058	0.91
111	W7	28	11898	2	804	12202	2	517	-303	0.98
111	W14	28	11886	2	24	12729	2	405	-843	0.93
111	W28	28	10917	2	368	11251	2	273	-334	0.97
111	W28	182	13689	2	297	13536	2	196	153	1.01
111	W28	365	13145	2	838	13102	2	54	44	1.00
111	W182	182	13507	2	351	13149	2	932	358	1.03
111	W365	365	13963	2	341	13410	2	145	554	1.04
112	H	1	11325	1		11793	1		-468	0.96
112	H	28	13221	1		12619	1		602	1.05
112	H	182	13023	2	24	13185	2	44	-162	0.99
112	H	365	12333	2	425	12362	2	628	-29	1.00
112	HW1	28	13200	2	469	12870	2	287	329	1.03
112	HW3	28	13228	2	152	13374	2	88	-146	0.99
112	W7	28	15861	2	419	14489	2	1118	1373	1.09
112	W14	28	15530	2	699	15613	2	1567	-84	0.99
112	W28	28	13871	2	663	15062	2	638	-1190	0.92
112	W28	182	15754	2	503	15976	2	621	-222	0.99
112	W28	365	15847	2	88	15709	2	169	138	1.01
112	W182	182	15205	2	679	15382	2	186	-177	0.99
112	W365	365	15150	2	466	15527	2	338	-377	0.98
113	H	1	11526	2	162	11996	2	476	-470	0.96
113	H	28	12908	2	638	13233	2	84	-325	0.98
113	H	182	13433	2	496	13283	2	128	150	1.01
113	H	365	13367	2	78	12488	2	125	879	1.07
113	HW1	28	13049	2	493	13228	2	213	-179	0.99
113	HW3	28	13321	2	284	13605	2	361	-284	0.98
113	W7	28	14548	2	810	14747	2	415	-198	0.99
113	W14	28	15785	2	547	15487	2	483	298	1.02
113	W28	28	14560	2	57	15043	2	577	-482	0.97
113	W28	182	16336	2	226	16240	2	212	96	1.01
113	W28	365	15563	2	334	15845	2	159	-282	0.98
113	W182	182	15202	2	255	15362	2	591	-161	0.99
113	W365	365	15162	2	685	15541	2	189	-380	0.98
114	H	1	10621	2	341	10165	2	88	456	1.04
114	H	28	11743	2	57	11290	2	3	454	1.04
114	H	182	11230	2	34	11395	2	145	-165	0.99
114	H	365	10972	2	122	11025	2	284	-53	1.00
114	HW1	28	11810	2	37	11707	2	135	103	1.01
114	HW3	28	12097	2	111	11858	2	30	239	1.02
114	W7	28	14930	2	34	14871	2	449	60	1.00
114	W14	28	15513	2	554	14639	2	162	874	1.06
114	W28	28	14653	2	668	15028	2	611	-375	0.98
114	W28	182	15983	2	152	15962	2	189	21	1.00
114	W28	365	15721	2	118	15783	2	37	-62	1.00

n = number of replicate specimens tested
STD = sample standard deviation (n > 1)
Diff. = $f_{undisturbed} - f_{disturbed}$
Ratio = $f_{undisturbed} / f_{disturbed}$

Table 5.1. Comparison of compressive strengths of undisturbed and disturbed specimens, 4 x 8 in. (100 x 200 mm) cylinders. Continued ...

No.	Cure	Age	$f_{undisturbed}$ psi	n	STD psi	$f_{disturbed}$ psi	n	STD psi	Diff. psi	Ratio
114	W182	182	14859	2	68	15296	2	240	-437	0.97
114	W365	365	15274	2	905	14610	2	1654	664	1.05
115	H	1	9929	2	307	9876	2	246	53	1.01
115	H	28	10881	2	34	10562	2	709	320	1.03
115	H	182	10554	2	78	10822	2	37	-267	0.98
115	H	365	10206	2	132	10760	2	273	-554	0.95
115	HW1	28	10645	2	577	11211	2	486	-566	0.95
115	HW3	28	11359	2	513	10941	2	577	418	1.04
115	W7	28	14606	2	128	14236	2	537	370	1.03
115	W14	28	15374	2	189	15119	2	625	255	1.02
115	W28	28	13968	2	436	13297	2	1377	671	1.05
115	W28	182	15830	2	321	15110	2	295	720	1.05
115	W28	365	15386	2	179	15291	2	132	95	1.01
115	W182	182	14411	2	55	14816	2	135	-405	0.97
115	W365	365	14510	2	47	14947	2	192	-437	0.97
116	H	1	9861	2	450	9566	2	159	295	1.03
116	H	28	13025	2	7	13049	2	101	-24	1.00
116	H	182	12810	2	54	12214	2	7	597	1.05
116	H	365	12471	2	81	12643	2	7	-172	0.99
116	HW1	28	13644	2	368	13324	2	172	320	1.02
116	HW3	28	13617	2	95	13381	2	348	236	1.02
116	W7	28	14541	2	658	13854	2	712	688	1.05
116	W14	28	14721	2	458	14434	2	182	287	1.02
116	W28	28	12574	2	1286	13796	2	652	-1222	0.91
116	W28	182	15257	2	915	14631	2	700	626	1.04
116	W28	365	14964	2	506	15176	2	422	-212	0.99
116	W182	182	14462	2	149	14515	2	560	-53	1.00
116	W365	365	14713	2	327	14966	2	780	-253	0.98
117	H	1	8981	2	905	10251	2	81	-1270	0.88
117	H	28	12543	2	378	13028	2	334	-485	0.96
117	H	182	13309	2	172	12555	2	37	754	1.06
117	H	365	12722	2	213	12946	2	78	-224	0.98
117	HW1	28	12686	2	250	13223	2	78	-537	0.96
117	HW3	28	12462	2	182	13374	2	527	-912	0.93
117	W7	28	13603	2	878	13297	2	966	306	1.02
117	W14	28	13414	2	996	14088	2	1124	-673	0.95
117	W28	28	12416	2	382	12791	2	412	-375	0.97
117	W28	182	14405	2	1209	14196	2	1015	209	1.01
117	W28	365	13605	2	523	14718	2	1212	-1112	0.92
117	W182	182	13505	2	679	14040	2	678	-535	0.96
117	W365	365	14372	2	750	14114	2	675	258	1.02
118	H	1	7773	2	263	7950	2	68	-177	0.98
118	H	28	10255	2	105	10514	2	0	-259	0.98
118	H	182	11067	2	28	11113	2	267	-46	1.00
118	H	365	10930	2	35	10571	2	655	359	1.03
118	HW1	28	10578	2	91	10545	2	260	33	1.00
118	HW3	28	11199	2	64	11223	2	24	-24	1.00
118	W7	28	13159	2	736	13288	2	500	-129	0.99
118	W14	28	13032	2	523	13094	2	246	-62	1.00
118	W28	28	11855	2	939	11909	2	156	-53	1.00
118	W28	182	14801	2	338	15045	2	392	-244	0.98
118	W28	365	14438	2	276	14861	2	523	-423	0.97
118	W182	182	14324	2	149	14357	2	101	-33	1.00
118	W365	365	14945	2	47	15052	2	118	-107	0.99
119	H	1	7179	2	71	7243	2	0	-64	0.99

n = number of replicate specimens tested
STD = sample standard deviation (n > 1)
Diff. = $f_{undisturbed} - f_{disturbed}$
Ratio = $f_{undisturbed} / f_{disturbed}$

Table 5.1. Comparison of compressive strengths of undisturbed and disturbed specimens, 4 x 8 in. (100 x 200 mm) cylinders. Continued ...

No.	Cure	Age	$f_{undisturbed}$ psi	n	STD psi	$f_{disturbed}$ psi	n	STD psi	Diff. psi	Ratio
119	H	28	9622	2	296	9518	2	44	103	1.01
119	H	182	9972	2	51	10301	2	422	-329	0.97
119	H	365	9549	2	122	9370	2	206	179	1.02
119	HW1	28	9922	2	14	10382	2	105	-461	0.96
119	HW3	28	9721	2	7	10285	2	101	-563	0.95
119	W7	28	11898	2	804	12202	2	517	-303	0.98
119	W14	28	11886	2	24	12729	2	405	-843	0.93
119	W28	28	10917	2	368	11251	2	273	-334	0.97
119	W28	182	13689	2	297	13536	2	196	153	1.01
119	W28	365	13145	2	838	13102	2	54	44	1.00
119	W182	182	13507	2	351	13149	2	932	358	1.03
119	W365	365	13963	2	341	13410	2	145	554	1.04
120	H	1	11934	2	17	11767	2	179	167	1.01
120	H	28	14197	2	787	13737	2	912	461	1.03
120	H	182	13486	2	78	13503	2	88	-17	1.00
120	H	365	13343	2	91	13374	2	270	-31	1.00
120	HW1	28	13801	2	463	14052	2	270	-251	0.98
120	HW3	28	13880	2	74	13476	2	402	403	1.03
120	W7	28	15861	2	419	14489	2	1118	1373	1.09
120	W14	28	15530	2	699	15613	2	1567	-84	0.99
120	W28	28	13871	2	663	15062	2	638	-1190	0.92
120	W28	182	15754	2	503	15976	2	621	-222	0.99
120	W28	365	15847	2	88	15709	2	169	138	1.01
120	W182	182	15205	2	679	15382	2	186	-177	0.99
120	W365	365	15150	2	466	15527	2	338	-377	0.98
121	H	1	11569	2	439	11395	2	321	174	1.02
121	H	28	13710	2	159	13264	2	736	446	1.03
121	H	182	13424	2	37	13295	2	78	129	1.01
121	H	365	12989	2	118	13145	2	439	-155	0.99
121	HW1	28	13283	2	398	13106	2	176	177	1.01
121	HW3	28	13644	2	267	12674	2	1320	969	1.08
121	W7	28	14548	2	810	14747	2	415	-198	0.99
121	W14	28	15785	2	547	15487	2	483	298	1.02
121	W28	28	14560	2	57	15043	2	577	-482	0.97
121	W28	182	16336	2	226	16240	2	212	96	1.01
121	W28	365	15565	2	331	15845	2	159	-279	0.98
121	W182	182	15226	2	290	15362	2	591	-136	0.99
121	W365	365	15162	2	685	15541	2	189	-380	0.98
122	H	1	11096	2	122	10934	2	176	162	1.01
122	H	28	12887	2	7	12638	2	216	248	1.02
122	H	182	12452	2	81	12001	2	64	451	1.04
122	H	365	12543	2	61	12020	2	145	523	1.04
122	HW1	28	13016	2	0	12870	2	105	146	1.01
122	HW3	28	13233	2	226	12935	2	108	298	1.02
122	W7	28	14930	2	34	14871	2	449	60	1.00
122	W14	28	15513	2	554	14639	2	162	874	1.06
122	W28	28	14653	2	668	15028	2	611	-375	0.98
122	W28	182	15983	2	152	15962	2	189	21	1.00
122	W28	365	15721	2	118	15783	2	37	-62	1.00
122	W182	182	14859	2	68	15296	2	240	-437	0.97
122	W365	365	15274	2	905	14610	2	1654	664	1.05
123	H	1	10671	2	344	10454	2	382	217	1.02
123	H	28	11330	2	358	11431	2	35	-101	0.99
123	H	182	11357	2	37	11068	2	473	289	1.03
123	H	365	11314	2	172	11309	2	105	5	1.00

n = number of replicate specimens tested
STD = sample standard deviation (n > 1)
Diff. = $f_{undisturbed} - f_{disturbed}$
Ratio = $f_{undisturbed} / f_{disturbed}$

Table 5.1. Comparison of compressive strengths of undisturbed and disturbed specimens, 4 x 8 in. (100 x 200 mm) cylinders. Continued ...

No.	Cure	Age	$f_{undisturbed}$ psi	n	STD psi	$f_{disturbed}$ psi	n	STD psi	Diff. psi	Ratio
123	HW1	28	12044	2	334	11736	2	257	308	1.03
123	HW3	28	11772	2	510	11796	2	199	-24	1.00
123	W7	28	14606	2	128	14236	2	537	370	1.03
123	W14	28	15374	2	189	15119	2	625	255	1.02
123	W28	28	13968	2	436	13297	2	1377	671	1.05
123	W28	182	15830	2	321	15110	2	295	720	1.05
123	W28	365	15386	2	179	15291	2	132	95	1.01
123	W182	182	14411	2	55	14816	2	135	-405	0.97
123	W365	365	14510	2	47	14947	2	192	-437	0.97
124	H	1	12089	2	285	12588	2	98	-500	0.96
124	H	28	15405	2	368	14894	2	133	512	1.03
124	H	182	15148	2	428	15119	2	111	29	1.00
124	H	365	14706	2	331	15222	2	169	-516	0.97
124	HW1	28	15520	2	118	14978	2	371	542	1.04
124	HW3	28	16045	2	901	15778	2	273	267	1.02
124	W7	28	17542	1		16726	1		816	1.05
124	W14	28	17103	1		17676	1		-573	0.97
124	W28	28	16439	1		16535	1		-95	0.99
124	W28	182	18335	1		17127	1		1208	1.07
124	W182	182	16563	1		17055	1		-492	0.97
124	W365	365	17232	1		16172	1		1060	1.07
125	H	1	13722	2	439	13935	2	78	-212	0.98
125	H	28	16790	2	314	16422	2	761	368	1.02
125	H	182	16447	2	428	16568	2	344	-121	0.99
125	H	365	16843	2	57	16900	2	125	-57	1.00
125	HW1	28	16804	2	469	17005	2	71	-201	0.99
125	HW3	28	16547	2	976	16974	2	203	-427	0.97
125	W7	28	16792	1		16721	1		72	1.00
125	W14	28	19070	1		17174	1		1896	1.11
125	W28	28	17265	1		16969	1		296	1.02
125	W28	182	18688	1		18311	1		377	1.02
125	W28	365	19399	1		19452	1		-53	1.00
125	W182	182	16945	1		17599	1		-654	0.96
125	W365	365	16855	1		17575	1		-721	0.96
126	H	1	9069	2	138	9368	2	149	-298	0.97
126	H	28	12414	2	358	12495	2	7	-81	0.99
126	H	182	12775	2	341	12202	2	30	573	1.05
126	H	365	12309	2	270	12376	2	338	-67	0.99
126	HW1	28	12818	2	71	12701	2	446	117	1.01
126	HW3	28	12870	2	294	13283	2	74	-413	0.97
126	W7	28	14391	1		14119	1		272	1.02
126	W14	28	14763	1		14443	1		320	1.02
126	W28	28	14224	1		14305	1		-81	0.99
126	W28	182	14873	1		14663	1		210	1.01
126	W28	365	15183	1		15241	1		-57	1.00
126	W182	182	14314	1		15914	1		-1600	0.90
126	W365	365	15169	1		16067	1		-898	0.94
127	H	1	11736	1		11898	1		-162	0.99
127	H	28	14100	2	101	13655	2	223	444	1.03
127	H	182	13892	2	496	13467	2	57	425	1.03
127	H	365	13350	2	398	13734	2	91	-384	0.97
127	HW1	28	14123	2	122	13973	2	165	150	1.01
127	HW3	28	14171	2	209	13715	2	213	456	1.03
127	W7	28	15909	1		15689	1		220	1.01
127	W14	28	15718	1		16339	1		-621	0.96

n = number of replicate specimens tested
STD = sample standard deviation (n > 1)
Diff. = $f_{undisturbed} - f_{disturbed}$
Ratio = $f_{undisturbed} / f_{disturbed}$

Table 5.1. Comparison of compressive strengths of undisturbed and disturbed specimens, 4 x 8 in. (100 x 200 mm) cylinders. Continued ...

No.	Cure	Age	$f_{undisturbed}$ psi	n	STD psi	$f_{disturbed}$ psi	n	STD psi	Diff. psi	Ratio
127	W28	28	15694	1		15413	1		282	1.02
127	W28	182	16893	1		16396	1		497	1.03
127	W28	365	14534	1		15016	1		-482	0.97
127	W182	182	16219	1		15895	1		325	1.02
127	W365	365	16172	1		16043	1		129	1.01
128	H	1	11435	2	182	11824	2	179	-389	0.97
128	H	28	12773	2	316	13094	2	37	-321	0.98
128	H	182	12605	2	47	12887	2	162	-282	0.98
128	H	365	12727	2	267	12715	2	290	12	1.00
128	HW1	28	13028	2	591	12927	2	98	100	1.01
128	HW3	28	13400	2	382	13137	2	287	263	1.02
128	W7	28	16024	1		16181	1		-158	0.99
128	W14	28	16453	1		16344	1		110	1.01
128	W28	28	15260	1		14801	1		458	1.03
128	W28	182	16874	1		16697	1		177	1.01
128	W28	365	16353	1		16406	1		-53	1.00
128	W182	182	16105	1		15699	1		406	1.03
128	W365	365	15809	1		15890	1		-81	0.99
129	H	1	11999	2	14	12168	2	415	-170	0.99
129	H	28	14353	2	425	14345	2	64	7	1.00
129	H	182	14522	2	327	13997	2	206	525	1.04
129	H	365	14212	2	219	14379	2	57	-167	0.99
129	HW1	28	14522	2	98	14498	2	314	24	1.00
129	HW3	28	15088	2	162	15152	2	402	-64	1.00
129	W7	28	16940	1		15904	1		1036	1.07
129	W14	28	17174	1		16917	1		258	1.02
129	W28	28	16043	1		15164	1		879	1.06
129	W28	182	17203	1		16931	1		272	1.02
129	W28	365	17657	1		17609	1		48	1.00
129	W182	182	16530	1		16477	1		53	1.00
129	W365	365	15771	1		16716	1		-945	0.94
130	H	1	9948	2	64	10017	2	216	-69	0.99
130	H	28	12476	2	189	12433	2	182	43	1.00
130	H	182	12624	2	128	12304	2	398	320	1.03
130	H	365	12273	2	10	12340	2	294	-67	0.99
130	HW1	28	12488	2	71	12868	2	243	-380	0.97
130	HW3	28	12767	2	196	13276	2	327	-509	0.96
130	W7	28	14911	1		15155	1		-244	0.98
130	W14	28	16057	1		15756	1		301	1.02
130	W28	28	14792	1		15284	1		-492	0.97
130	W28	182	16606	1		15799	1		807	1.05
130	W28	365	16067	1		16444	1		-377	0.98
130	W182	182	15742	1		16234	1		-492	0.97
130	W365	365	15486	1		16659	1		-1173	0.93
131	H	1	12023	2	20	12063	2	179	-41	1.00
131	H	28	12851	2	260	13429	2	78	-578	0.96
131	H	182	13140	2	304	12975	2	213	165	1.01
131	H	365	13121	2	182	12825	2	88	296	1.02
131	HW1	28	13157	2	286	13073	2	189	84	1.01
131	HW3	28	13536	2	20	13450	2	14	86	1.01
131	W7	28	16535	1		16501	1		33	1.00
131	W14	28	16592	1		16296	1		296	1.02
131	W28	28	15890	1		15933	1		-43	1.00
131	W28	182	17287	1		17041	1		247	1.01
131	W28	365	16816	1		17590	1		-773	0.96

n = number of replicate specimens tested
STD = sample standard deviation (n > 1)
Diff. = $f_{undisturbed} - f_{disturbed}$
Ratio = $f_{undisturbed} / f_{disturbed}$

Table 5.1. Comparison of compressive strengths of undisturbed and disturbed specimens, 4 x 8 in. (100 x 200 mm) cylinders. Continued ...

No.	Cure	Age	$f_{undisturbed}$ psi	n	STD psi	$f_{disturbed}$ psi	n	STD psi	Diff. psi	Ratio
131	W182	182	16325	1		16792	1		-468	0.97
131	W365	365	17743	1		16807	1		936	1.06
132	H	1	14580	2	513	14978	2	189	-398	0.97
132	H	28	16086	2	533	16511	2	277	-425	0.97
132	H	182	15728	2	123	15570	2	493	158	1.01
132	H	365	15723	2	317	15740	2	348	-17	1.00
132	HW1	28	15999	2	197	16642	2	138	-643	0.96
132	HW3	28	16243	2	311	16126	2	44	117	1.01
132	W7	28	16558	1		18249	1		-1690	0.91
132	W14	28	17776	1		18483	1		-707	0.96
132	W28	28	15551	1		16516	1		-964	0.94
132	W28	182	16738	1		17069	1		-331	0.98
132	W28	365	17685	1		17972	1		-286	0.98
132	W182	182	16086	1		16473	1		-387	0.98
132	W365	365	16482	1		17294	1		-812	0.95
133	H	1	14384	2	118	13792	2	348	592	1.04
133	H	28	16036	2	199	16749	2	338	-714	0.96
133	H	182	16995	2	152	15945	2	118	1050	1.07
133	H	365	16800	2	327	16644	2	263	155	1.01
133	HW1	28	15530	2	44	17270	2	230	-1740	0.90
133	HW3	28	16781	2	820	17454	2	294	-673	0.96
133	W7	28	17384	1		19323	1		-1939	0.90
133	W14	28	18764	1		18378	1		387	1.02
133	W28	28	16749	1		18397	1		-1647	0.91
133	W28	182	18949	1		19270	1		-321	0.98
133	W28	365	18830	1		19567	1		-737	0.96
133	W182	182	17766	1		17509	1		258	1.01
133	W365	365	18425	1		18416	1		10	1.00
134	H	1	10657	2	68	10719	2	270	-62	0.99
134	H	28	13567	2	442	14751	2	125	-1184	0.92
134	H	182	14813	2	132	14546	2	71	267	1.02
134	H	365	14396	2	135	14415	2	243	-19	1.00
134	HW1	28	14104	2	230	14878	2	338	-773	0.95
134	HW3	28	14054	2	334	15000	2	57	-945	0.94
134	W7	28	15083	1		14114	1		969	1.07
134	W14	28	16453	1		15923	1		530	1.03
134	W28	28	13952	1		15847	1		-1896	0.88
134	W28	182	17919	1		17292	1		627	1.04
134	W28	365	17408	1		17256	1		153	1.01
134	W182	182	16769	1		16621	1		148	1.01
134	W365	365	17490	1		16807	1		683	1.04
135	H	1	14061	2	1580	15150	2	47	-1089	0.93
135	H	28	15589	2	68	16659	2	135	-1070	0.94
135	H	182	16418	2	382	16141	2	78	277	1.02
135	H	365	16377	2	142	16160	2	334	217	1.01
135	HW1	28	16000	2	7	16909	2	78	-910	0.95
135	HW3	28	16079	2	463	16913	2	90	-835	0.95
135	W7	28	17571	1		18507	1		-936	0.95
135	W14	28	18306	1		18946	1		-640	0.97
135	W28	28	15336	1		16582	1		-1246	0.92
135	W28	182	17986	1		17719	1		267	1.02
135	W28	365	19552	1		18869	1		683	1.04
135	W182	182	17074	1		17733	1		-659	0.96
135	W365	365	17136	1		17852	1		-716	0.96
136	H	1	11538	2	354	11342	2	152	196	1.02

n = number of replicate specimens tested
STD = sample standard deviation (n > 1)
Diff. = $f_{undisturbed} - f_{disturbed}$
Ratio = $f_{undisturbed} / f_{disturbed}$

Table 5.1. Comparison of compressive strengths of undisturbed and disturbed specimens, 4 x 8 in. (100 x 200 mm) cylinders. Continued ...

No.	Cure	Age	$f_{undisturbed}$ psi	n	STD psi	$f_{disturbed}$ psi	n	STD psi	Diff. psi	Ratio
136	H	28	12660	2	3	12588	2	192	72	1.01
136	H	182	12486	2	405	12679	2	84	-193	0.98
136	H	365	12598	2	354	12643	2	230	-45	1.00
136	HW1	28	13214	2	37	13037	2	145	177	1.01
136	HW3	28	13565	2	176	13016	2	290	549	1.04
136	W7	28	14257	1		14458	1		-201	0.99
136	W14	28	15303	1		14057	1		1246	1.09
136	W28	28	14310	1		14233	1		76	1.01
136	W28	182	15909	1		15728	1		181	1.01
136	W28	365	16043	1		15360	1		683	1.04
136	W182	182	14588	1		15408	1		-820	0.95
136	W365	365	15136	1		14758	1		377	1.03
137	H	1	12439	2	775	12894	2	314	-455	0.96
137	H	28	13999	2	405	14255	2	17	-255	0.98
137	H	182	13983	2	233	13453	2	98	530	1.04
137	H	365	13550	2	34	13823	2	81	-272	0.98
137	HW1	28	13971	2	439	14606	1		-635	0.96
137	HW3	28	14193	2	463	14479	2	192	-286	0.98
137	W7	28	17518	1		17174	1		344	1.02
137	W14	28	16702	1		16883	1		-181	0.99
137	W28	28	16902	1		16344	1		559	1.03
137	W28	182	18191	1		17523	1		668	1.04
137	W28	365	17452	1		17872	1		-419	0.98
137	W182	182	16931	1		17480	1		-549	0.97
137	W365	365	16697	1		16630	1		67	1.00
138	H	1	10375	2	277	10203	2	311	172	1.02
138	H	28	11629	2	51	11829	2	442	-201	0.98
138	H	182	11885	2	141	11521	2	135	364	1.03
138	H	365	11789	2	7	11774	2	432	14	1.00
138	HW1	28	12328	2	149	12290	2	351	38	1.00
138	HW3	28	13419	2	240	13369	2	54	50	1.00
138	W7	28	14018	1		14701	1		-683	0.95
138	W14	28	13999	1		15532	1		-1533	0.90
138	W28	28	13550	1		14954	1		-1404	0.91
138	W28	182	15732	1		15050	1		683	1.05
138	W28	365	15861	1		15054	1		807	1.05
138	W182	182	15284	1		15546	1		-263	0.98
138	W365	365	15570	1		15618	1		-48	1.00
139	H	1	11163	2	662	11357	2	300	-193	0.98
139	H	28	12920	2	250	13056	2	78	-136	0.99
139	H	182	12980	2	37	12784	2	37	196	1.02
139	H	365	12896	2	386	13159	2	122	-263	0.98
139	HW1	28	13412	2	7	13746	2	270	-334	0.98
139	HW3	28	13965	2	595	14083	2	679	-118	0.99
139	W7	28	15109	1		15088	1		21	1.00
139	W14	28	15479	1		16788	1		-1308	0.92
139	W28	28	15460	1		16611	1		-1151	0.93
139	W28	182	17332	1		16697	1		635	1.04
139	W28	365	16692	1		17628	1		-936	0.95
139	W182	182	15413	1		16153	1		-740	0.95
139	W365	365	15717	1		16415	1		-699	0.96

n = number of replicate specimens tested
STD = sample standard deviation (n > 1)
Diff. = $f_{undisturbed} - f_{disturbed}$
Ratio = $f_{undisturbed} / f_{disturbed}$

Table 5.2. Comparison of compressive strengths of undisturbed and disturbed specimens, 6 x 12 in. (150 x 300 mm) cylinders.

No.	Cure	Age	$f_{undisturbed}$ psi	n	STD psi	$f_{disturbed}$ psi	n	STD psi	Diff. psi	Ratio
22	H	1	9732	1		10247	1		-516	0.95
22	H	28	13281	3	197	12667	1		614	1.05
23	H	28	12739	2	183	12086	2	302	653	1.05
24	H	28	10664	2	137	10772	2	72	-107	0.99
25	H	1	8144	1		8299	1		-155	0.98
25	H	28	9591	2	83	9715	2	231	-124	0.99
25	W28	28	10875	2	305	11345	2	60	-470	0.96
26	H	1	11296	1		11786	1		-490	0.96
26	H	28	12607	2	6	12569	2	477	38	1.00
26	W28	28	13803	2	221	13857	1		-54	1.00
27	H	1	9819	1		9963	1		-144	0.99
27	H	28	11229	2	65	10837	2	393	392	1.04
27	W28	28	12297	1		11998	1		299	1.02
28	H	1	7072	1		7126	1		-54	0.99
28	H	28	9277	2	1331	8361	2	234	915	1.11
28	W28	28	9734	1		9711	2	96	23	1.00
29	H	1	8503	1		8248	1		255	1.03
29	H	28	9751	2	168	9968	2	59	-218	0.98
50	H	1	9435	1		9452	1		-17	1.00
50	H	28	11505	2	80	11597	2	33	-92	0.99
50	W28	28	11852	1		11673	2	165	178	1.02
51	H	1	7784	1		7709	1		74	1.01
51	H	28	9632	2	57	9966	2	29	-334	0.97
51	W28	28	9908	2	81	10133	2	252	-225	0.98
52	H	1	10676	1		10566	1		110	1.01
52	H	28	12112	2	5	12364	2	56	-252	0.98
52	W28	28	13091	2	0	12896	2	411	195	1.02
53	H	1	5424	1		6027	1		-603	0.90
53	H	28	8872	2	9	9498	2	12	-626	0.93
53	W28	28	9986	2	216	9498	2	12	488	1.05
54	H	1	10434	1		10317	1		117	1.01
54	H	28	12401	2	312	12633	2	372	-231	0.98
54	W28	28	13498	2	16	13570	2	142	-72	0.99
55	H	1	9742	1		9863	1		-121	0.99
55	H	28	11458	2	17	11948	2	746	-490	0.96
55	W28	28	11939	2	315	12493	2	24	-554	0.96
56	H	1	10536	1		10313	1		223	1.02
56	H	28	11999	2	119	12271	2	98	-272	0.98
56	W28	28	12895	2	53	12845	1		50	1.00
57	H	1	10156	1		10381	1		-225	0.98
57	H	28	12059	2	19	12295	2	231	-236	0.98
57	W28	28	12031	2	92	12626	2	133	-595	0.95
58	H	1	10738	1		10568	1		170	1.02
58	H	28	12284	2	203	12015	2	42	268	1.02
58	W28	28	12237	2	32	11583	2	107	654	1.06
59	H	1	10678	1		10438	1		240	1.02
59	H	28	11989	2	244	11868	2	38	122	1.01
59	W28	28	12142	2	312	12010	2	38	133	1.01
60	H	1	8582	1		8437	1		144	1.02
60	H	28	11020	2	73	10528	2	258	492	1.05
60	W28	28	11327	2	89	11406	2	18	-80	0.99
61	H	1	9316	1		9515	1		-199	0.98
61	H	28	11318	2	200	11327	2	11	-8	1.00
61	W28	28	11713	2	248	11353	2	282	360	1.03
62	H	1	10216	1		9954	1		262	1.03

n = number of replicate specimens tested
STD = sample standard deviation (n > 1)
Diff. = $f_{undisturbed} - f_{disturbed}$
Ratio = $f_{undisturbed} / f_{disturbed}$

Table 5.2. Comparison of compressive strengths of undisturbed and disturbed specimens, 6 x 12 in. (150 x 300 mm) cylinders. Continued ...

No.	Cure	Age	$f_{undisturbed}$ psi	n	STD psi	$f_{disturbed}$ psi	n	STD psi	Diff. psi	Ratio
62	H	28	11959	2	461	11816	2	72	143	1.01
62	W28	28	12563	2	471	12792	1		-229	0.98
63	H	1	9305	1		8921	1		384	1.04
63	H	28	11216	2	182	11086	2	156	131	1.01
63	W28	28	11881	2	261	11472	1		410	1.04
64	H	1	9449	1		9505	1		-56	0.99
64	H	28	12293	2	114	11774	2	14	519	1.04
64	W28	28	12491	2	16	12708	2	380	-217	0.98
65	H	1	10228	1		10593	1		-365	0.97
65	H	28	12793	2	59	12584	2	3	209	1.02
65	W28	28	13786	2	61	12843	2	102	944	1.07
66	H	1	8796	1		8925	1		-129	0.99
66	H	28	11732	2	149	11623	2	159	110	1.01
66	W28	28	12864	2	411	11825	2	1004	1039	1.09
67	H	1	10356	1		10360	1		-4	1.00
67	H	28	11889	2	208	12680	2	694	-791	0.94
67	W28	28	12799	2	150	11546	1		1252	1.11
68	H	1	10070	1		10354	1		-284	0.97
68	H	28	11716	2	219	12032	2	24	-316	0.97
68	W28	28	12708	2	269	12722	2	519	-14	1.00
69	H	1	7824	1		7913	1		-89	0.99
69	H	28	10680	2	84	10425	2	56	256	1.02
69	W28	28	11321	2	210	10983	2	122	338	1.03
70	H	1	10296	1		10680	1		-384	0.96
70	H	28	11987	2	10	11589	2	318	399	1.03
70	W28	28	13741	2	203	12988	2	536	753	1.06
71	H	1	9706	1		9995	1		-289	0.97
71	H	28	11340	2	129	11095	2	224	245	1.02
71	W28	28	12814	2	53	12246	2	247	568	1.05
72	H	1	8834	1		8686	1		149	1.02
72	H	28	10611	2	344	10565	2	119	47	1.00
72	W28	28	11692	2	341	12109	1		-417	0.97
73	H	1	9774	1		9564	1		210	1.02
73	H	28	12152	2	110	12354	2	110	-202	0.98
73	W28	28	12969	2	92	12046	2	95	923	1.08
74	H	1	10146	1		10025	1		121	1.01
74	H	28	11953	2	380	11544	2	279	408	1.04
74	W28	28	12659	2	206	12720	2	177	-61	1.00
75	H	1	9278	1		8951	1		327	1.04
75	H	28	10865	2	189	10828	2	188	37	1.00
75	W28	28	11392	2	269	10982	2	423	411	1.04
76	H	1	9312	1		9358	1		-47	1.00
76	H	28	11128	2	141	11018	2	66	110	1.01
76	W28	28	11804	2	187	10879	2	692	926	1.09
77	H	1	10088	1		9963	1		125	1.01
77	H	28	11173	2	78	11178	2	158	-5	1.00
77	W28	28	12385	2	32	12429	2	237	-44	1.00
78	H	1	9460	1		9042	1		418	1.05
78	H	28	10633	2	224	10571	2	38	62	1.01
78	W28	28	12705	1		11111	2	97	1593	1.14
79	H	28	10762	2	62	10675	2	8	87	1.01
79	W28	28	12144	2	209	12488	2	12	-345	0.97
80	H	28	11042	2	119	11075	2	204	-33	1.00
80	W28	28	12009	2	516	11457	1		552	1.05
81	H	28	10600	2	84	10612	2	189	-13	1.00

n = number of replicate specimens tested
STD = sample standard deviation (n > 1)
Diff. = $f_{undisturbed} - f_{disturbed}$
Ratio = $f_{undisturbed} / f_{disturbed}$

Table 5.2. Comparison of compressive strengths of undisturbed and disturbed specimens, 6 x 12 in. (150 x 300 mm) cylinders. Continued ...

No.	Cure	Age	$f_{undisturbed}$ psi	n	STD psi	$f_{disturbed}$ psi	n	STD psi	Diff. psi	Ratio
81	W28	28	11562	2	530	11703	2	705	-141	0.99
82	H	1	7841	1		7898	1		-57	0.99
82	H	28	9102	2	201	9208	2	3	-106	0.99
82	W28	28	10354	2	173	10661	1		-307	0.97
83	H	1	8832	1		8724	1		108	1.01
83	H	28	9050	2	1573	9548	2	14	-498	0.95
83	W28	28	10623	1		11151	1		-528	0.95
84	H	1	9413	1		9982	1		-569	0.94
84	H	28	11740	2	14	11582	2	33	158	1.01
84	W28	28	11949	2	9	12083	2	372	-134	0.99
85	H	1	11154	1		10230	1		923	1.09
85	H	28	11306	2	336	11302	2	144	4	1.00
85	W28	28	12858	2	30	12687	2	89	171	1.01
86	H	1	7160	1		7073	1		87	1.01
86	H	28	8546	2	204	8720	2	57	-174	0.98
86	W28	28	9286	2	111	10198	2	227	-911	0.91
87	H	1	8478	1		7917	1		560	1.07
87	H	28	9025	2	15	8748	2	50	277	1.03
87	W28	28	9388	2	192	10343	2	147	-955	0.91
88	H	1	9157	1		9496	1		-340	0.96
88	H	28	10725	2	66	10763	1		-38	1.00
88	W28	28	12028	2	7	11586	2	315	441	1.04
89	H	1	9658	1		9808	1		-151	0.98
89	H	28	10355	2	242	9845	2	290	509	1.05
89	W28	28	11862	2	105	11447	2	215	415	1.04
90	H	1	6317	1		6453	1		-136	0.98
90	H	28	7516	2	9	7480	2	78	36	1.00
90	W28	28	8637	2	126	8861	2	209	-224	0.97
91	H	1	7650	1		7737	1		-87	0.99
91	H	28	7927	2	26	8017	2	210	-90	0.99
91	W28	28	9689	2	99	9604	2	24	85	1.01
100	H	1	7949	1		9411	1		-1462	0.84
100	H	28	10188	1		10207	1		-19	1.00
100	W28	28	10408	2	593	9867	2	311	541	1.05
101	H	1	8009	1		8166	1		-156	0.98
101	H	28	8191	1		8998	1		-806	0.91
101	W28	28	10408	2	593	9867	2	311	541	1.05
102	H	1	6146	1		6050	1		95	1.02
102	H	28	8034	1		7737	1		297	1.04
102	W28	28	9392	2	312	9651	2	363	-259	0.97
103	H	1	7033	1		7028	1		4	1.00
103	H	28	8403	1		8473	1		-70	0.99
103	W28	28	9392	2	312	9651	2	363	-259	0.97
104	H	1	10256	1		10343	1		-87	0.99
104	H	28	11336	1		10820	1		516	1.05
104	W28	28	12902	2	210	12832	2	582	70	1.01
105	H	1	9950	1		8934	1		1016	1.11
105	H	28	10381	1		10349	1		32	1.00
105	W28	28	12902	2	210	12832	2	582	70	1.01
106	H	1	8501	1		8940	1		-439	0.95
106	H	28	10368	1		9725	1		643	1.07
106	W28	28	12032	2	60	12094	2	132	-62	0.99
107	H	1	8028	1		8115	1		-87	0.99
107	H	28	8679	1		8985	1		-306	0.97
107	W28	28	12032	2	60	12094	2	132	-62	0.99

n = number of replicate specimens tested
STD = sample standard deviation (n > 1)
Diff. = $f_{undisturbed} - f_{disturbed}$
Ratio = $f_{undisturbed} / f_{disturbed}$

Table 5.2. Comparison of compressive strengths of undisturbed and disturbed specimens, 6 x 12 in. (150 x 300 mm) cylinders. Continued ...

No.	Cure	Age	$f_{undisturbed}$ psi	n	STD psi	$f_{disturbed}$ psi	n	STD psi	Diff. psi	Ratio
108	H	1	8359	1		8416	1		-57	0.99
108	H	28	11118	1		11423	1		-306	0.97
108	W28	28	12600	2	359	12692	2	324	-92	0.99
109	H	1	7805	1		7770	1		35	1.00
109	H	28	10578	1		10171	1		407	1.04
109	W28	28	11857	2	248	11804	2	455	53	1.00
110	H	1	7958	1		7973	1		-15	1.00
110	H	28	10035	1		9959	1		76	1.01
110	W28	28	11453	2	8	11450	2	134	4	1.00
111	H	1	7321	1		7298	1		23	1.00
111	H	28	9358	1		9297	1		62	1.01
111	W28	28	9864	2	278	10237	2	459	-372	0.96
112	H	1	10685	1		10799	1		-115	0.99
112	H	28	11867	1		11981	1		-115	0.99
112	W28	28	13755	2	196	13409	2	1002	346	1.03
113	H	1	10918	1		10780	1		138	1.01
113	H	28	11690	1		12312	1		-622	0.95
113	W28	28	13677	2	21	13973	2	689	-296	0.98
114	H	1	10228	1		10129	1		100	1.01
114	H	28	10852	1		11162	1		-310	0.97
114	W28	28	13442	2	437	13658	2	438	-215	0.98
115	H	1	9312	1		9445	1		-134	0.99
115	H	28	10502	1		10163	1		340	1.03
115	W28	28	13431	2	513	13317	2	89	114	1.01
116	H	1	9159	1		9199	1		-40	1.00
116	H	28	12092	1		11351	1		741	1.07
116	W28	28	12600	2	359	12692	2	324	-92	0.99
117	H	1	9220	1		9573	1		-352	0.96
117	H	28	11676	1		11839	1		-163	0.99
117	W28	28	11857	2	248	11804	2	455	53	1.00
118	H	1	7455	1		7177	1		278	1.04
118	H	28	9384	1		9594	1		-210	0.98
118	W28	28	11453	2	8	11450	2	134	4	1.00
119	H	1	7117	1		7164	1		-47	0.99
119	W28	28	9864	2	278	10237	2	459	-372	0.96
120	H	1	10721	1		10432	1		289	1.03
120	H	28	12792	1		13102	1		-310	0.98
120	W28	28	13755	2	196	13409	2	1002	346	1.03
121	H	1	10559	1		10487	1		72	1.01
121	H	28	12607	1		12671	1		-64	0.99
121	W28	28	13677	2	21	13973	2	689	-296	0.98
122	H	1	10114	1		10095	1		19	1.00
122	H	28	11705	1		11563	1		142	1.01
122	W28	28	13442	2	437	13658	2	438	-215	0.98
123	H	1	9602	1		9594	1		8	1.00
123	H	28	11062	1		11039	1		23	1.00
123	W28	28	13431	2	513	13317	2	89	114	1.01
124	H	1	10910	1		10116	1		794	1.08
124	H	28	14761	1		14816	1		-55	1.00
124	W28	28	14322	1		14727	1		-405	0.97
125	H	1	13040	1		12979	1		62	1.00
125	H	28	15357	1		15039	1		318	1.02
125	W28	28	11487	1		11661	1		-174	0.99
126	H	1	8781	1		8673	1		108	1.01
126	H	28	12123	1		11839	1		284	1.02

n = number of replicate specimens tested
STD = sample standard deviation (n > 1)
Diff. = $f_{undisturbed} - f_{disturbed}$
Ratio = $f_{undisturbed} / f_{disturbed}$

Table 5.2. Comparison of compressive strengths of undisturbed and disturbed specimens, 6 x 12 in. (150 x 300 mm) cylinders. Continued ...

No.	Cure	Age	$f_{undisturbed}$ psi	n	STD psi	$f_{disturbed}$ psi	n	STD psi	Diff. psi	Ratio
126	W28	28	13286	1		13189	1		98	1.01
127	H	1	11406	1		11043	1		363	1.03
127	H	28	12554	1		12705	1		-151	0.99
127	W28	28	14700	1		13942	1		758	1.05
128	H	1	10831	1		10929	1		-98	0.99
128	H	28	12278	1		12304	1		-25	1.00
128	W28	28	13248	1		12843	1		405	1.03
129	H	1	11043	1		11162	1		-119	0.99
129	H	28	13000	1		12667	1		333	1.03
129	W28	28	14029	1		13199	1		830	1.06
130	H	1	9144	1		9547	1		-403	0.96
130	H	28	11620	1		11767	1		-146	0.99
130	W28	28	13010	1		12022	1		989	1.08
131	H	1	11018	1		10969	1		49	1.00
131	H	28	12085	1		12440	1		-354	0.97
131	W28	28	14536	1		14124	1		412	1.03
132	H	1	12568	1		13655	1		-1087	0.92
132	H	28	14504	1		14116	1		388	1.03
132	W28	28	14419	1		13471	1		949	1.07
133	H	1	12898	1		13513	1		-615	0.95
133	H	28	15841	1		14882	1		959	1.06
133	W28	28	14875	1		14388	1		487	1.03
134	H	1	9829	1		9804	1		25	1.00
134	H	28	11994	1		13095	1		-1101	0.92
134	W28	28	14670	1		13201	1		1468	1.11
135	H	1	12442	1		13800	1		-1358	0.90
135	H	28	15177	1		14995	1		182	1.01
135	W28	28	13965	1		13488	1		477	1.04
136	H	1	10791	1		10065	1		726	1.07
136	H	28	11710	1		11845	1		-136	0.99
136	W28	28	13787	1		13844	1		-57	1.00
137	H	1	12183	1		12159	1		23	1.00
137	H	28	12732	1		12919	1		-187	0.99
137	W28	28	15004	1		13305	1		1698	1.13
138	H	1	8732	1		8883	1		-151	0.98
138	H	28	11264	1		10742	1		522	1.05
138	W28	28	12981	1		13344	1		-363	0.97
139	H	1	10740	1		10536	1		204	1.02
139	H	28	12223	1		12000	1		223	1.02
139	W28	28	14080	1		12637	1		1443	1.11

n = number of replicate specimens tested
STD = sample standard deviation (n > 1)
Diff. = $f_{undisturbed} - f_{disturbed}$
Ratio = $f_{undisturbed} / f_{disturbed}$

Table 5.3. Descriptive statistics of the compressive strength ratios of all undisturbed and disturbed specimens ($f_{undisturbed}/f_{disturbed}$).

Statistics	
Mean	0.998
Standard Error	0.0012
Median	0.998
Standard Deviation	0.037
Variance	0.0014
Kurtosis	1.450
Skewness	-0.017
Range	0.300
Minimum	0.8446
Maximum	1.1434
Count	971

Table 5.4-A. Comparison of the ACI 209 equations with the derived equations from this study, moist-cured specimens.

	7-day	182-day	365-day	ultimate
Moist-cured concrete, Type I cement				
ACI 209: normal strength concrete	$0.70\,(f'_c)_{28d}$	$1.15\,(f'_c)_{28d}$	$1.16\,(f'_c)_{28d}$	$1.18\,(f'_c)_{28d}$
All mixes: high strength concrete	$0.75\,(f'_c)_{28d}$	$1.11\,(f'_c)_{28d}$	$1.12\,(f'_c)_{28d}$	$1.13\,(f'_c)_{28d}$
Moist-cured concrete, Type III cement				
ACI 209: normal strength concrete	$0.80\,(f'_c)_{28d}$	$1.07\,(f'_c)_{28d}$	$1.08\,(f'_c)_{28d}$	$1.09\,(f'_c)_{28d}$
All mixes: high strength concrete	$0.91\,(f'_c)_{28d}$	$1.03\,(f'_c)_{28d}$	$1.04\,(f'_c)_{28d}$	$1.04\,(f'_c)_{28d}$
Ref. mixes: high strength concrete	$0.91\,(f'_c)_{28d}$	$1.03\,(f'_c)_{28d}$	$1.03\,(f'_c)_{28d}$	$1.03\,(f'_c)_{28d}$
FA mixes: high strength concrete	$0.71\,(f'_c)_{28d}$	$1.13\,(f'_c)_{28d}$	$1.14\,(f'_c)_{28d}$	$1.16\,(f'_c)_{28d}$
SF mixes: high strength concrete	$0.90\,(f'_c)_{28d}$	$1.03\,(f'_c)_{28d}$	$1.03\,(f'_c)_{28d}$	$1.04\,(f'_c)_{28d}$
FA+SF mixes: high strength concrete	$0.91\,(f'_c)_{28d}$	$1.03\,(f'_c)_{28d}$	$1.04\,(f'_c)_{28d}$	$1.04\,(f'_c)_{28d}$

Table 5.4-B. Comparison of the ACI 209 equations with the derived equations from this study, heat-cured specimens.

	1-day	2-day	182-day	ultimate
Heat-cured concrete, Type I cement				
ACI 209: normal strength concrete	$0.51\,(f'_c)_{28d}$	$0.69\,(f'_c)_{28d}$	$1.05\,(f'_c)_{28d}$	$1.05\,(f'_c)_{28d}$
All mixes: high strength concrete	$0.88\,(f'_c)_{28d}$	$0.94\,(f'_c)_{28d}$	$1.01\,(f'_c)_{28d}$	$1.01\,(f'_c)_{28d}$
Ref. mixes: high strength concrete	$0.82\,(f'_c)_{28d}$	$0.91\,(f'_c)_{28d}$	$1.01\,(f'_c)_{28d}$	$1.02\,(f'_c)_{28d}$
FA mixes: high strength concrete	$0.82\,(f'_c)_{28d}$	$0.91\,(f'_c)_{28d}$	$1.02\,(f'_c)_{28d}$	$1.02\,(f'_c)_{28d}$
SF mixes: high strength concrete	$0.93\,(f'_c)_{28d}$	$0.97\,(f'_c)_{28d}$	$1.01\,(f'_c)_{28d}$	$1.01\,(f'_c)_{28d}$
FA+SF mixes: high strength concrete	$0.91\,(f'_c)_{28d}$	$0.95\,(f'_c)_{28d}$	$1.00\,(f'_c)_{28d}$	$1.00\,(f'_c)_{28d}$
Heat-cured concrete, Type III cement				
ACI 209: normal strength concrete	$0.60\,(f'_c)_{28d}$	$0.75\,(f'_c)_{28d}$	$1.02\,(f'_c)_{28d}$	$1.02\,(f'_c)_{28d}$
All mixes: high strength concrete	$0.83\,(f'_c)_{28d}$	$0.91\,(f'_c)_{28d}$	$1.00\,(f'_c)_{28d}$	$1.00\,(f'_c)_{28d}$
Ref. mixes: high strength concrete	$0.79\,(f'_c)_{28d}$	$0.88\,(f'_c)_{28d}$	$1.01\,(f'_c)_{28d}$	$1.01\,(f'_c)_{28d}$
FA mixes: high strength concrete	$0.79\,(f'_c)_{28d}$	$0.88\,(f'_c)_{28d}$	$1.01\,(f'_c)_{28d}$	$1.01\,(f'_c)_{28d}$
SF mixes: high strength concrete	$0.86\,(f'_c)_{28d}$	$0.92\,(f'_c)_{28d}$	$1.00\,(f'_c)_{28d}$	$1.00\,(f'_c)_{28d}$
FA+SF mixes: high strength concrete	$0.86\,(f'_c)_{28d}$	$0.93\,(f'_c)_{28d}$	$1.00\,(f'_c)_{28d}$	$1.00\,(f'_c)_{28d}$

Table 5.5. Comparison of compressive strengths of 4 x 8 in. (100 x 200 mm) and 6 x 12 in. (150 x 300 mm) cylinders, heat-cured specimens.

No.	Age	f_{4x8} psi	n	STD psi	f_{6x12} psi	n	STD psi	Diff. psi	Ratio
4	28	10533	3	776	9820	3	934	713	1.07
4	7	10121	5	370	10032	2	230	89	1.01
5	7	9947	4	1241	9555	2	779	392	1.04
5	28	10552	4	839	9891	4	1087	660	1.07
5	1	8531	5	447	8041	3	344	491	1.06
22	1	10800	5	314	9990	2	365	811	1.08
22	28	13933	5	693	13127	4	347	806	1.06
23	1	10754	3	142	10330	1		424	1.04
23	28	13110	5	303	12412	4	428	698	1.06
24	28	10975	5	203	10718	4	109	257	1.02
24	1	8257	3	246	7812	1		445	1.06
25	1	8335	5	179	8222	2	110	113	1.01
25	28	10035	5	172	9653	4	159	383	1.04
26	28	13870	5	329	12588	4	276	1282	1.10
26	1	12199	5	532	11541	2	347	658	1.06
27	28	11493	5	379	11033	4	322	459	1.04
27	1	10309	4	238	9891	2	102	418	1.04
28	28	8985	4	157	8819	4	942	166	1.02
28	1	7312	5	203	7099	2	38	213	1.03
29	28	10313	5	197	9860	4	162	453	1.05
29	1	8574	5	281	8376	2	180	199	1.02
50	28	12258	5	243	11551	4	73	707	1.06
50	1	9918	5	158	9443	2	12	475	1.05
51	28	10018	4	182	9799	4	196	218	1.02
51	1	7812	5	271	7747	2	53	66	1.01
52	28	13060	5	109	12238	4	149	822	1.07
52	1	11245	5	94	10621	2	78	624	1.06
53	1	6151	5	259	5725	2	426	425	1.07
53	28	8867	5	177	9185	4	362	-318	0.97
54	28	13859	4	658	12517	4	311	1342	1.11
54	1	11329	5	203	10376	2	83	953	1.09
55	1	10487	5	134	9803	2	86	684	1.07
55	28	12387	4	529	11703	4	515	683	1.06
56	28	12999	5	223	12135	4	180	863	1.07
56	1	11170	5	172	10425	2	158	745	1.07
57	1	11029	5	147	10269	2	159	761	1.07
57	28	12342	5	359	12177	4	191	165	1.01
58	1	11383	4	208	10653	2	120	730	1.07
58	28	12705	5	166	12149	4	196	556	1.05
59	28	12649	5	516	11928	4	159	721	1.06
59	1	11077	5	192	10558	2	170	519	1.05
60	28	11557	5	418	10774	4	323	783	1.07
60	1	9274	5	189	8509	2	102	765	1.09
61	1	10045	5	112	9416	2	141	629	1.07
61	28	11988	5	592	11322	4	115	666	1.06
62	1	10910	5	371	10085	2	185	825	1.08
62	28	12616	5	243	11887	4	282	728	1.06
63	1	10133	5	383	9113	2	272	1020	1.11
63	28	11687	5	462	11151	4	157	536	1.05
64	1	11003	4	817	9477	2	40	1526	1.16
64	28	13059	4	222	12034	4	307	1025	1.09
65	28	13677	4	352	12688	4	125	989	1.08
65	1	11495	4	1091	10411	2	258	1084	1.10
66	28	12080	4	544	11677	4	141	402	1.03
66	1	9466	5	203	8861	2	92	605	1.07

n = number of replicate specimens tested
STD = sample standard deviation (n > 1)
Diff. = $f_{4x8} - f_{6x12}$
Ratio = f_{4x8} / f_{6x12}

Table 5.5. Comparison of compressive strengths of 4 x 8 in. (100 x 200 mm) and 6 x 12 in. (150 x 300 mm) cylinders, heat-cured specimens. Continued ...

No.	Age	f_{4x8} psi	n	STD psi	f_{6x12} psi	n	STD psi	Diff. psi	Ratio
67	1	10737	5	398	10358	2	3	379	1.04
67	28	12192	4	404	12284	4	619	-92	0.99
68	1	10655	5	420	10212	2	201	443	1.04
68	28	12836	5	276	11874	4	223	962	1.08
69	1	8603	5	453	7869	2	63	734	1.09
69	28	11653	4	174	10553	4	159	1100	1.10
70	1	11370	5	224	10488	2	272	882	1.08
70	28	12246	5	294	11788	4	294	458	1.04
71	28	11986	5	302	11218	4	206	768	1.07
71	1	10476	5	243	9851	2	204	625	1.06
72	28	10833	5	197	10588	4	212	245	1.02
72	1	9193	5	444	8760	2	105	433	1.05
73	28	13055	5	384	12253	4	147	802	1.07
73	1	10052	5	546	9669	2	149	382	1.04
74	1	9951	5	292	10085	2	86	-134	0.99
74	28	12990	5	399	11748	4	360	1242	1.11
75	1	9761	5	300	9114	2	231	647	1.07
75	28	11276	5	103	10846	4	155	430	1.04
76	28	11697	4	196	11073	4	110	624	1.06
76	1	9986	5	313	9335	2	33	651	1.07
77	1	10664	5	147	10026	2	89	638	1.06
77	28	11741	4	93	11175	4	102	566	1.05
78	28	11483	5	142	10602	4	136	881	1.08
78	1	10117	5	144	9251	2	296	865	1.09
79	28	11532	4	75	10719	4	62	813	1.08
79	1	10606	5	126	9590	1		1017	1.11
80	28	11643	5	192	11059	4	138	585	1.05
80	1	10373	5	300	9318	1		1055	1.11
81	28	11435	5	74	10606	4	120	829	1.08
81	1	10324	5	79	9201	1		1122	1.12
82	1	8680	5	90	7870	2	41	811	1.10
82	28	9439	5	212	9155	4	131	285	1.03
83	1	9635	5	197	8778	2	77	857	1.10
83	28	10626	5	184	9299	4	953	1326	1.14
84	1	10673	5	264	9698	2	402	975	1.10
84	28	12552	5	76	11661	4	94	890	1.08
85	28	12485	5	297	11304	4	211	1181	1.10
85	1	11948	5	179	10692	2	653	1256	1.12
86	1	7625	5	270	7116	2	62	509	1.07
86	28	9753	5	216	8633	4	158	1121	1.13
87	1	8729	5	298	8198	2	396	531	1.06
87	28	9648	5	127	8887	4	163	762	1.09
88	1	9953	4	80	9326	2	240	626	1.07
88	28	11639	5	105	10738	3	52	901	1.08
89	1	10555	5	214	9733	2	107	822	1.08
89	28	11133	5	127	10100	4	366	1033	1.10
90	1	6778	5	44	6385	2	96	393	1.06
90	28	8003	5	231	7498	4	50	505	1.07
91	28	8590	5	199	7972	4	133	618	1.08
91	1	8092	5	106	7694	2	62	399	1.05
100	1	8548	4	118	8680	2	1034	-132	0.98
100	28	10610	4	344	10198	2	14	413	1.04
101	1	8625	4	59	8088	2	111	538	1.07
101	28	10297	4	562	8594	2	570	1702	1.20
102	28	8508	4	218	7886	2	210	623	1.08

n = number of replicate specimens tested
STD = sample standard deviation (n > 1)
Diff. = $f_{4x8} - f_{6x12}$
Ratio = f_{4x8} / f_{6x12}

Table 5.5. Comparison of compressive strengths of 4 x 8 in. (100 x 200 mm) and 6 x 12 in. (150 x 300 mm) cylinders, heat-cured specimens. Continued ...

No.	Age	f_{4x8} psi	n	STD psi	f_{6x12} psi	n	STD psi	Diff. psi	Ratio
102	1	6663	4	436	6098	2	68	565	1.09
103	28	8572	4	446	8438	2	50	133	1.02
103	1	7436	3	372	7030	2	3	405	1.06
104	28	11742	4	796	11078	2	365	664	1.06
104	1	11023	4	107	10299	2	62	724	1.07
105	28	11093	4	696	10365	2	23	727	1.07
105	1	10325	4	409	9442	2	719	883	1.09
106	1	9626	4	77	8721	2	311	905	1.10
106	28	10706	4	522	10047	2	455	659	1.07
107	1	8777	4	313	8071	2	62	706	1.09
107	28	9528	4	443	8832	2	216	696	1.08
108	1	8843	2	81	8387	2	41	455	1.05
108	28	11218	2	165	11270	2	216	-52	1.00
109	28	11132	4	174	10375	2	288	757	1.07
109	1	8633	4	356	7788	2	25	845	1.11
110	1	8475	4	189	7965	2	11	510	1.06
110	28	10908	4	366	9997	2	54	911	1.09
111	1	7898	4	559	7309	2	17	589	1.08
111	28	10257	4	237	9328	2	44	930	1.10
112	28	12920	2	425	11924	2	81	996	1.08
112	1	11559	2	331	10742	2	81	818	1.08
113	1	11761	4	398	10849	2	98	912	1.08
113	28	13071	4	416	12001	2	440	1069	1.09
114	1	10393	4	333	10178	2	71	215	1.02
114	28	11516	4	264	11007	2	219	509	1.05
115	28	10721	4	450	10332	2	240	389	1.04
115	1	9903	4	229	9378	2	95	524	1.06
116	1	9714	4	324	9179	2	29	535	1.06
116	28	13037	4	60	11721	2	524	1316	1.11
117	28	12785	4	404	11757	2	116	1028	1.09
117	1	9616	4	902	9397	2	249	220	1.02
118	28	10384	4	161	9489	2	149	896	1.09
118	1	7861	4	187	7316	2	197	546	1.07
119	28	9570	4	183	8726	1		844	1.10
119	1	7211	4	55	7141	2	33	70	1.01
120	28	13967	4	744	12947	2	219	1020	1.08
120	1	11851	4	142	10576	2	204	1274	1.12
121	1	11482	4	330	10523	2	51	959	1.09
121	28	13487	4	505	12639	2	45	848	1.07
122	1	11015	4	155	10104	2	14	911	1.09
122	28	12763	4	190	11634	2	101	1128	1.10
123	1	10563	4	322	9598	2	6	965	1.10
123	28	11381	4	216	11051	2	17	330	1.03
124	28	15150	4	372	14789	2	39	361	1.02
124	1	12338	4	337	10513	2	561	1826	1.17
125	1	13829	4	285	13009	2	44	819	1.06
125	28	16606	4	521	15198	2	225	1408	1.09
126	28	12455	4	212	11981	2	201	473	1.04
126	1	9219	4	208	8727	2	77	492	1.06
127	1	11817	2	115	11225	2	257	593	1.05
127	28	13878	4	293	12629	2	107	1248	1.10
128	1	11630	4	269	10880	2	69	750	1.07
128	28	12934	4	261	12291	2	18	643	1.05
129	28	14349	4	248	12833	2	236	1516	1.12
129	1	12083	4	259	11103	2	84	981	1.09

n = number of replicate specimens tested
STD = sample standard deviation (n > 1)
Diff. = $f_{4x8} - f_{6x12}$
Ratio = f_{4x8} / f_{6x12}

Table 5.5. Comparison of compressive strengths of 4 x 8 in. (100 x 200 mm) and 6 x 12 in. (150 x 300 mm) cylinders, heat-cured specimens. Continued ...

No.	Age	f_{4x8} psi	n	STD psi	f_{6x12} psi	n	STD psi	Diff. psi	Ratio
130	1	9983	4	136	9346	2	285	637	1.07
130	28	12455	4	154	11694	2	104	761	1.07
131	1	12043	4	107	10993	2	35	1049	1.10
131	28	13140	4	369	12262	2	251	877	1.07
132	28	16298	4	425	14310	2	275	1988	1.14
132	1	14779	4	390	13112	2	769	1667	1.13
133	1	14088	4	402	13206	2	435	882	1.07
133	28	16393	4	470	15362	2	678	1031	1.07
134	1	10688	4	165	9817	2	18	871	1.09
134	28	14159	4	733	12545	2	779	1615	1.13
135	1	14606	4	1108	13121	2	960	1485	1.11
135	28	16124	4	624	15086	2	129	1038	1.07
136	28	12624	4	119	11777	2	96	847	1.07
136	1	11440	4	250	10428	2	513	1012	1.10
137	1	12666	4	550	12171	2	17	495	1.04
137	28	14127	4	277	12826	2	132	1301	1.10
138	28	11729	4	282	11003	2	369	726	1.07
138	1	10289	4	260	8807	2	107	1482	1.17
139	1	11260	4	434	10638	2	144	622	1.06
139	28	12988	4	170	12112	2	158	877	1.07

n = number of replicate specimens tested
STD = sample standard deviation (n > 1)
Diff. = $f_{4x8} - f_{6x12}$
Ratio = f_{4x8} / f_{6x12}

Table 5.6. Comparison of compressive strengths of 4 x 8 in. (100 x 200 mm) and 6 x 12 in. (150 x 300 mm) cylinders, moist-cured specimens.

No.	Age	f_{4x8} psi	n	STD psi	f_{6x12} psi	n	STD psi	Diff. psi	Ratio
20	28	13949	5	131	13369	3	380	580	1.04
20	7	11570	4	164	11127	2	197	443	1.04
21	28	14047	4	281	13758	2	128	289	1.02
21	14	13229	4	237	12646	3	103	583	1.05
22	28	13448	2	348	12688	2	426	760	1.06
23	28	13178	3	306	12773	2	312	405	1.03
24	28	12034	3	437	11612	1		422	1.04
25	28	10841	2	375	11110	4	325	-269	0.98
26	28	13627	2	385	13821	3	159	-194	0.99
27	28	13023	2	436	12148	2	212	875	1.07
28	28	10280	1		9718	3	69	561	1.06
29	28	11211	3	381	11071	2	381	140	1.01
50	28	12273	2	429	11733	3	156	540	1.05
51	28	10527	2	312	10020	4	201	507	1.05
52	28	13716	2	434	12993	4	263	723	1.06
53	28	10411	2	37	9742	4	308	669	1.07
54	28	14094	2	21	13534	4	92	560	1.04
55	28	12080	2	277	12216	4	368	-136	0.99
56	28	13576	2	36	12878	3	47	698	1.05
57	28	13051	2	63	12328	4	356	722	1.06
58	28	11662	2	273	11910	4	383	-248	0.98
59	28	13142	2	78	12076	4	197	1066	1.09
60	28	11137	2	361	11366	4	70	-229	0.98
61	28	12190	2	371	11533	4	300	657	1.06
62	28	13231	2	68	12639	3	358	592	1.05
63	28	12381	2	228	11745	3	300	637	1.05
64	28	13200	2	327	12600	4	253	600	1.05
65	28	13783	2	380	13315	4	549	468	1.04
66	28	12968	2	392	12345	4	867	623	1.05
67	28	12808	2	361	12381	3	731	427	1.03
68	28	13309	2	706	12715	4	338	595	1.05
69	28	11144	2	621	11152	4	240	-8	1.00
70	28	14417	2	233	13365	4	546	1052	1.08
71	28	13211	2	297	12530	4	359	681	1.05
72	28	12359	2	294	11831	3	341	529	1.04
73	28	13338	2	354	12507	4	538	831	1.07
74	28	14053	2	141	12690	4	160	1363	1.11
75	28	12553	2	182	11187	4	374	1366	1.12
76	28	12727	2	611	11342	4	676	1385	1.12
77	28	13035	2	351	12407	4	140	628	1.05
78	28	13250	2	358	11643	3	922	1607	1.14
79	28	13613	2	122	12316	4	233	1297	1.11
80	28	13288	2	290	11825	3	484	1463	1.12
81	28	12975	2	395	11633	4	516	1342	1.12
82	28	11053	2	81	10457	3	215	597	1.06
83	28	12326	2	267	10887	2	374	1438	1.13
84	28	13152	2	71	12016	4	228	1136	1.09
85	28	14185	2	20	12772	4	112	1413	1.11
86	28	10562	2	169	9742	4	546	820	1.08
87	28	10488	2	773	9865	4	569	622	1.06
88	28	12192	2	30	11807	4	313	385	1.03
89	28	13216	2	54	11655	4	276	1561	1.13
90	28	9767	2	186	8749	4	191	1018	1.12
91	28	10523	2	365	9647	4	77	876	1.09
100	28	11158	4	572	10137	4	497	1021	1.10

n = number of replicate specimens tested
STD = sample standard deviation (n > 1)
Diff. = $f_{4x8} - f_{6x12}$
Ratio = f_{4x8} / f_{6x12}

Table 5.6. Comparison of compressive strengths of 4 x 8 in. (100 x 200 mm) and 6 x 12 in. (150 x 300 mm) cylinders, moist-cured specimens. Continued ...

No.	Age	f_{4x8} psi	n	STD psi	f_{6x12} psi	n	STD psi	Diff. psi	Ratio
101	28	11158	4	572	10137	4	497	1021	1.10
102	28	10272	4	541	9522	4	314	751	1.08
103	28	10272	4	541	9522	4	314	751	1.08
104	28	13897	4	667	12867	4	360	1030	1.08
105	28	13897	4	667	12867	4	360	1030	1.08
106	28	12141	4	658	12063	4	91	78	1.01
107	28	12141	4	658	12063	4	91	78	1.01
108	28	13185	4	1091	12646	4	284	539	1.04
109	28	12604	4	390	11831	4	300	773	1.07
110	28	11882	4	550	11452	4	77	431	1.04
111	28	11084	4	328	10051	4	377	1034	1.10
112	28	14466	4	869	13582	4	622	884	1.07
113	28	14801	4	436	13825	4	433	977	1.07
114	28	14841	4	566	13550	4	378	1291	1.10
115	28	13633	4	920	13374	4	308	259	1.02
116	28	13185	4	1091	12646	4	284	539	1.04
117	28	12604	4	390	11831	4	300	773	1.07
118	28	11882	4	550	11452	4	77	431	1.04
119	28	11084	4	328	10051	4	377	1034	1.10
120	28	14466	4	869	13582	4	622	884	1.07
121	28	14801	4	436	13825	4	433	977	1.07
122	28	14841	4	566	13550	4	378	1291	1.10
123	28	13633	4	920	13374	4	308	259	1.02
124	28	16487	2	68	14524	2	287	1962	1.14
126	28	14264	2	57	13237	2	69	1027	1.08
127	28	15553	2	199	14321	2	536	1233	1.09
128	28	15031	2	324	13045	2	287	1985	1.15
129	28	15604	2	621	13614	2	587	1989	1.15
130	28	15038	2	348	12516	2	699	2522	1.20
131	28	15912	2	30	14330	2	291	1581	1.11
132	28	16033	2	682	13945	2	671	2088	1.15
133	28	17573	2	1165	14631	2	345	2942	1.20
134	28	14899	2	1340	13936	2	1038	964	1.07
135	28	15959	2	881	13727	2	338	2233	1.16
136	28	14271	2	54	13816	2	41	456	1.03
137	28	16623	2	395	14155	2	1201	2468	1.17
138	28	14252	2	993	13162	2	257	1090	1.08
139	28	16036	2	814	13358	2	1020	2677	1.20

n = number of replicate specimens tested
STD = sample standard deviation (n > 1)
Diff. = $f_{4x8} - f_{6x12}$
Ratio = f_{4x8} / f_{6x12}

Table 5.7. Number of replicate specimens tested for each specimen size.

Compressive strength based on testing:	4 x 8 in. (100 x 200 mm)		6 x 12 in. (150 x 300 mm)	
1 specimen	1	1x1=1	7	7x1=7
2 specimens	66	66x2=132	148	148x2=296
3 specimens	7	7x3=21	16	16x3=48
4 specimens	120	120x4=480	107	107x4=428
5 specimens	84	84x5=420	0	0x5=0
Total:	278 observations	1054 cylinders	278 observations	779 cylinders

Table 5.8. Descriptive statistics of the coefficient of variation of the compressive strength test results for two sizes of specimens.

Statistics	4 x 8 in. (100 x 200 mm)		6 x 12 in. (150 x 300 mm)	
	Heat-cured	Moist-cured	Heat-cured	Moist-cured
Mean	2.838	3.144	2.115	2.960
Standard Error	0.1353	0.2174	0.1592	0.1835
Median	2.311	2.824	1.431	2.651
Standard Deviation	1.840	2.097	2.165	1.770
Minimum	0.462	0.143	0.024	0.293
Maximum	12.479	8.996	11.910	8.484
Count	179	91	179	91

Table 5.9. Comparison of compressive strengths of 4 x 8 in. (100 x 200 mm) high strength concrete specimens capped with a high strength sulfur-based capping compound versus specimens with an unbonded capping system.

No.	Cure	Age	$f_{neoprene}$ psi	n	STD psi	f_{cap} psi	n	STD psi	Diff. psi	Ratio
19	W	7	12308	4	264.94	12858	4	137.94	-550	0.96
19	W	14	14113	4	228.63	14335	4	384.08	-222	0.98
19	W	28	15806	4	123.06	15537	4	701.14	270	1.02
19	W	56	14809	4	340.34	14782	3	128.38	26	1.00
20	W	7	11491	5	198.35	11570	4	164.45	-79	0.99
20	W	14	13116	4	220.67	13353	4	153.85	-238	0.98
20	W	28	14294	4	193.73	13949	5	131.13	345	1.02
20	W	91	14829	5	368.38	13926	5	544.67	903	1.06
21	W	7	11580	4	122.13	11598	4	560.72	-18	1.00
21	W	14	13117	4	159.00	13229	4	236.67	-112	0.99
21	W	28	14401	5	214.60	14047	4	280.96	354	1.03
21	W	91	15237	5	301.45	14451	5	392.66	786	1.05
22	H	28	13778	3	207.70	13933	5	693.21	-155	0.99
23	H	28	13399	3	123.99	13110	5	302.85	289	1.02
24	H	28	11395	3	179.25	10975	5	203.21	420	1.04
25	H	28	10212	3	203.63	10035	5	171.97	177	1.02
26	H	28	13932	2	155.30	13870	5	329.26	62	1.00
27	H	28	11949	2	84.40	11493	5	378.81	456	1.04
28	H	28	9011	3	249.10	8985	4	157.41	26	1.00
29	H	28	10509	3	153.68	10313	5	196.83	196	1.02

n = number of replicate specimens tested
STD = sample standard deviation (n > 1)
Diff. = $f_{neoprene} - f_{cap}$
Ratio = $f_{neoprene} / f_{cap}$

Table 5.10. Comparison of compressive strengths of 4 x 8 in. (100 x 200 mm) high strength concrete specimens capped with a high strength sulfur-based capping compound versus specimens with ground ends.

No.	Cure	Age	f_{ground} psi	n	STD psi	f_{cap} psi	n	STD psi	Diff. psi	Ratio
4	H	7	10204	5	772.52	10121	5	369.77	83	1.01
4	H	14	10802	3	679.70	10688	4	833.59	114	1.01
4	H	28	11049	3	265.28	10533	3	775.61	516	1.05
5	H	1	8715	5	447.00	8531	5	447.19	184	1.02
5	H	3	9754	5	387.75	9410	5	500.63	343	1.04
5	H	7	10588	4	94.09	10533	3	500.06	55	1.01
5	H	28	11250	4	599.12	10552	4	839.43	698	1.07
6	H	56	11970	5	291.61	11739	5	519.92	231	1.02
7	H	14	9465	4	431.26	9077	5	475.88	387	1.04
7	H	56	10382	5	361.73	10355	5	312.32	27	1.00
9	H	14	12497	3	79.08	12698	5	317.35	-201	0.98
9	H	56	11521	5	287.47	12086	5	330.06	-564	0.95
10	H	14	13874	5	302.17	13654	5	232.60	221	1.02
10	H	56	13163	5	346.39	13374	4	78.84	-211	0.98
11	H	14	13598	5	169.11	13411	5	135.99	187	1.01
11	H	56	13882	4	68.70	13602	5	516.53	280	1.02
12	H	14	12753	5	210.63	12334	4	462.30	419	1.03
12	H	56	12629	4	548.15	12315	5	396.17	314	1.03
13	H	14	14616	4	89.36	14266	5	354.68	351	1.02
13	H	56	15043	4	266.65	14785	4	305.34	258	1.02
14	H	14	14671	5	547.49	14460	5	177.66	210	1.01
14	H	56	14807	4	358.27	14634	4	973.85	173	1.01

n = number of replicate specimens tested
STD = sample standard deviation (n > 1)
Diff. = $f_{ground} - f_{cap}$
Ratio = f_{ground} / f_{cap}

Table 5.11. Descriptive statistics of the coefficient of variation of the compressive strength test results for the three end conditions.

Statistics	Case 1		Case 2	
	Sulfur cap	Neoprene pad	Sulfur cap	Ground ends
Mean	2.404	1.594	3.932	3.012
Standard Error	0.286	0.125	0.463	0.411
Median	1.954	1.540	3.70	2.466
Standard Deviation	1.278	0.560	2.172	1.929
Minimum	0.868	0.706	0.590	0.495
Maximum	4.975	2.764	7.955	7.570
Count	20	20	22	22

Table 5.12. Comparison of compressive strengths of 6 x 12 in. (150 x 300 mm) high strength concrete specimens cast in single-use plastic molds to those of companion specimens cast in heavy-gauge steel molds.

No.	Age	$f_{plastic}$ psi	n	STD psi	f_{steel} psi	n	STD psi	Diff. psi	Ratio
4	1	6304	2	603	6489	2	516	-185	0.97
4	3	8729	4	601	8783	3	371	-53	0.99
4	7	10032	2	230	9989	2	81	44	1.00
4	28	9820	3	934	10190	2	15	-371	0.96
5	1	8041	3	344	8149	3	372	-109	0.99
5	3	8414	3	85	8721	3	373	-307	0.96
5	7	9555	2	779	9917	2	512	-363	0.96
5	28	9891	4	1087	10435	2	308	-544	0.95

n = number of replicate specimens tested
STD = sample standard deviation (n > 1)
Diff. = $f_{plastic} - f_{steel}$
Ratio = $f_{plastic} / f_{steel}$

Table 5.13. Chemical and physical properties of the high-range water reducers (HRWR) used in this study based on the manufacturer's laboratory reports.

High-range water reducer	Properties
HRWR #1	ASTM C 494 Type A and F; HRWR Aqueous solution of a modified naphthalene sulfonate. % Solids: 40% Specific Gravity: 1.20 Manufacturer's Recommended Dosage: 6-20 oz/cwt (4-13 ml/kg)
HRWR #2	ASTM C 494 Type A and F; HRWR Melamine formaldehyde-based water soluble polymer. % Solids: 33% Specific Gravity: 1.20 Manufacturer's Recommended Dosage: 6-30 oz/cwt (4-20 ml/kg)
HRWR #3	ASTM C 494 Type F; HRWR Water-soluble sulphonated naphthalene condensate. % Solids: 42% Specific Gravity: 1.20 Manufacturer's Recommended Dosage: 6-18 oz/cwt (4-12 ml/kg)
HRWR #4	ASTM C 494 Type D and G; HRWR Based on sodium salts of an unsaturated carboxylic acid and the hydroxyalkyl ester of such acids. % Solids: 22% Specific Gravity: 1.11 Manufacturer's Recommended Dosage: 6-18 oz/cwt (4-12 ml/kg)
HRWR #5	ASTM C 494 Type A and F; HRWR Combination of a water-soluble anionic melamine polycondensate and a naphthalene condensate. % Solids: 39% Specific Gravity: 1.23 Manufacturer's Recommended Dosage: 6-25 oz/cwt (4-16 ml/kg)

Table 5.14. Compressive strength of high strength concrete mixes made with five different high-range water reducers. Also shown are compressive strength values expressed as a percentage of compressive strength of high strength concrete mixes made with high-range water reducer No. 1 at equal ages.

Mix ID Code	No.	Cure	Compressive strength psi			Compressive strength % HRWR No. 1		
			1-Day	14-Day	28-Day	1-Day	14-Day	28-Day
131-XAL1-F00M00-130	30	H	10024	12775	13250	100	100	100
131-XAL1-F00M00-230	31	H	9233	11644	11955	92	91	90
131-XAL1-F00M00-330	44	H	8129	12126	12957	81	95	98
131-XAL1-F00M00-430	45	H	6815	10258	10703	68	80	81
131-XAL1-F00M00-530	46	H	7372	11244	11900	74	88	90
131-XAL1-F00M75-130	32	H	10098	12354	12699	100	100	100
131-XAL1-F00M75-230	33	H	9635	11262	11516	95	91	91
131-XAL1-F00M75-330	47	H	10476	11852	12694	104	96	100
131-XAL1-F00M75-430	48	H	8061	10337	11087	80	84	87
131-XAL1-F00M75-530	49	H	9529	11795	11876	94	95	94
131-XAR2-F00M00-130	34	H	10095	12490	13208	100	100	100
131-XAR2-F00M00-230	35	H	9085	11290	11698	90	90	89
131-XAR2-F00M00-330	38	H	8720	10982	10834	86	88	82
131-XAR2-F00M00-430	39	H	8535	9604	10117	85	77	77
131-XAR2-F00M00-530	40	H	7310	8817	9759	72	71	74
131-XAR2-F00M75-130	36	H	9880	11852	12209	100	100	100
131-XAR2-F00M75-230	37	H	10065	11531	11532	102	97	94
131-XAR2-F00M75-330	41	H	10424	11345	11590	105	96	95
131-XAR2-F00M75-430	42	H	7059	8806	8967	71	74	73
131-XAR2-F00M75-530	43	H	7530	9328	9858	76	79	81
131-XAL1-F00M00-130	30	W	7649	12409	13347	100	100	100
131-XAL1-F00M00-230	31	W	7405	11555	12107	97	93	91
131-XAL1-F00M00-330	44	W	7370	10893	11834	96	88	89
131-XAL1-F00M00-430	45	W	6070	8779	10374	79	71	78
131-XAL1-F00M00-530	46	W	5449	9785	11426	71	79	86
131-XAL1-F00M75-130	32	W	6928	12007	13232	100	100	100
131-XAL1-F00M75-230	33	W	6997	11521	13022	101	96	98
131-XAL1-F00M75-330	47	W	6982	11542	13382	101	96	101
131-XAL1-F00M75-430	48	W	5196	8986	11262	75	75	85
131-XAL1-F00M75-530	49	W	5957	10679	12656	86	89	96
131-XAR2-F00M00-130	34	W	6373	12746	12448	100	100	100
131-XAR2-F00M00-230	35	W	6159	10885	11634	97	85	93
131-XAR2-F00M00-330	38	W	6782	10953	12734	106	86	102
131-XAR2-F00M00-430	39	W	6059	8616	10958	95	68	88
131-XAR2-F00M00-530	40	W	2492	10044	11092	39	79	89
131-XAR2-F00M75-130	36	W	7267	12600	13194	100	100	100
131-XAR2-F00M75-230	37	W	6911	11953	12903	95	95	98
131-XAR2-F00M75-330	41	W	6243	11690	13100	86	93	99
131-XAR2-F00M75-430	42	W	4794	7958	10380	66	63	79
131-XAR2-F00M75-530	43	W	4316	9926	11512	59	79	87

Table 5.15. Compressive strength of 4 x 8 in. (100 x 200 mm) specimens from high strength concrete mixes made with five different types of coarse aggregates.

Mix ID Code	No.	Compressive strength, psi Heat-cured				Compressive strength, psi Moist-cured		
		1-Day	28-Day	182-Day	365-Day	28-Day	182-Day	365-Day
131-XAR1-F00M00-130	108	8843	11218	11415	11373	13185	14489	14840
131-XAR1-F20M00-130	110	8475	10908	11300	10826	11882	14341	14998
131-XAR1-F00M75-130	112	11559	12920	13104	12347	14466	15293	15339
131-XAR1-F20M75-130	114	10393	11516	11312	10998	14841	15077	14942
131-XAL1-F00M00-130	124	12338	15150	15134	14964	16487	16809	16702
131-XAL1-F20M00-130	125	13829	16606	16508	16871	17117	17272	17215
131-XAL1-F00M75-130	126	9219	12455	12488	12342	14264	15114	15618
131-XAL1-F20M75-130	127	11817	13878	13679	13542	15553	16057	16107
131-XAR2-F00M00-130	128	11630	12934	12746	12721	15031	15902	15849
131-XAR2-F20M00-130	129	12083	14349	14259	14295	15604	16504	16243
131-XAR2-F00M75-130	130	9983	12455	12464	12307	15038	15988	16072
131-XAR2-F20M75-130	131	12043	13140	13057	12973	15912	16558	17275
131-XAL2-F00M00-130	132	14779	16298	15649	15731	16033	16279	16888
131-XAL2-F20M00-130	133	14088	16393	16470	16722	17573	17638	18421
131-XAL2-F00M75-130	134	10688	14159	14680	14405	14899	16695	17148
131-XAL2-F20M75-130	135	14606	16124	16279	16268	15959	17404	17494
131-XAG2-F00M00-130	136	11440	12624	12582	12621	14271	14998	14947
131-XAG2-F20M00-130	137	12666	14127	13718	13687	16623	17205	16664
131-XAG2-F00M75-130	138	10289	11729	11703	11781	14252	15415	15594
131-XAG2-F20M75-130	139	11260	12988	12882	13027	16036	15783	16066

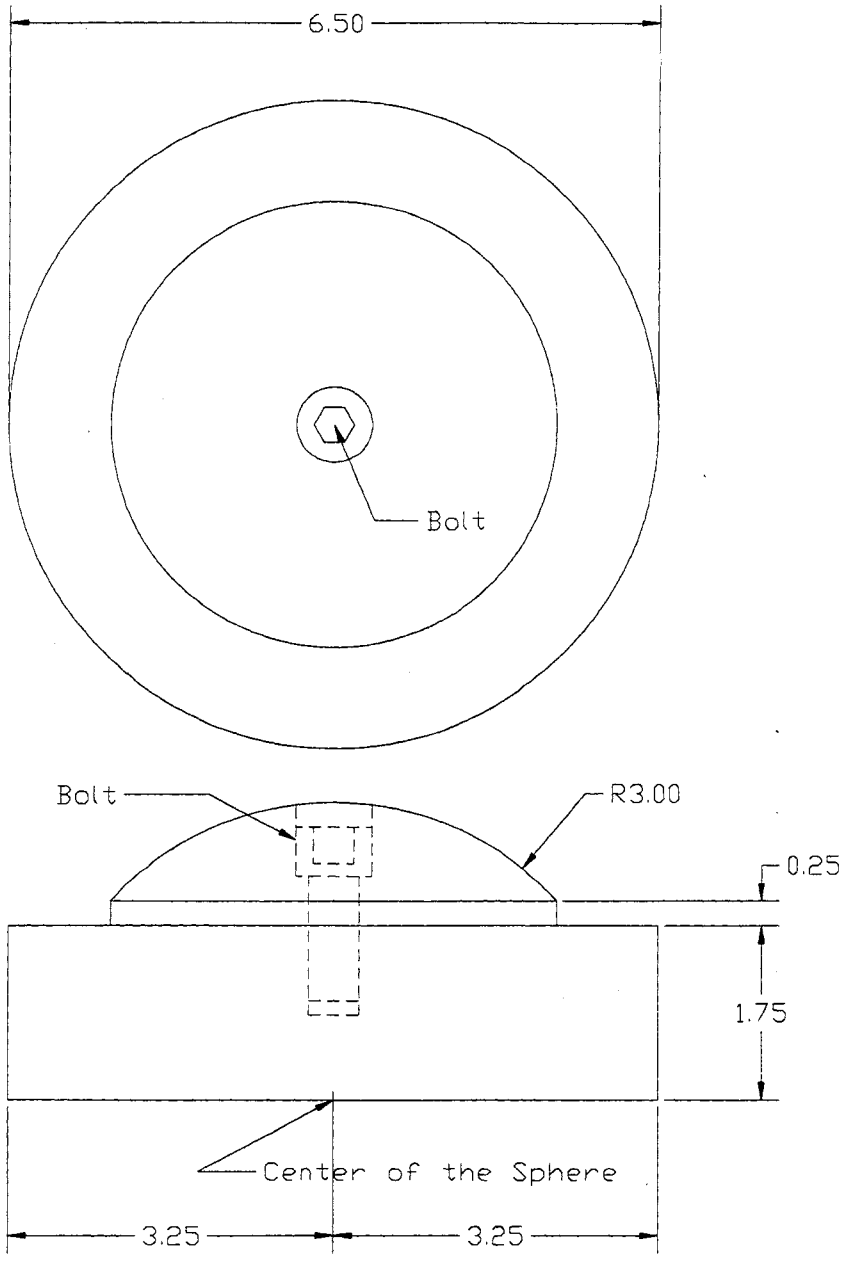

Figure 5.1. Schematic sketch of the testing machine spherical bearing block. [PLATTEN.PLT]

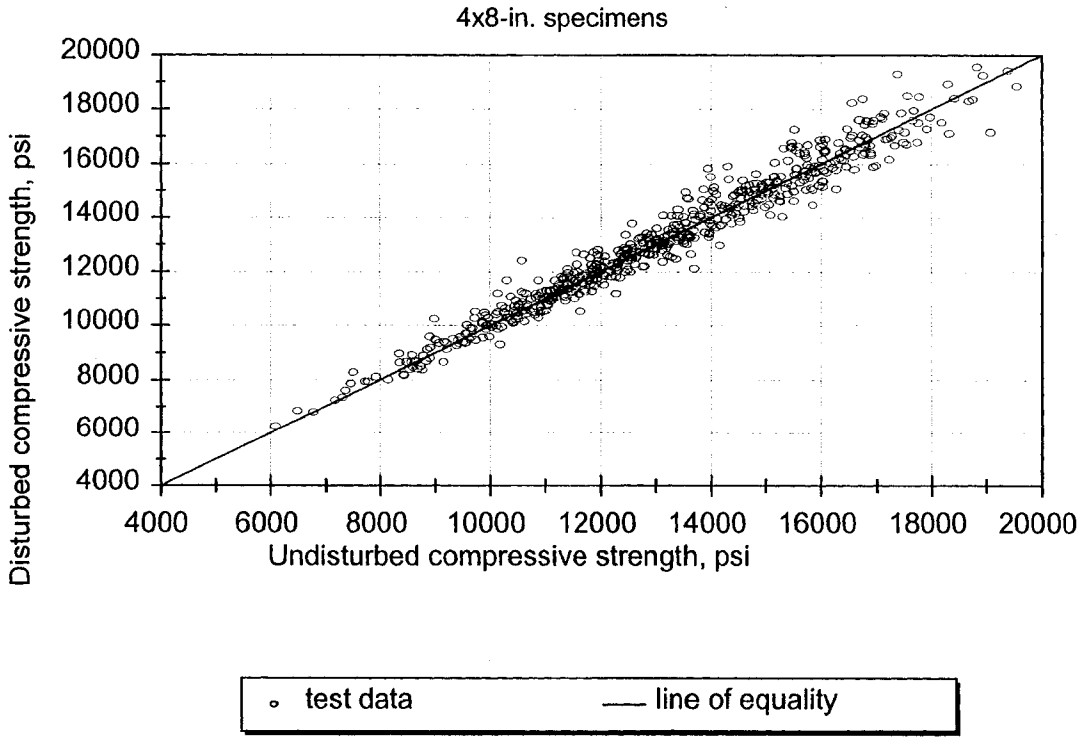

Figure 5.2. Comparison of the compressive strengths of disturbed and undisturbed 4 x 8 in. (100 x 200 mm) high strength concrete cylinders for all curing conditions.
[4D_VS_U.WMF]

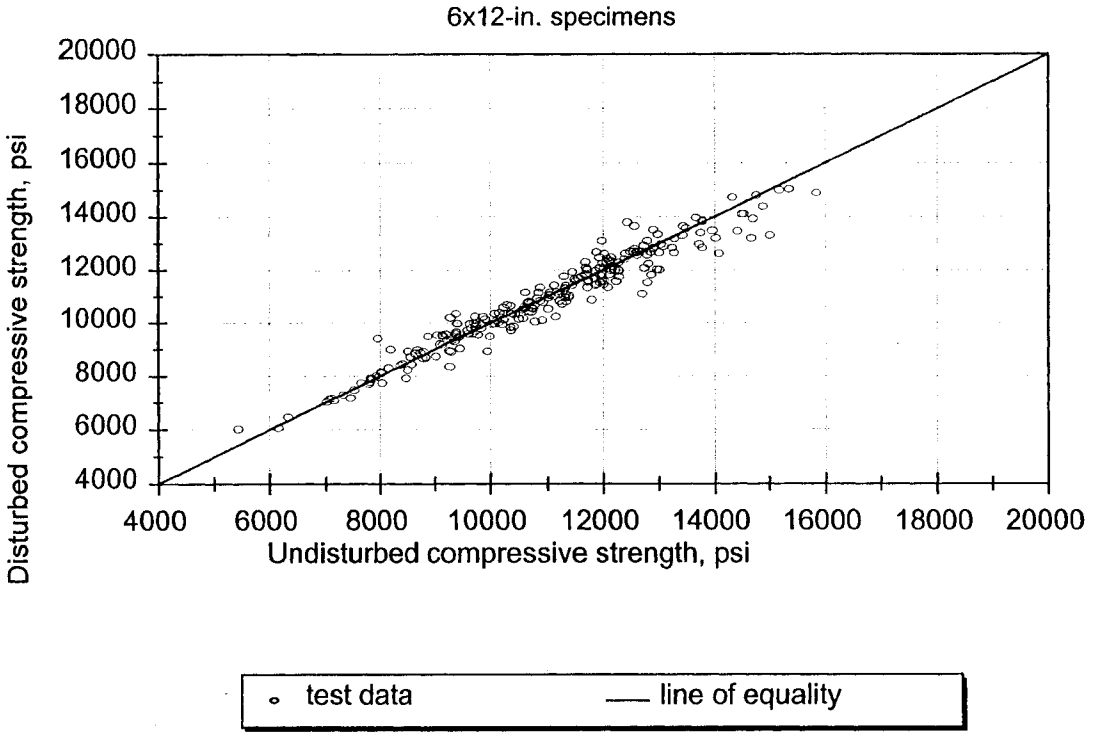

Figure 5.3. Comparison of the compressive strengths of disturbed and undisturbed 6 x 12 in. (150 x 300 mm) high strength concrete cylinders for all curing conditions.
[6D_VS_U.WMF]

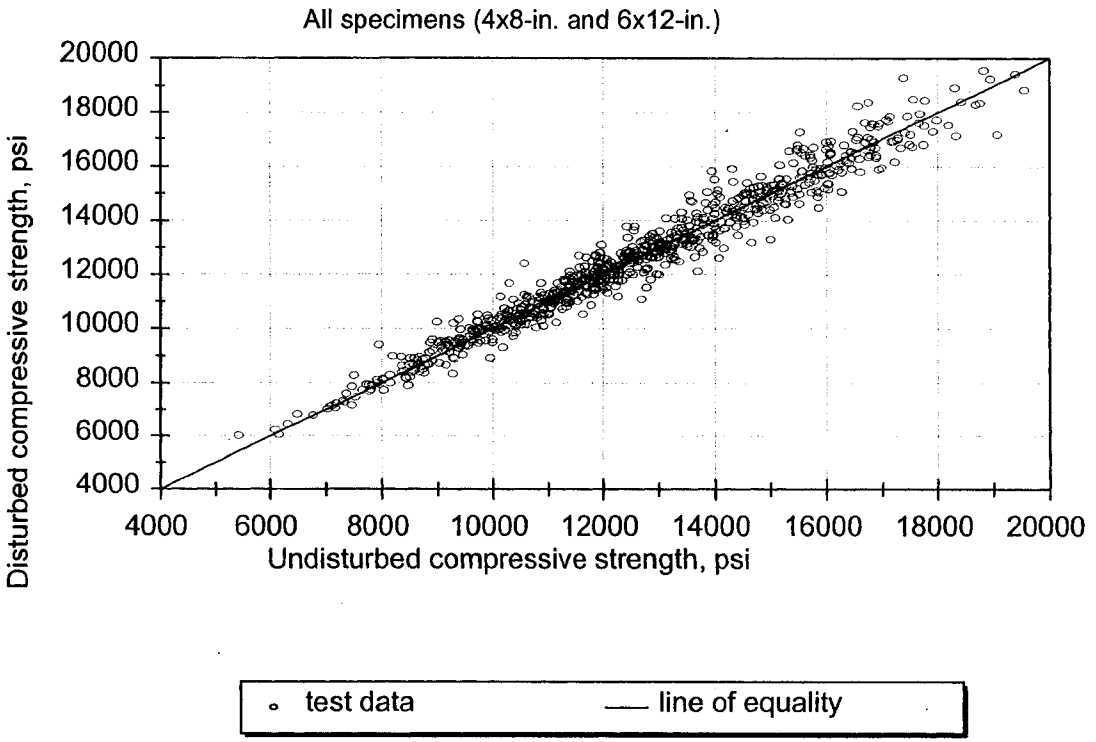

Figure 5.4. Comparison of the compressive strengths of disturbed and undisturbed 4 x 8 in. (100 x 200 mm) and 6 x 12 in. (150 x 300 mm) concrete cylinders for all curing conditions.
[D_VS_U.WMF]

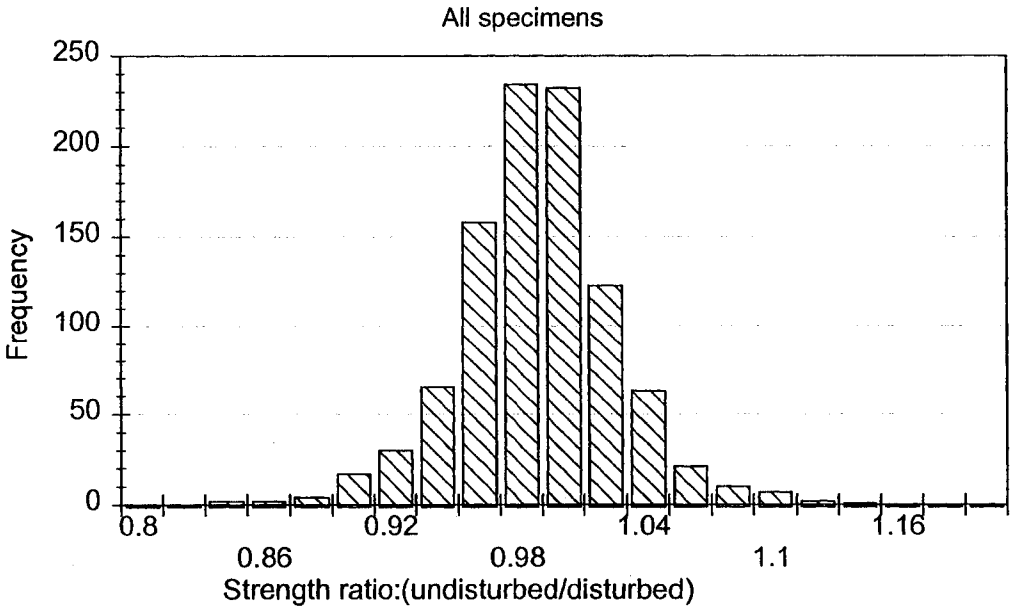

Figure 5.5. Histogram of the $f_{undisturbed}/f_{disturbed}$ ratios for all specimens.
[DVSUHIST.WMF]

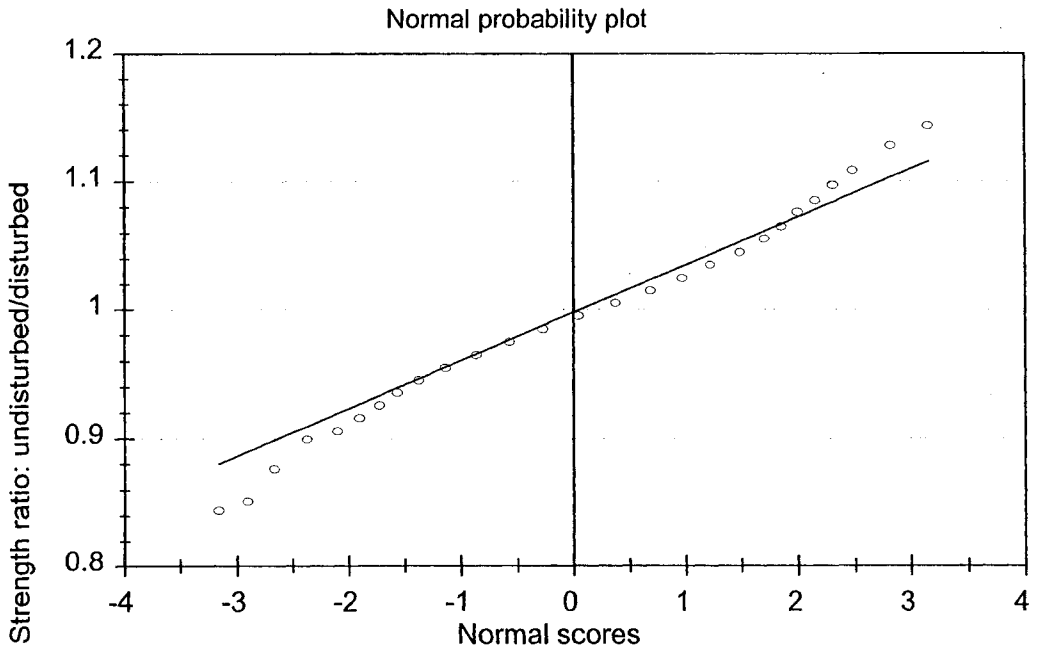

Figure 5.6. Normal probability plot of the $f_{undisturbed}/f_{disturbed}$ ratios for all specimens. The best fit line equation is: *(Strength ratio) = 0.998 + 0.0373(Normal score);* $R^2 = 0.98$.
[DVU_NORM.WMF]

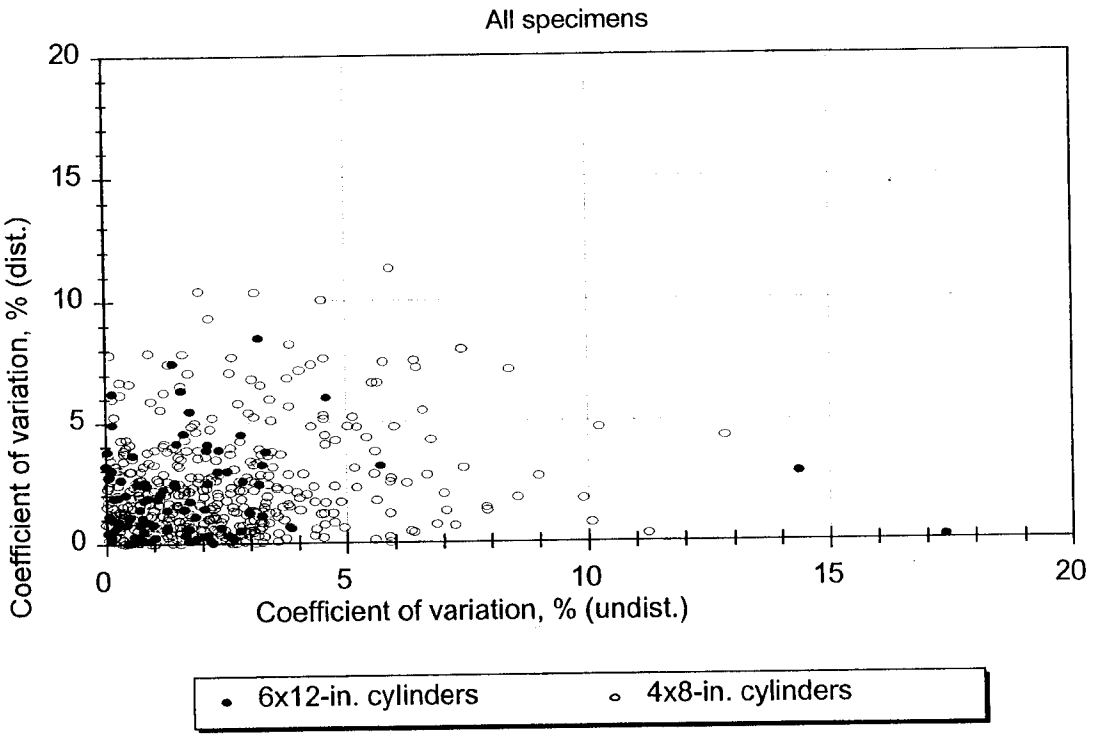

Figure 5.7. Comparison of the coefficient of variation of the compressive strengths of undisturbed and disturbed specimens for both 6 x 12 in. (150 x 300 mm) and 4 x 8 in. (100 x 200 mm) cylinders.
[ALLCOV.WMF]

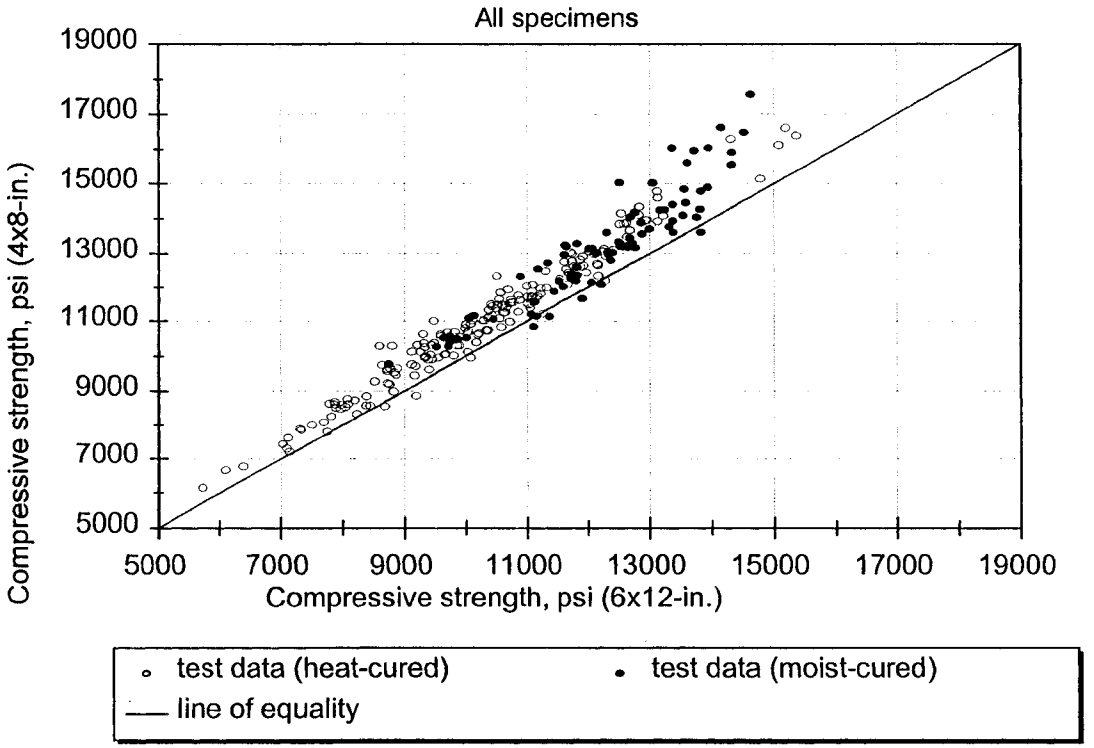

Figure 5.8. Comparison of the compressive strength of 4 x 8 in. (100 x 200 mm) and 6 x 12 in. (150 x 300 mm) high strength concrete cylinders for all data.
[ALL4VS6.WMF]

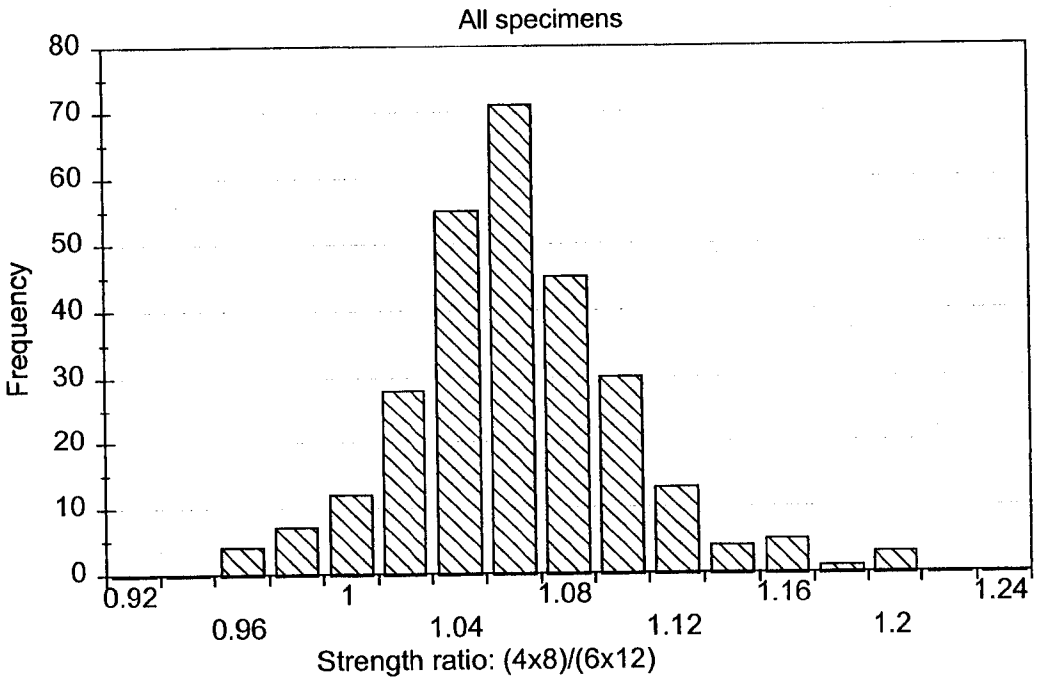

Figure 5.9. Histogram of the f_{4x8}/f_{6x12} ($f_{100x200}/f_{150x300}$) strength ratios.
[ALLHISTO.WMF]

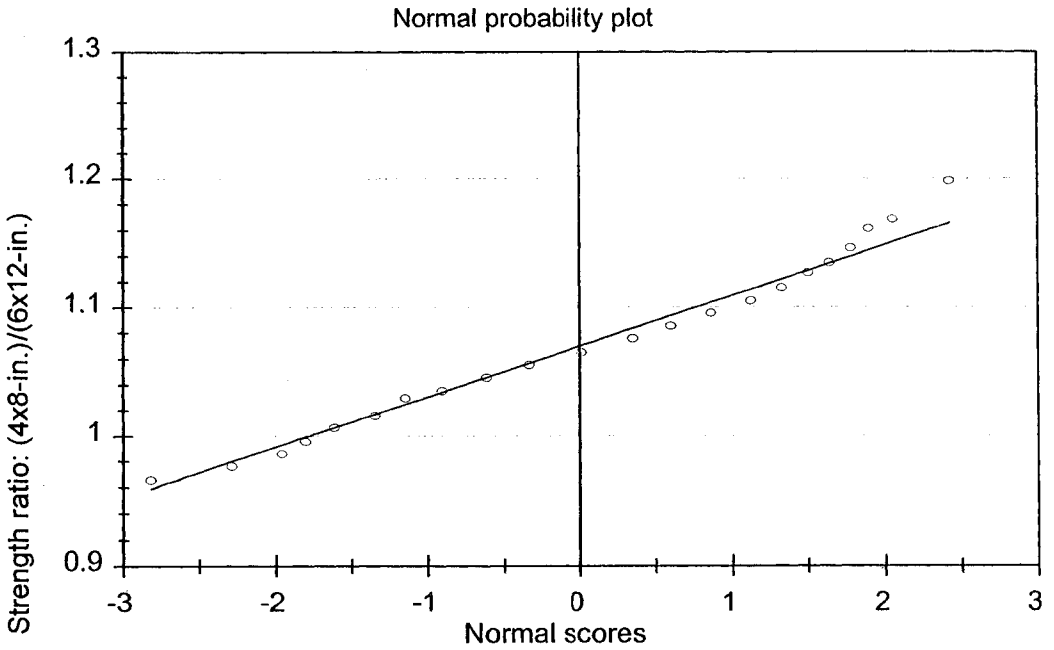

Figure 5.10. Normal probability plot of the f_{4x8}/f_{6x12} ratios for all specimens. The best fit line equation is: *(Strength ratio) = 1.070 + 0.0394(Normal score);* $R^2 = 0.98$.
[SIZENORM.WMF]

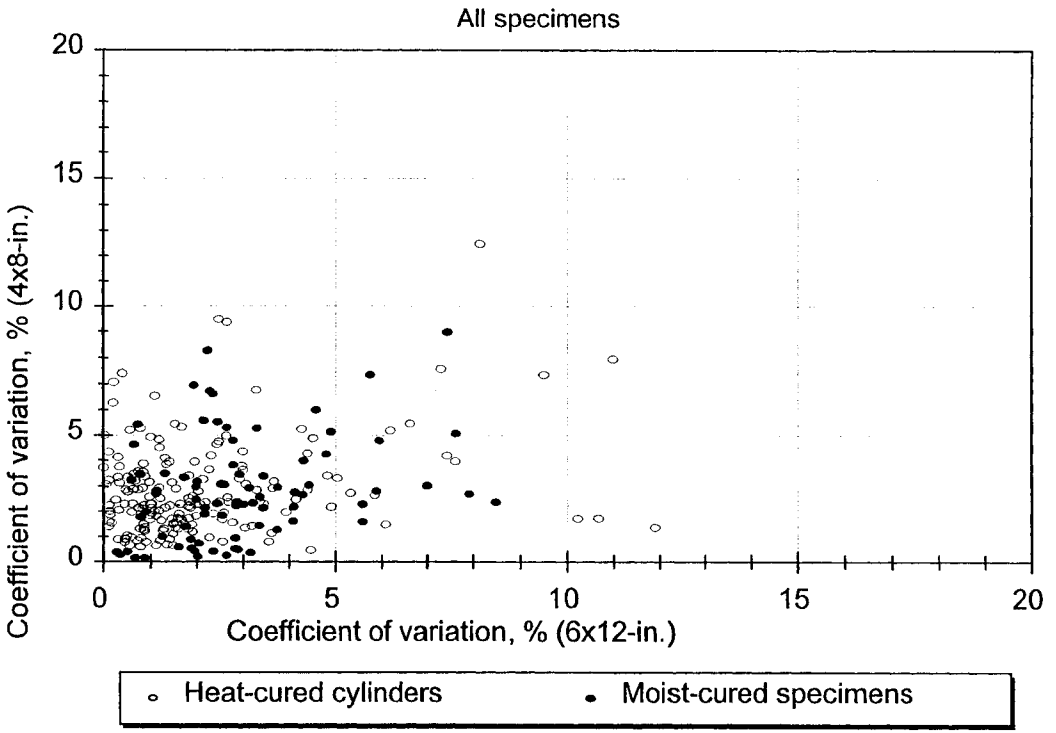

Figure 5.11. Comparison of the coefficient of variation of the compressive strength using 4 x 8 in. (100 x 200 mm) and 6 x 12 in. (150 x 300 mm) specimens.
[ALLCOV46.WMF]

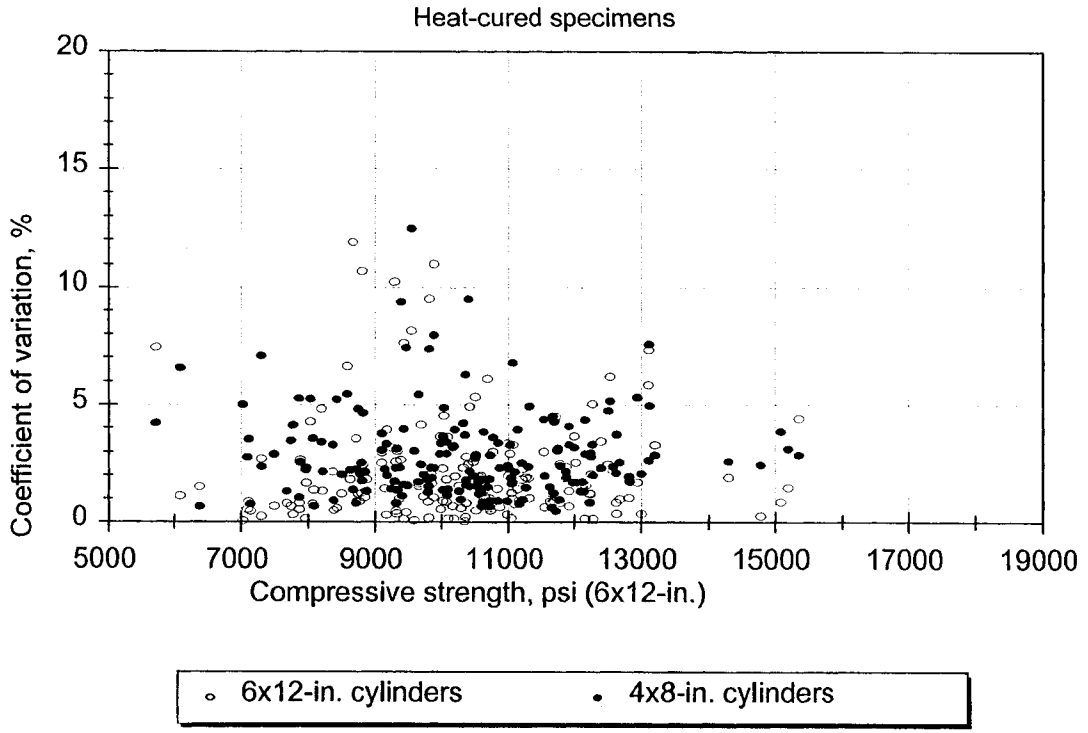

Figure 5.12. Coefficient of variation of the heat-cured specimens as a function of the strength level. [HCOV.WMF]

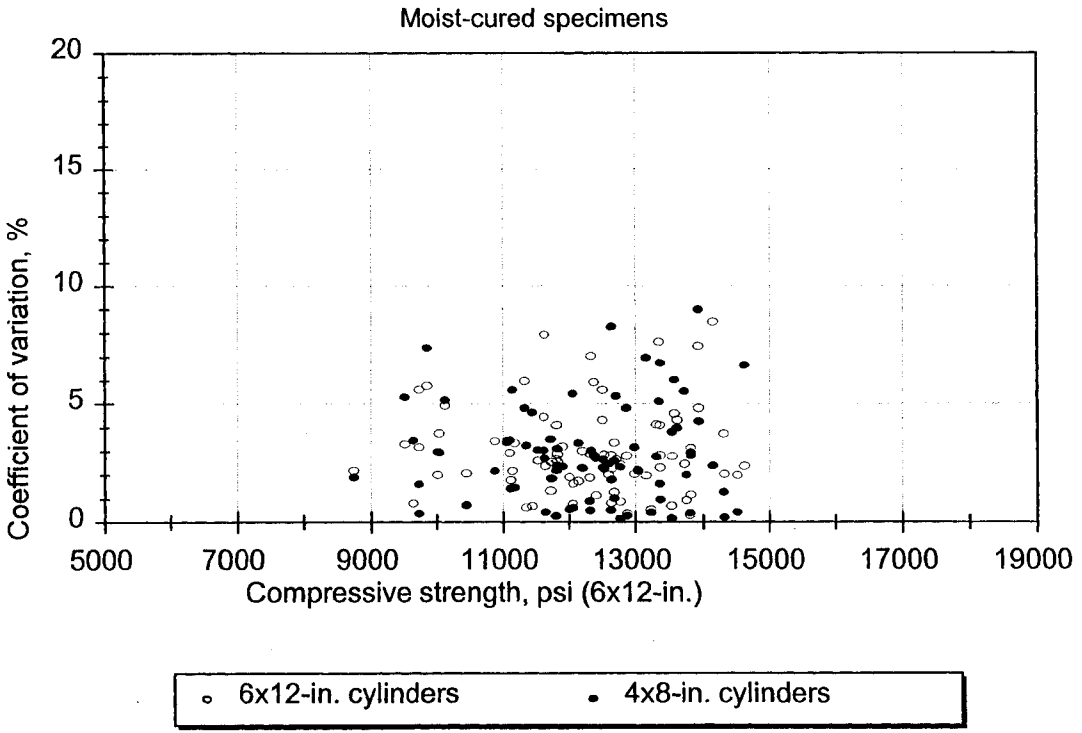

Figure 5.13. Coefficient of variation of the moist-cured specimens as a function of the strength level. [WCOV.WMF]

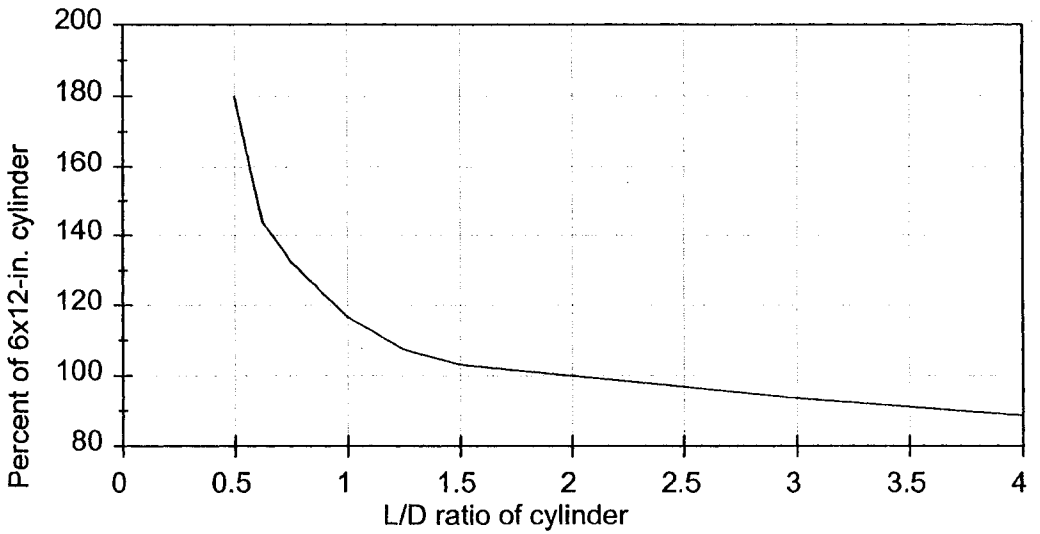

Figure 5.14. Effect of varying the length/diameter ratio on concrete strength (*Concrete Manual*, U.S. Bureau of Reclamation, 1975, pp. 574-75). Strength of a 4 x 11 in. (100 x 280 mm) cylinder is approximately 97% that of a standard 6 x 12 in. (150 x 300 mm) cylinder.
[LD_PRICE.WMF]

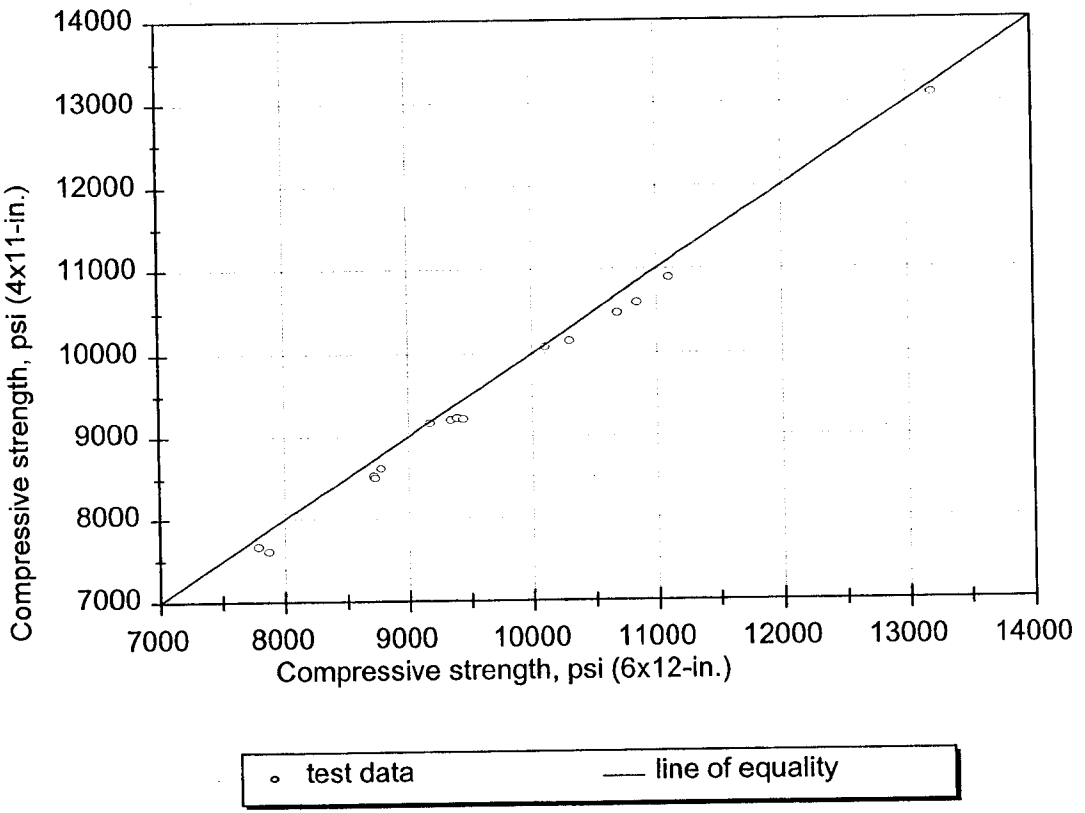

Figure 5.15. Comparison of the compressive strength of 4 x 11 in. (100 x 280 mm) and 6 x 12 in. (150 x 300 mm) high strength concrete cylinders.
[LD_RATIO.WMF]

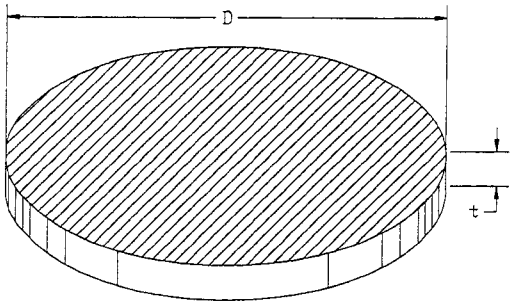

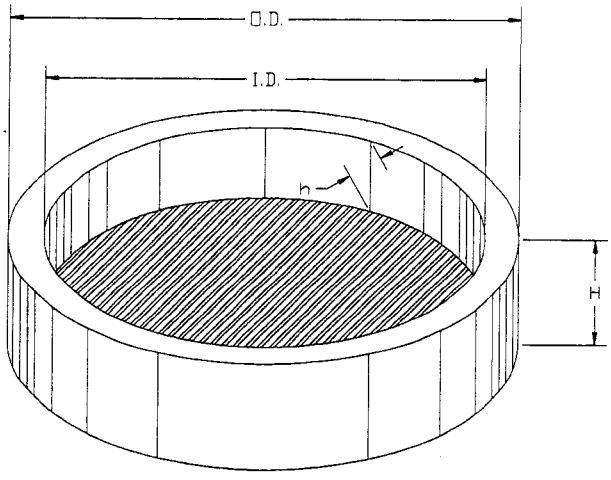

D	4.19 in.	(106.4 mm)
t	0.50 in.	(12.7 mm)
O.D.	5.00 in.	(127.0 mm)
I.D.	4.19 in.	(106.4 mm)
H	1.50 in.	(38.1 mm)
h	1.00 in.	(25.4 mm)
Pad Durometer Hardness	70	

Figure 5.16. Dimensions of the unbonded capping system used. [CAPDIM.PLT]

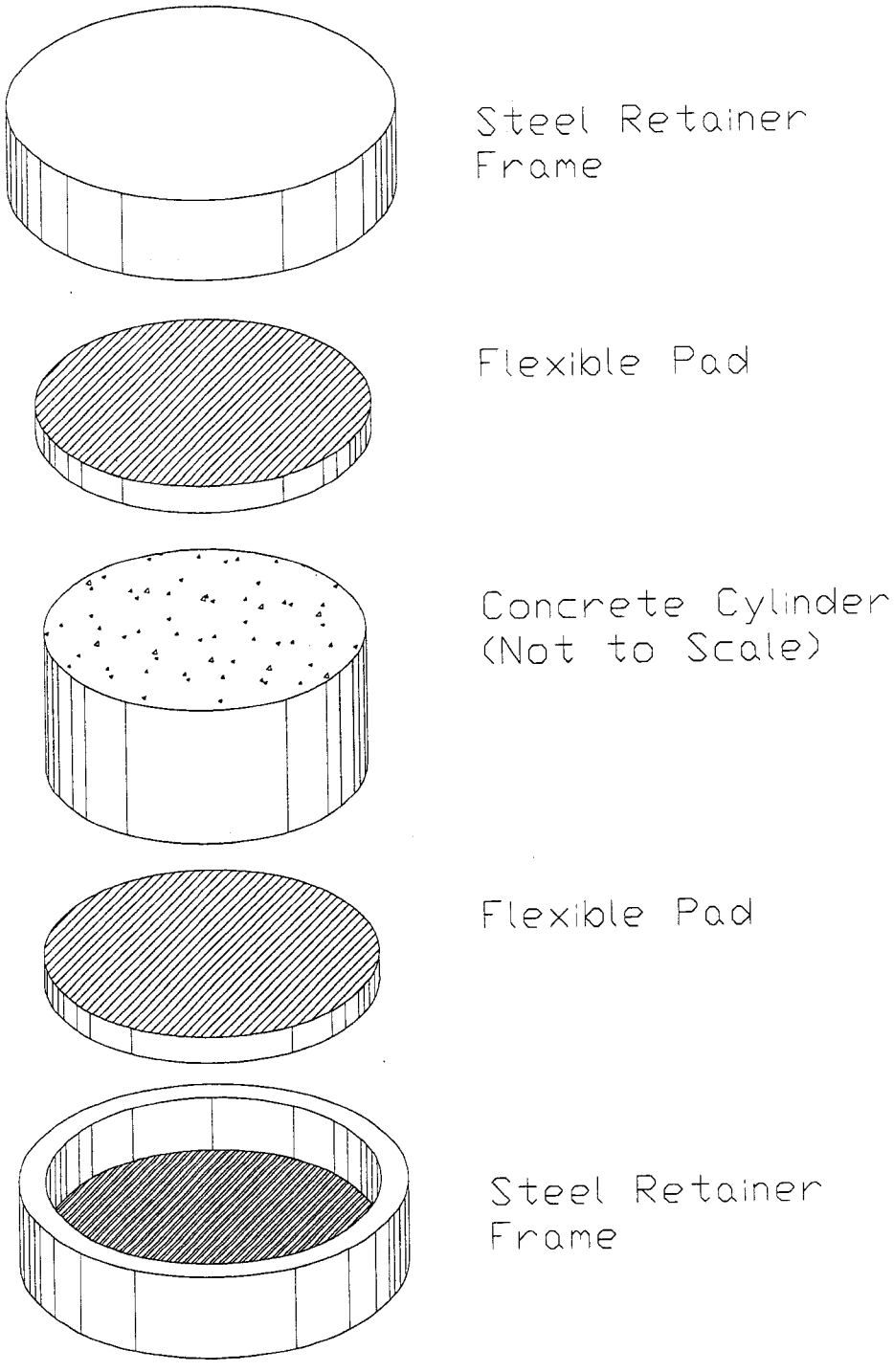

Figure 5.17. Unbonded capping system.
[2CAP.PLT]

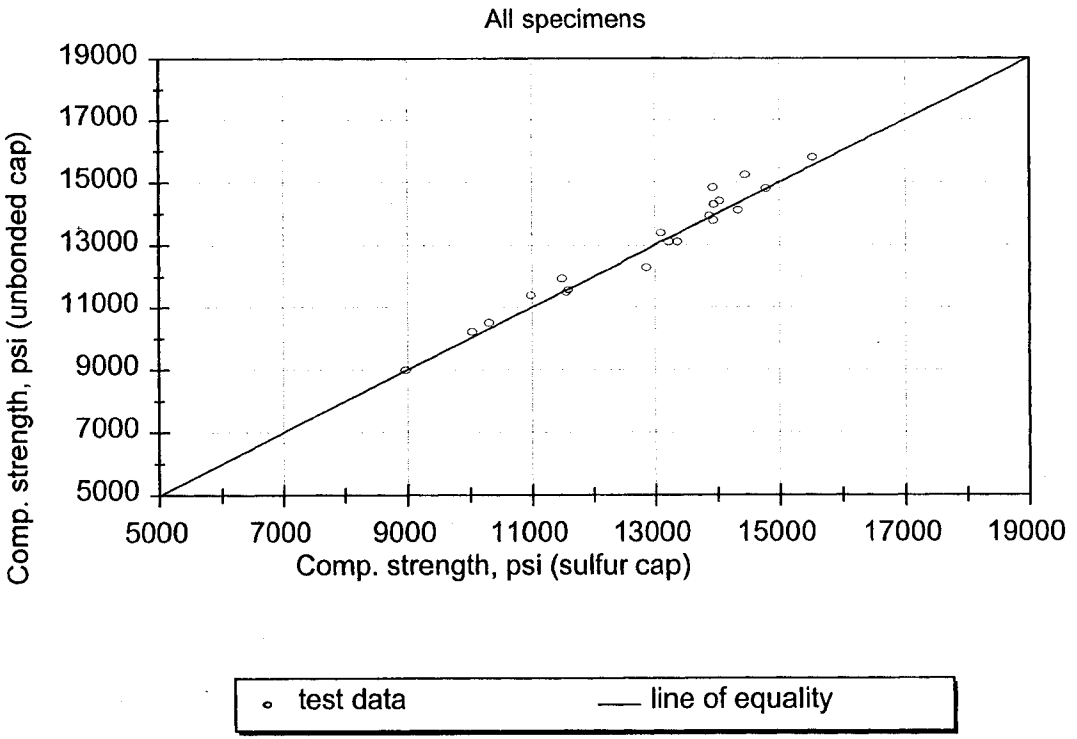

Figure 5.18. Comparison of the compressive strengths of 4 x 8 in. (100 x 200 mm) high strength concrete specimens tested with an unbonded capping system to those of companion specimens tested with a high strength sulfur-based capping compound.
[NEOP.WMF]

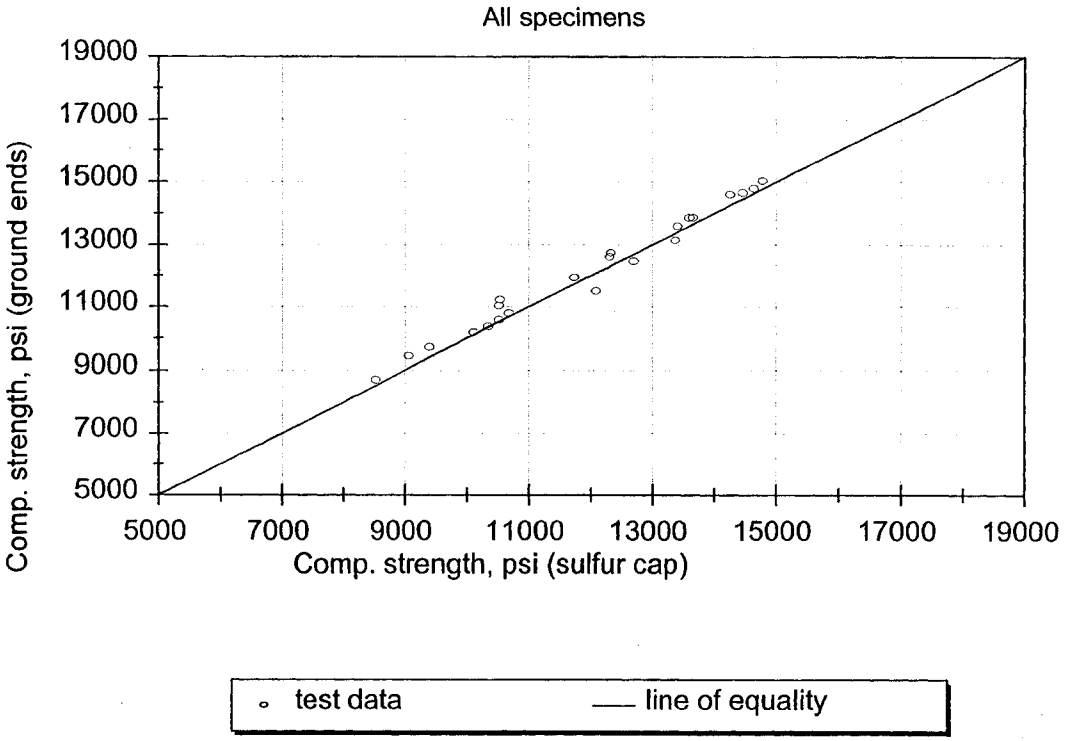

Figure 5.19. Comparison of the compressive strengths of 4 x 8 in. (100 x 200 mm) high strength concrete specimens tested with ground ends to those of companion specimens tested with a high strength sulfur-based capping compound. [GRND.WMF]

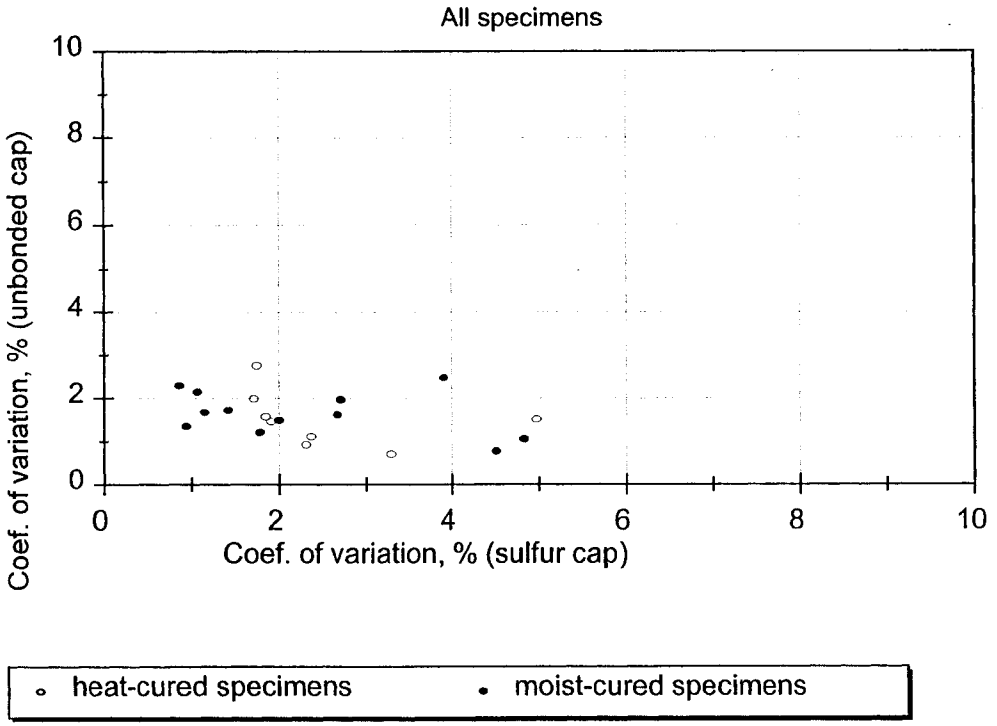

Figure 5.20. Comparison of the coefficient of variation of the compressive strengths of specimens tested using unbonded capping system to that of those tested using a high strength sulfur-based capping compound.
[NEOPCOV.WMF]

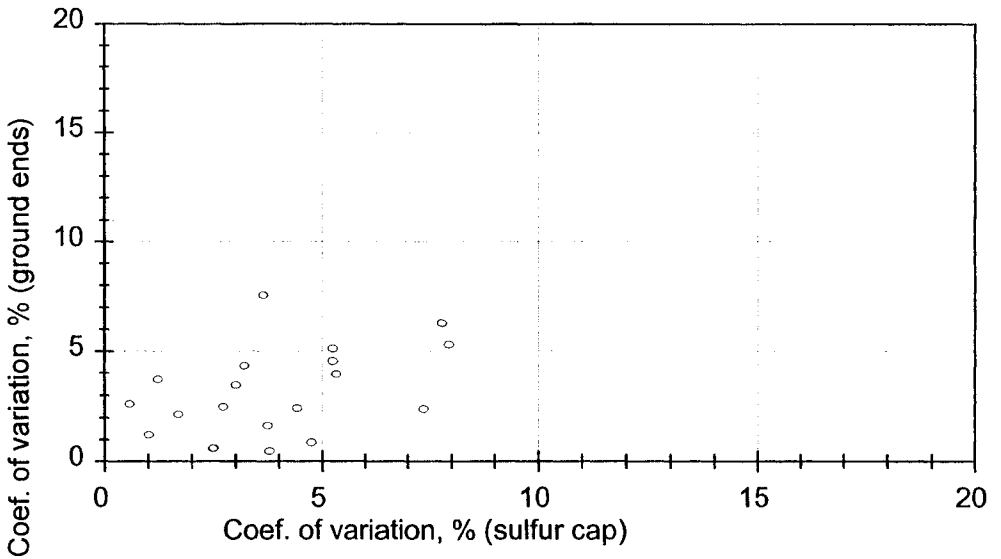

Figure 5.21. Comparison of the coefficient of variation of the compressive strengths of specimens tested with both ends ground to that of those tested using a high strength sulfur-based capping compound.
[GRNDCOV.WMF]

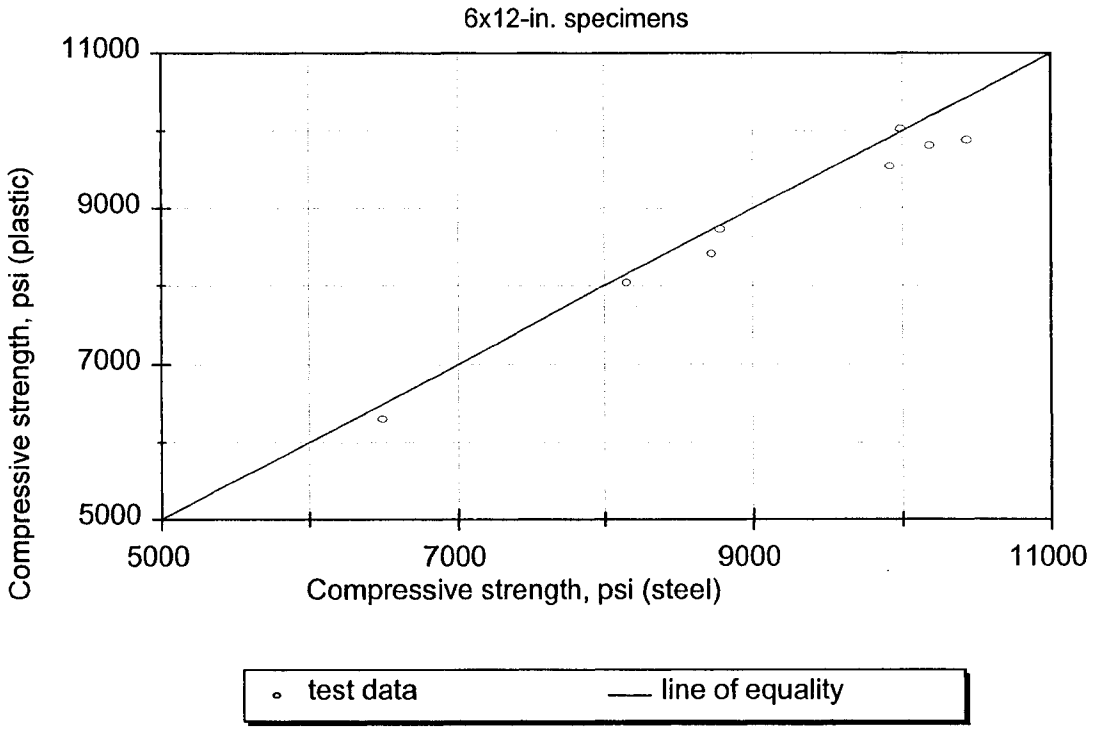

Figure 5.22. Comparison of the compressive strengths of high strength concrete specimens cast in single-use plastic molds to those of companion specimens cast in heavy-gauge reusable steel molds. The best fit line equation for these data is: $f_{plastic} = 0.97 f_{steel}$; $R^2 = 0.98$.
[MOLD.WMF]

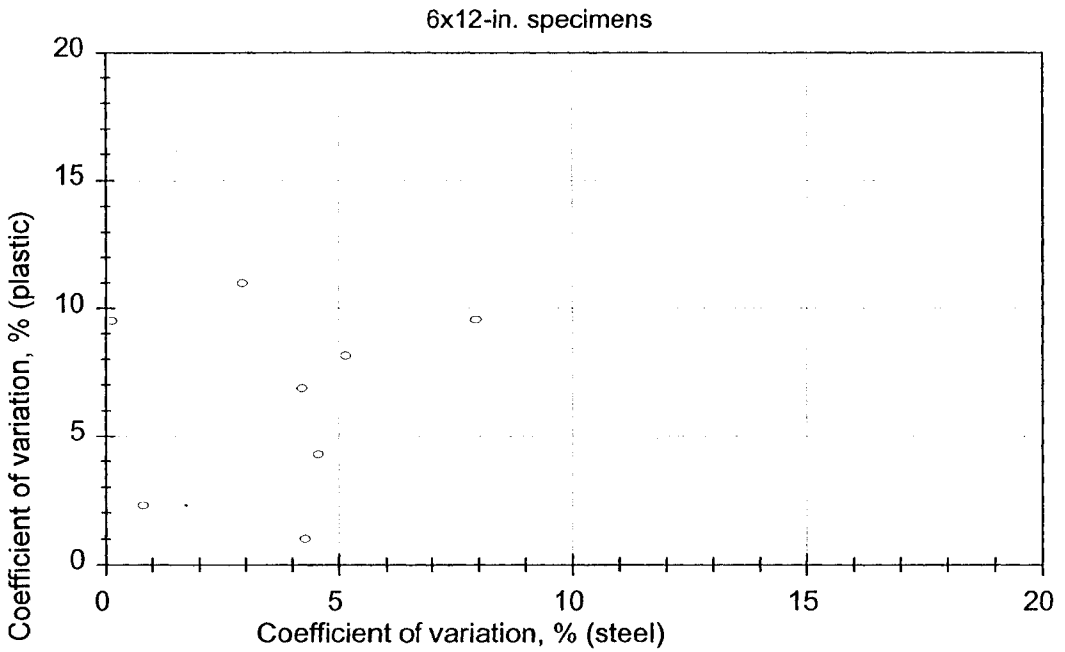

Figure 5.23. Comparison of the coefficient of variation of the compressive strength values of high strength concrete specimens cast in single-use plastic molds versus those of companion specimens cast in heavy-gauge reusable steel molds. [MOLDCOV.WMF]

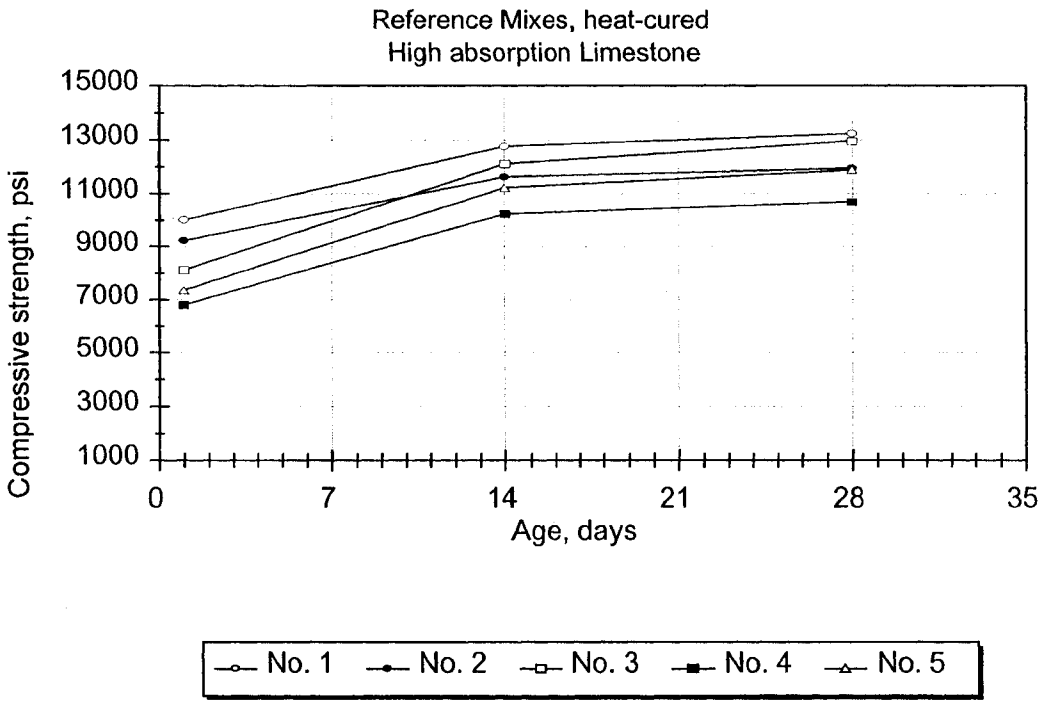

Figure 5.24. Compressive strength development in heat-cured specimens from reference mixes made with five different high-range water reducers and high absorption limestone.
[HREF_L1.WMF]

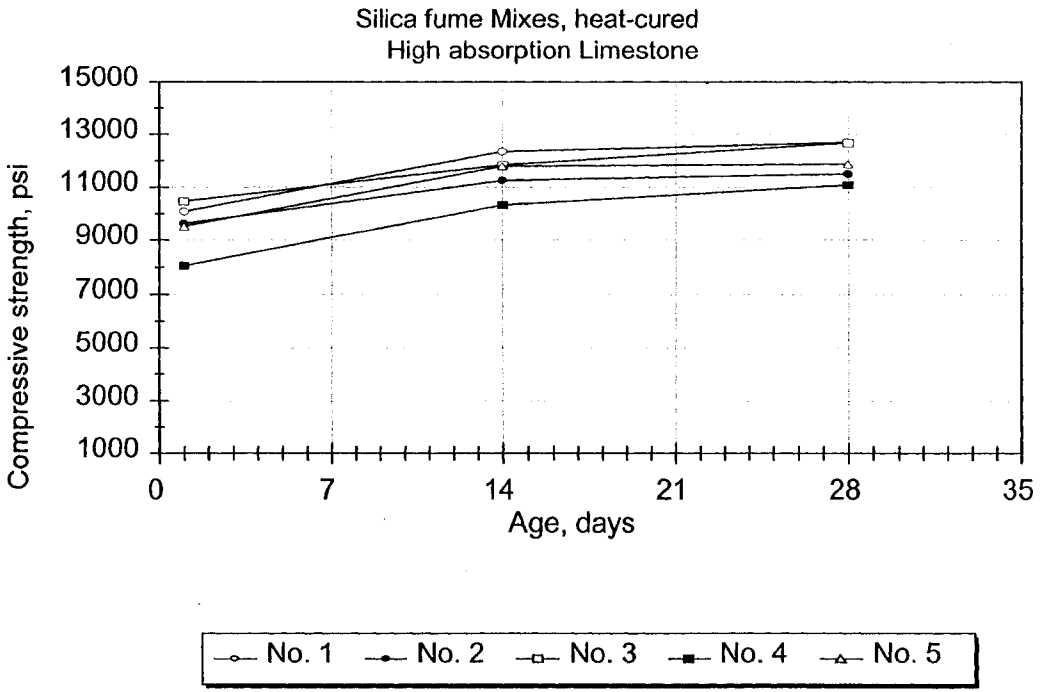

Figure 5.25. Compressive strength development in heat-cured specimens from silica fume mixes made with five different high-range water reducers and high absorption limestone.
[HS_L1.WMF]

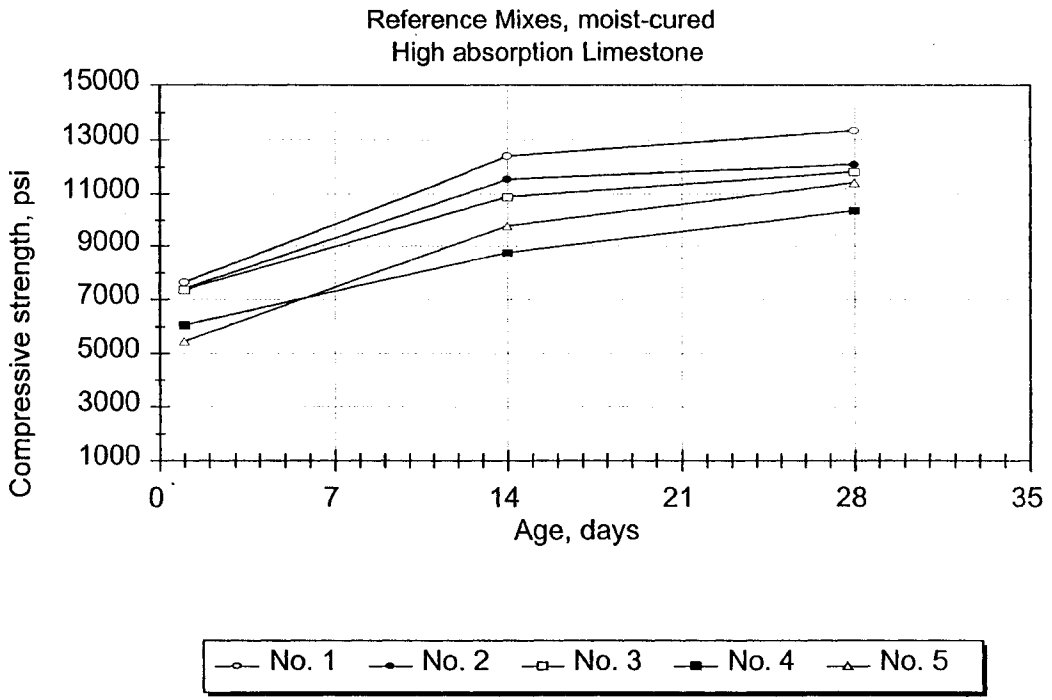

Figure 5.26. Compressive strength development in moist-cured specimens from reference mixes made with five different high-range water reducers and high absorption limestone.
[WREF_L1.WMF]

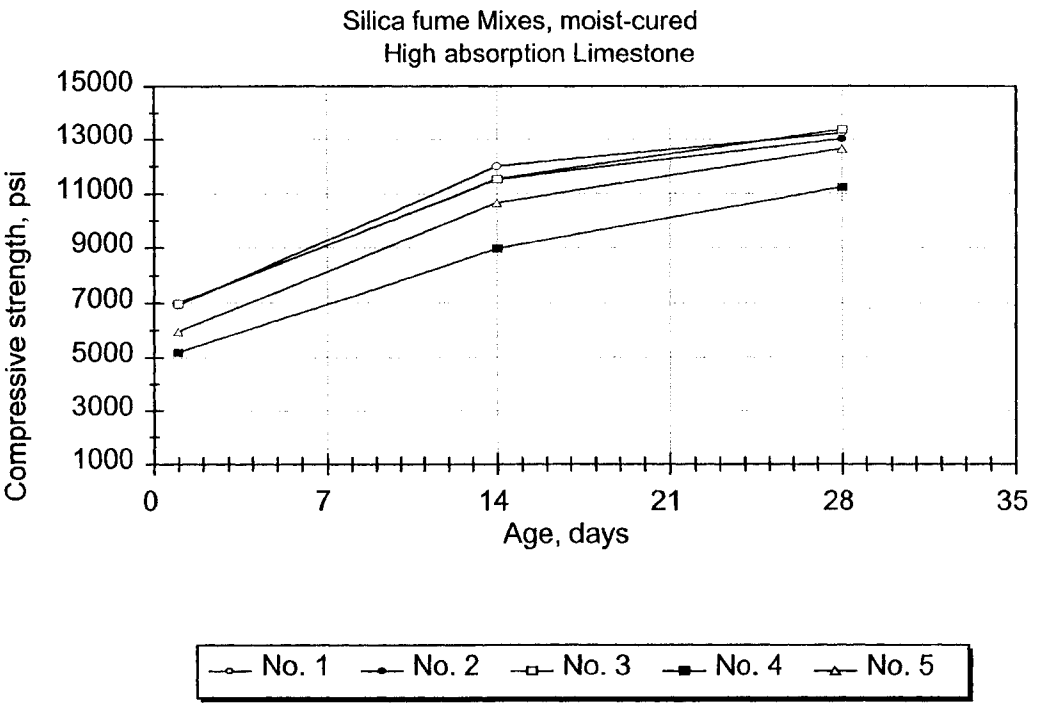

Figure 5.27. Compressive strength development in moist-cured specimens from silica fume mixes made with five different high-range water reducers and high absorption limestone.
[WS_L1.WMF]

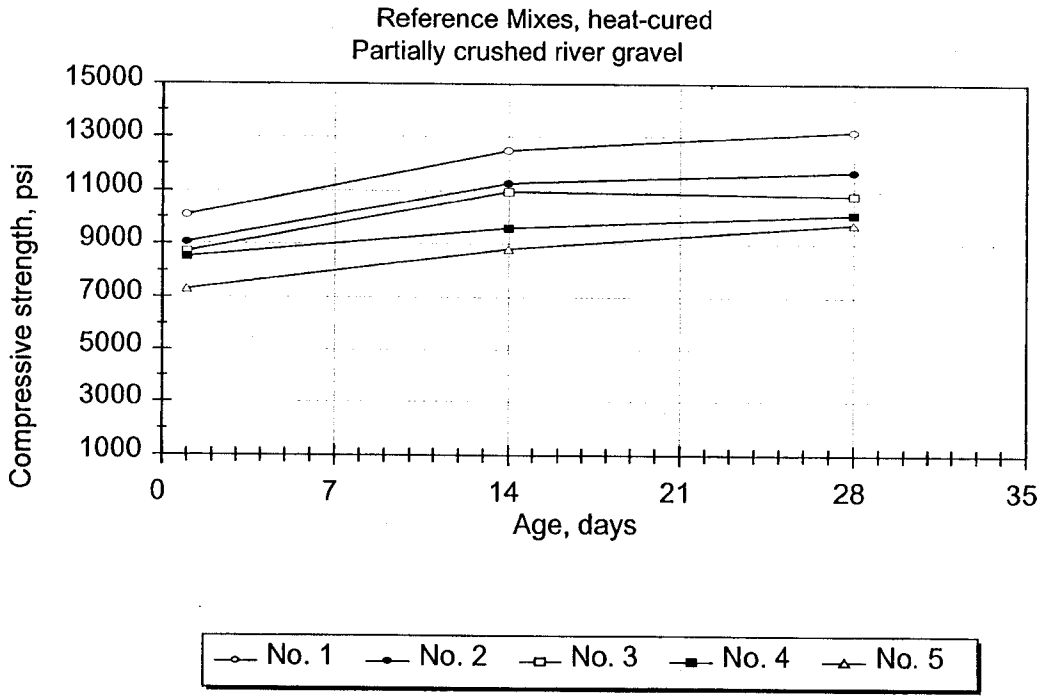

Figure 5.28. Compressive strength development in heat-cured specimens from reference mixes made with five different high-range water reducers and partially crushed river gravel.
[HREF_R2.WMF]

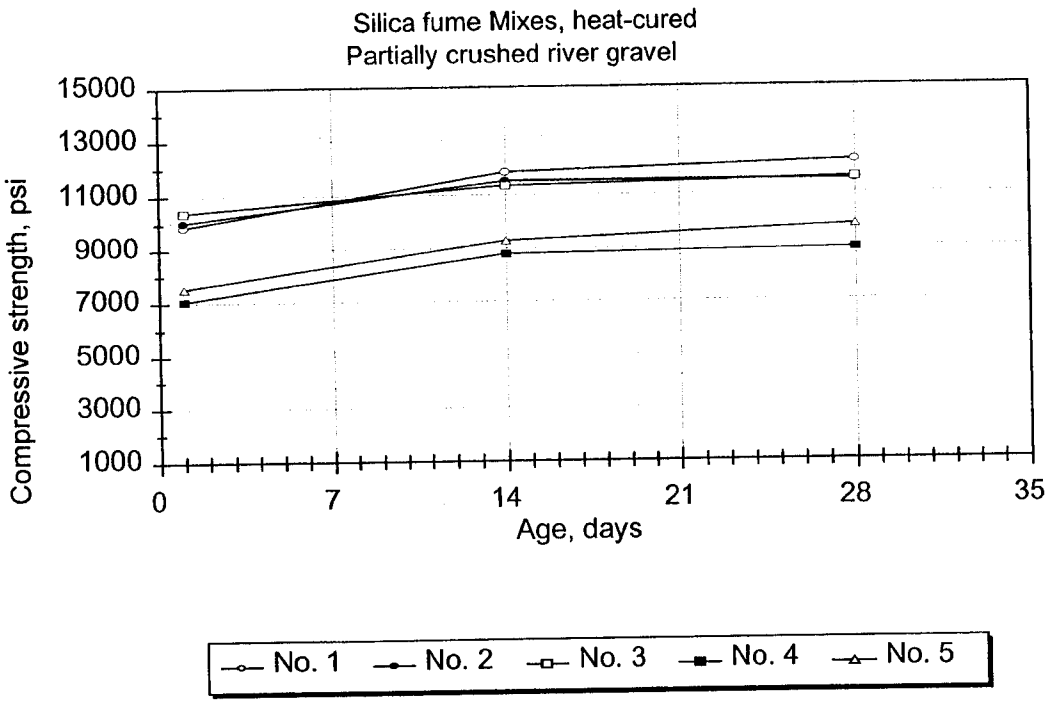

Figure 5.29. Compressive strength development in heat-cured specimens from silica fume mixes made with five different high-range water reducers and partially crushed river gravel.
[HS_R2.WMF]

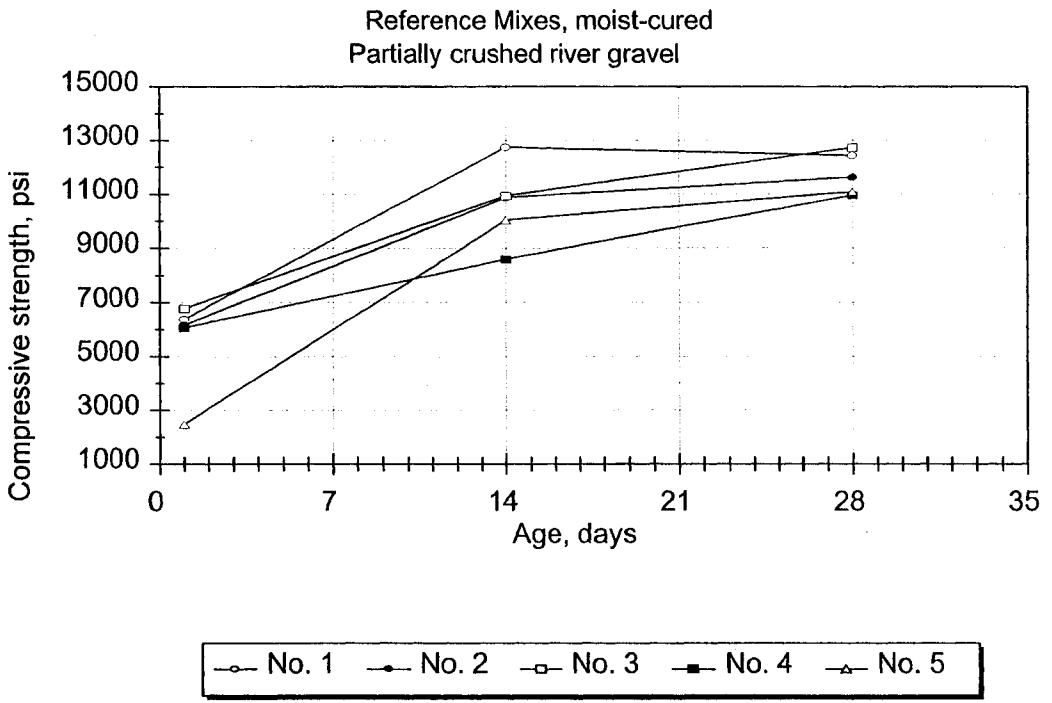

Figure 5.30. Compressive strength development in moist-cured specimens from reference mixes made with five different high-range water reducers and partially crushed river gravel.
[WREF_R2.WMF]

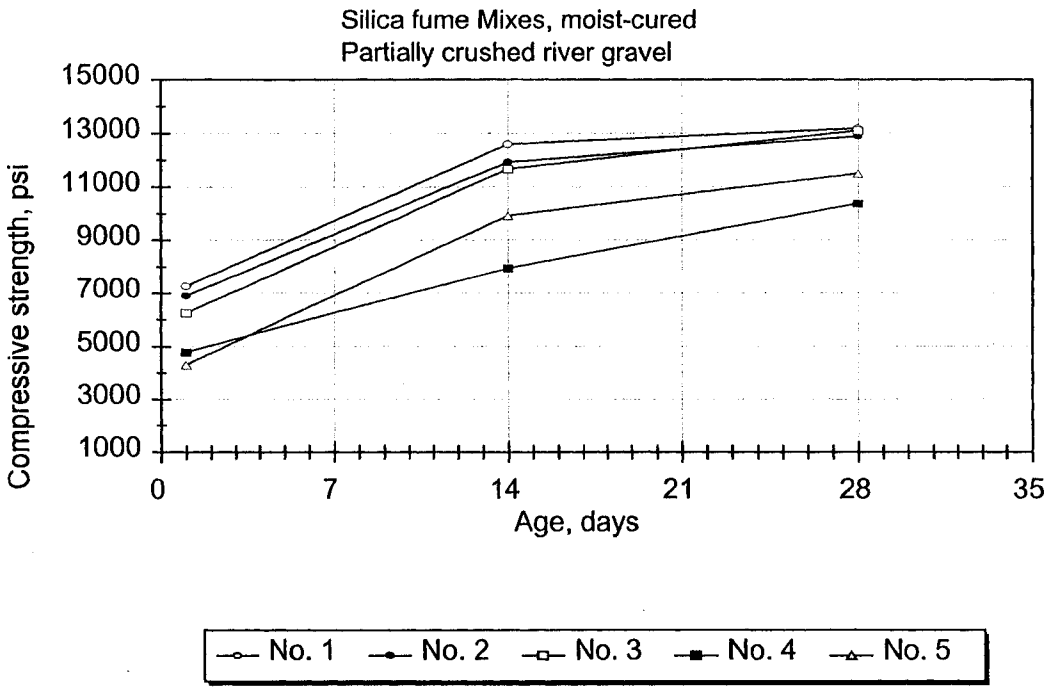

Figure 5.31. Compressive strength development in moist-cured specimens from silica fume mixes made with five different high-range water reducers and partially crushed river gravel.
[WS_R2.WMF]

CHAPTER 6
LITERATURE REVIEW:
MODULUS OF ELASTICITY OF HIGH STRENGTH CONCRETE

6.1 General

The static modulus of elasticity of concrete, E_C (also known as elastic modulus, Young's modulus or Young's modulus of elasticity) is defined as the ratio of normal stress to corresponding strain for tensile or compressive stresses. Knowing the static modulus of elasticity of concrete in analysis and design of both reinforced and prestressed concrete elements is as important as knowing the compressive strength of concrete.

Knowledge of the modulus of elasticity of concrete is essential in predicting deflections of concrete structures in service. Also, the estimate of the prestress losses due to the elastic shortening of prestressed elements, at the time of the prestress transfer, is based on the assumed value of the modulus of elasticity of the concrete. However, while concrete compressive strength can be easily determined experimentally, direct determination of static modulus of elasticity of concrete is laborious and time-consuming (ASTM standard C 469: Test Method for Static Modulus of Elasticity and Poisson's Ratio of Concrete in Compression). Concrete engineers have always been interested in predicting the value of static modulus of elasticity (with reasonable accuracy) through establishing a simple relationship between compressive strength and static modulus of elasticity of concrete. In fact for normal strength concrete, it has been found that the static modulus of elasticity of concrete increases with increase in its compressive strength and numerous empirical equations for predicting static modulus of elasticity of concrete from its compressive strength have been proposed by many investigators. These past investigations have typically been limited to concrete with standard cylinder strengths less than 6,000 psi (41.4 MPa).

Furthermore, in United States, values of compressive strength and static modulus of elasticity of normal strength concrete have been traditionally measured on 6 x 12 in.

(150 x 300 mm) standard cylindrical specimens. As most concrete suppliers and precast/prestressed plants have testing machines with a nominal compressive capacity of approximately 250,000 lb (1,100 kN), the maximum compressive strength of concrete that can be tested on a 6 x 12 in. (150 x 300 mm) cylinder is about 8,800 psi (60.7 MPa) at full load (which is not a safe practice on a routine basis). This testing capacity is not high enough for today's high strength concretes with compressive strengths reaching 20,000 psi (138 MPa) levels. This limitation on the capacity of testing machines has led companies to use 4 x 8 in. (100 x 200 mm) cylindrical test specimens where high strength concretes with compressive strengths up to 19,900 psi (137 MPa) can be tested without need for a high-capacity testing machine. While the maximum capacity of the testing machine may not look critical for testing static modulus of elasticity of high strength concrete (since the maximum load applied to the specimen is limited to 40% of the ultimate load according to ASTM standard C 469) stiffness of existing testing machines may not be sufficient to sustain repeated high loading and unloading cycles involved in static modulus of elasticity measurements of high strength concrete specimens *[Baalbaki et al. 1992]*. Thus, use of 4 x 8 in. (100 x 200 mm) specimens is also beneficial in static modulus of elasticity testing of high strength concrete.

The use of 4 x 8 in. (100 x 200 mm) cylinders for modulus of elasticity tests requires an investigation to determine if the existing relationships are adequately accurate to predict high strength concrete static modulus of elasticity. In addition, the effect of the specimen size on compressive strength and static modulus of elasticity values is of interest. The following is a brief review of some of the research that has been conducted on static modulus of elasticity of both normal strength and high strength concrete and effect of specimen size on static modulus of elasticity values. Table 6.1 shows a number of empirical relationships that have been since proposed to predict the static modulus of elasticity of high strength concrete. Effect of specimen size on compressive strength of high strength concrete was discussed in detail in Chapter 5 of this report.

As a side note it should be mentioned that in addition to the static method of determining the modulus of elasticity of concrete, in which the stress-strain relationship is measured directly, the modulus of elasticity may be determined by dynamic methods through finding the natural frequency of vibration of a specimen or determining the velocity of sound waves through the material. Dynamic methods are used to determine the extent of deterioration of concrete specimens subjected to freezing and thawing tests or affected by alkali-aggregate reaction. These tests provide simple and rapid means for frequent measurements of the modulus of elasticity without damaging the specimen. A decrease in the modulus, measured by a lower natural frequency or wave velocity, indicates deterioration of the concrete.

In this report all measurements of modulus of elasticity of high strength concrete were conducted by the static method and the terms *"static modulus of elasticity"* and *"modulus of elasticity"* are used equivalently. The dynamic method of determining the modulus of elasticity of concrete was used to evaluate the freeze-thaw durability of some of the high strength concrete mixes considered in this part of the study. Those results are reported elsewhere *[Mokhtarzadeh et al. 1995]*.

6.2 Previous Research

[Pauw 1960]: In a study conducted by Adrian Pauw, results of experiments on both normal weight and lightweight normal strength concrete from several investigators were considered. Based on those results Pauw suggested the following empirical relationship between modulus of elasticity and compressive strength of both lightweight and normal weight concrete:

- USC, psi: $E_c = 33w^{1.5}(f_c)^{0.5}$ ***(6.1-a)***
- SI, MPa: $E_c = 0.043w^{1.5}(f_c)^{0.5}$ ***(6.1-b)***

where

E_c = modulus of elasticity of concrete, psi (MPa)

w = unit weight of concrete at time of test, pcf (kg/m^3)

f_C = compressive strength of concrete at time of test, psi (MPa)

In this equation the effect of coarse aggregate, in the form of difference in specific gravity, is represented by the unit weight of concrete (w). The same equation is recommended by ACI 318-89 for normal strength concrete with unit weight values between 90 and 155 pcf (1,440 and 2,480 kg/m^3).

[Carrasquillo, Nilson and Slate 1981]: Based on an experimental investigation of the properties of high-strength concrete Carrasquillo, Nilson and Slate concluded that the ACI 318 equation overestimates the stiffness of concrete with compressive strengths greater than 6,000 psi (41.4 MPa). They recommended that the modulus of elasticity of normal weight concrete be calculated as:

- USC, psi: $E_C = (40{,}000(f_C)^{0.5} + 10^6).(w/145)^{1.5}$

  for $3{,}000 < f_C < 12{,}000$ psi **(6.2-a)**

- SI, MPa: $E_C = (3{,}320(f_C)^{0.5} + 6{,}900).(w/2{,}320)^{1.}$

  for $21 < f_C < 83$ MPa **(6.2-b)**

where

E_C = modulus of elasticity of concrete, psi (MPa)

w = unit weight of concrete at time of test, pcf (kg/m^3)

f_C = compressive strength of concrete at time of test, psi (MPa)

The concrete specimens considered were 4 x 8 in. (100 x 200 mm) cylinders produced using Type I portland cement, gravel or crushed limestone as coarse aggregate and had water-to-cement ratios between 0.32 to 0.70. In the State-of-the-Art Report on High-Strength Concrete ACI Committee 363 - High-Strength Concrete (ACI 363R-92) proposed using this equation for predicting modulus of elasticity of high-strength concrete. However, ACI 363 warns designers of

deviations of actual values of modulus of elasticity from predicted values mainly due to properties and proportions of the coarse aggregate used in the concrete mixture. In this equation (similar in form to the ACI 318 equation) the effect of coarse aggregate, in the form of difference in specific gravity, on modulus of elasticity of high strength concrete is represented by the unit weight of concrete *(w)*.

[Ahmad and Shah 1985]: Ahmad et al. conducted an investigation into the mechanical properties of high-strength concrete with compressive strengths of up to 12,000 psi (84 MPa) using their own data as well as experimental data reported by other investigators. They concluded that the secant modulus of elasticity of medium- and high-strength concrete does not conform to values predicted by the ACI 318-89 proposed equation and that the ACI 318-89 equation predicted lower and higher values for modulus of elasticity for concrete with compressive strengths under and above 5,000 psi (34.5 MPa), respectively. Ahmad et al. proposed the following equation for the prediction of modulus of elasticity of both normal- and high-strength concrete:

- USC, psi: $E_c = w^{2.5} (f_c)^{0.325}$

  for $f_c < 12{,}000$ psi ***(6.3-a)***
- SI, MPa: $E_c = 3.385 \times 10^{-5} w^{2.5} (f_c)^{0.325}$

  for $f_c < 84$ MPa ***(6.3-b)***

where

E_c = modulus of elasticity of concrete, psi (MPa)

w = unit weight of concrete at time of test, pcf (kg/m^3)

f_c = compressive strength of concrete at time of test, psi (MPa)

This equation passes through the origin and is claimed to be comparable to the ACI 318-89 predicted values for low and normal strength concrete and more accurate for high-strength concrete. Similar to ACI 318-89 and ACI 363R-92 equations the effect of coarse aggregate, in

the form of difference in specific gravity, on modulus of elasticity of high strength concrete is represented by unit weight of concrete *(w)*. Ahmad et al. argued that since experimentally determined values of modulus of elasticity depend on many parameters such as properties and proportions of coarse aggregate, the wetness or dryness of test specimen at the time of test, and method of obtaining deformations, predictions of their proposed equation or proposed ACI 363R-92 equation are sufficiently accurate and development of more accurate equations may be unnecessary.

[Aïtcin and Mehta 1990]: Aïtcin et al., using identical materials and similar mix proportions, investigated the influence of four coarse aggregate types on the modulus of elasticity of high-strength concrete. The high-strength concrete mixes contained ASTM C150 Type I portland cement and condensed silica fume and had 28-day compressive strengths in the range of 12,300 to 14,600 psi (84.8 to 101 MPa). The aggregates considered were (i) round and smooth particles of a siliceous gravel; (ii) crushed diabase; (iii)crushed limestone; and (iv) crushed granite. It was found that concrete made with diabase and limestone resulted in significantly higher strengths and modulus of elasticity than concrete made with granite and river gravel. Also it was reported that the highest compressive strength values and the highest modulus of elasticity values were not found in the same concrete. In this study diabase aggregate produced the concrete with highest compressive strength and limestone aggregate produced concrete with highest modulus of elasticity.

[Baalbaki, Aïtcin and Ballivy 1992]: Baalbaki et al. carried out tests on high-strength concrete made with Type III portland cement, silica fume and seven types of coarse aggregates (two limestones, one granite, two quartzites and two sandstones) with a water-to-cementitious material ratio of 0.27. The 28-day compressive strengths of concrete considered, determined by testing 4 x 8 in. (100 x 200 mm) cylindrical specimens, were between 12,900 to 14,900 psi (89.2 to 103 MPa). They compared observed E_C values, measured on 4 x 8 in. (100 x 200 mm) specimens, with values predicted by seven two-phase (mortar and coarse aggregate) mathematical composite models (Voigt, Reuss, Hirsch-Dougill, Popovics, Counto, Hashin, and

Bache & Nepper-Christensen models, Figure 6.1). They also compared the observed experimental values for modulus of elasticity of high-strength concrete with predicted values obtained from proposed relationships between E_C and f_C recommended by ACI 363 [**USC**: $E_C = 40{,}000\,(f_C)^{0.5} + 1{,}000{,}000$; **SI**: $E_C = 3{,}320\,(f_C)^{0.5} + 6{,}900$], first predraft of CEB/FIP Model Code 1990 [**USC**: $E_C = 276{,}000(f_C + 1160)^{1/3}$; **SI**: $E_C = 10{,}000(f_C + 8)^{1/3}$] and Proposal 12 of Revised Norwegian Standard - NS 3473 [**USC**: $E_C = 309{,}500\,f_C^{0.3}$; **SI**: $E_C = 9{,}500\,f_C^{0.3}$] codes. Based on their study they concluded that it is unreliable to precisely predict modulus of elasticity of high-strength concrete from two phase composite models and existing code equations. They stated that until a better relationship for predicting E_C based on f_C and the modulus of elasticity of concrete components has been developed direct measurement of modulus of elasticity remains the best and the most reliable method. In their study except for the case of two sandstones (highly porous aggregates) code equations and mathematical models provided estimates of E_C within 20 percent difference after 28 days.

[Baalbaki, Baalbaki, Benmokrane and Aïtcin 1992]: Baalbaki et al. reported results from an experimental study on the influence of specimen size on static modulus of elasticity of high performance concrete. The concrete components used in this study were: Type III portland cement, silica fume, superplasticizer, natural sand with fineness modulus of 2.40 and seven types of coarse aggregate with maximum size of 0.4 in. (10 mm). The water-to-cementitious material ratio was kept at 0.27 for all concretes. The 28-day compressive strength of concretes, measured on 6 x 12 in. (150 x 300 mm) cylinders, ranged between 12,200 to 14,200 psi (84.1 to 98.1 MPa). Based on 56 cylinders tested in this investigation Baalbaki et al. concluded that the modulus of elasticity was higher for 6 x 12 in. (150 x 300 mm) cylinders than for 4 x 8 in. (100 x 200 mm) cylinders and suggested the following relation for calculating the modulus of elasticity of 6 x 12 in. (150 x 300 mm) cylinders from the values obtained on 4 x 8 in. (100 x 200 mm) cylinders:

- USC, psi: $(E_C)_{6x12} = 1.05\,(E_C)_{4x8}$ ***(6.4-a)***
- SI, MPa: $(E_C)_{150x300} = 1.05\,(E_C)_{100x200}$ ***(6.4-b)***

Baalbaki et al. provided two possible explanations for the observed differences: (i) the relative size of skin layer with more pores or higher *w/c* ratio is inversely proportional to the specimen diameter and therefore, variations in the external surface characteristics have greater impact on smaller cylinders (secondary scale effect); (ii) Higher friction force between the testing machine's bearing plates and the end faces of the tested specimen for larger specimens results in smaller transverse strain and subsequently smaller change in volume and decrease in longitudinal strain (or increase in elastic modulus).

[Burg and Ost 1992]: Burg et al. reported the results of their study on engineering properties of five commercially made high strength concretes. Considered concretes had 28-day compressive strengths in the range of 10,600 to 17,250 psi (73.1 to 119 MPa) measured on 6 x 12 in. (150 x 300 mm) moist-cured cylinders. Concretes had water-to-cementitious material ratios ranging from 0.22 to 0.32 and contained either no mineral admixtures, silica fume only, or both fly ash and silica fume. Burg and Ost reported that: (i) at equivalent strengths, modulus of elasticity values for moist-cured cylinders were somewhat higher than modulus of elasticity values for air-cured specimens; (ii) measured values of modulus of elasticity were between values predicted by ACI 318-89 and ACI 363R-92 equations; and (iii) modulus of elasticity values measured using 4 x 8 in. (100 x 200 mm) specimens were on average about 500,000 psi (3400 MPa) higher than values measured using 6 x 12 in. (150 x 300 mm) cylinders.

[Berke, Dallaire and Hicks 1992]: Berke et al. proposed the following equation for prediction of modulus of elasticity of concrete:

- USC, psi: ***(6.5-a)***

  $E_C = 2778(CF) + 6189(SF) + 452545(LN(AGE)) + 1796695$

- SI, MPa: ***(6.5-b)***

  $E_C = 32.297(CF) + 71.963(SF) + 3121(LN(AGE)) + 12391$

where

E_C = modulus of elasticity of concrete, psi (MPa)

CF = concrete cement factor, pcy (kg/m^3)

SF = concrete silica fume content, pcy (kg/m^3)

AGE = fog room curing period, days

The proposed formula was the result of a study on mechanical properties of silica fume concrete made with ASTM Type I cement and an ASTM C33 Grade 67 dense igneous rock (trap rock) coarse aggregate with compressive strength in the range of 2,900 to 14,500 psi (20 to 100 MPa). In this study both compressive strength and modulus of elasticity of the concrete were measured on 4 x 6 in. (100 x 150 mm) cylinders. They concluded that the effects of water-to-cementitious material ratio and air content were not significant and that on a mass basis, silica fume was three times more effective than cement in increasing the modulus of elasticity of concrete.

[Tomosawa and Noguchi 1993]: Tomosawa et al. proposed the following universal equation for predicting modulus of elasticity of concrete which takes into consideration types of coarse aggregate and types of mineral additives used through the use of two correction factors k_1 and k_2 :

- USC, psi: ***(6.6-a)***

$$E_C = 4.86 \times 10^6 \, k_1 \, k_2 \, (w/150)^2 \, (f_c/8{,}700)^{1/3}$$

- SI, MPa: ***(6.6-b)***

$$E_C = 3.35 \times 10^4 \, k_1 \, k_2 \, (w/2{,}400)^2 \, (f_c/60)^{1/3}$$

where

E_C = modulus of elasticity of concrete, psi (MPa)

k_1 = correction factor for coarse aggregate

k_2 = correction factor for mineral additives

w = unit weight of concrete at time of test, pcf (kg/m^3)

f_c = compressive strength of concrete at time of test, psi (MPa)

Values of k_1 fall in the range of 0.9 to 1.2. According to Tomosawa and Noguchi the effects of coarse aggregate on modulus of elasticity can be classified into three groups: (i) $k_1 = 1$ group, includes river gravel, crushed graywacke, etc.; (ii) $k_1 > 1$ group, includes crushed limestone and calcined bauxite; (iii) $k_1 < 1$ group, includes crushed quartzitic aggregate, crushed andesite, crushed cobble stone, crushed basalt, and crushed clayslate. As a practical guide, values of 1.00, 1.20 and 0.95 were proposed for k_1 for the three groups of aggregates, respectively, described above. The value of k_2, correction factor for mineral additives, depends on the type of coarse aggregate as well as type and level of addition. A detailed table showing the average values of k_2 for each type of coarse aggregate and for each type and level of additives was reported. However, for simplicity and as a practical guide, three values for k_2 were reported: (i) $k_2 = 0.95$ for addition of silica fume, ground granulated blast-furnace slag, and fly ash fume; (ii) $k_2 = 1.10$ for addition of fly ash; and (iii) $k_2 = 1.00$ for any other kind of addition. The proposed equation was obtained as part of the work of the Research Committee on High-Strength Concrete of the Architectural Institute of Japan (AIJ) and National Research and Development Project, also known as New RC Project, sponsored by the Ministry of Construction. The data investigated were obtained from concrete with compressive strengths in the range of 2,900 to 23,200 psi (20 to 160 MPa) collected by many investigators using concrete made with various materials.

[Radain, Samman and Wafa 1993]: Radain et al. reported results of their study on twenty high strength concrete mixes with 28-day compressive strengths in the range of 5,770 to 13,000 psi (39.8 to 90.0 MPa). This author noticed that the relationship printed in the above reference for modulus of elasticity of high strength concrete was misprinted ($E_c = 1456 + 2173 (f_{c150})^{0.5}$; MPa). Using the same regression model used by original authors a regression analysis was conducted by this author on their test data and the following equation for prediction of modulus of elasticity of 6 x 12 in. (150 x 300 mm) concrete specimens was derived:

- USC, psi: $E_c = 2{,}101{,}775 + 26{,}200\,(f_c)^{0.5}$ ***(6.7-a)***
- SI, MPa: $E_c = 14495 + 2176\,(f_c)^{0.5}$ ***(6.7-b)***

where

E_c = modulus of elasticity of concrete, psi (MPa)

f_c = compressive strength of concrete at time of test, psi (MPa)

Other Proposed Equations: The Norwegian Concrete Code NS 3473 suggests the following relationship between modulus of elasticity of high strength concrete and its compressive strength:

- USC, psi: $E_c = 309{,}500\,f_{cc}^{0.30}$ ***(6.8-a)***
- SI, MPa: $E_c = 9{,}500\,f_{cc}^{0.30}$ ***(6.8-b)***

where

E_c = modulus of elasticity of concrete, psi (MPa)

f_{cc} = compressive strength of concrete at time of test measured on cylinders with a height-to-diameter ratio of 2, psi (MPa)

The 0.30 power makes the calculated modulus of elasticity less sensitive to changes in the compressive strength than the more frequently used 0.5 value.

The relationship between modulus of elasticity and compressive strength of high strength concrete takes the following form in the CEB-FIP state-of-the-art report:

- USC, psi: $E_c = 276{,}000(f_{ck} + 1160)^{1/3}$ ***(6.9-a)***
- SI, MPa: $E_c = 10{,}000(f_{ck} + 8)^{1/3}$ ***(6.9-b)***

where

E_c = modulus of elasticity of concrete, psi (MPa)

f_{ck} = characteristic compressive strength of 6 x 12 in. (150 x 300 mm) cylinders, psi (MPa)

The following equation can be used if the actual compressive strength of concrete (f_{cm}) is known:

- USC, psi: $E_c = 276{,}000(f_{cm})^{1/3}$ ***(6.10-a)***
- SI, MPa: $E_c = 10{,}000(f_{cm})^{1/3}$ ***(6.10-b)***

6.3 Concluding Remarks

Ability to predict the modulus of elasticity of high strength concrete with reasonable accuracy is fundamental for its successful use in various structural applications. Since the development of high strength concrete, the prediction of its modulus of elasticity has been the subject of numerous studies. Results of these studies have led to the suggestion of several prediction equations and models that range from simple to complex. Two general methods have been used by researchers in these studies.

The method used in most cases comprises conducting experiments on compressive strength and modulus of elasticity of high strength concrete. Regression analysis is then used to establish a relationship between compressive strength and modulus of elasticity of high strength concrete. This method has been traditionally used to develop design code equations. The following are some of the advantages to this method:

1. It is a reasonable compromise of accuracy and simplicity;
2. It has been successfully used in the past to develop prediction equations for normal strength concrete;

3. Only such parameters which are known to the design engineer are used in the prediction equations;
4. The general form of the prediction equation can be further developed to include parameters which may affect the modulus of elasticity of high strength concrete such as type of aggregate, composition of cementitious material, etc.

However, there are disadvantages to this approach as well. For example:

1. It is empirical;
2. Depending on the type of regression model used, the same experimental data set can result in different equations;
3. Since these equations are based on the average of a large number of experimental data, they may not be valid for a specific concrete; therefore these equations are valid in general terms only.

Another method that has been used for prediction of modulus of elasticity of high strength concrete is the use of composite models, Figure 6.1. In these models the modulus of elasticity of high strength concrete is calculated as a function of the elastic modulus of aggregate and the cement paste and their respective volume proportions. While this method may look more scientific it has major disadvantages. For example:

1. This method also results in different prediction equations depending on the type of composite model which is applied to concrete;
2. Detailed information about concrete mix proportions, type of aggregate to be used as well as material properties of aggregate and the cement paste is required to compute modulus of elasticity of high strength concrete. In general, the design engineer does not have access to this information at the time of the design;

3. Recent research has shown that the values of modulus of elasticity predicted by composite models are as accurate as results predicted by some of the existing empirical equations *[Baalbaki, Aïtcin and Ballivy 1992].*

It appears that empirical equations between modulus of elasticity of high strength concrete with its compressive strength are satisfactory in many cases and at least in the early stages of the design process of major projects. However, if information about modulus of elasticity of high strength concrete is very important, the final design should be based on the direct measurement of modulus of elasticity on the concrete in question *[Nilsen and Gjorv 1993; Baalbaki, Aïtcin and Ballivy 1992].*

Furthermore, limitation on the capacity of testing machines has led to the use of smaller size test specimens. While the effect of specimen size on compressive strength test results for high strength concrete has been explored by several researchers, available information on the influence of the specimen size on the modulus of elasticity test results is sparse and contradictory.

TABLE 6.1. Some of the proposed equations for the calculation of modulus of elasticity of high strength concrete.

	Equations for Modulus of Elasticity	Compressive Strength Limitation
Pauw - ACI 318-89	$E_c = 33w^{1.5}(f_c)^{0.5}$ $E_c = 0.043w^{1.5}(f_c)^{0.5}$	psi, No max. strength specified MPa, No. max. strength specified
Carrasquillo, Nilson and Slate - ACI 363R-92	$E_c = (40{,}000(f_c)^{0.5}+10^6).(w/145)^{1.5}$ $E_c = (3{,}320(f_c)^{0.5}+6{,}900).(w/2{,}320)^{1.5}$	$3{,}000\ psi < f_c < 12{,}000\ psi$ $21\ MPa < f_c < 83\ MPa$
Ahmad and Shah	$E_c = w^{2.5}(f_c)^{0.325}$ $E_c = 3.385x10^{-5}\, w^{2.5}(f_c)^{0.325}$	$f_c < 12{,}000\ psi$ $f_c < 84\ MPa$
Berke, Dallaire and Hicks	$E_c = 2778\ (CF) + 6189\ (SF) + 452545\ (LN(AGE)) + 1796695$ $E_c = 32.297\ (CF) + 71.963\ (SF) + 3121\ (LN(AGE)) + 12391$	
Tomosawa and Noguchi	$E_c = 4.86x10^6\, k_1.k_2(w/150)^2(f_c/8{,}700)^{1/3}$ $E_c = 3.35x10^4\, k_1.k_2(w/2{,}400)^2(f_c/60)^{1/3}$	
Radain, Samman and Wafa	$E_c = 2{,}101{,}775 + 26{,}200(f_c)^{0.5}$ $E_c = 14{,}495 + 2{,}176(f_c)^{0.5}$	psi MPa
CEB/FIP MC 90	$E_c = 593{,}400\ [(f_{ck}+1160)/10]^{1/3}$ **or** $E_c = 593{,}400\ [(f_{cm})/10]^{1/3}$ $E_c = 21{,}500\ [(f_{ck}+8)/10]^{1/3}$ **or** $E_c = 21{,}500\ [(f_{cm})/10]^{1/3}$	$f_c < 11{,}600\ psi$ $f_c < 80\ MPa$
NS 3473	$E_c = 309{,}500\, f_{cc}^{0.3}$ $E_c = 9{,}500\, f_{cc}^{0.3}$	$3{,}600\ psi < f_{cc} < 12{,}300\ psi$ $25\ MPa < f_{cc} < 85\ MPa$

E_c = modulus of elasticity

f_c = compressive strength of 6 x 12 in. (150 x 300 mm) cylinder

k_1 = 1.20 for crushed limestone, calcined bauxite aggregates
0.95 for crushed quartzitic, crushed andesite, crushed basalt, crushed clayslate and crushed cobble stone aggregates
1.00 for coarse aggregates other than the above

k_2 = 0.95 for silica fume, ground granulated blast-furnace slag, fly ash fume
1.10 for fly ash
1.00 addition other than the above

= 1.2 for basalt, dense limestone aggregates
1.0 for quartizitic aggregates
0.9 for limestone aggregates
0.7 for sandstone aggregates

f_{ck} = characteristic compressive strength of 6 x 12 in. (150 x 300 mm) cylinder

f_{cm} = compressive strength at 28 days of 6 x 12 in. (150 x 300 mm) cylinder

f_{cc} = compressive strength of 6 x 12 in. (150 x 300 mm) cylinder

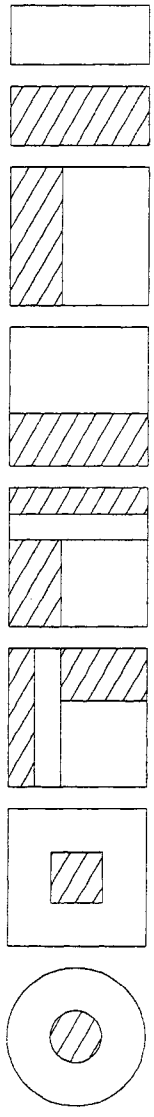

Phase 1: Mortar

Phase 2: Coarse Aggregate

Voigt Model: $E_c = E_1 c_1 + E_2 c_2$

Reuss Model: $\frac{1}{E_c} = \frac{c_1}{E_1} + \frac{c_2}{E_2}$

Hirsch-Dougill Model: $\frac{1}{E_c} = \frac{1}{2}\left(\frac{1}{E_{cVoigt}} + \frac{1}{E_{cReuss}}\right)$

Popovics Model: $E_c = \frac{1}{2}(E_{cVoigt} + E_{cReuss})$

Counto Model: $\frac{1}{E_c} = \frac{1-\sqrt{c_2}}{E_1} + \left(\frac{1-\sqrt{c_2}}{\sqrt{c_2}} E_1 + E_2\right)^{-1}$

Hashin Model: $E_c = \left[\frac{(E_1 + E_2) + (E_2 - E_1)c_2}{(E_1 + E_2) - (E_2 - E_1)c_2}\right] E_1$

Bache and Nepper-Christensen Model: $E_c = E_1^{c_1} . E_2^{c_2}$

Figure 6.1. Some of the proposed two phase composite models for prediction of modulus of elasticity of concrete; (c_i=V_i/V volumetric ratio of each phase)
[MODELS-2.PLT]

CHAPTER 7
TEST RESULTS: MODULUS OF ELASTICITY

7.1 Experimental Program

Modulus of elasticity of ninety-eight high strength concrete mixes with compressive strengths in the range of 6,000 to 19,500 psi (41.4 to 135 MPa) were studied (Mix Nos. 22 through 29 and 50 through 139 of Table 7.1). The water-to-cementitious material ratio was kept constant at 0.30 for all mixes. Seventeen of the concrete mixes contained no mineral admixtures, twenty-three contained fly ash only, another twenty-three of the mixes contained silica fume only and the rest (thirty-five mixes) contained both fly ash and silica fume. Inclusion of fly ash and silica fume was on a replacement by weight of cement basis and were limited to 10, 20 and 30 percent for fly ash and 7.5, 10 and 15 percent for silica fume.

Several different curing conditions were examined for 4 x 8 in. (100 x 200 mm) specimens:

1. **H** Condition: Specimens heat-cured and then tested *dry* at 1-, 28-, 182-, and 365-days.
2. **HW1** and **HW3** Conditions: Initial heat-curing of specimens followed by an additional 1- or 3-day moist-curing and then were tested *dry* at 28-days.
3. **W7** and **W14** Conditions: Specimens moist-cured for either 7- or 14-days and tested *dry* at 28-days.
4. **W28** Condition: Specimens moist-cured for 28-days and then tested *wet* at 28-, and *dry* at 182-, or 365-days.
5. **W182**, and **W365** Conditions: Specimens moist-cured for their entire life and then tested *wet* at 182-, or 365-days respectively.

Additional 6 x 12 in. (150 x 300 mm) cylinders were cast from ninety of the ninety-eight mixes to study the influence of specimen size on modulus of elasticity test results (Mix Nos. 22

through 29, 50 through 91, and 100 through 139 of Table 7.1). These specimens were either heat-cured (H) and tested *dry* at 1- and 28-days or moist-cured (W28) and tested *wet* at 28-days.

Six different types of coarse aggregates were used in the production of the concrete mixes:

1. High absorption limestone (*L1*): 46 mixes
2. Low absorption limestone (L2): 4 mixes
3. Round river gravel (*R1*): 24 mixes
4. Partially crushed river gravel (*R2*): 12 mixes
5. Granite (*G1*): 8 mixes
6. Granite (*G2*): 4 mixes

Except for eight mixes (Mix Nos. 100 through 107 of Table 7.1) where Type I portland cement was used, all other concrete mixes (ninety mixes) used Type III portland cement. Eight mixes used a different brand of Type III portland cement.

The test matrix for this portion of the study is shown in Table 7.1. A detailed description of the materials as well as the fabrication and curing procedures used in making high strength concrete specimens was given in Chapter 3 of this report. Appendix B presents measured modulus of elasticity values from this part of the study.

7.2 Apparatus

7.2.1 Testing Machine

The detailed description of the MTS testing machine and the loading rate used was given in Chapter 5 of this report.

7.2.2 Compressometer

The test setup for measuring the modulus of elasticity of concrete specimens is schematically shown in Figure 7.1. Two different compressometers were used to measure modulus of elasticity of 6 x 12 in. (150 x 300 mm) and 4 x 8 in. (100 x 200 mm) concrete cylinders.

Compressometer for 6 x 12 in. (150 x 300 mm) Specimens: For determining modulus of elasticity of 6 x 12 in. (150 x 300 mm) cylinders a commercially available compressometer very similar to that shown in the ASTM C 469, Standard Test Method for Static Modulus of Elasticity and Poisson's Ratio of Concrete in Compression, was used. This device consisted of two yokes (Figures 7.1). The bottom yoke was rigidly attached to the specimen by three pointed screws located on its circumference 120° apart from each other. The top yoke was attached to two diametrically opposite points of the specimen by means of two pointed screws, 180° apart, so that it was free to rotate. At a point midway between the supporting points a long pivot rod was used to maintain a constant 8 in. (200 mm) distance (gage line length) between one side of the two yokes such that at the opposite point on the circumference the change in distance between the yokes was equal to two times the average deformations of the two diametrically opposite gage lines ($e_r = e_g$). For 6 x 12 in. (150 x 300 mm) specimens, deformations were measured by a 0.0001 in. (2.54×10^{-3} mm) dial gage installed exactly opposite to the pivot rod between the two yokes ($e_r = e_g$).

Compressometer for 4 x 8 in. (100 x 200 mm) Specimens: For measuring modulus of elasticity of 4 x 8 in. (100 x 200 mm) specimens an electronic compressometer was constructed at the machine shop facility of the Structural Laboratory of the Department of Civil Engineering of the University of Minnesota, Figures 7.2-A to 7.2-C. The mechanism of action of compressometer on this apparatus was very similar to what was described earlier with some modifications to better fit test requirements. On this device the fixed yoke (bottom yoke) was rigidly attached to the specimen by means of four pointed screws located at 90° around the yoke's circumference (Figure 7.2-B). As recommended by ASTM C 469 (preferred length of

gage line = ½ the height of the specimen), the gage length on this device was selected to be 4 in. (100 mm). Deformations were measured by a ±0.010 in. (±0.25 mm) LVDT (Linear Variable Differential Transformer), accurate to 0.0001 in. (0.0025 mm), located opposite to the pivot rod with the same eccentricity from axis of the specimen. The body of the LVDT was mounted in the top yoke and the core was connected to the bottom yoke using a threaded bar and a zero-output adjusting mechanism (Figure 7.2-A).

The output of the LVDT from the compressometer as well as the loads from the testing machine were continuously recorded by computer at every second from the MTS 452 data acquisition system.

Referring to Figure 7.1 the axial deformation of the specimen for either of the two test setups was calculated as follows:

- $d = g.e_r / (e_r + e_g)$ *(7.1)*

where

d = total deformation of the specimen throughout the effective gage length, in. (mm)

g = gage (or LVDT) reading, in. (mm)

e_r = eccentricity of the pivot rod from the axis of specimen, in. (mm)

e_g = eccentricity of the gage (or LVDT) from the axis of specimen, in. (mm)

7.3 Procedure

Immediately before testing specimens for modulus of elasticity, the same size companion specimens were tested for compressive strength. The same procedures described in Chapter 5 for testing concrete specimens for compressive strength were followed. The compressometer was attached to each specimen immediately before testing. The axis of the specimen was carefully aligned with the axis of the compressometer to ensure equal eccentricities ($e_r = e_g$) for pivot rod and the deformation measuring device (dial gage or LVDT). The test specimen was then placed

on the lower platen of the testing machine. Using concentric circles inscribed on the lower platen, the axis of the test specimen was carefully aligned with the center of thrust of the spherical bearing block. The spherical bearing block was brought down slowly to lightly bear on the specimen. During this action the moveable part of the spherical bearing block was gently rotated back and forth by hand so that uniform seating was obtained. Side bars of the compressometer, needed for handling the compressometer, were then removed and the deformation measuring device on the compressometer was set to an initial value (zero for the case of the dial gage and +8.0 volts for the case of the LVDT).

The specimen was loaded and unloaded at least two times. During the first loading-unloading cycle, which was primarily for seating of the gages, no data was recorded. The performance of the testing machine and deformation measuring device was checked for any unusual behavior. If needed, corrections were made and a second seating load was applied. After unloading the specimen, the deformation measuring device was reset to initial values. The seating load was 30,000 lb (133.5 kN) for 6 x 12 in. (150 x 300 mm) specimens and 15,000 lb (66.8 kN) for 4 x 8 in. (100 x 200 mm) cylinders (equivalent to approximately 1,100 psi (7.6 MPa) compressive stress in the specimen).

Each test for modulus of elasticity was conducted as follows. Load was continuously applied to the test specimen by moving the upper spherical bearing block downward at a rate of 0.05 in./min (1.25 mm/min). For the case of 6 x 12 in. (150 x 300 mm) cylinders, the applied load and the corresponding dial gage readings were recorded (without interruption of loading) at 10,000 lb (44.5 kN) load intervals until the applied load was equal to 50 percent of the ultimate load (more than the 40 percent of the ultimate load required by ASTM C 469).

For the case of 4 x 8 in. (100 x 200 mm) specimens load and deformation data were recorded at every second by a computer through an MTS 452 data acquisition system until the applied load reached 50 percent of the ultimate load level.

After completion of each test the specimen was removed from the testing machine, the compressometer was removed and the cylinder was immediately tested for ultimate compressive strength. The ultimate compressive strength of the disturbed specimen (leftover from modulus of elasticity test) was compared to the compressive strength of undisturbed companion specimen as a test to check the validity of using the disturbed samples to determine compressive strength (see Section 5.2).

For all cases considered, the partial stress-strain curves obtained were, for all practical purposes, a line of constant slope. The modulus of elasticity was then obtained by conducting a linear regression analysis on stress-strain data and finding the slope of the best fit line through the origin (zero intercept). The coefficient of determination (R^2) was calculated as an indication of goodness of fit. In all cases values of R^2 were above 98 percent.

7.4 Repeatability of Results

In order to check the repeatability of the results, ASTM C 469 (Standard Test Method for Static Modulus of Elasticity and Poisson's Ratio of Concrete in Compression) recommends that the calculation of the modulus of elasticity of a concrete test specimen be based on the average of the results from at least two loading/unloading cycles. Therefore according to ASTM C 469 the loading/unloading cycles are carried out at 40 percent of the ultimate compressive strength and the modulus of elasticity of the test specimen is calculated as the average of the slopes of the two ascending parts of the stress-strain curves of these loadings.

During the course of this investigation it was noted that for high strength concrete and our test setup, the results obtained from the first and the second loading/unloading cycles were practically identical and that the additional accuracy and information obtained during the second loading/unloading cycle did not justify the amount of time, labor and resources it demanded. To investigate in more detail the feasibility of obtaining modulus of elasticity of high strength concrete with reasonable accuracy in only one loading/unloading cycle and also to avoid the potentially unnecessary laborious and time consuming second loading/unloading cycle, twenty-

two concrete test specimens were selected from eight concrete mixes (Mix Nos. 92 to 99 of Table 7.1) to investigate the repeatability of the results. All test specimens were 4 x 8 in. (100 x 200 mm) and were tested at 182-days. Fourteen of the specimens were moist-cured for 28-days. The other eight were initially heat-cured and then stored in the laboratory until time of test. Each test specimen was subjected to two loading/unloading cycles up to 50 percent of their ultimate compressive strengths and the modulus of elasticity from each cycle was computed.

Figures 7.3-A to 7.3-K show the stress-strain curves for these twenty-two concrete test specimens. Each figure contains a pair of experimental stress-strain curves obtained from two loading cycles. Table 7.2 summarizes the numerical results for modulus of elasticity values together with R^2 values of the linear regression line through experimental data. As is readily seen for each stress-strain curve pair, there was minimal difference in the observed modulus of elasticity values (slopes) obtained from the first and the second loading/unloading cycles.

To determine if the modulus of elasticity differentials were statistically significant, data from each pair were analyzed using a paired t-test (a statistical measure of similarity of test data). It was determined that differences in measured modulus of elasticity values were statistically insignificant (p value = 0.0012). Based on these tests it was concluded that for high strength concrete and our test setup, the measured modulus of elasticity values from the first loading/unloading cycle were sufficiently accurate. It seemed that conducting two or more loading/unloading cycles, as suggested by ASTM C 469, was not warranted.

Subsequently all other tests on modulus of elasticity of high strength concrete in this research program were conducted with only one loading/unloading cycle.

7.5 Effect of Wetness/Dryness of Test Specimen

Figure 7.4 plots measured modulus of elasticity versus compressive strength for 4 x 8 in. (100 x 200 mm) cylinders. In this plot different symbols are used for specimens tested in dry condition (specimens initially heat-cured or moist-cured and then stored in the laboratory until

time of test) and specimens tested in wet condition (specimens moist-cured until time of test). It can be seen from this plot that wet samples produced higher values of modulus of elasticity for a given level of compressive strength. Burg and Ost also reported somewhat higher modulus of elasticity values for moist specimens *[Burg and Ost 1992]*. A probable cause of this observation is as follows:

(a) Dry specimens have the tendency to yield higher compressive strengths. The explanation is that the surface layer of a dry specimen is subject to greater shrinkage. However, this shrinkage is restrained by the wetter inner core of the specimen and the result is that the surface layer is under tension and the inner core is under compression resulting in a non-uniform state of stress across the width of a concrete specimen. During the uniaxial compression test the outer surface can take more load to reach the ultimate stress due to the presence of the initial tensile stress and meanwhile acts as a confinement for the more stressed inner core. It should be noted that in this case the only components contributing to the stiffness of the specimen are the solid constituents.

(b) Low water-to-cementitious materials ratio in high strength concrete result in a dense and impermeable matrix. The result is that curing water will penetrate the specimen only superficially and the inner core of a water-cured specimen is almost unaffected by the surrounding water. In this case the state of stress across the width of a cylinder is reversed. The wet surface layer wants to expand but is restrained by the dryer inner core. This results in development of compressive stress in the surface layer and tensile stress in the inner core. When the wet specimens are subjected to uniaxial compressive tests, the surface layer reaches the ultimate stress first and results in spalling and loss of cross section and consequently failure of the entire specimen.

(c) Due to the denseness and impermeability of the cement matrix of high strength concrete, the movement of the interlayer water in concrete is restricted and thus the trapped water inside wet specimens also contributes to the total stiffness of the specimen. On the other hand,

during the uniaxial compression test, the trapped water inside the wet specimens exerts pressure to the surrounding matrix and further lowers the ultimate compressive strength of the specimen.

7.6 Effect of Specimen Size

Figure 7.5 shows modulus of elasticity data for 4 x 8 in. (100 x 200 mm) specimens plotted against data from testing 6 x 12 in. (150 x 300 mm) companion specimens. For the 202 data pairs considered, the modulus of elasticity values measured using 4 x 8 in. (100 x 200 mm) specimens were on average 620,000 psi (4.3 GPa) higher than modulus of elasticity values measured using 6 x 12 in. (150 x 300 mm) specimens. This observation agrees closely with results reported by Burg and Ost *(1992)*. Burg and Ost reported that the modulus of elasticity values of high strength concrete measured using 4-in. (100 mm) diameter cylinders were about 0.5 million psi (3.4 GPa) higher than the modulus of elasticity values measured using 6-in. (150 mm) diameter cylinders. However, this contradicts Baalbaki et al. observations *[Baalbaki, Baalbaki, Benmokrane and Aïtcin 1992]*. Baalbaki et al. reported that the modulus of elasticity was 5 percent higher for 6 x 12 in. (150 x 300 mm) cylinders than for 4 x 8 in. (100 x 200 mm) specimens.

7.7 Modulus of Elasticity versus Time

The effect of time on modulus of elasticity of concrete is taken into account implicitly when strength of concrete at any time *t*, rather than 28-day compressive strength, is inserted into the modulus of elasticity equations given in different codes. As an example, based on the ACI 318 code, the time-dependent modulus of elasticity of concrete is expressed as:

- $E_t = 33w^{1.5}(f_{ct})^{0.50}$ *(7.2)*

where

E_t = modulus of elasticity of concrete at time *t*, psi

w = unit weight of concrete, pcf

f_{ct} = compressive strength of concrete at time *t*, psi

The change in modulus of elasticity with time was studied for both heat-cured and moist-cured specimens. The early age modulus of elasticity is important to the precast/prestressed industry for investigating effects such as elastic shortening. The results obtained from 314 sets of heat-cured and 92 sets of moist-cured specimens indicate that at 1-day the modulus of elasticity of heat-cured specimens is approximately 98 percent of its 28-day value, Figure 7.6. Modulus of elasticity of heat-cured specimens did not change significantly with time and were, on average, 94 and 96 percent of the 28-day value after 182- and 365-days respectively. Drying of the specimens is the possible cause of the slight decrease in modulus of elasticity of heat-cured specimens observed at later ages. The modulus of elasticity of moist-cured specimens increased with time and were approximately 106 and 108 percent of their 28-day values at 182- and 365-days of age.

7.8 Effect of Aggregate Type, Curing Condition, Type of Cement and Composition of Cementitious Material

The effect of the aggregate type on the concrete modulus of elasticity is shown in Figure 7.7 for limestone and round gravel concretes. Superimposed on the data are the relationships given by ACI 318, ACI 363 and the bounds recommended by New RC. The data clearly indicates the influence of the aggregate type on the concrete stiffness. For similar compressive strengths, the limestone aggregate concrete investigated in the study was less stiff than the round river gravel concrete. Although the New RC relation is shown to bound the results, the coefficients correlating the aggregate type with modulus of elasticity produced opposite trends than those observed in this study (k1=1.20 for limestone, 1.00 for round river gravel). It is important to recognize the relationship between aggregate type and concrete stiffness; however, these results indicate that it is difficult to generalize a coefficient for a certain aggregate type because the relative aggregate properties may vary from one source to another. Figure 7.7 also shows that the current ACI code equation overpredicts the stiffness of high strength concrete. The ACI 363 relationship represents a reasonable lower bound to the data.

Figures 7.8-A to 7.8-F show modulus of elasticity of high strength 4 x 8 in. (100 x 200 mm) dry specimens for each of the six coarse aggregates used in this study. In each of these figures different symbols are used to distinguish between different cementitious material compositions of high strength concretes considered. Tables 7.3-A and 7.3-B present modulus of elasticity values for concretes with different cementitious material composition at different compressive strength levels for both dry and wet 4 x 8 in. (100 x 200 mm) specimens. From examination of these figures and tables it is clear that cementitious material composition, for the levels of replacement by weight of cement by fly ash and/or silica fume considered in this study, did not have a significant effect on the measured modulus of elasticity values.

To investigate what, if any, differences would result in modulus of elasticity of high-strength concrete if different types and brands of cements were used, comparisons were made between three sets of high-strength concretes made with three cements: Type III Brand 1 (TYPE III-1), Type III Brand 2 (TYPE III-2), and Type I Brand 2 (TYPE I-2) from two local cement manufacturers. Chemical and physical properties of the cements used are reported in Chapter 3. Each set included four high-strength concrete mixes made according to an identical basic mix design: 750 pcy cementitious material (445 kg/m^3), water-to-cementitious materials ratio of 0.30 and coarse aggregate-to-fine aggregate ratio of 1.5. Round river gravel (R1) was used as the coarse aggregate in these mixes. The variable within each set (the difference among the four high-strength concrete mixes made by each cement) was the cementitious materials composition. Each set comprised a control mix (Reference Mix) with no fly ash and no silica fume, a mix made with 20% of the weight of cement replaced by fly ash (FA Mix), a mix made with 7.5% of the weight of cement replaced by silica fume (SF Mix) and a mix made by replacing equal weight of cement by 20% fly ash and 7.5% silica fume (FA+SF Mix). Specimens from each set were heat-cured at 120 °F (50 °C) and 150 °F (65 °C). Companion specimens moist-cured in saturated lime-water from all three sets were also made to compare to the effects of heat-curing on modulus of elasticity of high-strength concrete. Figure 7.9 shows the test organization.

Results of the modulus of elasticity tests are reported in Tables 7.4-A through 7.4-C. For each curing condition, results are the average of two 4 x 8 in. (100 x 200-mm.) cylinders unless otherwise specified. Examination of the data shows that the modulus of elasticity of heat-cured high strength concrete at 1-day was affected only by the presence of 20 percent fly ash in the mix (FA mixes). Mixes with 20 percent fly ash resulted in the lowest values for modulus of elasticity while 1-day modulus of elasticity of all other high strength concrete mixes were practically the same. However, the difference between modulus of elasticity of mixes with 20 percent fly ash and all other mixes, for all curing conditions, was insignificant at all other ages.

No systematic differences due to difference in types and brands of cements were observed. High strength concretes made with different types and different brands of cement resulted in practically identical values of modulus of elasticity when cured and tested under identical conditions.

7.9 Measured Values versus Predicted Values

Figure 7.10 shows plots of proposed modulus of elasticity-compressive strength relationships which were discussed in detail in Chapter 6. All of these equations relate the modulus of elasticity of concrete to a less than unity power of compressive strength. Two of these equations, New RC and CEB-FIP equations, include parameters that account for the type of aggregate used in the concrete mix. The New RC equation includes an additional parameter which takes into consideration mineral additives such as fly ash and silica fume. For different values of these parameters, different plots can be obtained. In Figure 11 each of these two equations are represented by two curves one for the highest predicted values (upper bound) and one for the lowest predicted values (lower bound).

The modulus of elasticity was measured after 1-day (heat-cured specimens only), 28-, 182- and 365-days on 4 x 8 in. (100 x 200 mm) cylinders and after 1-day (heat-cured specimens only) and 28-days on 6 x 12 in. (150 x 300 mm) cylinders. Figures 7.11-A and 7.11-B show comparisons of the modulus of elasticity and compressive strengths measured on both 4 x 8 in. (100 x 200

mm) and 6 x 12 in. (150 x 300 mm) cylinders relative to these six equations. For forty mixes (Mix No. 100 to Mix No. 139 of Table 7.1), the differences between the predicted and measured values were calculated using actual unit weights of both heat-cured and moist-cured 6 x 12 in. (150 x 300 mm) concrete cylinders. The results are discussed below:

***ACI 318 Relationship*:** For high strength concrete, the ACI 318 equation overestimates the measured modulus of elasticity of 6 x 12 in. (150 x 300 mm) cylinders. The observed differentials were clearly a function of type of aggregate used and were the highest for concretes made with limestones (11% to 39%) and the lowest for concretes made with round river gravel (-6% to 23%). The range of differences observed for concretes made with partially crushed river gravel and granite were (9% to 34%) and (4% to 31%) respectively.

***ACI 363 Relationship*:** Good agreement was found between predicted and measured values for modulus of elasticity of high strength concrete made with all types of coarse aggregate and for both curing conditions. The ACI 363 relationship was a better predictor for moist-cured specimens and slightly overestimated heat-cured test results. The observed differences between predicted and measured values of modulus of elasticity ranged from -5% to 20% for concretes made with limestone, -8% to 13% for concretes made with granite, -17% to 5% for concretes made with round river gravel, and -5% to 14% for concretes made with partially crushed river gravel.

***Ahmad and Shah Relationship*:** Good agreement was found between predicted and measured values for modulus of elasticity of high strength concrete made with all types of coarse aggregate and for both curing conditions. The Ahmad and Shah relationship predicted modulus of elasticity of concretes made with low absorption limestone with better accuracy (differential range: 13% to 21% for heat-cured specimens and 7% to 15% for moist-cured specimens) than those for concretes made with high absorption limestone (differential range: 20% to 34% for heat-cured specimens and 4% to 20% for moist-cured specimens). As was the case for the ACI 363 relationship, the Ahmad and Shah relationship was a better predictor for moist-cured

specimens and slightly overestimated heat-cured test results. The observed differences between predicted and measured values of modulus of elasticity ranged from 4% to 34% for concretes made with limestone, 1% to 21% for concretes made with granite, -8% to 14% for concretes made with round river gravel, and 4% to 23% for concretes made with partially crushed river gravel.

New RC Relationship: Modulus of elasticity values of high strength concretes made with limestone were overestimated by the New RC relationship when the proposed New RC aggregate coefficients were used. The difference between predicted and measured values of modulus of elasticity ranged from 23% to 44% for heat-cured specimens and 10% to 37% for moist-cured specimens. Therefore due to variations in quality of aggregates at different locations, aggregate coefficients must be determined for local materials and a predetermined set of coefficients cannot always be used to predict high strength concrete modulus of elasticity. For other types of coarse aggregates used and both curing conditions the New RC equation had a tendency to slightly underestimate modulus of elasticity values of high strength concretes. The observed differences between predicted and measured values of modulus of elasticity ranged from -13% to 11% for concretes made with granite, -16% to 7% for concretes made with round river gravel, and -9% to 14% for concretes made with partially crushed river gravel.

CEB-FIP Relationship: The calculated values were in good agreement with the actual measured modulus of elasticity values. On average, the CEB-FIP relationship slightly overestimated the modulus of elasticity values for heat-cured specimens and slightly underestimated the modulus of elasticity values of moist-cured specimens. For heat-cured specimens the variations ranged between -2% to 11% for concretes made with limestone, -2% to 19% for concretes made with granite, -11% to 8% for concretes made with round river gravel, and 2% to 18% for concretes made with partially crushed river gravel. For moist-cured specimens the differences between predicted and measured values of modulus of elasticity ranged from -18% to -3% for concretes made with limestone, -18% to 5% for concretes made with granite, -17% to 2% for concretes made with round river gravel, and -14% to 1% for

concretes made with partially crushed river gravel. As was mentioned earlier, the CEB-FIP relationship includes an aggregate related correction factor.

NS 3473 Relationship: The modulus of elasticity obtained using Norwegian code equation underestimated the actual values of modulus of elasticity for all aggregate types and curing conditions. For concretes considered here, the variations ranged from -20% to 1% for concretes made with limestone, -19% to -2% for concretes made with granite, -25% to -10% for concretes made with round river gravel, and -20% to -3% for concretes made with partially crushed river gravel.

7.10 Concluding Remarks

The repeatability of modulus of elasticity tests was investigated with twenty tests by comparing the results of the first and second loading and unloading cycles. Negligible differences were observed among the two tests. Consequently, the remainder of the modulus of elasticity values were obtained conducting just one load cycle.

The effect of moisture condition of the specimens had a significant impact on the results. Higher modulus of elasticity values were observed for continuously moist-cured specimens relative to heat-cured or limited moist-cured specimens when tested at the same age. The opposite trend was observed for compressive strengths. The effect of testing specimens in a moist condition sometimes resulted in decreased compressive strengths observed relative to specimens tested in the dry condition.

The effect of specimen size was investigated by comparing the modulus of elasticity values of 4 x 8 in. (100 x 200 mm) specimens to those of 6 x 12 in. (150 x 300 mm) specimens. The 4 x 8 in. (100 x 200 mm) specimens exhibited an increase in stiffness of approximately 620,000 psi over that observed for the 6 x 12 in. (150 x 300 mm) specimens. This appeared as a constant offset in the results rather than a percentage increase with stiffness.

Changes in modulus of elasticity values with time were also investigated. The 1-day modulus of elasticity values were 98 percent of the 28-day values. At later ages (182-day and 365-day), the modulus of elasticity values were found to decrease slightly with respect to the 28-day values. In the case of the continuously moist-cured specimens, the modulus of elasticity values continued to increase with time (365-day value was 108 percent of the 28-day value).

The effect of aggregate type significantly affected the modulus of elasticity. Comparing the results of this study to the results of other researchers, it is difficult to generalize a coefficient for a certain type of aggregate source.

The type and brand of cement did not appear to have an effect on the modulus of elasticity. In addition, the effect of the cementitious material composition did not appear to have a significant effect on the results for the level of cement replacement considered in this study. The only exception was observed for the heat-cured specimens, which had 20 percent replacement of cement by weight with fly ash. These specimens had lower modulus of elasticity values at 1-day of age in comparison with the other mixes. With only this exception, the difference between modulus of elasticity values of all mixes for all curing conditions was insignificant at all ages.

In comparing the measured modulus of elasticity values relative to the predicted values, the ACI 318 relation was found to overestimate the results of the 6 x 12 in. (150 x 300 mm) cylinders as their compressive strength increased. In general, the ACI 363 relation was a conservative lower bound to the results. The New RC and CEB-FIP relations provide coefficients, which account for aggregate type. In addition the New RC relation includes coefficients to account for the cementitious composition. Both the New RC and CEB-FIP relations were found to bound the data observed in these tests; However, the aggregate coefficients provided in the New RC relations predicted bounds for the limestone and round gravel mixes which were opposite to those observed in these tests. As mentioned above, the aggregate type appears to dominate the stiffness of high strength concrete, but it is difficult to

generalize the effect of aggregate because of the variation in aggregate properties with geographical source.

TABLE 7.1. Test matrix for modulus of elasticity study.

No.	Mix ID Code	4 x 8 in. (100 x 200 mm)													6 x 12 in. (150 x 300 mm)		
		H				HW1	HW3	W7	W14	W28			W182	W365	H		W28
		1	28	182	365	28	28	28	28	28	182	365	182	365	1	28	28
22	131-MBL1-F00M00-130	X	X												X	X	
23	331-MBL1-F00M00-130		X													X	
24	131-MBL1-F30M00-130		X													X	
25	331-MBL1-F30M00-130		X												X	X	X
26	131-MBL1-F00M15-130		X												X	X	X
27	331-MBL1-F00M15-130	X	X												X	X	X
28	131-MBL1-F30M15-130	X	X												X	X	X
29	331-MBL1-F30M15-130	X	X												X	X	
50	231-MBL1-F00M00-130	X	X	X							X				X	X	X
51	231-MBL1-F30M00-130	X	X	X							X				X	X	X
52	231-MBL1-F00M15-130	X	X	X							X				X	X	X
53	231-MBL1-F30M15-130	X	X	X							X				X	X	X
54	131-MBL1-F00M75-130	X	X	X							X				X	X	X
55	131-MBL1-F00M10-130	X	X	X							X				X	X	X
56	231-MBL1-F00M75-130	X	X	X							X				X	X	X
57	231-MBL1-F00M10-130	X	X	X							X				X	X	X
58	331-MBL1-F00M10-130	X	X	X							X				X	X	X
59	331-MBL1-F00M75-130	X	X	X							X				X	X	X
60	131-MBL1-F10M00-130	X	X	X							X				X	X	X
61	131-MBL1-F10M75-130	X	X	X											X	X	X
62	131-MBL1-F10M10-130	X	X	X							X				X	X	X
63	231-MBL1-F10M00-130	X	X	X							X				X	X	X
64	231-MBL1-F10M75-130	X	X	X							X				X	X	X
65	231-MBL1-F10M10-130	X	X	X							X				X	X	X
66	331-MBL1-F10M00-130	X	X	X							X				X	X	X
67	331-MBL1-F10M75-130	X	X	X							X				X	X	X
68	331-MBL1-F10M10-130	X	X	X							X				X	X	X
69	131-MBL1-F20M00-130	X	X	X							X				X	X	X
70	131-MBL1-F20M75-130	X	X	X							X				X	X	X
71	131-MBL1-F20M10-130	X	X	X							X				X	X	X
72	231-MBL1-F20M00-130	X	X	X							X				X	X	X
73	231-MBL1-F20M75-130	X	X	X							X				X	X	X
74	231-MBL1-F20M10-130	X	X	X							X				X	X	X

TABLE 7.1. Test matrix for modulus of elasticity study. (continued ...)

No.	Mix ID Code	4 x 8 in. (100 x 200 mm)													6 x 12 in. (150 x 300 mm)		
		H				HW1	HW3	W7	W14	W28			W182	W365	H		W28
		1	28	182	365	28	28	28	28	28	182	365	182	365	1	28	28
75	331-MBL1-F20M00-130	X	X	X							X				X	X	X
76	231-MBL1-F20M75-130	X	X	X							X				X	X	X
77	331-MBL1-F20M10-130	X	X	X							X				X	X	X
78	131-MBL1-F30M75-130	X	X	X							X				X	X	X
79	131-MBL1-F30M10-130	X	X	X											X	X	X
80	231-MBL1-F30M75-130	X	X	X							X				X	X	X
81	231-MBL1-F30M10-130	X	X	X							X				X	X	X
82	331-MBL1-F30M75-130	X	X	X							X				X	X	X
83	331-MBL1-F30M10-130	X	X	X							X				X	X	X
84	131-XBR2-F00M00-130	X	X	X							X				X	X	X
85	131-XBR2-F00M15-130	X	X	X							X				X	X	X
86	131-XBR2-F30M00-130	X	X	X							X				X	X	X
87	131-XBR2-F30M15-130	X	X	X							X				X	X	X
88	331-XBR2-F00M00-130	X	X	X							X				X	X	X
89	331-XBR2-F00M15-130	X	X	X							X				X	X	X
90	331-XBR2-F30M15-130	X	X	X							X				X	X	X
91	331-XBR2-F30M15-130	X	X	X							X				X	X	X
92	131-SAG1-F00M00-130		X	X						X	X						
93	131-SAG1-F10M00-130		X	X						X	X						
94	131-SAG1-F00M75-130		X	X						X	X						
95	131-SAG1-F10M75-130		X	X						X	X						
96	131-XAG1-F00M00-130		X	X						X	X						
97	131-XAG1-F10M00-130		X	X						X	X						
98	131-XAG1-F00M75-130		X	X						X	X						
99	131-XAG1-F10M75-130		X	X						X	X						
100#	112-XAR1-F00M00-130	X	X	X	X	X	X	X	X	X	X	X	X	X	X	X	X
101	112-XAR1-F00M00-130	X	X	X	X	X	X								X	X	
102#	112-XAR1-F20M00-130	X	X	X	X	X	X	X	X	X	X	X	X	X	X	X	X
103	112-XAR1-F20M00-130	X	X	X	X	X	X								X	X	
104#	112-XAR1-F00M75-130	X	X	X	X	X	X	X	X	X	X	X	X	X	X	X	X
105	112-XAR1-F00M75-130	X	X	X	X	X	X								X	X	
106#	112-XAR1-F20M75-130	X	X	X	X	X	X	X	X	X	X	X	X	X	X	X	X
107	112-XAR1-F20M75-130	X	X	X	X	X	X								X	X	

Heat-cured at 120 °F

TABLE 7.1. Test matrix for modulus of elasticity study. (continued ...)

No.	Mix ID Code	4 x 8 in. (100 x 200 mm)													6 x 12 in. (150 x 300 mm)		
		H				HW1	HW3	W7	W14	W28			W182	W365	H		W28
		1	28	182	365	28	28	28	28	28	182	365	182	365	1	28	28
108	131-XAR1-F00M00-130	X	X	X	X	X	X	X	X	X	X	X	X	X	X	X	X
109	132-XAR1-F00M00-130	X	X	X	X	X	X	X	X	X	X	X	X	X	X	X	X
110	131-XAR1-F20M00-130	X	X	X	X	X	X	X	X	X	X	X	X	X	X	X	X
111	132-XAR1-F20M00-130	X	X	X	X	X	X	X	X	X	X	X	X	X	X	X	X
112	131-XAR1-F00M75-130	X	X	X	X	X	X	X	X	X	X	X	X	X	X	X	X
113	132-XAR1-F00M75-130	X	X	X	X	X	X	X	X	X	X	X	X	X	X	X	X
114	131-XAR1-F20M75-130	X	X	X	X	X	X	X	X	X	X	X	X	X	X	X	X
115	132-XAR1-F20M75-130	X	X	X	X	X	X	X	X	X	X	X	X	X	X	X	X
116#	131-XAR1-F00M00-130	X	X	X	X	X	X								X	X	
117#	132-XAR1-F00M00-130	X	X	X	X	X	X								X	X	
118#	131-XAR1-F20M00-130	X	X	X	X	X	X								X	X	
119#	132-XAR1-F20M00-130	X	X	X	X		X								X		
120#	131-XAR1-F00M75-130	X	X	X	X	X	X								X	X	
121#	132-XAR1-F00M75-130	X	X	X	X	X	X								X	X	
122#	131-XAR1-F20M75-130	X	X	X	X	X	X								X	X	
123#	132-XAR1-F20M75-130	X	X	X	X	X	X								X	X	
124	131-XAL1-F00M00-130	X	X	X	X	X	X	X	X	X	X	X	X	X	X	X	X
125	131-XAL1-F00M75-130	X	X	X	X	X	X	X	X	X	X	X	X	X	X	X	X
126	131-XAL1-F20M00-130	X	X	X	X	X	X	X	X	X	X	X	X	X	X	X	X
127	131-XAL1-F20M75-130	X	X	X	X	X	X	X	X	X	X	X	X	X	X	X	X
128	131-XAR2-F00M00-130	X	X	X	X	X	X	X	X	X	X	X	X	X	X	X	X
129	131-XAR2-F00M75-130	X	X	X	X	X	X	X	X	X	X	X	X	X	X	X	X
130	131-XAR2-F20M00-130	X	X	X	X	X	X	X	X		X	X	X	X	X	X	X
131	131-XAR2-F20M75-130	X	X	X	X	X	X	X	X	X	X	X	X	X	X	X	X
132	131-XAL2-F00M00-130	X	X	X	X	X	X	X	X	X	X	X	X	X	X	X	X
133	131-XAL2-F00M75-130	X	X	X	X	X	X	X	X	X	X	X	X	X	X	X	X
134	131-XAL2-F20M00-130	X	X	X	X	X	X	X	X	X	X	X	X	X	X	X	X
135	131-XAL2-F20M75-130	X	X	X	X	X	X	X	X	X	X	X	X	X	X	X	X
136	131-XAG2-F00M00-130	X	X	X	X	X	X	X	X	X	X	X	X	X	X	X	X
137	131-XAG2-F00M75-130	X	X	X	X	X	X	X	X	X	X	X	X	X	X	X	X
138	131-XAG2-F20M00-130	X	X	X	X	X	X	X	X	X	X	X	X	X	X	X	X
139	131-XAG2-F20M75-130	X	X	X	X	X	X	X	X	X	X	X	X	X	X	X	X

Heat-cured at 120 °F

TABLE 7.2. Modulus of elasticity of 4 x 8 in. (100 x 200 mm) high strength concretes specimens calculated for each of the two loading/unloading cycles

Mix No.	Moist-cured				Heat-cured	
	Specimen #1		Specimen #2		Specimen #1	
	Cycle #1 psi *(GPa)* R^2	Cycle #2 psi *(GPa)* R^2	Cycle #1 psi *(GPa)* R^2	Cycle #2 psi *(GPa)* R^2	Cycle #1 psi *(GPa)* R^2	Cycle #2 psi *(GPa)* R^2
92	7892771 *(54.43)* 0.9969	7854313 *(54.17)* 0.9988	7748299 *(53.44)* 0.9983	7621948 *(52.57)* 0.9993	6085716 *(41.97)* 0.9985	6097351 *(42.05)* 0.9996
93	7675371 *(52.93)* 0.9987	7597536 *(52.40)* 0.9996	7858438 *(54.20)* 0.9989	7667589 *(52.88)* 0.9997	5611545 *(38.70)* 0.9991	5495911 *(37.90)* 0.9990
94	7757149 *(53.50)* 0.9981	7833552 *(54.02)* 0.9992	7774351 *(53.62)* 0.9990	7742626 *(53.40)* 0.9998	5526825 *(38.12)* 0.9992	5473312 *(37.75)* 0.9986
95	7882607 *(54.36)* 0.9986	7767347 *(53.57)* 0.9998	NA	NA	5390364 *(37.17)* 0.9983	5328913 *(36.75)* 0.9975
96	7901822 *(54.50)* 0.9991	7800212 *(53.79)* 0.9999	8138752 *(56.13)* 0.9989	7980464 *(55.04)* 0.9998	6464812 *(44.58)* 0.9989	6357043 *(43.84)* 0.9996
97	7708408 *(53.16)* 0.9990	7795428 *(53.76)* 0.9994	NA	NA	5750642 *(39.66)* 0.9991	5662029 *(39.05)* 0.9987
98	8103781 *(55.89)* 0.9994	7965009 *(54.93)* 0.9997	7734437 *(53.34)* 0.9989	7836108 *(54.04)* 0.9997	6167880 *(42.54)* 0.9997	6000984 *(41.39)* 0.9986
99	7698035 *(53.09)* 0.9990	7633014 *(52.64)* 0.9999	7978862 *(55.03)* 0.9993	7997987 *(55.16)* 0.9991	5891832 *(40.63)* 0.9993	5797135 *(39.98)* 0.9986

TABLE 7.3-A. Average modulus of elasticity of 4 x 8 in. (100 x 200 mm) high strength concretes made with different cementitious material compositions at different compressive strength levels (Dry specimens).

Compressive Strength Level psi *(MPa)*	Reference Mixes psi *(GPa)*	Fly Ash Mixes psi *(GPa)*	Silica Fume Mixes psi *(GPa)*	Fly Ash + Silica Fume Mixes psi *(GPa)*
6000-8000 *(41-55)*		5935081 *(40.93)*		4761277 *(32.84)*
8000-10000 *(55-69)*	6229454 *(42.96)*	6116327 *(42.18)*		5574077 *(38.44)*
10000-12000 *(69-83)*	6480240 *(44.69)*	6046899 *(41.70)*	5942101 *(40.98)*	5805725 *(40.04)*
12000-14000 *(83-97)*	6481006 *(44.70)*	6671571 *(46.01)*	6256218 *(43.15)*	6002017 *(41.39)*
14000-16000 *(97-110)*	6897061 *(47.57)*	6699881 *(46.21)*	6876352 *(47.42)*	6793345 *(46.85)*
16000-18000 *(110-124)*	6853158 *(47.26)*	7129840 *(49.17)*	6847908 *(47.23)*	6971692 *(48.08)*
18000-20000 *(124-138)*	7437487 *(51.29)*		7288696 *(50.27)*	7215740 *(49.76)*

TABLE 7.3-B. Average modulus of elasticity of 4 x 8 in. (100 x 200 mm) high strength concretes made with different cementitious material compositions at different compressive strength levels (Wet specimens).

Compressive Strength Level psi *(MPa)*	Reference Mixes psi *(GPa)*	Fly Ash Mixes psi *(GPa)*	Silica Fume Mixes psi *(GPa)*	Fly Ash + Silica Fume Mixes psi *(GPa)*
6000-8000 *(41-55)*				
8000-10000 *(55-69)*				
10000-12000 *(69-83)*	7149000 *(49.30)*	6999200 *(48.27)*		
12000-14000 *(83-97)*	7547220 *(52.05)*	7664104 *(52.86)*	7039000 *(48.54)*	7308667 *(50.40)*
14000-16000 *(97-110)*	7518004 *(51.85)*	7643564 *(52.71)*	7641750 *(52.70)*	7522631 *(51.88)*
16000-18000 *(110-124)*	7754038 *(53.48)*	8078583 *(55.71)*	7659101 *(52.82)*	7873020 *(54.30)*
18000-20000 *(124-138)*			7699161 *(53.10)*	

TABLE 7.4-A. Modulus of elasticity development of continuously moist-cured high strength concrete mixes made with different types and brands of cement, psi (GPa).

Age	Control (Ref.)			20% Fly Ash (FA)		
Days	III-1	III-2	I-2	III-1	III-2	I-2
1	-	-	-	-	-	-
28	7486000 (51.6)	7311000 (50.4)	7149000 (49.3)	6993000 (48.2)	6994000 (48.2)	6732000 (46.4)
182	7749000 (53.4)	7679000 (53.0)	7843000 (54.1)	7625000 (52.6)	7604000 (52.4)	7685000 (53.0)
365	7777000 (53.6)	7940000 (54.8)	7997000 (55.2)	7801000 (53.8)	7918000 (54.6)	7450000 (51.4)

Age	7.5% Silica Fume (SF)			20% FA+7.5% SF (FA+SF)		
Days	III-1	III-2	I-2	III-1	III-2	I-2
1	-	-	-	-	-	-
28	7581000 (52.3)	7232000 (49.9)	7039000 (48.6)	7575000 (52.2)	7419000 (51.2)	7033000* (48.5)
182	7599000 (52.4)	7990000 (55.1)	7519000 (51.9)	7676000 (52.9)	7521000 (51.9)	7470000 (51.5)
365	7887000 (54.4)	7760000 (53.5)	7897000 (54.5)	7973000 (55.0)	7626000 (52.6)	7929000 (54.7)

* Measured on one 4 x 8-in. (100 x 200-mm.) cylinder.

TABLE 7.4-B. Modulus of elasticity development of heat-cured high strength concrete mixes made with different types and brands of cement [120 °F (50 °C)], psi (GPa).

Age	Control (Ref.)			20% Fly Ash (FA)		
Days	III-1	III-2	I-2	III-1	III-2	I-2
1	6723000 (46.4)	6580000 (45.4)	6340000 (43.7)	6300000 (43.4)	6514000 (44.9)	5675000 (39.1)
28	6643000 (45.8)	6689000 (46.1)	6918000 (47.7)	6774000 (46.7)	6765000 (46.7)	6742000 (46.5)
182	6665000 (46.0)	6511000 (44.9)	6506000 (44.9)	6314000 (43.5)	6330000 (43.7)	6375000 (44.0)
365	6596000 (45.5)	6743000 (46.5)	6317000 (43.6)	6342000 (43.7)	6469000 (44.6)	6204000 (42.8)

Age	7.5% Silica Fume (SF)			20% FA+7.5% SF (FA+SF)		
Days	III-1	III-2	I-2	III-1	III-2	I-2
1	6809000 (47.0)	6500000 (44.8)	6714000 (46.3)	6509000 (44.9)	6555000 (45.2)	6755000 (46.6)
28	6843000 (47.2)	6949000 (47.9)	6930000 (47.8)	6415000 (44.2)	6535000 (45.1)	6755000 (46.6)
182	6202000 (42.8)	6124000 (42.2)	6231000 (43.0)	6146000 (42.4)	6258000 (43.2)	6262000 (43.2)
365	6318000 (43.6)	6402000 (44.2)	6441000 (44.4)	6101000 (42.1)	6162000 (42.5)	6456000 (44.5)

TABLE 7.4-C. Modulus of elasticity development of heat-cured high strength concrete mixes made with different types and brands of cement [150 °F (65 °C)], psi (GPa).

Age	Control (Ref.)			20% Fly Ash (FA)		
Days	III-1	III-2	I-2	III-1	III-2	I-2
1	6457000 (44.5)	6497000 (44.8)	6311000 (43.5)	6212000 (42.8)	6419000 (44.3)	6250000 (43.1)
28	6637000 (45.8)	6557000 (45.2)	6718000 (46.3)	6632000 (45.7)	6588000 (45.4)	6440000 (44.4)
182	6354000 (43.8)	6268000 (43.2)	6712000* (46.3)	6291000 (43.4)	6362000 (43.9)	6066000 (41.8)
365	6230000 (43.0)	6290000 (43.4)	6638000 (45.8)	6227000 (42.9)	6242000 (43.1)	6349000 (43.8)

Age	7.5% Silica Fume (SF)			20% FA+7.5% SF (FA+SF)		
Days	III-1	III-2	I-2	III-1	III-2	I-2
1	6460000 (44.6)	6705000 (46.2)	6807000 (47.0)	6438000 (44.4)	6756000 (46.6)	6559000 (45.2)
28	6670000 (46.0)	6680000 (46.1)	6758000 (46.6)	6559000 (45.2)	6499000 (44.8)	6599000 (45.5)
182	6134000 (42.3)	6406000 (44.2)	6074000 (41.9)	6057000 (41.8)	6036000 (41.6)	5892000 (40.6)
365	6258000 (43.2)	6287000 (43.4)	6341000 (43.7)	6339000 (43.7)	6097000 (42.1)	5915000 (40.8)

* Measured on one 4 x 8-in. (100 x 200-mm.) cylinder.

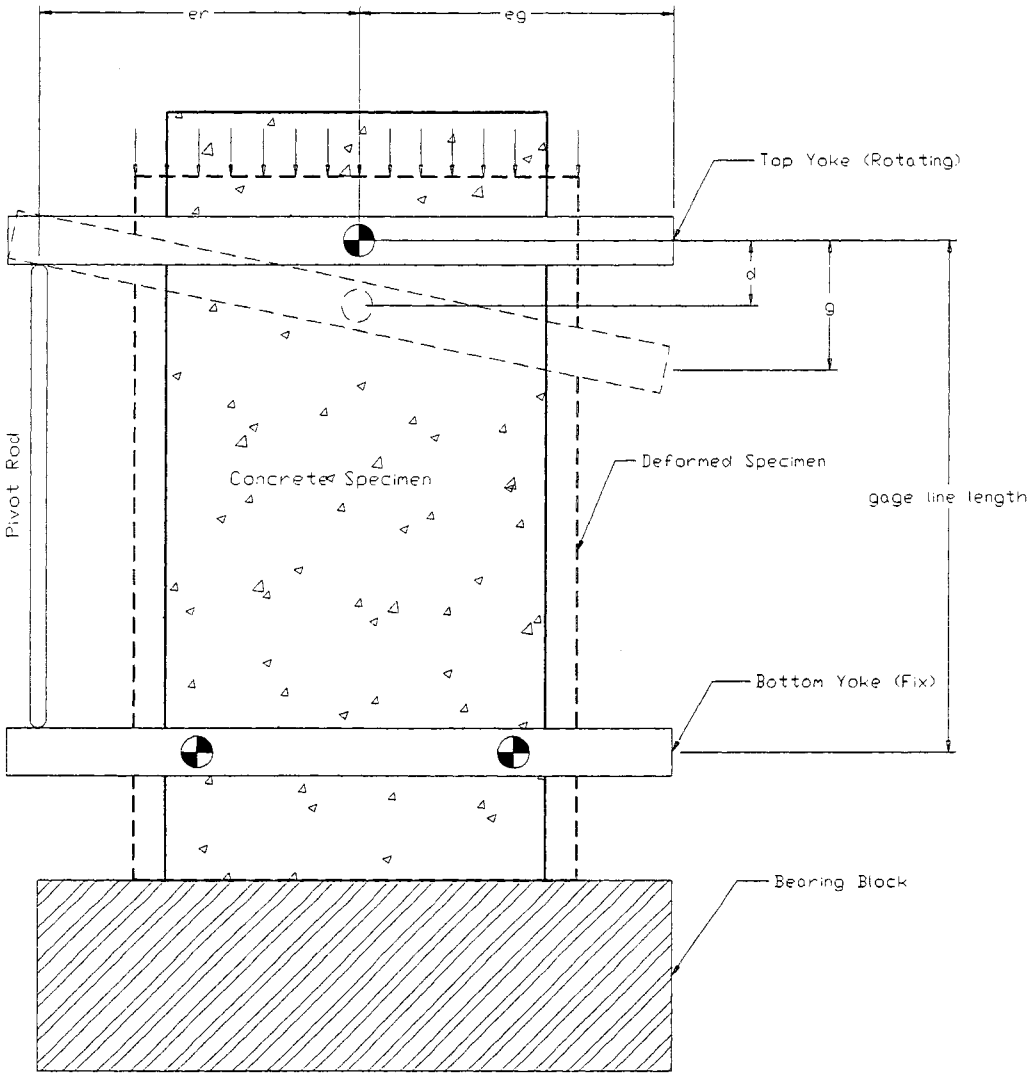

Figure 7.1. A typical compressometer with a lever multiplying system; $(d = ge_r/(e_r+e_g)$ [E-SETUP.PLT]

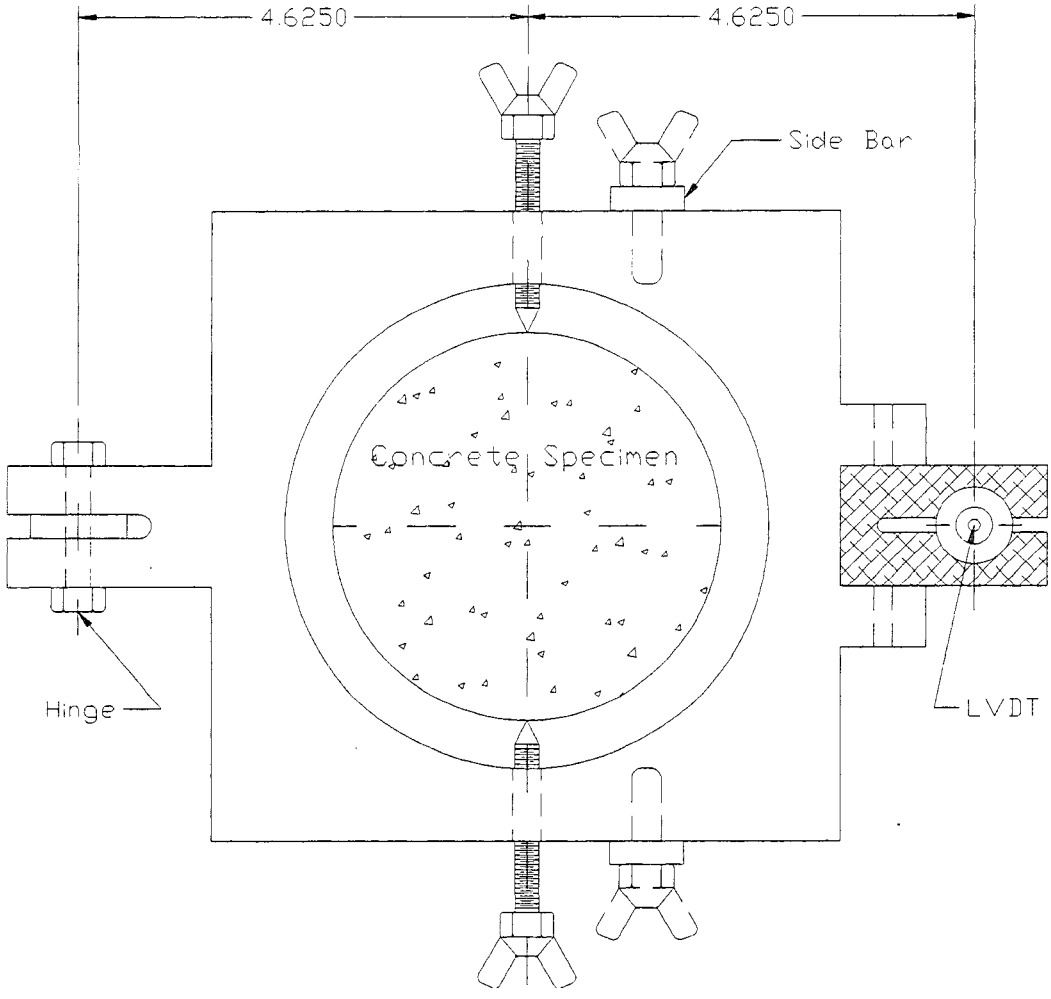

Figure 7.2-A. Top yoke (rotating yoke) of the electronic compressometer used for testing 4 x 8 in. (100 x 200 mm) specimens (top view)
[TOP-YOKE.PLT]

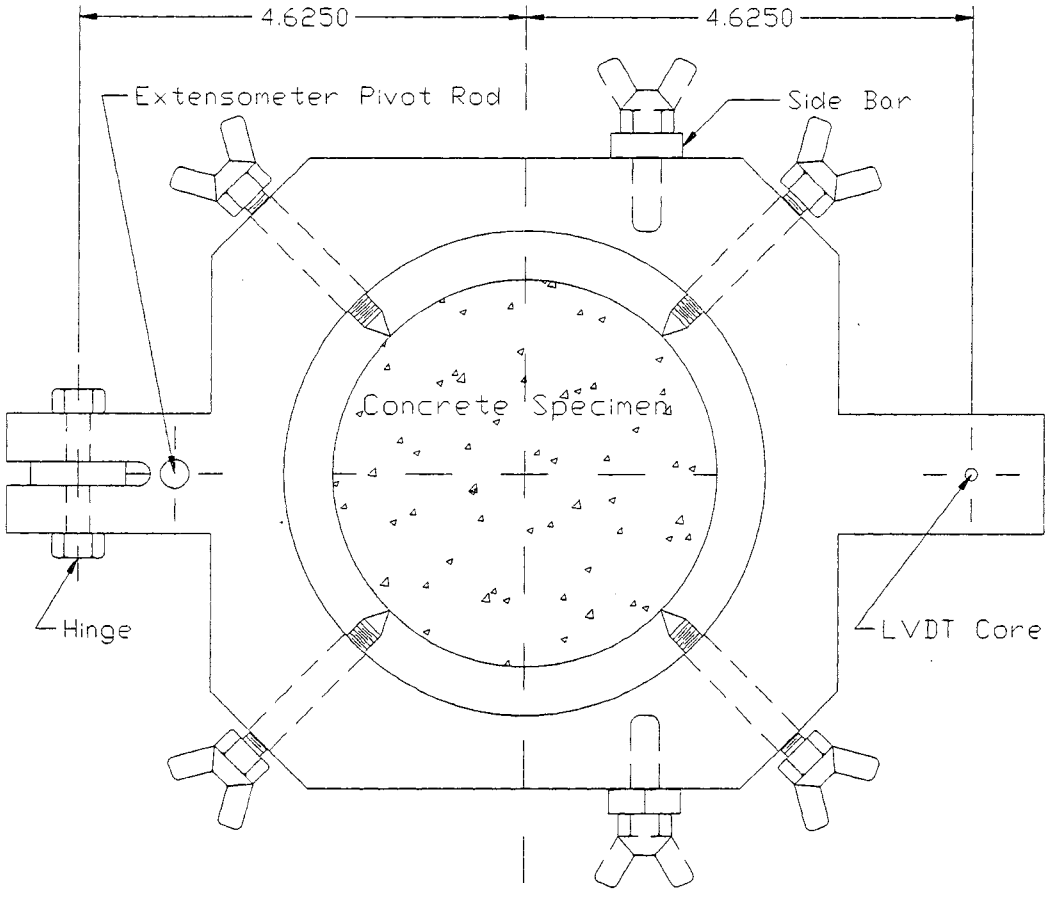

Figure 7.2-B. Bottom yoke (fixed yoke) of the electronic compressometer used for testing 4 x 8 in. (100 x 200 mm) specimens (top view)
[BOt-YOKE.PLT]

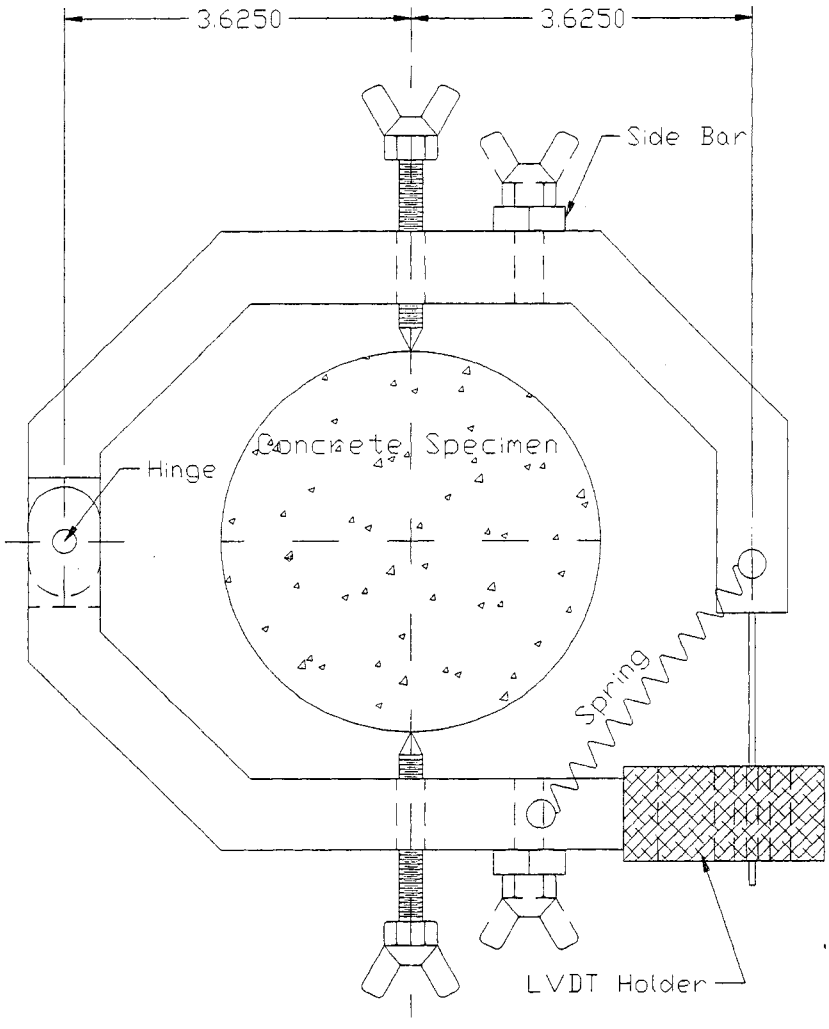

Figure 7.2-C. Middle yoke (extensometer) of the electronic compressometer for testing Poisson's ratio of 4 x 8 in. (100 x 200 mm) specimens (top view)
[MID-YOKE.PLT]

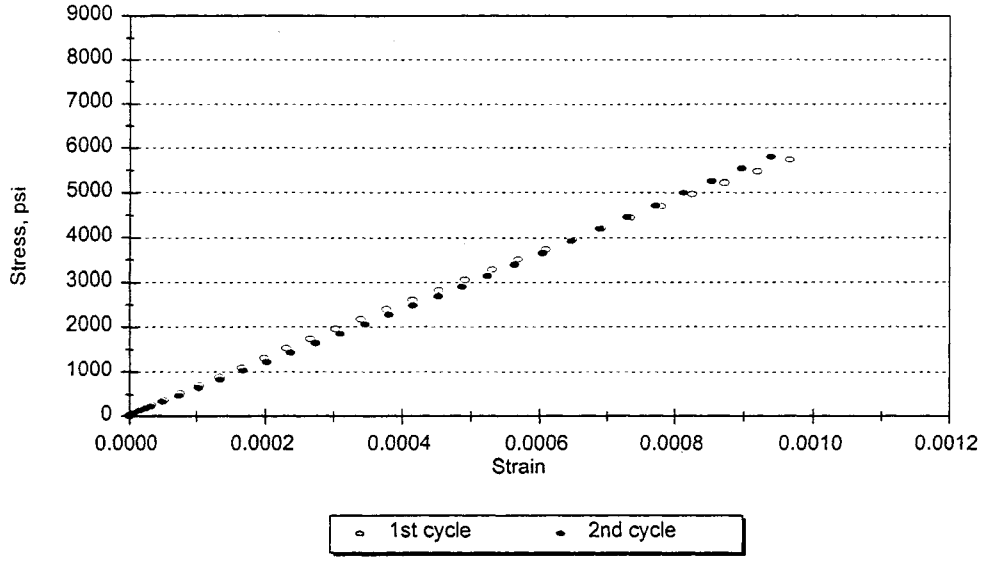

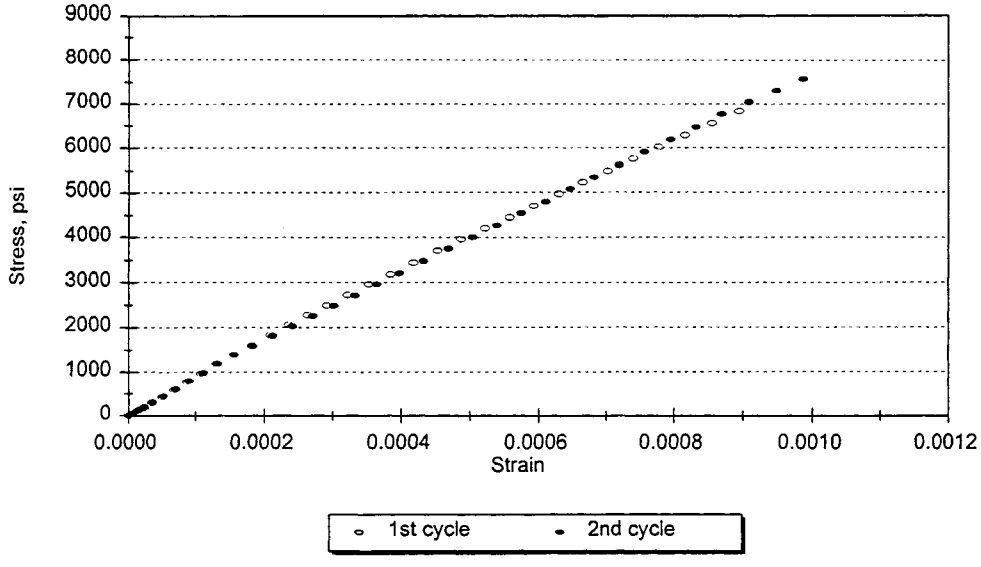

Figure 7.3-A. Stress-strain curves from two consecutive loading/unloading cycles at 50 percent of the ultimate compressive strength. Top: 92-H182-S1; Bottom: 92-W182-S1 [92H182S1.WMF & 92W182S1.WMF]

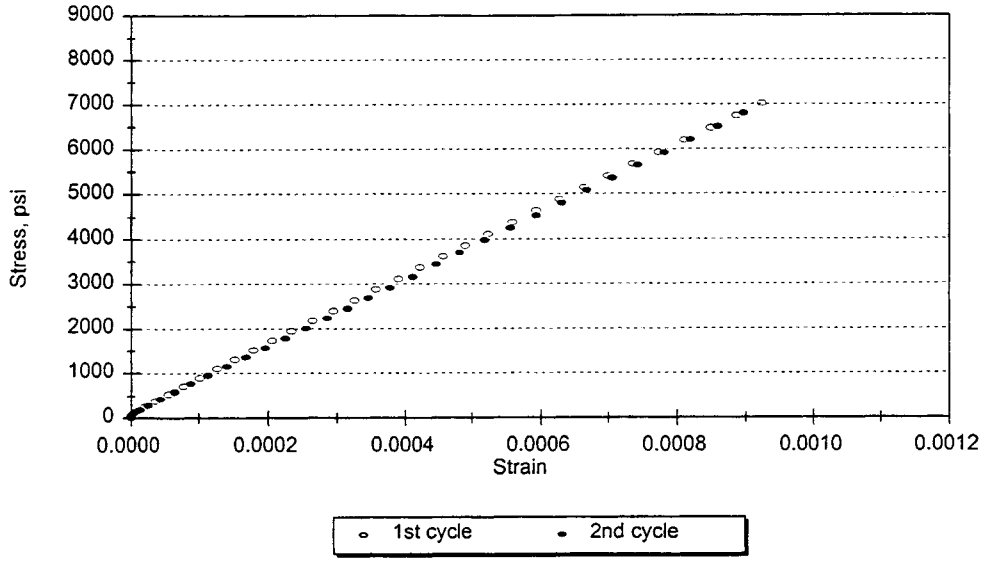

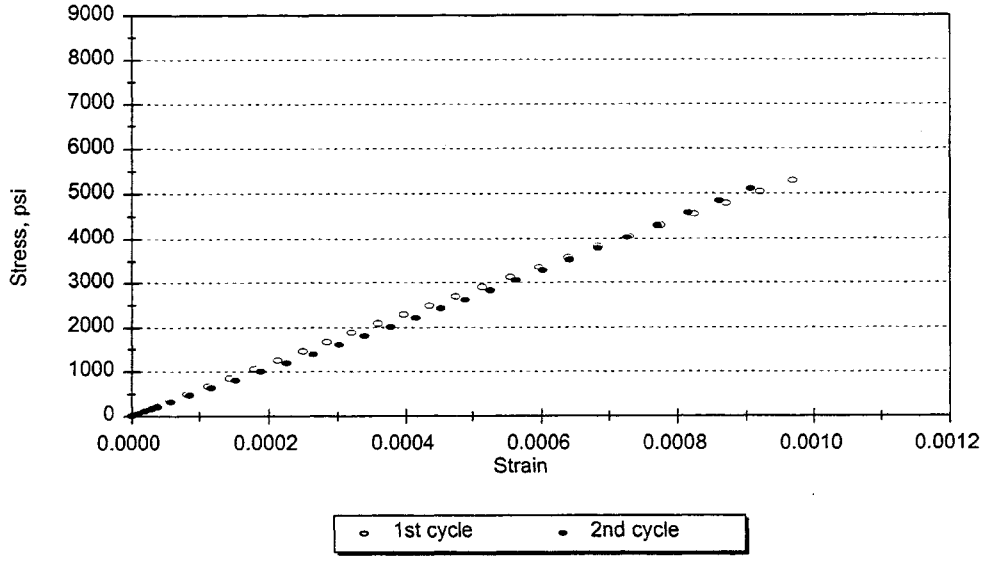

Figure 7.3-B. Stress-strain curves from two consecutive loading/unloading cycles at 50 percent of the ultimate compressive strength. Top: 92-W182-S2; Bottom: 93-H182-S1 [92W182S2.WMF & 93H182S1.WMF]

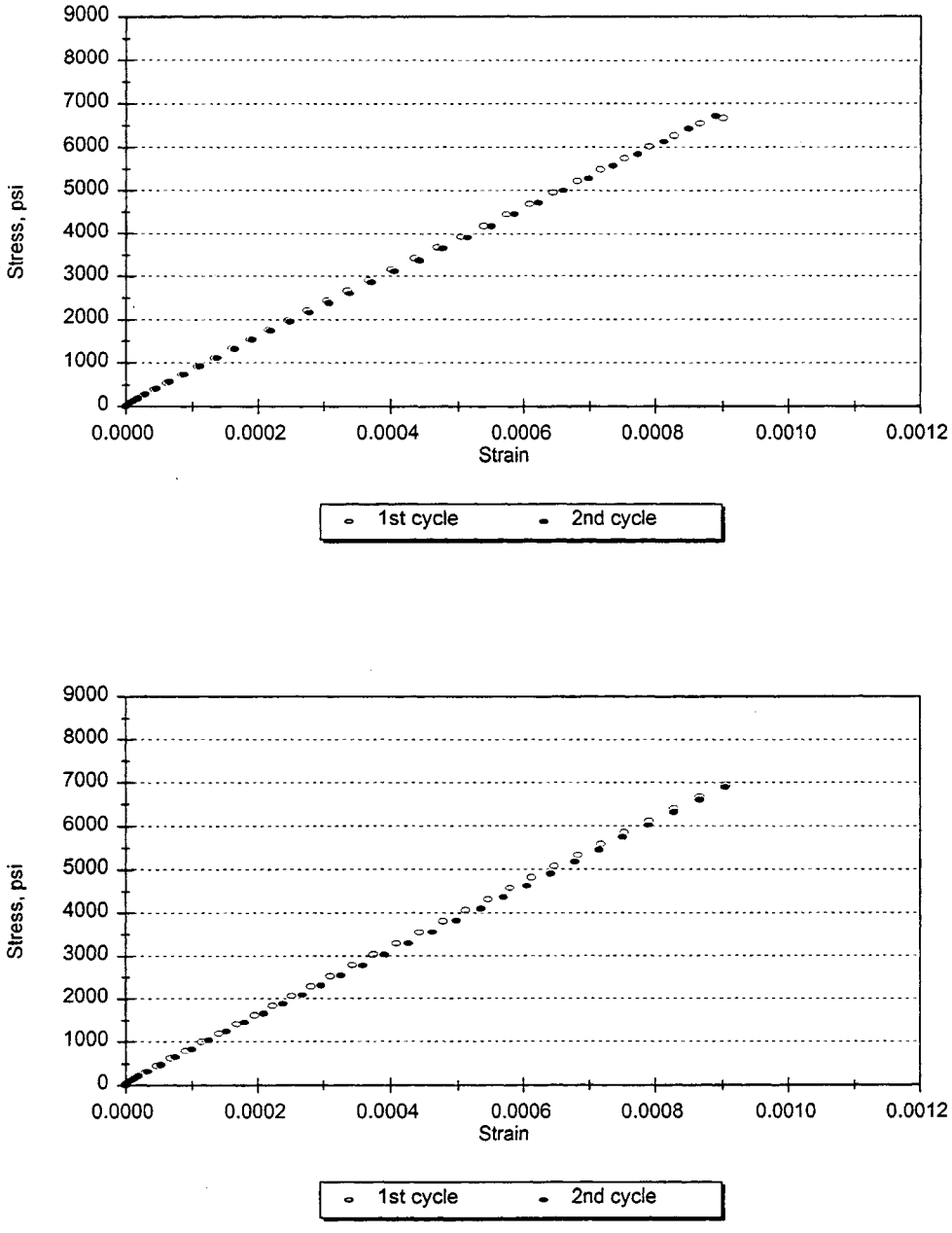

Figure 7.3-C. Stress-strain curves from two consecutive loading/unloading cycles at 50 percent of the ultimate compressive strength. Top: 93-W182-S1; Bottom: 93-W182-S2 [93W182S1.WMF & 93W182S2.WMF]

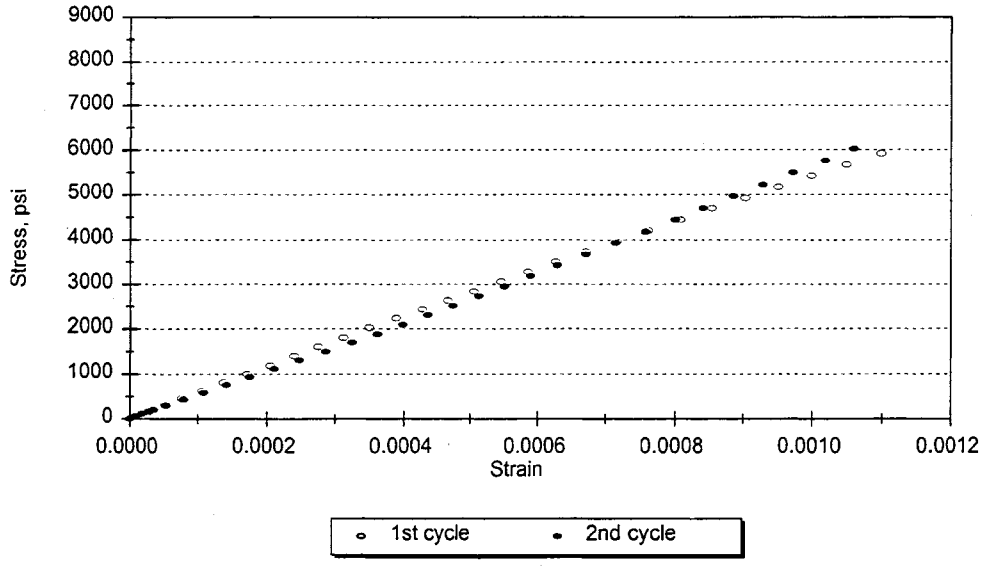

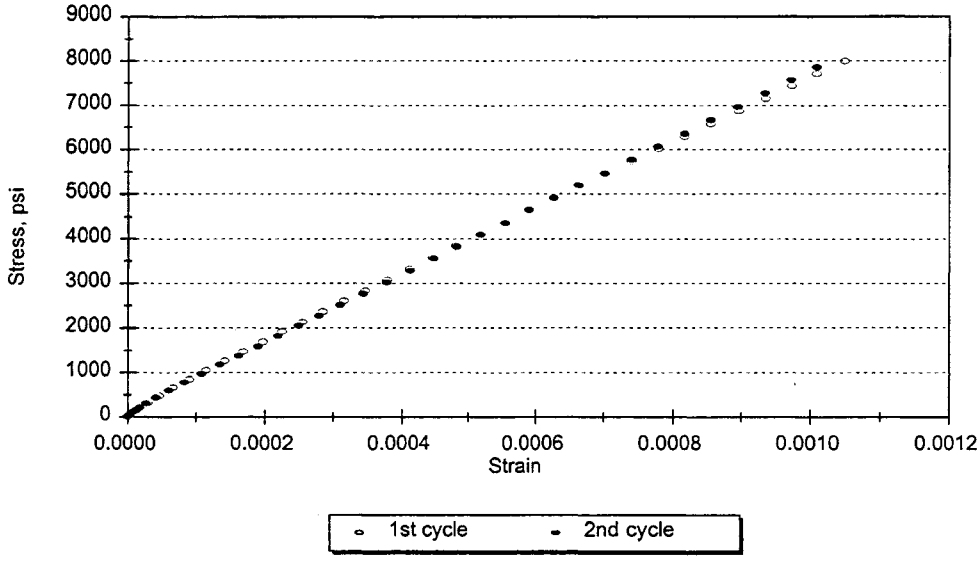

Figure 7.3-D. Stress-strain curves from two consecutive loading/unloading cycles at 50 percent of the ultimate compressive strength. Top: 94-H182-S1; Bottom: 94-W182-S1 [94H182S1.WMF & 94W182S1.WMF]

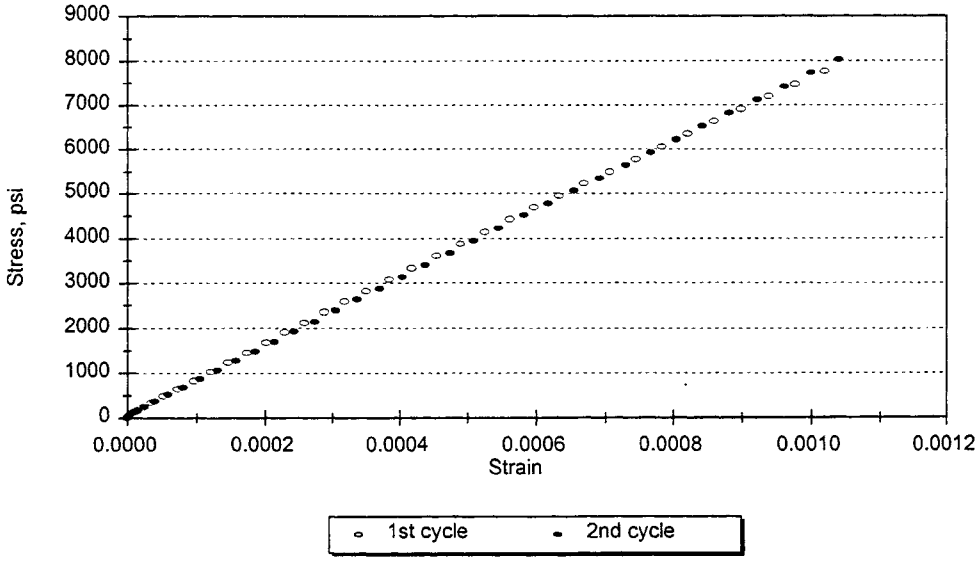

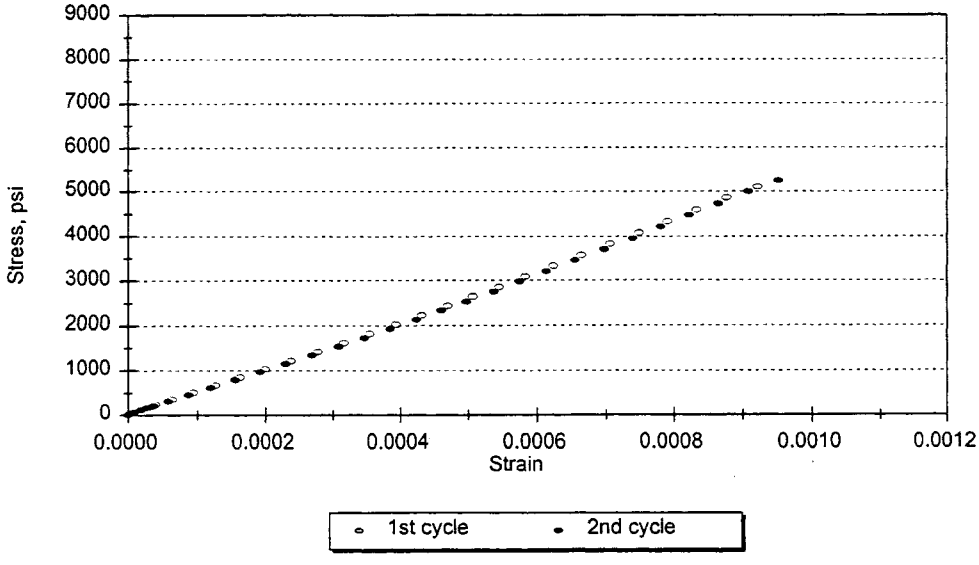

Figure 7.3-E. Stress-strain curves from two consecutive loading/unloading cycles at 50 percent of the ultimate compressive strength. Top: 94-W182-S2; Bottom: 95-H182-S1 [94W182S2.WMF & 95H182S1.WMF]

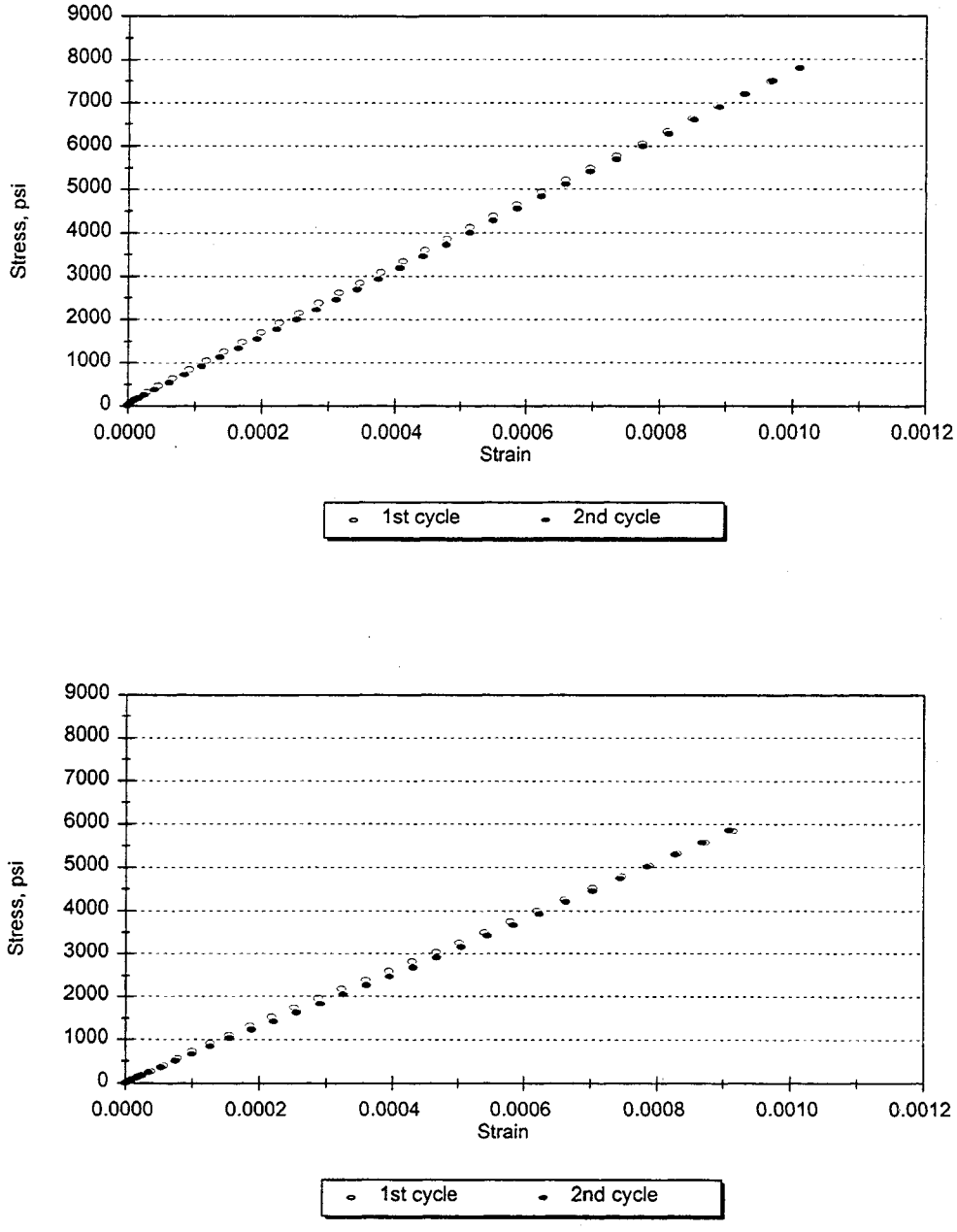

Figure 7.3-F. Stress-strain curves from two consecutive loading/unloading cycles at 50 percent of the ultimate compressive strength. Top: 95-W182-S1; Bottom: 96-H182-S1 [95W182S1.WMF & 96H182S1.WMF]

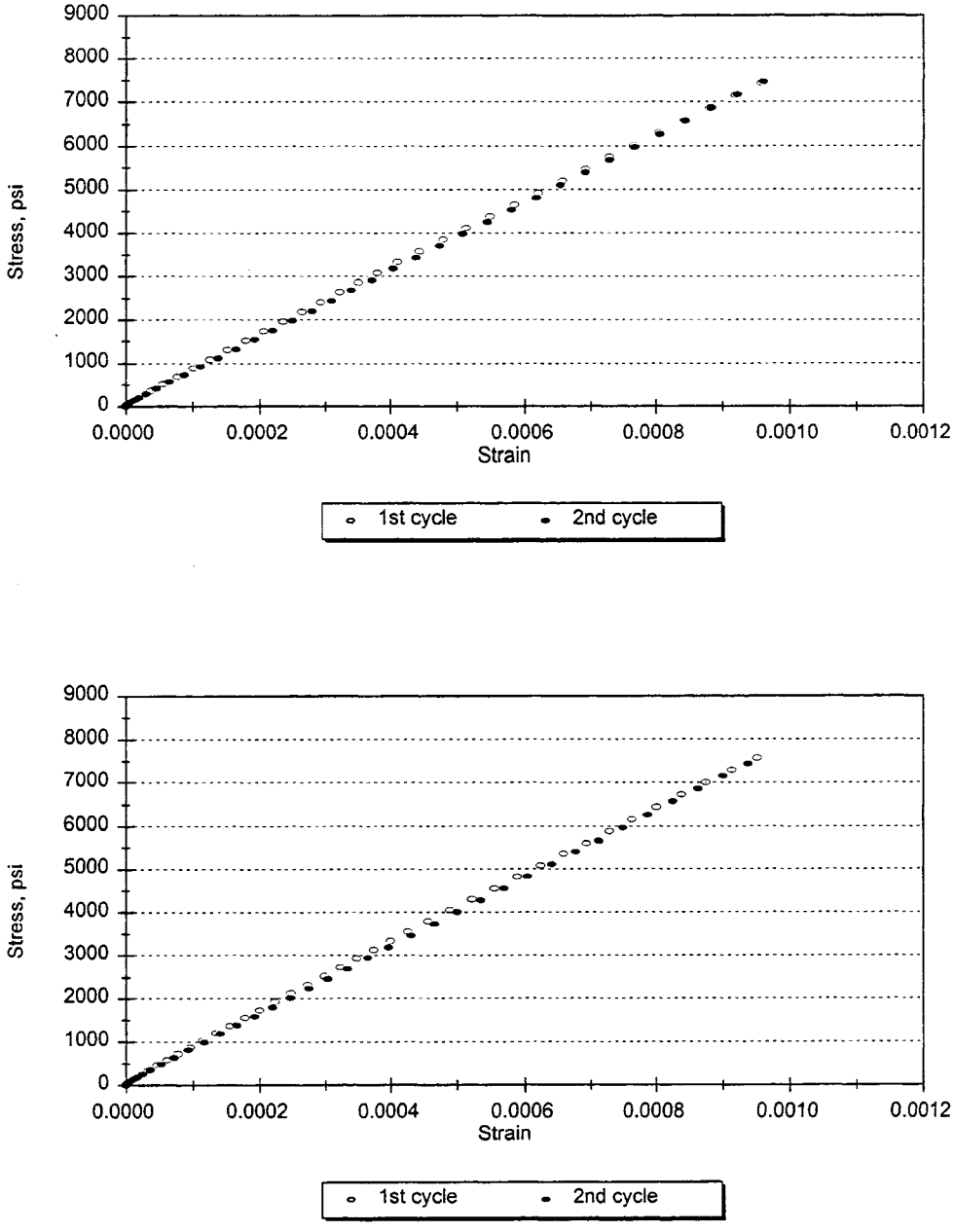

Figure 7.3-G. Stress-strain curves from two consecutive loading/unloading cycles at 50 percent of the ultimate compressive strength. Top: 96-W182-S1; Bottom: 96-W182-S2 [96W182S1.WMF & 96W182S2.WMF]

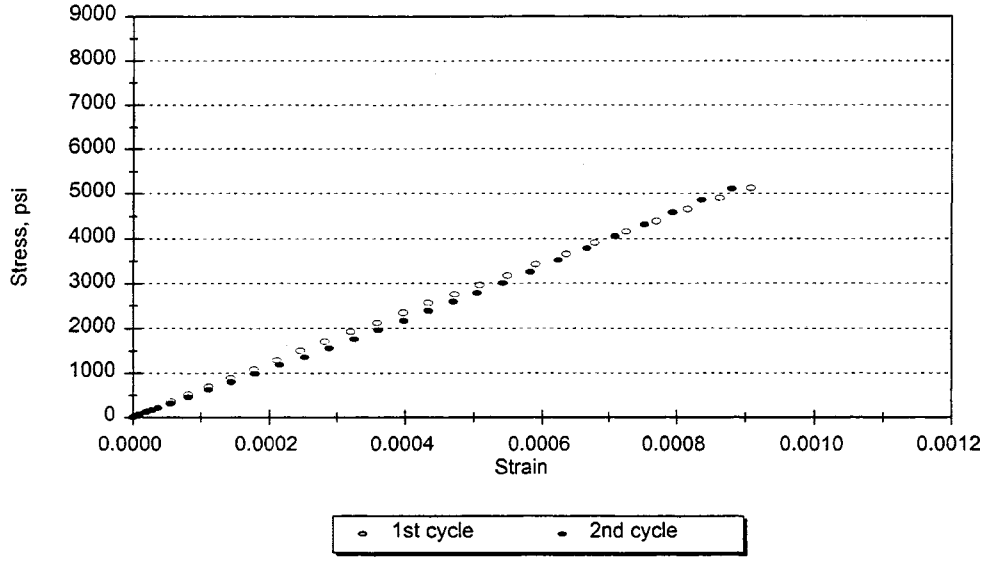

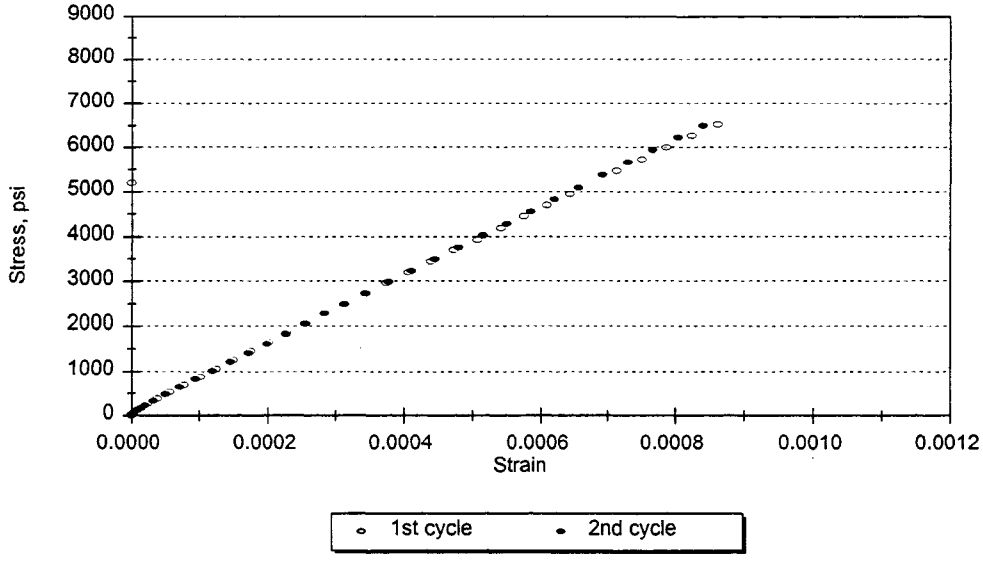

Figure 7.3-H. Stress-strain curves from two consecutive loading/unloading cycles at 50 percent of the ultimate compressive strength. Top: 97-H182-S1; Bottom: 97-W182-S1 [97H182S1.WMF & 97W182S1.WMF]

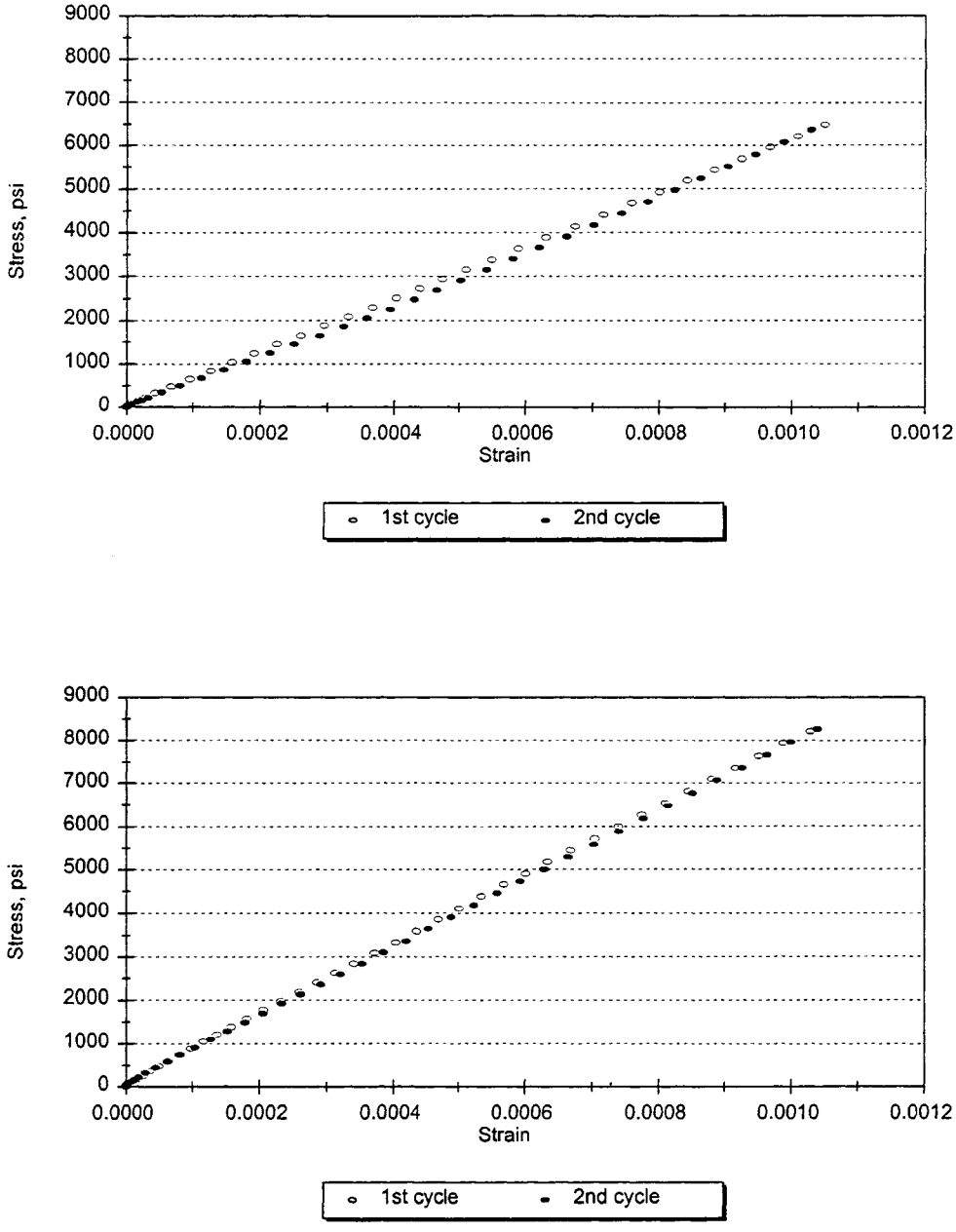

Figure 7.3-I. Stress-strain curves from two consecutive loading/unloading cycles at 50 percent of the ultimate compressive strength. Top: 98-H182-S1; Bottom: 98-W182-S1 [98H182S1.WMF & 98W182S1.WMF]

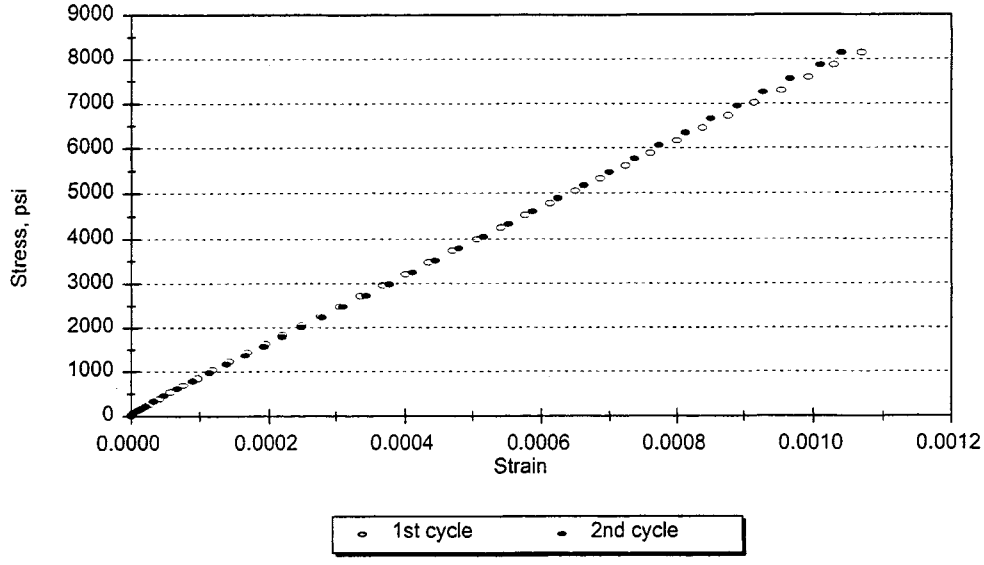

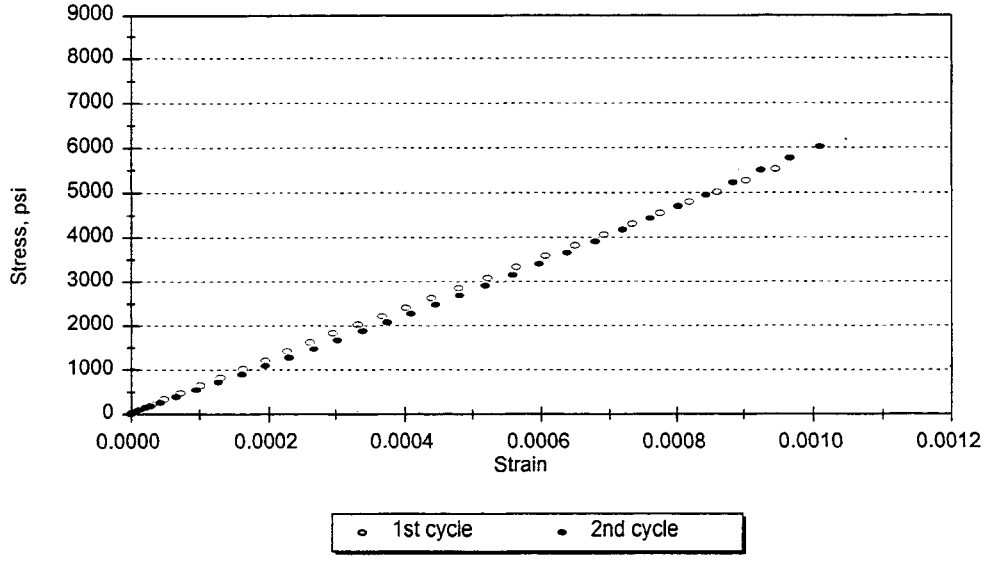

Figure 7.3-J. Stress-strain curves from two consecutive loading/unloading cycles at 50 percent of the ultimate compressive strength. Top: 98-W182-S2; Bottom: 99-H182-S1 [98W182S2.WMF & 99H182S1.WMF]

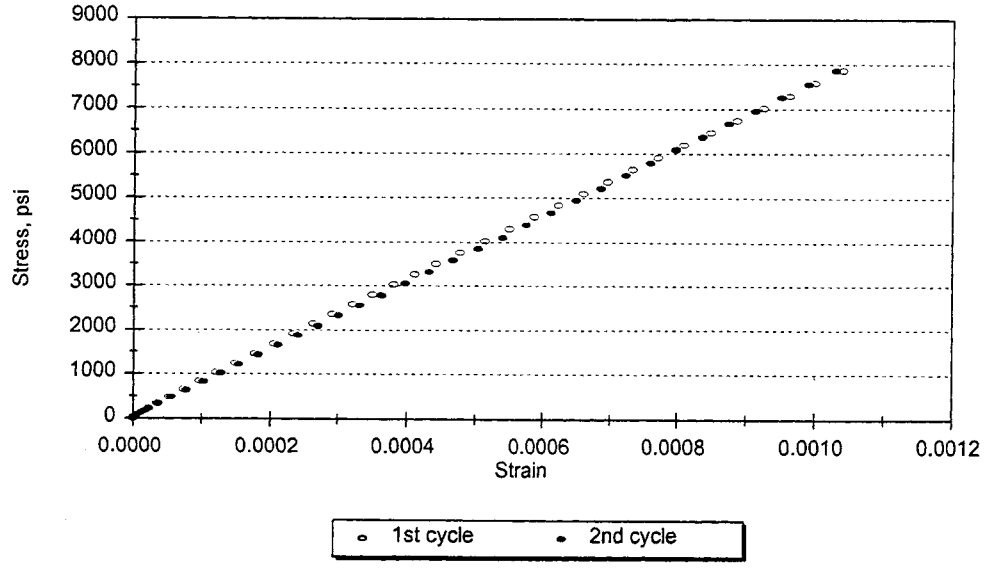

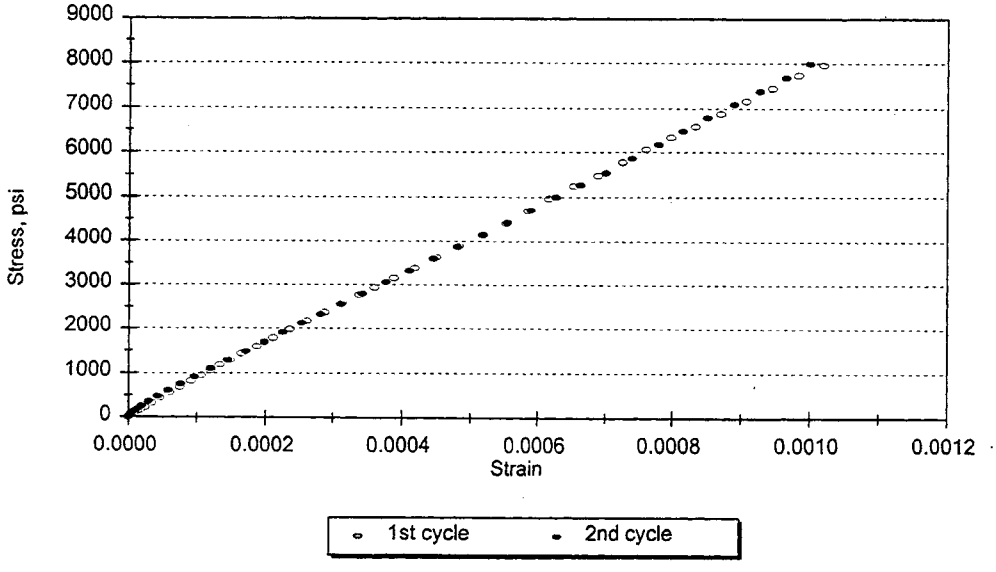

Figure 7.3-K. Stress-strain curves from two consecutive loading/unloading cycles at 50 percent of the ultimate compressive strength. Top: 99-W182-S1; Bottom: 99-W182-S2 [99W182S1.WMF & 99W182S2.WMF]

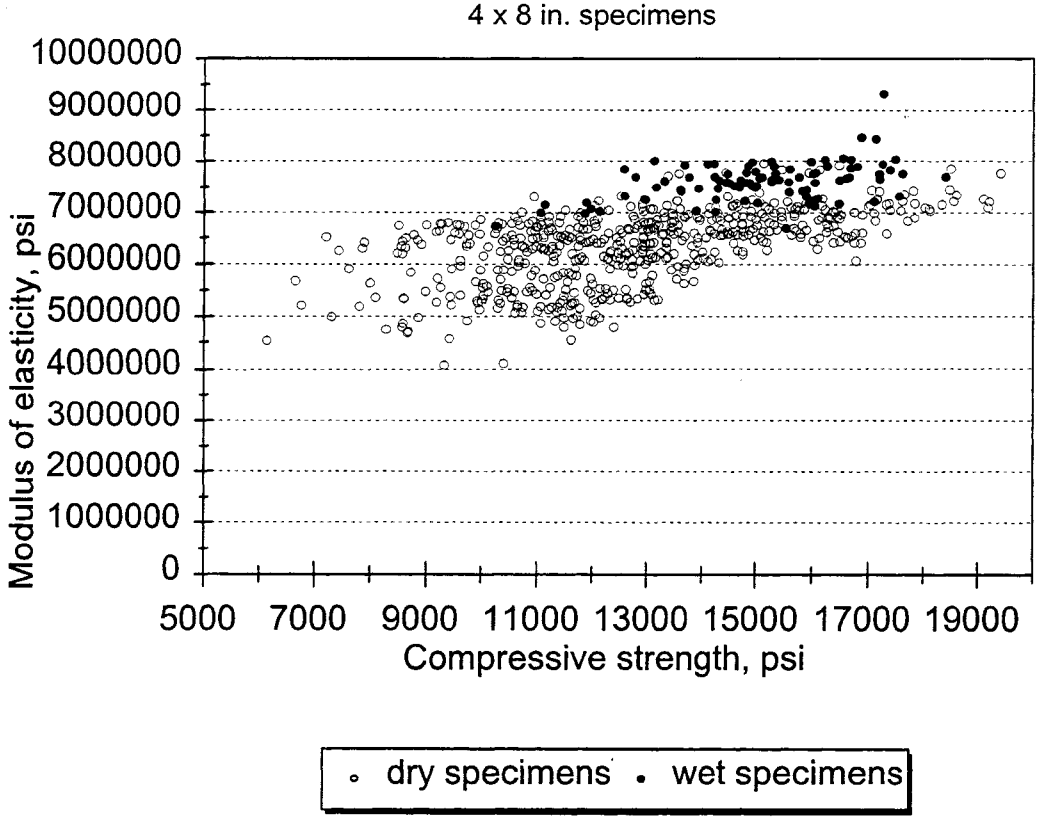

Figure 7.4. Measured static modulus of elasticity versus compressive strength for 4 x 8 in. (100 x 200 mm) cylinders.
[4WET_DRY.WMF]

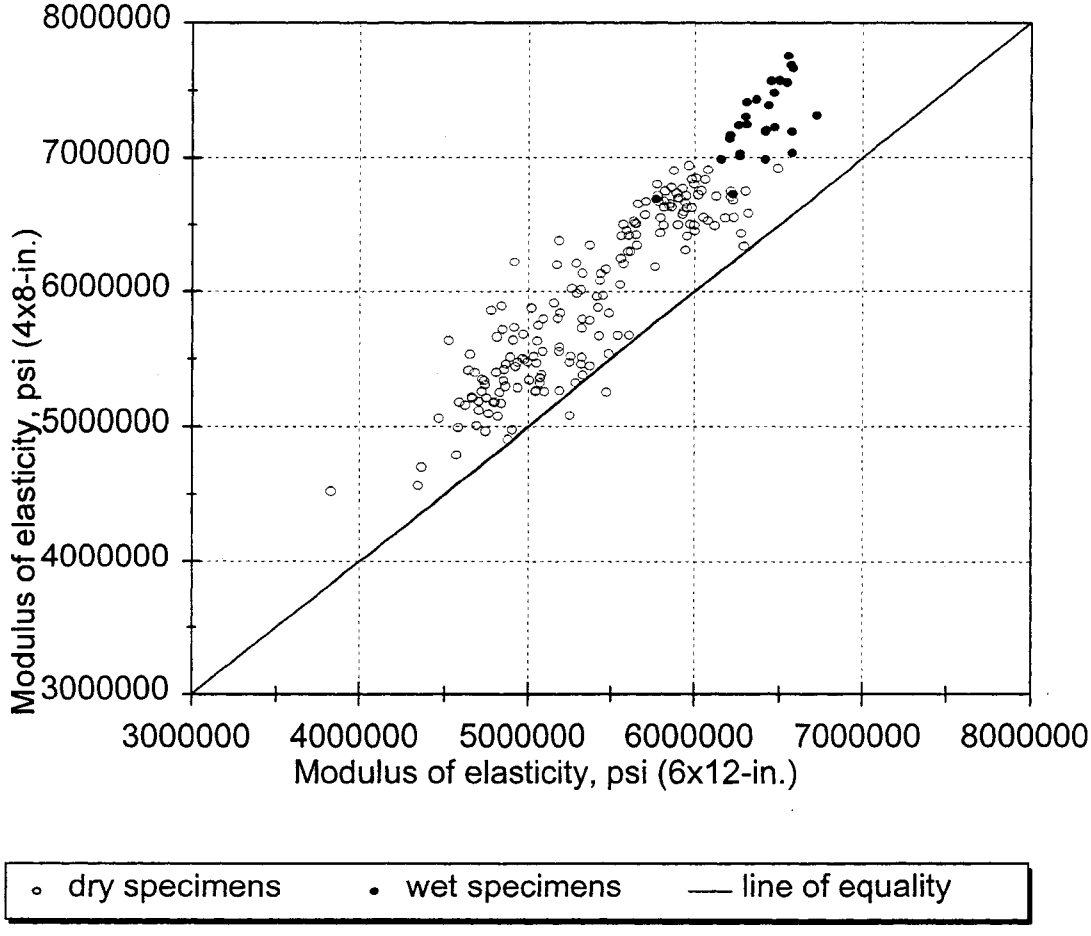

Figure 7.5. Effect of specimen size on measured static modulus of elasticity of high strength concrete.
[E_SIZE.WMF]

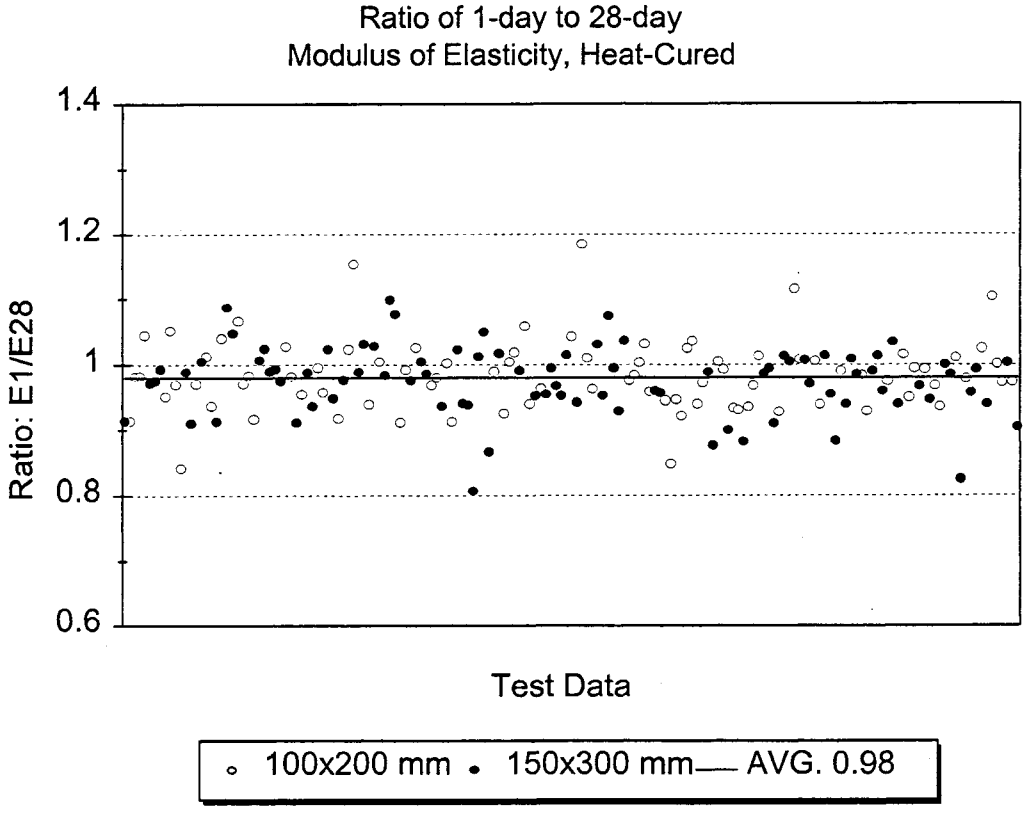

Figure 7.6. Ratios of 1-day modulus of elasticity of heat-cured specimens to their 28-day values.

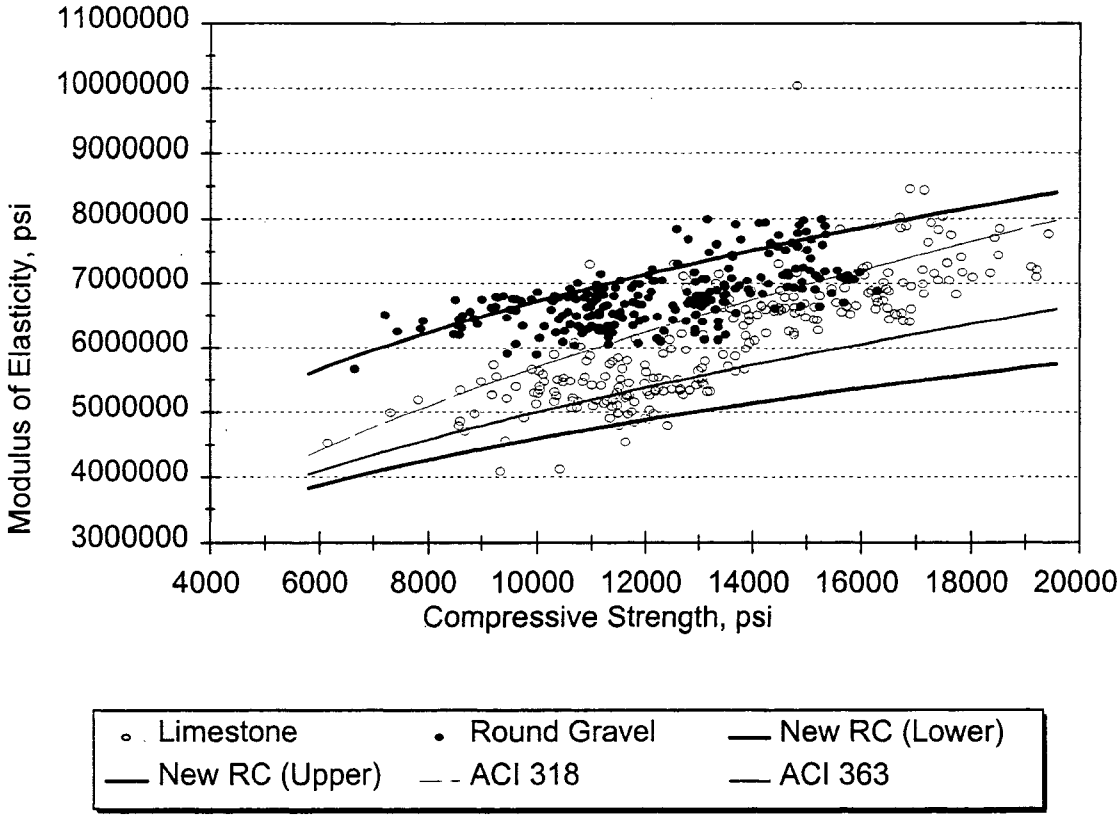

Figure 7.7. Effect of aggregate type on modulus of elasticity of high strength concrete.

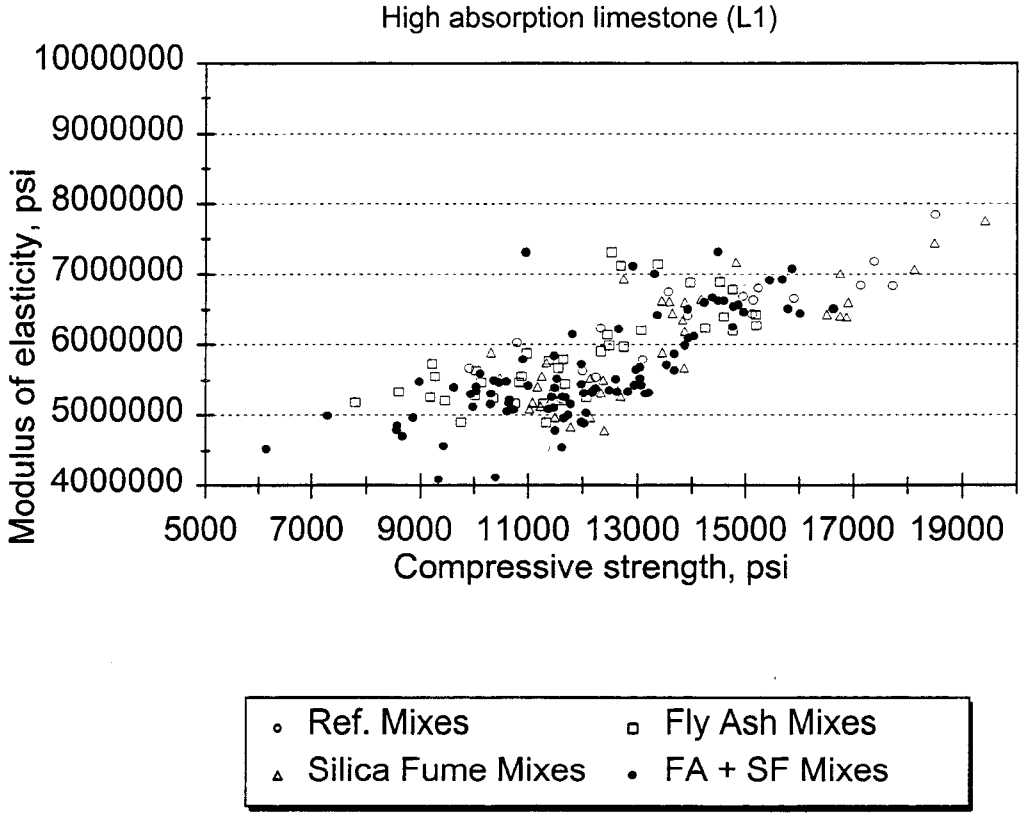

Figure 7.8-A. Effect of composition of cementitious material on measured static modulus of elasticity of high strength concrete made with high absorption limestone (L1); 4 x 8 in. (100 x 200 mm) dry specimens.
[E_COM_L1.WMF]

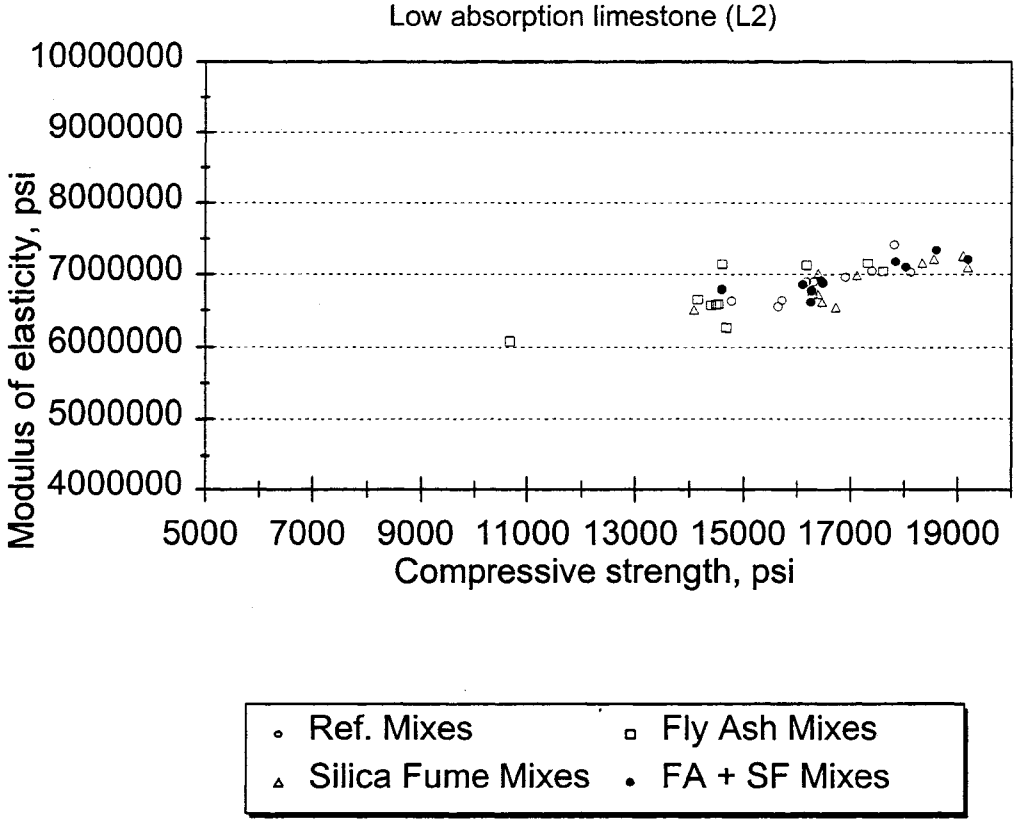

Figure 7.8-B. Effect of composition of cementitious material on measured static modulus of elasticity of high strength concrete made with low absorption limestone (L2); 4 x 8 in. (100 x 200 mm) dry specimens.
[E_COM_L2.WMF]

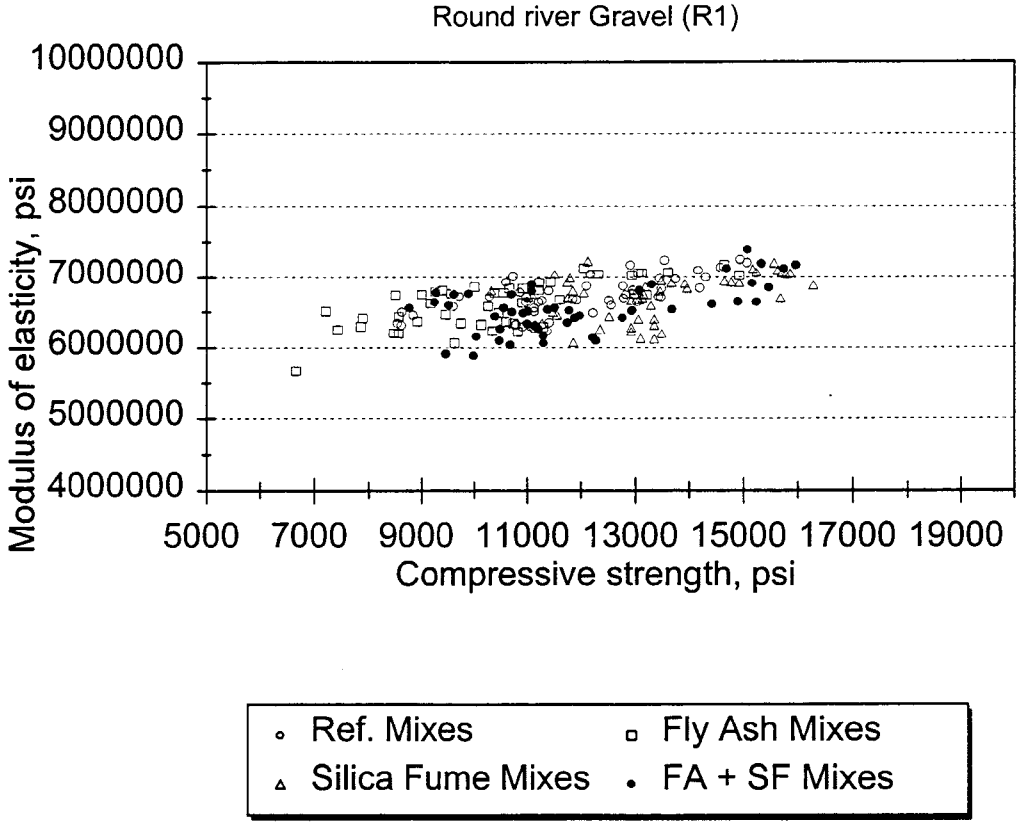

Figure 7.8-C. Effect of composition of cementitious material on measured static modulus of elasticity of high strength concrete made with round river gravel (R1); 4 x 8 in. (100 x 200 mm) dry specimens.
[E_COM_R1.WMF]

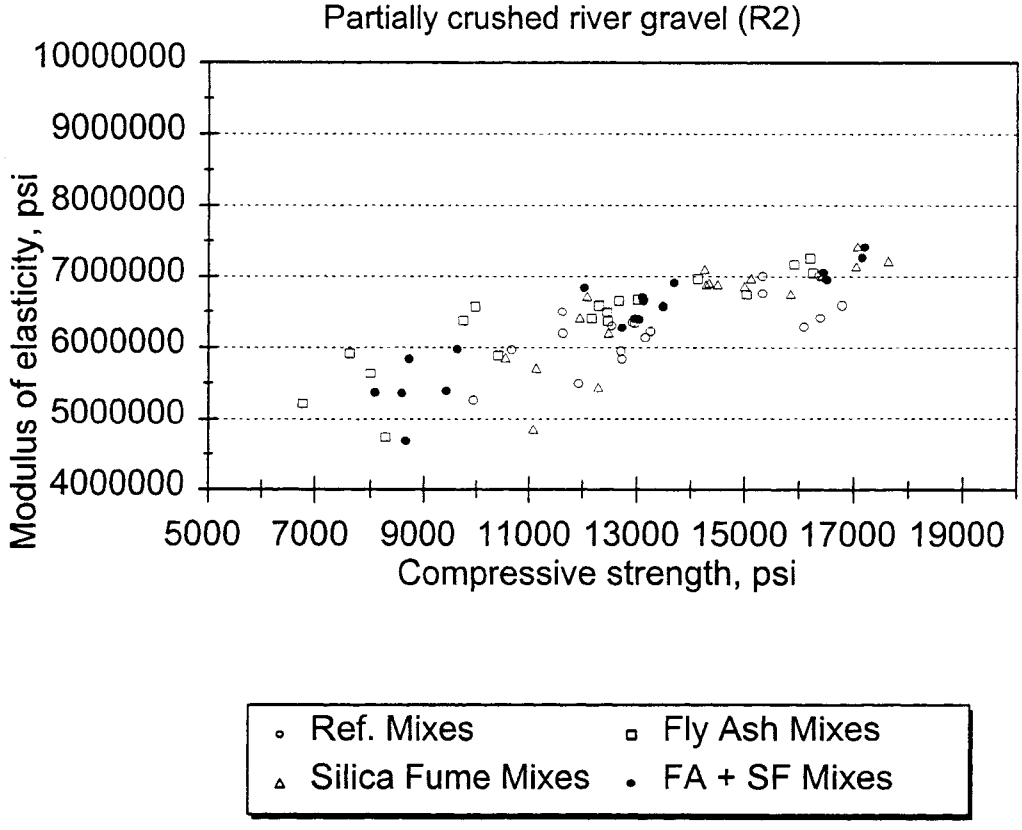

Figure 7.8-D. Effect of composition of cementitious material on measured static modulus of elasticity of high strength concrete made with partially crushed river gravel (R2); 4 x 8 in. (100 x 200 mm) dry specimens.
[E_COM_R2.WMF]

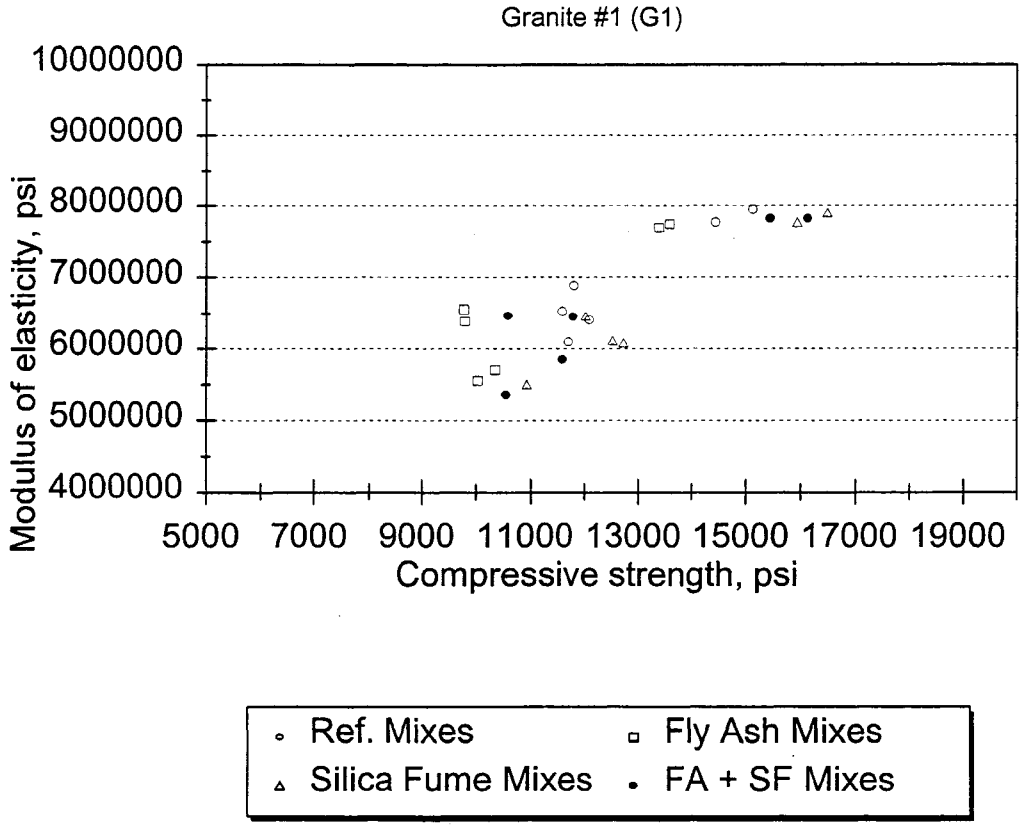

Figure 7.8-E. Effect of composition of cementitious material on measured static modulus of elasticity of high strength concrete made with granite from source #1 (G1); 4 x 8 in. (100 x 200 mm) dry specimens.
[E_COM_G1.WMF]

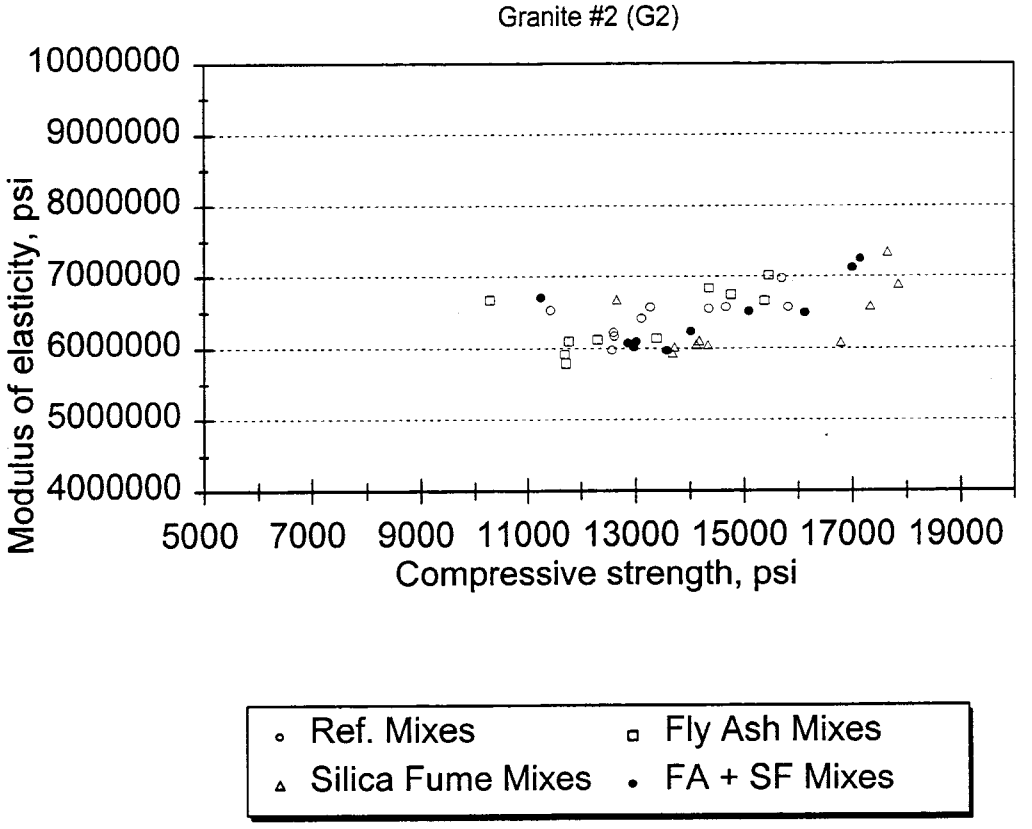

Figure 7.8-F. Effect of composition of cementitious material on measured static modulus of elasticity of high strength concrete made with partially crushed river gravel (G2); 4 x 8 in. (100 x 200 mm) dry specimens.
[E_COM_G2.WMF]

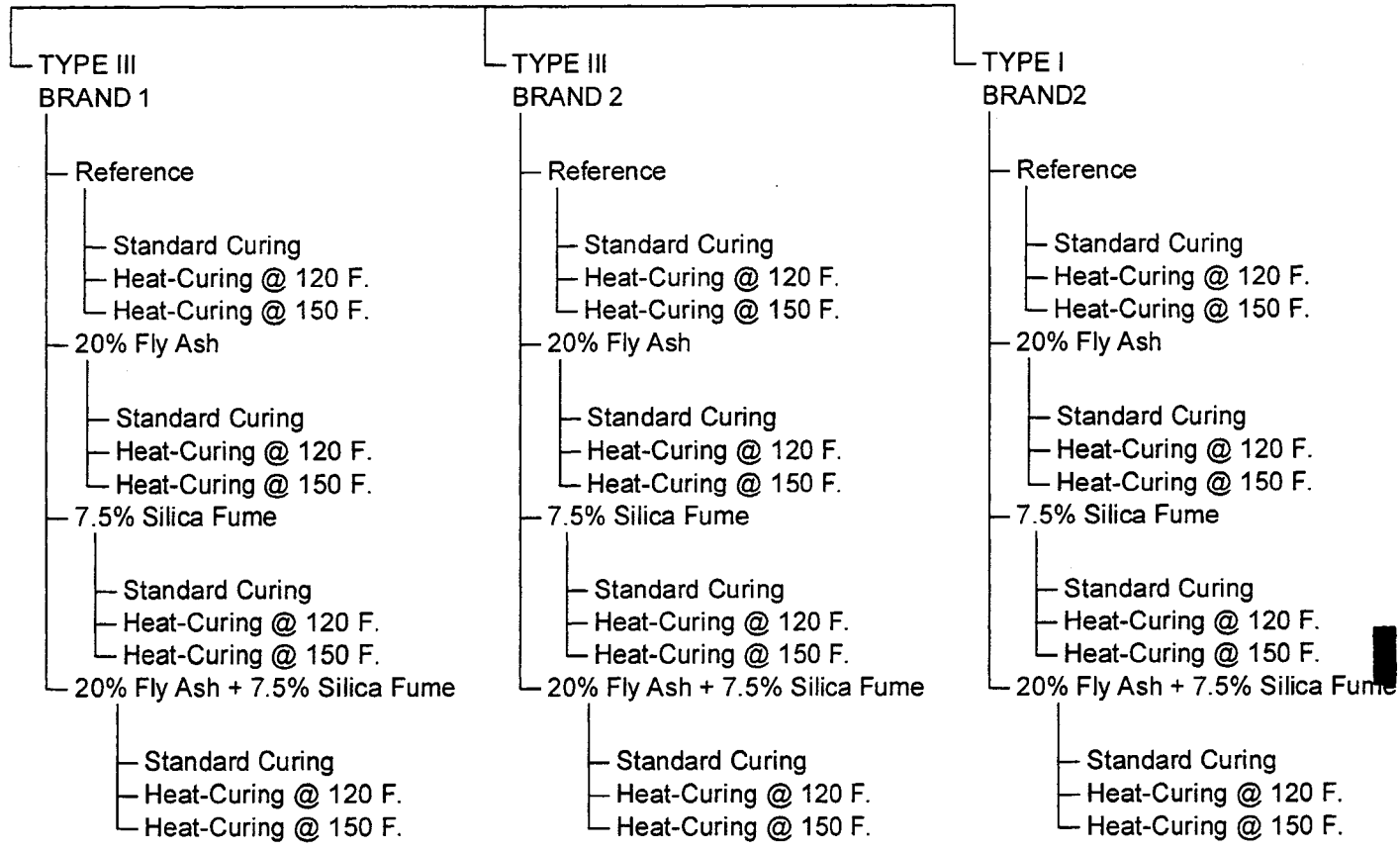

Figure 7.9. Test organization for investigation of the effects of curing condition as well as type and brand of cement on mechanical properties of high strength concrete

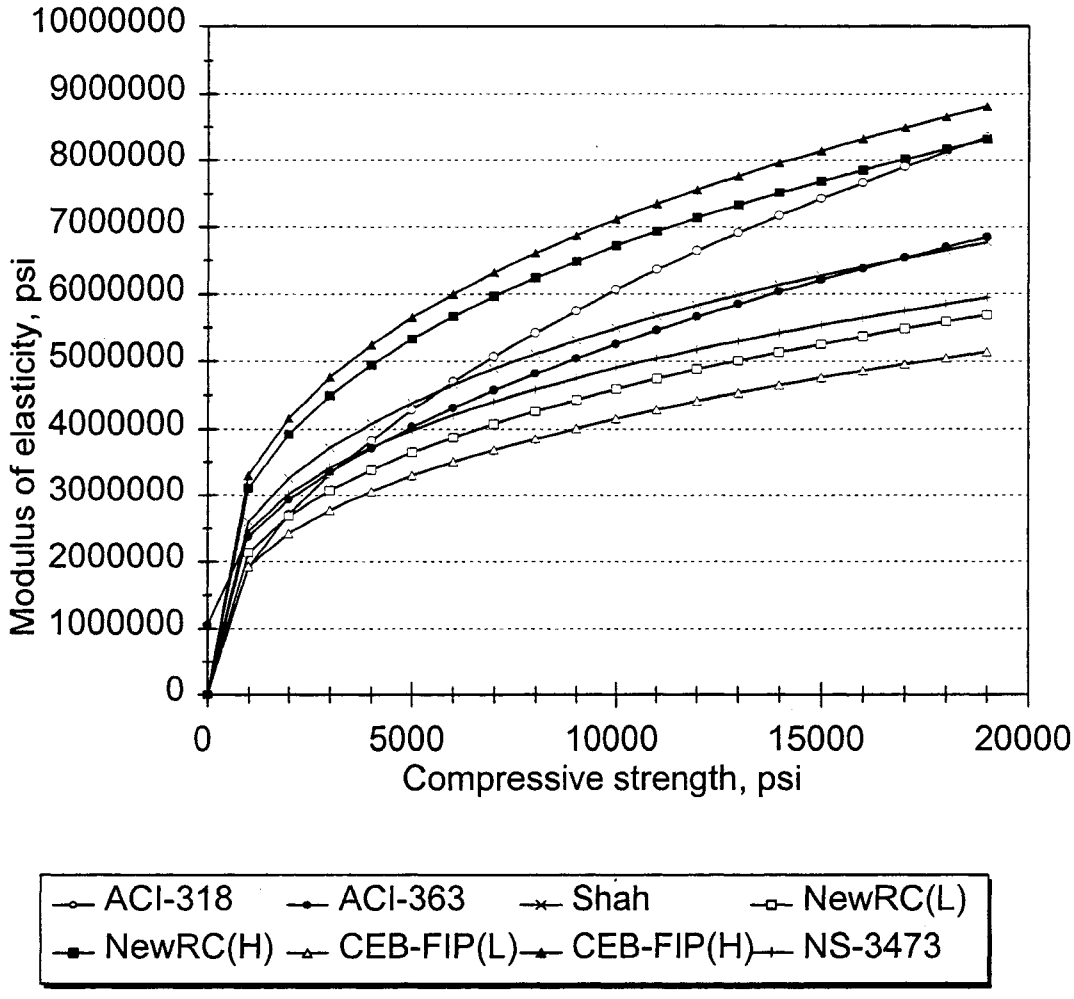

Figure 7.10. Comparison of six widely used prediction equations for modulus of elasticity. (L) and (H) indicate lower and upper bounds.
[E_CODE1.WMF]

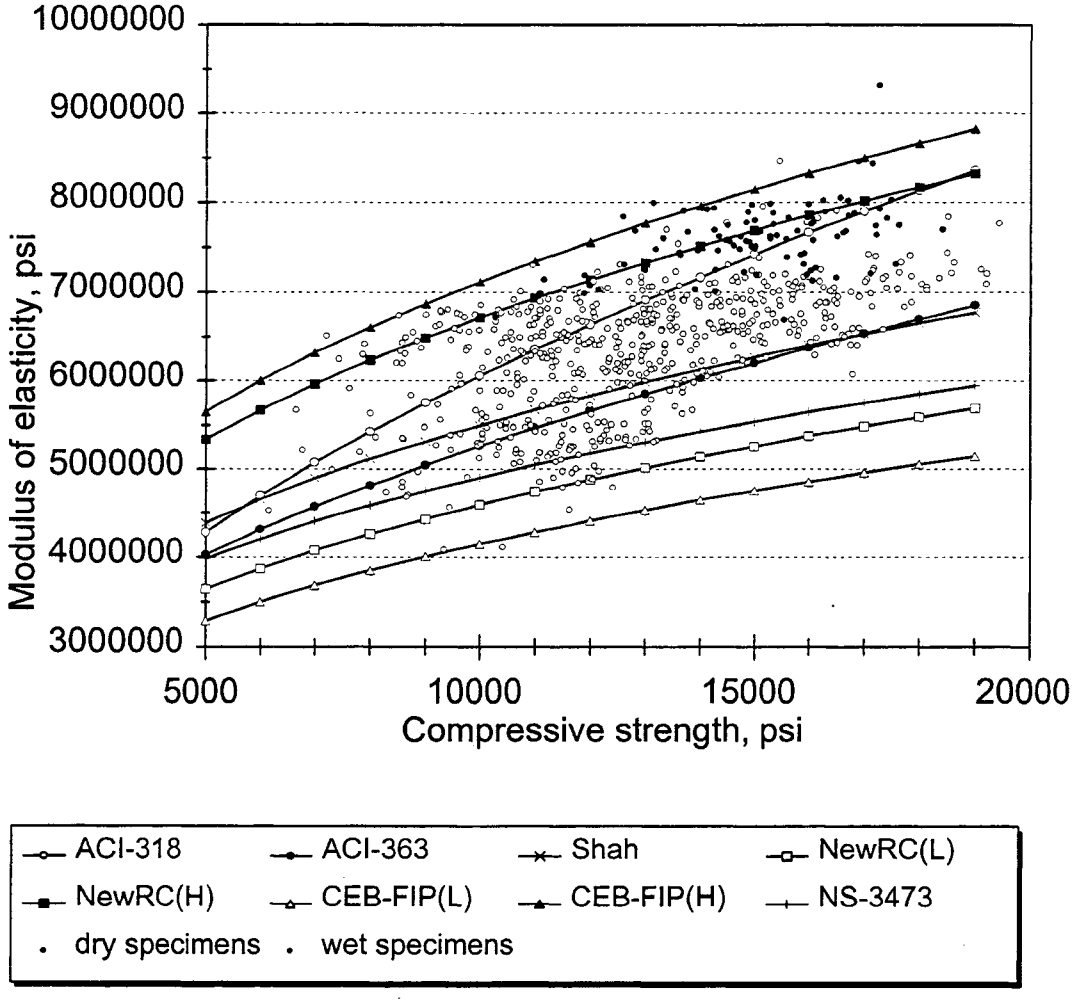

Figure 7.11-A. Comparison of measured modulus of elasticity values for 4 x 8 in. (100 x 200 mm) specimens with predictions of six widely used equations. (L) and (H) indicate lower and upper bounds.
[E_CODE4.WMF]

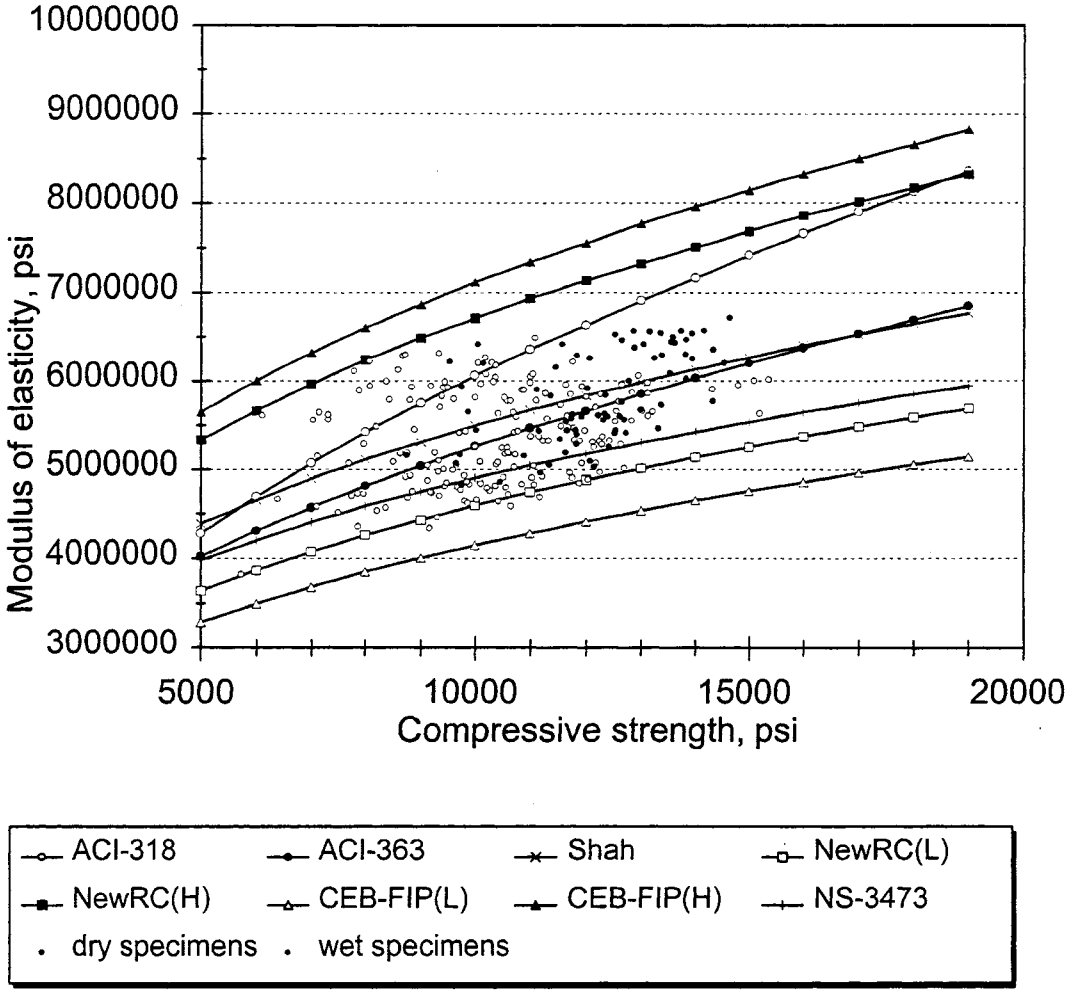

Figure 7.11-B. Comparison of measured modulus of elasticity values for 6 x 12 in. (150 x 300 mm) specimens with predictions of six widely used equations. (L) and (H) indicate lower and upper bounds.
[E_CODE6.WMF]

CHAPTER 8

TEST RESULTS: TENSILE STRENGTH

8.1 Background

Tensile strength of concrete is always expressed in terms of a specific test procedure. The direct tension test, the split cylinder test, and the beam test are the three kinds of tests that have been used. Due to the difficulty in applying direct tension to concrete specimens, the split cylinder test and the beam test have gained wide acceptance.

Split Cylinder Test: In the split cylinder test, also called Brazilian test, a cylinder is loaded in compression diametrically between two platens. Using theory of elasticity (for example see: Frocht, Max. M. (1948) "Photoelasticity," Volume II, John Wiley & Sons Inc., NY, Chapter 4), it can be shown that this loading produces a nearly uniform maximum principal tensile stress along the diameter, which causes the cylinder to fail by splitting. Splitting tensile strength of concrete is calculated as follows:

- $T = 2P/\pi Ld$ ***(8.1)***

where

T = splitting tensile strength, psi (MPa)

P = maximum applied load indicated by the testing machine, lb (N)

L = specimen length, in. (mm)

d = diameter of the specimen, in. (mm)

ASTM C 496, "Standard Test Method for Splitting Tensile Strength of Cylindrical Concrete Specimens," covers the determination of the splitting tensile strength of cylindrical concrete specimens.

Beam Test: In the beam test, also called modulus of rupture test, a simple supported prismatic beam with a clear span of three times its depth is subjected to two-point loading applied at the third points between the supports. The resulting bending moment within the middle third of the span length is constant and maximum and is equal to:

- $M = PL/6$ ***(8.2)***

where

M = maximum bending moment, constant throughout the middle third of the span length, lb-in. (N-mm)

P = maximum applied load indicated by the testing machine, lb (N)

L = span length, in. (mm)

When the fracture initiates in the tension surface within the middle third of the span length (region of constant maximum moment), the modulus of rupture is calculated as follows:

- $R = PL/bd^2$ ***(8.3)***

where

R = modulus of rupture, psi (MPa)

P = maximum applied load indicated by the testing machine, lb (N)

L = span length, in. (mm)

b = width of specimen, in. (mm)

d = depth of specimen, in. (mm)

ASTM C 78 test method, "Standard Test Method for Flexural Strength of Concrete (Using Simple Supported Beam with Third-Point Loading)," covers determination of the flexural strength of concrete by the use of a simple beam with third-point loading.

ACI Building Code (ACI 318-89) gives the following empirical relationships between tensile strength and the cylinder compressive strength for concrete with strength between 2,000 and 6,000 psi (13.8 to 41.4 MPa):

Splitting Tensile Strength:

- USC, psi: $f_{sp} = 6.7(f_c)^{0.5}$ ***(8.4-a)***
- SI, MPa: $f_{sp} = 0.56(f_c)^{0.5}$ ***(8.4-b)***

Flexural Tensile Strength (Modulus of Rupture):

- USC, psi: $f_r = 7.5(f_c)^{0.5}$ ***(8.5-a)***
- SI, MPa: $f_r = 0.62(f_c)^{0.5}$ ***(8.5-b)***

where

f_{sp} = splitting tensile strength of the concrete, psi (MPa)

f_c = compressive strength of the concrete, psi (MPa)

f_r = flexural tensile strength (modulus of rupture) of the concrete, psi (MPa)

In estimating tensile strength of high strength concrete, ACI Committee 363 - High Strength Concrete (ACI 363R-92) gives the following empirical relationships between tensile strength and the cylinder compressive strength for normal weight high strength concrete with strength between 3,000 and 12,000 psi (20.7 to 82.8 MPa):

Splitting Tensile Strength:

- USC, psi: $f_{sp} = 7.4(f_c)^{0.5}$ ***(8.6-a)***
- SI, MPa: $f_{sp} = 0.59(f_c)^{0.5}$ ***(8.6-b)***

Flexural Tensile Strength (Modulus of Rupture):

- USC, psi: $f_r = 11.7(f_c)^{0.5}$ ***(8.7-a)***
- SI, MPa: $f_r = 0.94(f_c)^{0.5}$ ***(8.7-b)***

where

f_{sp} = splitting tensile strength of the concrete, psi (MPa)

f_c = compressive strength of the concrete, psi (MPa)

f_r = flexural tensile strength (modulus of rupture) of the concrete, psi (MPa)

Recent test results have indicated that the relationship between compressive strength and tensile strength of concrete as used in ACI equations may not be representative of test data. A recent review by Oluokun *(1991)* provides an excellent summary of the proposed equations for prediction of tensile strength of concrete from cylinder compressive strength.

8.2 Apparatus and Test Procedure

8.2.1 Testing Machine

Detailed description of the testing machine together with the rate of loading used are given in Chapter 5.

8.2.2 Split Cylinder Tests

Apparatus for Marking the Diametral Lines on the Ends of the Specimens: A modified version of the apparatus described in ASTM C 496 for marking the diametral lines on the ends of the specimen in the same axial plane was constructed and used, Figure 1. The apparatus consisted of a base plate (a length of *C 4x5.4* steel channel) and a removable tee bar assembly which fit smoothly over the flanges of the channel. Mounted on the tee bar assembly was a vertical bar with its inner edge along the centerline of the steel channel. The inner edge of the vertical bar was used for guiding a pencil.

For marking the diametral lines on the ends of the specimen, the cylindrical specimen was placed on the base plate as shown in Figure 8.1. The tee bar assembly was placed over the flanges of the base plate in close contact with the end of the specimen. A diametral line was drawn on one end of the specimen. Without moving the specimen, the tee bar assembly was lifted and placed on the

other side of the specimen. The second diametral line was drawn. Because the specimen was not moved, the drawn diametral lines were in the same axial plane.

***Aligning jig*:** The aligning jig was used to prevent the specimen from rolling to the sides during the test setup. It also helped to position the specimen directly beneath the center of thrust of the spherical bearing block of the testing machine.

Two aligning jigs, similar to the one described in ASTM C 496, were constructed for the two sizes of the specimens studied, Figures 8.2 and 8.3. Each aligning jig consisted of four parts: lower bearing block, bearing bar, and two uprights for positioning the test cylinder, plywood bearing strips, and the bearing bar.

The specimen was placed on a plywood bearing strip, on the lower bearing block, between the two uprights. The two diametral lines drawn earlier on the ends of the specimen were used to align the axial plane of the specimen with the vertical axis of the uprights. A second plywood bearing strip was placed between the specimen and the bearing rod on top. The whole assembly was placed in the testing machine. The axis of the specimen was aligned with the center of thrust of the spherical bearing block of the testing machine. The spherical bearing block was brought to bear on the bearing bar. The two uprights were then removed and the test was conducted, Figure 8.4.

8.2.3 Modulus of Rupture Tests (Simple Beam with Third-Point Loading)

An apparatus similar to one suggested by ASTM C 78, Standard Test Method for Flexural Strength of Concrete (Using Simple Beam with Third-Point Loading), was used for the third-point flexure tests. Support points and loading points on the specimen were marked in advance. The specimen was turned on its side with respect to its molding position and was placed on the support blocks. Plywood bearing strips, extending across the full width of the specimen, were placed between the specimen and the support and the load-applying blocks. The load was then applied uniformly and continuously by the testing machine to the load-applying block.

Continuously moist-cured specimens were sprayed with water during the test to eliminate the effect of drying shrinkage on the test results.

8.3 Test Results

8.3.1 Split Cylinder Tests

A total of 314 6 x 12 in. (150 x 300 mm) specimens from 90 high strength concrete mixes were cast during the course of the study to investigate the relationship between the splitting tensile strength of high strength concrete with its cylinder compressive strength. Test results are presented in Appendix C. High strength concrete mixes considered were made with five different types of coarse aggregate (R1, R2, G2, L1, and L2), and had a variety of cementitious materials compositions. The 28-day compressive strengths of concrete mixes ranged from 7,500 to 15,360 psi (51.7 to 106 MPa) and 8,750 to 14,630 psi (60.3 to 101 MPa) for heat-cured and moist-cured specimens, respectively. In addition, a total of 247 companion 4 x 8 in. (100 x 200 mm) specimens were cast from 50 of the studied mixes to investigate the size effect on splitting tensile strength test results. All specimens were tested at 28-days of age. The test results are shown in Tables 8.1, 8.2 and Figure 8.5. Also shown in Figure 8.5 are the equations proposed by ACI Building Code (ACI 318-89) and ACI Committee 363 - High Strength Concrete (ACI 363R-92).

A regression analysis, based on the generally accepted simple power model, $f_{sp} = \alpha(f_c)^{\beta}$, was done on the collected experimental data. The following empirical equations for predicting the average splitting tensile strength (f_{sp}) of high strength concrete from its compressive strength (f_c) were determined:

For Moist-Cured Specimens:

- USC, psi: $f_{sp} = 0.42(f_c)^{0.79}$ **(8.8-a)**
- SI, MPa: $f_{sp} = 0.15(f_c)^{0.79}$ **(8.8-b)**

For Heat-Cured Specimens:

- USC, psi: $f_{sp} = 3.63(f_c)^{0.57}$ **(8.9-a)**

- SI, MPa: $f_{sp} = 0.42(f_c)^{0.57}$ **(8.9-b)**

For All Data (Moist-Cured and Heat-Cured Specimens):

- USC, psi: $f_{sp} = 1.98(f_c)^{0.63}$ **(8.10-a)**
- SI, MPa: $f_{sp} = 0.32(f_c)^{0.63}$ **(8.10-b)**

Figure 8.6 shows the plot of the derived equations for predicting the split cylinder strengths of high strength concrete mixes considered. Also shown in Figure 8.6 are the equations proposed by ACI Building Code (ACI 318-89), ACI Committee 363 - High Strength Concrete (ACI 363R-92), and an alternative equation proposed by Ahmad and Shah *(1985)* for concrete strengths up to 12,000 psi (82.8 MPa) based on the published experimental data of low, medium, and high strength concretes from different sources.

The equation proposed by ACI Committee 363 appeared to overestimate the values of tensile strengths for concrete with compressive strengths up to about 12,000 psi (82.8 MPa). Considering the wide spread of the experimental data (shown in Figure 8.5), for all practical purposes, the equation proposed by ACI 318 seemed to predict satisfactory average results. In fact, when the simple 0.5 power model, ($f_{sp} = \alpha(f_c)^{0.5}$), was used in the regression analysis of the experimental data, the coefficient α was determined to be 6.74 and 6.77 for heat-cured and moist-cured data respectively, compared to 6.7 suggested by ACI Building Code (ACI 318).

Figure 8.7 is the histogram of the ratio of the splitting tensile strength to compressive strength for all 6 x 12 in. (150 x 300 mm) high strength concrete specimens studied. Splitting tensile strength values were between 5 to 8 percent of the compressive strength. The average value of the strength ratio was 0.0627 (6.27%) with a standard error of 0.0005, indicating the brittle nature of high strength concrete. The average value of the strength ratio was not significantly affected by the type of curing condition used and had average values of 0.0640 and 0.0612 for heat- and moist-cured specimens. These values of strength ratio are in excellent agreement with the 5 to 10% range, published in the "State-of-the-Art Report on High-Strength

Concrete," reported for compressive strengths up to 12,105 psi (83.5 MPa) *[ACI 363R-92 1992]*. For normal strength concrete tensile strength of concrete is reported to be about 10 to 15% of its compressive strength *[Wang and Salmon 1992]*.

8.3.2 Beam Tests

A total of 280 6 x 6 x 24 in. (150 x 150 x 610 mm) specimens from 90 high strength concrete mixes were cast during the course of the study to investigate the relationship between the flexural strength of high strength concrete with respect to its cylinder compressive strength. Test results are presented in Appendix C. High strength concrete mixes considered were the same as those used for the splitting tensile strength study and were described in detail in Section 8.3.1. The test results are shown in Tables 8.3, 8.4 and Figure 8.8. Also shown in Figure 8.8 are the equations proposed by ACI Building Code (ACI 318-89) and ACI Committee 363 - High Strength Concrete (ACI 363R-92).

As seen in Figure 8.8, the type of curing significantly affected the modulus of rupture test results as evinced with the moist-cured specimens exhibiting higher flexural tensile strengths. This can be explained as follows. Drying shrinkage strain in heat-cured beams (maximum on the surfaces of the beam) are added to the flexural tensile strain (maximum on the outermost fibers) during two point loading of the beams causing the heat-cured beams to break at a lower load. The moist-cured samples (moist up to the time of test) did not suffer from shrinkage strain, therefore a higher load was needed to break the moist-cured beams.

The type of curing did not affect the splitting tensile strength of high strength concrete samples, Figure 8.5. The reason is that during the splitting tensile strength test the elements along the diagonal plane inside the concrete (with the least amount of shrinkage strain) are under tension and therefore pre-existing shrinkage strain (mostly on the surface) does not interfere with the test result. Data obtained for flexural tensile strength of heat-cured specimens ranged between ACI 318-89 Code equation and ACI High Strength Committee 363 proposed equation.

A regression analysis, based on the generally accepted simple power model, $f_r = \alpha(f_c)^{\beta}$, was done on the collected experimental data. The following empirical equations for predicting the average flexural strength (f_r) of high strength concrete from its compressive strength (f_c) were determined:

For Moist-Cured Specimens:

- USC, psi: $f_{sp} = 5.92(f_c)^{0.57}$ ***(8.11-a)***
- SI, MPa: $f_{sp} = 0.70(f_c)^{0.57}$ ***(8.11-b)***

For Heat-Cured Specimens:

- USC, psi: $f_{sp} = 23.57(f_c)^{0.40}$ ***(8.12-a)***
- SI, MPa: $f_{sp} = 1.19(f_c)^{0.40}$ ***(8.12-b)***

For All Data (Moist-Cured and Heat-Cured Specimens):

- USC, psi: $f_{sp} = 0.71(f_c)^{0.79}$ ***(8.13-a)***
- SI, MPa: $f_{sp} = 0.25(f_c)^{0.79}$ ***(8.13-b)***

Figure 8.9 shows the plot of the derived equations for predicting the flexural strengths of high strength concrete mixes considered. Also shown in Figure 8.9 are the equations proposed by ACI Building Code (ACI 318-89), ACI Committee 363 - High Strength Concrete (ACI 363R-92), and an alternative equation proposed by Ahmad and Shah *(1985)* for concrete strengths up to 12,000 psi (82.8 MPa) based on the published experimental data of low, medium, and high strength concretes from different sources. The derived best fit equation for moist-cured specimens was very close to the equations proposed by ACI Committee 363 and Ahmad and Shah. The best fit equation for heat-cured specimens fell between the values predicted by the ACI 318 and ACI 363 equations.

When the simple 0.5 power model, ($f_r = \alpha(f_c)^{0.5}$), was used in the regression analysis of the experimental data, the coefficient α was determined to be 9.29 and 11.50 for heat-cured and

moist-cured data respectively, compared to 11.7 suggested by ACI Committee 363 equation. Considering the wide scatter of the data, it is believed that the 0.50 power used by ACI equations is a relatively good estimator for use in prediction models of flexural tensile strength of high strength concrete. For heat-cured specimens a coefficient of 9.30 instead of 11.70 is recommended. The 11.70 coefficient proposed by ACI 363 seems to be satisfactory for moist-cured specimens.

8.4 Conclusions

1. The ACI 318 equation for predicting splitting tensile strength of concrete from its cylinder compressive strength was found to be applicable to high strength concretes studied in this research program.
2. While the splitting tensile strength of high strength concrete was not proportional to the 0.5 power of the compressive strength, the scatter of the test data did not warrant the proposal of a new equation. For all practical purposes the equations derived from regression analysis of the data resulted in predictions reasonably close to those from the ACI 318 equation.
3. Splitting tensile strengths of high strength concrete specimens considered, were between 5 to 8 percent of compressive strength values. The average value of the ratio of the splitting tensile strength to compressive strength was not significantly affected by the type of curing and was determined to be 0.0627 (6.27%), with a standard error of 0.0005.
4. The type of curing significantly affected the flexural strength of high strength concrete specimens. Reduced flexural tensile strength of heat-cured specimens was attributed to the presence of drying shrinkage strain on the outermost fibers of the specimen.
5. The flexural tensile strength of moist-cured high strength concrete can be satisfactorily predicted by the 0.5 power relation suggested by ACI 363 ($11.70 f_c^{0.50}$). For heat-cured specimens a new equation in the form of $9.30 f_c^{0.50}$ is proposed.

Table 8.1. Splitting tensile strength of 4 x 8 in. (100 x 200 mm) and 6 x 12 in. (150 x 300 mm) cylinders, heat-cured specimens.

No.	$(f_c)_{6x12}$ psi	$(f_{sp})_{6x12}$ psi	n	STD psi	$(f_{sp})_{4x8}$ psi	n	STD psi	Diff. psi	Ratio
22	13127	758	1		793	3	51	35	1.05
23	12412	638	2	9	723	3	52	85	1.13
24	10718	618	2	84	687	3	45	69	1.11
25	9653	518	2	43	730	3	76	212	1.41
26	12588	804	2	12	997	3	109	192	1.24
27	11033	698	2	11	918	3	107	220	1.32
28	8819	563	2	62	775	3	67	213	1.38
29	9860	591	2	120	768	3	92	177	1.30
50	11551	677	2	16	988	3	110	312	1.46
51	9799	666	2	49	869	3	29	203	1.31
52	12238	836	2	48	1086	3	58	250	1.30
53	9185	626	2	76	784	3	20	158	1.25
54	12517	849	2	91	1010	3	13	161	1.19
55	11703	740	2	1	896	3	41	156	1.21
56	12135	751	2	141	1000	2	128	249	1.33
57	12177	770	2	97	969	3	90	199	1.26
58	12149	812	2	37	851	3	30	38	1.05
59	11928	654	2	3	1019	3	83	365	1.56
60	10774	655	2	55	949	3	26	294	1.45
61	11322	679	2	83	944	3	36	266	1.39
62	11887	730	2	18	1014	3	90	284	1.39
63	11151	685	2	15	975	3	30	290	1.42
64	12034	752	2	126	1009	2	85	258	1.34
65	12688	872	2	23	941	2	146	69	1.08
66	11677	710	2	48	975	3	63	265	1.37
67	12284	734	2	30	1062	2	90	328	1.45
68	11874	704	1		901	3	51	197	1.28
69	10553	651	2	46	829	3	33	179	1.27
70	11788	744	2	18	1010	3	101	266	1.36
71	11218	707	2	13	1048	3	25	341	1.48
72	10588	601	1		911	3	10	309	1.51
73	12253	725	2	43	1068	3	103	342	1.47
74	11748	764	2	0	1013	3	66	250	1.33
75	10846	690	2	41	854	3	39	164	1.24
76	11073	706	2	112	927	2	20	221	1.31
77	11175	749	2	11	926	2	40	177	1.24
78	10602	589	2	11	882	3	95	293	1.50
79	10719	647	2	55	869	3	32	223	1.34
80	11059	651	2	7	843	3	17	192	1.30
81	10606	657	2	125	817	3	43	160	1.24
82	9155	612	2	66	746	3	34	135	1.22
83	9299	570	2	42	817	3	50	248	1.43
84	11661	690	2	65	904	3	54	214	1.31
85	11304	749	2	140	955	2	27	206	1.28
86	8633	580	2	11	840	3	3	260	1.45
87	8887	602	2	43	753	2	83	151	1.25
88	10738	701	2	16	882	3	13	181	1.26
89	10100	730	2	7	934	3	41	204	1.28
90	7498	535	2	14	721	3	27	187	1.35
91	7972	587	2	11	765	3	17	178	1.30
100	10198	743	2	32	-	-	-	-	-
101	8594	689	2	12	-	-	-	-	-
102	7886	598	2	77	-	-	-	-	-
103	8438	678	2	2	-	-	-	-	-
104	11078	711	2	98	-	-	-	-	-

n = number of replicate specimens tested
STD = sample standard deviation (n > 1)
Diff. = $f_{4x8} - f_{6x12}$
Ratio = f_{4x8} / f_{6x12}

Table 8.1. Splitting tensile strength of 4 x 8 in. (100 x 200 mm) and 6 x 12 in. (150 x 300 mm) cylinders, heat-cured specimens. Continued ...

No.	$(f_c)_{6x12}$ psi	$(f_{sp})_{6x12}$ psi	n	STD psi	$(f_{sp})_{4x8}$ psi	n	STD psi	Diff. psi	Ratio
105	10365	722	2	3	-	-	-	-	-
*106	10047	679	2	7	-	-	-	-	-
107	8832	679	2	56	-	-	-	-	-
108	11270	779	2	96	-	-	-	-	-
109	10375	757	2	86	-	-	-	-	-
110	9997	670	2	10	-	-	-	-	-
111	9328	657	2	47	-	-	-	-	-
112	11924	736	2	40	-	-	-	-	-
113	12001	681	2	13	-	-	-	-	-
114	11007	778	2	28	-	-	-	-	-
115	10332	695	2	49	-	-	-	-	-
116	11721	833	2	82	-	-	-	-	-
117	11757	798	2	26	-	-	-	-	-
118	9489	746	2	125	-	-	-	-	-
119	8726	664	2	64	-	-	-	-	-
120	12947	703	2	23	-	-	-	-	-
121	12639	751	2	19	-	-	-	-	-
122	11634	749	2	40	-	-	-	-	-
123	11051	809	2	32	-	-	-	-	-
124	14789	839	2	18	-	-	-	-	-
125	15198	829	2	173	-	-	-	-	-
126	11981	746	2	10	-	-	-	-	-
127	12629	824	2	125	-	-	-	-	-
128	12291	796	2	28	-	-	-	-	-
129	12833	688	2	14	-	-	-	-	-
130	11694	679	2	25	-	-	-	-	-
131	12262	761	2	0	-	-	-	-	-
132	14310	828	2	71	-	-	-	-	-
133	15362	818	2	155	-	-	-	-	-
134	12545	819	2	87	-	-	-	-	-
135	15086	834	2	123	-	-	-	-	-
136	11777	658	2	17	-	-	-	-	-
137	12826	714	2	13	-	-	-	-	-
138	11003	705	2	10	-	-	-	-	-
139	12112	821	2	82	-	-	-	-	-

n = number of replicate specimens tested
STD = sample standard deviation (n > 1)
Diff. = $f_{4x8} - f_{6x12}$
Ratio = f_{4x8} / f_{6x12}

Table 8.2. Splitting tensile strength of 4 x 8 in. (100 x 200 mm) and 6 x 12 in. (150 x 300 mm) cylinders, moist-cured specimens.

No.	$(f_c)_{6x12}$ psi	$(f_{sp})_{6x12}$ psi	n	STD psi	$(f_{sp})_{4x8}$ psi	n	STD psi	Diff. psi	Ratio
23	12773	731	2	39	717	3	54	-14	0.98
24	11612	595	2	41	732	3	70	138	1.23
25	11110	602	2	48	795	3	45	193	1.32
26	13821	729	2	134	1016	3	27	287	1.39
27	12148	651	2	17	894	3	185	243	1.37
28	9718	626	2	41	716	3	35	89	1.14
29	11071	570	2	88	804	3	114	234	1.41
50	11733	716	2	46	951	2	30	235	1.33
51	10020	670	2	7	751	2	37	81	1.12
52	12993	741	2	21	955	2	28	214	1.29
53	9742	568	2	51	719	2	13	150	1.26
54	13534	840	2	19	933	2	91	93	1.11
55	12216	752	2	17	910	2	46	158	1.21
56	12878	772	1		955	2	56	183	1.24
57	12328	602	2	24	934	2	89	332	1.55
58	11910	675	2	36	794	2	43	119	1.18
59	12076	715	2	96	927	2	3	212	1.30
60	11366	749	2	32	935	2	67	186	1.25
61	11533	734	2	76	1021	2	69	287	1.39
62	12639	809	2	44	901	2	132	92	1.11
63	11745	824	2	34	874	2	63	50	1.06
64	12600	777	2	54	963	2	29	186	1.24
65	13315	803	2	22	1035	2	71	232	1.29
66	12345	775	2	9	1053	2	59	278	1.36
67	12381	678	2	134	990	2	47	312	1.46
68	12715	722	2	25	880	2	22	158	1.22
69	11152	794	2	6	857	2	3	63	1.08
70	13365	712	2	9	996	2	39	284	1.40
71	12530	616	2	44	943	2	55	326	1.53
72	11831	791	2	30	946	2	2	155	1.20
73	12507	753	2	16	896	2	92	143	1.19
74	12690	725	2	21	914	2	85	189	1.26
75	11187	699	2	100	813	2	33	114	1.16
76	11342	662	2	39	837	2	47	175	1.26
77	12407	746	2	77	885	2	24	139	1.19
78	11643	729	2	40	894	2	30	165	1.23
79	12316	609	2	62	955	2	72	346	1.57
80	11825	775	2	56	881	2	36	106	1.14
81	11633	765	2	5	738	2	50	-27	0.96
82	10457	679	2	3	757	2	22	79	1.12
83	10887	672	2	5	902	2	25	229	1.34
84	12016	807	2	47	917	2	74	110	1.14
85	12772	795	2	76	1022	2	105	227	1.29
86	9742	589	2	4	767	2	87	178	1.30
87	9865	649	2	37	714	2	12	65	1.10
88	11807	790	2	36	921	2	119	131	1.17
89	11655	768	2	0	836	2	82	68	1.09
90	8749	644	2	68	777	2	47	132	1.21
91	9647	601	2	17	767	2	56	166	1.28
100	10137	679	2	28	-	-	-	-	-
102	9522	582	2	13	-	-	-	-	-
104	12867	768	2	41	-	-	-	-	-
106	12063	752	2	61	-	-	-	-	-
108	12646	839	2	8	-	-	-	-	-
109	11831	746	2	11	-	-	-	-	-

n = number of replicate specimens tested
STD = sample standard deviation (n > 1)
Diff. = $f_{4x8} - f_{6x12}$
Ratio = f_{4x8} / f_{6x12}

Table 8.2. Splitting tensile strength of 4 x 8 in. (100 x 200 mm) and 6 x 12 in. (150 x 300 mm) cylinders, moist-cured specimens. Continued ...

No.	$(f_c)_{6x12}$ psi	$(f_{sp})_{6x12}$ psi	n	STD psi	$(f_{sp})_{4x8}$ psi	n	STD psi	Diff. psi	Ratio
110	11452	725	2	36	-	-	-	-	-
111	10051	636	2	37	-	-	-	-	-
112	13582	728	2	43	-	-	-	-	-
113	13825	705	2	46	-	-	-	-	-
114	13550	805	2	70	-	-	-	-	-
115	13374	721	2	5	-	-	-	-	-
124	14524	963	1		-	-	-	-	-
125	11574	847	1		-	-	-	-	-
126	13237	790	1		-	-	-	-	-
127	14321	789	1		-	-	-	-	-
128	13045	891	1		-	-	-	-	-
129	13614	963	1		-	-	-	-	-
130	12516	791	1		-	-	-	-	-
131	14330	858	1		-	-	-	-	-
132	13945	968	1		-	-	-	-	-
133	14631	1030	1		-	-	-	-	-
134	13936	898	1		-	-	-	-	-
135	13727	957	1		-	-	-	-	-
136	13816	711	1		-	-	-	-	-
137	14155	834	1		-	-	-	-	-
138	13162	794	1		-	-	-	-	-
139	13358	787	1		-	-	-	-	-

n = number of replicate specimens tested
STD = sample standard deviation (n > 1)
Diff. = $f_{4x8} - f_{6x12}$
Ratio = f_{4x8} / f_{6x12}

Table 8.3. Flexural tensile strength of 6 x 6 x 24 in. (150 x 150 X 610 mm) high strength concrete simple supported beams with 18 in. (457 mm) clear span and third-point loading, heat-cured specimens.

No.	$(f_c)_{6x12}$ psi	f_r psi	n	STD psi	No.	$(f_c)_{6x12}$ psi	f_r psi	n	STD psi
22	13127	999	2	27	**87**	8887	837	2	22
23	12412	1084	2	10	**88**	10738	781	2	27
24	10718	973	2	14	**89**	10100	870	2	26
25	9653	864	2	16	**90**	7498	728	2	11
26	12588	815	2	45	**91**	7972	875	2	30
27	11033	1001	2	1	**100**	10198	878	1	
28	8819	903	2	32	**101**	8594	947	1	
29	9860	859	2	34	**102**	7886	880	1	
50	11551	1051	2	28	**103**	8438	943	1	
51	9799	909	2	6	**104**	11078	1087	1	
52	12238	1067	2	15	**105**	10365	1055	1	
53	9185	823	2	3	**106**	10047	1073	1	
54	12517	941	2	74	**107**	8832	992	1	
55	11703	1049	2	48	**108**	11270	992	1	
56	12135	1098	2	2	**109**	10375	1038	1	
57	12177	1081	2	29	**110**	9997	861	1	
58	12149	995	2	75	**111**	9328	896	1	
59	11928	963	2	67	**112**	11924	1058	1	
60	10774	937	2	5	**113**	12001	1108	1	
61	11322	859	2	51	**114**	11007	1053	1	
62	11887	829	2	70	**115**	10332	993	1	
63	11151	1003	2	35	**116**	11721	838	1	
64	12034	939	2	44	**117**	11757	1061	1	
65	12688	853	2	25	**118**	9489	776	1	
66	11677	1013	2	1	**119**	8726	887	1	
67	12284	1041	2	34	**120**	12947	1066	1	
68	11874	1053	2	11	**121**	12639	1000	1	
69	10553	1026	2	37	**122**	11634	1048	1	
70	11788	1105	2	33	**123**	11051	972	1	
71	11218	1070	2	15	**124**	14789	1188	1	
72	10588	958	2	81	**125**	15198	1015	1	
73	12253	1106	2	28	**126**	11981	1240	1	
74	11748	1024	2	37	**127**	12629	968	1	
75	10846	1053	2	25	**128**	12291	947	1	
76	11073	1068	2	106	**129**	12833	952	1	
77	11175	1012	2	58	**130**	11694	822	1	
78	10602	896	2	49	**131**	12262	1315	1	
79	10719	990	2	24	**132**	14310	1233	1	
80	11059	1081	2	13	**133**	15362	1058	1	
81	10606	1031	2	98	**134**	12545	1072	1	
82	9155	986	2	26	**135**	15086	1023	1	
83	9299	1025	2	61	**136**	11777	952	1	
84	11661	889	2	53	**137**	12826	1108	1	
85	11304	965	2	68	**138**	11003	888	1	
86	8633	804	2	24	**139**	12112	937	1	

n = number of replicate specimens tested
STD = sample standard deviation (n > 1)

Table 8.4. Flexural tensile strength of 6 x 6 x 24 in. (150 x 150 X 610 mm) high strength concrete simple supported beams with 18 in. (457 mm) clear span and third-point loading, moist-cured specimens.

No.	$(f_c)_{6x12}$ psi	f_r psi	n	STD psi	No.	$(f_c)_{6x12}$ psi	f_r psi	n	STD psi
22	12688	1207	2	16	**81**	11633	979	2	75
23	12773	1497	2	101	**82**	10457	887	2	91
24	11612	1160	2	33	**83**	10887	958	2	120
25	11110	1122	2	27	**84**	12016	1558	2	54
26	13821	1266	2	80	**85**	12772	1506	2	48
27	12148	1252	2	31	**86**	9742	1266	2	107
28	9718	989	2	45	**87**	9865	971	2	103
29	11071	872	2	12	**88**	11807	1358	2	117
50	11733	1256	2	70	**89**	11655	1471	2	15
51	10020	1111	2	22	**90**	8749	1230	2	42
52	12993	1332	2	9	**91**	9647	1146	2	41
53	9742	988	2	68	**100**	10137	1256	2	98
54	13534	1221	2	41	**102**	9522	1217	2	82
55	12216	1116	2	135	**104**	12867	1510	2	54
56	12878	1087	2	97	**106**	12063	1333	2	81
57	12328	1047	2	24	**108**	12646	1493	2	142
58	11910	1218	2	29	**109**	11831	1420	2	10
59	12076	1274	2	2	**110**	11452	1428	2	84
60	11366	1075	2	16	**111**	10051	1389	2	81
61	11533	1033	2	25	**112**	13582	1520	2	54
62	12639	1218	2	52	**113**	13825	1552	2	22
63	11745	1118	2	53	**114**	13550	1438	2	53
64	12600	1268	2	24	**115**	13374	1430	2	14
65	13315	1220	2	18	**124**	14524	1521	1	
66	12345	1498	2	6	**125**	11574	1446	1	
67	12381	1377	2	40	**126**	13237	1262	1	
68	12715	1299	2	4	**127**	14321	1258	1	
69	11152	1152	2	19	**128**	13045	1743	1	
70	13365	1037	2	120	**129**	13614	1652	1	
71	12530	834	2	9	**130**	12516	1661	1	
72	11831	898	2	25	**131**	14330	1543	1	
73	12507	1138	2	85	**132**	13945	1496	1	
74	12690	1178	2	81	**133**	14631	1598	1	
75	11187	1105	2	116	**134**	13936	1455	1	
76	11342	1069	2	67	**135**	13727	1422	1	
77	12407	1092	2	59	**136**	13816	1380	1	
78	11643	1196	2	7	**137**	14155	1422	1	
79	12316	1061	2	60	**138**	13162	1341	1	
80	11825	1112	2	38	**139**	13358	1327	1	

n = number of replicate specimens tested
STD = sample standard deviation (n > 1)

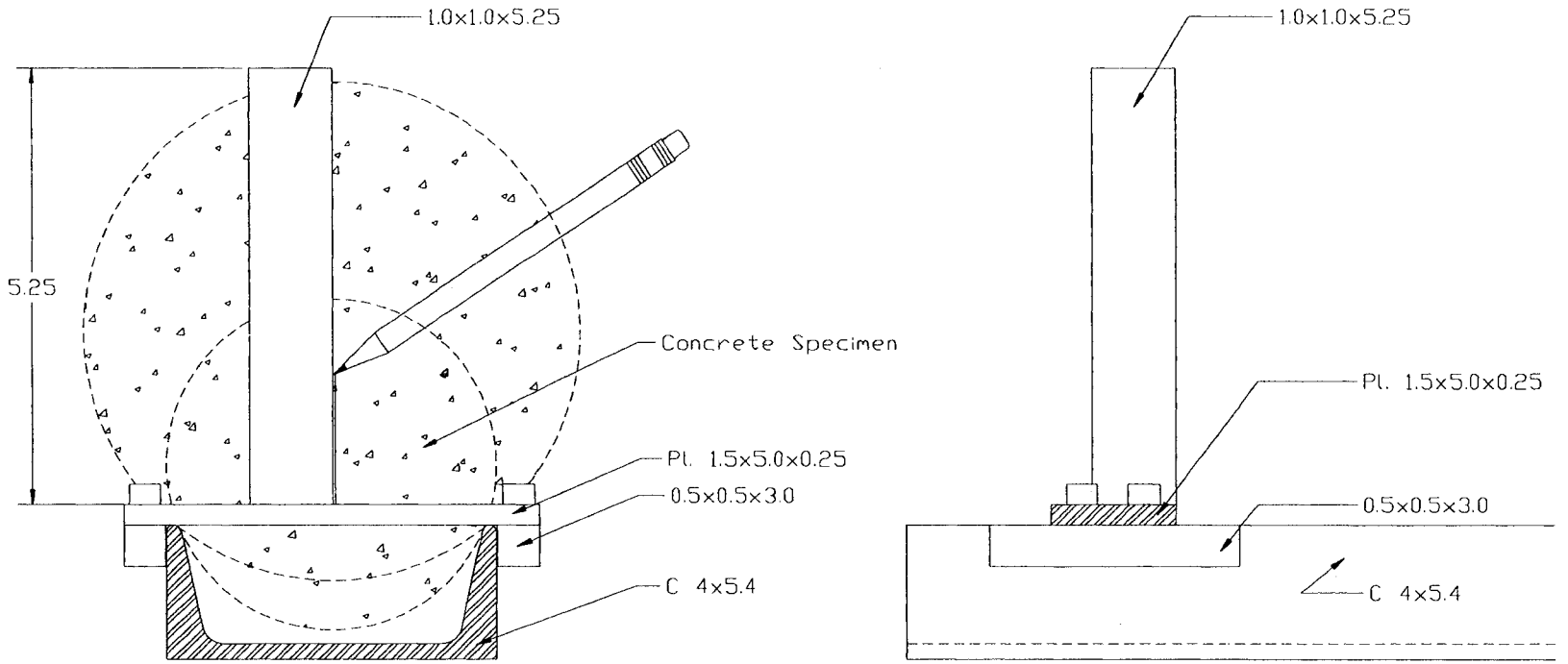

Figure 8.1. Detailed view of the apparatus constructed and used for marking diametral lines on ends of the specimens. [MRKSPLT.PLT]

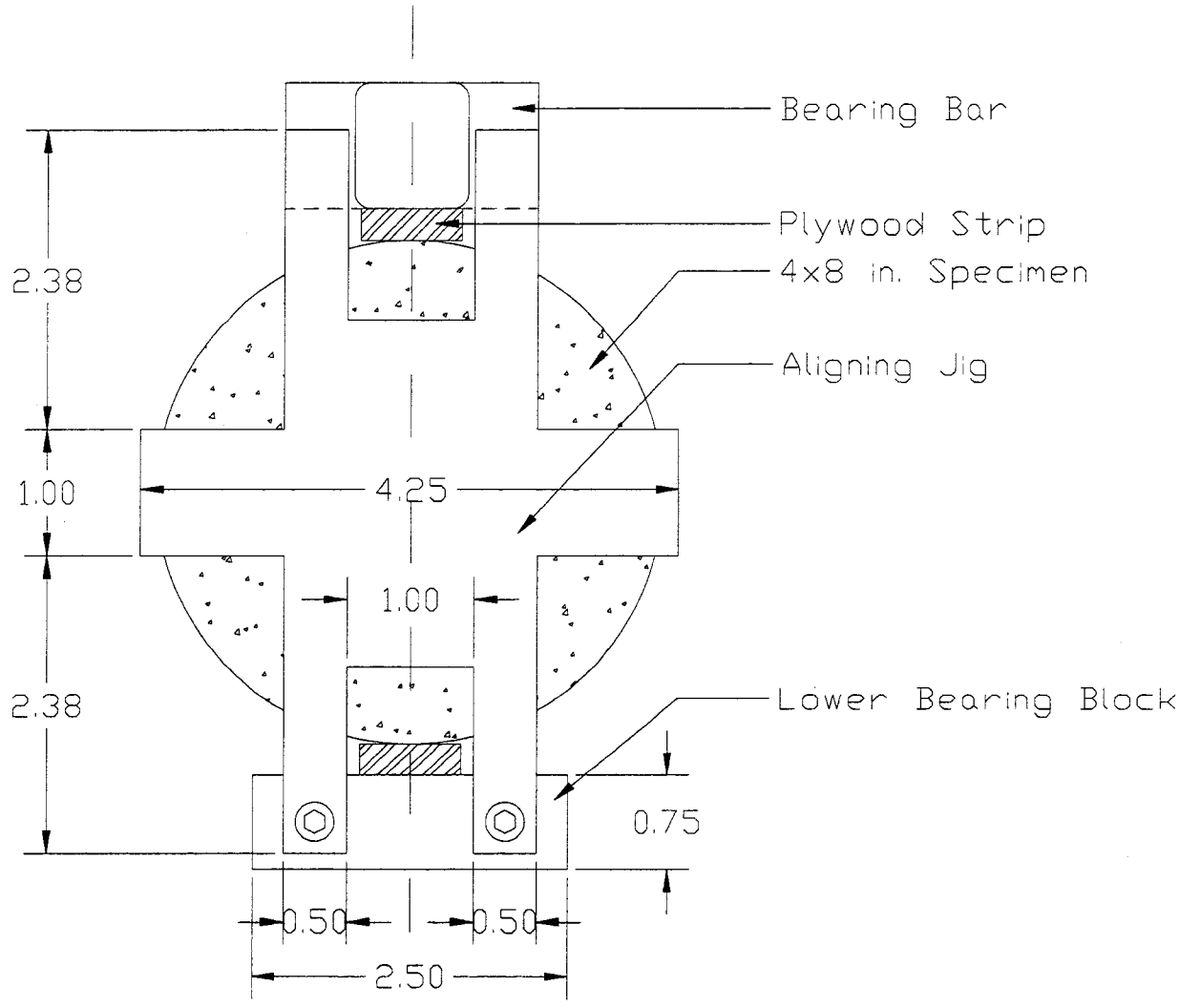

Figure 8.2. Front view of the jig constructed and used for aligning concrete cylinder and bearing strips. A similar aligning jig was constructed for use with 6 x 12 in. (150 x 300 mm) specimens. [SPLT4.PLT]

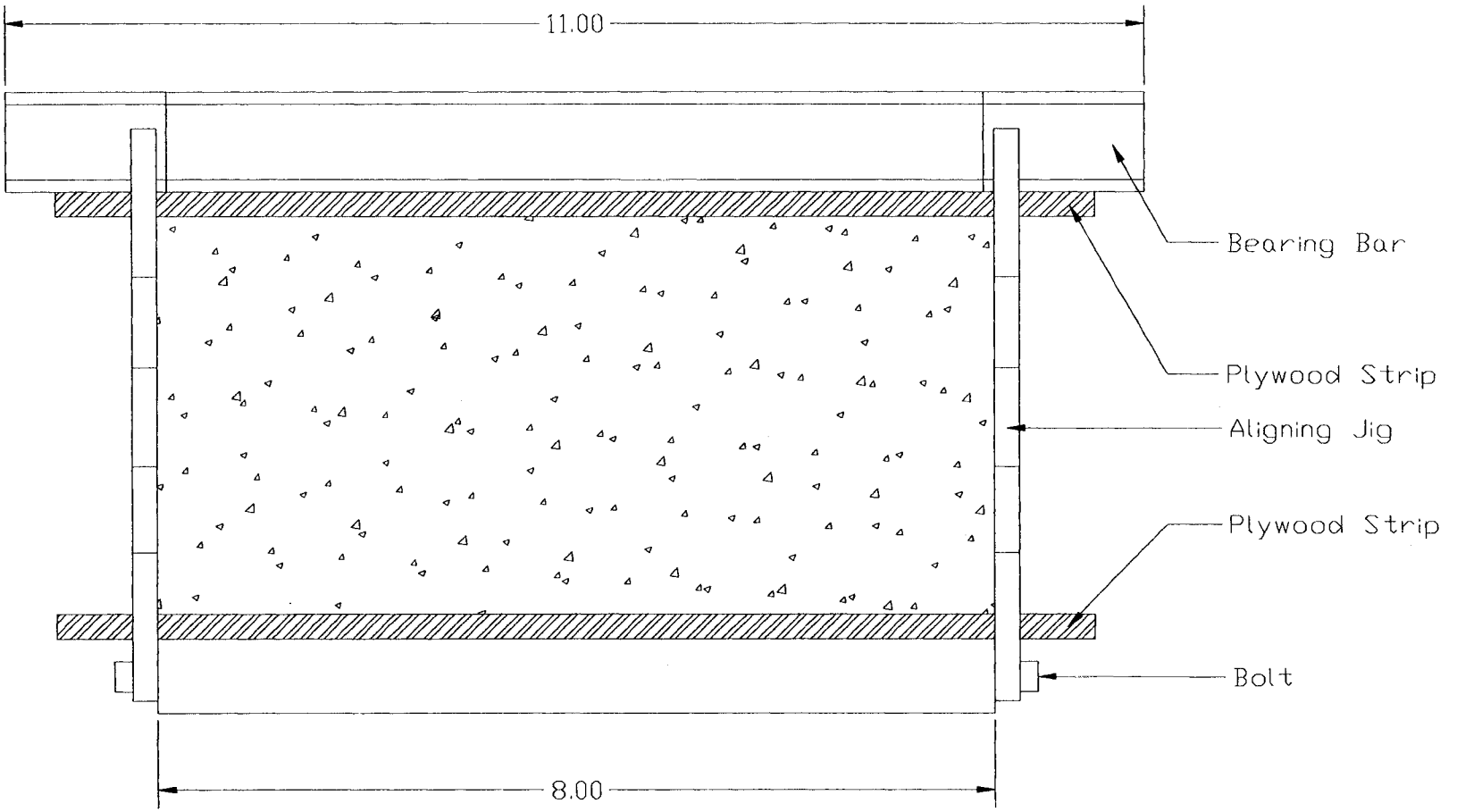

Figure 8.3. Side view of the jig used for aligning concrete cylinder and bearing strips. A similar aligning jig was constructed for use with 6 x 12 in. (150 x 300 mm) specimens.
[SPLT4_1.PLT]

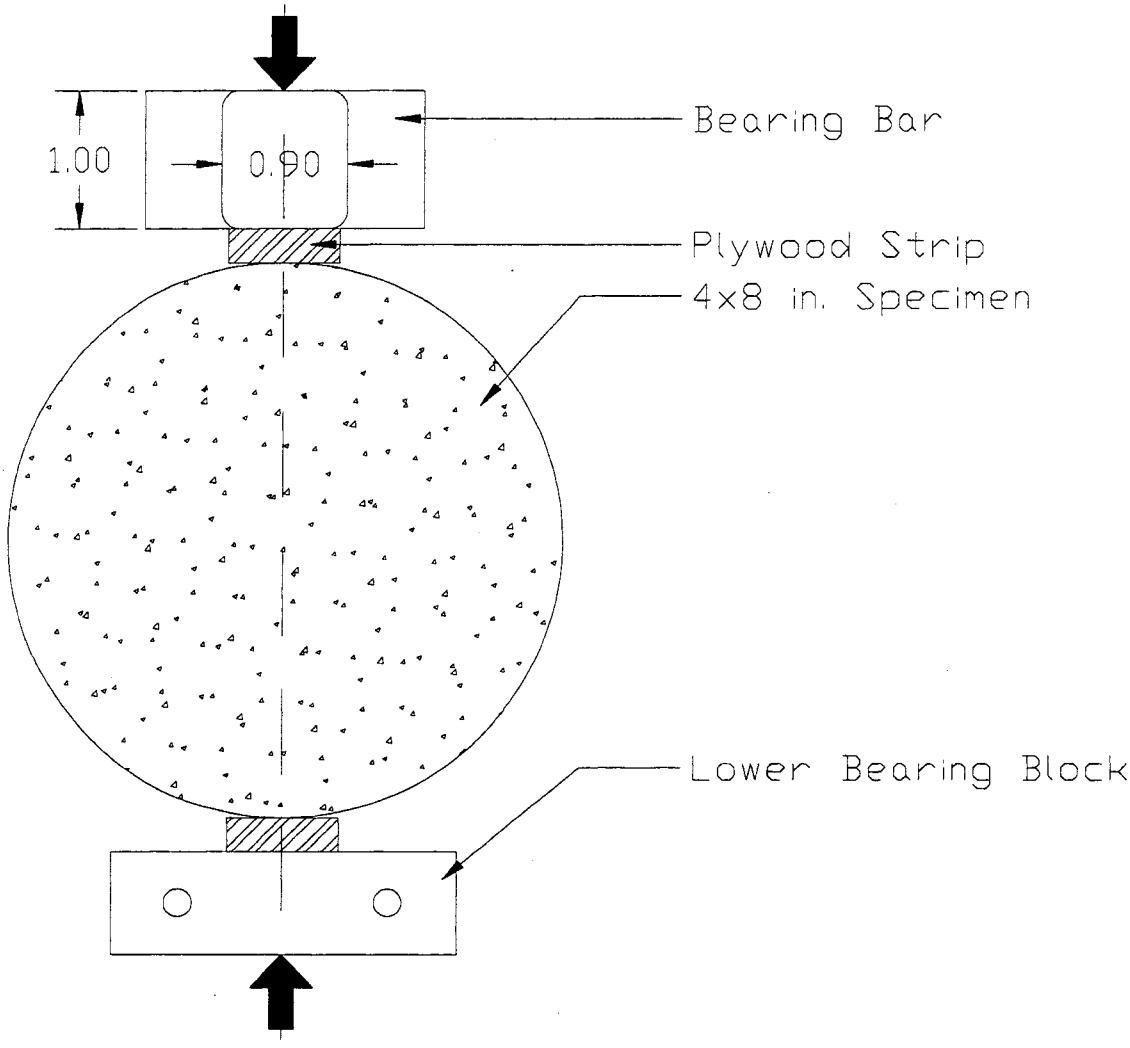

Figure 8.4. Specimen in testing position for determination of splitting tensile strength. [SPLT4_2.PLT]

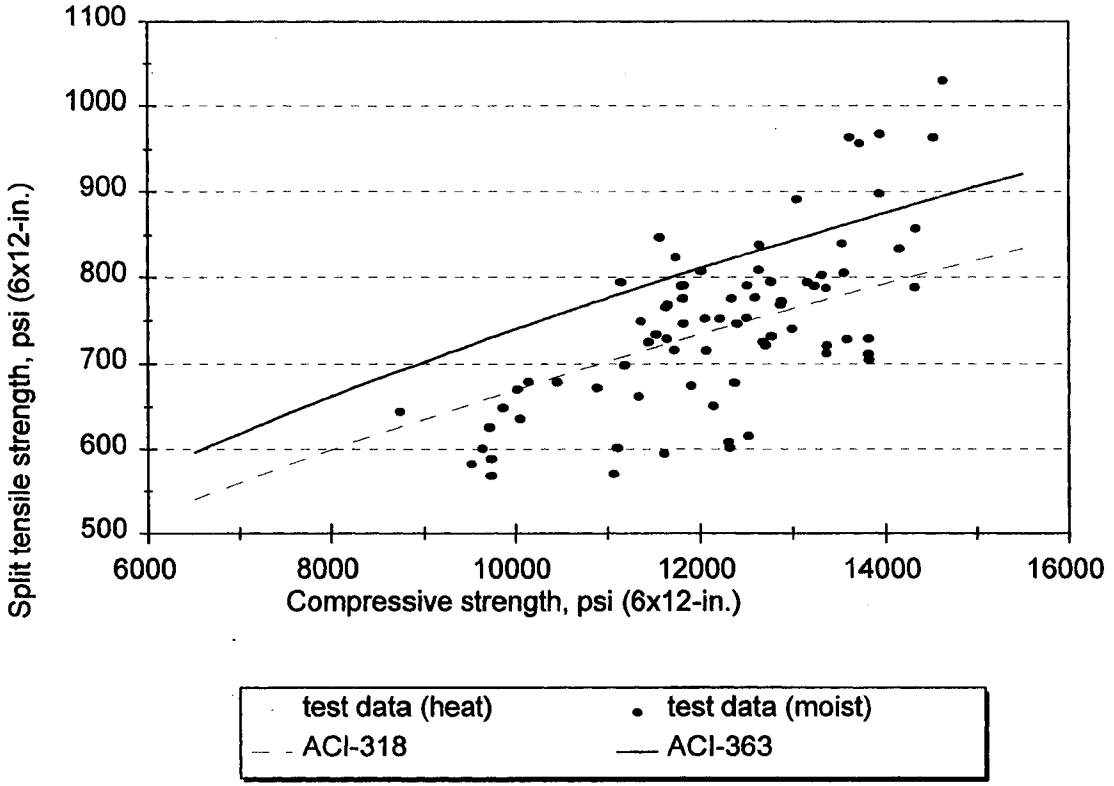

Figure 8.5. Scatter plot of 28-day splitting tensile strength versus compressive strength for all high strength concrete specimens studied. Also shown are proposed relationships by ACI-318 and ACI Committee 363.
[DATASPLT.WMF]

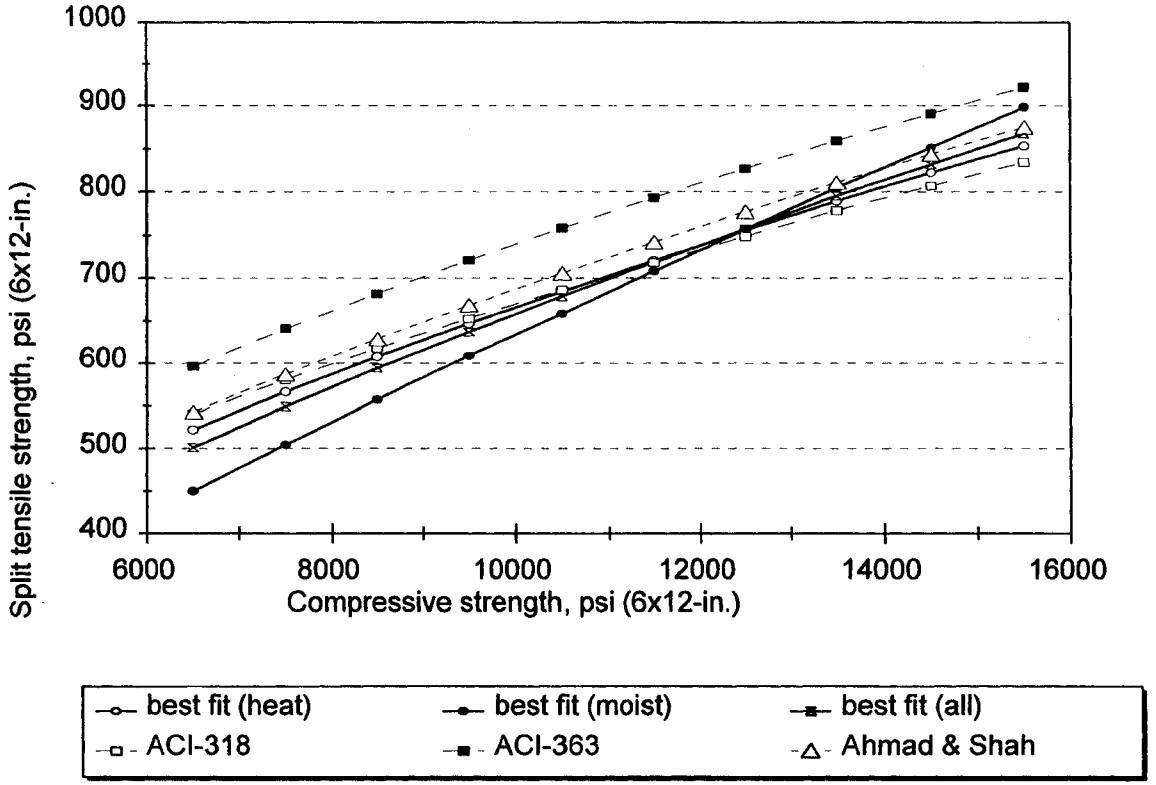

Figure 8.6. Comparison of the best-fit-lines from regression analysis on the experimental data from this study with proposed relationships by ACI-318 and ACI-363. Also shown is a proposed relationship by Ahmad and Shah (1985) for high strength concrete strength up to 12,000 psi (82.8 MPa).
[FITSPLT.WMF]

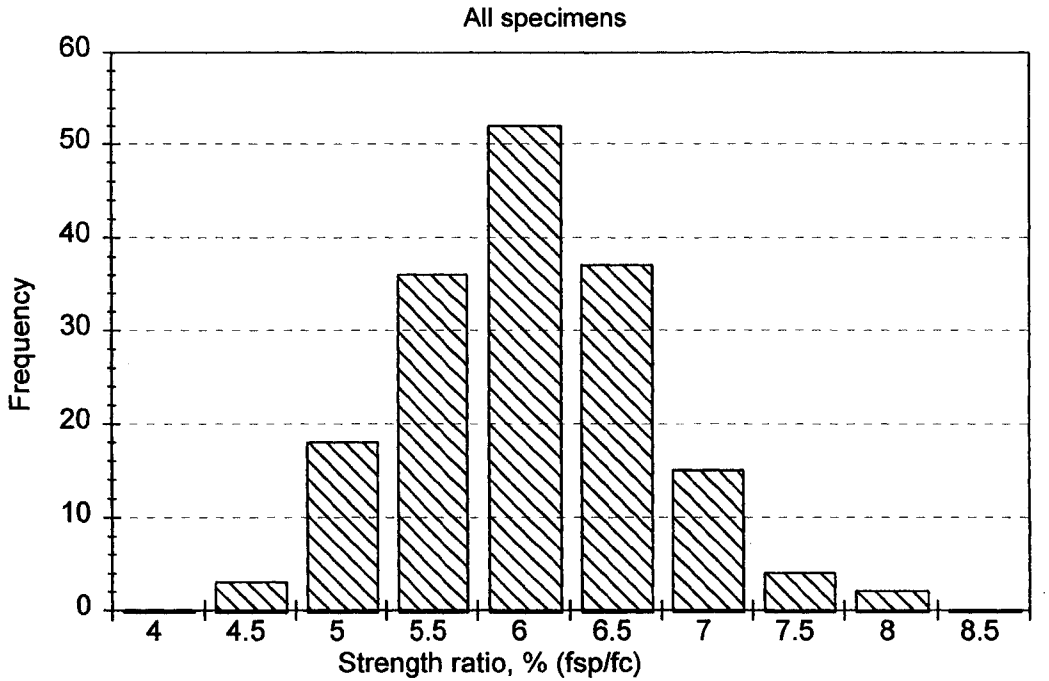

Figure 8.7. Histogram of the f_{sp}/f_c ratios for all specimens. The average value of the strength ratio was 0.0627 (6.27%) with a standard error of 0.0005.
[HISTSPLT.WMF]

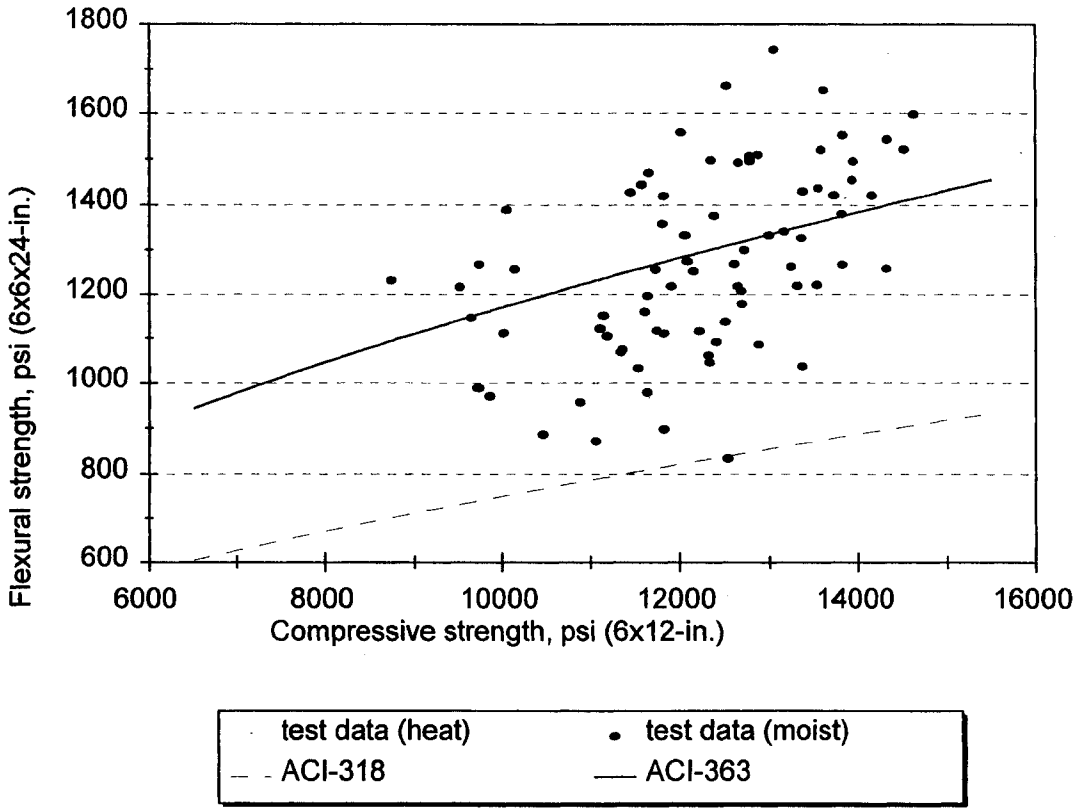

Figure 8.8. Scatter plot of 28-day flexural tensile strength versus compressive strength for all high strength concrete specimens studied. Also shown are proposed relationships by ACI-318 and ACI Committee 363.
[DATAFLX.WMF]

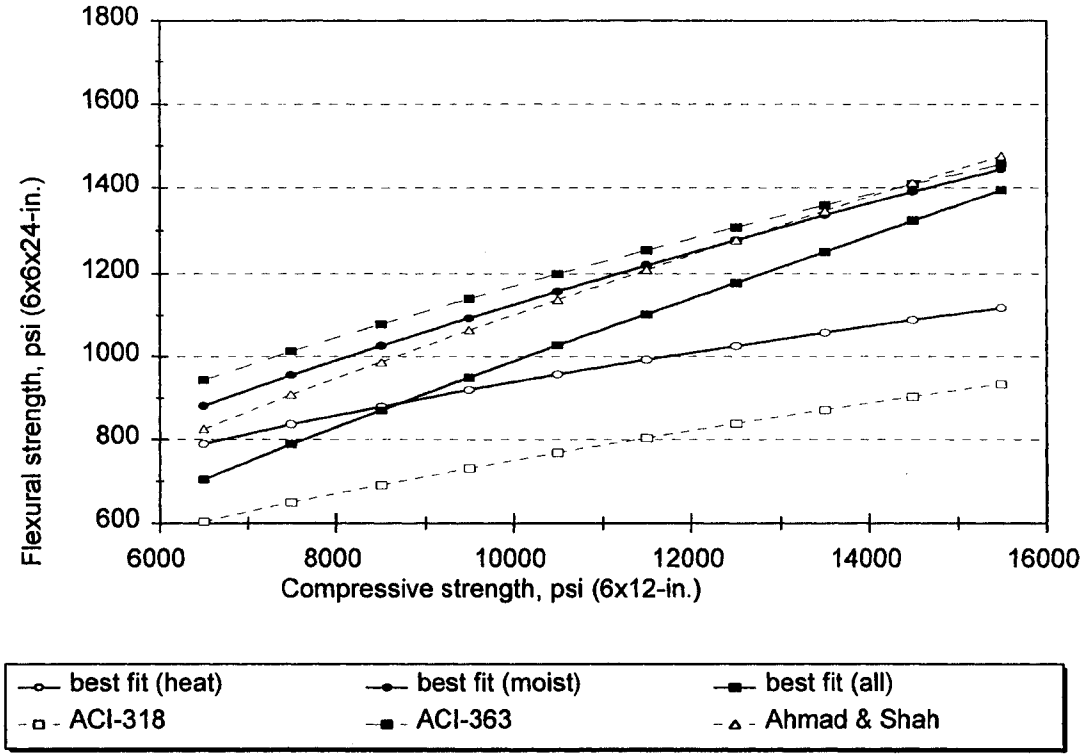

Figure 8.9. Comparison of the best-fit-lines resulting from regression analysis on the experimental data from this study with proposed relationships by ACI-318 and ACI-363. Also shown is relationship by Ahmad and Shah (1985) for high strength concrete strength up to 12,000 psi (82.8 MPa).
[FITFLX.WMF]

CHAPTER 9
TEST RESULTS: EFFECT OF COARSE AGGREGATE ON MECHANICAL PROPERTIES OF HIGH STRENGTH CONCRETE

9.1 Experimental Program

Mechanical properties (compressive strength, modulus of elasticity, modulus of rupture, and splitting tensile strength) of high strength concrete specimens cast from concretes of given mix proportions and made with six different coarse aggregates (R1, R2, G1, G2, L1, L2) were investigated. The coarse aggregates considered were:

- A siliceous river gravel with round and smooth particles (*R1*) with a maximum size of 1/2 in. (13 mm) and 1.44% absorption;
- Another siliceous river gravel with a significant proportion of crushed particles (*R2*) with a maximum size of 1/2 in. (13 mm) and 1.39% absorption;
- Two crushed granites (*G1* and *G2*) with 3/4 in. (19 mm) maximum size and 1.00% absorption from two sources;
- The other two aggregate types consisted of crushed limestone particles with a 1/2 in. (13 mm) maximum size. One of the crushed limestones (*L1*) had an absorption of 2.05% and the other (*L2*) had an absorption of 1.50%.

Gradation curves for the coarse aggregates used were presented in Chapter 3 of this report. All high strength concrete mixes considered had a total cementitious material content of 750 lb/yd^3 (445 kg/m^3), were made with ASTM Type III portland cement, and had a water-to-cementitious material ratio of 0.30. These mixes formed the following four groups with different cementitious material compositions:

1. *Reference mixes* (Mix Nos. 96, 108, 124, 128, 132, and 136): had no fly ash or silica fume as part of their cementitious material.
2. *Fly Ash (FA) mixes* (Mix Nos. 110, 125, 129, 133, and 137): 20% of the total weight of the cementitious material was replaced by an ASTM Class C fly ash. This group did not include a mix with G1 coarse aggregate.
3. *Silica Fume (SF) mixes* (Mix Nos. 98, 112, 126, 130, 134, and 138): 7.5% of the total weight of the cementitious material was replaced by silica fume; and
4. *Fly Ash and Silica Fume (FA + SF) mixes* (Mix Nos. 114, 127, 131, 135, and 139): 20% and 7.5% of the total weight of the cementitious material was replaced by an ASTM Class C fly ash and silica fume respectively. This group did not include a mix with G1 coarse aggregate.

9.2 Effect of Coarse Aggregate on Compressive Strength

Compressive strength test results are given in Table 9.1 and plotted in Figures 9.1 through 9.8. As can be seen from the test results, high strength concrete of the same mix proportions produced different compressive strengths, depending on the type of aggregate used. The maximum range in the compressive strength test results of heat-cured specimens from high strength concretes of the same mix proportions and tested at the same age, was 52, 46, 23, and 39 percent for reference, fly ash, silica fume and FA+SF mixes respectively. For moist-cured specimens maximum compressive strength range values were 24, 36, 11, and 16 percent respectively (Table 9.1). The average range for compressive strengths of reference, fly ash, silica fume, and FA+SF mixes was 39, 41, 21, and 36 percent for heat-cured and 17, 25, 9, and 13 percent for moist-cured specimens. Therefore the effect of different aggregate on compressive strength depended on both curing condition and the composition of cementitious material of the mix. The effect of type of coarse aggregate was significantly less for moist-cured specimens. However, the effects were still considered as significant.

The effect of different coarse aggregates on compressive strength was the most noticeable when 20% of the weight of portland cement was replaced with ASTM Class C fly ash. After fly ash mixes, the effect of type of coarse aggregate on compressive strength test results was the most for the reference mixes and the least for silica fume mixes. the Combination of moist-curing and replacement of 7.5% of portland cement with silica fume significantly decreased the effect of type of coarse aggregate on compressive strength test results at all ages (average range 9%).

In general, the highest compressive strength values were produced by specimens made with the low-absorption limestone (L2) followed by those made with the high-absorption limestone (L1), granite #2 or the partially crushed river gravel (G2, or R2), granite #1 (G1), and the round river gravel (R1), Figures 9.1 through 9.8. The only exceptions were the silica fume mixes (concretes in which 7.5% of the weight of the portland cement was replaced by silica fume) for which case the effect of type of coarse aggregate on compressive strength was minimal.

The observation that the low-absorption limestone produced higher compressive strengths than the high-absorption limestone, in otherwise identical mixes, may appear to contradict the published results from an earlier study conducted at early stages of this research program where two high strength concrete reference mixes (Mix Nos. 4 and 5), with water-to-cement ratio of 0.32, were made using two limestone aggregates from the same sources with absorption rates of 1.50% and 2.96% *[French and Mokhtarzadeh 1993]*. Figure 9.9 shows the results from that study. Compressive strength test results were measured at 3, 7, and 28-days on 6 x 12 in. (150 x 300 mm) heat-cured cylinders. No significant difference in compressive strength test results was observed.

It should be reminded that at lower compressive strength levels, the influence of aggregate types on the compressive strength of concrete is generally negligible and the compressive strength of the concrete system is predominantly controlled by the strength of the cement paste and the bond between the cement paste and the coarse aggregate (transition zone). However, at higher strength levels where the strengths of the hardened cement paste and the bond between the cement paste and the aggregate is improved, the type of the coarse aggregate can have a significant effect on the compressive strength of the concrete. Aïtcin et al. *(1987, 1990)* found that the mineralogy and the strength of the coarse aggregate greatly influenced the strength of very high strength concrete.

It is of interest to see that the results described earlier, from the two parts of this study, are in complete agreement with the above argument and do not represent any contradiction. A close look at the data of high strength concrete specimens made with the two types of limestones L1 and L2, presented in Table 9.1, shows that the compressive strengths of concrete considered ranged between 9,219 to 16,871 psi (63.6 to 116 MPa) and 14,264 to 17,573 psi (98.3 to 121 MPa) for heat- and moist-cured specimens, respectively. These strength levels represent very high strength concrete and as is expected are greatly influenced by the type of coarse aggregate used in the mix. However, for the other part of this study, the range of compressive strength data presented in Figure 9.9 was 8,780 to 10,440 psi (60.0 to 72.0 MPa), lower than the ranges studied in the other case.

9.3 Effect of Coarse Aggregate on Modulus of Elasticity

The effects of different types of coarse aggregate on modulus of elasticity were not as great as on the compressive strength of high strength concrete. Nevertheless, the effects were considerable. The maximum range in the modulus of elasticity test results of heat-cured specimens from high strength concretes of the same mix proportions and

tested at the same age, was 12, 17, 15, and 18 percent for reference, fly ash, silica fume and FA+SF mixes, respectively. For moist-cured specimens, the maximum modulus of elasticity range values were 13, 9, 11, and 14 percent respectively (Table 9.2). The average range for compressive strengths of reference, fly ash, silica fume, and FA+SF mixes was 10, 13, 12, and 14 percent for heat-cured and 8, 6, 8 and 13 percent for moist-cured specimens. Moist-curing or composition of cementitious material did not influence the effects of coarse aggregate-type on modulus of elasticity variations significantly. No single aggregate-type consistently resulted in the highest modulus of elasticity values. However, high strength concrete mixes made with low-absorption limestone (L2) and partially crushed river gravel (R2) were the most likely to test the highest and high strength concrete mixes made with the high-absorption limestone (L1) were the most likely to test the lowest modulus of elasticity values.

9.4 Effect of Coarse Aggregate on Flexural Tensile Strength

The effects of different types of coarse aggregate on flexural tensile strength of high strength concrete of the same mix proportions were observed to be significant, Table 9.3. As was the case for compressive strength test results, the heat-cured specimens were most affected by the type of coarse aggregate used. The maximum range in flexural strength of concrete varied between 25 to 41 percent for heat-cured and 15 to 28 percent for moist-cured specimens. The maximum range in flexural strength of concrete varied between 22 to 33 percent and 25 to 36 percent when initial heat-curing was followed by 1 and 3 days of moist-curing (HW1 and HW3), respectively. For moist-cured specimens high strength concrete mixes made with the partially crushed river gravel (R2) consistently resulted in the highest flexural strength values. Lowest values of flexural strength in moist-cured specimens were observed to be those of high strength concrete mixes made with granite #2 (G2) and low-absorption limestone (L1) for high strength concrete mixes without silica fume (reference and fly ash mixes) and with silica fume

(silica fume and FA + SF mixes), respectively. In the case of heat-cured specimens, the large scatter of the test results does not permit a strong conclusion in this regard. However, in general, flexural strength of high strength concrete mixes made with crushed limestone were among the highest values observed.

9.5 Effect of Coarse Aggregate on Splitting Tensile Strength

Coarse aggregate type also influenced the 28-day splitting tensile strength of 6 x 12 in. (150 x 300 mm) high strength concrete specimens made from mixes of the same proportions, Table 9.4. The maximum range in splitting tensile strength varied between 9 to 23 percent for heat-cured specimens and 20 to 35 percent for moist-cured specimens of all cementitious material compositions. Moist-curing slightly increased the effect of coarse aggregate type on splitting tensile strength of high strength concrete. Cementitious material composition did not seem to have a significant influence on the effect of the coarse aggregate on the splitting tensile strength of concrete.

9.6 Concluding Remarks

The aggregate type was observed to have a dominant effect on the mechanical properties of high strength concrete. This chapter summarizes the effect on the compressive strength, modulus of elasticity, and tensile strength.

With respect to compressive strength, the effect of aggregate type was dependent on the curing condition and cementitious material composition of mixes. Aggregate type had less of an effect for the moist-cured specimens compared with the heat-cured specimens. Relative to the cementitious material composition, the aggregate type had the most noticeable effect on the mixes which incorporated fly ash, and the least effect on the silica fume mixes. The aggregate type tend to have a greater effect influence as the compressive strengths increased.

The effect of aggregate type on modulus of elasticity was considerable, but not as pronounced as it was on the compressive strength. The cementiotious material composition and curing condition did not have a significant influence on the effect of aggregate type on the modulus of elasticity values.

The aggregate type had a significant effect on both the modulus of rupture and split cylinder tensile tests. The effect of heat-curing had the greatest effect on the tensile strength results with respect to aggregate type; whereas, the cementitious material composition did not have a significant effect on the tensile strength results with respect to aggregate type.

A companion study by Kriesel *[Mokhtarzadeh et al. 1995]* concluded that aggregate was the dominant variable in the freeze thaw durability of high strength concrete. The effect of the aggregate type on the creep and shrinkage properties of high strength concrete are described in the following chapter.

Table 9.1. Variations in compressive strength of 4 x 8 in. (100 x 200 mm) high strength concrete specimens made with 6 different types of coarse aggregates, psi.

Mix ID Code	No.	Age, day(s)						
		Heat-cured				Moist-cured		
		1	28	182	365	28	182	365
Reference Mixes								
131-XAR1-F00M00-130	108	8843	11218	11415	11373	13185	14489	14840
131-XAR2-F00M00-130	128	11630	12934	12746	12721	15031	15902	15849
131-XAG1-F00M00-130	96	9462	11808	12094	-	12986	-	-
131-XAG2-F00M00-130	136	11440	12624	12582	12621	14271	14998	14947
131-XAL1-F00M00-130	124	12338	15150	15134	14964	16487	16809	16702
131-XAL2-F00M00-130	132	14779	16298	15649	15731	16033	16279	16888
Maximum:		***14779***	***16298***	***15649***	***15731***	***16487***	***16809***	***16888***
Minimum:		***8843***	***11218***	***11415***	***11373***	***12986***	***14489***	***14840***
Range:		***5936***	***5080***	***4234***	***4358***	***3501***	***2320***	***2048***
Average:		***11415***	***13339***	***13270***	***13482***	***14666***	***15695***	***15845***
Range, percent:		***52***	***38***	***32***	***32***	***24***	***15***	***13***
Fly Ash Mixes								
131-XAR1-F20M00-130	110	8475	10908	11300	10826	11882	14341	14998
131-XAR2-F20M00-130	129	12083	14349	14259	14295	15604	16504	16243
131-XAG1-F20M00-130	-	-	-	-	-	-	-	-
131-XAG2-F20M00-130	137	12666	14127	13718	13687	16623	17205	16664
131-XAL1-F20M00-130	125	13829	16606	16508	16871	17117	17272	17215
131-XAL2-F20M00-130	133	14088	16393	16470	16722	17573	17638	18421
Maximum:		***14088***	***16606***	***16508***	***16871***	***17573***	***17638***	***18421***
Minimum:		***8475***	***10908***	***11300***	***10826***	***11882***	***14341***	***14998***
Range:		***5613***	***5698***	***5208***	***6045***	***5691***	***3297***	***3423***
Average:		***12228***	***14477***	***14451***	***14480***	***15760***	***16592***	***16708***
Range, percent:		***46***	***39***	***36***	***42***	***36***	***20***	***20***
Silica Fume Mixes								
131-XAR1-F00M75-130	112	11559	12920	13104	12347	14466	15293	15339
131-XAR2-F00M75-130	130	9983	12455	12464	12307	15038	15988	16072
131-XAG1-F00M75-130	98	11096	12529	12729	-	15292	-	-
131-XAG2-F00M75-130	138	10289	11729	11703	11781	14252	15415	15594
131-XAL1-F00M75-130	126	9219	12455	12488	12342	14264	15114	15618
131-XAL2-F00M75-130	134	10688	14159	14680	14405	14899	16695	17148
Maximum:		***11559***	***14159***	***14680***	***14405***	***15292***	***16695***	***17148***
Minimum:		***9219***	***11729***	***11703***	***11781***	***14252***	***15114***	***15339***
Range:		***2340***	***2430***	***2977***	***2624***	***1040***	***1581***	***1809***
Average:		***10472***	***12708***	***12861***	***12636***	***14702***	***15701***	***15954***
Range, percent:		***22***	***19***	***23***	***21***	***7***	***10***	***11***
FA + SF Mixes								
131-XAR1-F20M75-130	114	10393	11516	11312	10998	14841	15077	14942
131-XAR2-F20M75-130	131	12043	13140	13057	12973	15912	16558	17275
131-XAG1-F20M75-130	-	-	-	-	-	-	-	-
131-XAG2-F20M75-130	139	11260	12988	12882	13027	16036	15783	16066
131-XAL1-F20M75-130	127	11817	13878	13679	13542	15553	16057	16107
131-XAL2-F20M75-130	135	14606	16124	16279	16268	15959	17404	17494
Maximum:		***14606***	***16124***	***16279***	***16268***	***16036***	***17404***	***17494***
Minimum:		***10393***	***11516***	***11312***	***10998***	***14841***	***15077***	***14942***
Range:		***4213***	***4608***	***4967***	***5270***	***1195***	***2327***	***2552***
Average:		***12024***	***13529***	***13442***	***13362***	***15660***	***16176***	***16377***
Range, percent:		***35***	***34***	***37***	***39***	***8***	***14***	***16***

Range, percent = [(Maximum - Minimum)/(Average)]*100

Table 9.2. Variations in static modulus of elasticity of 4 x 8 in. (100 x 200 mm) high strength concrete specimens made with 6 different types of coarse aggregates, ksi.

Mix ID Code	No.	Age, day(s)						
		Heat-cured				Moist-cured		
		1	28	182	365	28	182	365
Reference Mixes								
131-XAR1-F00M00-130	108	6457	6637	6353	6230	7486	7749	7777
131-XAR2-F00M00-130	128	6503	6347	5836	5950	7198	7318	7421
131-XAG1-F00M00-130	96	-	6888	6411	-	7254	-	-
131-XAG2-F00M00-130	136	6529	6167	5974	6216	7254	7491	7514
131-XAL1-F00M00-130	124	6222	6630	6442	6684	7173	7888	7859
131-XAL2-F00M00-130	132	6629	6704	6554	6638	7247	7897	8460
Maximum:		*6629*	*6888*	*6554*	*6684*	*7486*	*7897*	*8460*
Minimum:		*6222*	*6167*	*5836*	*5950*	*7173*	*7318*	*7421*
Range:		*407*	*720*	*718*	*734*	*314*	*579*	*1040*
Average:		*6468*	*6562*	*6262*	*6343*	*7269*	*7669*	*7806*
Range, percent:		*6*	*11*	*11*	*12*	*4*	*8*	*13*
Fly Ash Mixes								
131-XAR1-F20M00-130	110	6212	6632	6291	6227	6993	7625	7801
131-XAR2-F20M00-130	129	6721	6916	7109	6889	7396	7624	8022
131-XAG1-F20M00-130	-	-	-	-	-	-	-	-
131-XAG2-F20M00-130	137	6679	6054	6016	5929	7666	7740	7684
131-XAL1-F20M00-130	125	6350	6529	6437	6406	7212	7933	7639
131-XAL2-F20M00-130	133	6510	6730	6617	6541	7320	7751	7699
Maximum:		*6721*	*6916*	*7109*	*6889*	*7666*	*7933*	*8022*
Minimum:		*6212*	*6054*	*6016*	*5929*	*6993*	*7624*	*7639*
Range:		*509*	*862*	*1093*	*960*	*672*	*310*	*383*
Average:		*6494*	*6572*	*6494*	*6398*	*7317*	*7735*	*7769*
Range, percent:		*8*	*13*	*17*	*15*	*9*	*4*	*5*
Silica Fume Mixes								
131-XAR1-F00M75-130	112	6460	6670	6134	6258	7581	7599	7887
131-XAR2-F00M75-130	130	6578	6509	6376	6596	7426	7983	7780
131-XAG1-F00M75-130	98	-	6109	6084	-	7628	-	-
131-XAG2-F00M75-130	138	6676	5785	5911	6096	7693	7636	7595
131-XAL1-F00M75-130	126	5735	6133	5985	5911	7017	7685	7834
131-XAL2-F00M75-130	134	6083	6658	6263	6571	7567	8021	8435
Maximum:		*6676*	*6670*	*6376*	*6596*	*7693*	*8021*	*8435*
Minimum:		*5735*	*5785*	*5911*	*5911*	*7017*	*7599*	*7595*
Range:		*941*	*884*	*465*	*685*	*676*	*421*	*840*
Average:		*6306*	*6311*	*6126*	*6286*	*7485*	*7785*	*7906*
Range, percent:		*15*	*14*	*8*	*11*	*9*	*5*	*11*
FA + SF Mixes								
131-XAR1-F20M75-130	114	6438	6559	6057	6339	7575	7676	7973
131-XAR2-F20M75-130	131	6844	6662	6398	6404	7440	8055	8317
131-XAG1-F20M75-130	-	-	-	-	-	-	-	-
131-XAG2-F20M75-130	139	6705	6011	6067	6094	7759	7681	7580
131-XAL1-F20M75-130	127	6140	5986	5635	5717	6696	7136	7279
131-XAL2-F20M75-130	135	6785	6855	6771	6607	7198	7826	8032
Maximum:		*6844*	*6855*	*6771*	*6607*	*7759*	*8055*	*8317*
Minimum:		*6140*	*5986*	*5635*	*5717*	*6696*	*7136*	*7279*
Range:		*704*	*868*	*1136*	*890*	*1063*	*919*	*1037*
Average:		*6582*	*6415*	*6186*	*6232*	*7334*	*7675*	*7836*
Range, percent:		*11*	*14*	*18*	*14*	*14*	*12*	*13*

Range, percent = [(Maximum - Minimum)/(Average)]*100

Table 9.3. Variations in 28-days flexural strengths of high strength concrete specimens made with 6 different types of coarse aggregates, psi.

Mix ID Code	No.	Flexural strength			
		Heat-cured	HW1-cured	HW3-cured	Moist-cured
Reference Mixes					
131-XAR1-F00M00-130	108	992	1032	1152	1493
131-XAR2-F00M00-130	128	947	1001	930	1743
131-XAG1-F00M00-130	96	-	-	-	-
131-XAG2-F00M00-130	136	952	1057	1053	1380
131-XAL1-F00M00-130	124	1188	1083	1330	1521
131-XAL2-F00M00-130	132	1233	1272	1205	1496
Maximum:		***1233***	***1272***	***1330***	***1743***
Minimum:		***947***	***1001***	***930***	***1380***
Range:		***285***	***271***	***400***	***363***
Average:		***1062***	***1089***	***1134***	***1527***
Range, percent:		***27***	***25***	***35***	***24***
Fly Ash Mixes					
131-XAR1-F20M00-130	110	861	857	826	1428
131-XAR2-F20M00-130	129	952	910	897	1652
131-XAG1-F20M00-130	-	-	-	-	-
131-XAG2-F20M00-130	137	1108	933	1066	1422
131-XAL1-F20M00-130	125	1015	1078	1023	1446
131-XAL2-F20M00-130	133	1058	978	1035	1598
Maximum:		***1108***	***1078***	***1066***	***1652***
Minimum:		***861***	***857***	***826***	***1422***
Range:		***247***	***221***	***240***	***231***
Average:		***999***	***951***	***969***	***1509***
Range, percent:		***25***	***23***	***25***	***15***
Silica Fume Mixes					
131-XAR1-F00M75-130	112	1058	963	1103	1520
131-XAR2-F00M75-130	130	822	998	1011	1661
131-XAG1-F00M75-130	98	-	-	-	-
131-XAG2-F00M75-130	138	888	818	831	1341
131-XAL1-F00M75-130	126	1240	1148	1193	1262
131-XAL2-F00M75-130	134	1072	1036	1000	1455
Maximum:		***1240***	***1148***	***1193***	***1661***
Minimum:		***822***	***818***	***831***	***1262***
Range:		***418***	***330***	***362***	***399***
Average:		***1016***	***993***	***1027***	***1448***
Range, percent:		***41***	***33***	***35***	***28***
FA + SF Mixes					
131-XAR1-F20M75-130	114	1053	1002	1033	1438
131-XAR2-F20M75-130	131	1315	1182	1213	1543
131-XAG1-F20M75-130	-	-	-	-	-
131-XAG2-F20M75-130	139	937	955	971	1327
131-XAL1-F20M75-130	127	968	1148	1111	1258
131-XAL2-F20M75-130	135	1023	966	836	1422
Maximum:		***1315***	***1182***	***1213***	***1543***
Minimum:		***937***	***955***	***836***	***1258***
Range:		***378***	***227***	***377***	***285***
Average:		***1059***	***1050***	***1033***	***1397***
Range, percent:		***36***	***22***	***36***	***20***

Range, percent = [(Maximum - Minimum)/(Average)]*100

Table 9.4. Variations in 28-days splitting tensile strengths of 6 x 12 in. (150 x 300 mm) high strength concrete specimens made with 6 different types of coarse aggregates, psi.

Mix ID Code	No.	Splitting tensile strength	
		Heat-cured	Moist-cured
Reference Mixes			
131-XAR1-F00M00-130	108	779	839
131-XAR2-F00M00-130	128	796	891
131-XAG1-F00M00-130	96	-	-
131-XAG2-F00M00-130	136	658	711
131-XAL1-F00M00-130	124	839	963
131-XAL2-F00M00-130	132	828	968
Maximum:		***839***	***968***
Minimum:		***658***	***711***
Range:		***181***	***257***
Average:		***780***	***874***
Range, percent:		***23***	***29***
Fly Ash Mixes			
131-XAR1-F20M00-130	110	670	725
131-XAR2-F20M00-130	129	688	963
131-XAG1-F20M00-130	-	-	-
131-XAG2-F20M00-130	137	714	834
131-XAL1-F20M00-130	125	829	847
131-XAL2-F20M00-130	133	818	1030
Maximum:		***829***	***1030***
Minimum:		***670***	***725***
Range:		***158***	***305***
Average:		***744***	***880***
Range, percent:		***21***	***35***
Silica Fume Mixes			
131-XAR1-F00M75-130	112	736	728
131-XAR2-F00M75-130	130	679	791
131-XAG1-F00M75-130	98	-	-
131-XAG2-F00M75-130	138	705	794
131-XAL1-F00M75-130	126	746	790
131-XAL2-F00M75-130	134	819	898
Maximum:		***819***	***898***
Minimum:		***679***	***728***
Range:		***140***	***170***
Average:		***737***	***800***
Range, percent:		***19***	***21***
FA + SF Mixes			
131-XAR1-F20M75-130	114	778	805
131-XAR2-F20M75-130	131	761	858
131-XAG1-F20M75-130	-	-	-
131-XAG2-F20M75-130	139	821	787
131-XAL1-F20M75-130	127	824	789
131-XAL2-F20M75-130	135	834	957
Maximum:		***834***	***957***
Minimum:		***761***	***787***
Range:		***73***	***170***
Average:		***804***	***839***
Range, percent:		***9***	***20***

Range, percent = [(Maximum - Minimum)/(Average)]*100

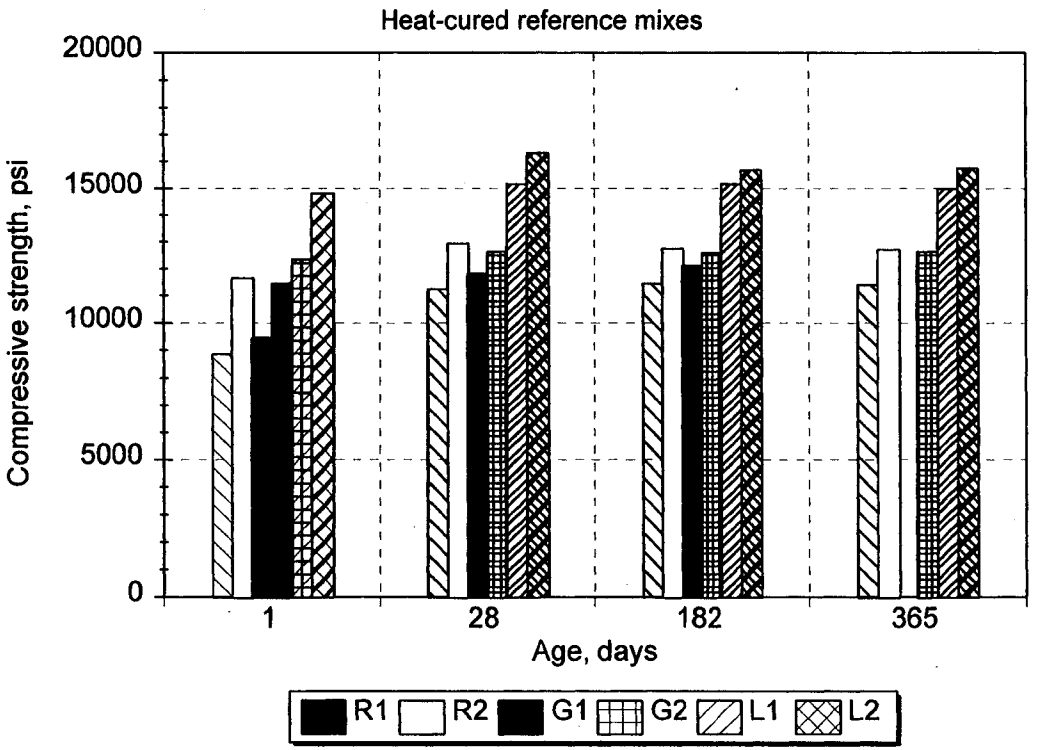

Figure 9.1. Aggregate-type effect on compressive strength of heat-cured 4 x 8 in. (100 x 200 mm) specimens of the same mix proportions, reference mixes.
[H_REF.WMF]

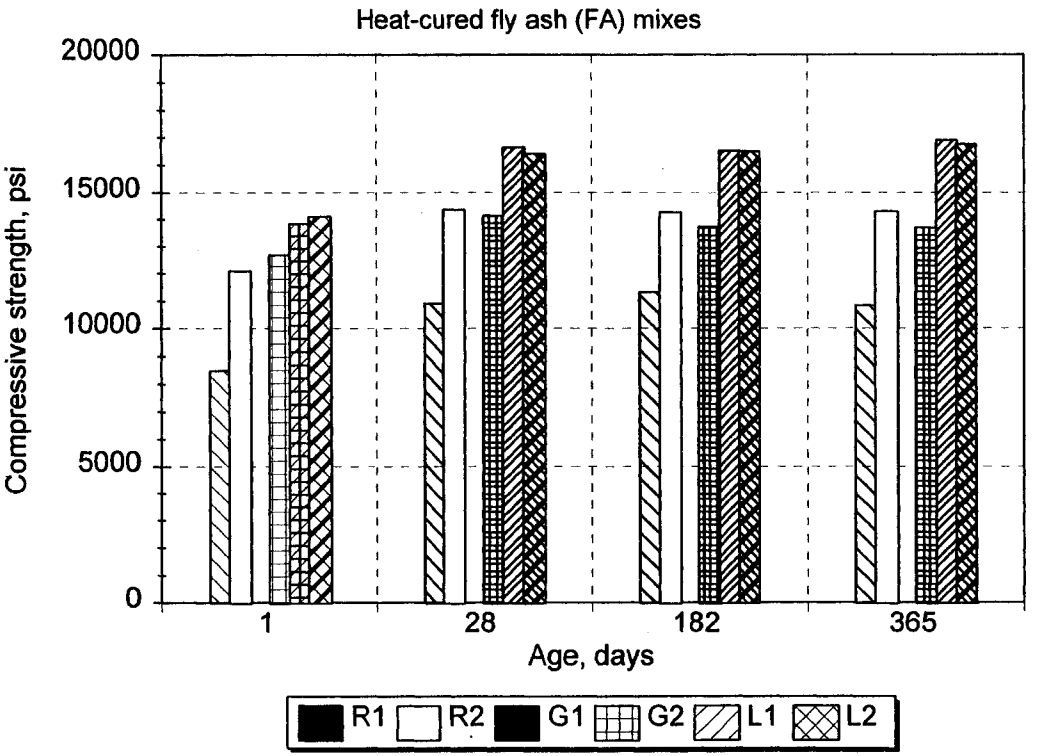

Figure 9.2. Aggregate-type effect on compressive strength of heat-cured 4 x 8 in. (100 x 200 mm) specimens of the same mix proportions, fly ash (FA) mixes.
[H_FA.WMF]

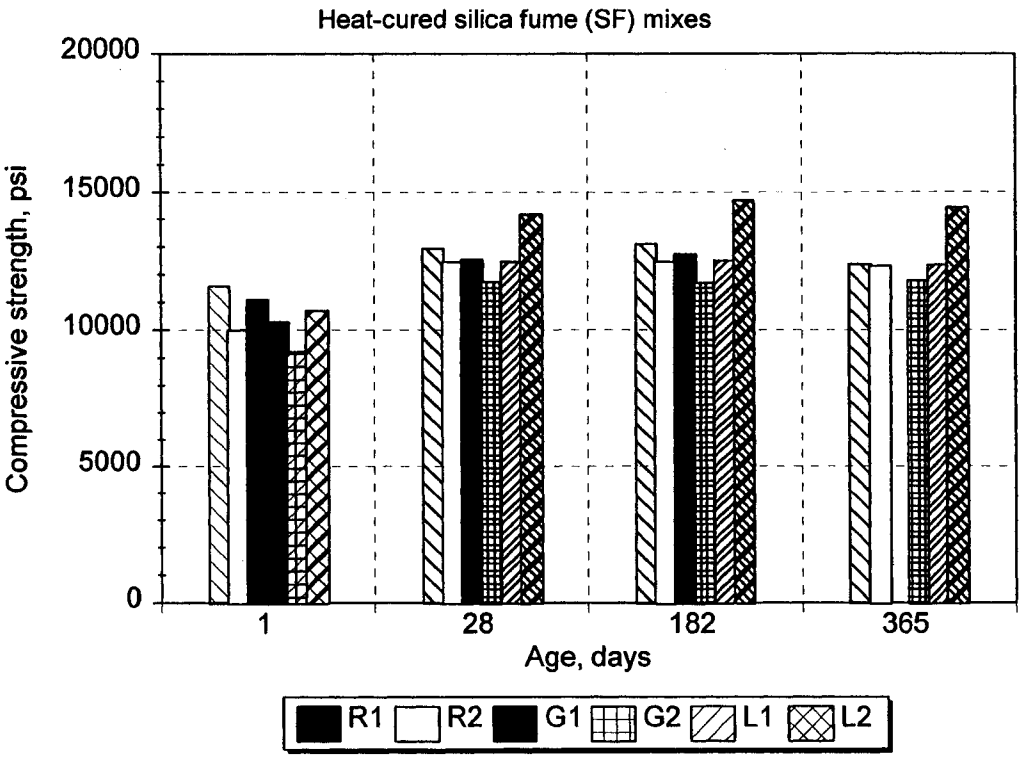

Figure 9.3. Aggregate-type effect on compressive strength of heat-cured 4 x 8 in. (100 x 200 mm) specimens of the same mix proportions, silica fume (SF) mixes.
[H_SF.WMF]

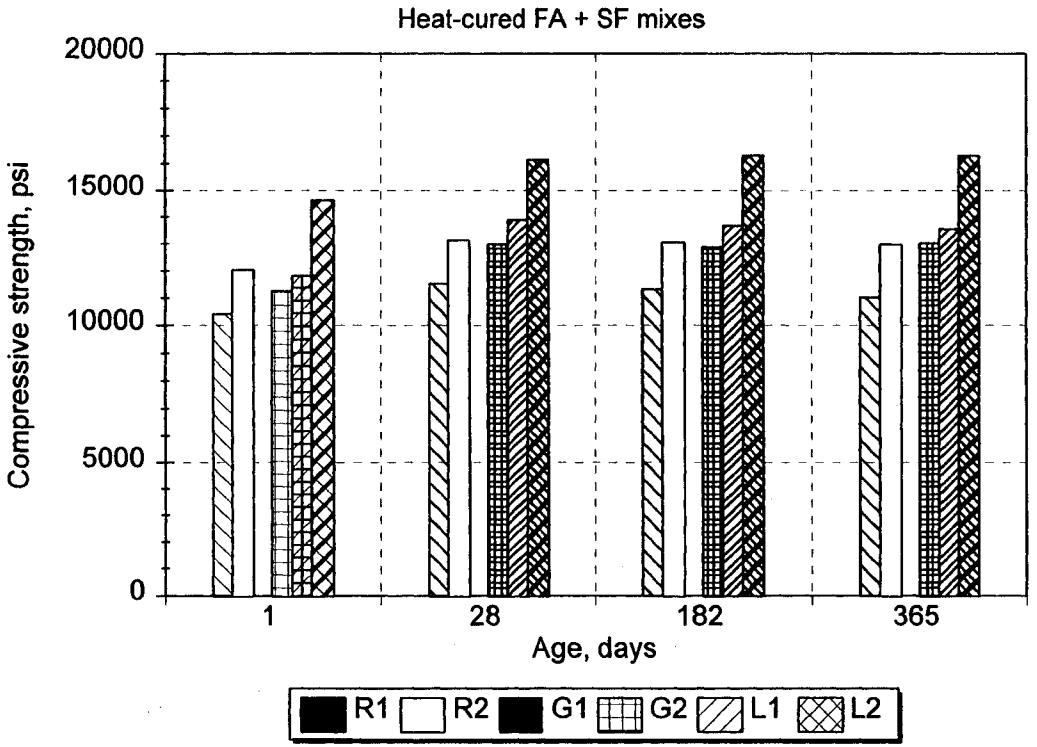

Figure 9.4. Aggregate-type effect on compressive strength of heat-cured 4 x 8 in. (100 x 200 mm) specimens of the same mix proportions, fly ash and silica fume (FA + SF) mixes.
[H_FASF.WMF]

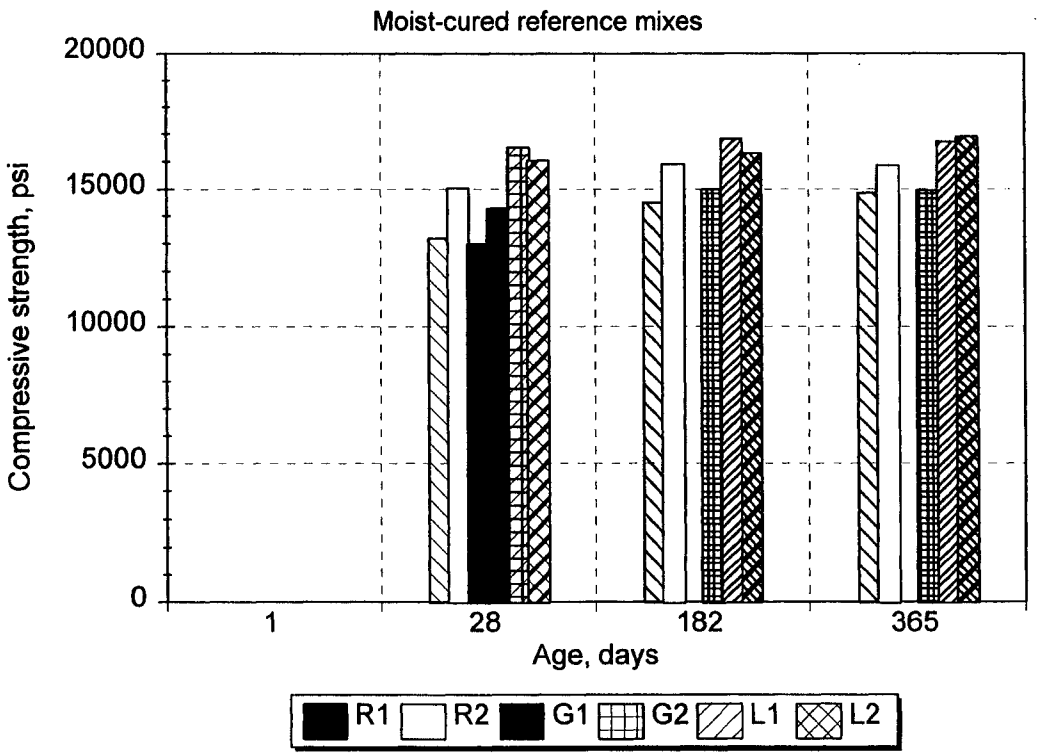

Figure 9.5. Aggregate-type effect on compressive strength of moist-cured 4 x 8 in. (100 x 200 mm) specimens of the same mix proportions, reference mixes.
[W_REF.WMF]

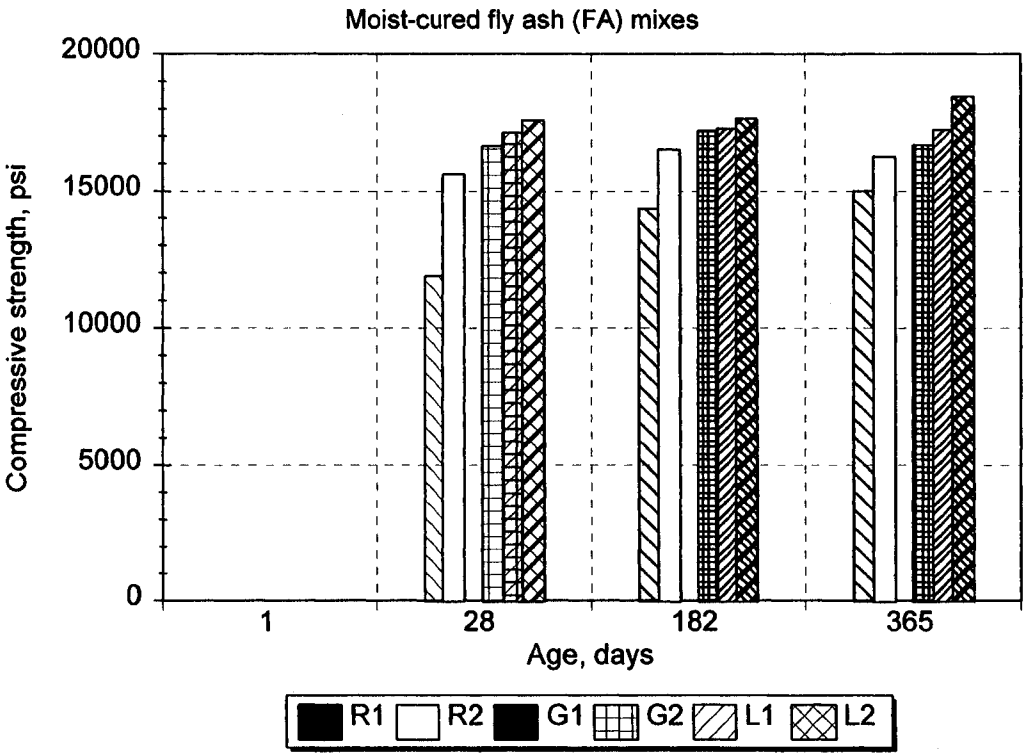

Figure 9.6. Aggregate-type effect on compressive strength of moist-cured 4 x 8 in. (100 x 200 mm) specimens of the same mix proportions, fly ash (FA) mixes.
[W_FA.WMF]

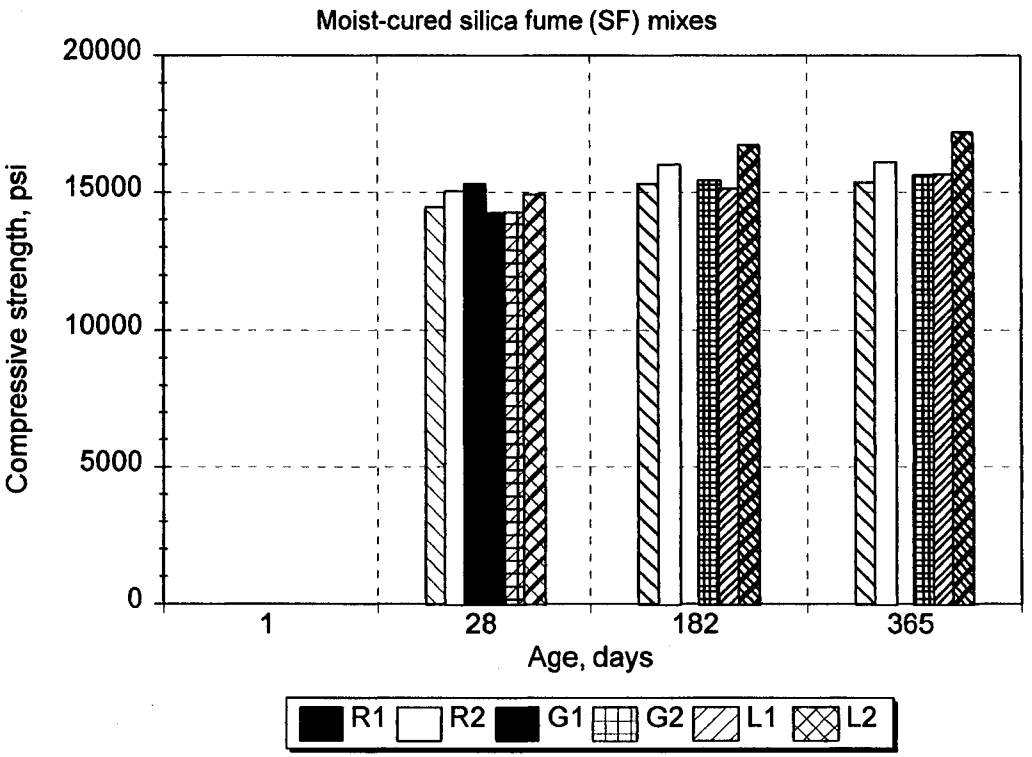

Figure 9.7. Aggregate-type effect on compressive strength of moist-cured 4 x 8 in. (100 x 200 mm) specimens of the same mix proportions, silica fume (SF) mixes.
[W_SF.WMF]

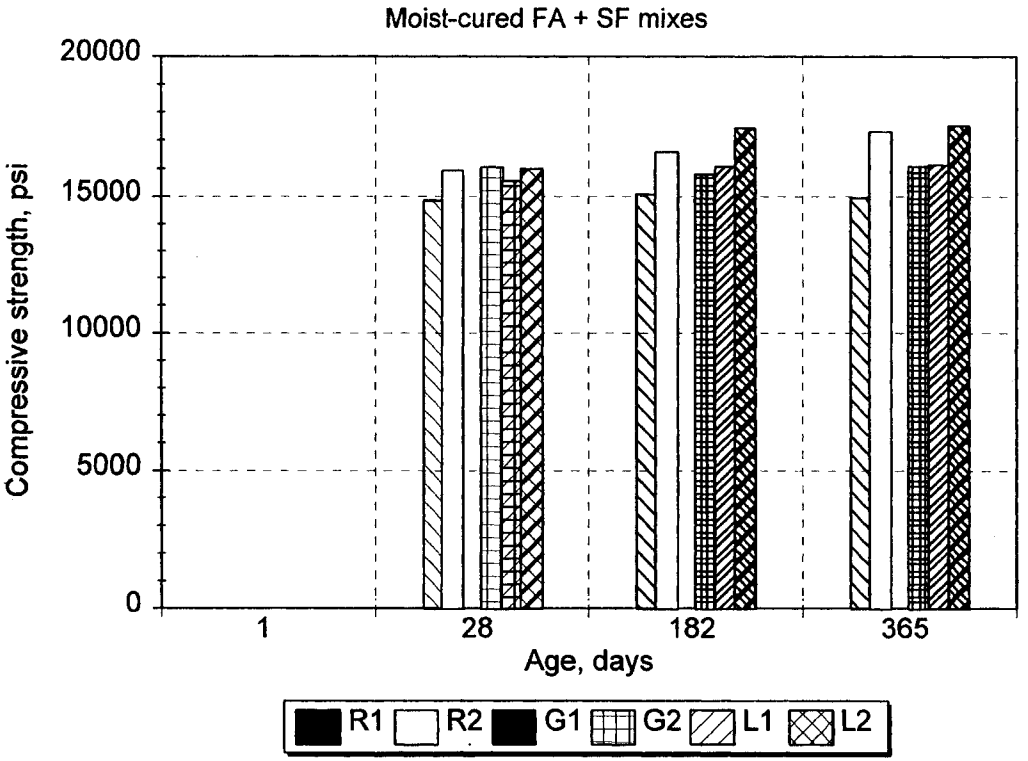

Figure 9.8. Aggregate-type effect on compressive strength of moist-cured 4 x 8 in. (100 x 200 mm) specimens of the same mix proportions, fly ash and silica fume (FA + SF) mixes.
[W_FASF.WMF]

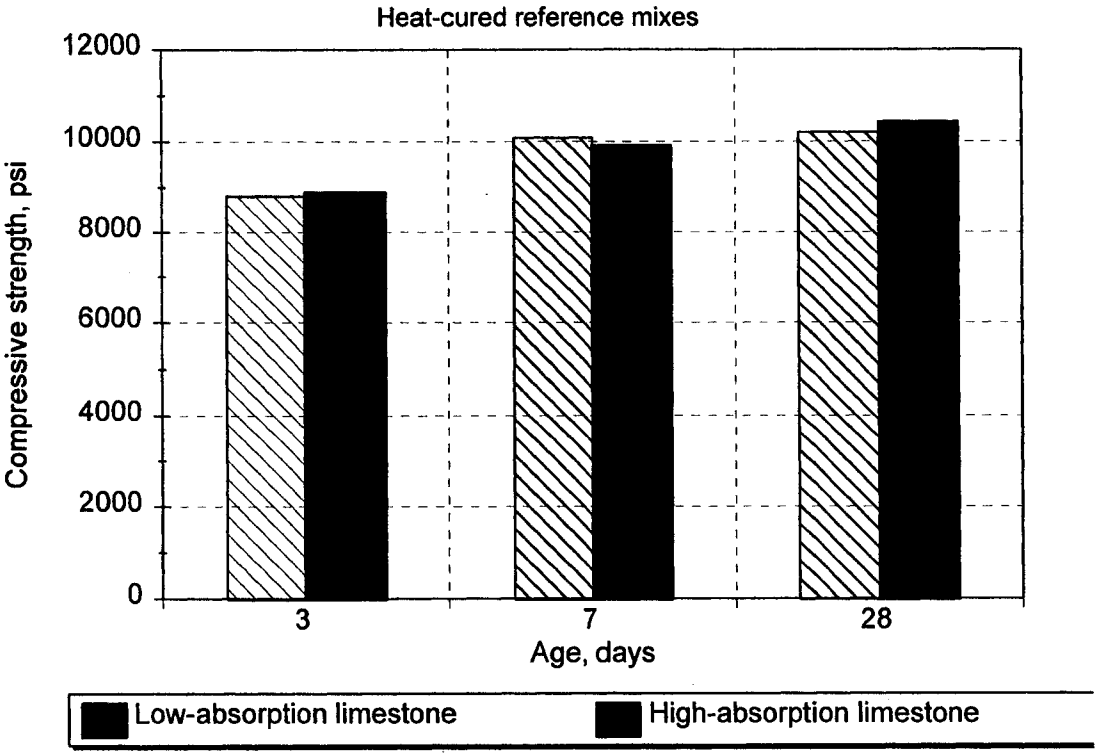

Figure 9.9. Aggregate-type effect on compressive strength of heat-cured 6 x 12 in. (150 x 300 mm) specimens, low-absorption limestone versus high-absorption limestone [French and Mokhtarzadeh, 1993]. [W_LLVSHL.WMF]

CHAPTER 10
SHRINKAGE AND CREEP

10.1 General

The use of high strength concrete in both cast-in-place and precast methods of construction has been increasing steadily for the past two decades and will continue in the future. The primary reasons are the economic advantages that high strength concrete offers over conventional normal strength concrete and the need for more durable and stronger concrete in different construction applications. In high-rise buildings, the total shortening of columns and walls due to gravity loads, creep and shrinkage may be as high as 1 in. (2.54 mm) for every 80 ft. (24.4 m) of height. The possibly large absolute amount of cumulative column shortening over the height of the structure in high-rise buildings is of consequence in its effects on the cladding, finishes, partitions, and so on. Elastic and time dependent deformations (creep and shrinkage) increase prestress losses. Loss of prestress in flexural members reduces the stiffness of the member causing further increases in deflections. Creep and shrinkage characteristics of high strength concrete, with or without supplementary cementitious materials (such as fly ash and silica fume), were the subject of this part of this research program.

Figure 10.1 illustrates the deformation history of a typical concrete element loaded at a relatively early age after casting. The subsequent deformations of this concrete element may be divided into two parts: Immediate elastic deformations and long term deformations. Upon application of the load, the element will have an elastic deformation which is dependent on the elastic properties of the concrete and occurs immediately but would entirely disappear on immediate removal of the load. Under sustained load, the combination of the following effects will result in total long term deformation: shrinkage, creep, temperature and relative humidity effects, and the variation of the modulus of elasticity of concrete with time. Upon removal of the load at a later age, because of the increased age of the concrete at the time of unloading, the element will recover only some of its initial elastic and long term creep deformations, the result being a nonrecoverable deformation of the element.

The word shrinkage as used in this report refers to the contraction of concrete due to drying (drying shrinkage) and physio-chemical changes (autogenous and carbonation shrinkage), dependent on time but not on stresses induced by external loading. Usually the concrete mix contains more water than is needed for hydration. Drying shrinkage occurs in the cement paste when concrete loses part of this free water to the surrounding environment. Autogenous shrinkage of concrete (of practical importance only in large mass concrete structures) is due to continued hydration of cement. Continued hydration, when a supply of water is present, leads to expansion. However, when no moisture movement to or from the paste is permitted (such as interior of a large concrete mass) shrinkage occurs. Carbonation shrinkage occurs when CO_2 present in the atmosphere reacts, in the presence of moisture, with $Ca(OH)_2$ present in the cement paste:

- $Ca(OH)_2 + (H_2O + CO_2) \rightarrow CaCO_3 + 2H_2O$ ***(10.1)***

For carbonation shrinkage to occur, the water produced from this reaction must be lost to the environment.

From the above brief discussion, it should be clear that although both drying shrinkage and carbonation shrinkage occur when concrete internal moisture is lost to the environment, they are quite distinct in nature. Most of the published studies on drying shrinkage of concrete include the effects of carbonation. In most cases, no distinction is made between drying shrinkage and autogenous shrinkage of concrete and drying shrinkage results include contractions due to autogenous changes.

The word creep, as used here, is defined as the time-dependent deformation of hardened concrete subjected to sustained stress. In this creep definition, creep is considered as a deformation in excess of shrinkage and no distinction is made between creep of concrete under

conditions of no moisture movement to or from the surrounding environment (basic creep) and the additional creep caused by drying (drying creep).

This research program studied the effects of the following variables on shrinkage and creep properties of high strength concrete: composition of cementitious material, type of coarse aggregate, heat-curing temperature, and accelerated heat- and standard moist-curing procedures. No attempt was made to study the mechanisms of shrinkage and creep, but rather the overall shrinkage and creep characteristics of high strength concrete as affected by the stated variables were studied. The results from this research program were used to investigate if the current guidelines for shrinkage and creep of conventional normal strength concrete are applicable to high strength concrete.

The following section summarizes the findings from some of the studies on the creep and shrinkage properties of high strength concrete.

10.2 Previous Research

[Smadi, Slate, and Nilson 1982]: In an experimental investigation Smadi et al. studied shrinkage and creep characteristics of low, medium and high strength concretes having 28-day uniaxial compressive strengths in the range of 3,000 to 10,000 psi (20.7 to 69.0 MPa) measured on 4 x 8 in. (100 x 200 mm) cylinders. For the creep study, the sustained stress level was chosen as the main variable and was varied between 40 to 95 percent of concrete's short-term ultimate strength. The period of sustained loading varied from 30 to 60 days. The low, medium and high strength concrete mixes had water-to-cement ratios of 0.32, 0.65, and 0.87 and had total cement contents of 996, 517, and 376 lb/yd^3 (590, 307, and 223 kg/m^3) respectively. Portland cement ASTM Type I, natural sand, and a 3/4 in. (19 mm) crushed limestone was used in the production of all concretes considered in this study. The high strength concrete mix also contained a commercially available ASTM Type A water-reducing admixture. All specimens were tested after 28-days of moist-curing in a testing room at approximately 72 °F (22 °C) and 50 percent relative humidity.

Reported shrinkage strain measurements, on unloaded specimens, after 60 days of drying indicated a greater magnitude of shrinkage strain for low strength concrete as compared with those of medium and high strength concretes. However, they reported greater shrinkage strain for high strength concrete than for medium strength concrete. The average magnitudes of shrinkage strains after 60 days for low, medium, and high strength concretes were reported to be 365, 200, and 266 $\mu\varepsilon$, respectively.

As it has been long practiced, Smadi et al. calculated creep strain by deducting from total strain, the initial elastic strain (occurring immediately after the application of load) and the average shrinkage of the companion unloaded specimen. It was reported that the rate and the magnitude of total strain and creep strain increased as load increased for the three types of concretes investigated. The rate of deformation of high strength concrete specimens subjected to stress levels up to 70 percent of ultimate strength was reported to almost stabilize 60 days after loading. When high strength concrete specimens were loaded to 80 percent of ultimate strength, the specimens either continued to deform at significantly high rates at 60 days or failed after 14 days. Of four medium strength concrete specimens loaded to 75 percent of their ultimate strength, two failed after 49 days. For medium strength concrete, the rates of time-dependent deformations were described as "significantly high" at stress levels above 60 percent of the ultimate. The highest stress level investigated for low strength concrete was 75 percent of ultimate strength. While the magnitudes of deformations at this stress level were reported as "extremely large" none of the specimens failed under the load up to 60 days. From the observations cited above, Smadi et al. concluded that the long-term strength (i.e. the maximum compressive stress which can be maintained permanently without causing failure) is close to 80 percent of 28-day ultimate strength for high strength concrete and 75 percent of 28-day ultimate strength for low and medium strength concretes. Table 10.1 compares the average magnitudes of time-dependent deformations in terms of total strain, creep strain, creep coefficient and specific creep at 60 days after loading for high, medium, and low strength concretes considered at two stress levels.

[Paulson, Nilson, and Hover 1989]: Paulson et al. conducted an experimental program to study the influence of high strength concrete on sustained load deflections of reinforced concrete beams. As a part of this program they studied creep and shrinkage of concrete cylinders from three high strength concrete mixes for a period of one year. All mixes were made with ASTM C 150 Type I cement. Two of the mixes contained combination of an ASTM C 618 Class F fly ash and a slurry form of silica fume as part of their cementitious material, 8.4% FA + 12.6% SF and 4.4% FA + 12.2% SF, and had 28-day compressive strengths of 11,760 psi (81.1 MPa) and 9,750 psi (67.2 MPa) respectively. The third mix was a reference mix and had 28-day compressive strength of 5,650 psi (39.0 MPa). The coarse aggregate used was a 0.5 in. (13 mm) crushed aggregate consisted of 35-40% limestone, 30-35% sandstone/siltstone, 10-15% siltstone/shale, 8-10% granite and less than 5% quartzite. Creep and shrinkage tests were conducted on 4 x 16 in. (100 x 406 mm) cylinders. For the duration of test, the temperature and relative humidity of the testing area varied between 68 °F to 78 °F (20 °C to 26 °C) and 30% to 72% respectively. The age of concrete at which creep and shrinkage tests started were 60, 39, and 45 days for the three mixes respectively. Creep specimens were loaded to approximately 45% of their ultimate strength.

Using the suggested percentage of 20 year shrinkage which occurs in the first two weeks, first 3 months, and the first year already reported in literature, and considering the age of the concretes when shrinkage measurements were started, Paulson et al. computed ultimate shrinkage strains based on their experimental data from one year. The predicted ultimate shrinkage strains were found to be: 540 με (microstrains) for 13,100 psi (90.3 MPa) concrete, 620 με for 9,600 psi (66.2 MPa) concrete, and 800 με for 5,400 psi (37.2 MPa) reference concrete. It was concluded that the predicted values of the ultimate shrinkage strains were within the usual range of values presented elsewhere in the literature for normal strength concrete. Also concluded was that concrete compressive strength had only a small influence on drying shrinkage. The latter conclusion was based on the fact that there exists contradicting values in the

literature, with some investigations reporting greater shrinkage strains for high strength concrete than for normal strength concrete (in contrast to the trend observed in Paulson et al. study).

Comparison of creep strains from the three high strength concrete mixes was conducted with no adjustment to account for different ages of concretes at the time of loading. Ultimate creep coefficients were computed for the three high strength concrete mixes by two different methods. In the first method, the suggested percentage of 20 year creep which occurs in the first two weeks, first 3 months, and the first year already reported in literature, were used to predict the ultimate creep of each mix. Percentages of the ultimate creep used were: 25% after 2 weeks, 50% after 3 months, and 75% after one year. The average values of the ultimate creep strains were found to be: 1,940 με (microstrains) for 13,100 psi (90.3 MPa) concrete, 2,440 με for 9,600 psi (66.2 MPa) concrete, and 1,930 με for 5,400 psi (37.2 MPa) reference concrete which corresponded to ultimate creep coefficients of 1.3, 2.1 and 2.6 respectively.

Ultimate creep coefficients for the three mixes considered were also computed based on the ACI Committee 209 recommendation. ACI 209 recommends that the relationship between the creep coefficient at any time and the ultimate creep coefficient be calculated by the following equation:

- $v_t = [t^{0.6}/(10+t^{0.6})]v_u$ ***(10.2)***

where

v_t = creep coefficient at time t (ratio of creep strain to initial elastic strain)

v_u = ultimate creep coefficient

A least square regression of the above equation with the data resulted in predicted ultimate creep coefficients of 1.1 for 13,100 psi (90.3 MPa) concrete, 1.9 for 9,600 psi (66.2 MPa) concrete, and 2.0 for 5,400 psi (37.2 MPa) reference concrete. Inherent approximations involved in prediction of the ultimate creep coefficients from 1 year data were presented as the

reason for the observed differences in predicted ultimate creep coefficients by the two methods. It was also concluded that the creep coefficient of concrete decreases with an increase in concrete compressive strength.

[Collins 1989]: Therese M. Collins reported the results of an experimental program on five high strength concrete mixes. All five mixes were made with an ASTM C 150 Type I cement, an ASTM C 618 Class C fly ash and had a water/(cement + fly ash) ratios of 0.35 or 0.36. In all five mixes, fly ash consisted approximately 15% of the total weight of cementitious material. Aggregates used consisted of either of two natural sands with fineness modulus of 2.6 and 2.8 and two crushed dolomitic limestones with maximum size of 1.5 and 1 in. (38.1 and 25.4 mm). High strength concrete batches contained either a Type A water-reducing admixture or a Type F high-range water-reducing admixture conforming to ASTM standard C 494. High strength concrete mixes had 28-day compressive strengths in the range of 8,050 to 9,280 psi (55.5 to 64.0 MPa). Compressive strength, creep, and shrinkage measurements were conducted on 6 x 12 in. (150 x 300 mm) moist-cured cylinders. Creep and shrinkage tests were conducted in an environmental room maintained at 70 °F (21 °C) and 50% R.H. Shrinkage testing was performed on specimens moist-cured for 7- and 28-days. Creep loads of $0.2f_c'$, $0.3f_c'$, and $0.4f_c'$ were applied to specimens after 28-days of moist-curing. From this work Collins drew the following conclusions:

1. The shrinkage deformation was inversely proportional to the moist-curing time. For one of the mixes, the shrinkage of a 7-day moist-cured specimen was approximately 50% higher than that of a 28-day moist-cured specimen.
2. The creep deformation increased directly with an increase in the applied stress level. The average creep strain at $0.3f_c'$ was approximately 50% higher than that of $0.2f_c'$, and the average creep strain at $0.4f_c'$ was 125% higher.
3. By comparing the results from two of the concrete mixes, it was suggested that a high strength concrete with larger maximum aggregate size and lower paste content could result in less creep and shrinkage strains.

4. The use of high-range water-reducing admixture did not have a significant effect on the creep and shrinkage deformations.

[Burg and Ost 1992]: R. G. Burg and B. W. Ost reported the results of their study on drying shrinkage and creep of five commercially made high strength concretes (due to limitations on the number of available creep test frames only four of the five high strength concrete mixes were subjects of the creep study). Considered concretes had 28-day compressive strengths in the range of 10,600 to 17,250 psi (73.1 to 119 MPa) measured on 6 x 12 in. (150 x 300 mm) moist-cured specimens. Concretes were made with ASTM C 150 Type I cement and had water-cementitious materials ratios of 0.22 to 0.32 and contained either no mineral admixtures, silica fume only (8.8% or 13.6%), or both fly ash and silica fume (10.6% FA + 4.2% SF or 15.9% FA + 11.4% SF). In all cases the coarse aggregate was a 3/8 in. (9.5 mm) maximum size crushed dolomite.

Drying shrinkage was measured at 73.4±3 °F (23±1.7 °C) and 50±4% R.H. on both 3 x 3 x 11.25 in. (76 x 76 x 286 mm) prisms and 6 x 12 in. (150 x 300 mm) cylinders. Specimens were 28-days old at the start of the test having previously been kept continuously in a standard moist room. Companion 6 x 12 in. (150 x 300 mm) cylinders were tested for creep at the same environmental condition after approximately six weeks of air drying beyond the initial 28-days of moist-curing. The applied load for creep tests was approximately 39% of compressive strength. Based on a method presented in ACI 209, Creep test results were fitted to a so-called modified Ross equation of the form:

- $v_t = [t^{\psi}/(d+t^{\psi})]v_u$ ***(10.3)***

where

v_t = creep coefficient at time t (ratio of creep strain to initial elastic strain)

v_u = ultimate creep coefficient

t = time in days after loading

ψ = time-ratio

d = time to one-half ultimate creep, days

The following findings were reported by Burg and Ost:

1. Prisms had higher overall shrinkage because of the smaller volume-to-surface ratio.
2. Drying shrinkage strains after one year for mixes containing silica fume were in the range of 300 to 450 με for 6 x 12 in. (150 x 300 mm) cylinders and 450 to 600 με for 3 x 3 x 11.25 in. (76 x 76 x 286 mm) prisms. For the reference mix that did not contain silica fume, the corresponding values were 550 and 700 με for the cylinders and prisms, respectively.
3. Specific creep (measured creep strain divided by applied stress) at one year measured on 6 x 12 in. (150 x 300 mm) cylinders was 0.15 to 0.25 με/psi (22 to 36 με/MPa) for mixes containing silica fume and 0.44 με/psi (64 με/MPa) for the reference mix without silica fume.

Specific creep was lowest for the concretes with the highest compressive strength. The reference mix, which contained no mineral admixtures, had a specific creep somewhat in excess of what other researchers have reported for concretes of similar water-cement ratio.

[Strategic Highway Research Program (SHRP) 1993]: A 5-year nationally coordinated research program, supported by the Strategic Highway Research Program (SHRP), was conducted by a consortium of researchers at North Carolina State University, the University of Arkansas, and the University of Michigan on the mechanical behavior of high performance concrete for highway applications. High performance concrete was defined as concrete with much higher early strength and greatly enhanced durability against freezing and thawing compared with conventional concrete. Very high strength concrete (VHS, with Type I cement and $f_c' > 10{,}000$ psi (70 MPa) in 28 days) and high early strength concrete (HES, with Type III cement and $f_c > 5{,}000$ psi (35 MPa) in 24 hours) were two of the three categories of high

performance concrete investigated in this program. VHS concretes included either 19.4% fly ash, VHS(F), or 4.4% silica fume, VHS(S), in their cementitious material. HES concretes contained no mineral admixtures. Four different types of coarse aggregates were used in this investigation: marine marl, crushed granite, dense crushed limestone, and washed rounded gravel. Shrinkage tests were conducted on both VHS and HES concretes. However, creep tests were conducted only on VHS concretes.

Shrinkage tests were conducted on 4 x 4 x 11.25 in. (100 x 100 x 281 mm) prisms for a period of up to 90 days. Specimens were cured in lime-saturated water for 28 days. During this period, the specimens were removed from the water only for measurements. Subsequently, they were stored in air under normal laboratory conditions.

Creep tests were conducted on 4 x 8 in. (100 x 200 mm) cylinders for a period of 90 days. The creep specimens were loaded to 40% of their compressive strength and were located in a room where temperature and humidity were maintained at 73 °F (23 °C) and 50% R.H.

The main observations from this study were:

1. Shrinkage of VHS and HES concretes follow the general trend of conventional concrete.
2. VHS(S) concrete had less shrinkage potential than VHS(F) concrete. At 90 days, the average shrinkage strain of VHS(F) concrete made with crushed granite aggregate was 521 με (approximately 70% of the ultimate shrinkage strain recommended by ACI Committee 209). On the other hand, the average 90-day shrinkage strains of VHS(S) concrete varied from -72 με for concrete with washed rounded gravel (expansion) to 361 με for concrete with crushed granite aggregate.
3. The average 90-day shrinkage of HES concrete ranged from 210 to 690 με, depending on the type of coarse aggregate used. At 90 days, the largest shrinkage strain occurred

for HES made with dense crushed limestone followed by HES concretes made with crushed granite, marine marl, and washed round gravel.

4. The observed creep strains of the different groups of VHS concrete ranged from 20% to 50% of that of conventional concrete. The total creep strains as well as the specific creep values of VHS(S) concretes made with rounded gravel and crushed granite were lower than companion VHS(F) concretes. However, for VHS(S) concrete with marine marl, the resultant specific creep values appeared to be inconsistently higher than those values for VHS(F) concrete with marine marl as coarse aggregate.

10.3 Experimental Program

This part of the study was undertaken to provide information on drying shrinkage and creep characteristics of high strength concretes made with varying materials and subjected to 7-days of moist-curing (W7 condition) or heat-curing (H condition) process similar to the curing process practiced in precast-prestressed plants.

Drying shrinkage and creep strains were measured on 4 x 11 in. (100 x 280 mm) cylinders instrumented with three sets of Whittemore type gage points equidistantly located around each cylinder, forming three 8 in. (200 mm) gage lines central along the height of each cylinder. Specimens were stored and tested at 72±4 °F (22±2 °C) and 50±5% R.H. Heat-cured specimens were 1-day old at the start of the test. The 7-day moist-cured specimens were 28-days old at the start of the test and were stored in the same controlled environmental condition after initially being moist-cured for 7-days. For each test and for each curing condition two 4 x 11 in. (100 x 280 mm) cylinders were made (a total of 8 specimens per mix when both heat- and moist-cured specimens were tested for shrinkage and creep characteristics).

To study drying shrinkage characteristics of high strength concrete, length change and weight change of both H and W7 specimens were monitored for a period of one year. Companion 4 x 11 in. (100 x 280 mm) cylinders were tested for creep for a period of one year. A total of 14 mix-curing condition combinations were considered (Mix Nos.: 108^{H}, 116^{H}, $124^{H,W7}$, $128^{H,W7}$,

129^{W7}, $131^{H,W7}$, $132^{H,W7}$, 136^{H}, and $139^{H,W7}$). The applied loads for creep tests were 60% of 1-day compressive strength for H specimens and 45% of 28-day compressive strength for W7 specimens.

A detailed description of materials as well as the fabrication and curing procedures used in making high strength concrete specimens was given in Chapter 3 of this report.

10.4 Apparatus

Specimen Molds: 4 x 11 in. (100 x 280 mm) cylindrical molds were constructed using commercially available PVC sewer pipe and end caps. Constructed molds performed exceptionally well and had superior dimensional stability compared to commercially available single-use plastic molds and were reused several times. Three pairs of brass inserts were bolted to the inner side of each mold (equidistantly located around each mold) to form three 8 in. (200 mm) gage lines central along the height of mold, Figures 10.2-A and 10.2-B.

Balance: A 44 lb. (20,000 g) maximum capacity high precision electronic balance with 0.0035 oz (0.1 g) resolution (A&D Model EP-20KA) was used to measure the weight change of the 4 x 11 in. (100 x 280 mm) shrinkage specimens. The changes in weight and deformation of shrinkage specimens were measured at the same time intervals.

Dehumidifier, Humidifier and Electric Heater: Commercially available dehumidifier, humidifier and electric heater were used to control the humidity and temperature of the laboratory. All these units had automatic controls and were adjusted to maintain the temperature and relative humidity of the laboratory close to 72±4 °F (22±2 °C) and 50±5% R.H. Although the temperature and relative humidity were maintained within the prescribed range for the major portion of the test period, on some isolated days the temperature and relative humidity of the laboratory fell outside the specified range.

Sling Psychrometer: Relative humidity (R.H.) of the laboratory environment was determined using a sling psychrometer. The unit consisted of two 20-120 °F x 1 °F thermometers, one dry-bulb and one wet-bulb, in a plastic casing with a swivel handle. An internal water reservoir fed the wet-bulb wick. The instrument was spun, away from the body, using the swivel handle for one minute and the wet-bulb temperatures was recorded. The whirling operation was repeated until two or more wet-bulb readings agreed with the least recorded value. The relative humidity was then determined by reading wet- and dry-bulb temperatures and then referring to a relative humidity chart.

Creep Load Frames: A typical creep load frame constructed for the purpose of this study is shown schematically in Figure 10.3. Each creep load frame consisted of four 10 x 10 x 1.5 in. (254 x 254 x 38 mm) steel plates (upper and lower jack plates and upper and lower base plates), four 1.25 DIA. x 48 in. (3.2 DIA. x 1220 mm) tension bars, four pairs of disk springs (Key Bellevilles, Inc. K4250-M-375) each pair stacked in series, and a spherical bearing block assembly attached to the center of the lower jack plate. The load was applied by a 150 ton compact hydraulic cylinder placed between the upper jack plate and the lower jack plate, placing the concrete specimens in compression and the tension bars in tension.

To determine the compressive force applied to the creep specimens each tension bar was instrumented with four electrical resistance strain gages positioned in a Wheatstone bridge as shown in Figure 10.4, acting as a load cell. The strain gages each had a 120 ohm resistance and a 0.125 in. (3.175 mm) active gage length. Lead wires from the strain gages were numbered and were equipped with color coded pin connectors at their ends. Similar numbering and color coding were used on the connectors of the strain measuring device "*strain indicator with switch and balance unit*" to make measurements fast, easy and reliable.

All tension bars from each of the creep load frames were calibrated by a standard 100,000 lb. (445 kN) load cell such that the load in the system could be determined from the readings of the strain gages. The accuracy of the system was verified by placing a load cell in series with the

hydraulic cylinder to measure the total load in all four tension bars. A steel cylinder was placed in the load frame, in place of concrete specimens, to resist the applied load. The system was loaded several times to verify the repeatability and accuracy of readings.

Two stacked 4 x 11 in. (100 x 280 mm) unsealed cylinders from each of the selected mixes were placed in each creep load frame. After centering the creep specimens, about 75% of the target load was applied and the tension forces in the tension bars were checked. If the tension forces in the tension rods were unequal, the load was released and the flat jack was repositioned until a nearly uniform loading was obtained. Once the desired loading of the system was obtained, the full target load was applied to the system, the four nuts above the lower jack plate were tightened, and the hydraulic pressure was removed. The system was then checked and readjusted if necessary for loss of tension due to seating of the nuts. Four pairs of disk springs were used to maintain a nearly constant compressive load in the specimens as concrete creep occurred. However, periodically the nuts on top of the lower jack plate had to be tightened to restore the compressive force in the specimen to its initial value.

Strain Indicator with Switch and Balance Units: A portable, battery-powered strain indicator (Measurements Group, Inc. Model P-3500) in conjunction with a 10-channel switch and balance unit (Measurements Group, Inc. Model SB-10) was used to measure the strains in each of the four tension bars of each creep load frame. Strain measurements were read directly from a LCD readout with 1 resolution. Combination of the strain indicator and the switch and balance unit allowed fast and convenient reading of strains from all four tension rods of each creep load frame.

Hydraulic Cylinder (Jack) and Hydraulic Hand Pump: A 150 ton hydraulic cylinder (Enerpac Flat-Jac Model RSM-1500) with a retracted height of less than 4 in. (100 mm) and extended height of 4.5 in. (114 mm) was used together with a hydraulic hand pump to load the creep load frames used in this study, Figure 10.3. The compact design of this jack together with its carrying handle made it well suited for insertion between the upper and lower jack plates of

the creep load frames and reduced the total height of each creep load frame to a convenient 48 in. (1220 mm).

Whittemore Gage: Concrete creep and shrinkage deformations on the specimens were measured using a Whittemore Gage shown in Figure 10.5. The gage is designed to mechanically measure the relative displacement of stainless steel contact seats threaded in place in brass inserts mounted in a specimen at a selected spacing. The instrument adjusts for measuring 2, 4, 6, 8, or 10 in. (50, 100, 150, 200, 250 mm) spacings (gage lengths). The gage used in this study had a dial indicator with 0.0001 in. (0.00254 mm) graduations and maximum travel of 0.5 in. (12.7 mm). Three sets of stainless steel contact seats were threaded in brass inserts mounted in each of the 4 x 11 in. (100 x 280 mm) concrete creep or shrinkage specimen to form three 8 in. (200 mm) gage lines, central along the height of each cylinder, oriented at 120° around the specimen, Figures 10.6-A and 10.6-B. Deformations of creep specimens and companion shrinkage specimens were measured at the same time intervals.

10.5 Procedure

***Shrinkage Tests*:** To provide the same exposed surface area for the shrinkage specimens and the creep specimens, ends of two 4 x 11 in. (100 x 280 mm) shrinkage specimens from each of the selected high strength concrete mixes were first sealed with two coats of a two part epoxy coating. This prevented shrinkage specimens from exchanging moisture with the environment through their ends. Six stainless steel contact seats were then threaded in place in the embedded brass inserts on the side of each specimen to form three 8 in. (200 mm) gage lines around each specimen 120° apart and central along the height of the specimen. Each gage line was numbered and initial length of each gage line was measured three times, using the Whittemore gage, and recorded. Initial weight of each shrinkage specimen was also measured three times and recorded at the same time. For the duration of test, at predetermined time intervals, the same measurements were repeated and recorded.

Shrinkage specimens were stored on shelves in the vertical position in the creep laboratory at 72±4 °F (22±2 °C) and 50±5% R.H. for the duration of test. For proper air circulation, a minimum 2 in. (50 mm) clear distance between shrinkage specimens was maintained during storage. Handling of the specimens was done with great care to ensure that the weight change of each specimen was only due to exchange of moisture and not chipping of concrete or epoxy coatings.

Heat-cured specimens (H) were 1-day old at the start of the test. Moist-cured specimens (W7) were 28-days old at the start of the test and were stored in the creep laboratory at 72±4 °F (22±2 °C) and 50±5% R.H. after 7-days of initial moist-curing. Shrinkage experimental data are presented in Appendix D.

***Creep Tests*:** From each set of selected high strength concrete mixes two unsealed 4 x 11 in. (100 x 280 mm) creep test specimens were first capped with a sulfur based high strength capping compound. Six stainless steel contact seats were then threaded in place in the embedded brass inserts on the side of each specimen to form three 8 in. (200 mm) gage lines around each specimen 120° apart and central along the height of the specimen. Each gage line was numbered and the initial length of each gage line was measured three times, using the Whittemore gage, and recorded (unloaded condition). Initial gage lengths of companion shrinkage specimens were measured at the same time.

The two capped specimens were then placed (stacked in series) at the center of the upper base plate of the creep frame, Figure 10.3. The spherical bearing block assembly together with the lower jack plate were lowered to sit on the specimens. The lower jack plate was leveled and was secured by nuts. The hydraulic cylinder and a 100,000 lb. (445 kN) capacity load cell were placed in series on top of the lower jack plate and the upper jack plate was then placed above the load cell, leveled and was secured with nuts. Initially about 75% of the target load was applied and the tension forces in the tension bars were checked. If the tension forces in the tension bars were unequal, the load was released and the hydraulic cylinder was repositioned until a nearly

uniform loading was obtained. Once the desired load distribution was obtained, the full target load was applied to the system and the four nuts above the lower jack plate were tightened and the hydraulic pressure was removed. The system was then checked and readjusted if necessary for loss of tension due to seating of the nuts. Immediately after loading each gage line was measured in the same manner (each measurement was repeated three times) to determine the initial elastic deformation of the two specimens in compression.

Heat-cured specimens (H) were loaded at 1-day to 60% of their ultimate 1-day strength and moist-cured (W7) specimens were stored in the creep laboratory at 72±4 °F (22±2 °C) and 50±5% R.H. after 7-days of initial moist-curing and were loaded at 28-days to 45% of their ultimate 28-day strength as determined by separate compression tests.

Four pairs of disk springs positioned between upper and lower base plates of the creep load frame maintained a nearly constant compressive load in the specimens as concrete creep occurred. However, periodically tensile forces in the tension bars were checked and if necessary nuts on top of the lower jack plate were tightened to restore the compressive force in the specimen to its initial value. For the duration of test, at predetermined time intervals, gage lengths of creep specimens were measured and recorded. Creep experimental data are included in Appendix D.

10.6 Results

***Shrinkage Tests*:** Figures 10.7 and 10.8 show the measured shrinkage strains of heat-cured (H) and moist-cured (W7) specimens after 380 days of drying, for reference high strength concretes made with different types of coarse aggregates. Also shown in these figures are the predicted values base on the ACI 209R-92 *[ACI 209R-92, 1992]* equations for conventional normal weight concrete. Figure 10.7 indicates greater magnitude of shrinkage strain for high strength concrete made with round river gravel (R1) as compared with those made with crushed aggregates (R2, L1, L2, and G2). The coarse aggregate affects shrinkage characteristics of concrete by providing a restraining effect on the drying shrinkage of the pure cement paste.

Figures 10.7 and 10.8 show that when the amount and the maximum size of the coarse aggregate in a high strength concrete mix is held constant (such as the cases considered in this study), the amount of the restraint provided by the coarse aggregate depended more on the surface characteristics of the coarse aggregate than the mineralogy of the coarse aggregate and that the latter had only very minor effects on the shrinkage results. However, the reader should be reminded that the main factor influencing the amount of final shrinkage is the water content of the fresh concrete. In this part of the study the water-to-cementitious material ratio and the amount of cement were held constant. The average magnitudes of shrinkage strains after 380 days of drying were 565, 485, 469, 443, and 492 με for heat-cured reference high strength concrete specimens made with R1, R2, L1, L2 and G2 coarse aggregates, respectively (approximately 65 to 83 percent of the shrinkage strain values recommended by the ACI Committee 209 equation at equal age). The average magnitudes of shrinkage strains after 380 days of drying were 517, 452, and 485 με for moist-cured reference high strength concrete specimens made with R2, L1, and L2 coarse aggregates, respectively (approximately 63 to 72 percent of the shrinkage strain values recommended by ACI Committee 209 equation at equal age).

Figures 10.9 through 10.12 compare shrinkage characteristics of reference mixes to companion mixes containing supplementary cementing materials (7.5% silica fume or combination of 20% fly ash and 7.5% silica fume) for both heat-cured and moist-cured high strength concretes. Clearly, for the cases studied, the composition of the cementitious material did not have a significant effect on the shrinkage characteristics of high strength concretes made with crushed coarse aggregates. An FIP State of the Art Report also reports that shrinkage of concrete is little influenced by silica fume contents less than 10 percent by weight of the cement *[FIP Commission on Concrete, 1988]*. No comparison was made on the effect of inclusion of supplementary cementing materials on the shrinkage characteristics of high strength concrete made with round river gravel.

American Concrete Institute Committee 209 *[ACI 209R-92 1992]* suggested the following general equation for predicting shrinkage of concrete at any time:

- $(\varepsilon_{sh})_t = [t^{\alpha}/(f+t^{\alpha})]*(\varepsilon_{sh})_u$ ***(10.4)***

where

$(\varepsilon_{sh})_t$ = shrinkage strain at any time t

t = time in days

α = constant, $(0.90 < \alpha < 1.10)$

f = constant, $(20 < f < 130$ days)

$(\varepsilon_{sh})_u$ = ultimate shrinkage strain,

$(415\text{x}10^{-6} < (\varepsilon_{sh})_u < 1070\text{x}10^{-6})$

For normal weight, sand lightweight, and all lightweight concrete and under standard conditions ACI Committee 209 *[ACI 209R-92, 1992]* recommends the following values for the constants in the above equation:

- $\alpha = 1.00$
- $f = 35$, for 7-day moist-cured concrete
- $f = 55$, for steam-cured concrete
- $(\varepsilon_{sh})_u = 780\text{x}10^{-6}$ in/in (m/m)

A nonlinear least-square analysis of all the experimental data from this study (with $\alpha = 1$) resulted in ultimate shrinkage strain values in the range of 506 to 631 με for heat-cured and 477 to 539 με for 7-day moist-cured specimens. These values are between 65 to 86 percent and 61 to 69 percent of the ultimate shrinkage strain value recommended by the ACI Committee 209 for heat- and moist-cured specimens respectively. The time to one-half ultimate shrinkage strain (f) was determined to be between 58 to 72 days for heat-cured and between 42 to 50 days for 7-day moist-cured specimens as compared to 55 and 35 days recommended by the ACI Committee 209

for the two curing conditions. Lower water-to-cementitious material ratio required in the production of high strength concrete and the resulting denser matrix are believed to be the reasons for the observed smaller ultimate shrinkage strain for high strength concrete. High strength concrete dries out more slowly than conventional concrete and has less evaporable water. This also explains the higher f values (time to one-half ultimate shrinkage) computed in this study. The computed values of $(\varepsilon_{sh})_u$ and f are well within the ranges presented in ACI 209R-92 *[ACI 209R-92, 1992]* and reported by other researchers *[Smadi et al. 1982, Paulson et al. 1989, Burg et al. 1992]*.

Based on the data collected and analyzed during this study the following two equations are suggested for predicting shrinkage strain of high strength concrete at any time:

- Moist-cured concrete (W7);

$$\Rightarrow (\varepsilon_{sh})_t = [t/(45+t)]*(\varepsilon_{sh})_u \qquad \textbf{(10.5)}$$

- Heat-cured concrete (H):

$$\Rightarrow (\varepsilon_{sh})_t = [t/(65+t)]*(\varepsilon_{sh})_u \qquad \textbf{(10.6)}$$

where

$(\varepsilon_{sh})_t$ = shrinkage strain at any time t

t = time in days

$(\varepsilon_{sh})_u = 530\text{x}10^{-6}$ in/in, (m/m)

The amount of drying shrinkage measured with respect to time for high strength concrete specimens made with round river gravel, heat-cured at two different temperatures, is shown in Figure 10.13. In general, the drying shrinkage of concrete is expected to decrease with the increase in curing temperature. The decrease in shrinkage due to higher curing temperature may be explained by the maturity concept (i.e. the amount of curing) for the hardened concrete. A concrete cured at a higher temperatures is usually stronger, has a higher modulus of elasticity and therefore exhibits less shrinkage *[Soroka 1979]*. The data presented in Figure 10.13 confirms this expected effect. The average magnitudes of shrinkage strains after 380 days of drying were 603

and 565 με for specimens heat-cured at 120 °F and 150 °F, respectively. However, tests on companion specimens showed no significant difference in the compressive strength and modulus of elasticity tests results due to different curing temperatures and in cases specimens cured at 120 °F exhibited slightly higher compressive strength and modulus of elasticity values.

Creep Tests: Creep tests were conducted for a duration of 380 days on companion 4 x 11 in. (100 x 280 mm) cylinders. Tests for creep on heat-cured specimens started 1-day after casting the specimens under a constant initial stress equivalent to 60% of the compressive strength at the time of loading. The creep tests on moist-cured (W7) specimens started at the age of 28-days, after 3 weeks of air drying in 72±4 °F (22±2 °C) and 50±5% R.H. beyond the initial 7 days period of moist-curing, under a constant initial stress representing 45% of the compressive strength at the time of loading. Immediately after loading, the initial deformation, representing the elastic responses of the concrete specimens, were measured. The modulus of elasticity values were then calculated and were compared to the values obtained from testing companion 4 x 8 in. (100 x 200 mm) specimens. The results are presented in Table 10.2.

As explained earlier creep strains were calculated by deducting from total strain, the initial elastic strain (which occurred immediately after application of the load) and the average shrinkage of the companion unloaded specimens. Each data point represents the average of six strain measurements taken from two companion specimens loaded in the same frame. The variations of creep strain and specific creep (creep strain divided by the applied stress) with time for all the mixes and for both curing conditions are given in Figures 10.14 through 10.20 and 10.21 through 10.27, respectively.

Figure 10.28 compares the specific creep values observed in this study with the typical specific creep values suggested in the literature *[Nilson et al. 1986]* for the various compressive strengths. The examination of the behavior of high strength concrete specimens from each curing condition reveals that specific creep of high strength concrete follows the general trend of conventional concrete, i.e. concrete specific creep decreases as compressive strength increases.

However, heat-cured high strength concrete specimens made with round river gravel (R1) exhibited higher specific creep values than concretes having similar compressive strengths and made with other types of coarse aggregates. It is believed that the young age of concrete at loading together with the small amount of restraint provided by the smooth surface of this type of coarse aggregate are the main causes of observed higher specific creep values. The coarse aggregate itself normally used in the production of concrete mixes do not experience creep; however, the presence of the coarse aggregate influences the creep of concrete as a whole. The extent of the aggregate effect on creep depends on its mechanical and physical properties as well as its concentration in the concrete. It is well known that creep of concrete made with soft aggregate is higher than that of concrete of the same mix design made with hard aggregate. In contrast to normal strength concrete, grading, particle size, and shape of coarse aggregate particles affect creep characteristics of high strength concrete. Under high levels of sustained loads encountered in testing high strength concrete specimens for creep, local regions along the aggregate-paste interface are potential sites for the initiation of microcracks. Surface characteristics of the aggregate affect the strength of the aggregate-paste interface. The use of smooth aggregate involves lower strength and hence higher creep.

Because the strength of heat-cured and moist-cured specimens from the same mixes were not the same at the time of loading, no direct comparison can be made about the effect of curing condition on the creep characteristic of high strength concrete. However, results of this study suggest that moist-curing reduced the effect of the type of coarse aggregate and/or variations in the composition of cementitious materials on creep of high strength concrete mixes, Figures 10.21, 10.22, 10.25 and 10.26. In fact, for the cases considered, for high strength concrete mixes with identical basic mix designs, moist-curing supressed the effect of variations in the mix design on the specific creep of concrete. For instance moist-cured high strength concretes containing 7.5% silica fume or combination of 20% fly ash and 7.5% silica fume, made with crushed river gravel (R2) had almost identical specific creep values compared with the reference mix over the entire test period, Figure 10.26. moist-curing together with loading specimens at a later age (28-

days) resulted in hydrated cement paste of similar microstructure and hence similar creep characteristics.

Replacement of cement with a combination of 20% fly ash and 7.5% silica fume slightly decreased the specific creep values of heat-cured high strength concrete made with crushed river gravel (R2) compared with the reference mix over the entire test period, Figure 10.25. Replacement of cement with a combination of 20% fly ash and 7.5% silica fume had a more pronounced effect on specific creep values of high strength concrete made with granite (G2), Figure 10.24.

Lower curing temperature resulted in lower specific creep values for heat-cured high strength concrete reference mixes made with round river gravel (R1), Figure 10.27.

American Concrete Institute Committee 209 *[ACI 209R-92 1992]* suggests the following general equation for predicting the creep coefficient (ratio of creep strain to initial elastic strain) of concrete at any time:

- $v_t = [t^{\psi}/(d+t^{\psi})]^* v_u$ ***(10.7)***

where

v_t = creep coefficient at any time t

t = time in days

ψ = constant, $(0.40 < \psi < 0.80)$

d = constant, $(6 < d < 30$ days$)$

v_u = ultimate creep coefficient,

$(1.30 < v_u < 4.15)$

Table 10.3 shows the results when the creep tests data were fitted into the above equation.

The values of ψ, d, and v_u obtained from this study are close and comparable to the ranges presented in ACI 209 that were developed based on conventional concretes. Considering the inherent variability of the experimental data, it is likely that any of the obtained set of parameters can be used for estimating the creep coefficient of high strength concrete. Therefore, the recommended form of ACI 209 equation ($\psi = 0.60$ and $d = 10$), given below, was used to estimate the ultimate creep coefficient values based on the experimental data from this study.

For normal strength concrete cured under standard conditions ACI Committee 209 *[ACI 209R-92, 1992]* recommends the following equation for the creep coefficient, v_t, for a loading age at 7 days for moist-cured concrete, and at 1-3 days, for steam-cured concrete:

- $v_t = [t^{0.60}/(10+t^{0.60})]*v_u$ ***(10.8)***

where $v_u = 2.35$

Using this form of the equation to fit the experimental data results in the values given in Table 10.4. The experimental data fit the equation with reasonable accuracy, as shown by the R^2 values also shown in Table 10.4 ($R^2 = 1$ represents a perfect fit of data to the equation). The range of ultimate creep coefficients predicted in this study varied between 0.92 to 2.46 as compared to the 1.30 to 4.15 range reported by ACI 209 for normal strength concretes.

10.7 Concluding Remarks

Greater shrinkage strains were observed for specimens fabricated with round river gravel mixes compared to those for specimens fabricated with crushed aggregate mixes. Only reference mixes were included in this portion of the study for the round river gravel mixes. Consequently, no comparisons could be made regarding the effect of cementitious materials composition on the shrinkage characteristics of round river gravel mixes.

The time to one-half of the ultimate shrinkage strain was longer for the high strength concrete specimens observed in this study in comparison to the values presented in ACI 209 *[ACI 209R-92 1992]*. Consequently, the shrinkage of high-strength concrete appears to occur at a slower rate than that predicted by ACI 209. The specimens heat-cured at higher temperatures (150 °F) had less shrinkage strains at 380 days of drying relative to those of specimens heat-cured at lower temperatures (120 °F).

The specific creep of high-strength concrete followed the general trend of conventional concrete (decreased with increased f'c). Moist-curing reduced the effect of type of coarse aggregate and/or variation in cementitious composition on creep. The heat-cured round gravel concrete had a higher specific creep than heat-cured concrete of similar strength made with crushed aggregates considered in this study. The lower heat-curing temperature resulted in lower specific creep.

Table 10.1. Average magnitudes of time-dependent deformations in terms of total strain, creep strain, creep coefficient and specific creep at 60 days after loading for high, medium, and low strength concretes considered at two stress levels *[Smadi et al. 1982]*.

Type of Concrete	Stress Level % Ultimate	Total Strain με	Creep Strain με	Creep Coefficient	Specific Creep
High Strength	80	4,321	2,248	1.293	0.311
8,500-10,000 psi	40	1,890	732	0.895	0.211
Medium Strength	75	4,622	3218	2.769	0.858
5,000-6,000 psi	40	1,864	1,067	1.862	0.503
Low Strength	75	6,009	4,566	4.200	1.845
3,000-3,500 psi	40	2,005	1,222	2.829	0.976

Table 10.2. Comparison of the calculated modulus of elasticity of 4 x 11 in. (100 x 280 mm) creep test specimens from elastic response upon loading with the values obtained from testing companion 4 x 8 in. (100 x 200 mm) specimens at the same age.

No.	Cure	$(E_c)_{4x11}$, psi	$(E_c)_{4x8}$, psi	$(E_c)_{4x11}/(E_c)_{4x8}$
108	H	6244636	6456726	0.97
116	H	6843571	6723056	1.02
124	H	6219588	6221877	1.00
128	H	6650865	6503213	1.02
131	H	6587495	6843818	0.96
132	H	6375940	6629059	0.96
136	H	6392244	6528943	0.98
139	H	6770394	6705378	1.01
124	W7	6787913	6839613	0.99
128	W7	6054232	6294232	0.96
129	W7	7118928	7012595	1.02
131	W7	7158579	6958797	1.03
132	W7	6821574	7049430	0.97
139	W7	6315211	6516043	0.97

Table 10.3. Results obtained when the creep test results were fitted into ACI 209 *[ACI 209R-92 1992]* general equation ($v_t = [t^{\psi}/(d+t^{\psi})]*v_u$).

Mix	Ult. Creep Coef. v_u	Ult. Specific Creep, 10^{-6}/psi	Time-ratio (ψ)	Constant (d)
H108,R1,REF	2.68	0.43	0.49	7.60
H116,R1,REF	2.45	0.36	0.56	7.87
H136,G2,REF	2.37	0.37	0.43	8.34
H139,G2,FASF	2.63	0.39	0.40	11.57
H128,R2,REF	1.19	0.18	0.65	8.87
H131,R2,FASF	2.43	0.37	0.36	13.82
H124,L1,REF	2.28	0.37	0.40	18.47
H132,L2,REF	3.36	0.53	0.36	27.67
W139,G2,FASF	3.02	0.48	0.34	18.69
W128,R2,REF	3.08	0.51	0.30	18.75
W129,RS,SF	1.83	0.26	0.44	12.36
W131,R2,FASF	2.16	0.30	0.38	12.68
W124,L1,REF	1.22	0.18	0.39	6.47
W132,L2,REF	3.62	0.53	0.31	22.84

Table 10.4. Results obtained when the creep test results were fitted into equation: $v_t = [t^{0.60}/(10+t^{0.60})]*v_u$).

Mix	Ult. Creep Coef. v_u	Ult. Specific Creep, 10^{-6}/psi	R^2
H108,R1,REF	2.45	0.39	0.99
H116,R1,REF	2.46	0.36	0.99
H136,G2,REF	1.83	0.29	0.99
H139,G2,FASF	1.59	0.23	0.98
H128,R2,REF	1.31	0.20	0.99
H131,R2,FASF	1.15	0.18	0.98
H124,L1,REF	1.03	0.17	0.97
H132,L2,REF	0.94	0.15	0.95
W139,G2,FASF	1.07	0.17	0.98
W128,R2,REF	0.92	0.15	0.97
W129,RS,SF	1.20	0.17	0.98
W131,R2,FASF	1.13	0.16	0.98
W124,L1,REF	0.96	0.14	0.97
W132,L2,REF	0.95	0.14	0.96

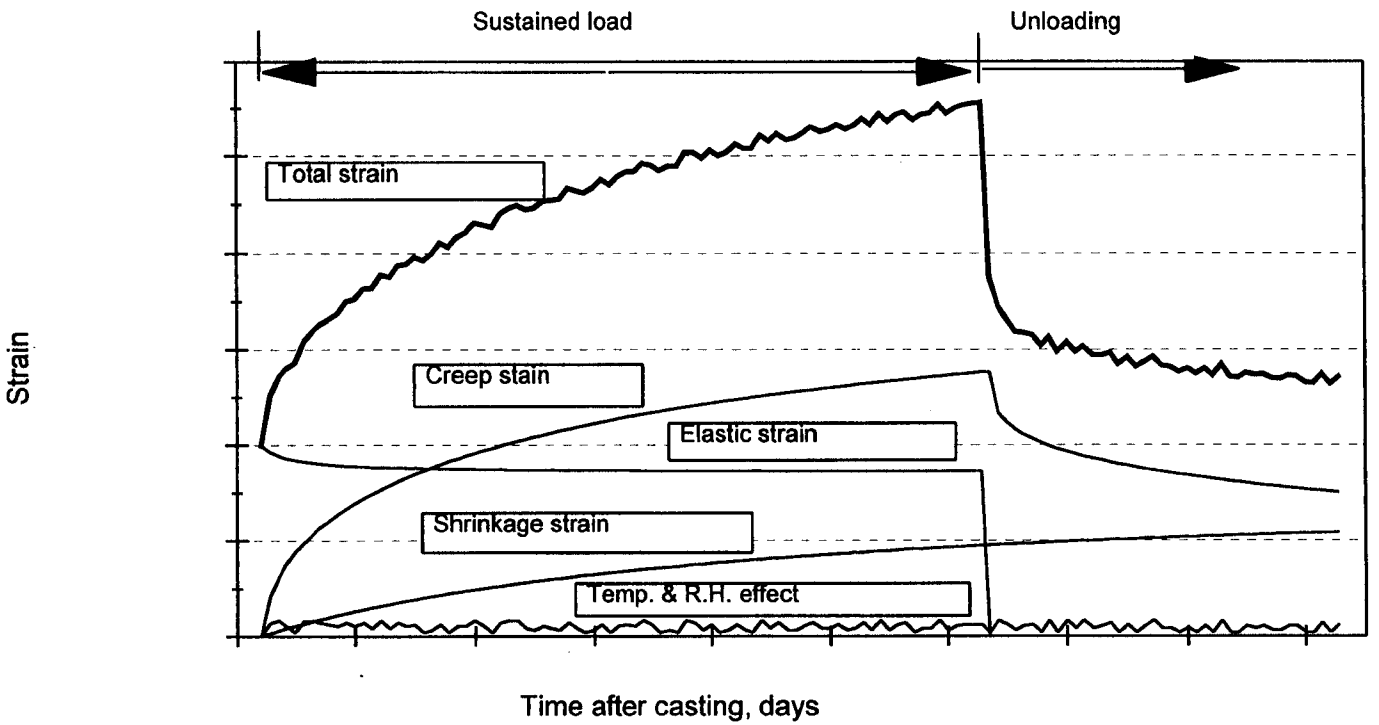

Figure 10.1. Deformation history of a typical concrete element loaded at a relatively early age after casting.

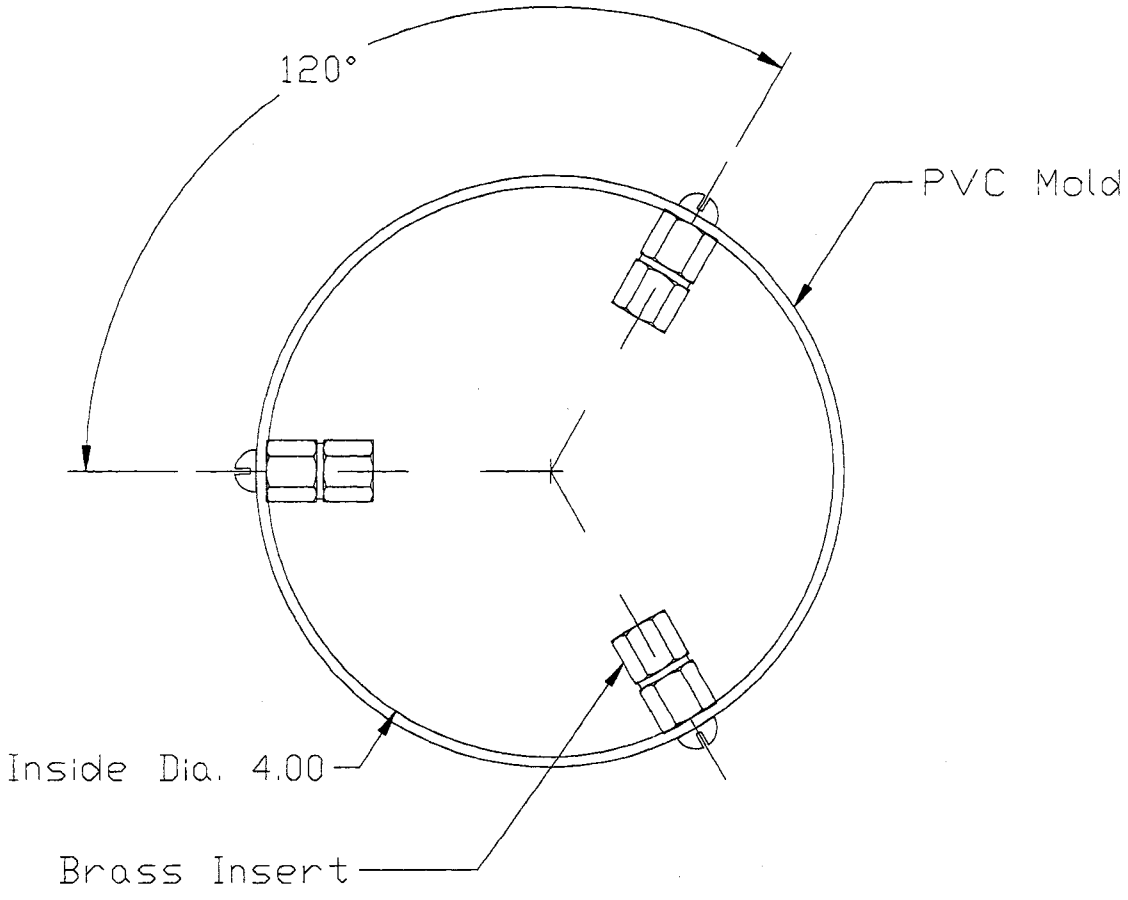

Figure 10.2-A. Top view of a PVC mold used for casting 4 x 11 in. (100 x 280 mm) creep and shrinkage specimens. Also shown are brass inserts mounted inside the mold prior to casting concrete.
[CR-MOLD.PLT]

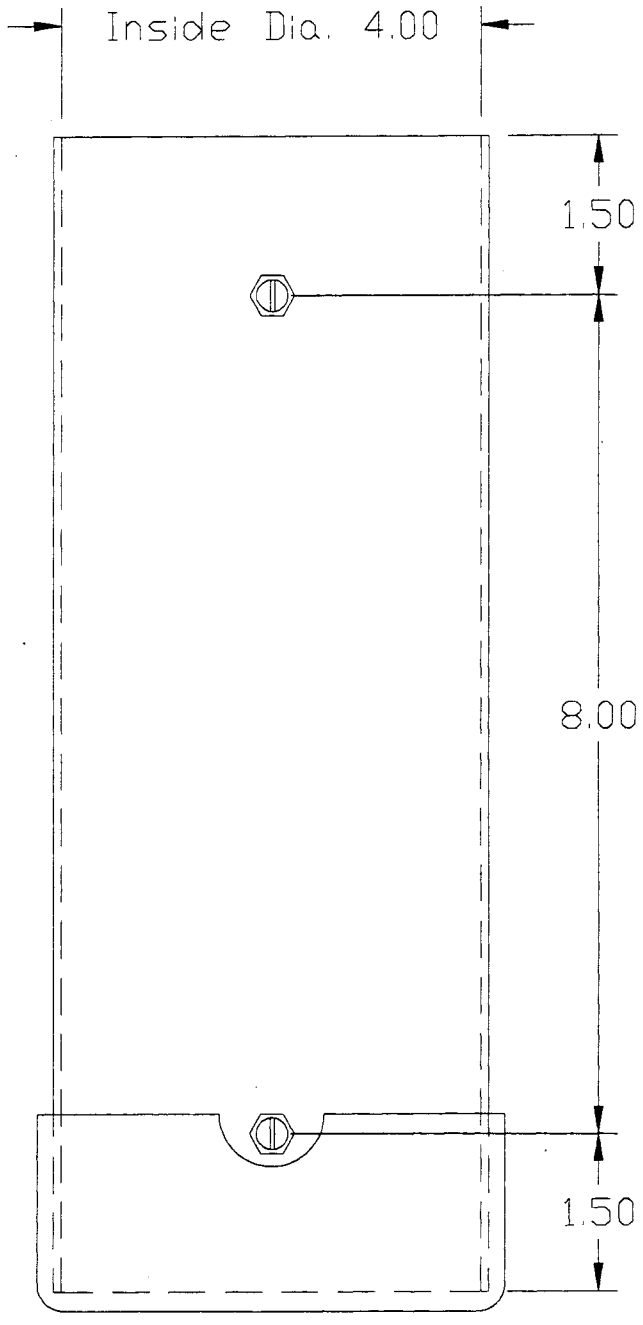

Figure 10.2-B. Side view of a PVC mold used for casting 4 x 11 in. (100 x 280 mm) creep and shrinkage specimens. Also shown are bolts used to hold brass inserts in place during casting of concrete.
[CR-MOLD2.PLT]

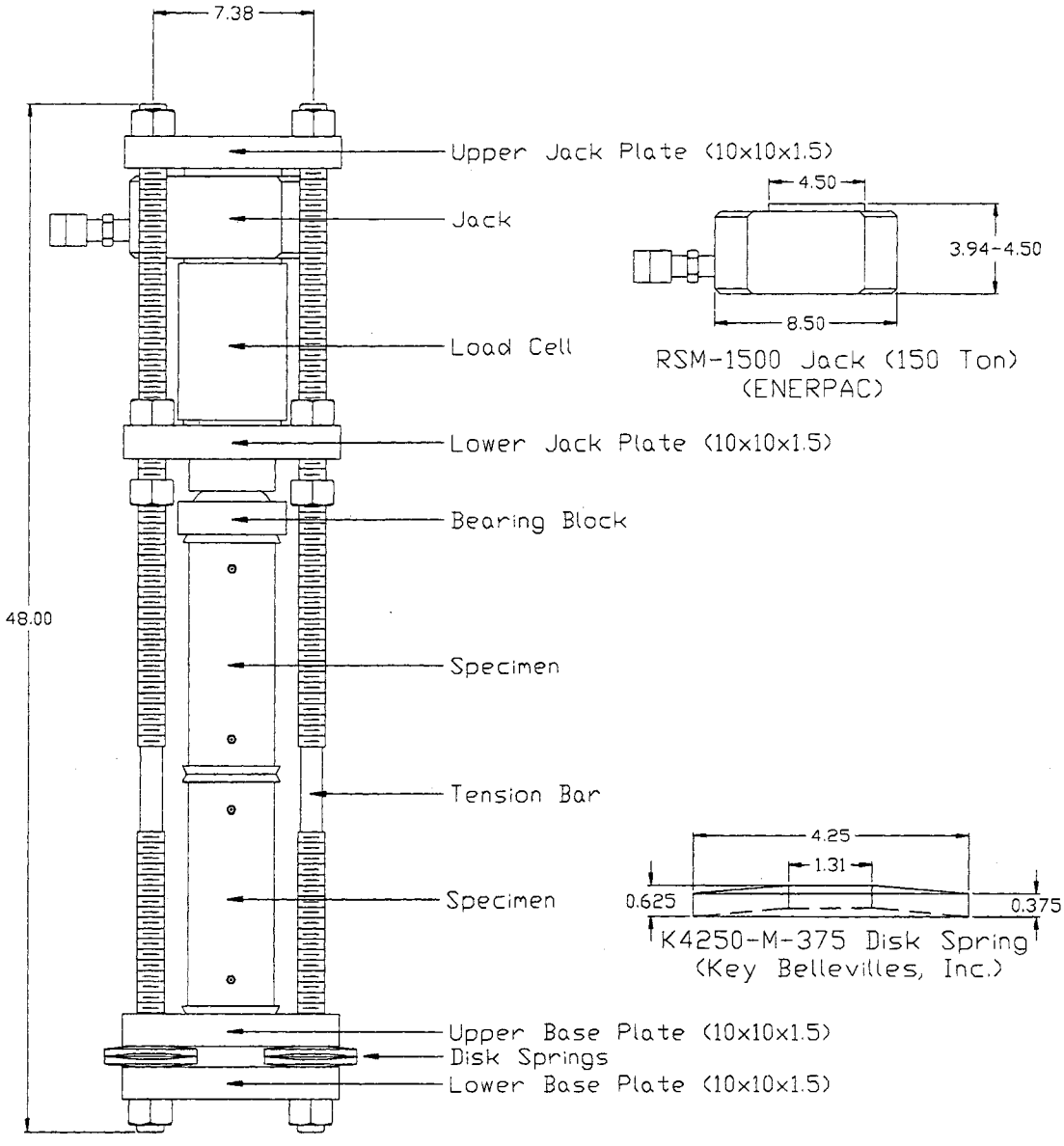

Figure 10.3. The creep load frame constructed and used for the purpose of this study. Details of the instrumentation of the tension bars are shown in Figure 10.4.
[FRAME1.PLT]

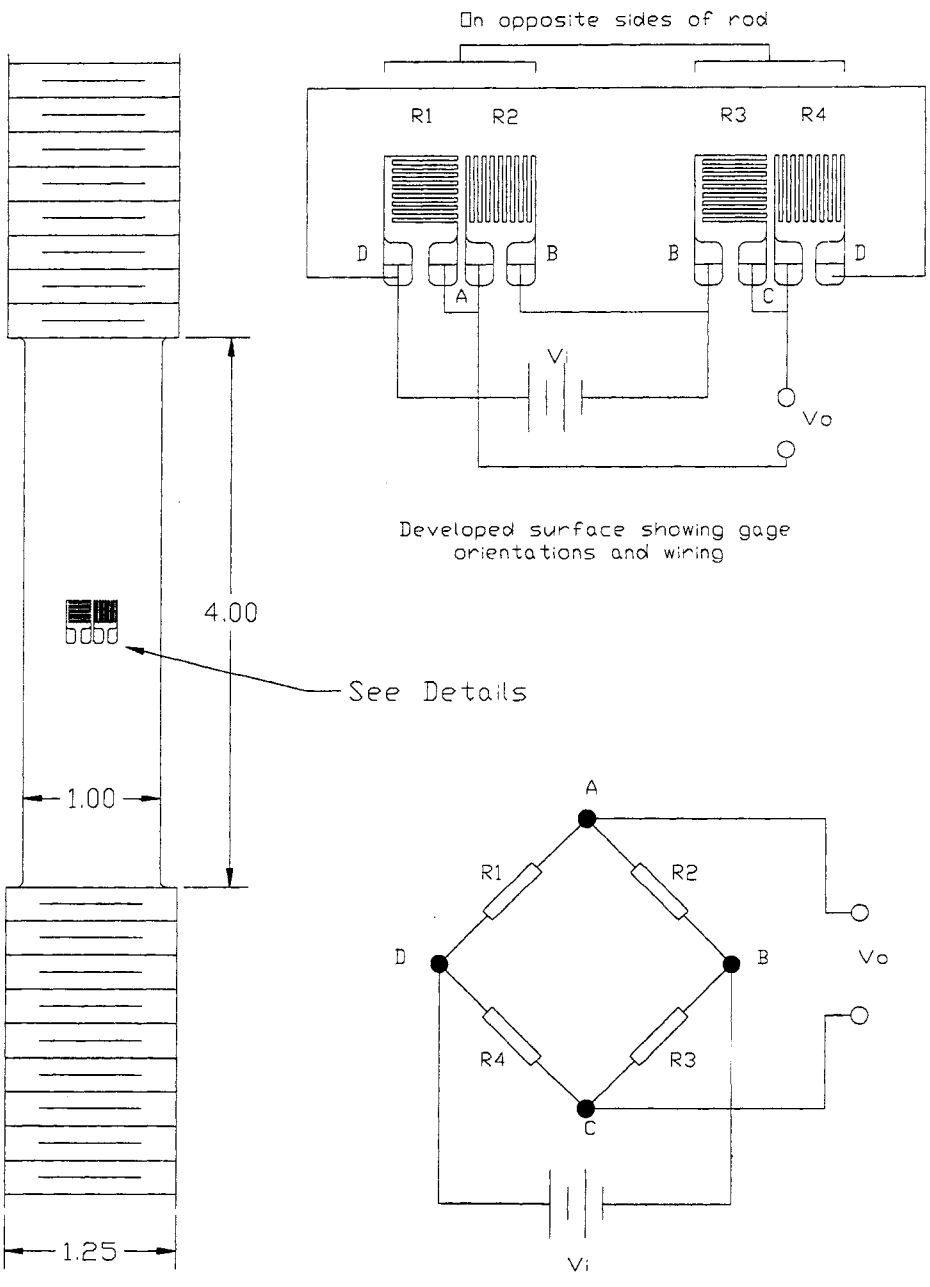

Figure 10.4. Two rectangular two-element strain gages (CEA-06-125UT-120) were mounted on each tension bar, in the Wheatstone bridge, to produce a load cell.
[ROD1.PLT]

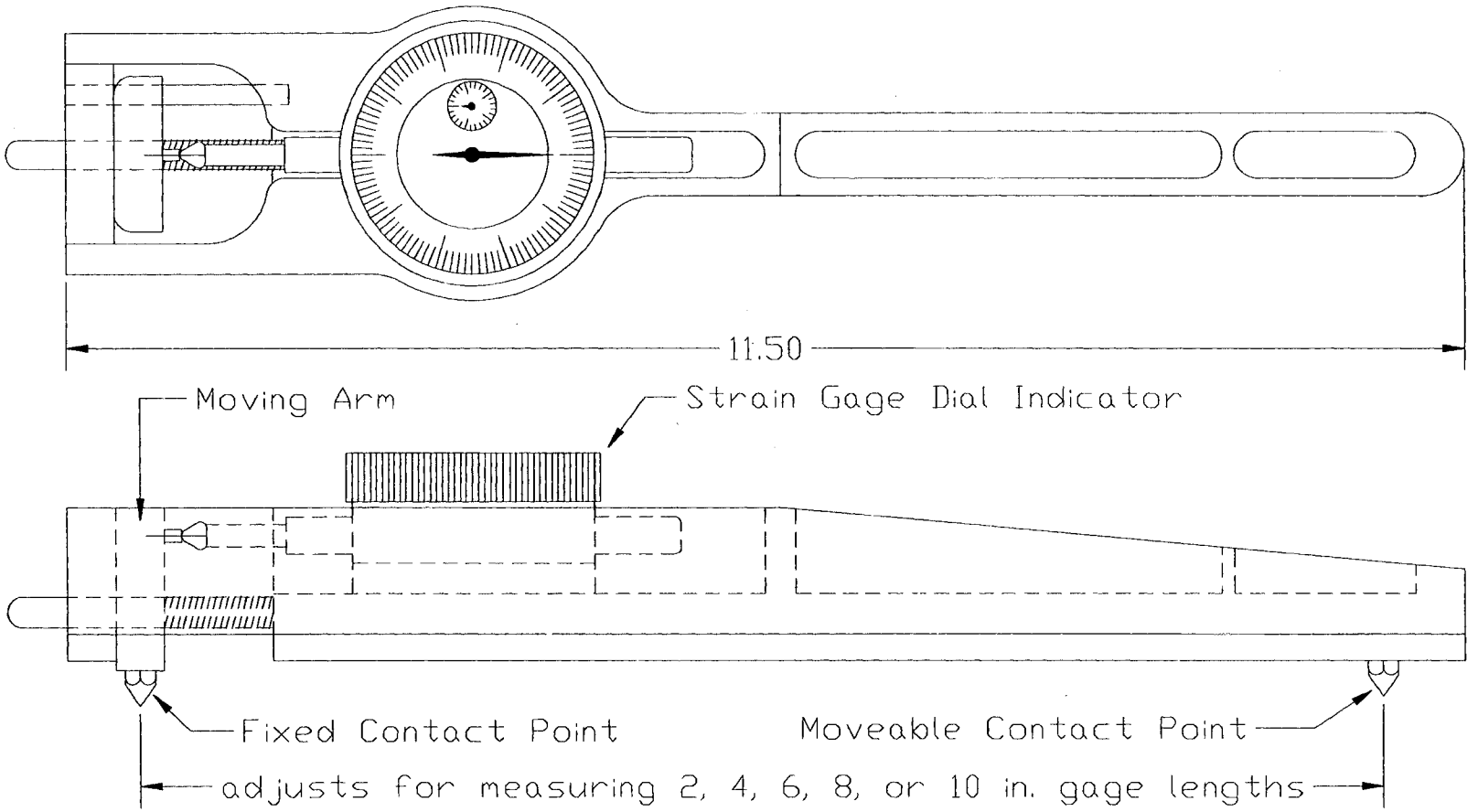

Figure 10.5. Creep and Shrinkage deformations of concrete specimens were measured by using a Whittemore gage similar to one shown here. The strain gage dial indicator had 0.0001 in. (0.00254 mm) graduations and maximum travel of 0.5 in. (12.7 mm). [WGAGE.PLT]

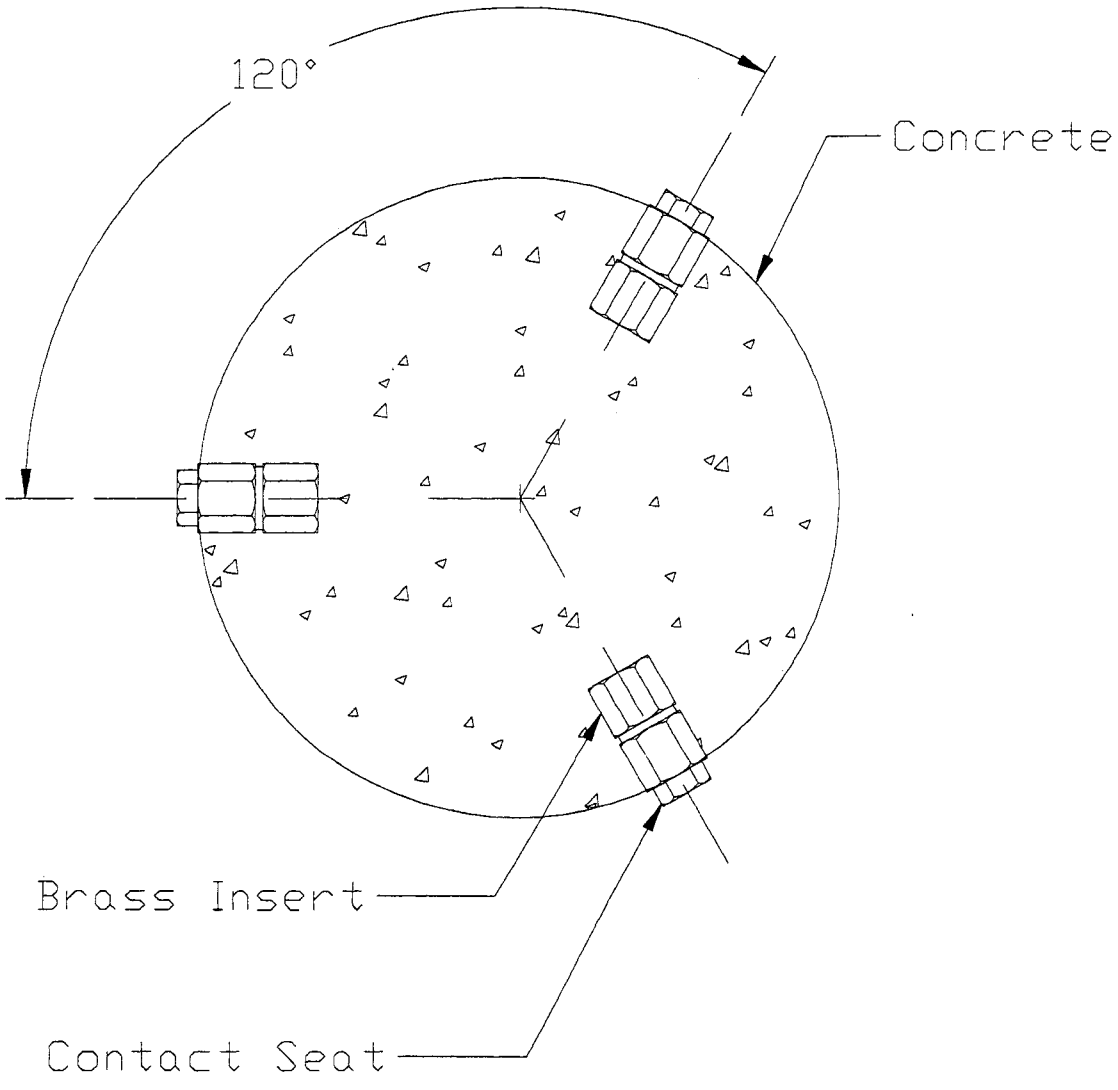

Figure 10.6-A. Cross section of a 4 x 11 in. (100 x 280 mm) concrete cylinder used for measuring creep and shrinkage deformations. Also shown are the stainless steel contact seats (DEMEC points) threaded in the embedded brass inserts.
[CR-SAMP.PLT]

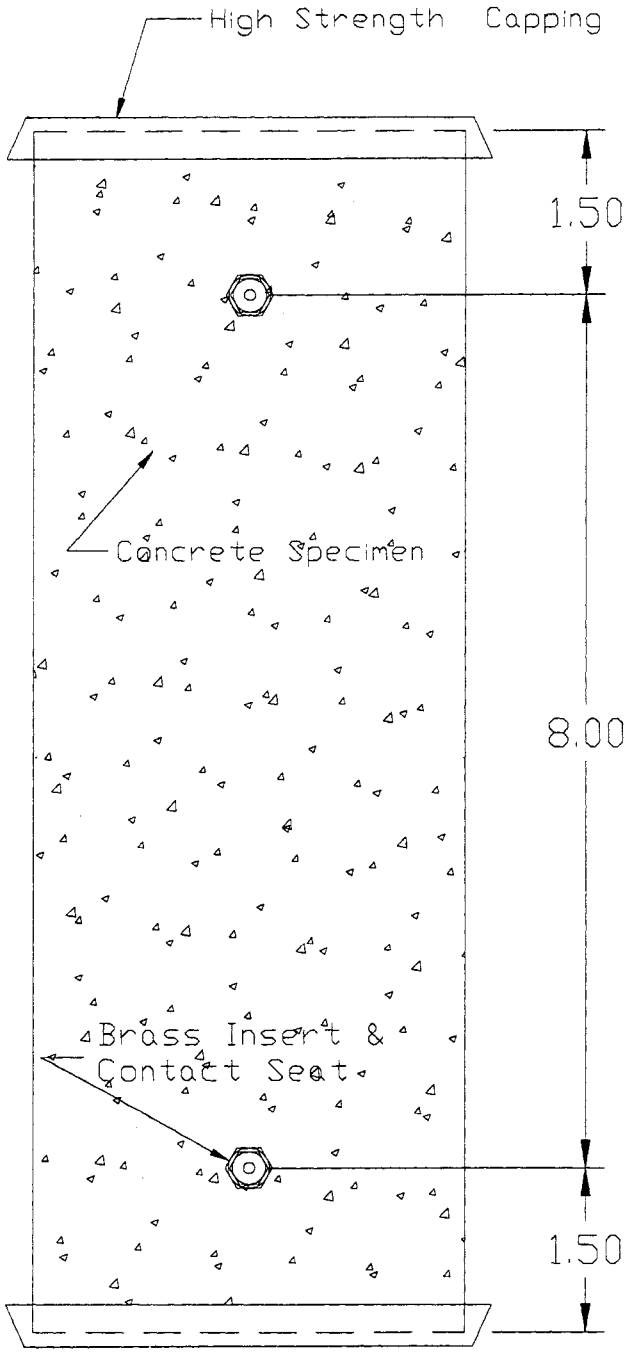

Figure 10.6-B. Side view of capped 4 x 11 in. (100 x 280 mm) creep and shrinkage specimens. Also shown are the contact seats threaded into embedded brass inserts to form 8 in. (200 mm) gage lines.
[CR-SAMP2.PLT]

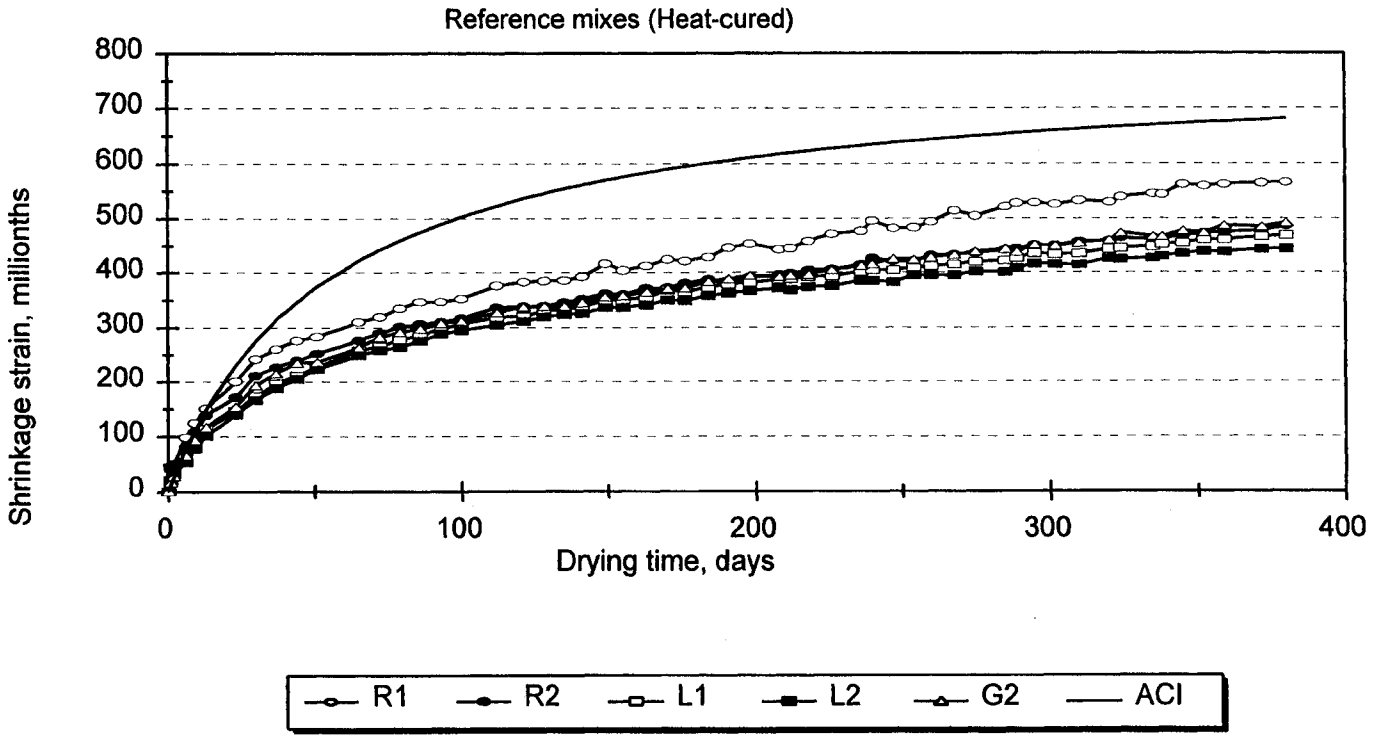

Figure 10.7. Drying shrinkage of heat-cured high strength concrete specimens made with different types of coarse aggregates. [10_7.WMF]

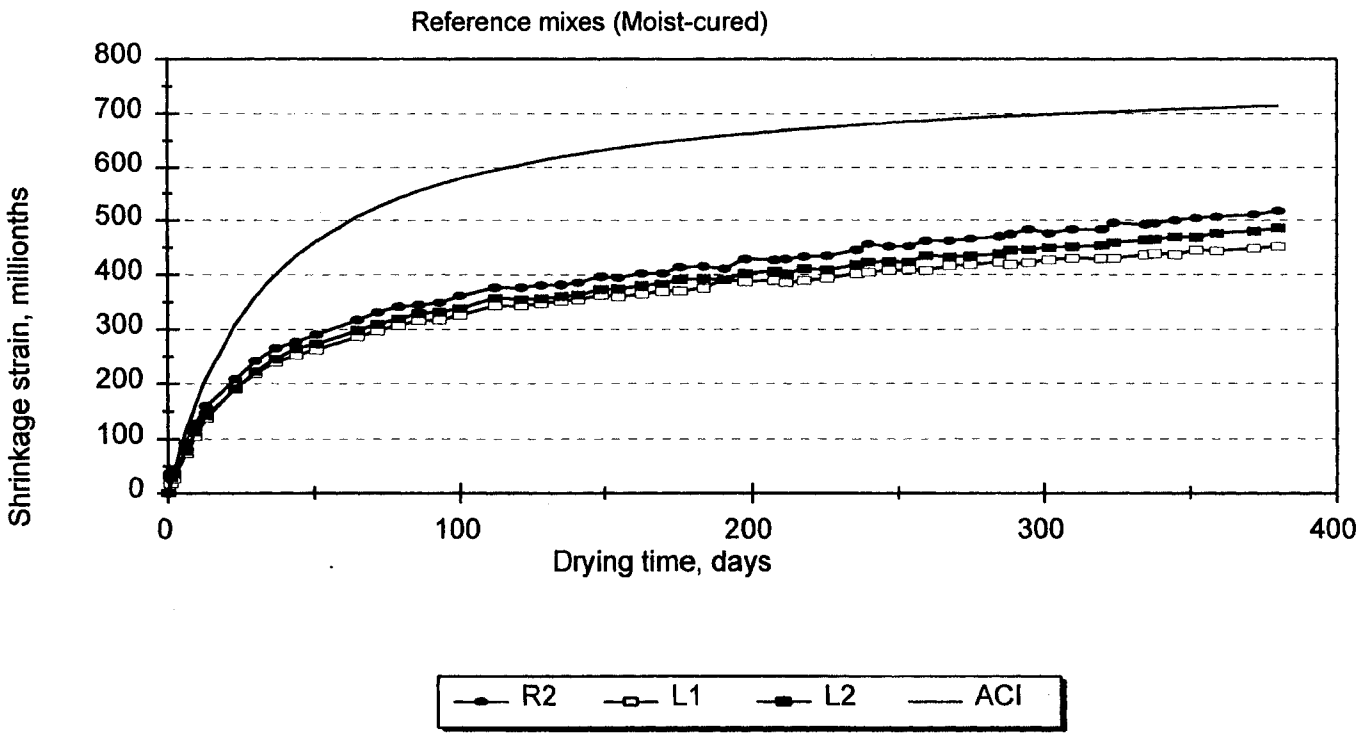

Figure 10.8. Drying shrinkage of moist-cured (W7) high strength concrete specimens made with different types of coarse aggregates. [10_8.WMF]

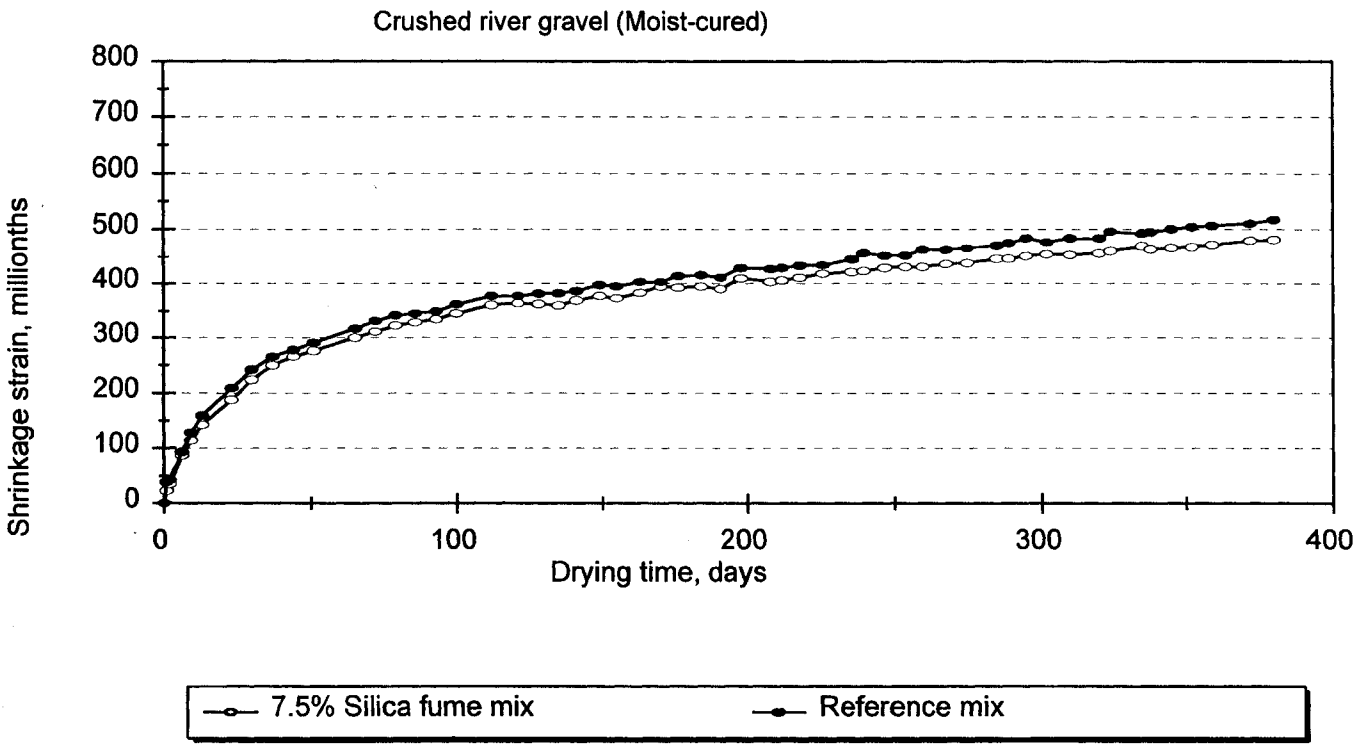

Figure 10.9. Comparison of the drying shrinkage characteristics of moist-cured (W7) high strength concretes made with partially crushed river gravel (R2), having different cementitious material compositions.
[10_9.WMF]

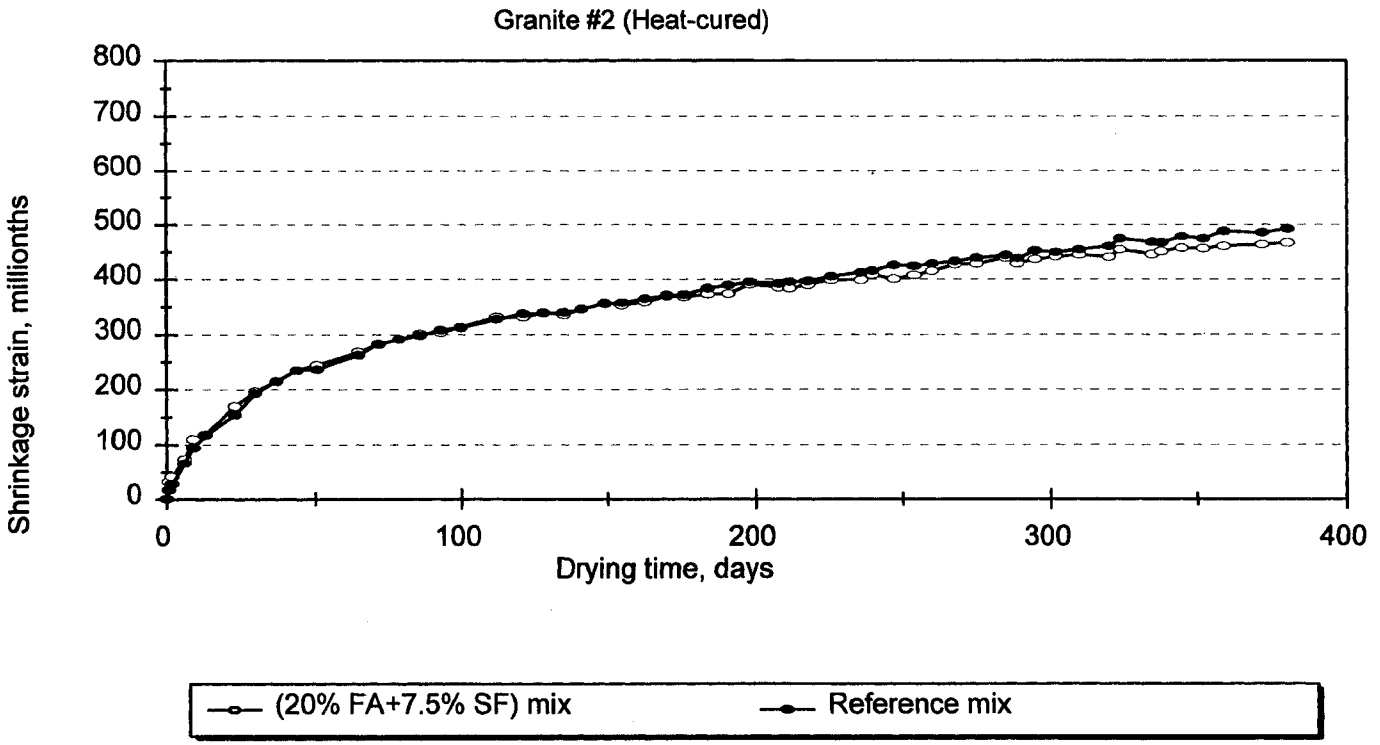

Figure 10.10. Comparison of the drying shrinkage characteristics of heat-cured (H) high strength concretes made with granite #2 (G2), having different cementitious material compositions.
[10_10.WMF]

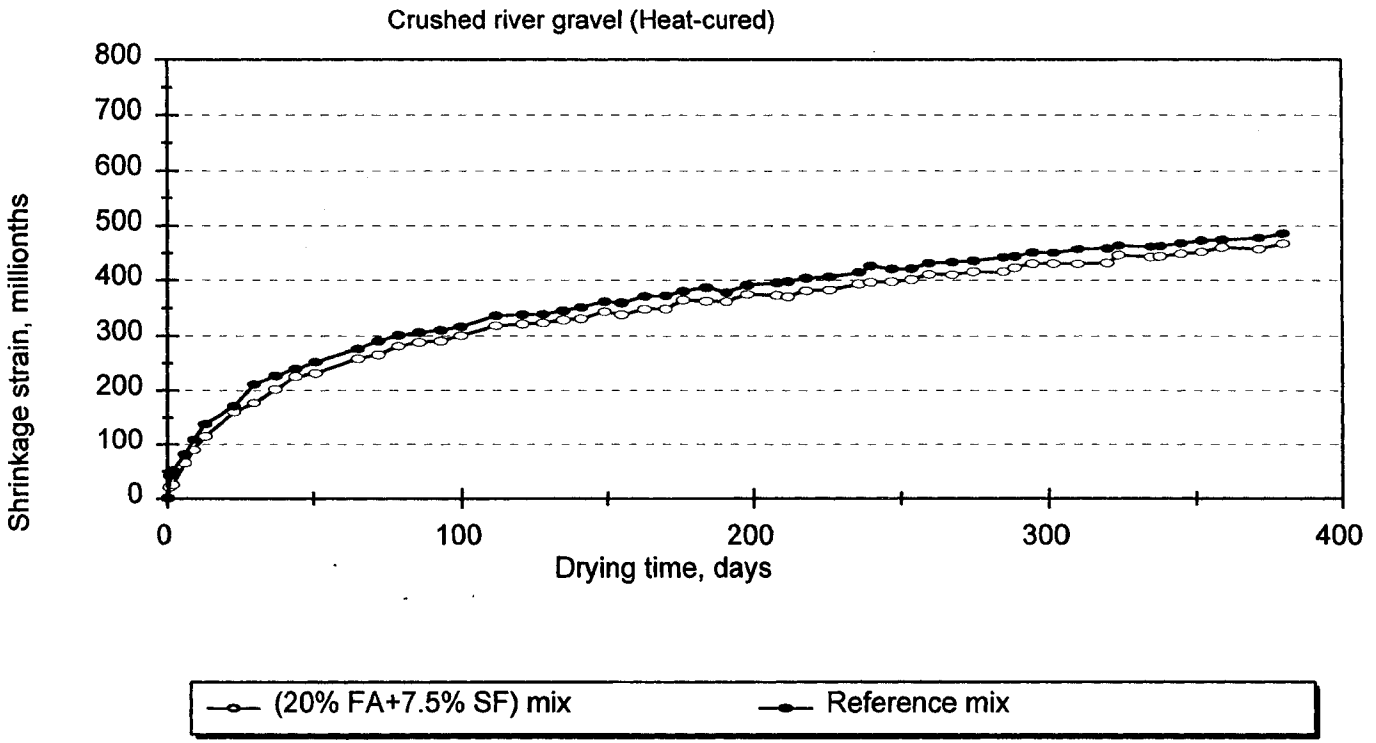

Figure 10.11. Comparison of the drying shrinkage characteristics of heat-cured (H) high strength concretes made with partially crushed river gravel (R2), having different cementitious material compositions.
[10_11.WMF]

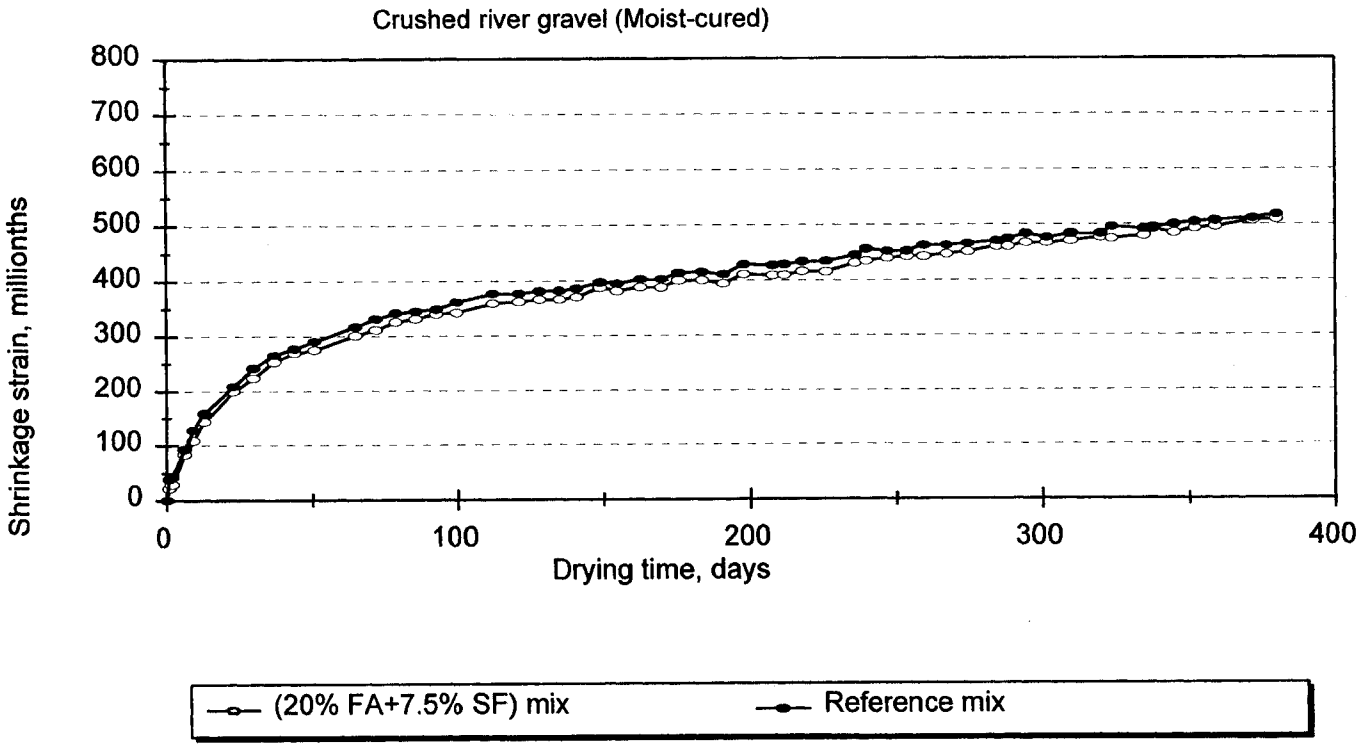

Figure 10.12. Comparison of the drying shrinkage characteristics of moist-cured (W7) high strength concretes made with partially crushed river gravel (R2), having different cementitious material compositions.
[10_12.WMF]

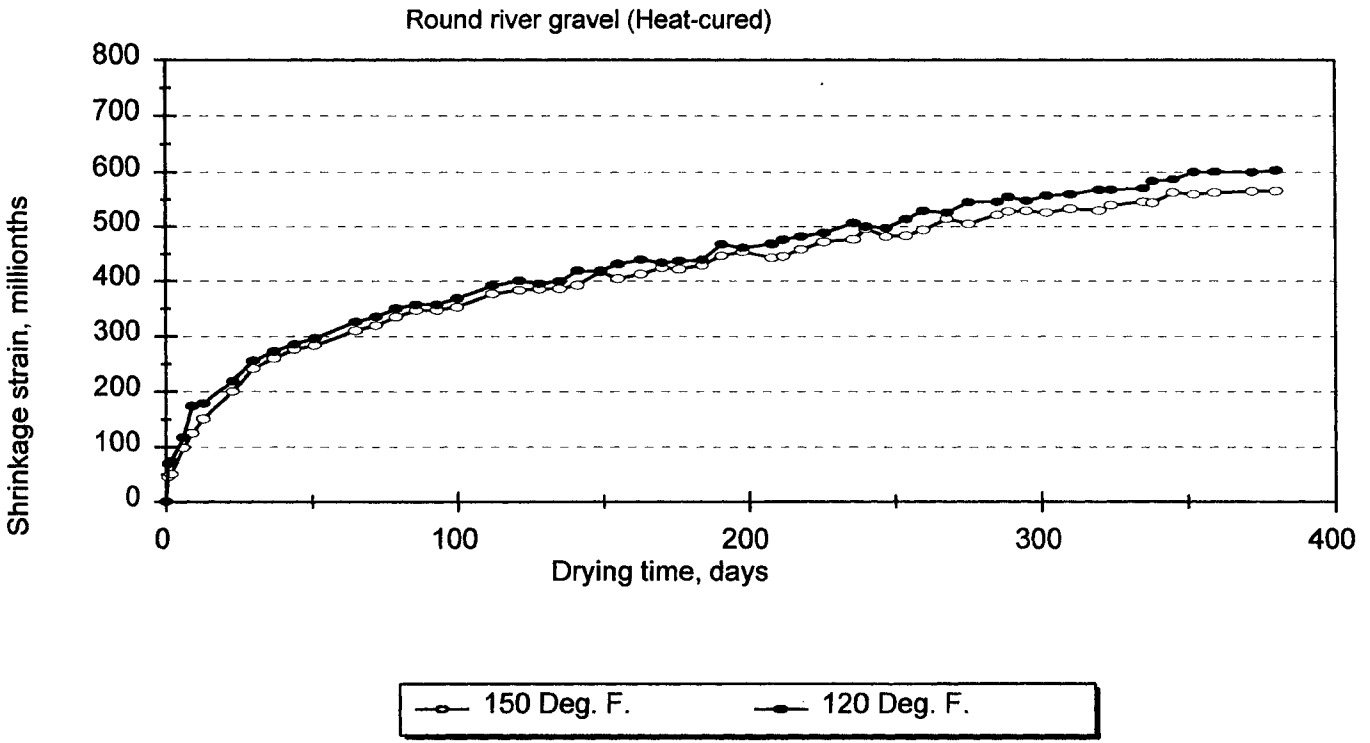

Figure 10.13. Comparison of the drying shrinkage characteristics of high strength concrete specimens heat-cured at 150 °F and 120 °F. [10_13.WMF]

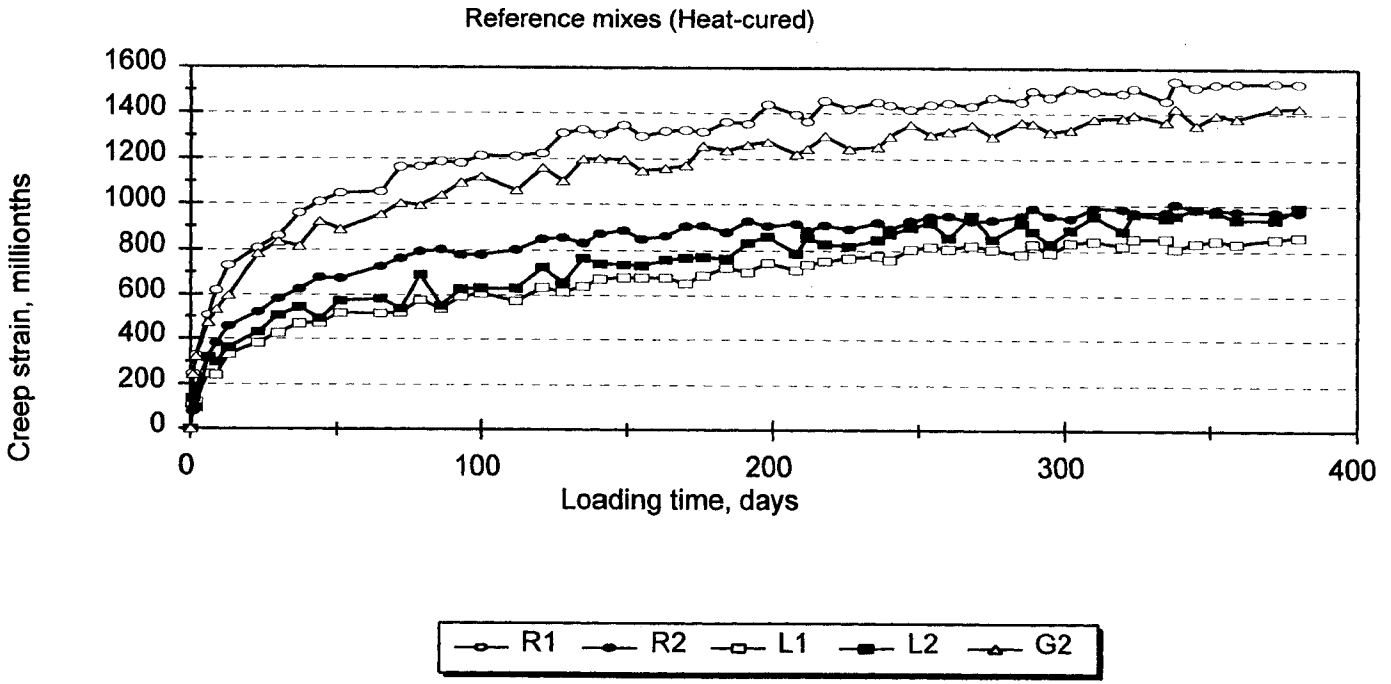

Figure 10.14. Creep strain of heat-cured high strength concrete specimens made with different types of coarse aggregates. [10_14.WMF]

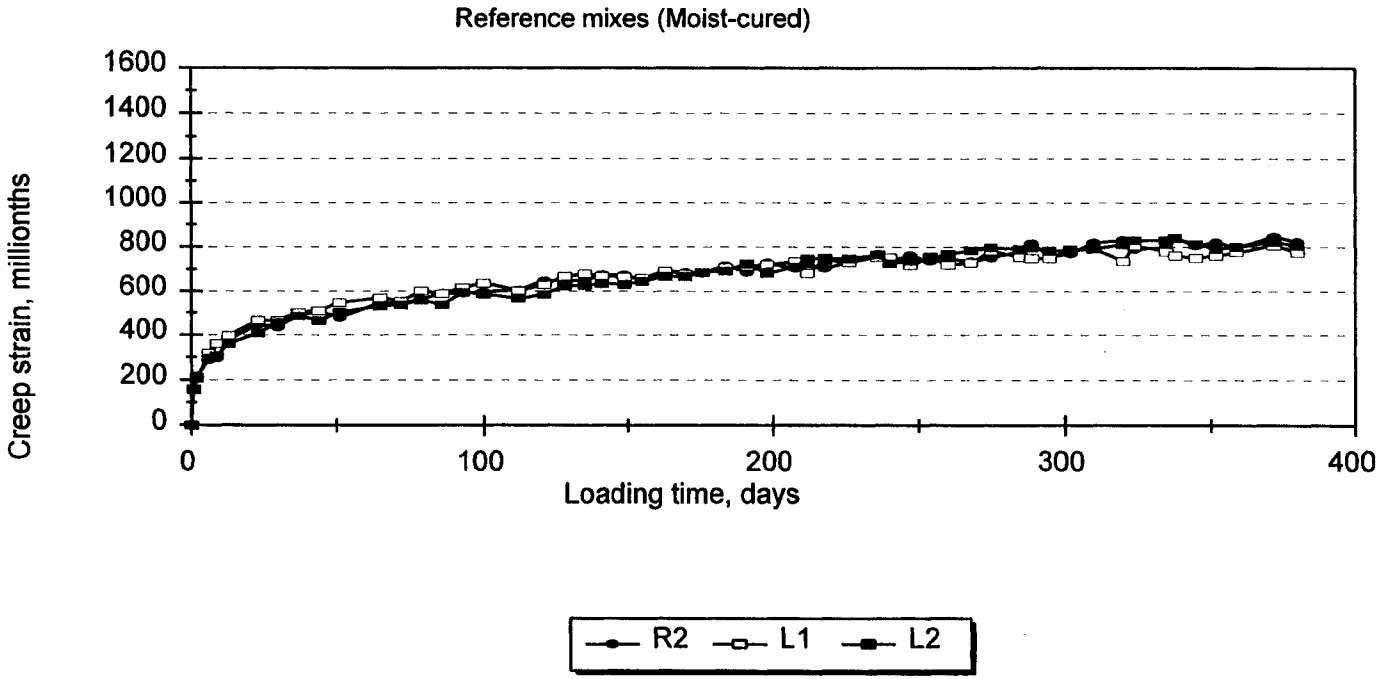

Figure 10.15. Creep strain of moist-cured (W7) high strength concrete specimens made with different types of coarse aggregates. [10_15.WMF]

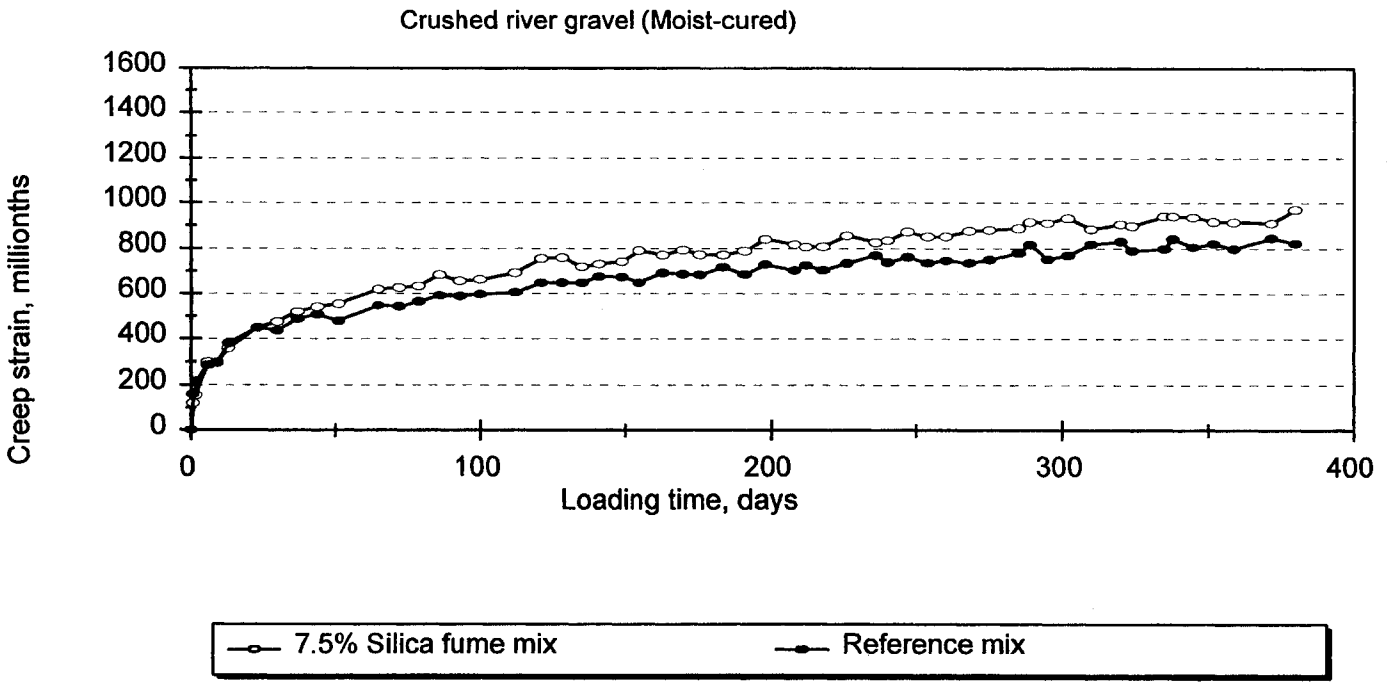

Figure 10.16. Comparison of the creep characteristics of moist-cured (W7) high strength concretes made with partially crushed river gravel (R2), having different cementitious material compositions.
[10_16.WMF]

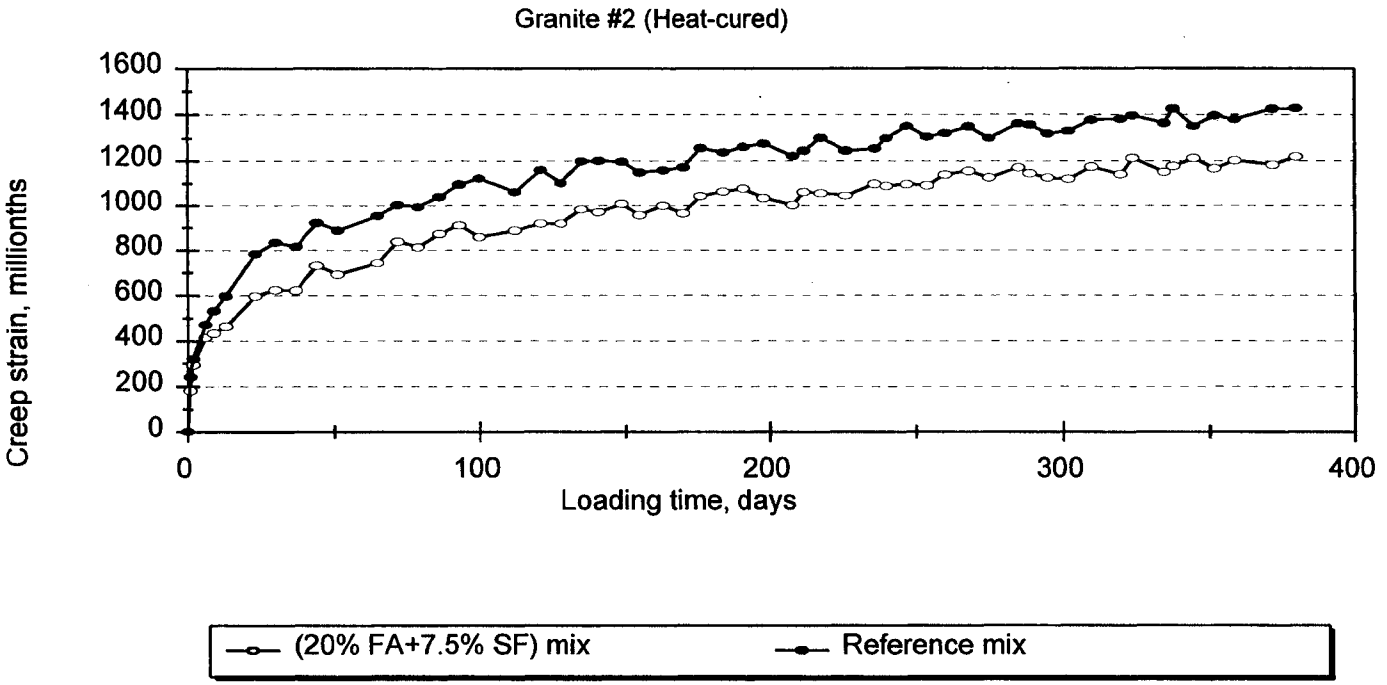

Figure 10.17. Comparison of the creep characteristics of heat-cured (H) high strength concretes made with granite #2 (G2), having different cementitious material compositions.
[10_17.WMF]

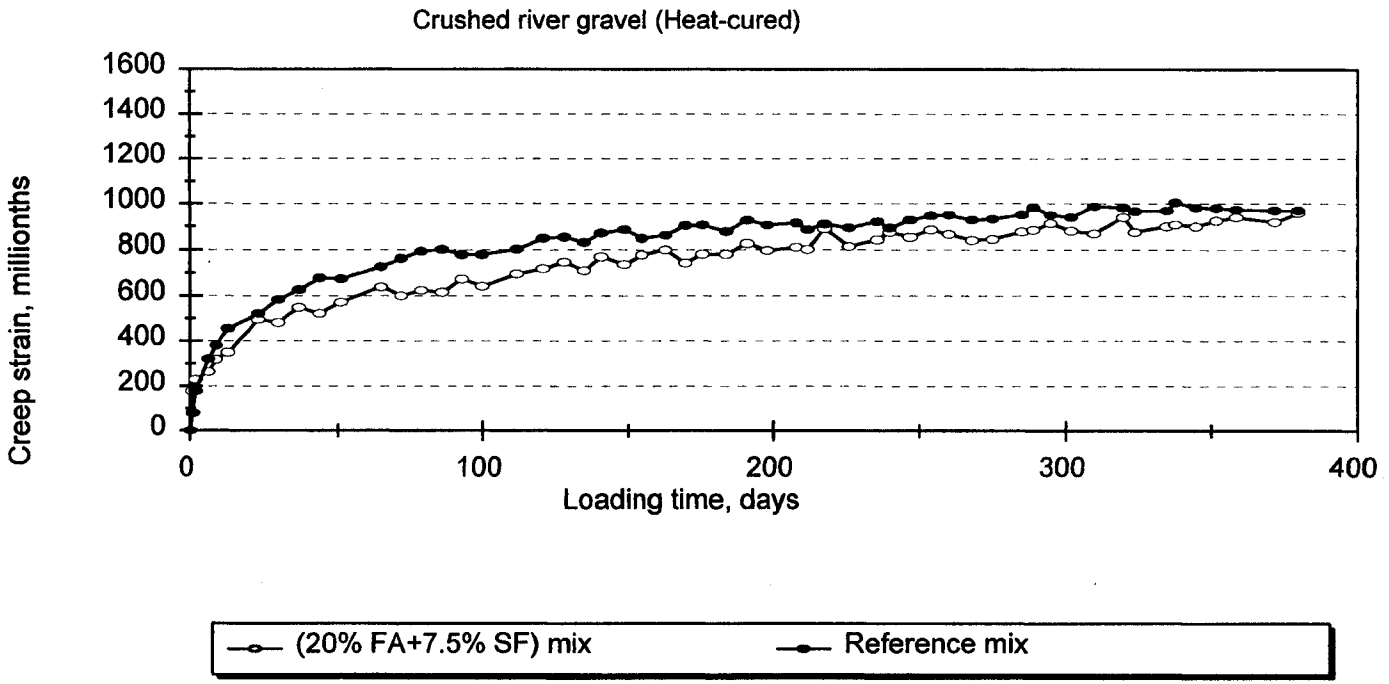

Figure 10.18. Comparison of the creep characteristics of heat-cured (H) high strength concretes made with partially crushed river gravel (R2), having different cementitious material compositions.
[10_18.WMF]

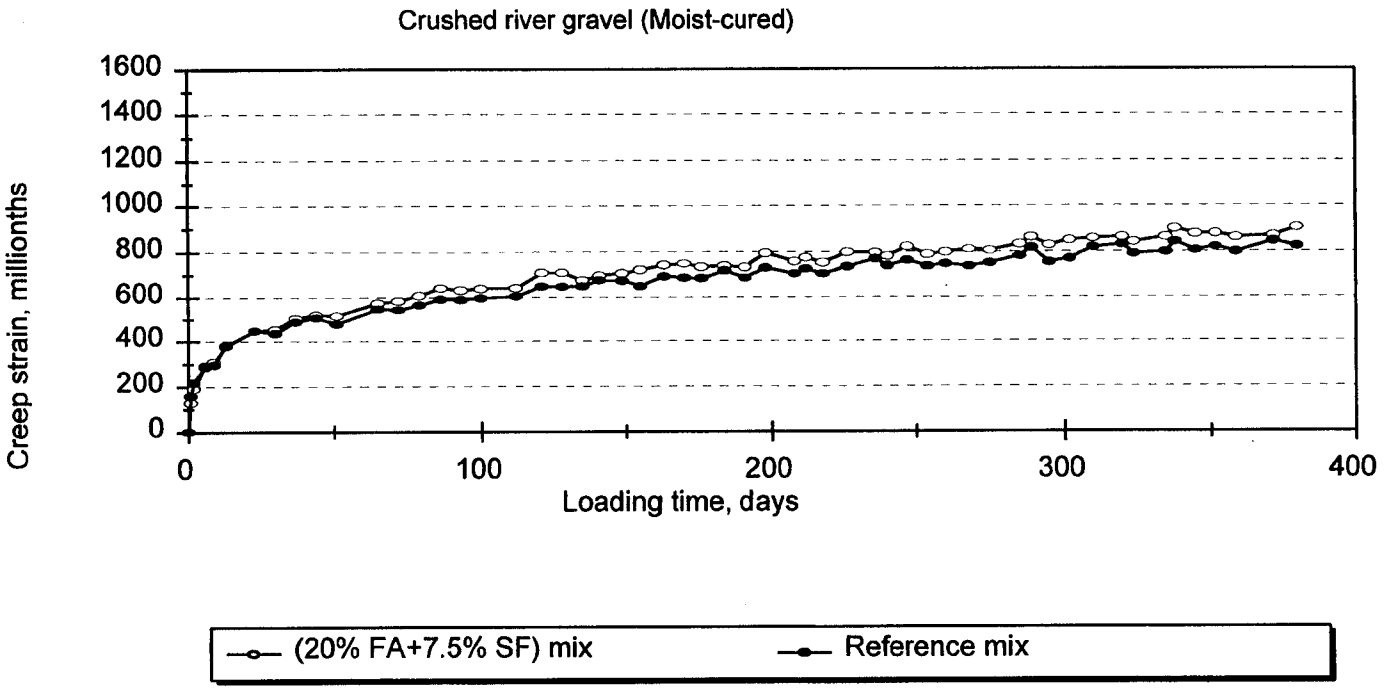

Figure 10.19. Comparison of the creep characteristics of moist-cured (W7) high strength concretes made with partially crushed river gravel (R2), having different cementitious material compositions.
[10_19.WMF]

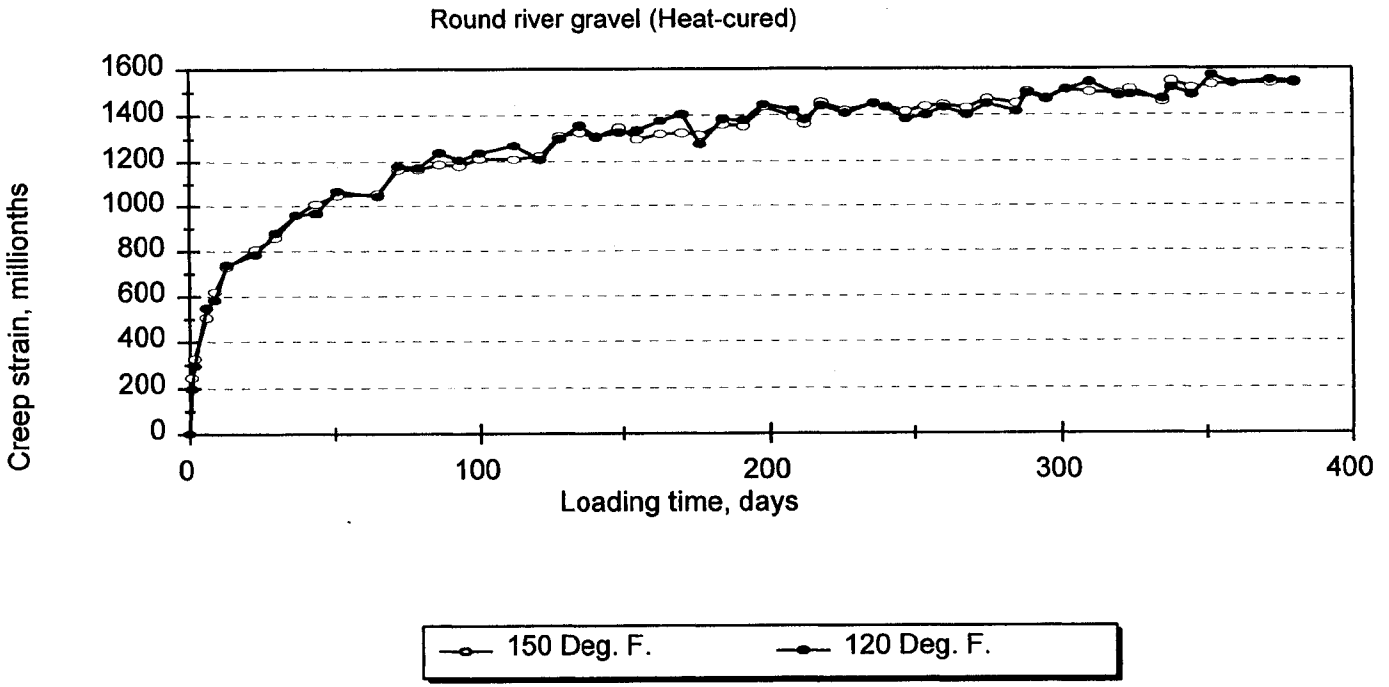

Figure 10.20. Comparison of the creep characteristics of high strength concrete specimens heat-cured at 120 °F and 150 °F. [10_20.WMF]

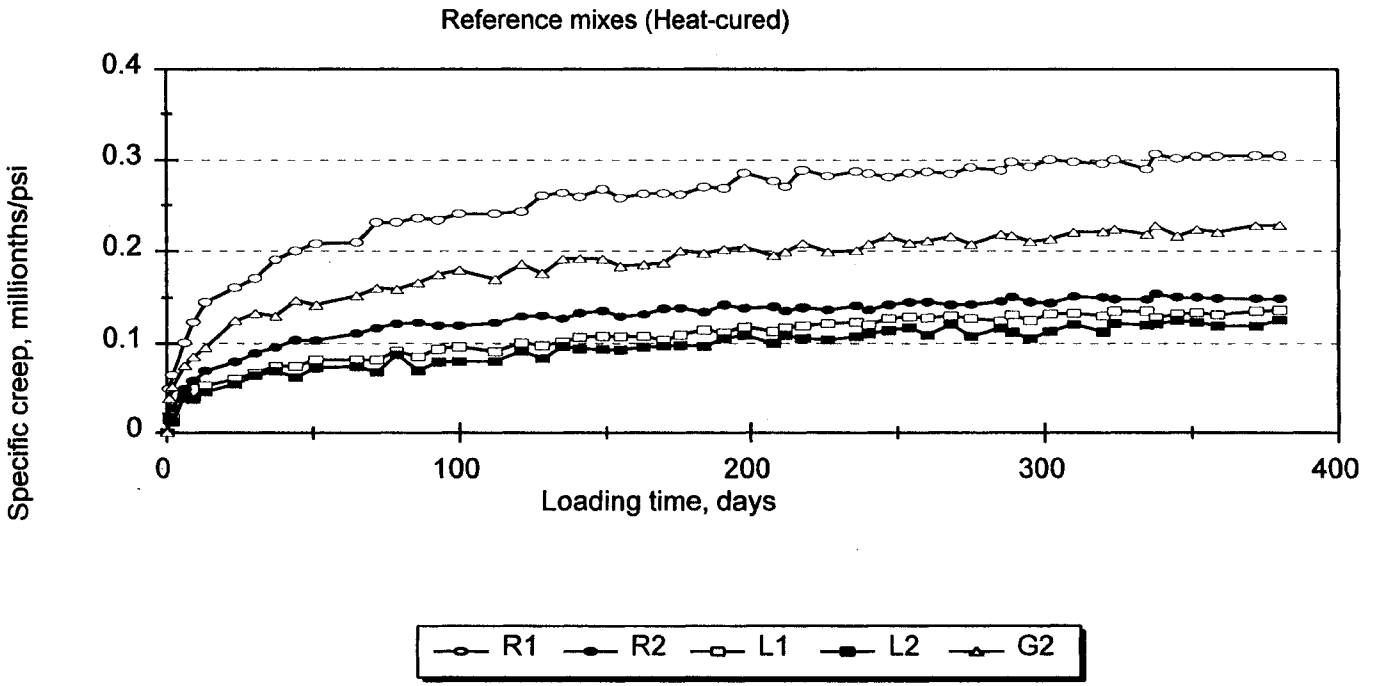

Figure 10.21. Specific creep of heat-cured high strength concrete specimens made with different types of coarse aggregates. [10_21.WMF]

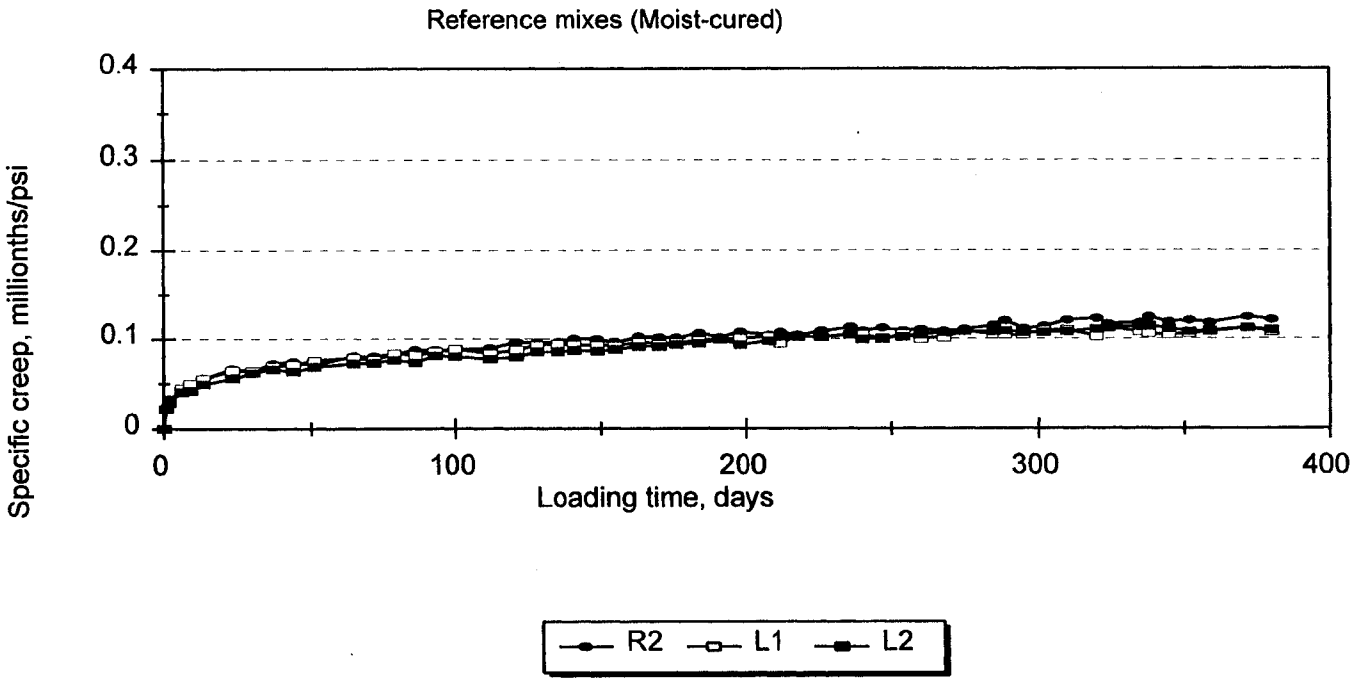

Figure 10.22. Specific creep of moist-cured (W7) high strength concrete specimens made with different types of coarse aggregates. [10_22.WMF]

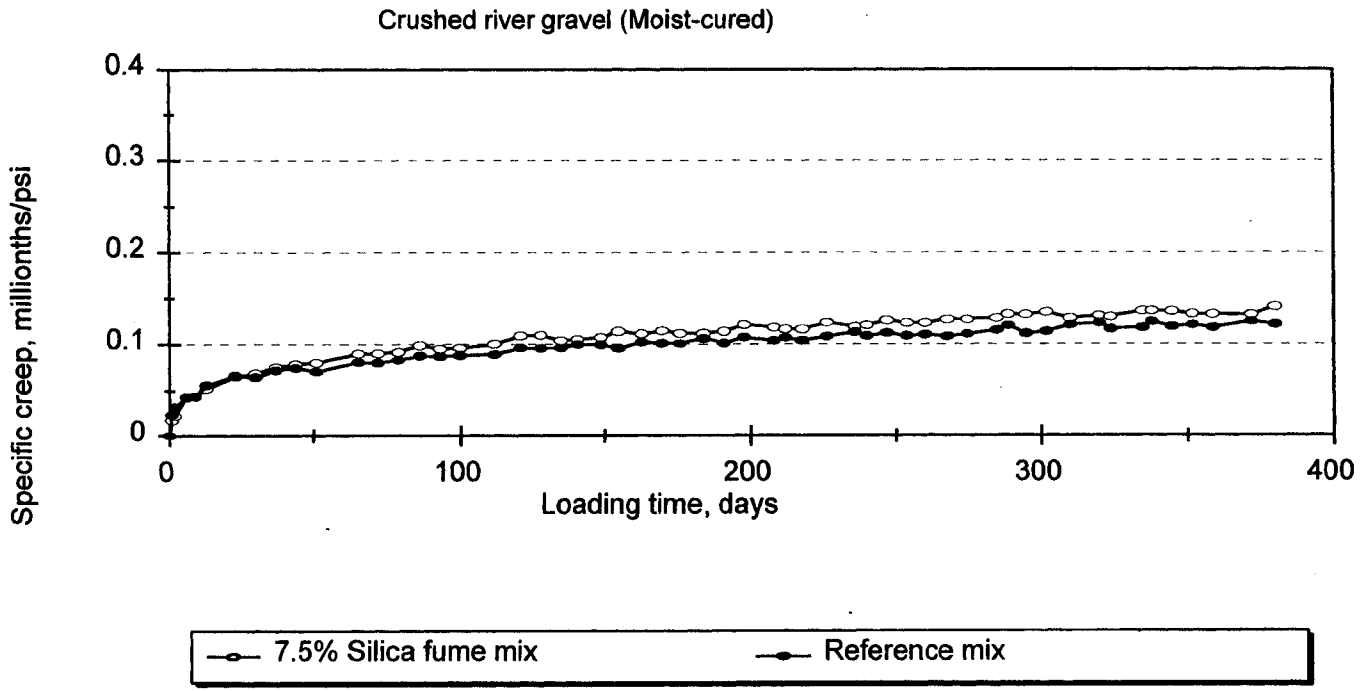

Figure 10.23. Comparison of the specific creeps of moist-cured (W7) high strength concretes made with partially crushed river gravel (R2), having different cementitious material compositions.
[10_23.WMF]

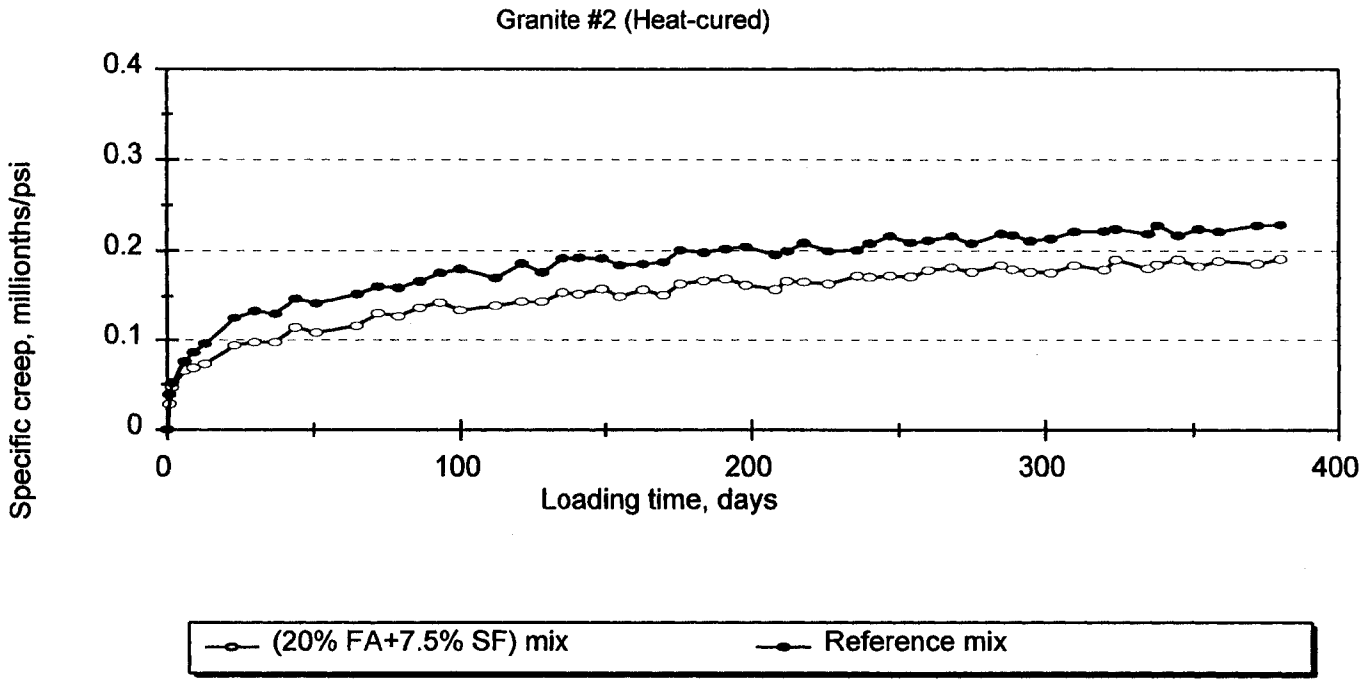

Figure 10.24. Comparison of the specific creeps of heat-cured (H) high strength concretes made with granite #2 (G2), having different cementitious material compositions.
[10_24.WMF]

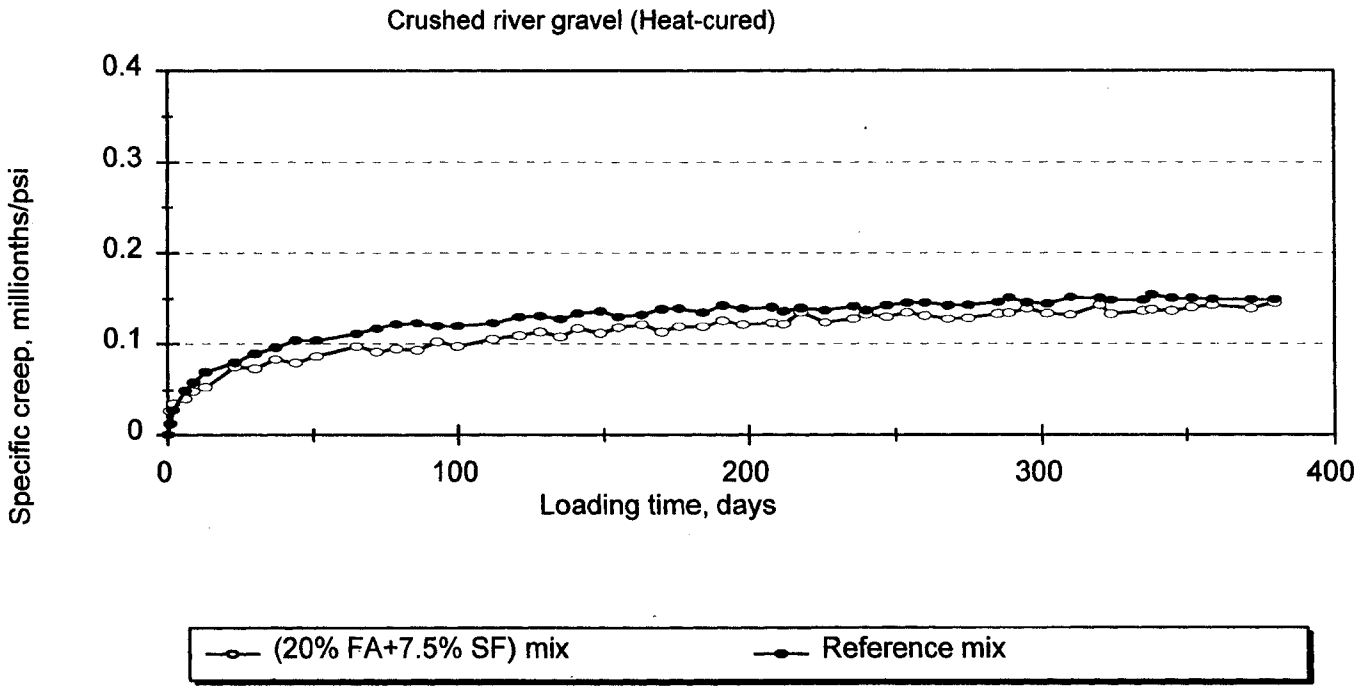

Figure 10.25. Comparison of the specific creeps of heat-cured (H) high strength concretes made with partially crushed river gravel (R2), having different cementitious material compositions.
[10_25.WMF]

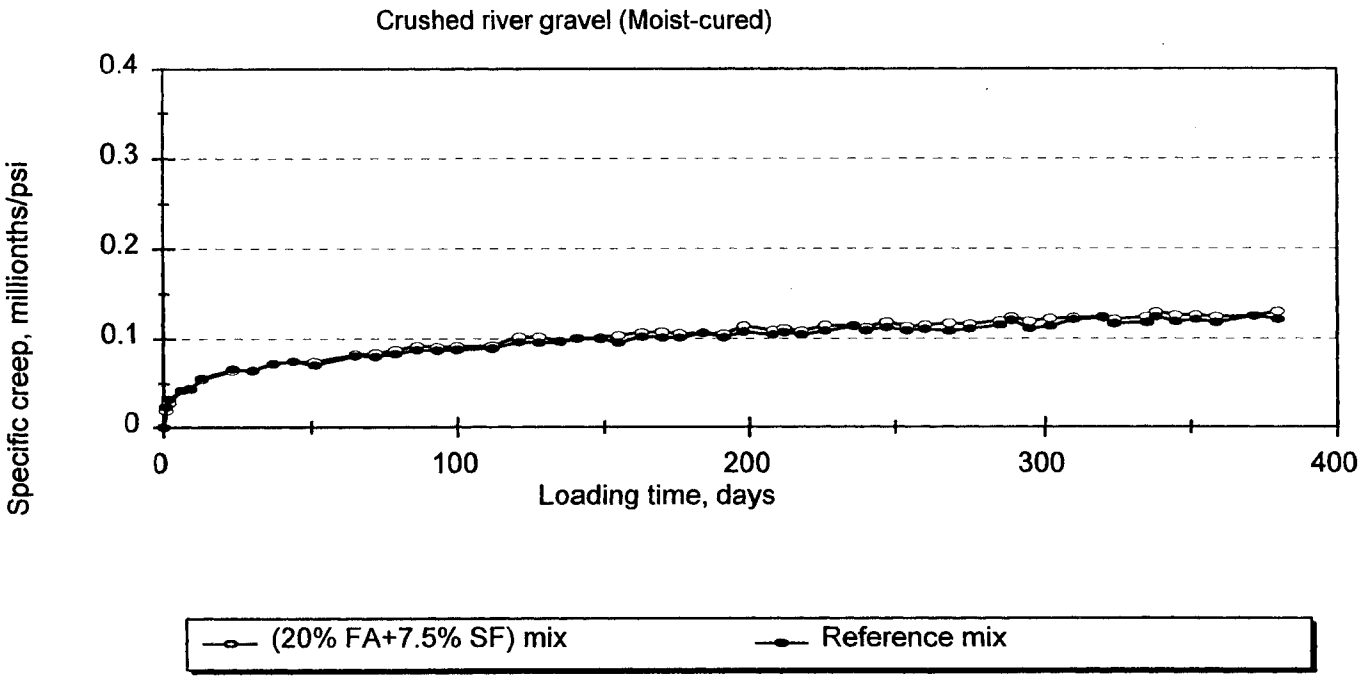

Figure 10.26. Comparison of the specific creeps of moist-cured (W7) high strength concretes made with partially crushed river gravel (R2), having different cementitious material compositions.
[10_26.WMF]

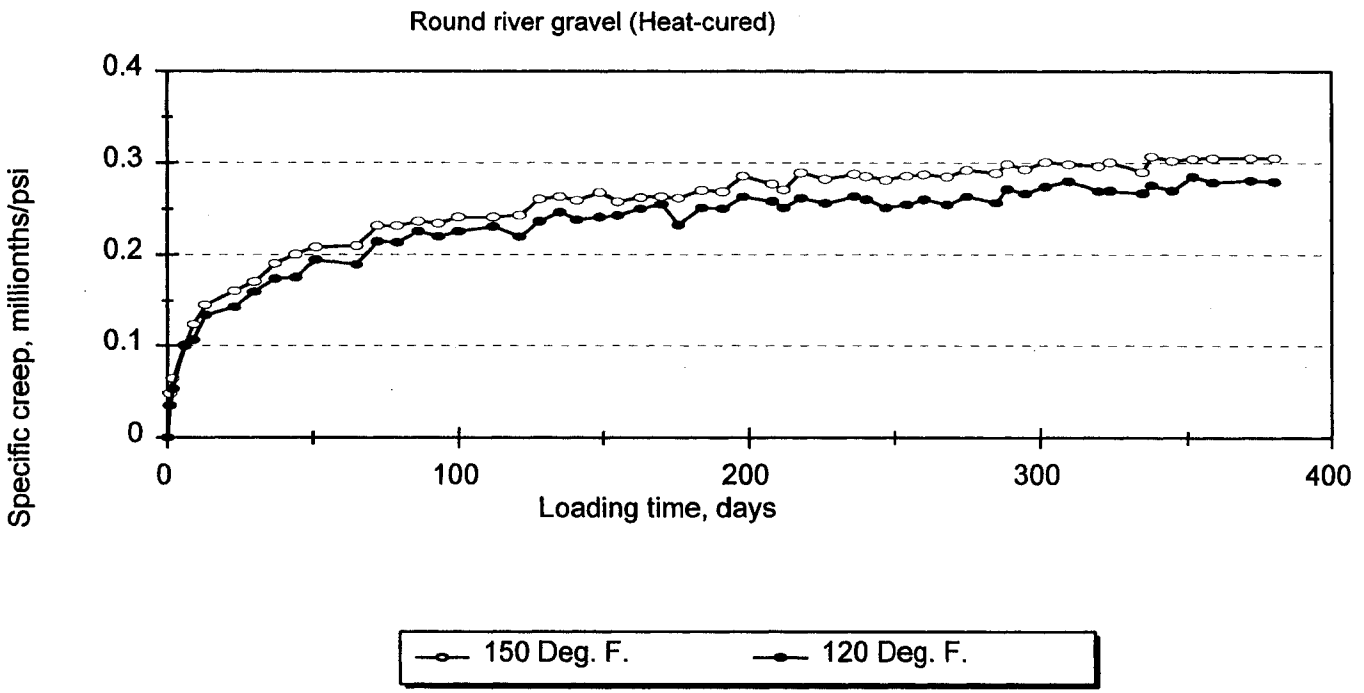

Figure 10.27. Comparison of the specific creeps of high strength concrete specimens heat-cured at 120 °F and 150 °F. [10_27.WMF]

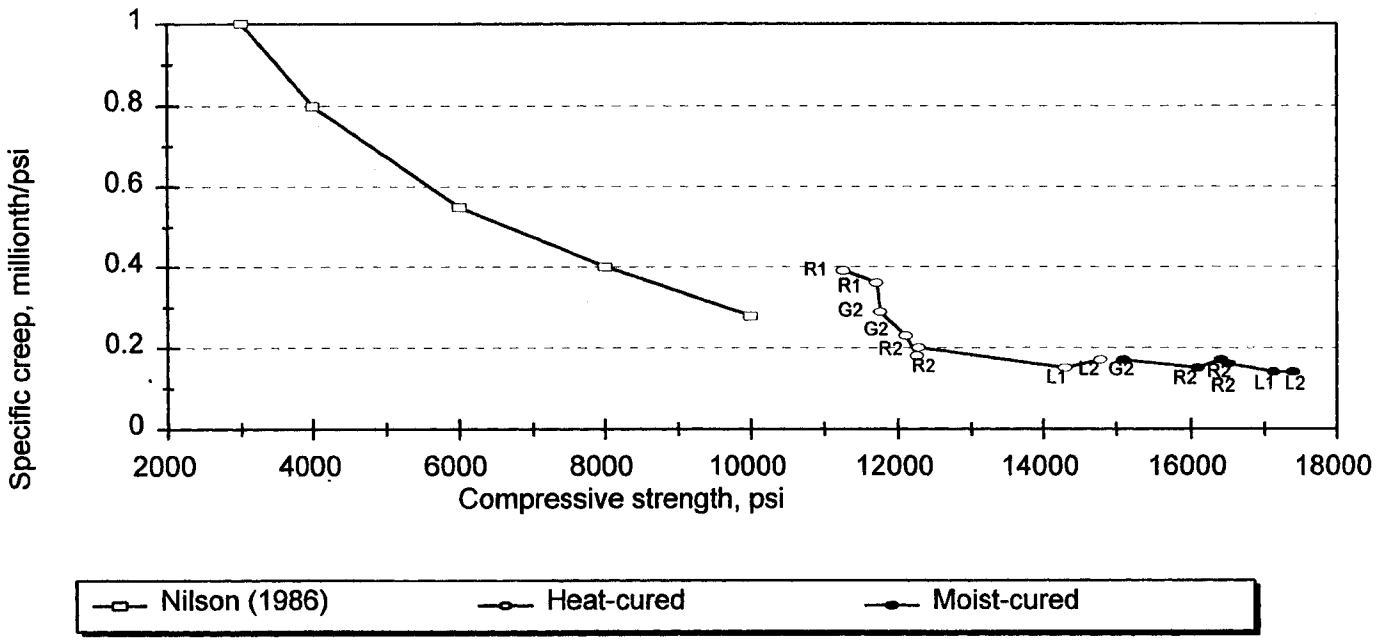

Figure 10.28. Comparison of the observed specific creep values for high strength concrete from this study with the typical values suggested by Nilson et al. *[Nilson and Winter Design of Concrete Structures 1986]* for various compressive strengths. [10_28.WMF]

CHAPTER 11
WATER ABSORPTION TESTS

11.1 Experimental Program

Water absorption characteristics of forty mixes (Mix Nos. 100 to 139) were investigated by placing two 4 x 8 in. (100 x 200 mm) cylinders in a tank of water and measuring weight gain as a function of time stored under water. Heat-cured specimens (H) were placed in the tank at an age of 1-day. Moist-cured (W7) specimens were stored in the laboratory at 72±4 °F (22± °C) and 50±5% R.H. after 7-days of initial moist-curing and were placed in the tank at 28-days. Weight change of specimens was measured by a 44 lb. (20,000 g) maximum capacity high precision electronic balance with 0.0035 ounce (0.1 g) resolution.

11.2 Results

Test results are presented in Figures 11.1 to 11.25 and in Appendix F. For any given type of coarse aggregate and for both curing conditions the weight gain was highest for mixes with 20% fly ash (20% FA) followed by the reference mixes, and the mixes containing a combination of 20% fly ash and 7.5% silica fume (20% FA+7.5% SF). Weight gain was the lowest for mixes containing 7.5% silica fume (7.5% SF), Figures 11.1 to 11.17. However, moist-curing reduced the influence of the type of aggregate on absorption potential of high strength concrete specimens significantly. After 385 days storage under water, the moist-cured specimens gained between 0.915 and 2.099 pcf (14.655 and 33.619 kg/m^3). Companion heat-cured specimens gained between 1.379 and 3.592 pcf (22.087 and 57.532 kg/m^3) in the same period. It is believed that the differential thermal expansion of concrete constituents during the heat-curing process results in internal cracking and hence, increased porosity.

At early ages, due to the slow rate of reactivity of fly ash, a high strength concrete mix with 20% fly ash has a higher effective water-to-cementitious materials ratio than a reference mix and hence, produces a more porous matrix. Higher porosity of the fly ash mix together with the consumption of water during continuous pozzolanic reaction of fly ash in the ideal

submerged condition of the test environment can explain the observed higher weight gain of fly ash mixes. On the other hand incorporation of fine particles of silica fume in high strength concrete mixes reduces porosity of concrete by creating a denser cement matrix through the filler effect as well as formation of additional cementitious hydrates. Therefore, at the beginning of the absorption test there are less pores to fill with water and, in the long term, there are less unhydrated particles left to react with water.

Comparison of the data presented in Figures 11.1, 11.4 and 11.7 with those presented in Figures 11.2, 11.5 and 11.8 suggests that specimens heat-cured at lower temperatures may absorb less water in an absorption test than those cured at a higher temperature. For the cases studied, on average, specimens heat-cured at 120 °F (50 °C) gained 8.36% less weight than those cured at 150 °F (65 °C) during the test period.

The effect of type of cement on absorption potential of high strength concrete results from differences in fineness of the two types of cement. Figures 11.1 through 11.6 indicate that for all curing conditions the use of ASTM Type III cement reduces the absorption potential of high strength concrete specimens. The more complete hydration of the finer Type III cement and its filler effect result in formation of a denser cement matrix and hence, the potential for water absorption is decreased.

It is clear that concretes made with absorptive coarse aggregates have a greater potential for water absorption. However, the effect of the type of coarse aggregate on absorption test results is secondary and was greater in mixes made with 20% fly ash and to a lesser extent in the reference mixes, Figures 11.18 through 11.25. The amount of water which reaches the coarse aggregate particles and becomes absorbed by the coarse aggregate particles depends on the permeability of the cement matrix. The type of coarse aggregate did not influence the absorption test results in high strength concrete mixes incorporating 7.5% silica fume. The dense cement matrix prevented water from reaching the aggregate particles.

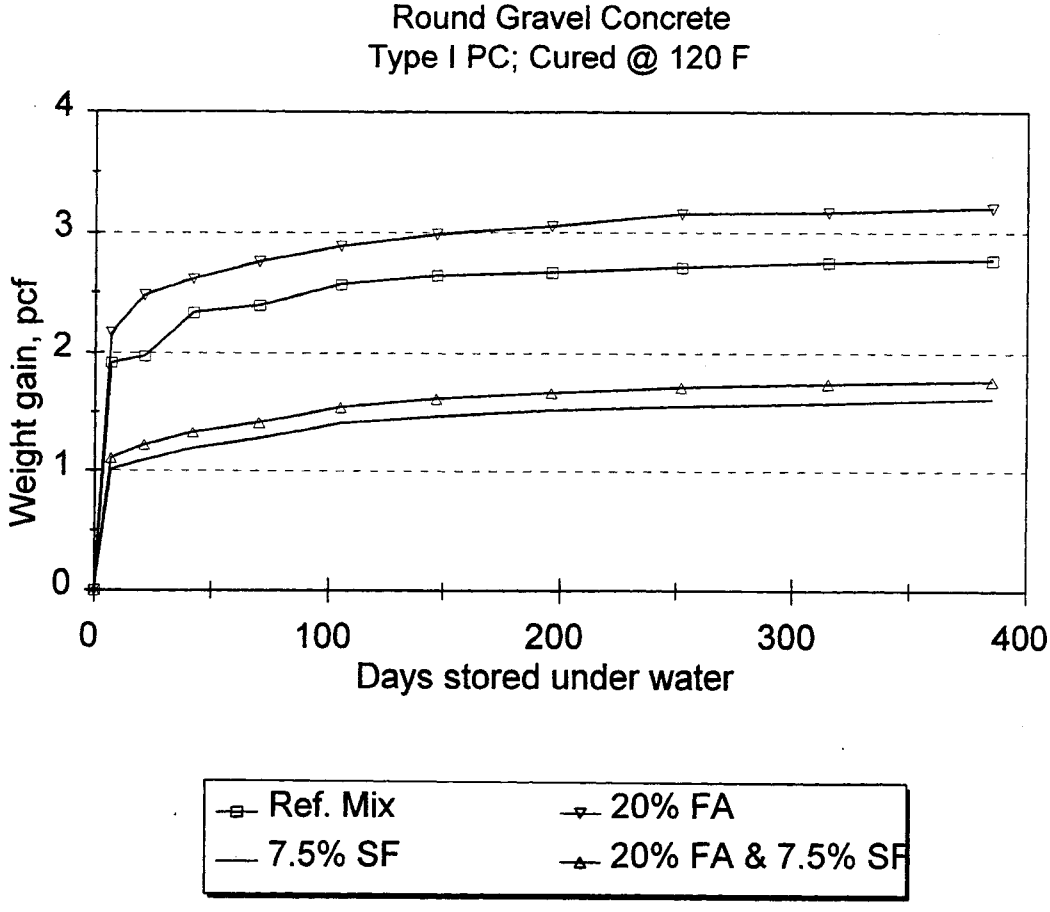

Figure 11.1. Weight-gain of high strength concrete mixes of different cementitious material compositions, heat-cured at 120 °F, made with round river gravel (R1) and ASTM Type I portland cement.

[APFIG1.WMF]

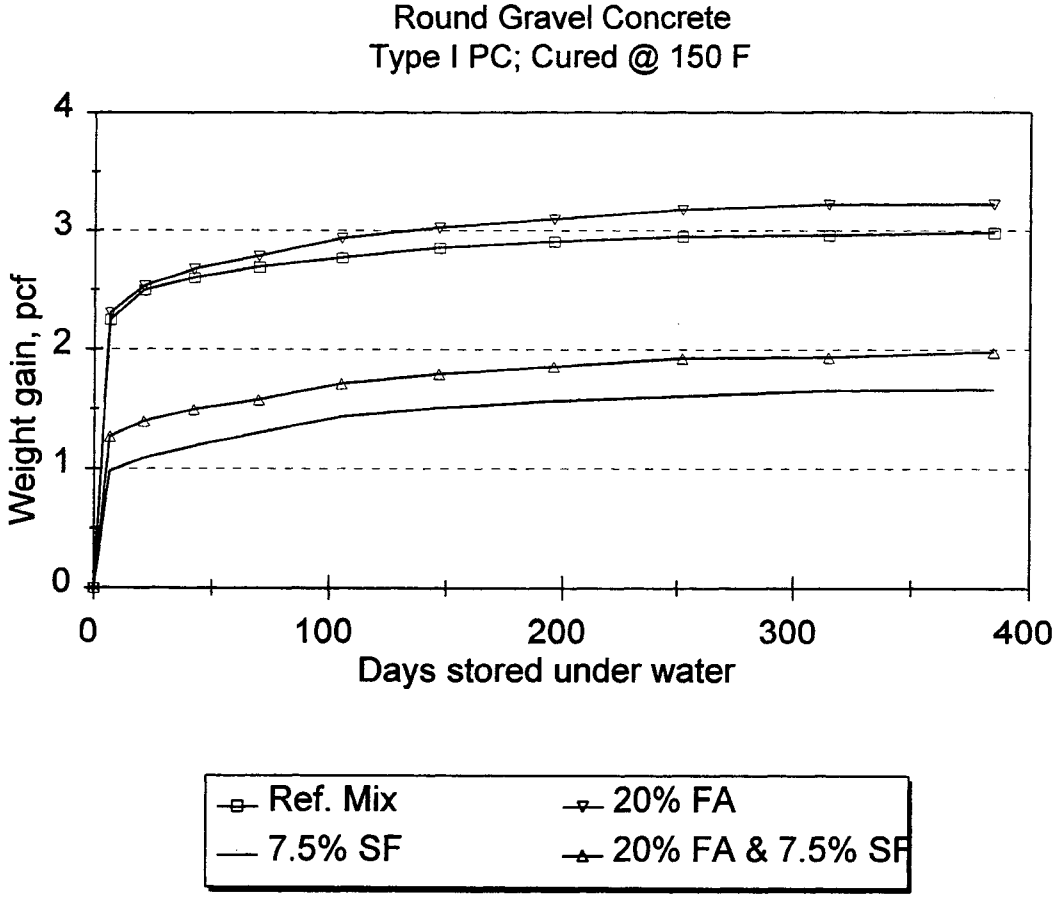

Figure 11.2. Weight-gain of high strength concrete mixes of different cementitious material compositions, heat-cured at 150 °F, made with round river gravel (R1) and ASTM Type I portland cement.

[APFIG2.WMF]

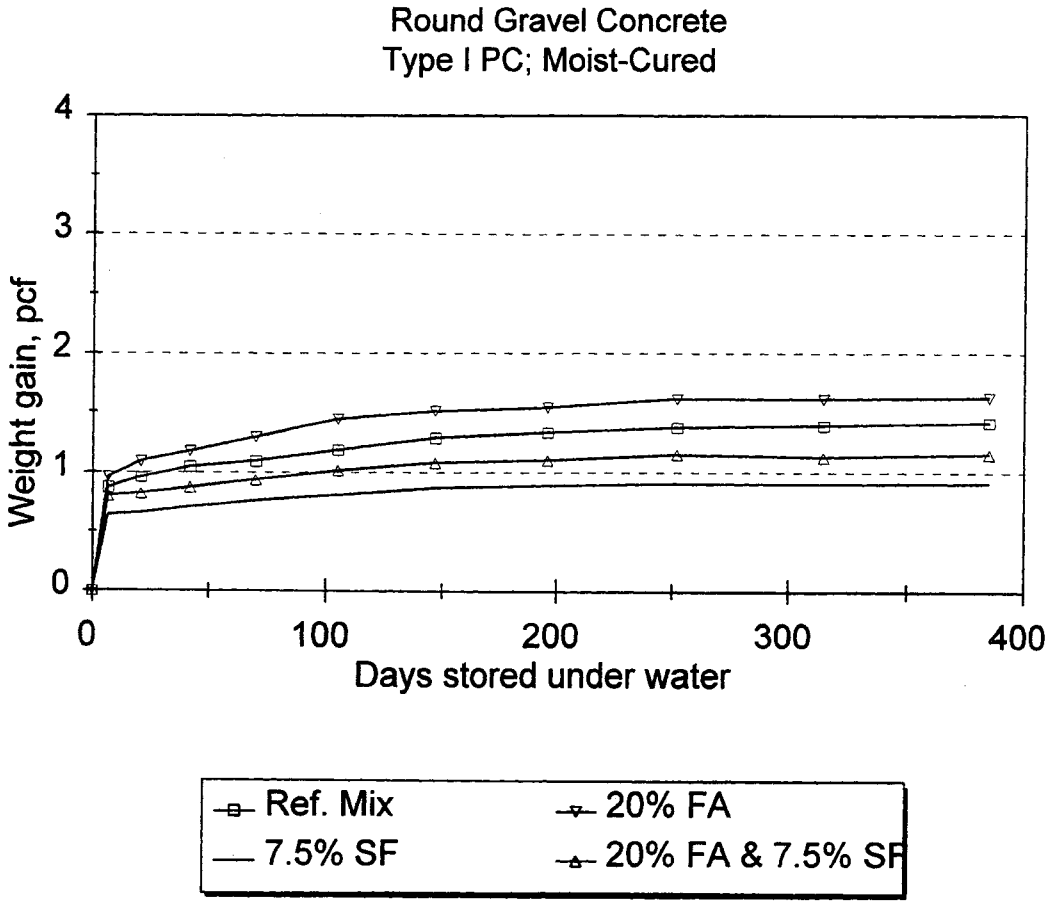

Figure 11.3. Weight-gain of high strength concrete mixes of different cementitious material compositions, moist-cured, made with round river gravel (R1) and ASTM Type I portland cement.

[APFIG3.WMF]

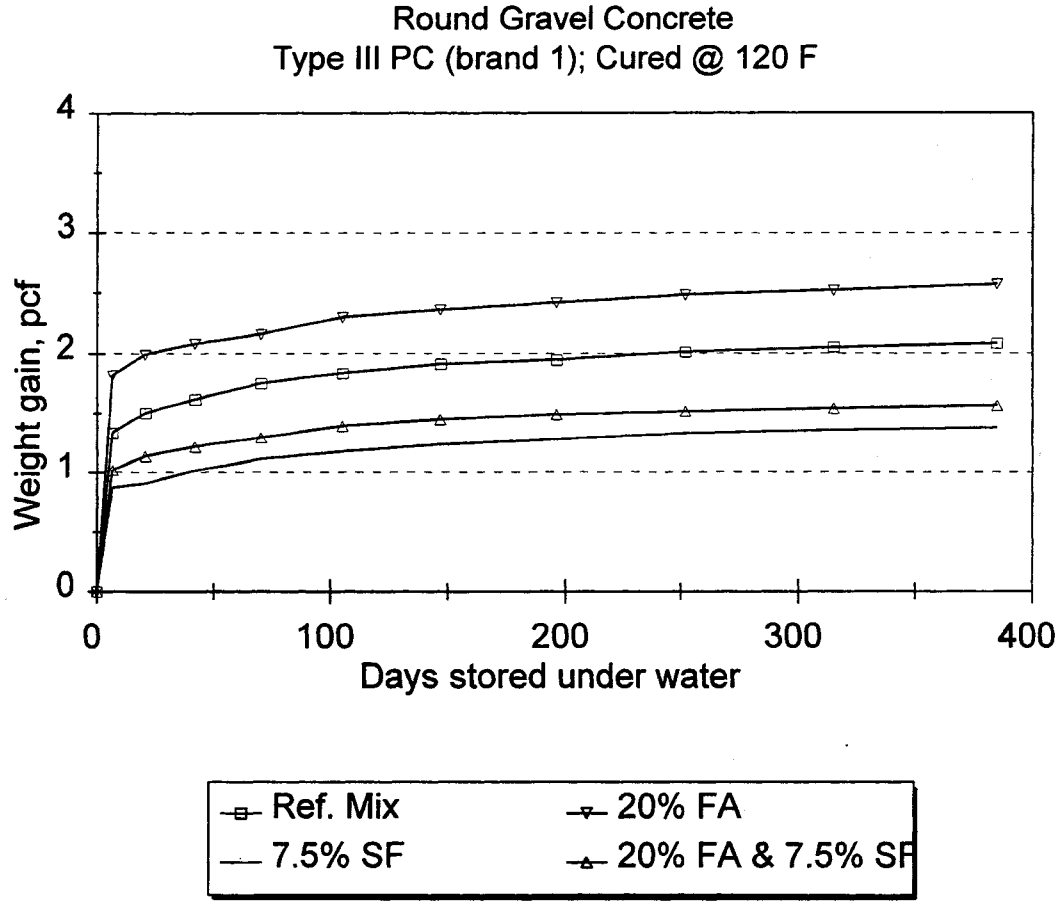

Figure 11.4. Weight-gain of high strength concrete mixes of different cementitious material compositions, heat-cured at 120 °F, made with round river gravel (R1) and ASTM Type III portland cement (Brand 1).

[APFIG4.WMF]

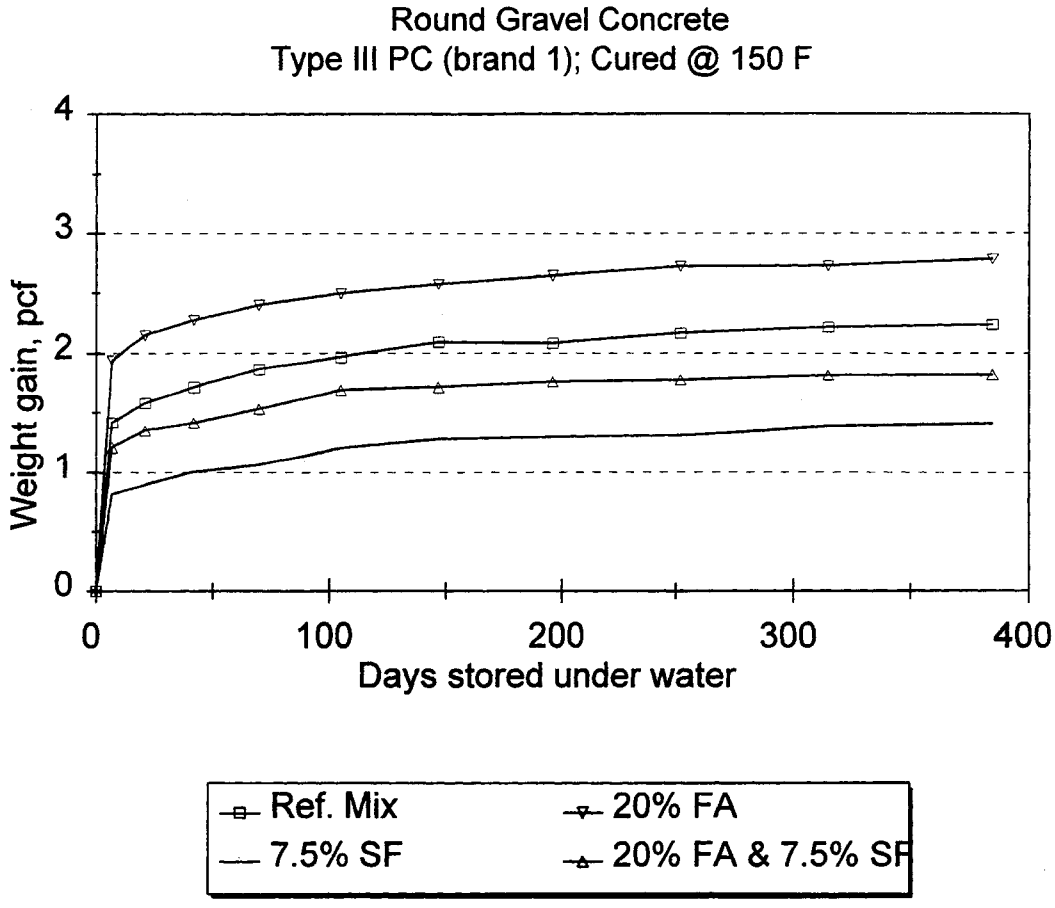

Figure 11.5. Weight-gain of high strength concrete mixes of different cementitious material compositions, heat-cured at 150 °F, made with round river gravel (R1) and ASTM Type III portland cement (Brand 1).

[APFIG5.WMF]

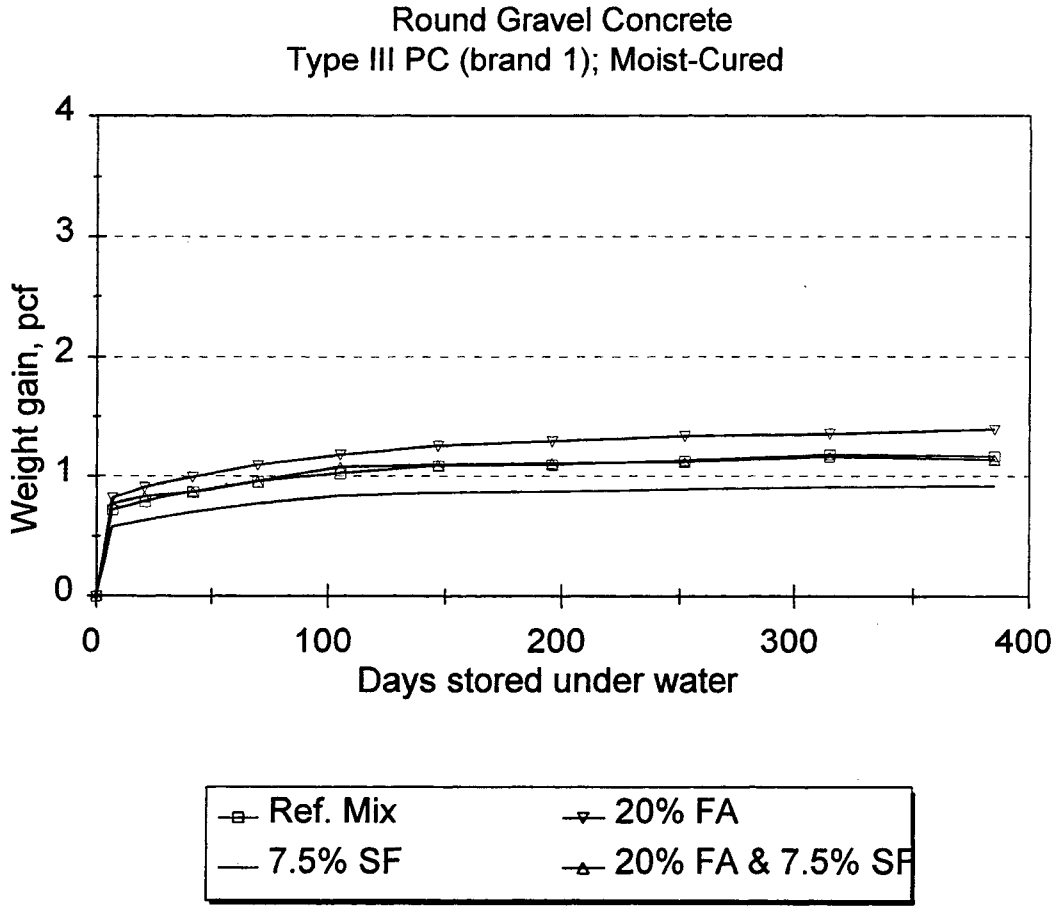

Figure 11.6. Weight-gain of high strength concrete mixes of different cementitious material compositions, moist-cured, made with round river gravel (R1) and ASTM Type III portland cement (Brand 1).

[APFIG6.WMF]

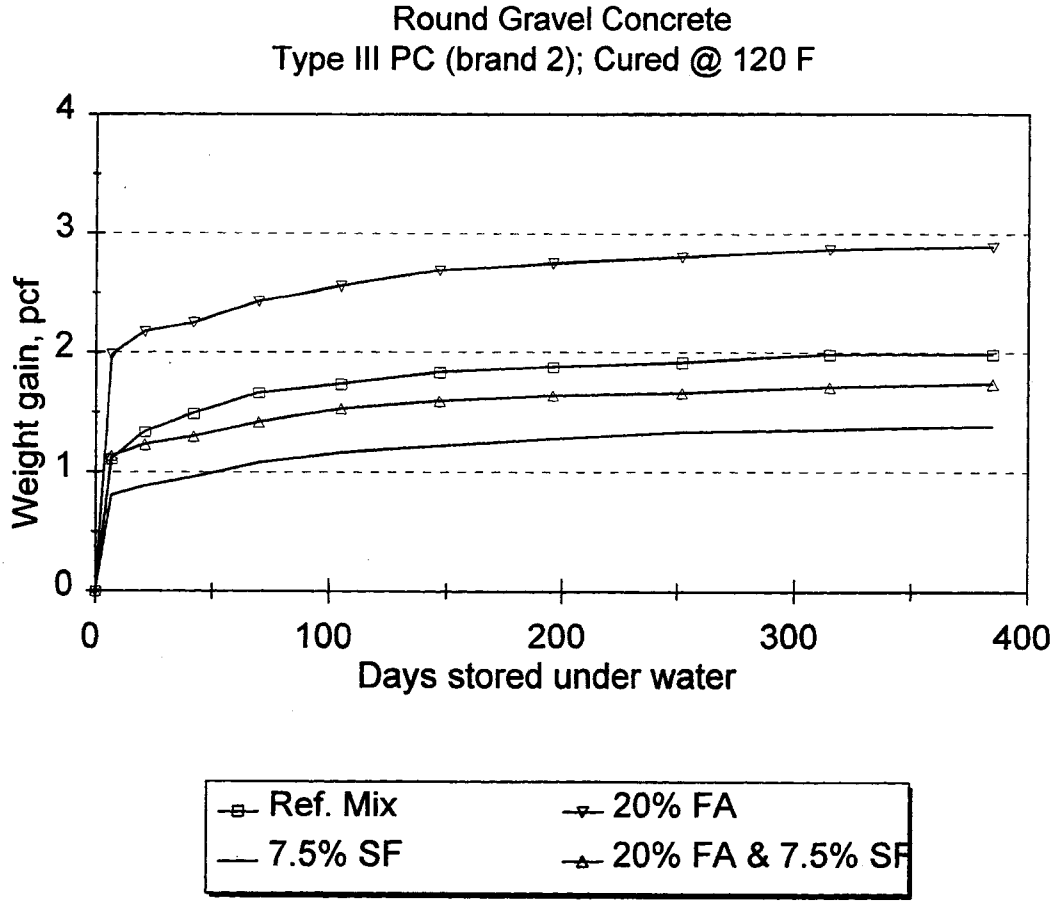

Figure 11.7. Weight-gain of high strength concrete mixes of different cementitious material compositions, heat-cured at 120 °F, made with round river gravel (R1) and ASTM Type III portland cement (Brand 2).

[APFIG7.WMF]

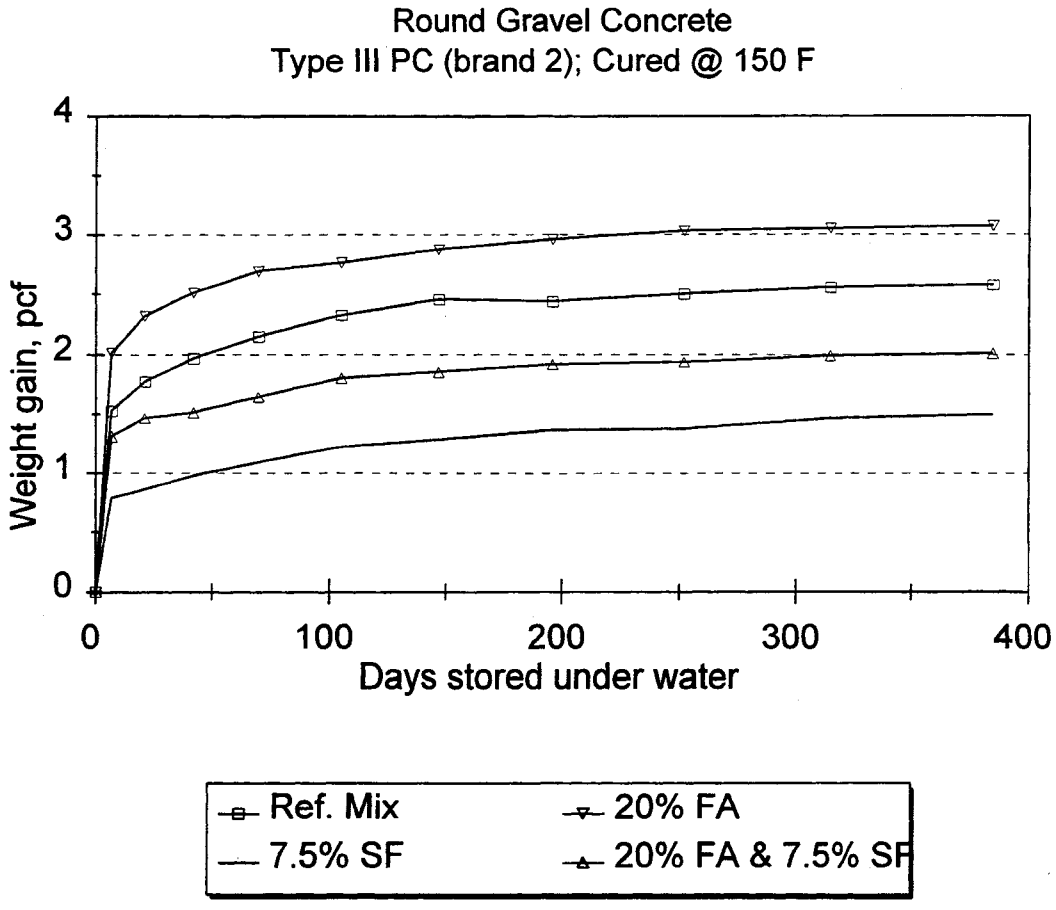

Figure 11.8. Weight-gain of high strength concrete mixes of different cementitious material compositions, heat-cured at 150 °F, made with round river gravel (R1) and ASTM Type III portland cement (Brand 2).

[APFIG8.WMF]

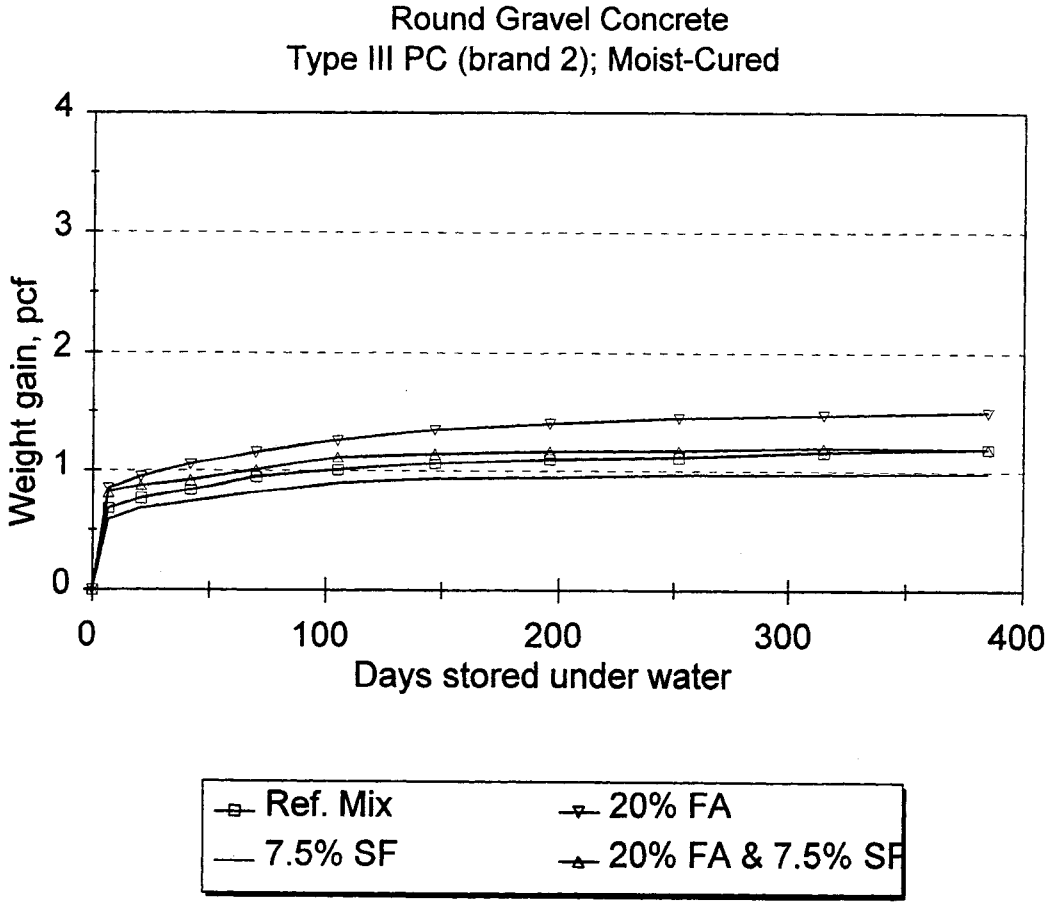

Figure 11.9. Weight-gain of high strength concrete mixes of different cementitious material compositions, moist-cured, made with round river gravel (R1) and ASTM Type III portland cement (Brand 2).

[APFIG9.WMF]

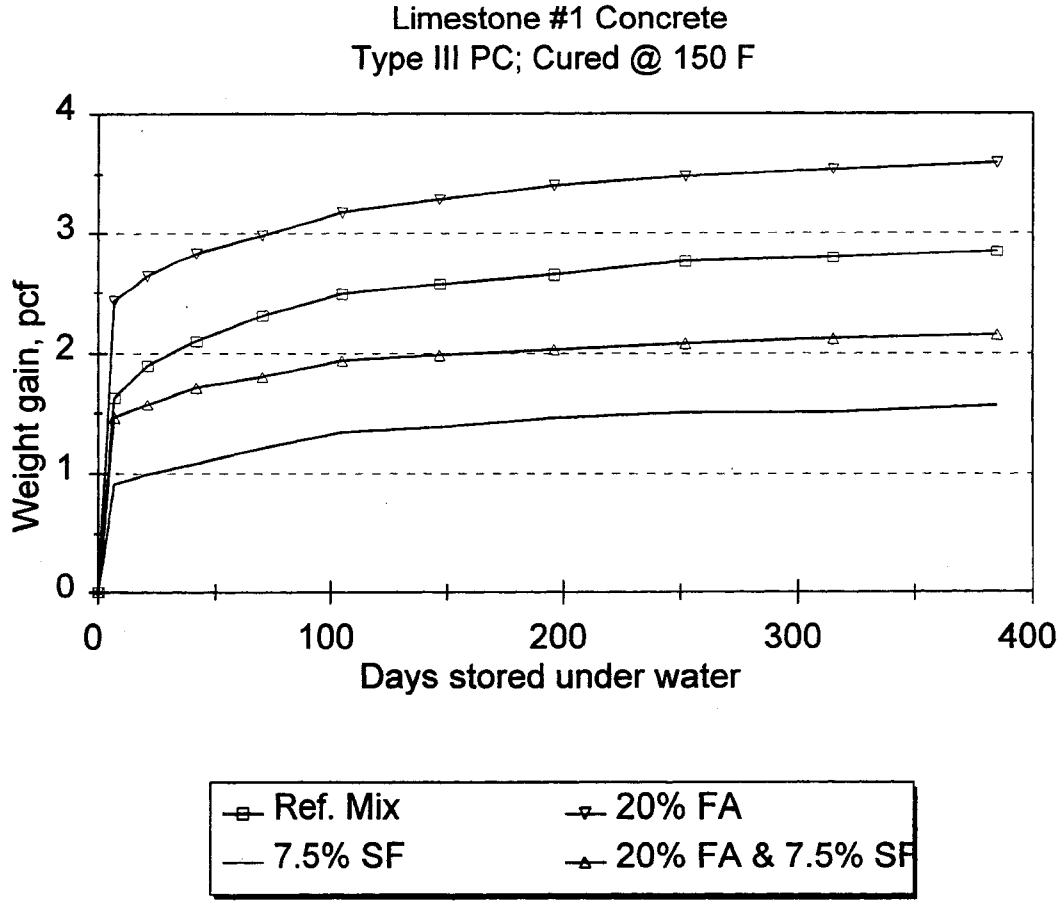

Figure 11.10. Weight-gain of high strength concrete mixes of different cementitious material compositions, heat-cured at 150 °F, made with high absorption limestone (L1) and ASTM Type III portland cement (Brand 1).

[APFIG10.WMF]

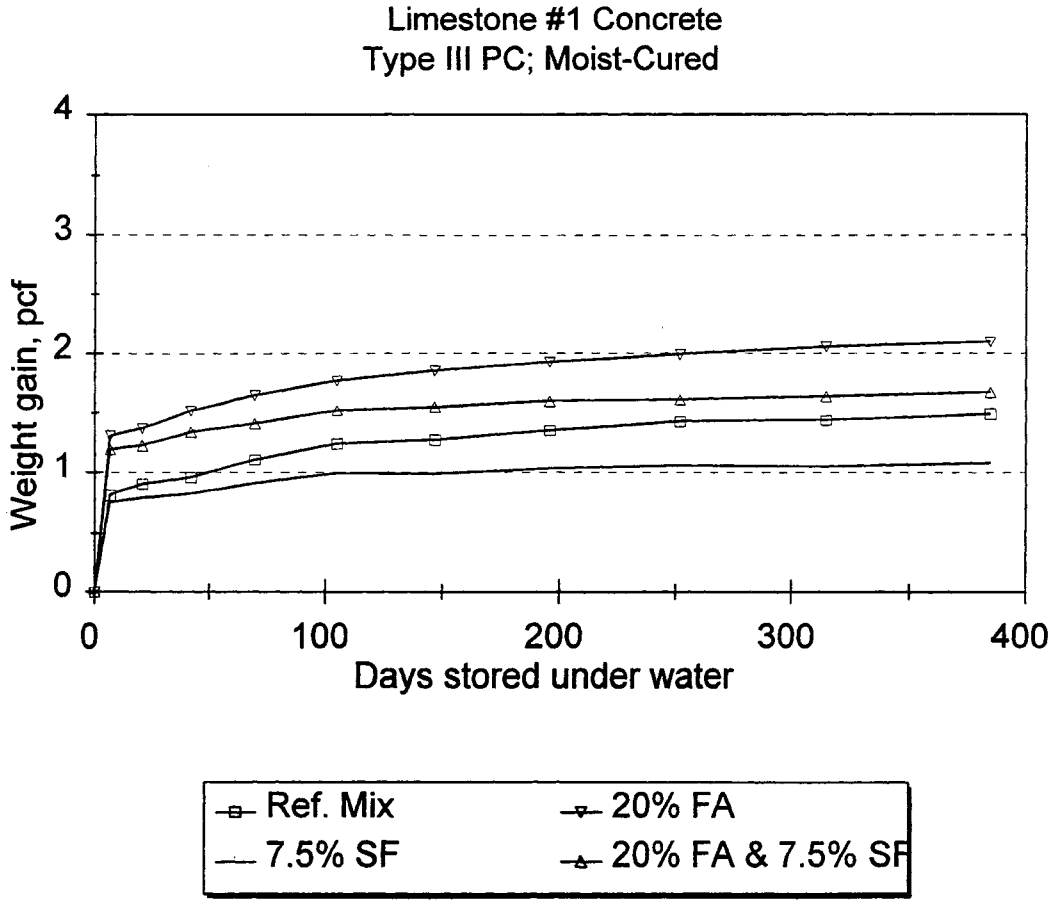

Figure 11.11. Weight-gain of high strength concrete mixes of different cementitious material compositions, moist-cured, made with high absorption limestone (L1) and ASTM Type III portland cement (Brand 1).

[APFIG11.WMF]

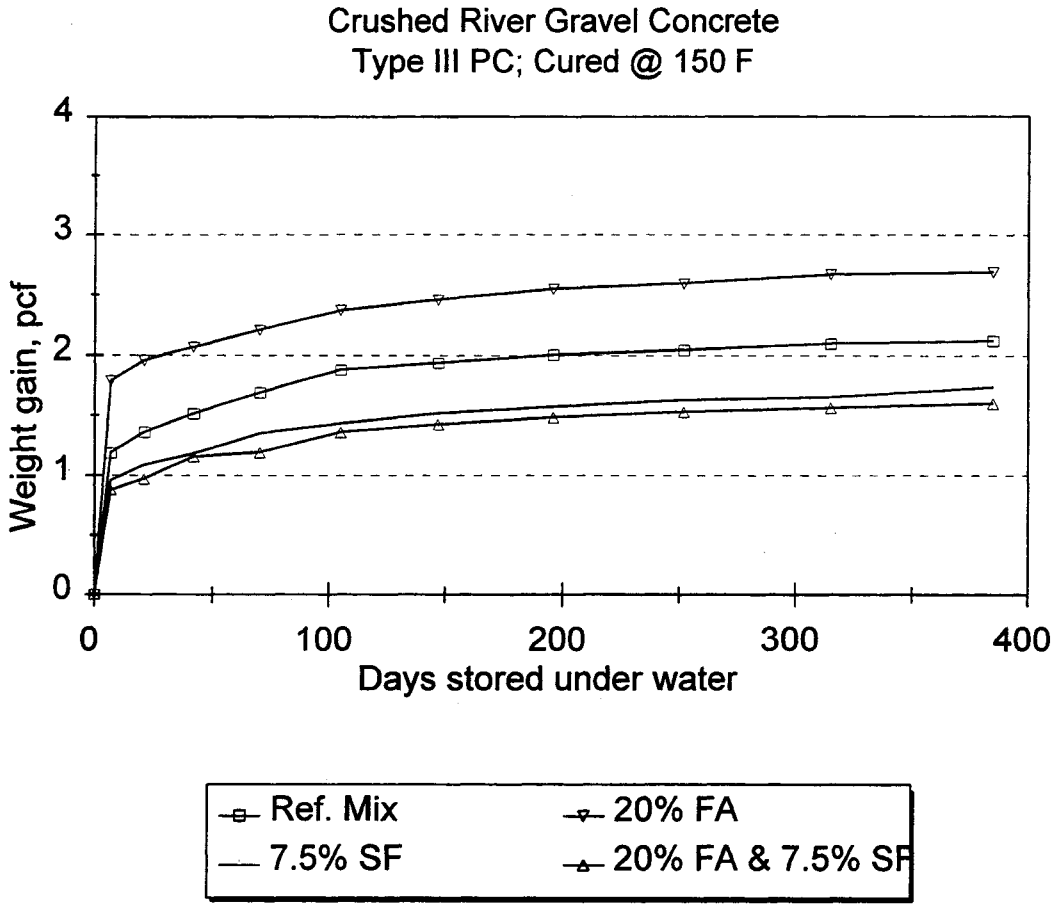

Figure 11.12. Weight-gain of high strength concrete mixes of different cementitious material compositions, heat-cured at 150 °F, made with partially crushed river gravel (R2) and ASTM Type III portland cement (Brand 1).

[APFIG12.WMF]

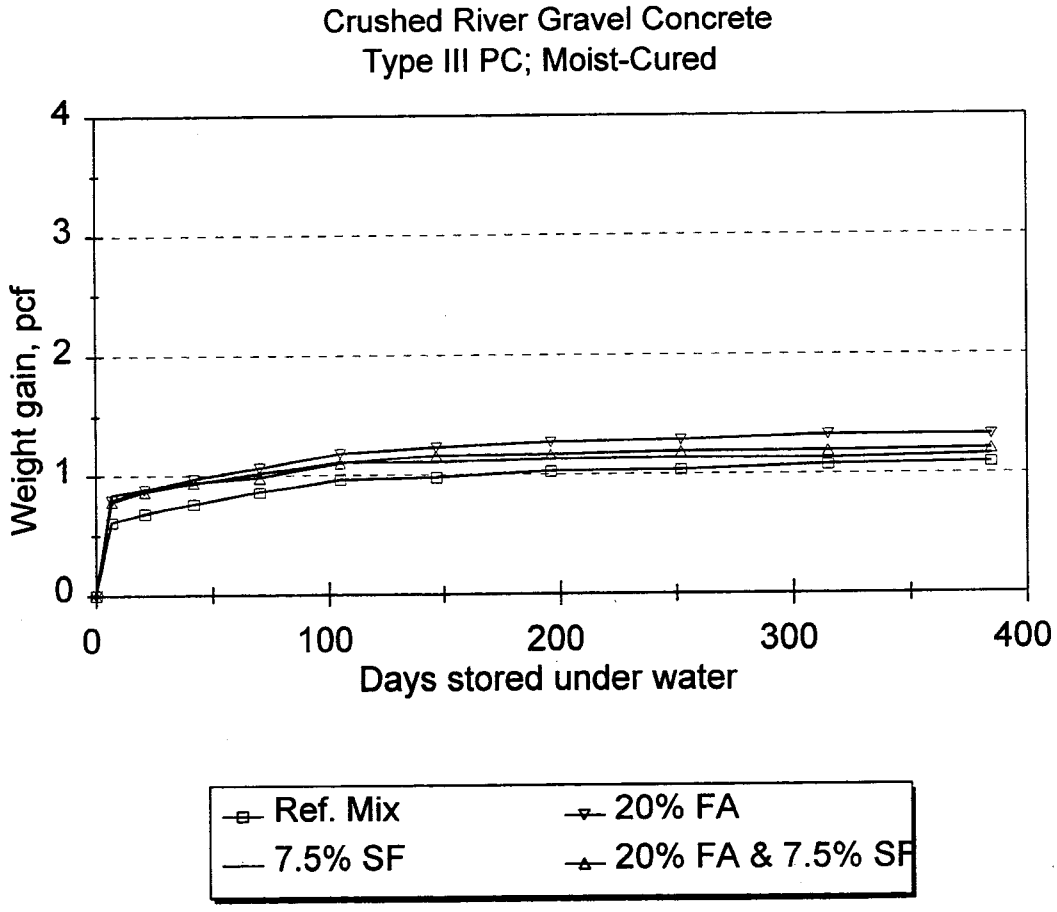

Figure 11.13. Weight-gain of high strength concrete mixes of different cementitious material compositions, moist-cured, made with partially crushed river gravel (R2) and ASTM Type III portland cement (Brand 1).

[APFIG13.WMF]

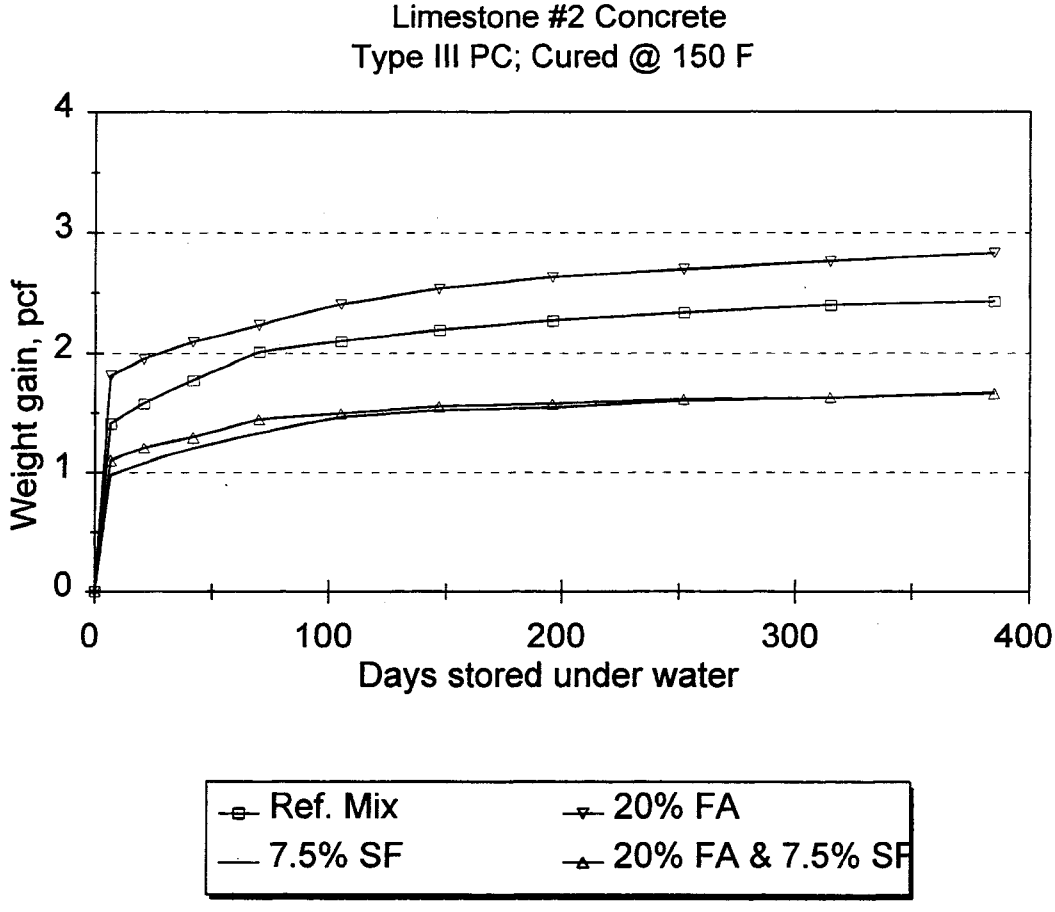

Figure 11.14. Weight-gain of high strength concrete mixes of different cementitious material compositions, heat-cured at 150 °F, made with low absorption limestone (L2) and ASTM Type III portland cement (Brand 1).

[APFIG14.WMF]

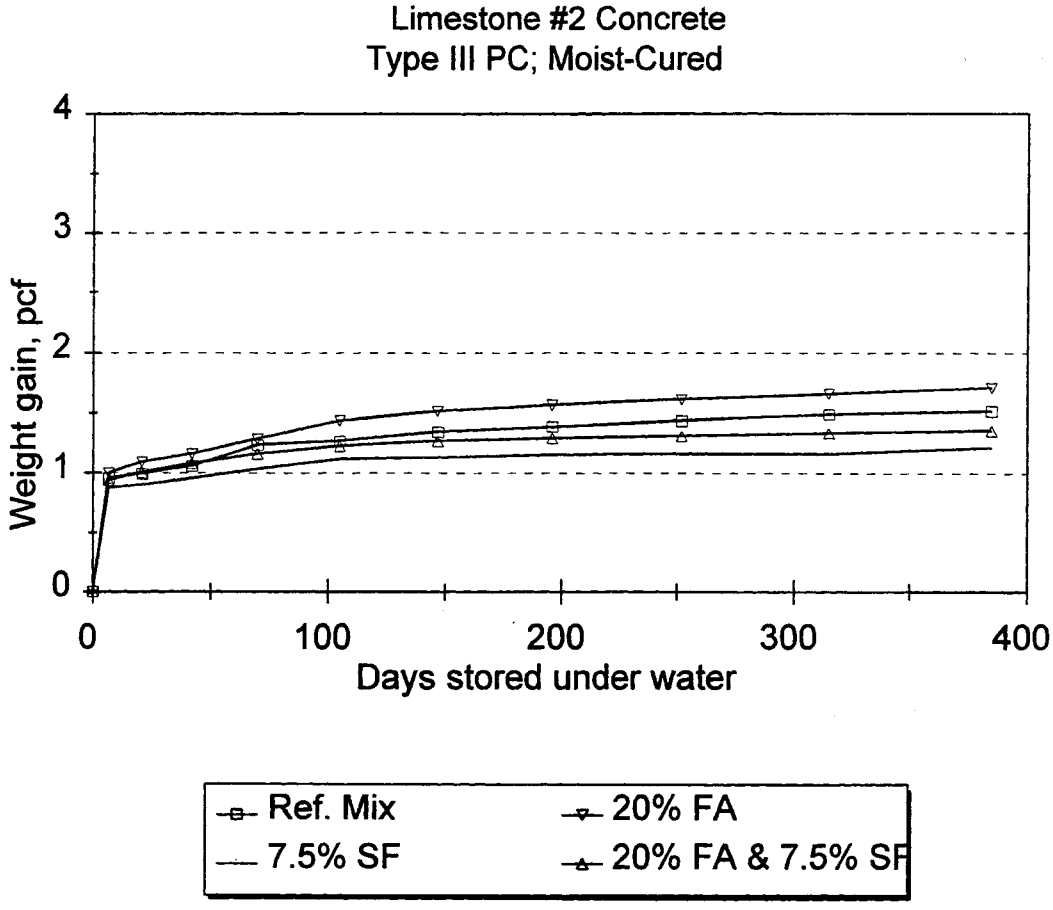

Figure 11.15. Weight-gain of high strength concrete mixes of different cementitious material compositions, moist-cured, made with low absorption limestone (L2) and ASTM Type III portland cement (Brand 1).

[APFIG15.WMF]

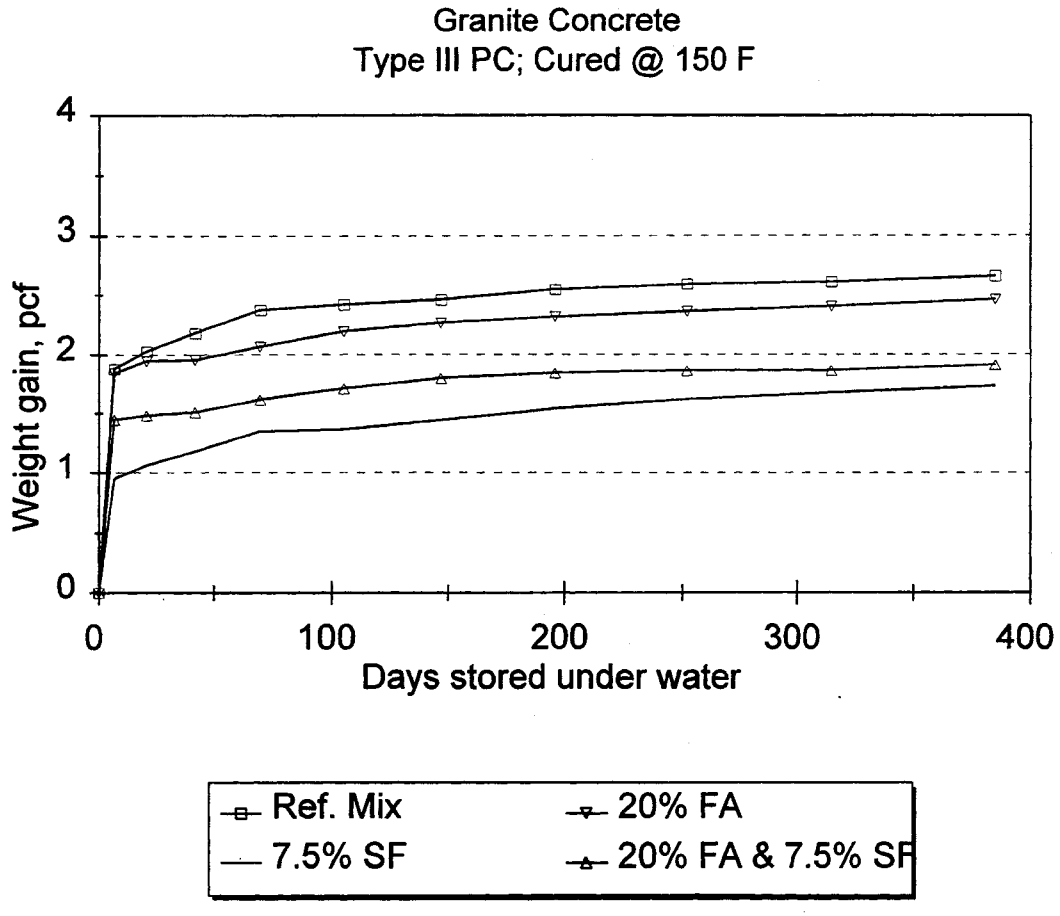

Figure 11.16. Weight-gain of high strength concrete mixes of different cementitious material compositions, heat-cured at 150 °F, made with crushed granite (G2) and ASTM Type III portland cement (Brand 1).

[APFIG16.WMF]

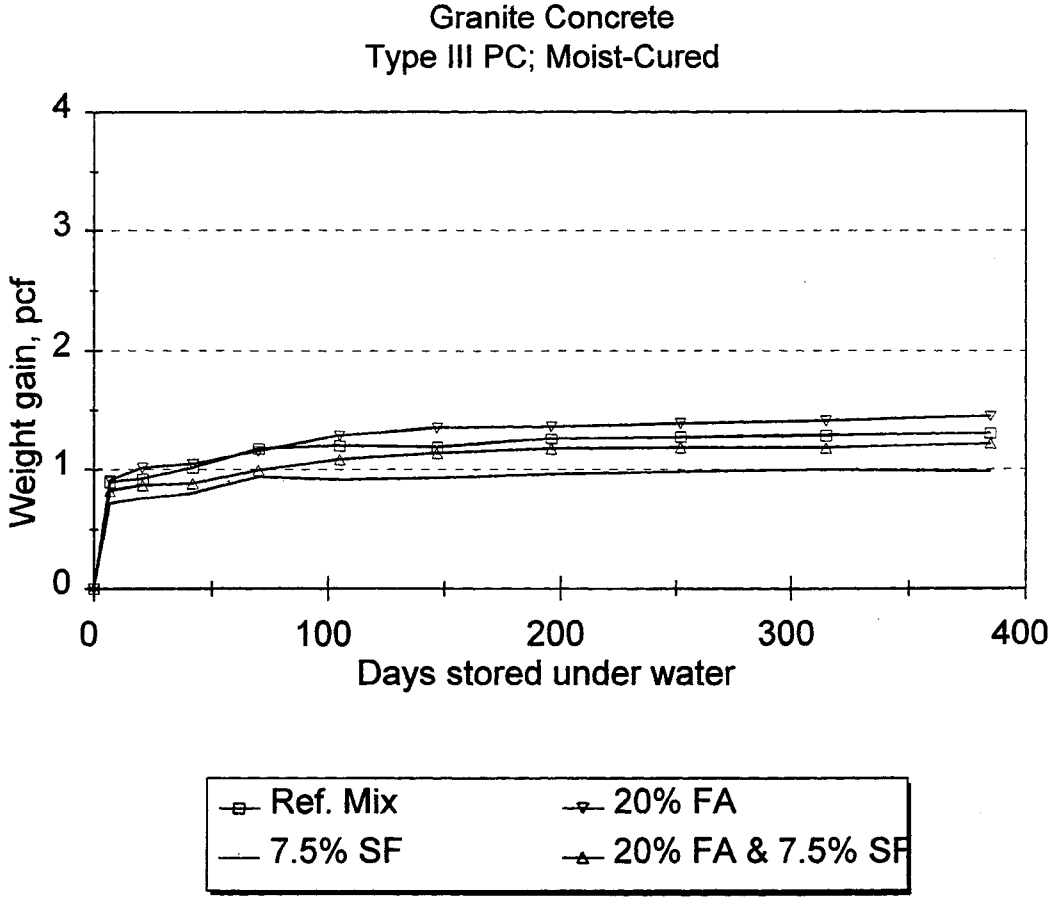

Figure 11.17. Weight-gain of high strength concrete mixes of different cementitious material compositions, moist-cured, made with crushed granite (G2) and ASTM Type III portland cement (Brand 1).

[APFIG17.WMF]

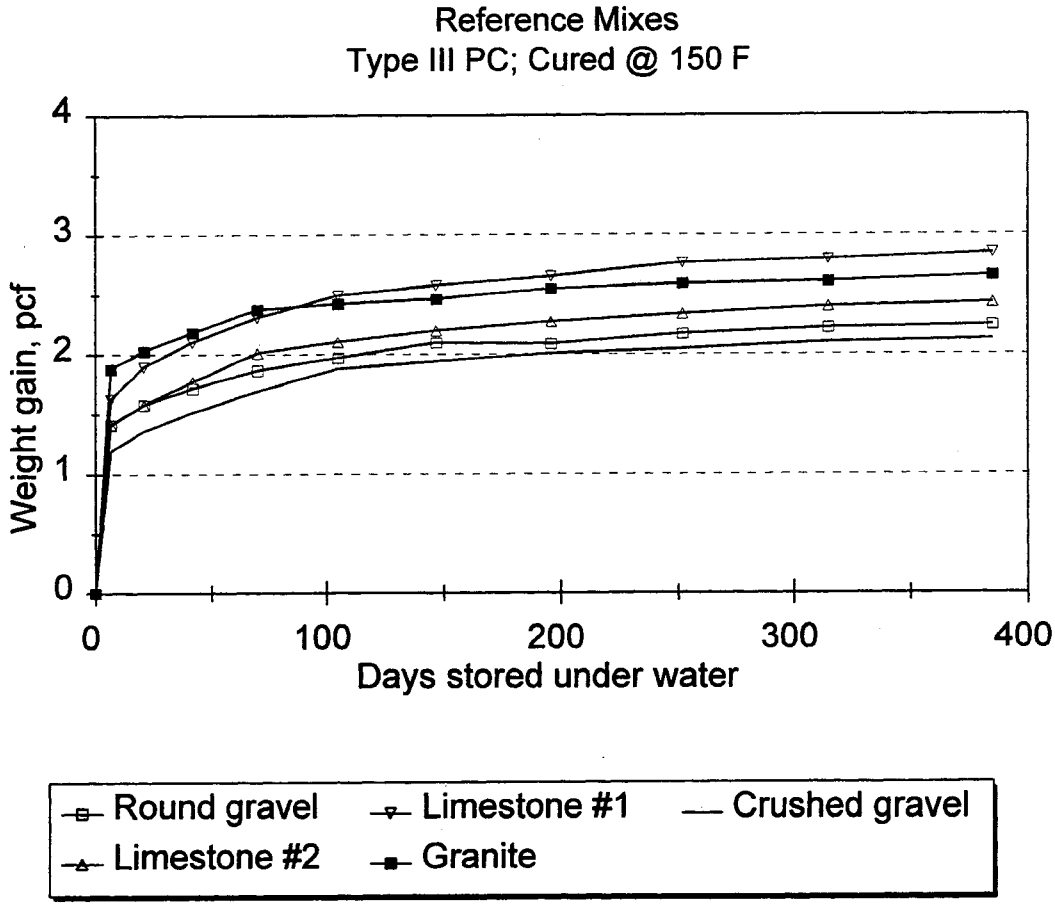

Figure 11.18. Weight-gain of reference high strength concrete mixes made with different coarse aggregates and ASTM Type III portland cement (Brand 1), heat-cured at 150 °F.

[APFIG18.WMF]

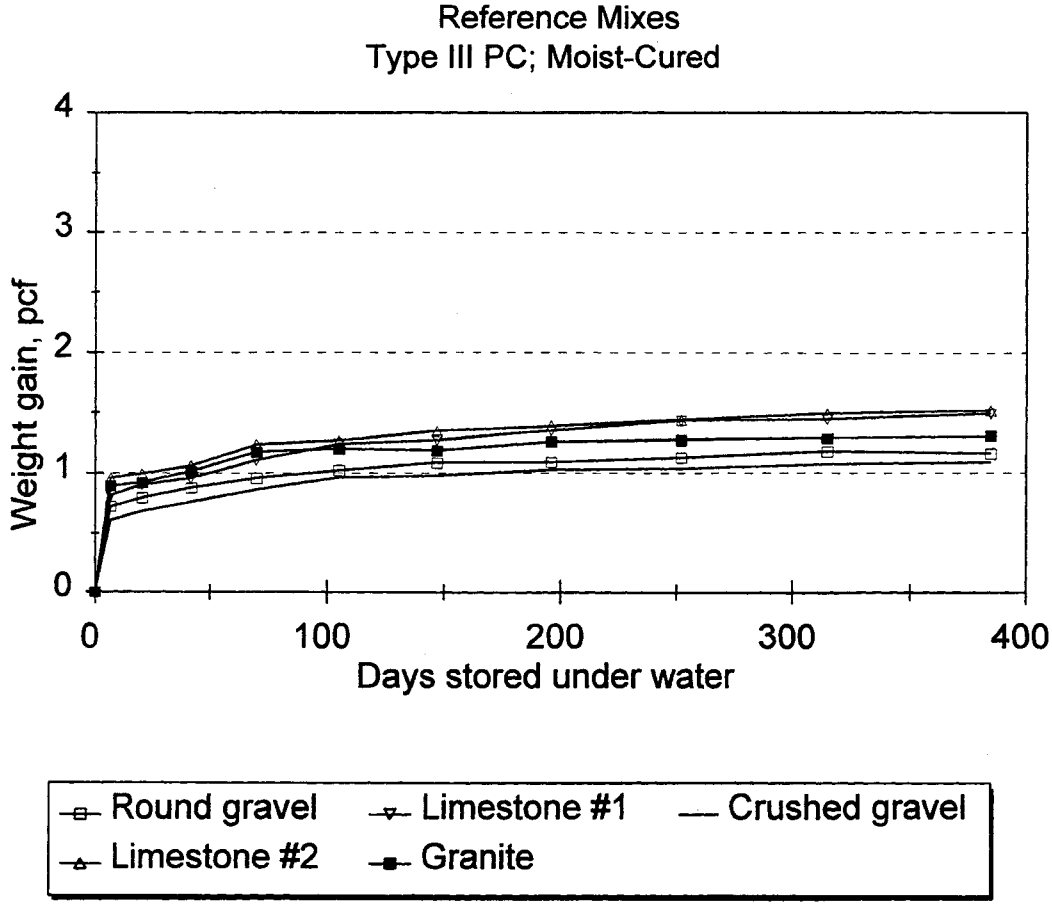

Figure 11.19. Weight-gain of moist-cured reference high strength concrete mixes made with different coarse aggregates and ASTM Type III portland cement (Brand 1).

[APFIG19.WMF]

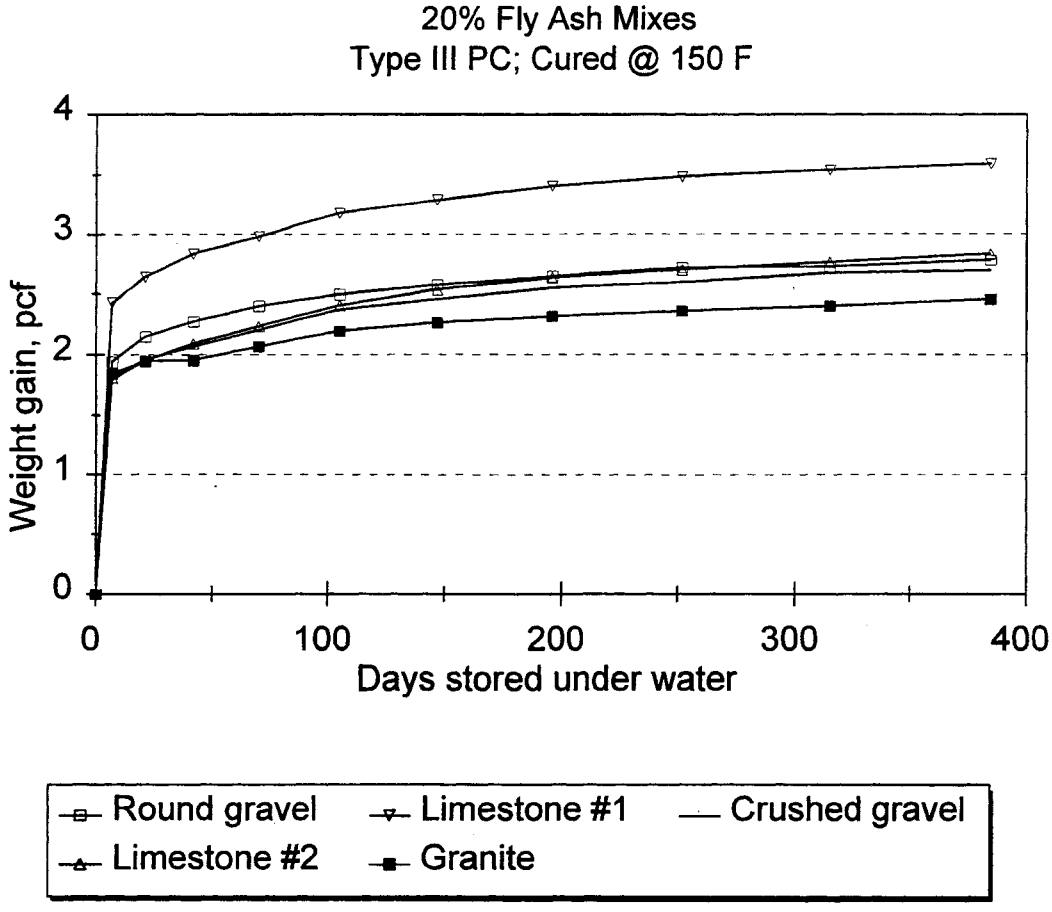

Figure 11.20. Weight-gain of high strength concrete mixes containing 20% fly ash replacement by weight of cement, made with different coarse aggregates and ASTM Type III portland cement (Brand 1), heat-cured at 150 °F.

[APFIG20.WMF]

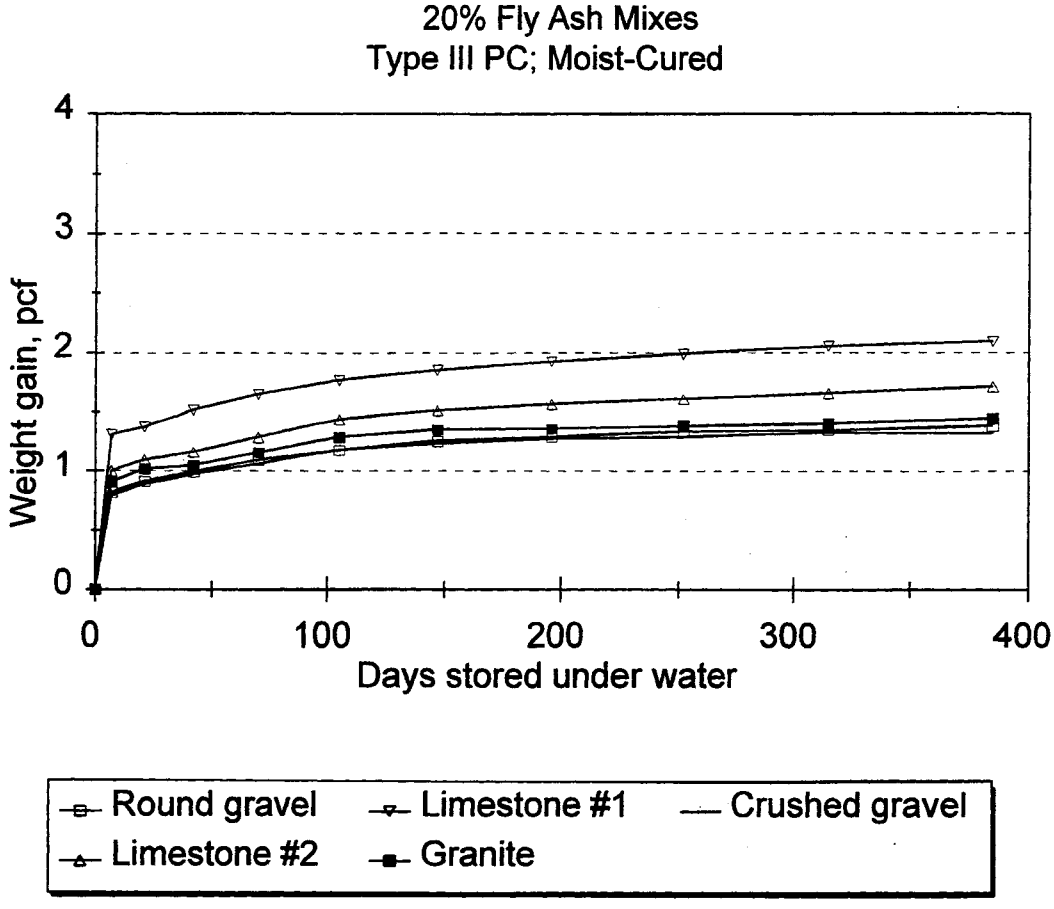

Figure 11.21. Weight-gain of moist-cured high strength concrete mixes containing 20% fly ash replacement by weight of cement, made with different coarse aggregates and ASTM Type III portland cement (Brand 1).

[APFIG21.WMF]

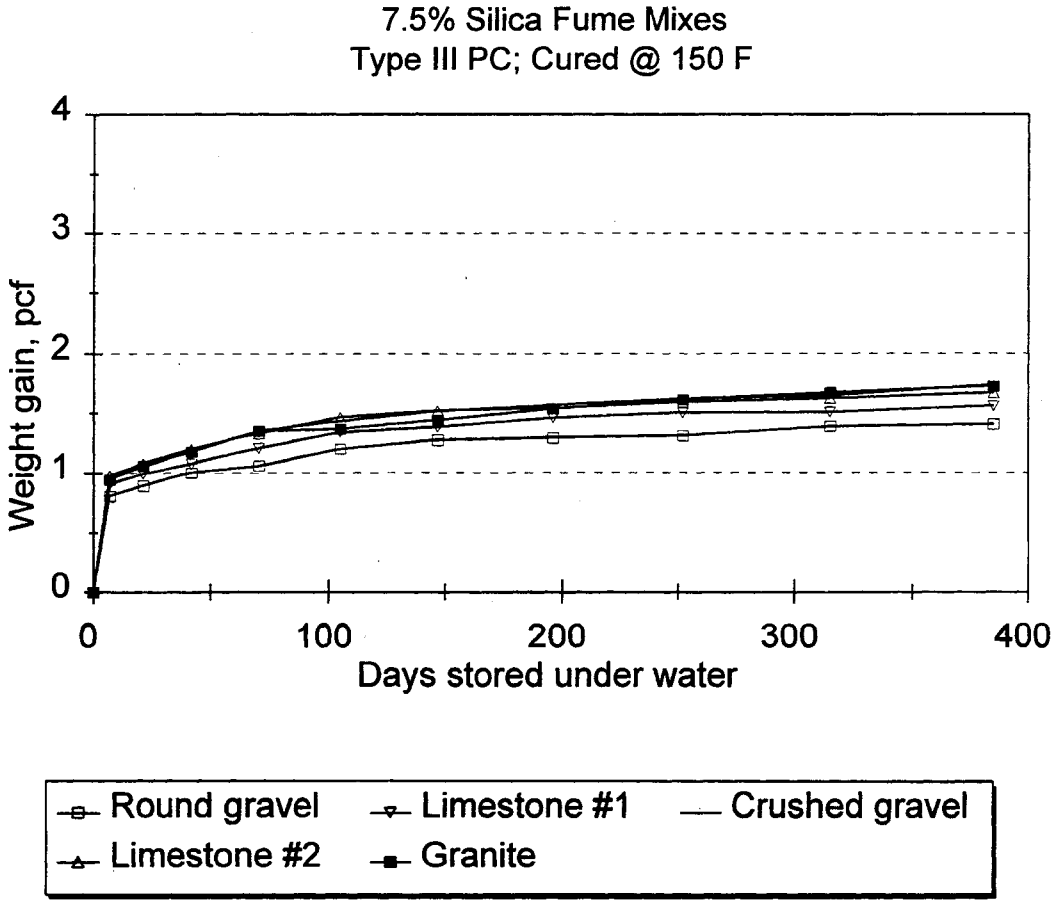

Figure 11.22. Weight-gain of high strength concrete mixes containing 7.5% silica fume replacement by weight of cement, made with different coarse aggregates and ASTM Type III portland cement (Brand 1), heat-cured at 150 °F.

[APFIG22.WMF]

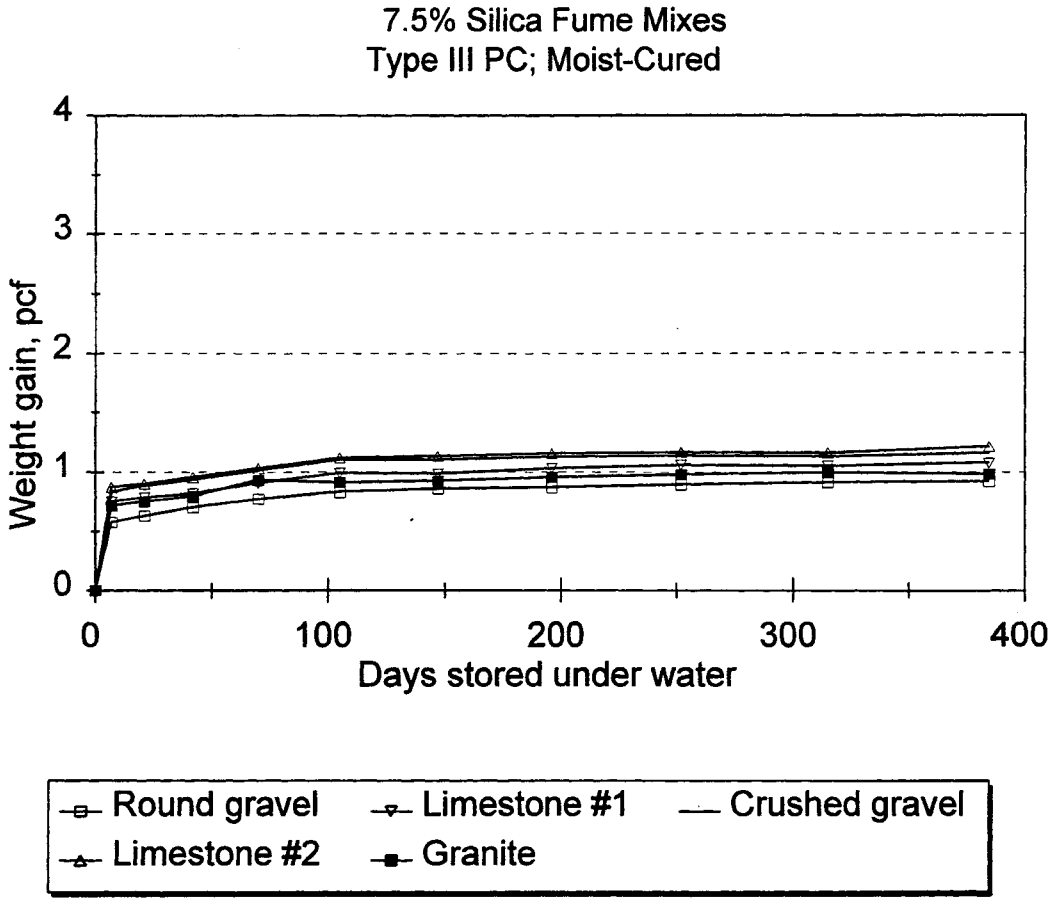

Figure 11.23. Weight-gain of moist-cured high strength concrete mixes containing 7.5% silica fume replacement by weight of cement, made with different coarse aggregates and ASTM Type III portland cement (Brand 1).

[APFIG23.WMF]

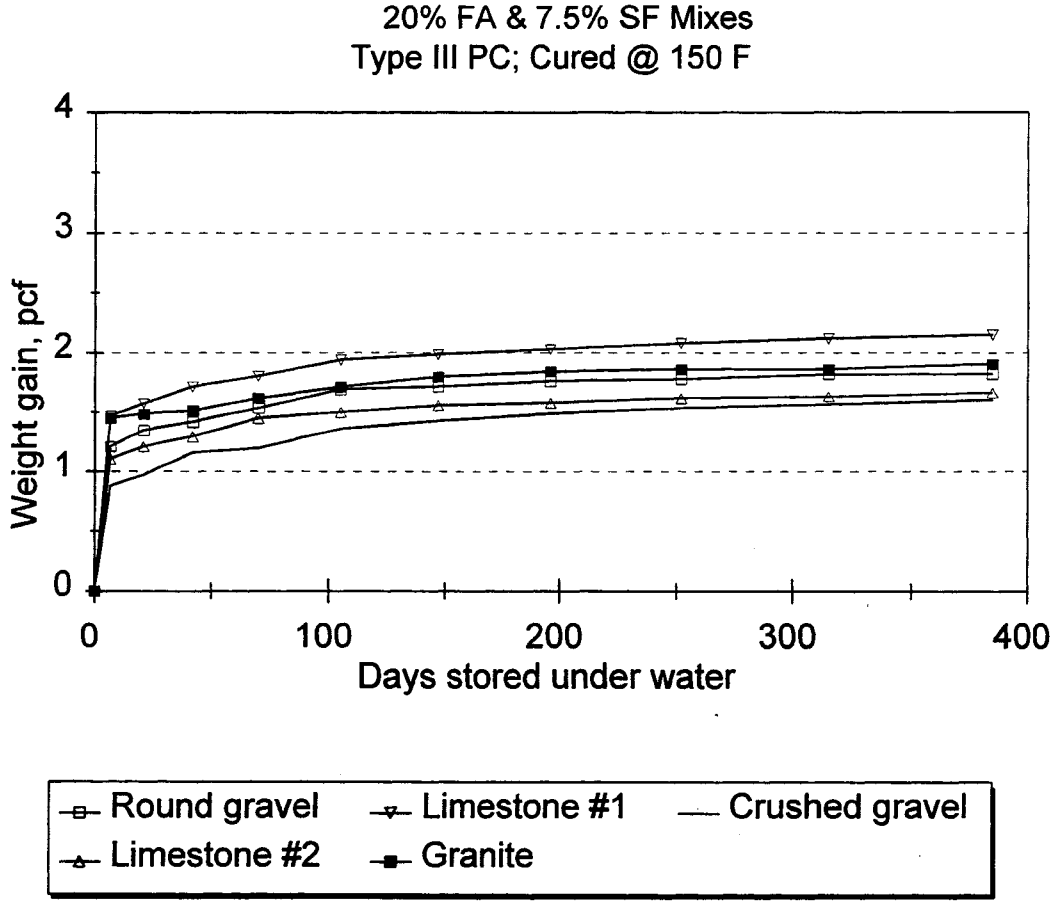

Figure 11.24. Weight-gain of high strength concrete mixes containing 20% fly ash and 7.5% silica fume replacement by weight of cement, made with different coarse aggregates and ASTM Type III portland cement (Brand 1), heat-cured at 150 °F.

[APFIG24.WMF]

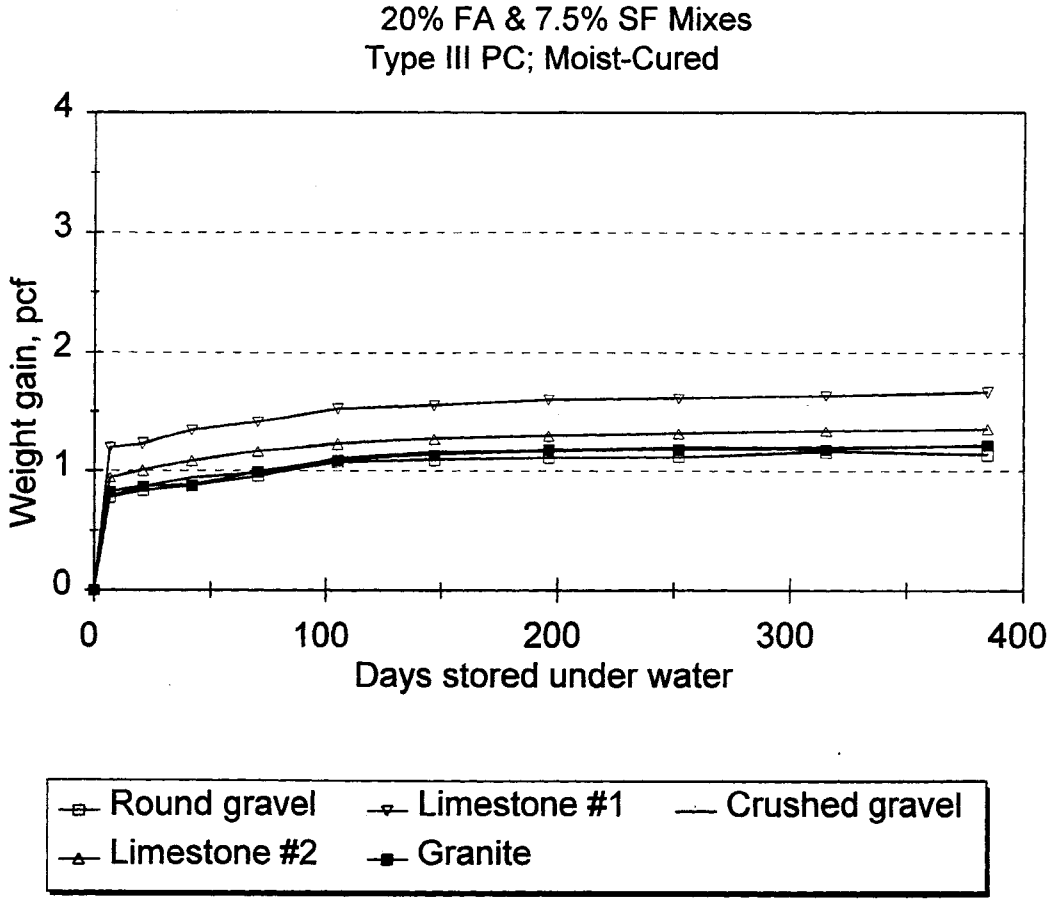

Figure 11.25. Weight-gain of moist-cured high strength concrete mixes containing 20% fly ash and 7.5% silica fume replacement by weight of cement, made with different coarse aggregates and ASTM Type III portland cement (Brand 1).

[APFIG25.WMF]

CHAPTER 12
DISCUSSION OF THE RESULTS

12.1 General

Concrete may be considered as a three-phase composite material consisting of cement matrix, aggregate, and the transition zone between cement matrix and aggregate. Therefore, mechanical properties of concrete, like any other composite material, are dependent on the characteristics of its constituents.

The following sections present a discussion of the experimental results.

12.2 Curing

Porosity of concrete and, therefore, its mechanical properties are significantly affected by the degree of hydration of cement in concrete. As discussed in Chapter 2, Section 2.2, hydration of portland cement is conditional on the presence of moisture. In the production of normal strength concrete, where water-to-cement ratios (*w/c*) greater than about 0.45 are used, hydration of cement will take place uninterrupted, provided that the concrete is prevented from drying out by sealing its exposed surfaces. In this process part of the mix water will be chemically combined in the hydration products, part will be physically adsorbed onto the surfaces of the gel particles and any excess amount of water will be eventually evaporated.

High strength concrete is made with a low water-to-cementitious material ratio (*w/cm*), usually lower than 0.32, and contains therefore less water than required for the complete hydration of the cementitious materials. Hence, under these conditions, a significant portion of the cementitious material remains unhydrated. Inclusion of very fine supplementary cementing materials, such as silica fume, or use of crushed stones with high surface area increase the amount of the adsorbed water and furthermore reduce the amount of available water for hydration of cementitious materials. Subsequently the amount of unhydrated cementitious materials in the hardened concrete will be higher. In view of the preceding discussion, it may be

concluded that providing adequate moisture for completion of hydration through moist-curing benefits the strength and other mechanical properties of high strength concrete significantly. Higher strengths (compressive and tensile) and stiffness due to improved cement matrix and better aggregate-matrix bond together with significantly lower shrinkage, creep, and absorption potential observed in moist-cured specimens were reflections of this conclusion in the data collected during this research program.

In precast/prestressed plants, the concrete must reach a strength sufficient to permit release of the strands in about 16 hours. This is mainly achieved by heat-curing the concrete and by using high-early strength cement. Heat-curing accelerates hydration, and consequently increases the initial strength of concrete. Results from this research program indicated that for high strength concretes considered, approximately 85 percent of the 28-day compressive strength of heat-cured concrete was reached in 1-day. On the other hand, heat-curing adversely affects the concrete ultimate strength which, under certain conditions, may be significantly less than the ultimate strength of otherwise similar concrete which is moist cured. It is believed that differential thermal expansion of concrete constituents increases porosity and results in internal cracking. At later ages, the adverse effect of increased porosity and internal cracking become prevalent and the ultimate concrete strength is therefore reduced. In heat-cured high strength concrete specimens, with low *w/cm* ratios, a large portion of the cementitious material remains unhydrated. Lack of moisture and limited amount of calcium hydroxide hampers the pozzolanic reaction. In this case the benefits from inclusion of supplementary cementing materials will be limited to filler effect. For the high strength concrete mixes considered in this study, in all cases, compressive strength of moist-cured specimens exceeded that of companion heat-cured specimens when tested at ages of 28-days or later.

Mineralogical and structural changes associated with the heat-curing process are also reflected in other mechanical properties of high strength concrete. More porous cement paste and the presence of internal microcracks, which also affect the paste-aggregate bond strength,

necessarily have adverse effects on the tensile strength, stiffness, shrinkage, creep, and absorption potential of high strength concrete.

12.3 Total Cementitious Material Content

Fresh Concrete: In general, the use of excessive portland cement in any concrete mix design should be avoided. Successful application of high strength concrete requires achievement of adequate workability and serviceability. Excess cement, which is sometimes used in production of high strength concrete, results in more expensive and unworkable concrete and causes larger volume change, higher temperature gradients between the inside and outside of the members, and possible unwanted cracking.

Hardened Concrete: Although the production of high strength concrete requires higher levels of total cementitious material than normal strength concrete, contrary to the belief of many, at a given water-to-cementitious material (*w/cm*) ratio, use of more cement will not necessarily result in higher strengths. For the same *w/cm* ratio, a mix with a higher amount of cementitious material has a lower aggregate content. As it is schematically shown in Figure 12.1, due to the difference in stiffness of the cement matrix and the aggregate, the presence of the aggregate in the cement matrix induces stress concentrations. However, overlapping of the regions of stress concentration will increase with increase in the aggregate content of the mix and consequently, the average stress concentration due to the presence of aggregate particles decreases. This, in turn, will produce a more uniform state of stress in the concrete and will result, therefore, in higher compressive or tensile strengths. Concrete with a more linear stress-strain relationship and higher stiffness can be obtained by keeping the total amount of cementitious material content of the mix to a minimum (maximum aggregate concentration). While the two components of concrete (i.e. cement paste and aggregate), individually exhibit a linear stress-strain relation, it is the development of microcracking at the interface between the cement paste and aggregate that makes the stress-strain relation bend over (become nonlinear). A more uniform state of stress resulting from reduction in total cementitious material content (increase in aggregate concentration) increases the region of linear stress-strain relationship for

concrete. Aggregate generally has a higher modulus of elasticity than the cement paste and therefore the modulus of elasticity of the composite material, concrete, increases with increased aggregate concentration.

No shrinkage and creep tests were performed on high strength concretes containing different amounts of total cementitious materials content. However, it is easy to visualize the effect of the latter on shrinkage and creep characteristics of concrete. Because the aggregates do not experience significant shrinkage or creep (shrinkage and creep of aggregates normally used for concrete are much smaller than those of the paste), the volume changes due to shrinkage and creep are highly dependent on those of the cement paste and its total concentration in the concrete. Therefore, an increase in the total cementitious material content can result in higher deformations due to shrinkage or creep.

In general, for the three total cementitious material contents investigated [750, 850, and 950 lb/yd^3 (445, 505, and 565 kg/m^3)], no significant overall advantage was observed to justify the use of higher cement contents. Subsequently the majority of the high strength concrete mixes used in this study were designed with a total cementitious material content of 750 lb/yd^3 (445 kg/m^3).

12.4 Effect of the Type of Coarse Aggregate

Fresh Concrete: In normal strength concrete mixes with higher levels of *w/c* ratios, the fresh concrete tends to segregate. However, in high strength concrete mixes with low *w/cm* ratios, and containing high volumes of fine materials, this tendency was observed to be generally low and of limited practical importance.

The shape and the texture of coarse aggregate particles had a significant effect on the workability of the high strength concrete mixes. Higher surface area to volume ratio of crushed aggregates, and in particular elongated and flaky aggregates, increased the high-range water

reducer (HRWR) demand for a given slump, lowered workability of the mix and demanded more effort for achieving full consolidation.

Selection of the type of coarse aggregate for use in the production of high strength concrete should also be based on the available means of consolidation. At lower *w/cm* ratios, necessary in the production of high strength concrete, concrete mixes made with round and smooth aggregate particles are easier to consolidate than identical mixes made with crushed stones. The presence of air voids due to incomplete consolidation of concrete will result in concrete of inferior quality.

Hardened Concrete: In normal strength concrete the strength of the cement matrix or the transition zone is usually the strength limiting factor and the properties of coarse aggregate do not have a significant effect on the compressive strength of the concrete. In normal strength concrete, cracking takes place in the cement matrix. The aggregate particles only delay fracture by preventing the extension of cracking into the stronger aggregate particles and, therefore, increasing the strength by preventing crack propagation and by allowing the formation of a number of microcracks, rather than a single crack. A decrease in *w/c* ratio increases the paste compressive strength as well as the strength of the transition zone. This explains why the *w/c* ratio is the most important factor in determining the strength of normal strength concrete.

The compressive strength of high strength concrete observed in this study depended largely on the type, shape, texture, and strength of coarse aggregates used. Except in mixes where 7.5 percent of the weight of portland cement was replaced by silica fume, use of smooth round gravel led to lower compressive strengths than rough and angular crushed rocks. It appeared that surface properties and the shape of the coarse aggregate influenced the bond between the cement matrix and the coarse aggregate. Superior bond between the cement matrix and crushed stone particles was attributed to the increased surface area and improved mechanical interlocking.

The limit on compressive strength of concrete made with crushed aggregates is reached when the strength of the aggregate becomes the limiting factor and then the plane of failure passes through almost all of the coarse aggregate particles. It is interesting to note that the famous *w/c* ratio law is valid when the strength of the cement matrix or the transition zone are the strength limiting factor. When the strength of concrete becomes limited by the strength of the coarse aggregate, further reduction of the *w/c* ratio does not result in the expected increase in compressive strength and only produces mixes which are not workable enough to allow full compaction of the fresh mix. In this context, high strength concrete is very different from normal strength concrete.

Replacement of 7.5 percent of weight of cement by silica fume significantly improved the compressive strength of high strength concrete made with round gravel. This was attributed to improved bond between the round gravel aggregate and the cement matrix due to reduced porosity of the cement matrix and the strengthened transition zone between the aggregate and the cement paste as a result of the filler effect and pozzolanic reaction associated with inclusion of silica fume. More aggregate fractures were noted in the round gravel mixes containing silica fume than in those round gravel mixes without silica fume.

When the strength of the cement matrix was the strength limiting factor, the influence of the type of coarse aggregate became insignificant. At concrete strength levels up to 10,440 psi (72.0 MPa), and in concrete of the same mix proportions, no difference in the compressive strengths of concretes made with two high- and low- absorption crushed limestones (*L1* and *L2*) was observed, Figure 12.2. However, at higher strength levels, between 9,219 to 17,573 psi (63.6 to 121 MPa), the low absorption limestone (*L2*) resulted in strengths up to 24 percent higher than when the obtained high-absorption limestone (*L1*) was used, Table 12.1.

While it is generally expected that aggregate strength be reflected in concrete strength, the results from this study indicated that concretes made with either of the two crushed limestones (*L1* or *L2*) were stronger than otherwise similar concretes made with either of the two

crushed granites (*G1* or *G2*). Limestone particles exhibited better bond with the cement matrix. It is believed that the porosity of limestone allows for moisture exchange between the aggregate and the surrounding paste, consequently reducing porosity of the transition zone by preventing the formation of a water film around coarse aggregate particles. Absorbed moisture in porous limestone serves as an internal source of curing water, thus promoting further formation of cementitious hydrates by continued hydration of unhydrated cement particles and pozzolans in the transition zone.

The influence of the type of coarse aggregate on compressive strength of concrete varied in magnitude and depended on the curing condition and the cementitious material composition of the mix. Moist-curing results in better bond between the aggregate particle and the cement matrix by allowing better hydration of portland cement and promoting pozzolanic reaction and producing a denser cement matrix and transition zone. In the absence of adequate moisture, the beneficial effect of inclusion of supplementary cementing materials, such as fly ash and silica fume, will be only limited, if at all, to refinement of pore structure through filler effect.

For all cementitious material compositions considered, moist-curing decreased the influence of the type of coarse aggregate on compressive strength of concrete, presumably because of the improved bond between cement matrix and the coarse aggregate as a result of better hydration of the cementitious materials. The range of variations in compressive strengths of concretes, of the same mix proportions, made with six different types of coarse aggregate reduced from 19 to 52 percent for heat-cured specimens to 7 to 36 percent when moist-cured, Table 12.2. The compressive strength of high strength concrete made with round gravel was more sensitive to curing condition than that of companion mixes made with crushed limestones. In all cases, the compressive strength of moist-cured specimens exceeded that of companion heat-cured specimens when tested at an age of 28-days or later.

The preceding discussion was limited to the effect of the type of coarse aggregate on the compressive strength of high strength concrete. The type of coarse aggregate also affects other

mechanical properties of high strength concrete. For example surface characteristics of the coarse aggregate affect the paste aggregate bond and hence concrete tensile strength. The use of smooth round river gravel resulted in lower tensile and particularly flexural strengths.

Generally speaking, the modulus of elasticity of concrete is related to its compressive strength. However, not all factors which affect compressive strength, affect modulus of elasticity of the concrete in the same manner. Examples of these factors are the effect of moisture content of the concrete specimen and the effect of surface roughness of the coarse aggregate which affect the two properties differently.

The effect of moisture content of the concrete specimen on the modulus of elasticity of concrete was discussed in detail in Chapter 7, Section 7.5. It was shown that saturating the test specimens decreased the compressive strength and increased the modulus of elasticity values.

As it was mentioned earlier, in most cases considered, the use of smooth round gravel led to lower compressive strengths than crushed limestone. However, the data presented in Figure 7.8 of Chapter 7 clearly indicates that for a given compressive strength, the limestone aggregate concrete was less stiff than the one made with round river gravel. In determining the modulus of elasticity of concrete, test specimens are subjected to stress levels not exceeding 40 to 50% of their ultimate strength. For such low stress levels, the aggregate and the paste work together, forming an ideal composite material (nearly perfect paste-aggregate bond) and the stress-strain curve is approximately linear. This was experimentally verified and data were presented in Figures 7.4-A to 7.4-K of Chapter 7. It should be kept in mind that because the stiffness of the aggregate and of the paste are different, the stress and strain throughout the concrete will not be uniform. Regardless of the choice of the mathematical model for predicting modulus of elasticity of concrete (Figure 6.1 of Chapter 6), it may be concluded that the modulus of elasticity of concrete increases with increase in modulus of elasticity of aggregate. This explains why high strength concretes made with the stiffer round river gravel resulted in higher modulus of elasticity values than those made with softer limestone coarse aggregates.

At higher stress levels, encountered during the compressive strength tests, the stress-strain curve departs from linearity, generally due to the deterioration of the aggregate-paste bond and development of cracking. The surface characteristics of the aggregate will affect the stress at which the curve departs from a straight line. This implies that the strength of concrete made with round river gravel, in general, is determined mainly by the strength of the paste-aggregate bond, rather than the strength of the aggregate. When the strength of the aggregate-paste bond was improved by inclusion of 7.5% silica fume, concretes made with the stiffer round river gravel led to higher compressive strength values than concrete made with crushed limestone in otherwise identical mixes.

Some of the newly developed equations relating modulus of elasticity of concrete to its compressive strength include coefficients accounting for parameters such as: the aggregate type, cementitious material composition, etc. While all proposed relationships are valuable and applicable within certain limitations, none can be applied with confidence to all situations. As indicated in Chapter 7, it is difficult to generalize the properties of an aggregate as they may vary significantly from one source to another.

The test results presented in Chapter 10 suggest similar shrinkage characteristics for all crushed coarse aggregates in otherwise identical mixes. Shrinkage strain for heat-cured high strength concrete made with round river gravel was slightly higher than those of concretes made with crushed coarse aggregates. The amount of adsorbed water for round gravel with smooth surfaces would be less than for crushed coarse aggregates and consequently, the effective water-to-cementitious material (*w/cm*)ratio at the time of mixing would be slightly higher. The higher effective *w/cm* ratio may explain the slightly higher observed shrinkage of high strength concrete made with round river gravel compared to those made with crushed coarse aggregates. In some practical applications, the comparison of the shrinkage characteristics of high strength concretes of equal strength made with different types of coarse aggregate may also be of interest. In this case, to obtain the same strength, concretes made with different types of coarse aggregate must

be made with different *w/cm* ratios and consequently may exhibit different shrinkage characteristics.

The coarse aggregate in concrete does not experience creep and its presence only restrains creep of the paste to an extent which depends on the aggregate stiffness and surface characteristics. Accordingly, the creep of concrete depends mainly on the total amount of the paste and the quality of the cement paste and the aggregate-paste bond. Therefore, all factors which improve the strength of the paste and the aggregate-paste bond similarly will improve its creep characteristics. This was confirmed by the creep test results of this study. Table 12.3 summarizes the compressive strength test results together with observed ultimate values of creep coefficient and specific creep. It is clearly seen that the ultimate creep coefficient and the ultimate specific creep of high strength concrete decreased with increased compressive strength for both heat and moist-cured specimens made with different types of aggregates and different cementitious materials compositions. It may be concluded that similar creep may be expected of high strength concretes of equal compressive strength made with different types of coarse aggregates.

The effect of the type of coarse aggregate on absorption potential tests was secondary and is determined by the permeability of the cement matrix. In general concretes made with more absorptive aggregates have a greater potential for water absorption. However, in a dense cement matrix where water is prevented from reaching the aggregate particles, the type of coarse aggregates does not influence the absorption potential test results.

12.5 Inclusion of Fly Ash

Fresh Concrete: Inclusion of fly ash reduced coarse aggregate segregation, surface bleeding, and improved finishability of fresh concrete. Inclusion of fly ash also reduced the amount of superplasticizer required for a given slump.

Hardened Concrete: In general, fly ash reacts as a pozzolan to form additional cementitious hydrates similar to those formed by portland cement, but at a much slower rate. However, the benefits claimed for the use of fly ash were not as apparent in some of the high strength concrete mixes considered. Decision on inclusion of fly ash in production of high strength concrete and successful prediction of concrete properties requires prompt knowledge of the performance of fly ash with selected mix parameters, coarse aggregates and curing methods.

For a concrete containing weights w of water, c of portland cement, and f of fly ash, the water-to-cementitious material ratio (w/cm) is $w/(c+f)$. At early ages, not much of an effect from the pozzolanic reaction is expected and the effective water-to-cement ratio of the mix $(w/c)_e$ is: $w/c > w/cm$. At this age any beneficial effects of fly ash on strength can be attributed to the more efficient packing of the cement matrix due to the presence of fly ash particles (filler effect). If adequate moisture is present (or provided through moist-curing), the pozzolanic reaction begins and these fly ash particles serve as potential nucleation sites for formation of additional cementitious hydrates, further improving the packing of the cement matrix and the transition zone between the cement matrix and the aggregate. However, if adequate moisture is not provided, the pozzolanic reaction will not take place and benefits from inclusion of fly ash (if any) will be limited to grain refinement of the cement matrix. In this case, no significant cement matrix-aggregate bond improvement should be expected.

For all replacement levels considered, replacement of portland cement with fly ash on a one-to-one basis decreased the compressive strength of heat-cured concretes made with round gravel at all ages up to 365-days. Apparently low water-to-cementitious material ratio of the mix, together with the accelerated heat-curing method slowed down or completely stopped the pozzolanic reaction and adversely affected the bond between the smooth round gravel aggregate particles and the cement matrix. Lack of progress of hydration or pozzolanic reaction with time was clear in strength development data presented in Section 5.3 of Chapter 5. No significant increase in compressive strength of heat-cured specimens was observed beyond 28-days. For

heat-cured specimens containing fly ash and made with Type I and Type III portland cements $(f'c)_{ultimate}/(f'c)_{28d}$ ratios of 1.02 and 1.01 were observed.

For 20 percent replacement of portland cement with fly ash 365-day compressive strengths of moist-cured specimens made with round gravel exceeded the compressive strength of companion specimens of the reference mix. As explained before, in the presence of adequate moisture, pozzolanic reaction of fly ash takes place at ages normally between 1 to 3 months after casting.

Replacement of 20 percent weight of portland cement with fly ash improved compressive strength of heat-cured concretes made with all crushed stones. Apparently the filler effect (physical mechanism of grain refinement) offered by fly ash improved packing of the cement paste and compensated for the reduced cement content of the concrete mix.

As expected, inclusion of fly ash had similar effects on tensile strength and modulus of elasticity of high strength concrete as on its compressive strength. No shrinkage test was performed on high strength mixes containing only fly ash in combination with cement. However, for both curing conditions, inclusion of 20% fly ash together with 7.5% silica fume as replacement by weight of cement did not influence shrinkage characteristics of high strength mixes considered. Apparently, the effect (if any) of the slow reactivity of fly ash was compensated by the presence of the highly reactive silica fume. As was discussed in Section 12.4 of the present chapter, the effect of inclusion of fly ash on compressive strength of high strength concrete mixes was directly reflected in creep test results.

Absorption potential of fly ash mixes, regardless of the type of coarse aggregate and curing condition, was the highest. At early ages, due to the slow rate of reactivity of fly ash, a high strength concrete mix with fly ash has higher effective water-to-cement ratio than a reference mix and hence, produces a more porous matrix. Higher porosity of the fly ash mix together with the consumption of water during continuous pozzolanic reaction of fly ash in the

ideal submerged condition of the test environment can explain the observed higher absorption potential of fly ash mixes.

12.6 Silica Fume

Fresh Concrete: The required amount of superplasticizer for a given slump increased when portland cement was replaced by silica fume on a one-to-one weight basis. The inclusion of silica fume increased cohesiveness and reduced segregation and bleeding of fresh concrete. The increased cohesiveness demanded a higher slump to match the workability of a plain portland cement (reference) mix.

Hardened Concrete: Silica fume, like fly ash, in the presence of adequate moisture reacts as a pozzolan to form additional cementitious hydrates similar to those formed by portland cement. Compared to portland cement and typical fly ashes, silica fume has particle size distributions that are two orders of magnitude finer. This high fineness, makes silica fume highly pozzolanic, but it also increases the water demand of the concrete mix. If the concrete mix is not properly designed, the greater specific surface area of the silica fume will hold a significant amount of water by its surface forces, leaving a major portion of the portland cement unhydrated and adversely will affect compressive strength and other mechanical properties of the resulting concrete. Moist-curing is essential for getting full advantage of silica fume in a mix. If adequate moisture is not provided, benefits from inclusion of silica fume will be limited to grain refinement of the cement matrix.

In some cases, inclusion of 7.5 percent silica fume resulted in decreased compressive strength of high strength concrete mixes made with crushed stones. Apparently the increased water demand of silica fume together with increased surface area of crushed stones did not leave adequate water for hydration of the cementitious materials. High strength concrete mixes made with crushed stones were, in general, stiff, harsh, rocky and occasionally difficult to work with. The compressive strength of silica fume concretes made with crushed stones may had been adversely affected due to inefficiency of the manual rodding consolidation method. However,

when used with smooth round river gravel, inclusion of 7.5% silica fume increased the compressive strength of concrete significantly. This was attributed to improved bond between the aggregate and the paste.

Inclusion of silica fume had similar effects on tensile strength and modulus of elasticity of high strength concrete as on its compressive strength. Effect of inclusion of silica fume in combination with fly ash on shrinkage and creep of high strength concrete mixes was discussed in Section 12.5 of the present chapter. High strength concrete mixes containing 7.5% silica fume by weight of cement exhibited the least absorption potential. Incorporation of fine particles of silica fume in high strength concrete mixes reduces porosity of concrete by creating a denser cement matrix through filler effect as well as formation of additional cementitious hydrates. Therefore, at the beginning of the absorption test there are less pores to fill with water and in the long term there are less unhydrated particles left to react with water.

Table 12.1. Variations in compressive strength of 4 x 8 in. (100 x 200 mm) high strength concrete specimens made with 2 different types of limestones, psi.

Mix ID Code	No.	Age, day(s)						
		Heat-cured				Moist-cured		
		1	28	182	365	28	182	365
Reference Mixes								
131-XAL1-F00M00-130	124	12338	15150	15134	14964	16487	16809	16702
131-XAL2-F00M00-130	132	14779	16298	15649	15731	16033	16279	16888
Range, Percent:		*20*	*8*	*3*	*5*	*3*	*3*	*1*
Fly Ash Mixes								
131-XAL1-F20M00-130	125	13829	16606	16508	16871	17117	17272	17215
131-XAL2-F20M00-130	133	14088	16393	16470	16722	17573	17638	18421
Range, Percent:		*2*	*1*	*0*	*1*	*3*	*2*	*7*
Silica Fume Mixes								
131-XAL1-F00M75-130	126	9219	12455	12488	12342	14264	15114	15618
131-XAL2-F00M75-130	134	10688	14159	14680	14405	14899	16695	17148
Range, Percent:		*16*	*14*	*18*	*17*	*4*	*10*	*10*
FA + SF Mixes								
131-XAL1-F20M75-130	127	11817	13878	13679	13542	15553	16057	16107
131-XAL2-F20M75-130	135	14606	16124	16279	16268	15959	17404	17494
Range, Percent:		*24*	*16*	*19*	*20*	*3*	*8*	*9*

Range, percent = [(Maximum - Minimum)/(Average)]*100

Table 12.2. Variations in compressive strength of 4 x 8 in. (100 x 200 mm) high strength concrete specimens made with 6 different types of coarse aggregates, psi.

Mix ID Code	No.	Age, day(s)						
		Heat-cured				Moist-cured		
		1	28	182	365	28	182	365
Reference Mixes								
131-XAR1-F00M00-130	108	8843	11218	11415	11373	13185	14489	14840
131-XAR2-F00M00-130	128	11630	12934	12746	12721	15031	15902	15849
131-XAG1-F00M00-130	96	9462	11808	12094	-	12986	-	-
131-XAG2-F00M00-130	136	11440	12624	12582	12621	14271	14998	14947
131-XAL1-F00M00-130	124	12338	15150	15134	14964	16487	16809	16702
131-XAL2-F00M00-130	132	14779	16298	15649	15731	16033	16279	16888
Maximum:		***14779***	***16298***	***15649***	***15731***	***16487***	***16809***	***16888***
Minimum:		***8843***	***11218***	***11415***	***11373***	***12986***	***14489***	***14840***
Range:		***5936***	***5080***	***4234***	***4358***	***3501***	***2320***	***2048***
Average:		***11415***	***13339***	***13270***	***13482***	***14666***	***15695***	***15845***
Range, percent:		***52***	***38***	***32***	***32***	***24***	***15***	***13***
Fly Ash Mixes								
131-XAR1-F20M00-130	110	8475	10908	11300	10826	11882	14341	14998
131-XAR2-F20M00-130	129	12083	14349	14259	14295	15604	16504	16243
131-XAG1-F20M00-130	-	-	-	-	-	-	-	-
131-XAG2-F20M00-130	137	12666	14127	13718	13687	16623	17205	16664
131-XAL1-F20M00-130	125	13829	16606	16508	16871	17117	17272	17215
131-XAL2-F20M00-130	133	14088	16393	16470	16722	17573	17638	18421
Maximum:		***14088***	***16606***	***16508***	***16871***	***17573***	***17638***	***18421***
Minimum:		***8475***	***10908***	***11300***	***10826***	***11882***	***14341***	***14998***
Range:		***5613***	***5698***	***5208***	***6045***	***5691***	***3297***	***3423***
Average:		***12228***	***14477***	***14451***	***14480***	***15760***	***16592***	***16708***
Range, percent:		***46***	***39***	***36***	***42***	***36***	***20***	***20***
Silica Fume Mixes								
131-XAR1-F00M75-130	112	11559	12920	13104	12347	14466	15293	15339
131-XAR2-F00M75-130	130	9983	12455	12464	12307	15038	15988	16072
131-XAG1-F00M75-130	98	11096	12529	12729	-	15292	-	-
131-XAG2-F00M75-130	138	10289	11729	11703	11781	14252	15415	15594
131-XAL1-F00M75-130	126	9219	12455	12488	12342	14264	15114	15618
131-XAL2-F00M75-130	134	10688	14159	14680	14405	14899	16695	17148
Maximum:		***11559***	***14159***	***14680***	***14405***	***15292***	***16695***	***17148***
Minimum:		***9219***	***11729***	***11703***	***11781***	***14252***	***15114***	***15339***
Range:		***2340***	***2430***	***2977***	***2624***	***1040***	***1581***	***1809***
Average:		***10472***	***12708***	***12861***	***12636***	***14702***	***15701***	***15954***
Range, percent:		***22***	***19***	***23***	***21***	***7***	***10***	***11***
FA + SF Mixes								
131-XAR1-F20M75-130	114	10393	11516	11312	10998	14841	15077	14942
131-XAR2-F20M75-130	131	12043	13140	13057	12973	15912	16558	17275
131-XAG1-F20M75-130	-	-	-	-	-	-	-	-
131-XAG2-F20M75-130	139	11260	12988	12882	13027	16036	15783	16066
131-XAL1-F20M75-130	127	11817	13878	13679	13542	15553	16057	16107
131-XAL2-F20M75-130	135	14606	16124	16279	16268	15959	17404	17494
Maximum:		***14606***	***16124***	***16279***	***16268***	***16036***	***17404***	***17494***
Minimum:		***10393***	***11516***	***11312***	***10998***	***14841***	***15077***	***14942***
Range:		***4213***	***4608***	***4967***	***5270***	***1195***	***2327***	***2552***
Average:		***12024***	***13529***	***13442***	***13362***	***15660***	***16176***	***16377***
Range, percent:		***35***	***34***	***37***	***39***	***8***	***14***	***16***

Range, percent = [(Maximum - Minimum)/(Average)]*100

Table 12.3. Compressive strength test results together with observed ultimate values of creep coefficient and specific creep.

Mix	1-day Comp. Strength, psi	28-day Comp. Strength, psi	Ult. Creep Coef. v_u	Ult. Specific Creep, 10^{-6}/psi
H108,R1,REF	8387	11270	2.45	0.39
H116,R1,REF	9179	11721	2.46	0.36
H136,G2,REF	10428	11777	1.83	0.29
H139,G2,FASF	10638	12112	1.59	0.23
H128,R2,REF	10880	12291	1.31	0.20
H131,R2,FASF	10993	12262	1.15	0.18
H124,L1,REF	10513	14789	1.03	0.17
H132,L2,REF	13112	14310	0.94	0.15
W139,G2,FASF	-	14111	1.07	0.17
W128,R2,REF	-	15049	0.92	0.15
W129,RS,SF	-	15348	1.20	0.17
W131,R2,FASF	-	15437	1.13	0.16
W124,L1,REF	-	16013	0.96	0.14
W132,L2,REF	-	16265	0.95	0.14

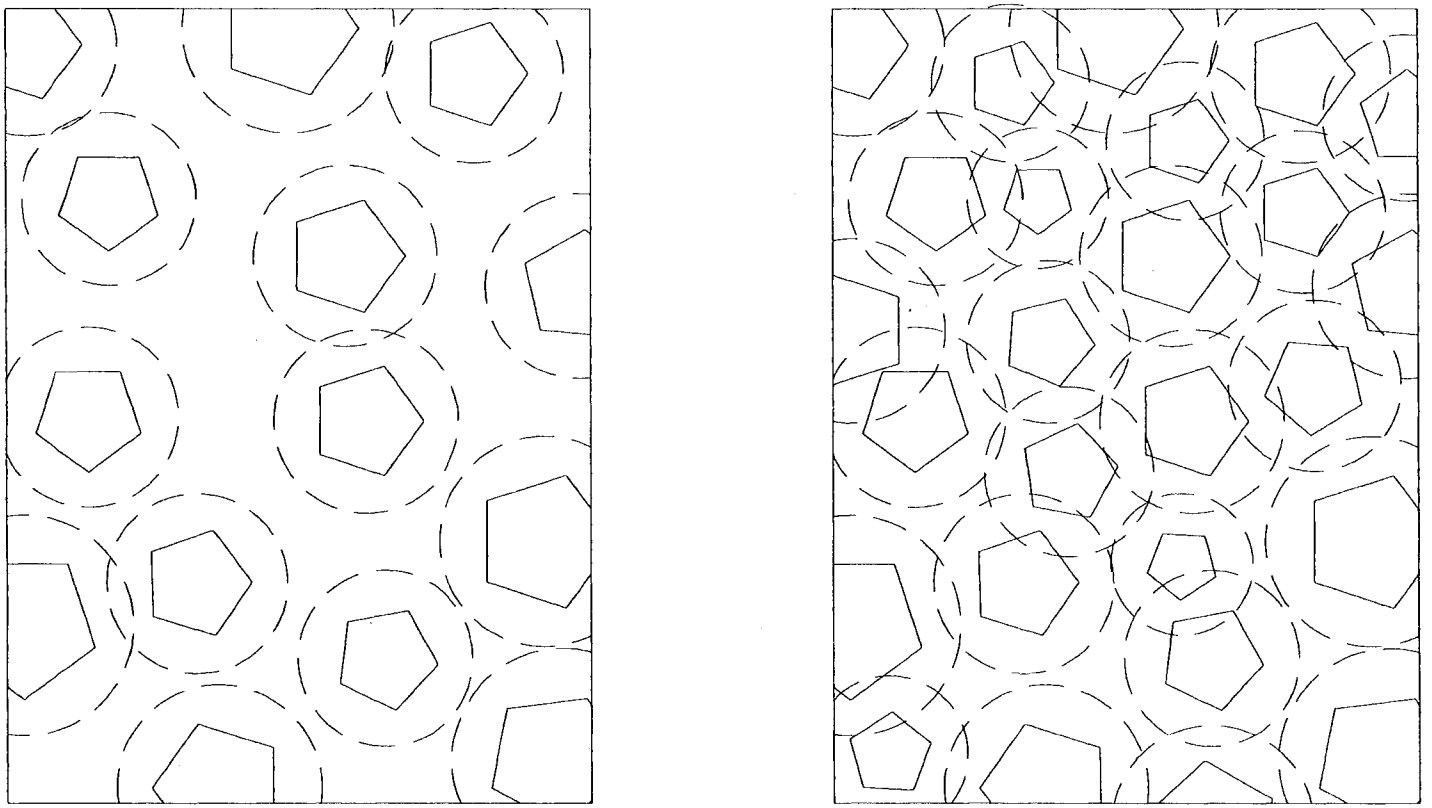

Figure 12.1. The regions of stress concentration around neighboring aggregate particles overlap more and more as the total volume of aggregate in the mix is increased.

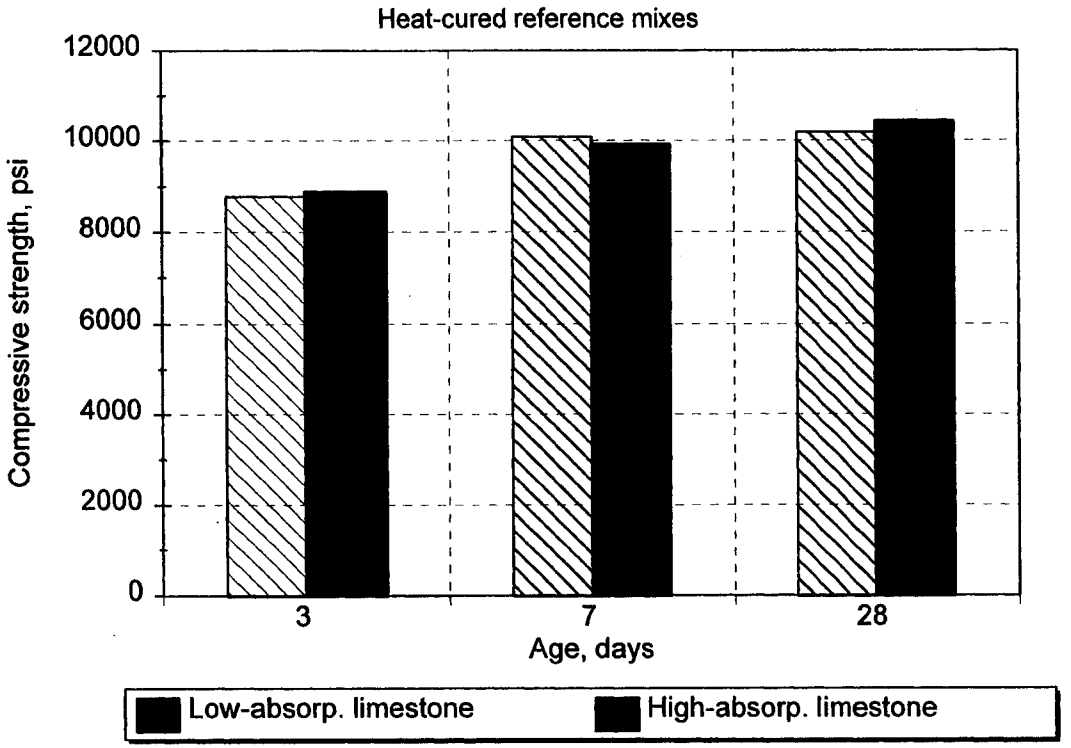

Figure 12.2. Effect of type of aggregate in medium strength concrete - high absorption limestone (L1) and low absorption limestone (L2).

CHAPTER 13
SUMMARY AND CONCLUSIONS

This chapter presents a summary and conclusions of this research program. The objective of the research was to investigate the effects of various test and material variables on the mechanical properties of high strength concrete. The main test variables included: mold material; mold size; specimen end condition; curing condition; heat-curing temperature; and age. The material variables investigated were: total cementitious material content of the mix; percent replacement of cement by weight with fly ash, silica fume or their combination; type and gradation of coarse aggregate; type of superplasticizer; and type and brand of cement. Efforts were made to use materials and procedures considered to be typical of those used by the precast/prestressed industry. In addition, standard tests were conducted on companion specimens, to correlate the results of this study with results reported elsewhere in the literature. High strength concretes with 28-day compressive strengths in the range of 8,000 to 18,600 psi (55.2 to 128 MPa) were produced.

In all, more than 6,300 concrete specimens from 142 high strength concrete mixes were tested for compressive and tensile strength, strength gain with time, modulus of rupture, static modulus of elasticity, shrinkage, creep, and absorption potential (indirect permeability). The following conclusions were obtained from the results:

I. ***Compressive Strength***

A. *Specimen Size*: On average, measured compressive strength of 4 x 8 in. (100 x 200 mm) cylinders was 7 percent higher than that of companion 6 x 12 in. (150 x 300 mm) cylinders ($f_{4x8} = 1.07 f_{6x12}$).

B. *Mold Material*: For the manual rodding consolidation method used in this study, the compressive strength of 6 x 12 in. (150 x 300 mm) cylinders cast in single-use plastic molds was 97 percent of companion cylinders cast in heavy-gauge reusable steel molds.

C. *End Condition*: Measured compressive strength of 4 x 8 in. (100 x 200 mm) cylinders with ground ends or capped with unbonded neoprene pads was, on average, 1.0 percent higher than that of companion specimens capped with high strength capping compound.

D. *Curing*: As expected, heat-cured specimens yielded higher early age compressive strengths than moist-cured specimens. At later ages, continuous application of moisture resulted in the continued increase in compressive strength of moist-cured specimens; whereas, the strength of the heat-cured specimens leveled off.

E. *Type of Cement*: The compressive strength developed at early ages was higher for moist-cured concrete made with rapid-hardening portland cement (Type III) than for ordinary portland cement (Type I). However, heat-cured high strength concrete specimens made with the two types of cement had basically the same strength development rate.

F. *Composition of Cementing Materials*: Use of supplementary cementing materials, such as fly ash and/or silica fume, do not necessarily translate into higher compressive strengths. It was shown that benefits from inclusion of fly ash and/or silica fume in the production of high strength concrete depended on factors such as mix proportions, type of coarse aggregate in the mix and method of curing. Moist-curing proved to be essential for getting full advantage of using fly ash and/or silica fume in a mix. In the absence of adequate moisture, any benefit from inclusion of fly ash and/or silica fume was limited to grain refinement of the cement matrix. Even when adequately cured, higher compressive strength resulting from inclusion of fly ash was delayed until 1 to 3 months after casting.

G. *Type of Superplasticizer*: Results from this study highlighted the importance of the selection of the superplasticizer. Selection of any superplasticizer should be based on its effects on both the properties of the fresh concrete and on long-term properties of hardened concrete.

H. *Rate of Strength Gain*: With the exception of moist-cured fly ash mixes, high strength concrete developed a significantly higher portion of its 28-day

compressive strength at early ages. Moist-cured high strength concrete specimens made with Type III cement, on average gained 91 percent of their 28-day compressive strength at 7-days. This ratio was 71 percent for moist-cured fly ash mixes. ACI 209 reports an 80 percent ratio for similarly cured normal strength concrete made with Type III cement. One-day to 28-day compressive strength ratios for heat-cured high strength concretes made with Type I and Type III cements were 88 and 83 percent, respectively. ACI 209 reports values of 51 and 60 percent for steam-cured normal strength concretes made with Type I and Type III cement, respectively.

I. <u>*Coarse Aggregate*</u>:

1. *Limestone versus Round Gravel*: *Concrete* made with limestone showed higher compressive strength than that made with round gravel. Limestone particles exhibited a superior bond characteristic with cement paste and the plane of fracture in limestone concrete crossed most of the coarse aggregate particles. In contrast, round gravel particles showed poor bond with cement paste and, except for small sized particles, the plane of fracture passed around coarse aggregate particles.
2. *Water-to-Cement Ratio*: When the strength of the high strength concrete was limited by failure of the aggregate, further reduction in the water-to-cementitious materials ratio will not increase strength, and may cause problems by reducing workability of the mix. The optimum value for water-to-cementitious materials ratio depends on the type of the coarse aggregate and the means of compaction.
3. *Silica Fume*: The influence of coarse aggregate type on the compressive strength of high strength concrete varied in magnitude and depended on the curing condition and the cementitious material composition of the mix. Addition of silica fume had the greatest effect on mixes made with round gravel. This was attributed to improved bond between the aggregate and the paste. More aggregate fractures were noted in the round gravel mixes

containing silica fume than in those round gravel mixes without silica fume. Because the fracture of the aggregate controlled the strength of the limestone mixes, the addition of silica fume had little effect on those mixes. For all aggregates, moist-curing enhanced the benefit obtained from inclusion of silica fume.

II. ***Modulus of Elasticity***

A. *Specimen Size*: In general, the static modulus of elasticity values measured using 4 x 8 in. (100 x 200 mm) specimens were 620,000 psi (4.3 GPa) higher than static modulus of elasticity values measured using 6 x 12 in. (150 x 300 mm) specimens.

B. *Curing*: At equivalent strengths, measured static modulus of elasticity values for moist-cured specimens tested in the wet condition were somewhat higher than the measured static modulus of elasticity values for heat-cured specimens or specimens moist-cured for a limited period of time and tested in a dry condition.

C. *Type of Cement*: High strength concretes made with different types and different brands of cement resulted in practically identical values of modulus of elasticity when cured and tested under identical conditions.

D. *Composition of Cementitious Materials*: For the levels of replacement by weight of cement by fly ash and/or silica fume considered in this study, cementitious material composition did not have a significant effect on the measured modulus of elasticity values of high strength concretes made with each of the six coarse aggregates used.

E. *Relationship with Time*: On average, 1-day modulus of elasticity of heat-cured specimens was 98 percent of its 28-day value. After 182- and 365-days, the modulus of elasticity of heat-cured specimens were, on average, 94 and 96 percent of the 28-day value. Modulus of elasticity of moist-cured specimens increased with time and was approximately 106 and 108 percent of the 28-day value at 182- and 365-days of age, respectively.

F. *Coarse Aggregate*: It is important to recognize the relationship between aggregate type and concrete stiffness; however, it is difficult to generalize a coefficient for a certain aggregate type because the relative aggregate properties may vary from one source to another.

G. *Design Equations*: Current design equations may overpredict the modulus of elasticity based on the concrete compressive strength and should be used with caution. Equations proposed by ACI 363 and CEB-FIP resulted the most reasonable predictions during this study.

III. ***Tensile Strength***

A. *Splitting Tensile Strength*: *The* splitting tensile strength of both heat-cured and moist-cured 6 x 12 in. (150 x 300 mm) cylinders were more closely predicted by the ACI 318 equation ($f_{sp}=6.7(f_c)^{0.5}$) than the proposed ACI 363 relationship ($f_{sp}=7.4(f_c)^{0.5}$).

B. *Modulus of Rupture*: Data obtained for flexural tensile strength of moist-cured specimens were closely predicted by the proposed ACI 363 equation ($f_r=11.7(f_c)^{0.5}$). For predicting flexural tensile strength of heat-cured specimens a new relationship yielding values between those predicted by the ACI 318 equation and the ACI 363 proposed equation is proposed ($f_r=9.30(f_c)^{0.5}$).

IV. ***Shrinkage***

A. *Relationship with Time:* Drying shrinkage strains observed in this study ranged between 63 to 83 percent of values predicted by ACI 209 equations. Based on the data collected the following two equations were suggested for predicting the shrinkage strain of high strength concrete:

Moist-cured concrete: $(\varepsilon_{sh})_t=[t/(45+t)]*(\varepsilon_{sh})_u$

Heat-cured concrete: $(\varepsilon_{sh})_t=[t/(65+t)]*(\varepsilon_{sh})_u$

where $(\varepsilon_{sh})_u$ =530 με.

Lower water-to-cementitious material ratio and denser matrix of high strength concrete were believed to be the main reasons for the observed smaller ultimate

shrinkage of high strength concrete and its increased time to one-half ultimate shrinkage strain value.

B. *Curing Temperature*: Specimens heat-cured at lower temperatures (120 °F) had slightly higher drying shrinkage strains than companion specimens cured at higher temperatures (150 °F).

C. *Cementitious Material Composition and Compressive Strength*: For the cases studied, concrete compressive strength and composition of cementitious material had no significant effect on drying shrinkage of high strength concrete mixes.

D. *Coarse Aggregate*: The drying shrinkage exhibited by high strength concrete reference mixes made with crushed gravels was less than that of the companion mix made with round gravel. Shrinkage strains after 380 days of drying were 565, 485, 469, 443, and 492 με for heat-cured reference mixes made with round gravel, crushed river gravel, high absorption limestone, low absorption limestone, and granite coarse aggregates respectively.

V. ***Creep***

A. *Relationship with Time*: The recommended form of ACI 209 equation: $V_t=[t^{0.60}/(10+t^{0.60})]*V_u$, was determined to be suitable for predicting the creep coefficient of high strength concrete at any time *t*. The range of ultimate creep coefficients (V_u) predicted in this study varied between 0.92 to 2.46 as compared to the 1.30 to 4.15 range reported by ACI 209 for normal strength concrete.

B. *Curing Temperature* : The specific creep of specimens heat-cured at a lower temperature (120 °F) was less than companion specimens cured at a higher temperature (150 °F).

C. *Compressive Strength*: The specific creep of high strength concrete followed the general trend of more conventional concrete, i.e. concrete specific creep decreased as compressive strength increased.

D. *Coarse Aggregate*: As was the case for the drying shrinkage of high strength concrete, the specific creep exhibited by high strength concrete reference mixes made with crushed gravel was less than that of the companion mix made with

round gravel. The young age of concrete at loading together with the small amount of restraint provided by the smooth surface of round gravel were considered to be the main causes for this observation. Moist-curing reduced the effect of the type of coarse aggregate and variations in composition of cementitious materials on creep characteristics of high strength concrete mixes considered.

VI. ***Absorption Potential (Indirect Permeability)***

A. *Curing Temperature*: Specimens heat-cured at a lower temperature (120 °F) absorbed less water than companion specimens cured at a higher temperature (150 °F).

B. *Type of Cement*: High strength concrete specimens made with Type III cement consistently absorbed less water than specimens made with Type I cement of identical mix design. More complete hydration of Type III cement due to its fineness was believed to be the reason for the denser cement matrix and resulting lower absorption potential.

C. *Composition of Cementitious Material*: For any type of coarse aggregate and for both curing conditions, the weight gain of submerged specimens was highest for mixes with 20 percent fly ash followed by reference mixes, and the mixes containing a combination of 20 percent fly ash and 7.5 percent silica fume. Weight gain was the lowest for mixes containing 7.5 percent silica fume.

D. *Coarse Aggregate*: The effect of the type of coarse aggregate on the absorption test results was concluded to be secondary. The amount of water that reaches and gets absorbed by coarse aggregate particles depends on the permeability of the cement matrix. Moist curing reduced the influence of the type of aggregate on absorption potential of high strength concrete specimens significantly.

LIST OF REFERENCES

1. ACI 212.4R Committee Report (1993), "Guide for the Use of High-Range Water-Reducing Admixtures(superplasticizers) in Concrete," Concrete International, 15(4), 40-47.
2. ACI Committee 116 (1967), "Cement and Concrete Terminology," Publication SP-19, American Concrete Institute, Detroit, Mich.
3. ACI Committee 209 (1971), "Prediction of Creep, Shrinkage, and Temperature Effects in Concrete Structures," Publication SP-27, American Concrete Institute, Detroit, Mich.
4. ACI Committee 209R-92 (1992), "Prediction of Creep, Shrinkage, and Temperature Effects in Concrete Structures," American Concrete Institute, Detroit, Mich.
5. ACI Committee 226 (1987), "Silica Fume in Concrete," ACI Materials Journal, 84(2), 158-166.
6. ACI Committee 363 (1987), "Research Needs for High-Strength Concrete," ACI Materials Journal, 84(6), 559-561.
7. ACI Committee 363 (1992), "State-of-the-Art Report on High-Strength Concrete," American Concrete Institute, Detroit, Mich., 55 pp.
8. Ahmad, Shuaib H.; and Shah, S. P. (1985), "Structural Properties of High Strength Concrete and its Implications for Precast Prestressed Concrete," PCI Journal, 30(6), 92-119.
9. Aïtcin, P. C.; Sarkar, S. L.; and Yaya, D. (1987) "Microstructural Study of Different Types of Very High-Strength Concrete," Proceedings, Material Research Society symposium, Material Research Society, Pittsburgh, Volume 85, 261-272.
10. Aïtcin, P.-C.; and Mehta, P. K. (1990), "Effect of Coarse-Aggregate Characteristics on Mechanical Properties of High-Strength Concrete," ACI Materials Journal, 87(2), 103-107.
11. Aïtcin, Pierre-Claude; and Laplante, P. (1990), "Long Term Compressive Strength of Silica-Fume Concrete," Journal of Materials in Civil Engineering, 2(3), 164-170.
12. Aïtcin, Pierre-Claude; Jolicoeur, Carmel; and MacGregor, James G. (1994), "Superplasticizers: How They Work and Why They Occasionally Don't," Concrete International, 16(5), 45-52.
13. Aïtcin, Pierre-Claude; Sarkar, Shondeep L; Ranc, Roger; and Levy, Christophe (1991), "A High Silica Modulus Cement for High-Performance Concrete," Ceramic Transactions, Volume 16, 795 pp.
14. Albinger, John M. (1988), "High Strength Concrete in the United States," Presented on November 7, 1988 in Paris, France.
15. ASTM C 125-93 (1993), "Annual Book of ASTM Standards," American Society for Testing and Materials, Philadelphia, PA.

16. Baalbaki, Walid; Aïtcin, Pierre-Claude; and Ballivy, Gerard (1992), "On Predicting Modulus of Elasticity in High-Strength Concrete," ACI Materials Journal, 89(5), 517-520. (see discussion July-August 93)

17. Baalbaki, Walid; Baalbaki, Moussa; Benmokrane, Brahim; and Aïtcin, Pierre-Claude (1992), "Influence of Specimen Size on Compressive Strength and Elastic Modulus of High-Performance Concrete," Cement, Concrete, and Aggregate, 14(2), 113-117.

18. Berke, N. S.; Dallaire, M. P.; and Hicks, M. C. (1992), "Plastic, Mechanical, Corrosion, and Chemical Resistance Properties of Silica Fume (Microsilica) Concretes," Fly Ash, Silica Fume, Slag, and Natural Pozzolans in Concrete, Proceedings Fourth International Conference, Istanbul, Turkey, Volume 2, 1125-1149.

19. Berry, E. E.; and Malhotra, M. (1980), "Fly Ash for Use in Concrete-A Critical Review," ACI Journal, 77(2), 59-73.

20. Blick, Ronald L., Petersen, Charles F., and Winter, Michael E. (1985), "Proportioning and Controlling High Strength Concrete" Proportioning Concrete Mixes, ACI SP-46, 141-163.

21. Bloem, Delmar L.; and Gaynor, Richard D. (1964), "Effects of Aggregate Properties on Strength of Concrete," ACI Journal, 60(10), 1429-1454.

22. Boulay, C.; and de Larrard, F. (1993), "Capping High-Performance Concrete Cylinders with the 'Sand-Box'," Proceedings of the Third International Symposium on Utilization of High-Strength Concrete, Lillehammer, Norway, Volume 2, 1015-1023.

23. Boulay, Claude; and de Larrard, Francois (1993), "A New Capping System for Testing HPC Cylinders: The Sand-Box," Concrete International, 15(4), 63-66.

24. Burg, R. G.; and Ost, B. W. (1992), "Engineering Properties of Commercially Available High-Strength Concretes," PCA Research and Development Bulletin RD104T, 55 pp.

25. Burgess, A. James; Ryell, John; and Bunting, John (1970), "High Strength Concrete for the Willows Bridge," ACI Journal, 67(8), 611-619.

26. Carette, G. G.; Malhotra, V. M.; and Aïtcin, P. C. (1987), "Preliminary data on long-term strength development on condensed silica-fume concrete," Proceedings, International Workshop on Condensed Silica Fume in Concrete.

27. Carrasquillo, P. M.; and Carrasquillo, R. L. (1986), "Guidelines for Use of High Strength Concrete in Texas Highways," Research Report 367-1F, Center for Transportation Research, The University of Texas at Austin, 227 pp.

28. Carrasquillo, P. M.; and Carrasquillo, R. L. (1988), "Effect of Using Unbonded Capping Systems on the Compressive Strength of Concrete Cylinders," ACI Materials Journal, 85(3), 141-147.

29. Carrasquillo, P. M.; and Carrasquillo, R. L. (1988), "Evaluation of the Use of Current Concrete Practice in Production of High-Strength Concrete," ACI Materials Journal, 85(1), 49-54.

30. Carrasquillo, Ramon L.; Nilson, Arthur H.; and Slate, Floyd O. (1981), "Properties of High Strength Concrete Subject to Short-Term Loads," ACI Journal, 87(3), 171-178.

31. Carrasquillo, Ramon L.; Nilson, Arthur H.; and Slate, Floyd O. (1981), "Properties of High Strength Concrete Subject to Short-Term Loads," ACI Journal, 87(3), 171-178.

32. Castrodale, Reid W.; Burns, Ned H.; and Kreger, Michael E. (1988), "A Study of Pretensioned High Strength Concrete Girders in Comosite Highway Bridges-Laboratory Tests," Research Report 381-3, Center for Transportation Research, The University of Texas at Austin, 210 pp.

33. Castrodale, Reid W.; Kreger, M. E.; and Burns, Ned H. (1988), "A Study of Pretensioned High Strength Concrete Girders in Composite Highway Bridges-Design Considerations," Research Report 381-4F, Center for Transportation Research, The University of Texas at Austin, 281 pp.

34. CERF (1993), "High-Performance Construction Materials and Systems: An Essential National Program for America and Its Infrastructure," prepared by the Civil Engineering Research Foundation and the Planning Committee for the Nationally-Coordinated Program on High-Performance Concrete and Steel, Technical Report 93-5011.

35. Chicago Committee on High-Rise Buildings (1977), "High Strength Concrete in Chicago High-Rise Buildings," Task Force Report No. 5, 63 pp.

36. Cohen, Menashi D.; and Olek, Jan (1989), "Silica Fume in PCC: The Effects of Form on Engineering Performance," Concrete International, 11(11), 43-47.

37. Collepardi, M. (1984), "Water Reducers/Retarders," Concrete Admixtures Handbook, V. S. Ramachandran ed., Noyes Publications, Park Ridge, New Jersey, 626 pp.

38. Day, R. L.; and Haque, M. N. (1993), "Correlation between Strength of Small and Standard Concrete Cylinders," ACI Materials Journal, 90(5), 452-462.

39. de Larrard, F.; and Lacroix, R. (1996), "Utilization of High Strength/High Performance Concrete," Proceedings of The Fourth International Symposium on Utilization of High Strength/High Performance Concrete, Paris, France, Volumes I, II & III, 1593 pp.

40. Detwiler, Rachel J.; and Mehta P. Kumar (1989), "Chemical and Physical Effects of Silica Fume on the Mechanical Behavior of Concrete," ACI Materials Journal, 86(6), 609-614.

41. FIP Commission on Concrete (1988), "Condensed Silica Fume in Concrete," Thomas Telford Ltd, London, 37 pp.

42. FIP/CEB (1990), "High Strength Concrete - State of the Art Report," SR 90/1 Bulletin d'Information No. 197, 61 pp.

43. French, Catherine W.; and Mokhtarzadeh, Alireza (1993), "High Strength Concrete: Effects of Materials, Curing and Test Procedures on Short-Term Compressive Strength," PCI Journal, 38(3), 76-87.

44. Gebler, S. H. (1982), "The Effects of High-Range Water Reducers on the Properties of Freshly Mixed and Hardened Flowing Concrete," PCA Research and Development Bulletin RD081.01T, 13 pp.

45. Goldman, Ariel; and Bentur, Arnon (1989), "Bond Effects in High-Strength Silica-Fume Concretes," ACI Materials Journal, 86(5), 440-447.

46. Gonnerman, Harrison F. (1925), "Effect of Size and Shape of Test Specimen on Compressive Strength of Concrete," Proceedings, ASTM, 25, Part 2, 237-250.

47. Helmuth, Richard (1987), "Fly Ash in Cement and Concrete," Portland Cement Association, 203 pp.

48. Hester, Weston T. (1977), "High Strength Air-Entrained Concrete," Concrete Construction, 22(2), 77-82.

49. Hester, Weston T. (1980), "Field Testing High-Strength Concretes: A Critical Review of the State-of-the-Art," Concrete International, 27-38.

50. Hester, Weston T. (1990), "High-Strength Concrete," ACI SP-121, The Second International Symposium on Utilization of High Strength Concrete, Berkely, California, 786 pp.

51. Hoff, George C. (1993), "Utilization of High Strength Concrete in North America," Proceedings of the Third International Symposium on Utilization of High-Strength Concrete, Lillehammer, Norway, Volume 1, 28-36.

52. Holand, Ivar (1987), "High-Strength Concrete," Proceedings of The First International Symposium on Utilization of High-Strength Concrete, Stavanger, Norway.

53. Holand, Ivar; and Sellevold, Erik (1993), "High-Strength Concrete," Proceedings of The Third International Symposium on Utilization of High Strength Cocrete, Lillehammer, Norway, Volumes I & II, 1287 pp.

54. Howard, Nathan L.; and Leatham, David M. (1989), "The Production and Delivery of High-Strength Concrete," Concrete International, 11(4), 26-30.

55. Ikeda, Shoji (1993), "Utilization of High Strength Concrete in Japan," Proceedings of the Third International Symposium on Utilization of High-Strength Concrete, Lillehammer, Norway, Volume 1, 37-44.

56. Janak, Karl J. (1985), "Comparative Compressive Strength of 4x8 in. Versus 6x12 in. Concrete Cylinders along with the Investigation of Concrete Compressive Strength at 56 Days," Texas State Department of Highways and Public Transportation, Materials and Tests Division Report #3-I-4-116, 36 pp.

57. Klieger, P. (1958), Proceedings of American Concrete Institute, 54, 1063.

58. Lambotte, H; and Taerwe, L. (1989), "The Use of High-Range Water-Reducers for High Strength Concrete," Book of Proceedings, ERMCO'89 The Norway to Concrete, 666-678.

59. Larbi, J. A.; and Bijen, J. M. J. (1991), "Orientation of Portlandite at the Paste-Aggregate Interface and Strength Development of the Paste-Aggregate Bond in Mortars in the Presence of Microsilica," Ceramic Transactions, Volume 16, 795 pp.

60. Lessard, Michel; Chaallal, Omar; and Aïtcin, Pierre-Claude (1993), "Testing High-Strength Concrete Compressive Strength," ACI Materials Journal, 90(4), 303-308.

61. Malhotra, M. (1976), "Are 4x8 Inch Concrete Cylinders as Good as 6x12 Inch Cylinders for Quality Control of Concrete?," ACI Journal, 73(1), 33-36.

62. Mehta P. K. (1984), "Mineral Admixtures," Concrete Admixtures Handbook, V. S. Ramachandran ed., Noyes Publications, Park Ridge, New Jersey, 626 pp.

63. Mehta, P. Kumar (1986), "Concrete - Structure, Properties, and Materials," Prentice-Hall, Inc., Englewood Cliffs, New Jersey, 450 pp.

64. Mokhtarzadeh, A.; Kriesel, R.; French ,C.; and Snyder, M. (1995), "Mechanical Properties and Durability of High-Strength Concrete for Prestressed Bridge Girders," Transportation Research Record No. 1478: Materials and Construction - Concrete and Concrete Pavement Construction, Transportation Research Board, Washington, D.C., 20-29.

65. Moreno, Jaime (1990), "Ultra-High-Strength Concrete for 225 W. Wacker Project, Chicago," PCA Engineered Concrete Structures, 3(1).

66. Neville, Adam M. (1966), "A General Relation for Strengths of Concrete Specimens of Different Shapes and Sizes," ACI Journal, Proceedings, 63(10), 1095-1109.

67. Neville, Adam M. (1975), " Properties of Concrete," Pitman Publishing Ltd., London, Great Britain, 687 pp.

68. Nilsen, Arne Ulrik; and Gjørv, Odd E. (1993), "Elastic Properties of High-Strength Concrete," Proceedings of the Third International Symposium on Utilization of High-Strength Concrete, Lillehammer, Norway, Volume 2, 1162-1168.

69. Novokshchenov, Vladimir (1993), "Factors Controlling the Compressive Strength of Silica Fume Concrete in the Range 100 to 150 MPa," Proceedings of the Third International Symposium on Utilization of High-Strength Concrete, Lillehammer, Norway, Volume 2, 863-873.

70. Oluokun, Francis A. (1991), "Prediction of Concrete Tensile Strength from its Compressive Strength: Evaluation of Existing Relations for Normal Weight Concrete," ACI Materials Journal, 88(3), 302-309.

71. Ozyildirim, Celik (1985), "Neoprene Pads for Capping Concrete Cylinders," Cement, Concrete, and Aggregate, 7(1), 25-28.

72. Parrott, L. J. (1988), "A Literature Review of High Strength Concrete Properties," British Cement Association Report, 85 pp.

73. Pauw, Adrian (1960), "Static Modulus of Elasticity of Concrete as Affected by Density," ACI Journal, 32(6), 679-687.

74. Peterman, M. B.; and Carrasquillo, R. L. (1983), "Production of High Strength Concrete," Noyes Publications, Park Ridge, NJ, 286 pp.

75. Ping, Xie; Beaudoin, J. J.; and Brousseau, R. (1991), "Effect of Aggregate Size on Transition Zone Properties at the Portland Cement Paste Interface," Cement and Concrete Reseach, 21, 999-1005.

76. Ping, Xie; Beaudoin, J. J.; and Brousseau, R. (1991), "Flat Aggregate-Portland Cement Paste Interfaces, I. Electrical Conductivity Models," Cement and Concrete Research, 21, 515-522.

77. Pistilli, Michael F.; and Willems, Terry (1993), "Evaluation of Cylinder Size and Capping Method in Compression Strength Testing of Concrete," Cement, Concrete, and Aggregate, 15(1), 59-69.

78. Price, Walter H. (1951), "Factors Influencing Concrete Strength," ACI Journal, 22(6), 417-432.

79. Radain, Talal A.; Samman, Tamim A.; and Wafa, Faisal F. (1993), "Mechanical Properties of High-Strength Concrete," Proceedings of the Third International Symposium on Utilization of High-Strength Concrete, Lillehammer, Norway, Volume 2, 1209-1216.

80. Ramachandran, V. S.; and Malhotra, V. M. (1984), "Superplasticizers," Concrete Admixtures Handbook, V. S. Ramachandran ed., Noyes Publications, Park Ridge, New Jersey, 626 pp.

81. Richardson, David N. (1990), "Effects of Testing Variables on the Comparison of Neoprene Pad and Sulfur Mortar-Capped Concrete Test Cylinders," ACI Materials Journal, 87(5), 489-495.

82. Sarkar, S. L.; and Aïtcin, P. C. (1987), "Dissolution Rate of Silica Fume in Very High Strength Concrete," Cement and Concrete Research, Vol. 17, 591-601.

83. Sarkar, Shondeep L.; Baalbaki, Moussa; and Aïtcin, Pierre-Claude (1991), "Microstructural Development in a High-Strength Concrete Containing a Ternary Cementitious System," Cement, Concrete and Aggregates, 13(2), 81-87.

84. Shin, Sung-Woo (1990), "High-Strength Concrete in Korea," PCA Engineered Concrete Structures, 3(2).

85. SHRP (1993), "Mechanical Behavior of High Performance Concretes, Volume 1: Summary Report," SHRP-C-361, Strategic Highway Research Program, National Academy of Science, Washington, DC, 98 pp.

86. SHRP (1993), "Mechanical Behavior of High Performance Concretes, Volume 2: Production of High Performance Concrete," SHRP-C-362, Strategic Highway Research Program, National Academy of Science, Washington, DC, 92 pp.

87. SHRP (1993), "Mechanical Behavior of High Performance Concretes, Volume 3: Very Early Strength Concrete," SHRP-C-363, Strategic Highway Research Program, National Academy of Science, Washington, DC, 116 pp.

88. SHRP (1993), "Mechanical Behavior of High Performance Concretes, Volume 4: High Early Strength Concrete," SHRP-C-364, Strategic Highway Research Program, National Academy of Science, Washington, DC, 179 pp.

89. SHRP (1993), "Mechanical Behavior of High Performance Concretes, Volume 5: Very High Strength Concrete," SHRP-C-365, Strategic Highway Research Program, National Academy of Science, Washington, DC, 101 pp.

90. SHRP (1993), "Mechanical Behavior of High Performance Concretes, Volume 6: High Early Strength Fiber Reinforced Concrete," SHRP-C-366, Strategic Highway Research Program, National Academy of Science, Washington, DC, 297 pp.

91. Slanicka, S. (1991), "The Influence of Fly Ash Fineness on the Strength of Concrete," Cement and Concrete Research, 21, 285-296.

92. Smith, E. F., Tynes, W. O., and Saucier, K. L. (1964), "High Compressive Strength Concrete - Development of Concrete Mixtures," U.S. Army Waterways Experiment Station, (WES) TDR-63-3114.

93. Smith, I. A. (1967), "The Design of Fly Ash Concretes," Proceedings, Institution of Civil Engineers, London, Vol. 36, 769-790.

94. Soroka, I. (1980), "Portland Cement Paste and Concrete," Chemical Publishing Co., New York, N. Y., 338 pp.

95. Swamy, R. N. (1986), "Cement Replacement Materials," Surrey University Press, London, 259 pp.

96. Tomosawa, Fuminori; and Noguchi, Takafumi (1993), "Relationship Between Compressive Strength and Modulus of Elasticity of High-Strength Concrete," Proceedings of the Third International Symposium on Utilization of High-Strength Concrete, Lillehammer, Norway, Volume 2, 1247-1254.

97. Tomosawa, Fuminori; Noguchi, Takafumi; and Onoyama, Kanzo (1993), "Test Method for Compressive Strength of High-Strength Concrete," Proceedings of the Third International Symposium on Utilization of High-Strength Concrete, Lillehammer, Norway, Volume 2, 1255-1262.

98. Tucker, John, Jr. (1941), "Statistical Theory of the Effect of Dimensions and of Method of Loading upon the Modulus of Rupture of Beams," Proceedings, ASTM, 41, 1072-1094.

99. Tucker, John, Jr. (1945), "Effect of Dimensions of Specimen Upon the Precision of Strength Data," Proceedings, ASTM, 45, 952-960.

100. Tucker, John, Jr. (1945), "Effect of Length on the Strength of Compression Test Specimens," Proceedings, ASTM, 45, 976-984.

101. Washa, G. W.; and Withey, N. H. (1953), "Strength and Durability of Concrete Containing Chicago Fly Ash," ACI Journal, 49(8), 701-713.

102. Whiting, David (1979), "Effects of High-Range Water Reducers on Some Properties of Fresh and Hardened Concretes," PCA Research and Development Bulletin RD061.01T, 15 pp.

APPENDIX A

COMPRESSIVE STRENGTH

Table A.1. Compressive strengths of 4 x 8 in. (100 x 200 mm) heat-cured cylindrical specimens, psi.

Mix	Age (days)										
No.	1	3	7	14	28	28-HW1	28-HW3	56	91	182	365
1											
2											
3											
4			10121	10688	10533						
5	8531	9410	9947		10552						
6	8647		10397	11406	11750			11739			
7	8092		8747	9077	10211			10355			
8											
9	10647		12229	12698	12808			12086			
10	10972		13022	13654	14243			13374			
11	10172		12749	13411	14027			13602			
12	11061		12318	12334	13098			12315			
13	12058		13581	14266	14340			14785			
14	12211		13660	14460	14373			14634			
15			13622	14231				15159	14918		
16			13024	13855				14572	14422		
17	11242		13439		14252			14852			
18	11697		13189		13932			14786			
19											
20											
21											
22	10800		13087		13933				13893		
23	10754		12591		13110				13162		
24	8257		10542		10975				11356		

Notes:

HW1: Heat-curing followed by 1-day of moist-curing.
HW3: Heat-curing followed by 3-days of moist-curing.

Table A.1. Compressive strengths of 4 x 8 in. (100 x 200 mm) heat-cured cylindrical specimens, psi.

Mix	Age (days)										
No.	1	3	7	14	28	28-HW1	28-HW3	56	91	182	365
25	8335		9459		10035				10270		
26	12199		13215		13870				13886		
27	10309		10668		11493						
28	7312		8270		8985						
29	8574		9766		10313				10283		
30	10024			12775	13250						
31	9233			11644	11955						
32	10098			12354	12699						
33	9635			11262	11516						
34	10095			12490	13208						
35	9085			11290	11698						
36	9880			11852	12209						
37	10065			11531	11532						
38	8720			10982	10834						
39	8535			9604	10117						
40	7310			8817	9759						
41	10424			11345	11590						
42	7059			8806	8967						
43	7530			9328	9858						
44	8129			12126	12957						
45	6815			10258	10703						
46	7372			11244	11900						
47	10476			11852	12694						
48	8061			10337	11087						

Notes:

HW1: Heat-curing followed by 1-day of moist-curing.
HW3: Heat-curing followed by 3-days of moist-curing.

Table A.1. Compressive strengths of 4 x 8 in. (100 x 200 mm) heat-cured cylindrical specimens, psi.

Mix	Age (days)										
No.	1	3	7	14	28	28-HW1	28-HW3	56	91	182	365
49	9529			11795	11876						
50	9918		10644		12258				12259	12015	
51	7812		9127		10018				10583	10354	
52	11245		12702		13060				12939	12408	
53	6151		7727		8867				8996	8586	
54	11329		12694		13859				14015	13452	
55	10487		11312		12387				12206	11225	
56	11170		12911		12999				13040	12150	
57	11029		12409		12342				11670	11651	
58	11383		12151		12705				12621	12153	
59	11077		11688		12649				12169	11784	
60	9274		10598		11557				11797	11380	
61	10045		11512		11988				12698	11792	
62	10910		11669		12616				13377	13086	
63	10133		10674		11687				11905	11472	
64	11003		11658		13059				13191	12497	
65	11495		12011		13677				13881	13210	
66	9466		11987		12080				12296	11620	
67	10737		11684		12192				12474	11469	
68	10655		12141		12836				12519	11988	
69	8603		11223		11653				11211	10881	
70	11370		11469		12246				12704	12638	
71	10476		11337		11986				12175	12075	
72	9193		10256		10833				11319	10762	

Notes:

HW1: Heat-curing followed by 1-day of moist-curing.
HW3: Heat-curing followed by 3-days of moist-curing.

Table A.1. Compressive strengths of 4 x 8 in. (100 x 200 mm) heat-cured cylindrical specimens, psi.

Mix	Age (days)										
No.	1	3	7	14	28	28-HW1	28-HW3	56	91	182	365
73	10052		12758		13055				13515	13153	
74	9951		12490		12990				13531	12957	
75	9761		11018		11276				11249	11335	
76	9986		11574		11697				11666	11661	
77	10664		11655		11741				11462	11627	
78	10117		10965		11483				11655	12190	
79	10606		11037		11532				11798	12037	
80	10373		10977		11643				11720	12042	
81	10324		10834		11435				11255	11499	
82	8680		9333		9439				9271	9342	
83	9635		10237		10626				10396	10414	
84	10673				12552				12857	13168	
85	11948				12485				12519	12301	
86	7625				9753				10054	10418	
87	8729				9648				9721	9447	
88	9953				11639				12107	11937	
89	10555				11133				10948	11076	
90	6778				8003				8118	8287	
91	8092				8590				8674	8663	
92	9482		11103	11354	11592				11724	11703	
93	8270		9649	9583	9800				10297	10041	
94	10424		11826	12205	12023				12054	10929	
95	9815		10867	11146	10592				10865	10557	
96	9462		11470	11662	11808				12237	12094	

Notes:

HW1: Heat-curing followed by 1-day of moist-curing.
HW3: Heat-curing followed by 3-days of moist-curing.

Table A.1. Compressive strengths of 4 x 8 in. (100 x 200 mm) heat-cured cylindrical specimens, psi.

Mix	Age (days)										
No.	1	3	7	14	28	28-HW1	28-HW3	56	91	182	365
97	7890		9460	9769	9795				10268	10356	
98	11096		12032	12698	12529				12915	12729	
99	10203		11177	11705	11785				12245	11586	
100	8548				10610	11409	12107			11130	10786
101	8625				10297	10737	10864			10994	10979
102	6663				8508	9005	9259			8919	8575
103	7436				8572	9182	9404			9632	9746
104	11023				11742	12124	12055			12924	12513
105	10325				11093	11516	11801			11867	11284
106	9626				10706	11085	11083			10498	10051
107	8777				9528	9287	9253			9996	9475
108	8843				11218	11929	12221			11415	11373
109	8633				11132	11280	11853			11132	10920
110	8475				10908	10922	11604			11300	10826
111	7898				10257	10460	10668			10606	10348
112	11559				12920	13035	13301			13104	12347
113	11761				13071	13139	13463			13358	12927
114	10393				11516	11759	11977			11312	10998
115	9903				10721	10928	11150			10688	10483
116	9714				13037	13484	13499			12512	12557
117	9616				12785	12955	12918			12932	12834
118	7861				10384	10562	11211			11090	10751
119	7211				9570	10152	10003			10137	9460
120	11851				13967	13926	13678			13494	13358

Notes:

HW1: Heat-curing followed by 1-day of moist-curing.
HW3: Heat-curing followed by 3-days of moist-curing.

Table A.1. Compressive strengths of 4 x 8 in. (100 x 200 mm) heat-cured cylindrical specimens, psi.

Mix	Age (days)										
No.	1	3	7	14	28	28-HW1	28-HW3	56	91	182	365
121	11482				13487	13195	13159			13359	13067
122	11015				12763	12943	13084			12227	12282
123	10563				11381	11890	11784			11212	11311
124	12338				15150	15249	15912			15134	14964
125	13829				16606	16905	16760			16508	16871
126	9219				12455	12759	13077			12488	12342
127	11817				13878	14048	13943			13679	13542
128	11630				12934	12977	13269			12746	12721
129	12083				14349	14510	15120			14259	14295
130	9983				12455	12678	13022			12464	12307
131	12043				13140	13115	13493			13057	12973
132	14779				16298	16321	16185			15649	15731
133	14088				16393	16400	17117			16470	16722
134	10688				14159	14491	14527			14680	14405
135	14606				16124	16455	16496			16279	16268
136	11440				12624	13126	13290			12582	12621
137	12666				14127	14182	14336			13718	13687
138	10289				11729	12309	13394			11703	11781
139	11260				12988	13579	14024			12882	13027

Notes:

HW1: Heat-curing followed by 1-day of moist-curing.
HW3: Heat-curing followed by 3-days of moist-curing.

Table A.2. Compressive strengths of 4 x 8 in. (100 x 200 mm) moist-cured cylindrical specimens, psi.

Mix	Age (days)											
No.	1	7	14	28-W7	28-W14	28	56	91	182-W28	182-W182	365-W28	365-W365
1												
2												
3												
4												
5												
6	7357	10113	10915	11897			13298					
7	7019	9560	9375	11303			11507					
8												
9	8013	12065	13932	14899			13805					
10	9079	12405	13445	14391			13035					
11	8872	11982	13408	14188			14609					
12	7234	12023	13688	14524			13952					
13	9095	13335	15096	14805			14687					
14	8529	13394	15139	15145			15331					
15		12489	13579				14700					
16		11949	14004				15048					
17	8775	11982		13460			13296					
18	6817	12009		13975			13528					
19		12858	14335	15537			14782					
20		11570	13353	13949				13926				
21		11598	13229	14047				14451				
22				13448				14399				
23				13178				14690				
24				12034				13677				

Note:

(Age)-W*(number of days)*: Moist-cured for *(number of days)* and tested at the indicated *age* (for example 182-W28 is a high strength concrete specimen that had been moist-cured for 28 days and was tested at 182-days).

Table A.2. Compressive strengths of 4 x 8 in. (100 x 200 mm) moist-cured cylindrical specimens, psi.

Mix	Age (days)											
No.	1	7	14	28-W7	28-W14	28	56	91	182-W28	182-W182	365-W28	365-W365
25				10841				13320				
26				13627				15354				
27				13023								
28				10280								
29				11211				11876				
30	7649			13347								
31	7405			12107								
32	6928			13232								
33	6997			13022								
34	6373			12448								
35	6159			11634								
36	7267			13194								
37	6911			12903								
38	6782			12734								
39	6059			10958								
40	2492			11092								
41	6243			13100								
42	4794			10380								
43	4316			11512								
44	7370			11834								
45	6070			10374								
46	5449			11426								
47	6982			13382								
48	5196			11262								

Note:

(Age)-W*(number of days)*: Moist-cured for *(number of days)* and tested at the indicated *age* (for example 182-W28 is a high strength concrete specimen that had been moist-cured for 28 days and was tested at 182-days).

Table A.2. Compressive strengths of 4 x 8 in. (100 x 200 mm) moist-cured cylindrical specimens, psi.

Mix	Age (days)											
No.	1	7	14	28-W7	28-W14	28	56	91	182-W28	182-W182	365-W28	365-W365
49	5957			12656								
50				12273				13686	13570			
51				10527				12366	12533			
52				13716				14236	13638			
53				10411				11812	10958			
54				14094				14003	14821			
55				12080				13348	12755			
56				13576				14095	13873			
57				13051				12847	14176			
58				11662				14555	13579			
59				13142				13983	13445			
60				11137				13640	12701			
61				12190				13796				
62				13231				15067	14491			
63				12381				14298	14524			
64				13200				14984	14787			
65				13783				15435	15467			
66				12968				14625	15196			
67				12808				14316	13930			
68				13309				14233	14601			
69				11144				13340	13366			
70				14417				14184	15876			
71				13211				13562	14245			
72				12359				12893	13975			

Note:

(Age)-W*(number of days)*: Moist-cured for *(number of days)* and tested at the indicated *age* (for example 182-W28 is a high strength concrete specimen that had been moist-cured for 28 days and was tested at 182-days).

Table A.2. Compressive strengths of 4 x 8 in. (100 x 200 mm) moist-cured cylindrical specimens, psi.

Mix	Age (days)											
No.	1	7	14	28-W7	28-W14	28	56	91	182-W28	182-W182	365-W28	365-W365
73				13338				15212	15699			
74				14053				14978	14978			
75				12553				13716	14758			
76				12727				13487	14388			
77				13035				13768	14880			
78				13250				13687	14491			
79				13613				13482	14823			
80				13288				13078	12920			
81				12975				13143	13316			
82				11053				11297	12674			
83				12326				12280	13367			
84				13152				14555	15336			
85				14185				15203	15849			
86				10562				13337	14138			
87				10488				12745	13698			
88				12192				14634	15339			
89				13216				14647	15007			
90				9767				10983	12168			
91				10523				11792	12746			
92		11176	12393	12965				14485	14458			
93		10219	11287	11898				12923	13387			
94		11853	13312	14535				15678	15954			
95		11069	12744	13952				14680	15467			
96		11018	12605	12986				14895	15144			

Note:

(Age)-W*(number of days)*: Moist-cured for *(number of days)* and tested at the indicated *age* (for example 182-W28 is a high strength concrete specimen that had been moist-cured for 28 days and was tested at 182-days).

Table A.2. Compressive strengths of 4 x 8 in. (100 x 200 mm) moist-cured cylindrical specimens, psi.

Mix	Age (days)											
No.	1	7	14	28-W7	28-W14	28	56	91	182-W28	182-W182	365-W28	365-W365
97		9809	11271	11988				13237	13592			
98		11913	14057	15292				16500	16490			
99		10955	13128	14713				15791	16141			
100				11158	12775	12179			13467	12584	13551	13142
101				11158	12775	12179			13467	12584	13550	13142
102				10272	11228	11438			12975	12800	12937	13618
103				10272	11228	11438			12975	12800	12937	13618
104				13897	14921	14773			15684	15019	15240	14865
105				13897	14921	14773			15684	15019	15240	14865
106				12141	13320	13689			15164	14315	14682	14122
107				12141	13320	13689			15164	14315	14682	14122
108				13185	14197	14577			14944	14489	15070	14840
109				12604	13450	13751			14301	13773	14162	14243
110				11882	13223	13063			14923	14341	14649	14998
111				11084	12050	12308			13613	13328	13124	13687
112				14466	15175	15571			15865	15293	15778	15339
113				14801	14647	15636			16288	15282	15704	15352
114				14841	14900	15076			15972	15077	15752	14942
115				13633	14421	15247			15470	14613	15339	14729
116				13185	14197	14577			14944	14489	15070	14840
117				12604	13450	13751			14301	13773	14162	14243
118				11882	13223	13063			14923	14341	14649	14998
119				11084	12050	12308			13613	13328	13124	13687
120				14466	15175	15571			15865	15293	15778	15339

Note:

(Age)-W*(number of days)*: Moist-cured for *(number of days)* and tested at the indicated *age* (for example 182-W28 is a high strength concrete specimen that had been moist-cured for 28 days and was tested at 182-days).

Table A.2. Compressive strengths of 4 x 8 in. (100 x 200 mm) moist-cured cylindrical specimens, psi.

Mix	Age (days)											
No.	1	7	14	28-W7	28-W14	28	56	91	182-W28	182-W182	365-W28	365-W365
121				14801	14647	15636			16288	15294	15705	15352
122				14841	14900	15076			15972	15077	15752	14942
123				13633	14421	15247			15470	14613	15339	14729
124				16487	17134	17389			17731	16809	18516	16702
125				17117	16757	18122			18499	17272	19426	17215
126				14264	14255	14603			14768	15114	15212	15618
127				15553	15799	16028			16644	16057	14775	16107
128				15031	16103	16399			16785	15902	16379	15849
129				15604	16422	17045			17067	16504	17633	16243
130				15038	15033	15907			16203	15988	16255	16072
131				15912	16518	16444			17164	16558	17203	17275
132				16033	17404	18129			16904	16279	17829	16888
133				17573	18354	18571			19110	17638	19198	18421
134				14899	14598	16188			17606	16695	17332	17148
135				15959	18039	18626			17852	17404	19211	17494
136				14271	14357	14680			15818	14998	15701	14947
137				16623	17346	16792			17857	17205	17662	16664
138				14252	14360	14766			15391	15415	15458	15594
139				16036	15098	16134			17014	15783	17160	16066

Note:
(Age)-W*(number of days)*: Moist-cured for *(number of days)* and tested at the indicated *age* (for example 182-W28 is a high strength concrete specimen that had been moist-cured for 28 days and was tested at 182-days).

Table A.3. Compressive strengths of 6 x 12 in. (150 x 300 mm) heat- and moist-cured cylindrical specimens, psi.

Mix	Heat-Cured Age (days)				Moist-Cured Age (days)			
No.	1	3	7	28	7	14	28	56
1								
2								
3								
4	6304	8729	10032	9820				
5	8041	8414	9555	9891				
6								
7								
8								
9								
10								
11								
12								
13								
14								
15								
16								
17								
18								
19								13858
20					11127		13369	
21						12646	13758	
22	9990			13127			12688	
23	10330			12412			12773	
24	7812			10718			11612	

Table A.3. Compressive strengths of 6 x 12 in. (150 x 300 mm) heat- and moist-cured cylindrical specimens, psi.

Mix	Heat-Cured Age (days)				Moist-Cured Age (days)			
No.	1	3	7	28	7	14	28	56
25	8222			9653			11110	
26	11541			12588			13821	
27	9891			11033			12148	
28	7099			8819			9718	
29	8376			9860			11071	
30								
31								
32								
33								
34								
35								
36								
37								
38								
39								
40								
41								
42								
43								
44								
45								
46								
47								
48								

Table A.3. Compressive strengths of 6 x 12 in. (150 x 300 mm) heat- and moist-cured cylindrical specimens, psi.

Mix	Heat-Cured Age (days)				Moist-Cured Age (days)			
No.	1	3	7	28	7	14	28	56
49								
50	9443			11551			11733	
51	7747			9799			10020	
52	10621			12238			12993	
53	5725			9185			9742	
54	10376			12517			13534	
55	9803			11703			12216	
56	10425			12135			12878	
57	10269			12177			12328	
58	10653			12149			11910	
59	10558			11928			12076	
60	8509			10774			11366	
61	9416			11322			11533	
62	10085			11887			12639	
63	9113			11151			11745	
64	9477			12034			12600	
65	10411			12688			13315	
66	8861			11677			12345	
67	10358			12284			12381	
68	10212			11874			12715	
69	7869			10553			11152	
70	10488			11788			13365	
71	9851			11218			12530	
72	8760			10588			11831	

Table A.3. Compressive strengths of 6 x 12 in. (150 x 300 mm) heat- and moist-cured cylindrical specimens, psi.

Mix	Heat-Cured Age (days)				Moist-Cured Age (days)			
No.	1	3	7	28	7	14	28	56
73	9669			12253			12507	
74	10085			11748			12690	
75	9114			10846			11187	
76	9335			11073			11342	
77	10026			11175			12407	
78	9251			10602			11643	
79	9590			10719			12316	
80	9318			11059			11825	
81	9201			10606			11633	
82	7870			9155			10457	
83	8778			9299			10887	
84	9698			11661			12016	
85	10692			11304			12772	
86	7116			8633			9742	
87	8198			8887			9865	
88	9326			10738			11807	
89	9733			10100			11655	
90	6385			7498			8749	
91	7694			7972			9647	
92								
93								
94								
95								
96								

Table A.3. Compressive strengths of 6 x 12 in. (150 x 300 mm) heat- and moist-cured cylindrical specimens, psi.

Mix	Heat-Cured Age (days)				Moist-Cured Age (days)			
No.	1	3	7	28	7	14	28	56
97								
98								
99								
100	8680			10198			10137	
101	8088			8594			10137	
102	6098			7886			9522	
103	7030			8438			9522	
104	10299			11078			12867	
105	9442			10365			12867	
106	8721			10047			12063	
107	8071			8832			12063	
108	8387			11270			12646	
109	7788			10375			11831	
110	7965			9997			11452	
111	7309			9328			10051	
112	10742			11924			13582	
113	10849			12001			13825	
114	10178			11007			13550	
115	9378			10332			13374	
116	9179			11721			12646	
117	9397			11757			11831	
118	7316			9489			11452	
119	7141			8726			10051	
120	10576			12947			13582	

Table A.3. Compressive strengths of 6 x 12 in. (150 x 300 mm) heat- and moist-cured cylindrical specimens, psi.

Mix	Heat-Cured Age (days)				Moist-Cured Age (days)			
No.	1	3	7	28	7	14	28	56
121	10523			12639			13825	
122	10104			11634			13550	
123	9598			11051			13374	
124	10513			14789			14524	
125	13009			15198			11574	
126	8727			11981			13237	
127	11225			12629			14321	
128	10880			12291			13045	
129	11103			12833			13614	
130	9346			11694			12516	
131	10993			12262			14330	
132	13112			14310			13945	
133	13206			15362			14631	
134	9817			12545			13936	
135	13121			15086			13727	
136	10428			11777			13816	
137	12171			12826			14155	
138	8807			11003			13162	
139	10638			12112			13358	

APPENDIX B

STATIC MODULUS OF ELASTICITY

Table B.1. Static modulus of elasticity of 4 x 8 in. (100 x 200 mm) heat-cured cylindrical specimens, ksi.

Mix	Age (days)					
No.	1	28	28-HW1	28-HW3	182	365
1						
2						
3						
4						
5						
6						
7						
8						
9						
10						
11						
12						
13						
14						
15						
16						
17						
18						
19						
20						
21						
22	6023	6418				
23		5795				
24		5883				

Notes:

HW1: Heat-curing followed by 1-day of moist-curing.
HW3: Heat-curing followed by 3-days of moist-curing.

Table B.1. Static modulus of elasticity of 4 x 8 in. (100 x 200 mm) heat-cured cylindrical specimens, ksi.

Mix	Age (days)					
No.	1	28	28-HW1	28-HW3	182	365
25		5635				
26		6187				
27	5894	4979				
28	4996	5479				
29	4795	5162				
30						
31						
32						
33						
34						
35						
36						
37						
38						
39						
40						
41						
42						
43						
44						
45						
46						
47						
48						

Notes:

HW1: Heat-curing followed by 1-day of moist-curing.
HW3: Heat-curing followed by 3-days of moist-curing.

Table B.1. Static modulus of elasticity of 4 x 8 in. (100 x 200 mm) heat-cured cylindrical specimens, ksi.

Mix	Age (days)					
No.	1	28	28-HW1	28-HW3	182	365
49						
50	5665	5538			5626	
51	5193	5289			5248	
52	5557	5460			4790	
53	4527	4970			4857	
54	5748	5676			5896	
55	5534	5505			5136	
56	5416	5520			5534	
57	5099	5323			5243	
58	5183	5270			4976	
59	5188	5362			4843	
60	5558	5673			5785	
61	5347	5728			5161	
62	5796	5514			5431	
63	5473	5452			5308	
64	5423	5518			5357	
65	5389	5877			5326	
66	5217	5258			5213	
67	5078	5324			5110	
68	5179	5342			4907	
69	5343	5802			5553	
70	5085	5382			5334	
71	5463	5447			5036	
72	5269	5475			5175	

Notes:

HW1: Heat-curing followed by 1-day of moist-curing.
HW3: Heat-curing followed by 3-days of moist-curing.

Table B.1. Static modulus of elasticity of 4 x 8 in. (100 x 200 mm) heat-cured cylindrical specimens, ksi.

Mix	Age (days)					
No.	1	28	28-HW1	28-HW3	182	365
73	5404	5684			5313	
74	5301	5644			5426	
75	4913	5176			4904	
76	5126	5256			4961	
77	5219	5009			4543	
78	5590	5844			5347	
79	5480	5519			5319	
80	5499	5266			4886	
81	5314	5265			4793	
82	4707	4567			4088	
83	5400	5062			4118	
84	5963	6300			6143	
85	6426	6207			5447	
86	5918	6382			5894	
87	5839	5970			5383	
88	5262	6200			5493	
89	5861	5722			4857	
90	5213	5637			4736	
91	5365	5354			4683	
92		6527			6092	
93		6391			5554	
94		6472			5500	
95		6472			5360	
96		6888			6411	

Notes:

HW1: Heat-curing followed by 1-day of moist-curing.
HW3: Heat-curing followed by 3-days of moist-curing.

Table B.1. Static modulus of elasticity of 4 x 8 in. (100 x 200 mm) heat-cured cylindrical specimens, ksi.

Mix	Age (days)					
No.	1	28	28-HW1	28-HW3	182	365
97		6560			5706	
98		6109			6084	
99		6457			5844	
100	6340	6918	6803	6872	6506	6317
101	6311	6718	7013	6784	6712	6638
102	5675	6742	6749	6788	6375	6204
103	6250	6439	6624	6807	6066	6349
104	6714	6930	7231	6779	6231	6441
105	6807	6757	7045	6995	6074	6341
106	6754	6754	6903	6804	6262	6156
107	6559	6598	6777	6642	5892	5915
108	6457	6637	6667	6485	6353	6230
109	6497	6557	6664	6673	6268	6290
110	6212	6632	6838	6674	6291	6227
111	6419	6588	6495	6837	6362	6242
112	6460	6670	6812	6594	6134	6258
113	6705	6680	6696	6805	6406	6287
114	6438	6559	6348	6444	6057	6339
115	6756	6499	6486	6305	6036	6097
116	6723	6643	6704	6836	6665	6596
117	6580	6689	6811	7176	6511	6743
118	6300	6774	6784	6819	6314	6342
119	6514	6765		6863	6330	6469
120	6809	6843	6909	6922	6202	6317

Notes:

HW1: Heat-curing followed by 1-day of moist-curing.
HW3: Heat-curing followed by 3-days of moist-curing.

Table B.1. Static modulus of elasticity of 4 x 8 in. (100 x 200 mm) heat-cured cylindrical specimens, ksi.

Mix	Age (days)					
No.	1	28	28-HW1	28-HW3	182	365
121	6500	6948	6868	6761	6124	6402
122	6509	6415	6525	6810	6146	6101
123	6555	6535	6418	6522	6257	6162
124	6222	6630	6805	6657	6442	6684
125	6350	6529	6605	6415	6437	6406
126	5735	6133	5975	6202	5985	5911
127	6140	5986	6116	6085	5635	5717
128	6503	6347	6336	6226	5836	5950
129	6721	6916	6896	6984	7109	6889
130	6578	6509	6663	6674	6376	6596
131	6844	6662	6707	6578	6398	6404
132	6629	6704	6890	6892	6554	6638
133	6510	6730	7018	6992	6617	6541
134	6083	6658	6578	6589	6263	6571
135	6785	6855	6912	6879	6771	6607
136	6529	6167	6417	6574	5974	6216
137	6679	6054	6103	6043	6016	5929
138	6676	5785	6118	6142	5911	6096
139	6705	6011	5964	6229	6067	6094

Notes:

HW1: Heat-curing followed by 1-day of moist-curing.
HW3: Heat-curing followed by 3-days of moist-curing.

Table B.2. Static modulus of elasticity of 4 x 8 in. (100 x 200 mm) moist-cured cylindrical specimens, ksi.

Mix	Age (days)						
No.	28-W7	28-W14	28	182-W28	182-W182	365-W28	365-W365
1							
2							
3							
4							
5							
6							
7							
8							
9							
10							
11							
12							
13							
14							
15							
16							
17							
18							
19							
20							
21							
22							
23							
24							

Note:

(Age)-W*(number of days)*: Moist-cured for *(number of days)* and tested at the indicated *age* (for example 182-W28 is a high strength concrete specimen that had been moist-cured for 28 days and was tested at 182-days).

Table B.2. Static modulus of elasticity of 4 x 8 in. (100 x 200 mm) moist-cured cylindrical specimens, ksi.

Mix	Age (days)						
No.	28-W7	28-W14	28	182-W28	182-W182	365-W28	365-W365
25							
26							
27							
28							
29							
30							
31							
32							
33							
34							
35							
36							
37							
38							
39							
40							
41							
42							
43							
44							
45							
46							
47							
48							

Note:

(Age)-W*(number of days)*: Moist-cured for *(number of days)* and tested at the indicated *age* (for example 182-W28 is a high strength concrete specimen that had been moist-cured for 28 days and was tested at 182-days).

Table B.2. Static modulus of elasticity of 4 x 8 in. (100 x 200 mm) moist-cured cylindrical specimens, ksi.

Mix	Age (days)						
No.	28-W7	28-W14	28	182-W28	182-W182	365-W28	365-W365
49							
50				6751			
51				7314			
52				6452			
53				7308			
54				7173			
55				6940			
56				6600			
57				6646			
58				6617			
59				6626			
60				7123			
61							
62				6626			
63				6894			
64				6540			
65				6913			
66				6431			
67				6506			
68				6622			
69				7146			
70				7080			
71				6595			
72				6886			

Note:

(Age)-W*(number of days)*: Moist-cured for *(number of days)* and tested at the indicated *age* (for example 182-W28 is a high strength concrete specimen that had been moist-cured for 28 days and was tested at 182-days).

Table B.2. Static modulus of elasticity of 4 x 8 in. (100 x 200 mm) moist-cured cylindrical specimens, ksi.

Mix	Age (days)						
No.	28-W7	28-W14	28	182-W28	182-W182	365-W28	365-W365
73				6923			
74				6471			
75				6789			
76				6668			
77				6567			
78				7315			
79				10043			
80				7112			
81				7003			
82				6218			
83				6428			
84				7002			
85				6758			
86				6974			
87				6912			
88				6759			
89				6871			
90				6412			
91				6274			
92			7261	7779			
93			7195	7700			
94			7570	7777			
95			7474	7825			
96			7254	7955			

Note:

(Age)-W*(number of days)*: Moist-cured for *(number of days)* and tested at the indicated *age* (for example 182-W28 is a high strength concrete specimen that had been moist-cured for 28 days and was tested at 182-days).

Table B.2. Static modulus of elasticity of 4 x 8 in. (100 x 200 mm) moist-cured cylindrical specimens, ksi.

Mix	Age (days)						
No.	28-W7	28-W14	28	182-W28	182-W182	365-W28	365-W365
97			7082	7752			
98			7628	7910			
99			7487	7827			
100	6872	7040	7149	6984	7843	7238	7997
101	6872	7040	7149	6984	7843	7238	7997
102	6924	6932	6732	6760	7685	7030	7450
103	6924	6932	6732	6760	7685	7030	7450
104	6919	6932	7039	6696	7519	7075	7897
105	6919	6932	7039	6696	7519	7075	7897
106	6894	6538	7033	6906	7470	7124	7929
107	6894	6538	7033	6906	7470	7124	7929
108	6843	7134	7486	7250	7749	7202	7777
109	6712	6972	7311	6999	7679	7097	7940
110	6742	7069	6993	7025	7625	7177	7801
111	7128	7049	6994	7081	7604	7070	7918
112	7126	7209	7581	7060	7599	7051	7887
113	6946	7099	7232	6882	7990	7068	7760
114	6650	7389	7575	7174	7676	7124	7973
115	6613	6642	7419	6848	7521	7193	7626
116	6843	7134	7486	7250	7749	7202	7777
117	6712	6972	7311	6999	7679	7097	7940
118	6742	7069	6993	7025	7625	7177	7801
119	7128	7049	6994	7081	7604	7070	7918
120	7126	7209	7581	7060	7599	7051	7887

Note:

(Age)-W*(number of days)*: Moist-cured for *(number of days)* and tested at the indicated *age* (for example 182-W28 is a high strength concrete specimen that had been moist-cured for 28 days and was tested at 182-days).

Table B.2. Static modulus of elasticity of 4 x 8 in. (100 x 200 mm) moist-cured cylindrical specimens, ksi.

Mix	Age (days)						
No.	28-W7	28-W14	28	182-W28	182-W182	365-W28	365-W365
121	6946		7232	6882	7990	7068	7760
122	6650		7575	7174	7676	7124	7973
123	6613		7419	6848	7521	7193	7626
124	6840		7173	6835	7888	7843	7859
125	7010		7212	7443	7933	7765	7639
126	6229		7017	6194	7685	6272	7834
127	6517		6696	6510	7136	6243	7279
128	6294		7198	6596	7318	7019	7421
129	7013		7396	7425	7624	7223	8022
130	6751			7263	7983	7056	7780
131	6959		7440	7269	8055	7411	9317
132	7049		7247	6958	7897	7415	8460
133	7164		7320	7260	7751	7100	7699
134	7144		7567	7045	8021	7158	8435
135	7098		7198	7181	7826	7213	8032
136	6553		7254	6575	7491	6977	7514
137	6585		7666	6893	7740	7346	7684
138	6844		7693	6663	7636	7020	7595
139	6516		7759	7126	7681	7246	7580

Note:

(Age)-W*(number of days)*: Moist-cured for *(number of days)* and tested at the indicated *age* (for example 182-W28 is a high strength concrete specimen that had been moist-cured for 28 days and was tested at 182-days).

Table B.3. Static modulus of elasticity of 6 x 12 in. (150 x 300 mm) heat- and moist-cured cylindrical specimens, ksi.

Mix	Heat-Cured Age (days)		Moist-Cured Age (days)
No.	1	28	28
1			
2			
3			
4			
5			
6			
7			
8			
9			
10			
11			
12			
13			
14			
15			
16			
17			
18			
19			
20			
21			
22	5263	5610	
23		5331	
24		5426	

Table B.3. Static modulus of elasticity of 6 x 12 in. (150 x 300 mm) heat- and moist-cured cylindrical specimens, ksi.

Mix	Heat-Cured Age (days)		Moist-Cured Age (days)
No.	1	28	28
25	4544	5053	5908
26	5735	5769	6024
27	4835	4903	5033
28	4585	4935	5173
29	4572	4624	
30			
31			
32			
33			
34			
35			
36			
37			
38			
39			
40			
41			
42			
43			
44			
45			
46			
47			
48			

Table B.3. Static modulus of elasticity of 6 x 12 in. (150 x 300 mm) heat- and moist-cured cylindrical specimens, ksi.

Mix	Heat-Cured Age (days)		Moist-Cured Age (days)
No.	1	28	28
49			
50	4809	5489	5579
51	4701	4935	5447
52	5186	5323	5681
53	3829	4743	4827
54	5060	5545	6094
55	4650	4965	5616
56	4641	5257	6386
57	4761	5071	5634
58	4590	5047	5599
59	4798	5071	5093
60	5088	5433	5836
61	5007	5327	5345
62	5093	5327	5772
63	5049	5374	5623
64	4854	4888	5604
65	5081	5020	5467
66	4748	5475	5839
67	4816	5287	5594
68	4792	4848	5420
69	4734	5181	5442
70	5253	5334	5734
71	4864	4921	5449
72	5190	5252	5397

Table B.3. Static modulus of elasticity of 6 x 12 in. (150 x 300 mm) heat- and moist-cured cylindrical specimens, ksi.

Mix	Heat-Cured Age (days)		Moist-Cured Age (days)
No.	1	28	28
73	4804	4970	5410
74	4861	4907	5566
75	4877	4836	4967
76	4701	4826	5053
77	4660	4690	5258
78	5191	5195	5541
79	4997	5033	5560
80	4978	5043	5295
81	4740	4720	5191
82	4365	4346	4866
83	4680	4466	5157
84	5419	5606	5926
85	5653	5578	6009
86	5155	5185	5941
87	5489	5454	5659
88	5099	5174	5450
89	4772	4842	5441
90	4665	4524	5164
91	5075	4724	5070
92			
93			
94			
95			
96			

Table B.3. Static modulus of elasticity of 6 x 12 in. (150 x 300 mm) heat- and moist-cured cylindrical specimens, ksi.

Mix	Heat-Cured Age (days)		Moist-Cured Age (days)
No.	1	28	28
97			
98			
99			
100	6286	6079	6205
101	5947	6128	6205
102	5612	5896	6222
103	5560	5795	6222
104	6211	6493	6573
105	5998	6043	6573
106	6298	6213	6262
107	6229	5937	6262
108	6000	5865	6468
109	6117	6179	6297
110	5294	5819	6156
111	5566	6316	6418
112	5596	5943	6501
113	5902	5821	6473
114	6269	6051	6450
115	5826	5997	6303
116	5950	5852	6468
117	5929	6224	6297
118	5618	5930	6156
119	5647		6418
120	5781	6062	6501

Table B.3. Static modulus of elasticity of 6 x 12 in. (150 x 300 mm) heat- and moist-cured cylindrical specimens, ksi.

Mix	Heat-Cured Age (days)		Moist-Cured Age (days)
No.	1	28	28
121	5818	5967	6473
122	5973	5958	6450
123	5799	6079	6303
124	4913	5953	6208
125	5661	5638	6420
126	4915	5441	6264
127	5330	5295	5773
128	5901	5372	6417
129	5783	5879	6438
130	5709	5575	6535
131	5985	5854	6361
132	5983	5913	6256
133	5655	6022	6722
134	5434	5664	6545
135	5864	6008	6572
136	5638	5473	6306
137	5711	5557	6579
138	5787	5376	6566
139	5783	5318	6552

APPENDIX C

SPLITTING TENSILE STRENGTH

&

MODULUS OF RUPTURE

Table C.1. Twenty eight-day splitting tensile strength and modulus of rupture of heat-cured specimens, psi.

Mix	Splitting Tensile Strength		Modulus of Rupture 6 x 6 x 24 -in. (Span = 18 in.)		
No.	4 x 8 -in.	6 x 12 -in.	28	HW1	HW3
1					
2					
3					
4					
5					
6					
7					
8					
9					
10					
11					
12					
13					
14					
15					
16					
17					
18					
19					
20					
21					
22	793	758	999		
23	723	638	1084		
24	687	618	973		

Notes:

HW1: Heat-curing followed by 1-day of moist-curing.
HW3: Heat-curing followed by 3-days of moist-curing.

Table C.1. Twenty eight-day splitting tensile strength and modulus of rupture of heat-cured specimens, psi.

Mix	Splitting Tensile Strength		Modulus of Rupture 6 x 6 x 24 -in. (Span = 18 in.)		
No.	4 x 8 -in.	6 x 12 -in.	28	HW1	HW3
25	730	518	864		
26	997	804	815		
27	918	698	1001		
28	775	563	903		
29	768	591	859		
30					
31					
32					
33					
34					
35					
36					
37					
38					
39					
40					
41					
42					
43					
44					
45					
46					
47					
48					

Notes:

HW1: Heat-curing followed by 1-day of moist-curing.
HW3: Heat-curing followed by 3-days of moist-curing.

Table C.1. Twenty eight-day splitting tensile strength and modulus of rupture of heat-cured specimens, psi.

Mix	Splitting Tensile Strength		Modulus of Rupture 6 x 6 x 24 -in. (Span = 18 in.)		
No.	4 x 8 -in.	6 x 12 -in.	28	HW1	HW3
49					
50	988	677	1051		
51	869	666	909		
52	1086	836	1067		
53	784	626	823		
54	1010	849	941		
55	896	740	1049		
56	1000	751	1098		
57	969	770	1081		
58	851	812	995		
59	1019	654	963		
60	949	655	937		
61	944	679	859		
62	1014	730	829		
63	975	685	1003		
64	1009	752	939		
65	941	872	853		
66	975	710	1013		
67	1062	734	1041		
68	901	704	1053		
69	829	651	1026		
70	1010	744	1105		
71	1048	707	1070		
72	911	601	958		

Notes:

HW1: Heat-curing followed by 1-day of moist-curing.
HW3: Heat-curing followed by 3-days of moist-curing.

Table C.1. Twenty eight-day splitting tensile strength and modulus of rupture of heat-cured specimens, psi.

Mix	Splitting Tensile Strength		Modulus of Rupture 6 x 6 x 24 -in. (Span = 18 in.)		
No.	4 x 8 -in.	6 x 12 -in.	28	HW1	HW3
73	1068	725	1106		
74	1013	764	1024		
75	854	690	1053		
76	927	706	1068		
77	926	749	1012		
78	882	589	896		
79	869	647	990		
80	843	651	1081		
81	817	657	1031		
82	746	612	986		
83	817	570	1025		
84	904	690	889		
85	955	749	965		
86	840	580	804		
87	753	602	837		
88	882	701	781		
89	934	730	870		
90	721	535	728		
91	765	587	875		
92					
93					
94					
95					
96					

Notes:

HW1: Heat-curing followed by 1-day of moist-curing.
HW3: Heat-curing followed by 3-days of moist-curing.

Table C.1. Twenty eight-day splitting tensile strength and modulus of rupture of heat-cured specimens, psi.

Mix	Splitting Tensile Strength		Modulus of Rupture 6 x 6 x 24 -in. (Span = 18 in.)		
No.	4 x 8 -in.	6 x 12 -in.	28	HW1	HW3
97					
98					
99					
100		743	878	963	963
101		689	948	1023	918
102		598	880	912	933
103		678	943	818	928
104		711	1087	1087	1218
105		722	1055	1106	1151
106		679	1073	1052	1133
107		679	992	991	1023
108		779	992	1032	1152
109		757	1038	1151	1035
110		670	861	858	826
111		657	896	912	920
112		736	1058	963	1103
113		681	1108	1033	1040
114		778	1053	1002	1033
115		695	993	1010	1005
116		833	838	991	921
117		798	1061	1133	963
118		746	776	848	895
119		664	887	945	950
120		703	1066	995	1023

Notes:

HW1: Heat-curing followed by 1-day of moist-curing.
HW3: Heat-curing followed by 3-days of moist-curing.

Table C.1. Twenty eight-day splitting tensile strength and modulus of rupture of heat-cured specimens, psi.

Mix	Splitting Tensile Strength		Modulus of Rupture 6 x 6 x 24 -in. (Span = 18 in.)		
No.	4 x 8 -in.	6 x 12 -in.	28	HW1	HW3
121		751	1000	1037	1053
122		749	1048	1003	963
123		809	972	1077	1073
124		839	1188	1083	1330
125		829	1015	1078	1023
126		746	1240	1148	1193
127		824	968	1148	1111
128		796	948	1001	930
129		688	952	910	897
130		679	823	998	1011
131		761	1315	1182	1213
132		828	1233	1272	1205
133		818	1058	978	1035
134		819	1072	1036	1000
135		834	1023	966	836
136		658	952	1057	1053
137		714	1108	933	1066
138		705	888	818	831
139		821	937	955	971

Notes:

HW1: Heat-curing followed by 1-day of moist-curing.
HW3: Heat-curing followed by 3-days of moist-curing.

Table C.2. Twenty eight-day splitting tensile strength and modulus of rupture of moist-cured specimens, psi.

Mix	Splitting Tensile Strength		Modulus of Rupture
No.	4 x 8 -in.	6 x 12 -in.	6 x 6 x 24 -in. (Span = 18 in.)
1			
2			
3			
4			
5			
6			
7			
8			
9			
10			
11			
12			
13			
14			
15			
16			
17			
18			
19			
20			
21			
22			1207
23	717	731	1497
24	732	595	1160

Notes:

HW1: Heat-curing followed by 1-day of moist-curing.
HW3: Heat-curing followed by 3-days of moist-curing.

Table C.2. Twenty eight-day splitting tensile strength and modulus of rupture of moist-cured specimens, psi.

Mix	Splitting Tensile Strength		Modulus of Rupture
No.	4 x 8 -in.	6 x 12 -in.	6 x 6 x 24 -in. (Span = 18 in.)
25	795	602	1122
26	1016	729	1266
27	894	651	1252
28	716	626	989
29	804	570	872
30			
31			
32			
33			
34			
35			
36			
37			
38			
39			
40			
41			
42			
43			
44			
45			
46			
47			
48			

Notes:

HW1: Heat-curing followed by 1-day of moist-curing.
HW3: Heat-curing followed by 3-days of moist-curing.

Table C.2. Twenty eight-day splitting tensile strength and modulus of rupture of moist-cured specimens, psi.

Mix	Splitting Tensile Strength		Modulus of Rupture
No.	4 x 8 -in.	6 x 12 -in.	6 x 6 x 24 -in. (Span = 18 in.)
49			
50	951	716	1256
51	751	670	1111
52	955	741	1332
53	719	568	988
54	933	840	1221
55	910	752	1116
56	955	772	1087
57	934	602	1047
58	794	675	1218
59	927	715	1274
60	935	749	1075
61	1021	734	1033
62	901	809	1218
63	874	824	1118
64	963	777	1268
65	1035	803	1220
66	1053	775	1498
67	990	678	1377
68	880	722	1299
69	857	794	1152
70	996	712	1037
71	943	616	834
72	946	791	898

Notes:

HW1: Heat-curing followed by 1-day of moist-curing.
HW3: Heat-curing followed by 3-days of moist-curing.

Table C.2. Twenty eight-day splitting tensile strength and modulus of rupture of moist-cured specimens, psi.

Mix	Splitting Tensile Strength		Modulus of Rupture
No.	4 x 8 -in.	6 x 12 -in.	6 x 6 x 24 -in. (Span = 18 in.)
73	896	753	1138
74	914	725	1178
75	813	699	1105
76	837	662	1069
77	885	746	1092
78	894	729	1196
79	955	609	1061
80	881	775	1112
81	738	765	979
82	757	679	887
83	902	672	958
84	917	807	1558
85	1022	795	1506
86	767	589	1266
87	714	649	971
88	921	790	1358
89	836	768	1471
90	777	644	1230
91	767	601	1146
92			
93			
94			
95			
96			

Notes:

HW1: Heat-curing followed by 1-day of moist-curing.
HW3: Heat-curing followed by 3-days of moist-curing.

Table C.2. Twenty eight-day splitting tensile strength and modulus of rupture of moist-cured specimens, psi.

Mix	Splitting Tensile Strength		Modulus of Rupture
No.	4 x 8 -in.	6 x 12 -in.	6 x 6 x 24 -in. (Span = 18 in.)
97			
98			
99			
100		679	1256
101		679	1256
102		582	1217
103		582	1217
104		768	1510
105		768	1510
106		752	1333
107		752	1333
108		839	1493
109		746	1420
110		725	1428
111		636	1389
112		728	1520
113		705	1552
114		805	1438
115		721	1430
116		839	1493
117		746	1420
118		725	1428
119		636	1389
120		728	1520

Notes:

HW1: Heat-curing followed by 1-day of moist-curing.
HW3: Heat-curing followed by 3-days of moist-curing.

Table C.2. Twenty eight-day splitting tensile strength and modulus of rupture of moist-cured specimens, psi.

Mix	Splitting Tensile Strength		Modulus of Rupture
No.	4 x 8 -in.	6 x 12 -in.	6 x 6 x 24 -in. (Span = 18 in.)
121		705	1552
122		805	1438
123		721	1430
124		963	1521
125		847	1446
126		790	1262
127		789	1258
128		891	1743
129		963	1653
130		791	1661
131		858	1543
132		968	1496
133		1030	1598
134		898	1455
135		957	1422
136		711	1380
137		834	1422
138		794	1341
139		787	1327

Notes:

HW1: Heat-curing followed by 1-day of moist-curing.
HW3: Heat-curing followed by 3-days of moist-curing.

APPENDIX D

SHRINKAGE & CREEP

Table D.1. Shrinkage strains of 4 x 11 in. (100 x 280 mm) heat- and moist-cured cylindrical specimens, με.

Time	Heat-Cured								Moist-Cured				
days	No. 108	No. 116	No. 124	No. 128	No. 131	No. 132	No. 136	No. 139	No. 124	No. 128	No. 129	No. 131	No. 132
0	0	0	0	0	0	0	0	0	0	0	0	0	0
1	46	70	22	42	21	19	17	32	18	39	23	22	30
2	51	74	35	51	25	32	28	42	27	43	35	29	36
6	98	117	61	81	65	54	66	73	74	93	87	84	79
9	124	173	83	109	90	79	94	109	105	128	113	109	113
13	151	178	114	138	115	101	117	119	139	159	142	143	143
23	200	219	146	171	160	140	154	170	191	208	187	199	190
30	242	256	173	211	177	166	193	196	218	242	224	224	222
37	261	273	196	227	201	187	214	215	239	266	250	253	246
44	277	286	211	239	225	205	235	235	253	277	266	270	265
51	284	296	227	252	232	223	236	244	263	291	276	275	274
65	311	326	258	277	259	249	264	269	287	318	301	301	298
72	320	337	267	291	265	259	283	282	298	332	312	312	310
79	336	350	278	301	282	265	291	292	307	342	323	326	320
86	347	357	286	307	289	276	299	301	316	345	329	331	329
93	347	357	299	311	291	288	308	304	317	349	335	340	332
100	353	369	306	317	301	295	312	314	326	362	345	343	339
112	377	392	320	337	319	305	327	332	343	377	360	359	357
121	383	400	320	339	322	311	338	332	343	377	364	362	355
128	385	395	331	339	324	320	339	339	348	381	362	367	357
135	387	399	333	346	329	324	339	337	352	382	360	366	361
141	392	419	339	352	332	326	346	345	355	386	369	370	363
149	417	419	350	363	345	337	356	357	363	397	377	387	374
155	404	431	351	360	339	337	358	353	360	395	373	381	374

Table D.1. Shrinkage strains of 4 x 11 in. (100 x 280 mm) heat- and moist-cured cylindrical specimens, με.

Time	Heat-Cured								Moist-Cured				
days	No. 108	No. 116	No. 124	No. 128	No. 131	No. 132	No. 136	No. 139	No. 124	No. 128	No. 129	No. 131	No. 132
163	413	439	355	372	349	341	365	359	365	403	383	389	381
170	425	434	369	372	350	351	371	369	371	403	395	388	383
176	422	437	366	382	366	350	372	368	371	414	392	400	392
184	429	439	374	388	363	358	384	372	376	415	395	400	393
191	446	468	380	378	362	363	389	373	392	411	390	395	392
198	453	461	382	392	375	367	395	391	388	429	410	411	403
208	443	468	388	396	374	372	392	386	390	428	404	409	407
212	445	477	389	398	371	369	394	384	386	429	406	410	402
218	458	482	392	404	382	374	396	390	390	434	410	416	412
226	473	488	394	406	383	376	405	399	394	434	418	415	409
236	477	507	402	415	394	385	412	399	403	445	422	431	419
240	495	500	405	426	397	385	416	408	405	457	423	435	423
247	482	497	405	421	398	383	425	400	409	451	430	440	425
254	483	514	409	422	402	396	424	407	410	453	431	443	423
260	494	528	412	432	412	396	428	415	408	463	432	443	435
268	514	526	416	433	411	396	433	427	417	463	437	447	433
275	505	545	420	436	416	402	439	428	418	466	438	451	435
285	522	546	423	442	416	401	444	439	423	471	446	460	439
289	528	554	427	444	423	409	439	429	420	475	446	460	445
295	528	547	436	451	431	417	452	437	423	483	451	467	446
302	526	556	433	450	431	415	450	442	428	476	455	467	450
310	533	559	435	457	431	415	455	445	430	484	453	471	452
320	529	567	444	459	432	427	461	441	430	483	457	477	454
324	539	568	446	464	446	425	474	454	431	496	461	475	460

Table D.1. Shrinkage strains of 4 x 11 in. (100 x 280 mm) heat- and moist-cured cylindrical specimens, με - Reference Mixes

Time	Heat-Cured								Moist-Cured				
days	No. 108	No. 116	No. 124	No. 128	No. 131	No. 132	No. 136	No. 139	No. 124	No. 128	No. 129	No. 131	No. 132
335	546	570	449	462	443	428	468	445	437	492	469	480	465
338	544	583	453	463	444	430	467	451	439	495	464	493	465
345	562	586	455	469	449	436	478	458	437	500	466	485	470
352	559	600	460	473	452	439	474	457	445	504	467	493	470
359	562	601	461	475	461	439	488	461	444	506	472	495	477
372	565	600	467	478	458	443	486	464	449	511	480	506	481
380	565	603	469	486	468	444	492	467	452	518	481	509	486

Table D.2. Creep strains of 4 x 11 in. (100 x 280 mm) cylindrical specimens from Mix No. 108, με.

Time Since Loading (days)	Heat-Cured Sustained Load=63240 lb. (Sustained Stress=5032 psi)					Moist-Cured				
	Shrinkage Strain	Total Strain	Creep Strain	Creep Coefficient	Specific Creep, με/psi	Shrinkage Strain	Total Strain	Creep Strain	Creep Coefficient	Specific Creep, με/psi
0	0	806	0	0.00	0.0000					
1	46	1098	246	0.31	0.0490					
2	51	1182	326	0.40	0.0647					
6	98	1411	507	0.63	0.1008					
9	124	1551	620	0.77	0.1233					
13	151	1686	730	0.91	0.1450					
23	200	1814	808	1.00	0.1605					
30	242	1907	859	1.07	0.1706					
37	261	2025	959	1.19	0.1905					
44	277	2090	1008	1.25	0.2003					
51	284	2138	1048	1.30	0.2082					
65	311	2172	1056	1.31	0.2098					
72	320	2289	1163	1.44	0.2311					
79	336	2306	1164	1.44	0.2314					
86	347	2340	1187	1.47	0.2359					
93	347	2332	1179	1.46	0.2342					
100	353	2371	1212	1.50	0.2409					
112	377	2394	1211	1.50	0.2406					
121	383	2412	1223	1.52	0.2430					
128	385	2503	1312	1.63	0.2606					
135	387	2519	1326	1.65	0.2636					
141	392	2504	1305	1.62	0.2594					
149	417	2571	1348	1.67	0.2679					
155	404	2508	1298	1.61	0.2578					

Table D.2. Creep strains of 4 x 11 in. (100 x 280 mm) cylindrical specimens from Mix No. 108, με.

Time Since Loading (days)	Heat-Cured Sustained Load=63240 lb. (Sustained Stress=5032 psi)					Moist-Cured				
	Shrinkage Strain	Total Strain	Creep Strain	Creep Coefficient	Specific Creep, με/psi	Shrinkage Strain	Total Strain	Creep Strain	Creep Coefficient	Specific Creep, με/psi
163	413	2540	1321	1.64	0.2625					
170	425	2557	1326	1.65	0.2635					
176	422	2545	1317	1.63	0.2617					
184	429	2596	1362	1.69	0.2706					
191	446	2607	1355	1.68	0.2692					
198	453	2697	1438	1.78	0.2857					
208	443	2643	1394	1.73	0.2769					
212	445	2614	1363	1.69	0.2708					
218	458	2718	1454	1.80	0.2890					
226	473	2699	1421	1.76	0.2823					
236	477	2732	1449	1.80	0.2879					
240	495	2736	1435	1.78	0.2852					
247	482	2704	1416	1.76	0.2814					
254	483	2727	1438	1.78	0.2857					
260	494	2745	1445	1.79	0.2871					
268	514	2753	1432	1.78	0.2846					
275	505	2782	1470	1.82	0.2922					
285	522	2779	1452	1.80	0.2884					
289	528	2836	1502	1.86	0.2984					
295	528	2807	1473	1.83	0.2927					
302	526	2843	1512	1.88	0.3004					
310	533	2839	1500	1.86	0.2980					
320	529	2827	1492	1.85	0.2965					
324	539	2858	1513	1.88	0.3006					

Table D.2. Creep strains of 4 x 11 in. (100 x 280 mm) cylindrical specimens from Mix No. 108, με.

Time Since Loading (days)	Heat-Cured Sustained Load=63240 lb. (Sustained Stress=5032 psi)					Moist-Cured				
	Shrinkage Strain	Total Strain	Creep Strain	Creep Coefficient	Specific Creep, με/psi	Shrinkage Strain	Total Strain	Creep Strain	Creep Coefficient	Specific Creep, με/psi
335	546	2811	1460	1.81	0.2901					
338	544	2894	1544	1.92	0.3069					
345	562	2887	1519	1.88	0.3018					
352	559	2896	1531	1.90	0.3042					
359	562	2904	1535	1.91	0.3051					
372	565	2908	1537	1.91	0.3055					
380	565	2907	1536	1.91	0.3052					

Table D.3. Creep strains of 4 x 11 in. (100 x 280 mm) cylindrical specimens from Mix No. 116, με.

Time Since Loading (days)	Heat-Cured Sustained Load=69208 lb. (Sustained Stress=5507 psi)					Moist-Cured				
	Shrinkage Strain	Total Strain	Creep Strain	Creep Coefficient	Specific Creep, με/psi	Shrinkage Strain	Total Strain	Creep Strain	Creep Coefficient	Specific Creep, με/psi
0	0	805	0	0.00	0.0000					
1	70	1071	196	0.24	0.0357					
2	74	1175	296	0.37	0.0537					
6	117	1471	549	0.68	0.0997					
9	173	1562	584	0.73	0.1061					
13	178	1721	738	0.92	0.1340					
23	219	1809	785	0.98	0.1425					
30	256	1941	880	1.09	0.1597					
37	273	2037	960	1.19	0.1742					
44	286	2057	966	1.20	0.1754					
51	296	2170	1069	1.33	0.1941					
65	326	2175	1044	1.30	0.1895					
72	337	2320	1179	1.47	0.2141					
79	350	2327	1172	1.46	0.2129					
86	357	2401	1239	1.54	0.2250					
93	357	2369	1207	1.50	0.2191					
100	369	2411	1237	1.54	0.2247					
112	392	2466	1269	1.58	0.2304					
121	400	2413	1208	1.50	0.2193					
128	395	2499	1300	1.61	0.2360					
135	399	2561	1356	1.69	0.2463					
141	419	2534	1310	1.63	0.2379					
149	419	2550	1326	1.65	0.2408					
155	431	2573	1337	1.66	0.2427					

Table D.3. Creep strains of 4 x 11 in. (100 x 280 mm) cylindrical specimens from Mix No. 116, με.

Time Since Loading (days)	Heat-Cured Sustained Load=69208 lb. (Sustained Stress=5507 psi)					Moist-Cured				
	Shrinkage Strain	Total Strain	Creep Strain	Creep Coefficient	Specific Creep, με/psi	Shrinkage Strain	Total Strain	Creep Strain	Creep Coefficient	Specific Creep, με/psi
163	439	2621	1377	1.71	0.2501					
170	434	2645	1406	1.75	0.2553					
176	437	2520	1278	1.59	0.2320					
184	439	2628	1385	1.72	0.2514					
191	468	2652	1380	1.71	0.2505					
198	461	2715	1449	1.80	0.2630					
208	468	2697	1424	1.77	0.2585					
212	477	2664	1383	1.72	0.2511					
218	482	2728	1441	1.79	0.2617					
226	488	2702	1410	1.75	0.2560					
236	507	2763	1452	1.80	0.2636					
240	500	2738	1433	1.78	0.2603					
247	497	2686	1384	1.72	0.2513					
254	514	2719	1401	1.74	0.2544					
260	528	2768	1435	1.78	0.2605					
268	526	2734	1403	1.74	0.2548					
275	545	2800	1450	1.80	0.2633					
285	546	2767	1417	1.76	0.2572					
289	554	2853	1494	1.86	0.2712					
295	547	2820	1468	1.82	0.2666					
302	556	2871	1510	1.88	0.2741					
310	559	2905	1542	1.92	0.2799					
320	567	2857	1485	1.85	0.2696					
324	568	2860	1488	1.85	0.2701					

Table D.3. Creep strains of 4 x 11 in. (100 x 280 mm) cylindrical specimens from Mix No. 116, με.

Time Since Loading (days)	Heat-Cured Sustained Load=69208 lb. (Sustained Stress=5507 psi)					Moist-Cured				
	Shrinkage Strain	Total Strain	Creep Strain	Creep Coefficient	Specific Creep, με/psi	Shrinkage Strain	Total Strain	Creep Strain	Creep Coefficient	Specific Creep, με/psi
335	570	2844	1470	1.83	0.2669					
338	583	2907	1518	1.89	0.2757					
345	586	2877	1486	1.85	0.2698					
352	600	2976	1571	1.95	0.2853					
359	601	2942	1536	1.91	0.2790					
372	600	2953	1548	1.92	0.2811					
380	603	2950	1542	1.92	0.2800					

Table D.4. Creep strains of 4 x 11 in. (100 x 280 mm) cylindrical specimens from Mix No. 124, με.

Time Since Loading (days)	Heat-Cured Sustained Load=79264 lb. (Sustained Stress=6308 psi)					Moist-Cured Sustained Load=90551 lb. (Sustained Stress=7206 psi)				
	Shrinkage Strain	Total Strain	Creep Strain	Creep Coefficient	Specific Creep, με/psi	Shrinkage Strain	Total Strain	Creep Strain	Creep Coefficient	Specific Creep, με/psi
0	0	1014	0	0.00	0.0000	0	1062	0	0.00	0.0000
1	22	1153	117	0.12	0.0186	18	1236	157	0.15	0.0217
2	35	1171	122	0.12	0.0193	27	1295	206	0.19	0.0286
6	61	1321	245	0.24	0.0389	72	1451	318	0.30	0.0441
9	83	1338	241	0.24	0.0382	101	1523	360	0.34	0.0500
13	114	1461	332	0.33	0.0527	133	1592	398	0.37	0.0552
23	146	1542	382	0.38	0.0606	182	1710	467	0.44	0.0648
30	173	1612	425	0.42	0.0674	208	1735	465	0.44	0.0645
37	196	1679	469	0.46	0.0743	230	1793	502	0.47	0.0697
44	211	1698	473	0.47	0.0749	243	1815	510	0.48	0.0708
51	227	1759	518	0.51	0.0821	252	1861	547	0.52	0.0759
65	258	1789	517	0.51	0.0819	275	1906	569	0.54	0.0790
72	267	1800	519	0.51	0.0823	284	1898	552	0.52	0.0766
79	278	1870	578	0.57	0.0917	293	1957	603	0.57	0.0837
86	286	1839	539	0.53	0.0854	302	1952	589	0.55	0.0817
93	299	1906	593	0.58	0.0940	304	1981	616	0.58	0.0855
100	306	1928	608	0.60	0.0963	311	2009	637	0.60	0.0883
112	320	1908	574	0.57	0.0910	327	1992	603	0.57	0.0837
121	320	1969	635	0.63	0.1006	327	2018	629	0.59	0.0873
128	331	1961	616	0.61	0.0977	332	2062	669	0.63	0.0928
135	333	1988	641	0.63	0.1017	336	2076	679	0.64	0.0943
141	339	2027	674	0.67	0.1069	339	2071	670	0.63	0.0930
149	350	2045	680	0.67	0.1078	347	2075	667	0.63	0.0925
155	351	2044	679	0.67	0.1077	345	2066	660	0.62	0.0915

Table D.4. Creep strains of 4 x 11 in. (100 x 280 mm) cylindrical specimens from Mix No. 124, με.

Time Since Loading (days)	Heat-Cured Sustained Load=79264 lb. (Sustained Stress=6308 psi)					Moist-Cured Sustained Load=90551 lb. (Sustained Stress=7206 psi)				
	Shrinkage Strain	Total Strain	Creep Strain	Creep Coefficient	Specific Creep, με/psi	Shrinkage Strain	Total Strain	Creep Strain	Creep Coefficient	Specific Creep, με/psi
163	355	2049	680	0.67	0.1078	348	2103	693	0.65	0.0962
170	369	2038	655	0.65	0.1039	352	2091	677	0.64	0.0940
176	366	2069	689	0.68	0.1093	354	2104	688	0.65	0.0954
184	374	2112	724	0.71	0.1148	359	2128	708	0.67	0.0982
191	380	2099	705	0.70	0.1118	373	2150	715	0.67	0.0992
198	382	2142	745	0.73	0.1182	369	2155	724	0.68	0.1005
208	388	2116	714	0.70	0.1132	373	2170	735	0.69	0.1021
212	389	2142	739	0.73	0.1172	370	2114	683	0.64	0.0948
218	392	2161	755	0.74	0.1196	373	2176	742	0.70	0.1029
226	394	2176	768	0.76	0.1218	376	2170	733	0.69	0.1017
236	402	2194	778	0.77	0.1233	384	2201	755	0.71	0.1048
240	405	2179	759	0.75	0.1204	385	2201	754	0.71	0.1046
247	405	2225	805	0.79	0.1277	389	2168	717	0.68	0.0995
254	409	2242	818	0.81	0.1297	390	2208	756	0.71	0.1049
260	412	2234	807	0.80	0.1280	389	2170	719	0.68	0.0998
268	416	2253	823	0.81	0.1304	398	2188	729	0.69	0.1011
275	420	2240	806	0.79	0.1278	399	2243	783	0.74	0.1086
285	423	2221	785	0.77	0.1244	405	2220	754	0.71	0.1046
289	427	2270	829	0.82	0.1314	400	2212	751	0.71	0.1042
295	436	2241	791	0.78	0.1254	403	2214	750	0.71	0.1041
302	433	2283	835	0.82	0.1324	406	2256	788	0.74	0.1093
310	435	2291	842	0.83	0.1335	411	2264	792	0.75	0.1099
320	444	2281	823	0.81	0.1305	411	2210	737	0.69	0.1023
324	446	2314	854	0.84	0.1355	411	2277	805	0.76	0.1117

Table D.4. Creep strains of 4 x 11 in. (100 x 280 mm) cylindrical specimens from Mix No. 124, με.

Time Since Loading (days)	Heat-Cured Sustained Load=79264 lb. (Sustained Stress=6308 psi)					Moist-Cured Sustained Load=90551 lb. (Sustained Stress=7206 psi)				
	Shrinkage Strain	Total Strain	Creep Strain	Creep Coefficient	Specific Creep, με/psi	Shrinkage Strain	Total Strain	Creep Strain	Creep Coefficient	Specific Creep, με/psi
335	449	2317	854	0.84	0.1353	417	2258	779	0.73	0.1081
338	453	2279	812	0.80	0.1287	420	2243	762	0.72	0.1058
345	455	2304	834	0.82	0.1323	417	2230	752	0.71	0.1043
352	460	2320	846	0.83	0.1341	424	2246	761	0.72	0.1056
359	461	2308	833	0.82	0.1321	423	2262	777	0.73	0.1079
372	467	2335	854	0.84	0.1354	428	2298	808	0.76	0.1121
380	469	2346	863	0.85	0.1368	432	2269	776	0.73	0.1077

Table D.5. Creep strains of 4 x 11 in. (100 x 280 mm) cylindrical specimens from Mix No. 128, με.

Time Since Loading (days)	Heat-Cured Sustained Load=82032 lb. (Sustained Stress=6528 psi)					Moist-Cured Sustained Load=85100 lb. (Sustained Stress=6772 psi)				
	Shrinkage Strain	Total Strain	Creep Strain	Creep Coefficient	Specific Creep, με/psi	Shrinkage Strain	Total Strain	Creep Strain	Creep Coefficient	Specific Creep, με/psi
0	0	982	0	0.00	0.0000	0	1119	0	0.00	0.0000
1	42	1103	80	0.08	0.0122	34	1311	158	0.14	0.0233
2	51	1211	179	0.18	0.0274	32	1368	217	0.19	0.0321
6	81	1383	321	0.33	0.0492	73	1478	287	0.26	0.0424
9	109	1470	379	0.39	0.0581	97	1512	296	0.26	0.0438
13	138	1575	456	0.46	0.0698	130	1628	379	0.34	0.0560
23	171	1675	522	0.53	0.0800	158	1724	448	0.40	0.0662
30	211	1776	583	0.59	0.0894	190	1744	436	0.39	0.0644
37	227	1834	625	0.64	0.0958	204	1810	487	0.44	0.0720
44	239	1898	677	0.69	0.1038	213	1837	506	0.45	0.0747
51	252	1908	674	0.69	0.1032	235	1832	478	0.43	0.0706
65	277	1983	725	0.74	0.1110	251	1916	546	0.49	0.0807
72	291	2034	762	0.78	0.1168	260	1922	543	0.49	0.0801
79	301	2075	792	0.81	0.1214	280	1962	563	0.50	0.0832
86	307	2088	800	0.82	0.1226	283	1994	592	0.53	0.0874
93	311	2072	780	0.79	0.1194	276	1983	588	0.53	0.0869
100	317	2078	779	0.79	0.1194	294	2009	596	0.53	0.0880
112	337	2119	800	0.82	0.1226	307	2029	604	0.54	0.0892
121	339	2167	847	0.86	0.1297	307	2076	650	0.58	0.0959
128	339	2174	853	0.87	0.1307	306	2070	646	0.58	0.0954
135	346	2158	831	0.85	0.1273	310	2077	649	0.58	0.0958
141	352	2205	872	0.89	0.1336	315	2108	675	0.60	0.0997
149	363	2231	887	0.90	0.1358	314	2107	674	0.60	0.0996
155	360	2189	847	0.86	0.1298	316	2082	648	0.58	0.0957

Table D.5. Creep strains of 4 x 11 in. (100 x 280 mm) cylindrical specimens from Mix No. 128, με.

Time Since Loading (days)	Heat-Cured Sustained Load=82032 lb. (Sustained Stress=6528 psi)					Moist-Cured Sustained Load=85100 lb. (Sustained Stress=6772 psi)				
	Shrinkage Strain	Total Strain	Creep Strain	Creep Coefficient	Specific Creep, με/psi	Shrinkage Strain	Total Strain	Creep Strain	Creep Coefficient	Specific Creep, με/psi
163	372	2214	861	0.88	0.1319	321	2132	693	0.62	0.1023
170	372	2258	904	0.92	0.1384	324	2129	686	0.61	0.1013
176	382	2269	906	0.92	0.1388	333	2136	684	0.61	0.1010
184	388	2247	878	0.89	0.1345	334	2171	718	0.64	0.1061
191	378	2286	927	0.94	0.1420	329	2133	686	0.61	0.1012
198	392	2278	905	0.92	0.1386	334	2182	729	0.65	0.1077
208	396	2293	916	0.93	0.1403	351	2174	704	0.63	0.1040
212	398	2266	887	0.90	0.1359	340	2184	725	0.65	0.1070
218	404	2295	909	0.93	0.1392	347	2171	705	0.63	0.1041
226	406	2280	892	0.91	0.1367	343	2197	735	0.66	0.1086
236	415	2317	921	0.94	0.1411	353	2240	769	0.69	0.1135
240	426	2299	892	0.91	0.1366	357	2214	738	0.66	0.1090
247	421	2331	928	0.95	0.1422	352	2233	762	0.68	0.1125
254	422	2350	947	0.96	0.1450	356	2212	737	0.66	0.1089
260	432	2362	949	0.97	0.1453	372	2238	747	0.67	0.1103
268	433	2343	928	0.95	0.1422	379	2234	736	0.66	0.1087
275	436	2349	931	0.95	0.1427	378	2247	750	0.67	0.1108
285	442	2375	952	0.97	0.1458	373	2271	780	0.70	0.1152
289	444	2410	984	1.00	0.1507	376	2312	817	0.73	0.1207
295	451	2382	949	0.97	0.1454	391	2263	754	0.67	0.1113
302	450	2372	940	0.96	0.1440	388	2277	770	0.69	0.1137
310	457	2427	988	1.01	0.1514	378	2316	820	0.73	0.1210
320	459	2422	982	1.00	0.1504	380	2329	831	0.74	0.1227
324	464	2412	967	0.98	0.1481	398	2307	791	0.71	0.1168

Table D.5. Creep strains of 4 x 11 in. (100 x 280 mm) cylindrical specimens from Mix No. 128, με.

Time Since Loading (days)	Heat-Cured Sustained Load=82032 lb. (Sustained Stress=6528 psi)					Moist-Cured Sustained Load=85100 lb. (Sustained Stress=6772 psi)				
	Shrinkage Strain	Total Strain	Creep Strain	Creep Coefficient	Specific Creep, με/psi	Shrinkage Strain	Total Strain	Creep Strain	Creep Coefficient	Specific Creep, με/psi
335	462	2413	969	0.99	0.1484	391	2307	798	0.71	0.1179
338	463	2450	1006	1.02	0.1540	389	2349	842	0.75	0.1243
345	469	2432	982	1.00	0.1504	404	2329	806	0.72	0.1190
352	473	2436	981	1.00	0.1503	400	2339	820	0.73	0.1211
359	475	2430	974	0.99	0.1492	401	2318	798	0.71	0.1179
372	478	2430	970	0.99	0.1486	411	2376	846	0.76	0.1249
380	486	2438	971	0.99	0.1488	416	2358	823	0.74	0.1215

Table D.6. Creep strains of 4 x 11 in. (100 x 280 mm) cylindrical specimens from Mix No. 129, με.

Time Since Loading (days)	Heat-Cured					Moist-Cured Sustained Load=86791 lb. (Sustained Stress=6907 psi)				
	Shrinkage Strain	Total Strain	Creep Strain	Creep Coefficient	Specific Creep, με/psi	Shrinkage Strain	Total Strain	Creep Strain	Creep Coefficient	Specific Creep, με/psi
0						0	970	0	0.00	0.0000
1						25	1115	120	0.12	0.0173
2						38	1163	155	0.16	0.0225
6						77	1348	300	0.31	0.0435
9						98	1367	298	0.31	0.0432
13						132	1460	358	0.37	0.0519
23						162	1582	450	0.46	0.0651
30						207	1651	474	0.49	0.0687
37						216	1707	521	0.54	0.0754
44						245	1758	542	0.56	0.0785
51						243	1768	555	0.57	0.0803
65						268	1858	620	0.64	0.0898
72						287	1882	625	0.64	0.0905
79						295	1899	634	0.65	0.0918
86						289	1942	683	0.70	0.0989
93						301	1927	656	0.68	0.0950
100						310	1942	663	0.68	0.0960
112						328	1992	693	0.71	0.1004
121						333	2059	756	0.78	0.1094
128						334	2064	760	0.78	0.1100
135						315	2004	719	0.74	0.1041
141						340	2040	730	0.75	0.1058
149						342	2054	742	0.76	0.1074
155						344	2105	790	0.81	0.1144

Table D.6. Creep strains of 4 x 11 in. (100 x 280 mm) cylindrical specimens from Mix No. 129, με.

Time Since Loading (days)	Heat-Cured					Moist-Cured Sustained Load=86791 lb. (Sustained Stress=6907 psi)				
	Shrinkage Strain	Total Strain	Creep Strain	Creep Coefficient	Specific Creep, με/psi	Shrinkage Strain	Total Strain	Creep Strain	Creep Coefficient	Specific Creep, με/psi
163						336	2077	771	0.79	0.1116
170						359	2121	792	0.82	0.1147
176						359	2102	773	0.80	0.1119
184						357	2098	771	0.79	0.1116
191						357	2117	789	0.81	0.1143
198						377	2187	840	0.87	0.1216
208						355	2144	818	0.84	0.1185
212						357	2132	805	0.83	0.1166
218						369	2146	807	0.83	0.1168
226						370	2197	856	0.88	0.1240
236						378	2175	827	0.85	0.1197
240						381	2185	834	0.86	0.1207
247						394	2237	872	0.90	0.1263
254						390	2211	851	0.88	0.1232
260						385	2207	851	0.88	0.1232
268						399	2247	877	0.90	0.1270
275						401	2251	880	0.91	0.1274
285						394	2253	889	0.92	0.1287
289						398	2282	914	0.94	0.1324
295						401	2283	912	0.94	0.1320
302						401	2303	932	0.96	0.1349
310						407	2262	885	0.91	0.1282
320						411	2286	905	0.93	0.1311
324						406	2273	897	0.93	0.1299

Table D.6. Creep strains of 4 x 11 in. (100 x 280 mm) cylindrical specimens from Mix No. 129, με.

Time Since Loading (days)	Heat-Cured					Moist-Cured Sustained Load=86791 lb. (Sustained Stress=6907 psi)				
	Shrinkage Strain	Total Strain	Creep Strain	Creep Coefficient	Specific Creep, με/psi	Shrinkage Strain	Total Strain	Creep Strain	Creep Coefficient	Specific Creep, με/psi
335						428	2338	940	0.97	0.1361
338						420	2330	940	0.97	0.1361
345						427	2335	937	0.97	0.1357
352						413	2300	917	0.95	0.1328
359						432	2318	916	0.94	0.1326
372						425	2306	911	0.94	0.1319
380						436	2376	970	1.00	0.1404

Table D.7. Creep strains of 4 x 11 in. (100 x 280 mm) cylindrical specimens from Mix No. 131, με.

Time Since Loading (days)	Heat-Cured Sustained Load=82888 lb. (Sustained Stress=6596 psi)					Moist-Cured Sustained Load=87296 lb. (Sustained Stress=6947 psi)				
	Shrinkage Strain	Total Strain	Creep Strain	Creep Coefficient	Specific Creep, με/psi	Shrinkage Strain	Total Strain	Creep Strain	Creep Coefficient	Specific Creep, με/psi
0	0	1001	0	0.00	0.0000	0	970	0	0.00	0.0000
1	21	1202	179	0.18	0.0272	28	1129	130	0.13	0.0187
2	25	1255	228	0.23	0.0346	20	1182	192	0.20	0.0276
6	65	1330	263	0.26	0.0399	72	1334	292	0.30	0.0420
9	90	1411	319	0.32	0.0484	111	1389	307	0.32	0.0442
13	115	1467	350	0.35	0.0531	127	1476	378	0.39	0.0544
23	160	1658	496	0.50	0.0752	185	1604	448	0.46	0.0645
30	177	1661	483	0.48	0.0732	208	1631	452	0.47	0.0651
37	201	1752	549	0.55	0.0832	232	1708	505	0.52	0.0727
44	225	1749	523	0.52	0.0793	254	1745	521	0.54	0.0750
51	232	1805	572	0.57	0.0867	249	1736	517	0.53	0.0744
65	259	1899	639	0.64	0.0969	290	1834	574	0.59	0.0826
72	265	1867	601	0.60	0.0911	289	1842	583	0.60	0.0839
79	282	1907	624	0.62	0.0946	301	1880	608	0.63	0.0875
86	289	1906	616	0.62	0.0934	308	1919	640	0.66	0.0922
93	291	1966	674	0.67	0.1022	314	1916	632	0.65	0.0910
100	301	1943	641	0.64	0.0972	328	1937	639	0.66	0.0919
112	319	2014	694	0.69	0.1052	334	1946	641	0.66	0.0923
121	322	2041	718	0.72	0.1089	344	2025	710	0.73	0.1022
128	324	2071	745	0.74	0.1130	349	2028	709	0.73	0.1021
135	329	2041	711	0.71	0.1078	335	1980	675	0.70	0.0971
141	332	2101	768	0.77	0.1165	337	2004	696	0.72	0.1003
149	345	2082	736	0.74	0.1116	356	2032	705	0.73	0.1015
155	339	2117	777	0.78	0.1178	358	2049	721	0.74	0.1037

Table D.7. Creep strains of 4 x 11 in. (100 x 280 mm) cylindrical specimens from Mix No. 131, με.

Time Since Loading (days)	Heat-Cured Sustained Load=82888 lb. (Sustained Stress=6596 psi)					Moist-Cured Sustained Load=87296 lb. (Sustained Stress=6947 psi)				
	Shrinkage Strain	Total Strain	Creep Strain	Creep Coefficient	Specific Creep, με/psi	Shrinkage Strain	Total Strain	Creep Strain	Creep Coefficient	Specific Creep, με/psi
163	349	2148	798	0.80	0.1209	367	2080	742	0.76	0.1068
170	350	2094	743	0.74	0.1127	360	2078	748	0.77	0.1077
176	366	2148	781	0.78	0.1184	370	2075	735	0.76	0.1058
184	363	2145	781	0.78	0.1183	374	2083	739	0.76	0.1063
191	362	2191	828	0.83	0.1255	368	2070	732	0.75	0.1054
198	375	2172	796	0.80	0.1207	374	2139	795	0.82	0.1144
208	374	2185	810	0.81	0.1229	373	2101	757	0.78	0.1090
212	371	2173	800	0.80	0.1213	391	2135	774	0.80	0.1115
218	382	2273	890	0.89	0.1349	384	2109	755	0.78	0.1087
226	383	2199	814	0.81	0.1234	395	2164	798	0.82	0.1149
236	394	2238	842	0.84	0.1277	402	2168	795	0.82	0.1145
240	397	2273	874	0.87	0.1326	398	2148	780	0.80	0.1123
247	398	2253	854	0.85	0.1294	405	2198	823	0.85	0.1185
254	402	2289	886	0.88	0.1343	418	2177	788	0.81	0.1134
260	412	2279	865	0.86	0.1312	404	2173	799	0.82	0.1150
268	411	2252	840	0.84	0.1273	411	2194	812	0.84	0.1169
275	416	2262	844	0.84	0.1280	425	2201	806	0.83	0.1160
285	416	2294	876	0.88	0.1329	438	2240	832	0.86	0.1198
289	423	2309	884	0.88	0.1341	431	2264	862	0.89	0.1241
295	431	2346	914	0.91	0.1385	426	2225	829	0.85	0.1193
302	431	2313	880	0.88	0.1335	425	2246	851	0.88	0.1225
310	431	2301	869	0.87	0.1318	443	2271	858	0.88	0.1236
320	432	2373	939	0.94	0.1424	444	2277	863	0.89	0.1242
324	446	2323	875	0.87	0.1327	435	2248	842	0.87	0.1212

Table D.7. Creep strains of 4 x 11 in. (100 x 280 mm) cylindrical specimens from Mix No. 131, με.

Time Since Loading (days)	Heat-Cured Sustained Load=82888 lb. (Sustained Stress=6596 psi)					Moist-Cured Sustained Load=87296 lb. (Sustained Stress=6947 psi)				
	Shrinkage Strain	Total Strain	Creep Strain	Creep Coefficient	Specific Creep, με/psi	Shrinkage Strain	Total Strain	Creep Strain	Creep Coefficient	Specific Creep, με/psi
335	443	2344	899	0.90	0.1364	441	2276	864	0.89	0.1244
338	444	2353	908	0.91	0.1376	460	2329	899	0.93	0.1294
345	449	2350	900	0.90	0.1365	447	2294	877	0.90	0.1263
352	452	2378	925	0.92	0.1403	464	2312	878	0.90	0.1264
359	461	2403	941	0.94	0.1426	465	2297	862	0.89	0.1241
372	458	2378	919	0.92	0.1394	461	2301	869	0.90	0.1251
380	468	2429	960	0.96	0.1455	467	2341	904	0.93	0.1301

Table D.8. Creep strains of 4 x 11 in. (100 x 280 mm) cylindrical specimens from Mix No. 132, με.

Time Since Loading (days)	Heat-Cured Sustained Load=98861 lb. (Sustained Stress=7867 psi)					Moist-Cured Sustained Load=91977 lb. (Sustained Stress=7319 psi)				
	Shrinkage Strain	Total Strain	Creep Strain	Creep Coefficient	Specific Creep, με/psi	Shrinkage Strain	Total Strain	Creep Strain	Creep Coefficient	Specific Creep, με/psi
0	0	1234	0	0.00	0.0000	0	1073	0	0.00	0.0000
1	19	1392	139	0.11	0.0176	28	1261	161	0.15	0.0220
2	32	1361	95	0.08	0.0121	33	1318	212	0.20	0.0290
6	54	1606	318	0.26	0.0404	72	1440	296	0.28	0.0404
9	79	1610	297	0.24	0.0378	104	1483	306	0.28	0.0418
13	101	1695	360	0.29	0.0458	130	1563	359	0.33	0.0491
23	140	1805	431	0.35	0.0548	173	1656	410	0.38	0.0560
30	166	1906	506	0.41	0.0643	202	1730	454	0.42	0.0621
37	187	1966	545	0.44	0.0693	224	1784	487	0.45	0.0665
44	205	1930	491	0.40	0.0624	241	1779	464	0.43	0.0635
51	223	2031	575	0.47	0.0731	249	1825	502	0.47	0.0686
65	249	2067	584	0.47	0.0743	271	1875	531	0.49	0.0725
72	259	2031	538	0.44	0.0684	283	1890	535	0.50	0.0731
79	265	2189	691	0.56	0.0878	291	1923	558	0.52	0.0763
86	276	2063	553	0.45	0.0703	300	1911	538	0.50	0.0735
93	288	2149	627	0.51	0.0797	303	1970	595	0.55	0.0813
100	295	2160	632	0.51	0.0803	308	1968	587	0.55	0.0802
112	305	2172	632	0.51	0.0804	325	1965	566	0.53	0.0774
121	311	2269	723	0.59	0.0919	324	1982	585	0.55	0.0799
128	320	2211	657	0.53	0.0835	325	2022	624	0.58	0.0853
135	324	2321	763	0.62	0.0970	328	2027	626	0.58	0.0855
141	326	2301	741	0.60	0.0942	331	2039	636	0.59	0.0869
149	337	2308	737	0.60	0.0937	340	2044	631	0.59	0.0862
155	337	2305	734	0.59	0.0933	341	2058	644	0.60	0.0881

Table D.8. Creep strains of 4 x 11 in. (100 x 280 mm) cylindrical specimens from Mix No. 132, με.

Time Since Loading (days)	Heat-Cured Sustained Load=98861 lb. (Sustained Stress=7867 psi)					Moist-Cured Sustained Load=91977 lb. (Sustained Stress=7319 psi)				
	Shrinkage Strain	Total Strain	Creep Strain	Creep Coefficient	Specific Creep, με/psi	Shrinkage Strain	Total Strain	Creep Strain	Creep Coefficient	Specific Creep, με/psi
163	341	2333	757	0.61	0.0963	347	2088	668	0.62	0.0913
170	351	2352	767	0.62	0.0975	350	2091	669	0.62	0.0914
176	350	2356	772	0.63	0.0981	357	2115	685	0.64	0.0936
184	358	2356	764	0.62	0.0971	358	2124	692	0.65	0.0946
191	363	2429	832	0.67	0.1058	357	2156	726	0.68	0.0991
198	367	2460	859	0.70	0.1092	367	2121	681	0.63	0.0930
208	372	2394	789	0.64	0.1002	371	2157	713	0.66	0.0974
212	369	2459	856	0.69	0.1088	366	2187	748	0.70	0.1022
218	374	2437	829	0.67	0.1054	375	2198	750	0.70	0.1024
226	376	2429	819	0.66	0.1041	373	2195	749	0.70	0.1024
236	385	2465	846	0.69	0.1075	382	2220	766	0.71	0.1046
240	385	2490	870	0.71	0.1106	385	2186	727	0.68	0.0994
247	383	2517	900	0.73	0.1144	387	2198	738	0.69	0.1008
254	396	2550	921	0.75	0.1171	386	2209	750	0.70	0.1024
260	396	2486	856	0.69	0.1088	397	2236	767	0.71	0.1047
268	396	2581	951	0.77	0.1209	394	2252	785	0.73	0.1072
275	402	2487	850	0.69	0.1081	396	2264	795	0.74	0.1087
285	401	2553	918	0.74	0.1167	399	2263	791	0.74	0.1081
289	409	2528	885	0.72	0.1125	406	2277	798	0.74	0.1090
295	417	2482	831	0.67	0.1056	406	2262	783	0.73	0.1069
302	415	2539	890	0.72	0.1131	410	2267	784	0.73	0.1071
310	415	2601	952	0.77	0.1210	412	2277	792	0.74	0.1083
320	427	2547	886	0.72	0.1127	414	2298	811	0.76	0.1108
324	425	2620	961	0.78	0.1221	419	2322	830	0.77	0.1134

Table D.8. Creep strains of 4 x 11 in. (100 x 280 mm) cylindrical specimens from Mix No. 132, με.

Time Since Loading (days)	Heat-Cured Sustained Load=98861 lb. (Sustained Stress=7867 psi)					Moist-Cured Sustained Load=91977 lb. (Sustained Stress=7319 psi)				
	Shrinkage Strain	Total Strain	Creep Strain	Creep Coefficient	Specific Creep, με/psi	Shrinkage Strain	Total Strain	Creep Strain	Creep Coefficient	Specific Creep, με/psi
335	428	2607	945	0.77	0.1201	423	2327	832	0.77	0.1136
338	430	2620	955	0.77	0.1214	424	2338	841	0.78	0.1148
345	436	2654	984	0.80	0.1251	428	2315	814	0.76	0.1112
352	439	2644	971	0.79	0.1234	427	2292	791	0.74	0.1081
359	439	2611	939	0.76	0.1193	435	2309	801	0.75	0.1094
372	443	2614	938	0.76	0.1192	438	2334	822	0.77	0.1124
380	444	2669	991	0.80	0.1260	443	2320	805	0.75	0.1100

Table D.9. Creep strains of 4 x 11 in. (100 x 280 mm) cylindrical specimens from Mix No. 136, με.

Time Since Loading (days)	Heat-Cured Sustained Load=78624 lb. (Sustained Stress=6257 psi)					Moist-Cured				
	Shrinkage Strain	Total Strain	Creep Strain	Creep Coefficient	Specific Creep, με/psi	Shrinkage Strain	Total Strain	Creep Strain	Creep Coefficient	Specific Creep, με/psi
0	0	979	0	0.00	0.0000					
1	17	1238	242	0.25	0.0387					
2	28	1328	321	0.33	0.0513					
6	66	1517	473	0.48	0.0756					
9	94	1606	534	0.55	0.0853					
13	117	1693	597	0.61	0.0954					
23	154	1915	782	0.80	0.1250					
30	193	2005	834	0.85	0.1333					
37	214	2008	815	0.83	0.1303					
44	235	2136	922	0.94	0.1474					
51	236	2102	887	0.91	0.1418					
65	264	2195	953	0.97	0.1523					
72	283	2265	1004	1.03	0.1604					
79	291	2263	993	1.01	0.1587					
86	299	2317	1039	1.06	0.1661					
93	308	2382	1095	1.12	0.1751					
100	312	2413	1122	1.15	0.1793					
112	327	2368	1062	1.09	0.1698					
121	338	2478	1161	1.19	0.1855					
128	339	2420	1102	1.13	0.1762					
135	339	2516	1198	1.22	0.1915					
141	346	2524	1200	1.23	0.1917					
149	356	2532	1197	1.22	0.1914					
155	358	2486	1149	1.17	0.1836					

Table D.9. Creep strains of 4 x 11 in. (100 x 280 mm) cylindrical specimens from Mix No. 136, με.

Time Since Loading (days)	Heat-Cured Sustained Load=78624 lb. (Sustained Stress=6257 psi)					Moist-Cured				
	Shrinkage Strain	Total Strain	Creep Strain	Creep Coefficient	Specific Creep, με/psi	Shrinkage Strain	Total Strain	Creep Strain	Creep Coefficient	Specific Creep, με/psi
163	365	2502	1158	1.18	0.1852					
170	371	2521	1172	1.20	0.1873					
176	372	2607	1256	1.28	0.2007					
184	384	2599	1237	1.26	0.1977					
191	389	2631	1262	1.29	0.2018					
198	395	2650	1276	1.30	0.2040					
208	392	2592	1221	1.25	0.1951					
212	394	2617	1244	1.27	0.1988					
218	396	2677	1302	1.33	0.2081					
226	405	2629	1244	1.27	0.1989					
236	412	2646	1255	1.28	0.2006					
240	416	2694	1299	1.33	0.2077					
247	425	2756	1352	1.38	0.2160					
254	424	2708	1305	1.33	0.2086					
260	428	2729	1322	1.35	0.2112					
268	433	2761	1349	1.38	0.2157					
275	439	2718	1300	1.33	0.2078					
285	444	2787	1364	1.39	0.2180					
289	439	2774	1357	1.39	0.2169					
295	452	2749	1318	1.35	0.2107					
302	450	2760	1331	1.36	0.2128					
310	455	2813	1379	1.41	0.2205					
320	461	2821	1382	1.41	0.2208					
324	474	2850	1398	1.43	0.2234					

Table D.9. Creep strains of 4 x 11 in. (100 x 280 mm) cylindrical specimens from Mix No. 136, με.

Time Since Loading (days)	Heat-Cured Sustained Load=78624 lb. (Sustained Stress=6257 psi)					Moist-Cured				
	Shrinkage Strain	Total Strain	Creep Strain	Creep Coefficient	Specific Creep, με/psi	Shrinkage Strain	Total Strain	Creep Strain	Creep Coefficient	Specific Creep, με/psi
335	468	2812	1366	1.40	0.2183					
338	467	2872	1426	1.46	0.2279					
345	478	2808	1352	1.38	0.2161					
352	474	2851	1398	1.43	0.2235					
359	488	2847	1380	1.41	0.2206					
372	486	2890	1426	1.46	0.2279					
380	492	2899	1428	1.46	0.2282					

Table D.10. Creep strains of 4 x 11 in. (100 x 280 mm) cylindrical specimens from Mix No. 139, με.

Time Since Loading (days)	Heat-Cured Sustained Load=80208 lb. (Sustained Stress=6383 psi)					Moist-Cured				
	Shrinkage Strain	Total Strain	Creep Strain	Creep Coefficient	Specific Creep, με/psi	Shrinkage Strain	Total Strain	Creep Strain	Creep Coefficient	Specific Creep, με/psi
0	0	943	0	0.00	0.0000					
1	32	1156	180	0.19	0.0283					
2	42	1281	297	0.31	0.0465					
6	73	1434	418	0.44	0.0654					
9	109	1485	433	0.46	0.0679					
13	119	1523	462	0.49	0.0724					
23	170	1710	597	0.63	0.0936					
30	196	1762	624	0.66	0.0977					
37	215	1780	622	0.66	0.0975					
44	235	1908	731	0.77	0.1145					
51	244	1879	692	0.73	0.1084					
65	269	1953	742	0.79	0.1162					
72	282	2062	837	0.89	0.1312					
79	292	2049	814	0.86	0.1275					
86	301	2118	874	0.93	0.1369					
93	304	2159	912	0.97	0.1429					
100	314	2115	858	0.91	0.1345					
112	332	2162	887	0.94	0.1390					
121	332	2193	919	0.97	0.1440					
128	339	2200	918	0.97	0.1439					
135	337	2262	983	1.04	0.1540					
141	345	2258	970	1.03	0.1520					
149	357	2307	1007	1.07	0.1578					
155	353	2252	957	1.01	0.1499					

Table D.10. Creep strains of 4 x 11 in. (100 x 280 mm) cylindrical specimens from Mix No. 139, με.

Time Since Loading (days)	Heat-Cured Sustained Load=80208 lb. (Sustained Stress=6383 psi)					Moist-Cured				
	Shrinkage Strain	Total Strain	Creep Strain	Creep Coefficient	Specific Creep, με/psi	Shrinkage Strain	Total Strain	Creep Strain	Creep Coefficient	Specific Creep, με/psi
163	359	2301	1000	1.06	0.1566					
170	369	2276	964	1.02	0.1510					
176	368	2354	1043	1.11	0.1634					
184	372	2379	1064	1.13	0.1667					
191	373	2395	1079	1.14	0.1690					
198	391	2367	1034	1.10	0.1620					
208	386	2332	1004	1.06	0.1572					
212	384	2388	1062	1.13	0.1664					
218	390	2389	1057	1.12	0.1655					
226	399	2387	1046	1.11	0.1638					
236	399	2440	1098	1.16	0.1721					
240	408	2440	1089	1.16	0.1706					
247	400	2441	1098	1.16	0.1720					
254	407	2442	1092	1.16	0.1711					
260	415	2497	1140	1.21	0.1786					
268	427	2526	1156	1.23	0.1811					
275	428	2497	1126	1.19	0.1765					
285	439	2554	1172	1.24	0.1837					
289	429	2517	1145	1.21	0.1794					
295	437	2505	1125	1.19	0.1763					
302	442	2506	1121	1.19	0.1756					
310	445	2560	1173	1.24	0.1838					
320	441	2524	1141	1.21	0.1787					
324	454	2608	1211	1.28	0.1898					

Table D.10. Creep strains of 4 x 11 in. (100 x 280 mm) cylindrical specimens from Mix No. 139, με.

Time Since Loading (days)	Heat-Cured Sustained Load=80208 lb. (Sustained Stress=6383 psi)					Moist-Cured				
	Shrinkage Strain	Total Strain	Creep Strain	Creep Coefficient	Specific Creep, με/psi	Shrinkage Strain	Total Strain	Creep Strain	Creep Coefficient	Specific Creep, με/psi
335	445	2538	1151	1.22	0.1803					
338	451	2571	1177	1.25	0.1845					
345	458	2613	1212	1.29	0.1899					
352	457	2566	1166	1.24	0.1827					
359	461	2606	1203	1.28	0.1885					
372	464	2590	1184	1.26	0.1855					
380	467	2629	1220	1.29	0.1911					

APPENDIX E

WEIGHT-LOSS

Table E.1.A. Weight-loss of 4 x 11 in. (100 x 280 mm) heat-cured cylindrical specimens, stored in a controlled environment of 50% R.H. and 72 °F (Mix Nos. 100 to 119), pcf.

Days	Mix Numbers																			
Stored	100	101	102	103	104	105	106	107	108	109	110	111	112	113	114	115	116	117	118	119
0	0.000	0.000	0.000	0.000	0.000	0.000	0.000	0.000	0.000	0.000	0.000	0.000	0.000	0.000	0.000	0.000	0.000	0.000	0.000	0.000
1	0.081	0.084	0.078	0.051	0.033	0.021	0.038	0.046	0.055	0.059	0.159	0.154	0.019	0.019	0.057	0.069	0.116	0.100	0.069	0.067
3	0.208	0.233	0.230	0.207	0.113	0.071	0.129	0.102	0.157	0.168	0.272	0.275	0.057	0.057	0.104	0.119	0.200	0.175	0.188	0.185
5	0.276	0.365	0.324	0.328	0.176	0.122	0.199	0.181	0.248	0.265	0.321	0.330	0.084	0.087	0.125	0.143	0.272	0.238	0.241	0.237
7	0.320	0.393	0.354	0.376	0.199	0.173	0.234	0.222	0.283	0.302	0.377	0.391	0.136	0.138	0.136	0.159	0.334	0.296	0.315	0.311
9	0.385	0.486	0.396	0.471	0.253	0.199	0.282	0.277	0.370	0.393	0.414	0.435	0.156	0.160	0.182	0.212	0.406	0.365	0.337	0.331
11	0.445	0.531	0.445	0.526	0.298	0.239	0.332	0.291	0.426	0.454	0.452	0.470	0.168	0.170	0.192	0.221	0.434	0.390	0.369	0.361
14	0.464	0.604	0.493	0.607	0.355	0.298	0.390	0.317	0.469	0.500	0.482	0.506	0.201	0.207	0.262	0.299	0.464	0.463	0.405	0.397
17	0.514	0.655	0.559	0.668	0.370	0.341	0.406	0.331	0.513	0.544	0.542	0.570	0.239	0.243	0.311	0.354	0.525	0.474	0.427	0.420
20	0.551	0.719	0.609	0.689	0.389	0.360	0.426	0.344	0.548	0.582	0.564	0.599	0.291	0.295	0.360	0.408	0.564	0.510	0.464	0.454
23	0.605	0.771	0.628	0.712	0.401	0.373	0.439	0.377	0.576	0.610	0.602	0.641	0.330	0.336	0.384	0.435	0.585	0.533	0.487	0.481
26	0.648	0.790	0.649	0.733	0.413	0.388	0.448	0.382	0.600	0.637	0.639	0.678	0.386	0.393	0.410	0.461	0.604	0.549	0.496	0.486
31	0.672	0.813	0.668	0.781	0.440	0.424	0.474	0.408	0.640	0.680	0.717	0.754	0.411	0.416	0.437	0.492	0.621	0.565	0.558	0.543
36	0.691	0.851	0.709	0.782	0.462	0.423	0.498	0.472	0.703	0.742	0.780	0.821	0.435	0.443	0.469	0.531	0.688	0.633	0.627	0.613
41	0.721	0.873	0.707	0.858	0.521	0.490	0.553	0.532	0.728	0.767	0.815	0.855	0.464	0.473	0.503	0.570	0.719	0.657	0.685	0.670
46	0.724	0.900	0.777	0.914	0.573	0.542	0.603	0.553	0.791	0.837	0.838	0.878	0.497	0.510	0.536	0.606	0.754	0.689	0.717	0.699
51	0.771	0.976	0.831	0.957	0.592	0.587	0.620	0.593	0.802	0.843	0.876	0.919	0.525	0.540	0.563	0.632	0.781	0.717	0.738	0.721
58	0.852	1.024	0.876	1.000	0.634	0.630	0.660	0.635	0.846	0.893	0.914	0.961	0.567	0.575	0.597	0.668	0.826	0.756	0.774	0.758
65	0.891	1.075	0.919	1.039	0.669	0.714	0.693	0.675	0.946	0.995	0.958	1.001	0.597	0.606	0.638	0.712	0.918	0.843	0.815	0.796
72	0.918	1.110	0.954	1.074	0.713	0.796	0.739	0.716	0.988	1.045	0.987	1.035	0.635	0.644	0.738	0.827	0.951	0.881	0.847	0.828
79	0.954	1.144	0.998	1.111	0.743	0.755	0.764	0.754	1.034	1.089	1.029	1.072	0.731	0.746	0.772	0.863	0.977	0.904	0.871	0.855
86	1.000	1.186	1.025	1.138	0.769	0.789	0.855	0.791	1.072	1.126	1.107	1.154	0.768	0.777	0.792	0.888	1.030	0.947	0.906	0.881
100	1.050	1.246	1.079	1.251	0.898	0.933	0.915	0.937	1.129	1.185	1.163	1.211	0.833	0.852	0.880	0.983	1.075	0.994	1.017	0.994
114	1.155	1.357	1.197	1.304	0.965	0.992	0.981	1.013	1.169	1.229	1.235	1.281	0.884	0.902	0.934	1.041	1.116	1.034	1.080	1.058

Table E.1.A. Weight-loss of 4 x 11 in. (100 x 280 mm) heat-cured cylindrical specimens, stored in a controlled environment of 50% R.H. and 72 °F (Mix Nos. 100 to 119), pcf.

Days	Mix Numbers																			
Stored	100	101	102	103	104	105	106	107	108	109	110	111	112	113	114	115	116	117	118	119
128	1.225	1.421	1.260	1.375	1.028	1.080	1.041	1.053	1.244	1.303	1.280	1.327	0.925	0.944	0.988	1.101	1.163	1.081	1.126	1.108
142	1.286	1.457	1.304	1.404	1.079	1.118	1.088	1.094	1.298	1.365	1.327	1.374	1.004	1.027	1.005	1.119	1.209	1.126	1.162	1.142
156	1.335	1.492	1.340	1.434	1.127	1.158	1.134	1.155	1.332	1.395	1.339	1.388	1.061	1.076	1.063	1.179	1.235	1.152	1.225	1.206
177	1.385	1.558	1.416	1.499	1.208	1.242	1.212	1.247	1.385	1.458	1.400	1.452	1.094	1.123	1.103	1.221	1.255	1.176	1.273	1.251
198	1.432	1.607	1.473	1.543	1.259	1.302	1.267	1.318	1.409	1.482	1.438	1.497	1.111	1.142	1.105	1.228	1.292	1.203	1.302	1.286
219	1.471	1.636	1.508	1.589	1.283	1.375	1.297	1.335	1.458	1.533	1.477	1.536	1.113	1.148	1.148	1.276	1.316	1.236	1.309	1.295
240	1.490	1.665	1.525	1.586	1.292	1.380	1.304	1.396	1.473	1.546	1.510	1.581	1.152	1.191	1.151	1.279	1.333	1.248	1.338	1.321
261	1.520	1.695	1.562	1.632	1.340	1.442	1.354	1.405	1.495	1.572	1.529	1.609	1.160	1.196	1.174	1.304	1.350	1.265	1.345	1.331
289	1.535	1.723	1.582	1.638	1.349	1.458	1.363	1.439	1.494	1.565	1.556	1.633	1.160	1.206	1.166	1.290	1.344	1.265	1.355	1.343
317	1.553	1.731	1.592	1.643	1.363	1.472	1.378	1.404	1.458	1.524	1.496	1.574	1.109	1.160	1.111	1.225	1.324	1.246	1.352	1.339
345	1.508	1.673	1.536	1.575	1.290	1.403	1.290	1.347	1.480	1.541	1.503	1.574	1.124	1.174	1.126	1.237	1.346	1.266	1.325	1.311
373	1.532	1.689	1.534	1.578	1.303	1.414	1.299	1.350	1.494	1.553	1.512	1.579	1.147	1.197	1.135	1.250	1.372	1.290	1.350	1.337

Table E.1.B. Weight-loss of 4 x 11 in. (100 x 280 mm) heat-cured cylindrical specimens, stored in a controlled environment of 50% R.H. and 72 °F (Mix Nos. 120 to 139), pcf.

Days	Mix Numbers																			
Stored	120	121	122	123	124	125	126	127	128	129	130	131	132	133	134	135	136	137	138	139
0	0.000	0.000	0.000	0.000	0.000	0.000	0.000	0.000	0.000	0.000	0.000	0.000	0.000	0.000	0.000	0.000	0.000	0.000	0.000	0.000
1	0.042	0.041	0.045	0.052	0.134	0.074	0.122	0.071	0.000	0.049	0.067	0.029	0.057	0.073	0.074	0.000	0.089	0.045	0.026	0.025
3	0.071	0.069	0.081	0.099	0.295	0.168	0.271	0.151	0.097	0.099	0.133	0.059	0.114	0.141	0.150	0.096	0.177	0.090	0.052	0.050
5	0.101	0.098	0.108	0.130	0.419	0.252	0.379	0.220	0.174	0.142	0.228	0.078	0.199	0.202	0.208	0.195	0.207	0.108	0.080	0.074
7	0.128	0.123	0.169	0.200	0.525	0.326	0.409	0.252	0.185	0.151	0.274	0.133	0.283	0.222	0.300	0.247	0.252	0.139	0.130	0.121
9	0.175	0.169	0.177	0.211	0.553	0.341	0.464	0.276	0.211	0.193	0.326	0.164	0.365	0.279	0.350	0.279	0.290	0.182	0.181	0.166
11	0.195	0.190	0.238	0.278	0.581	0.357	0.515	0.312	0.254	0.236	0.347	0.193	0.428	0.335	0.401	0.310	0.333	0.196	0.204	0.190
14	0.206	0.199	0.300	0.342	0.661	0.415	0.569	0.349	0.271	0.278	0.407	0.244	0.501	0.390	0.475	0.344	0.373	0.219	0.221	0.205
17	0.243	0.236	0.340	0.388	0.684	0.432	0.627	0.388	0.367	0.327	0.466	0.277	0.537	0.445	0.517	0.399	0.421	0.246	0.254	0.251
20	0.293	0.285	0.373	0.424	0.720	0.456	0.748	0.481	0.423	0.360	0.520	0.282	0.584	0.485	0.535	0.428	0.452	0.267	0.327	0.294
23	0.347	0.332	0.381	0.433	0.775	0.489	0.790	0.524	0.457	0.364	0.562	0.328	0.613	0.492	0.592	0.463	0.497	0.301	0.338	0.303
26	0.377	0.366	0.416	0.471	0.830	0.520	0.836	0.560	0.462	0.401	0.572	0.363	0.657	0.541	0.626	0.488	0.505	0.305	0.353	0.317
31	0.410	0.398	0.435	0.492	0.881	0.584	0.895	0.608	0.528	0.445	0.637	0.459	0.681	0.587	0.661	0.541	0.555	0.342	0.405	0.359
36	0.450	0.437	0.461	0.526	0.911	0.609	0.950	0.666	0.568	0.478	0.678	0.423	0.738	0.628	0.712	0.675	0.605	0.382	0.465	0.415
41	0.463	0.448	0.495	0.560	0.991	0.678	0.975	0.681	0.601	0.518	0.721	0.451	0.793	0.665	0.762	0.686	0.697	0.477	0.533	0.474
46	0.503	0.488	0.517	0.584	0.996	0.687	1.021	0.734	0.637	0.633	0.760	0.539	0.868	0.790	0.850	0.736	0.734	0.506	0.576	0.510
51	0.539	0.526	0.548	0.610	1.045	0.728	1.079	0.794	0.712	0.655	0.840	0.576	0.910	0.818	0.893	0.783	0.766	0.532	0.612	0.543
58	0.567	0.557	0.568	0.638	1.102	0.788	1.166	0.888	0.755	0.712	0.888	0.618	0.966	0.867	0.938	0.837	0.803	0.565	0.664	0.587
65	0.597	0.584	0.597	0.678	1.167	0.870	1.229	0.953	0.807	0.748	0.937	0.662	1.007	0.918	0.992	0.891	0.855	0.612	0.711	0.621
72	0.634	0.615	0.695	0.774	1.224	0.921	1.270	1.016	0.839	0.799	0.980	0.701	1.059	0.978	1.037	0.898	0.885	0.639	0.724	0.630
79	0.723	0.702	0.723	0.802	1.264	0.961	1.335	1.063	0.877	0.829	1.020	0.711	1.076	1.006	1.055	0.906	0.906	0.664	0.751	0.654
86	0.742	0.721	0.756	0.839	1.318	1.013	1.350	1.079	0.898	0.871	1.039	0.765	1.121	1.052	1.111	0.960	0.928	0.689	0.780	0.678
100	0.805	0.783	0.810	0.907	1.373	1.077	1.420	1.151	0.945	0.915	1.088	0.821	1.167	1.099	1.167	1.012	0.983	0.742	0.857	0.746
114	0.851	0.836	0.858	0.954	1.429	1.140	1.470	1.211	1.011	0.981	1.156	0.858	1.209	1.164	1.206	1.064	1.021	0.779	0.899	0.784

Table E.1.B. Weight-loss of 4 x 11 in. (100 x 280 mm) heat-cured cylindrical specimens, stored in a controlled environment of 50% R.H. and 72 °F (Mix Nos. 120 to 139), pcf.

Days Stored	Mix Numbers																			
	120	121	122	123	124	125	126	127	128	129	130	131	132	133	134	135	136	137	138	139
128	0.887	0.872	0.902	1.000	1.468	1.187	1.564	1.321	1.062	1.035	1.213	0.908	1.242	1.227	1.252	1.098	1.046	0.806	0.905	0.784
142	0.931	0.918	0.931	1.031	1.503	1.227	1.555	1.315	1.073	1.060	1.226	0.947	1.279	1.240	1.295	1.149	1.085	0.846	0.923	0.797
156	0.975	0.961	0.966	1.068	1.542	1.276	1.597	1.367	1.101	1.067	1.250	0.960	1.293	1.257	1.294	1.153	1.084	0.832	0.932	0.792
177	1.011	1.004	0.994	1.105	1.534	1.290	1.598	1.366	1.112	1.094	1.261	0.952	1.302	1.284	1.305	1.158	1.083	0.835	0.919	0.768
198	1.056	1.049	0.994	1.105	1.553	1.286	1.639	1.409	1.145	1.124	1.291	0.983	1.332	1.312	1.341	1.194	1.112	0.858	0.949	0.791
219	1.057	1.052	1.023	1.132	1.584	1.315	1.645	1.411	1.156	1.137	1.301	0.979	1.334	1.331	1.341	1.182	1.127	0.861	0.948	0.780
240	1.088	1.083	1.026	1.138	1.600	1.333	1.660	1.423	1.177	1.137	1.319	0.986	1.353	1.327	1.354	1.195	1.130	0.849	0.948	0.763
261	1.105	1.100	1.049	1.142	1.602	1.333	1.665	1.413	1.184	1.126	1.330	0.987	1.357	1.320	1.357	1.186	1.131	0.831	0.928	0.733
289	1.117	1.118	1.027	1.130	1.555	1.279	1.600	1.325	1.142	1.070	1.279	0.939	1.317	1.271	1.321	1.132	1.093	0.784	0.899	0.706
317	1.071	1.077	0.974	1.062	1.573	1.305	1.626	1.354	1.166	1.107	1.303	0.964	1.339	1.310	1.343	1.163	1.125	0.816	0.925	0.725
345	1.102	1.107	0.991	1.079	1.589	1.328	1.634	1.365	1.184	1.109	1.326	0.983	1.354	1.314	1.353	1.178	1.162	0.843	0.951	0.748
373	1.116	1.116	1.007	1.088	1.591	1.333	1.638	1.372	1.195	1.148	1.336	1.017	1.390	1.352	1.388	1.224	1.197	0.872	0.981	0.773

Table E.2.A. Weight-loss of 4 x 11 in. (100 x 280 mm) moist-cured cylindrical specimens, stored in a controlled environment of 50% R.H. and 72 °F (Mix Nos. 100 to 119), pcf.

Days	Mix Numbers																			
Stored	100	101	102	103	104	105	106	107	108	109	110	111	112	113	114	115	116	117	118	119
0	0.000	0.000	0.000	0.000	0.000	0.000	0.000	0.000	0.000	0.000	0.000	0.000	0.000	0.000	0.000	0.000	0.000	0.000	0.000	0.000
2	0.079	0.079	0.077	0.077	0.045	0.045	0.065	0.065	0.084	0.077	0.041	0.038	0.052	0.045	0.128	0.127	0.084	0.077	0.041	0.038
4	0.164	0.164	0.171	0.171	0.114	0.114	0.208	0.208	0.200	0.186	0.089	0.079	0.160	0.142	0.231	0.245	0.200	0.186	0.089	0.079
6	0.232	0.232	0.250	0.250	0.177	0.177	0.281	0.281	0.270	0.251	0.141	0.125	0.206	0.181	0.324	0.316	0.270	0.251	0.141	0.125
9	0.287	0.287	0.341	0.341	0.254	0.254	0.370	0.370	0.348	0.325	0.193	0.174	0.264	0.231	0.447	0.438	0.348	0.325	0.193	0.174
12	0.343	0.343	0.427	0.427	0.296	0.296	0.413	0.413	0.387	0.362	0.250	0.224	0.322	0.284	0.519	0.511	0.387	0.362	0.250	0.224
15	0.396	0.396	0.474	0.474	0.322	0.322	0.456	0.456	0.431	0.407	0.292	0.261	0.388	0.349	0.581	0.572	0.431	0.407	0.292	0.261
18	0.457	0.457	0.503	0.503	0.343	0.343	0.500	0.500	0.462	0.436	0.333	0.301	0.443	0.401	0.609	0.600	0.462	0.436	0.333	0.301
21	0.485	0.485	0.529	0.529	0.358	0.358	0.520	0.520	0.486	0.459	0.363	0.326	0.492	0.449	0.650	0.642	0.486	0.459	0.363	0.326
26	0.507	0.507	0.571	0.571	0.398	0.398	0.569	0.569	0.518	0.489	0.445	0.405	0.525	0.479	0.685	0.678	0.518	0.489	0.445	0.405
31	0.535	0.535	0.602	0.602	0.413	0.413	0.628	0.628	0.586	0.556	0.524	0.480	0.560	0.513	0.728	0.723	0.586	0.556	0.524	0.480
36	0.560	0.560	0.649	0.649	0.476	0.476	0.692	0.692	0.615	0.581	0.576	0.529	0.611	0.535	0.768	0.764	0.615	0.581	0.576	0.529
41	0.575	0.575	0.726	0.726	0.525	0.525	0.727	0.727	0.667	0.631	0.609	0.559	0.621	0.572	0.800	0.794	0.667	0.631	0.609	0.559
46	0.639	0.639	0.784	0.784	0.551	0.551	0.757	0.757	0.690	0.653	0.642	0.590	0.647	0.608	0.838	0.823	0.690	0.653	0.642	0.590
53	0.709	0.709	0.838	0.838	0.589	0.589	0.795	0.795	0.735	0.696	0.685	0.631	0.681	0.630	0.857	0.858	0.735	0.696	0.685	0.631
60	0.757	0.757	0.885	0.885	0.620	0.620	0.827	0.827	0.835	0.795	0.727	0.673	0.706	0.658	0.896	0.898	0.835	0.795	0.727	0.673
67	0.789	0.789	0.924	0.924	0.655	0.655	0.861	0.861	0.875	0.834	0.764	0.706	0.739	0.693	0.980	0.981	0.875	0.834	0.764	0.706
74	0.826	0.826	0.971	0.971	0.681	0.681	0.886	0.886	0.911	0.872	0.797	0.741	0.811	0.764	1.008	1.011	0.911	0.872	0.797	0.741
81	0.872	0.872	1.006	1.006	0.703	0.703	0.914	0.914	0.959	0.914	0.858	0.799	0.829	0.782	1.032	1.038	0.959	0.914	0.858	0.799
95	0.931	0.931	1.102	1.102	0.809	0.809	1.018	1.018	1.014	0.947	0.944	0.886	0.889	0.844	1.097	1.108	1.014	0.947	0.944	0.886
109	1.053	1.053	1.194	1.194	0.853	0.853	1.069	1.069	1.057	1.009	1.023	0.965	0.927	0.884	1.140	1.154	1.057	1.009	1.023	0.965
123	1.121	1.121	1.272	1.272	0.911	0.911	1.112	1.112	1.123	1.074	1.075	1.017	0.957	0.913	1.183	1.200	1.123	1.074	1.075	1.017
137	1.175	1.175	1.318	1.318	0.942	0.942	1.142	1.142	1.175	1.129	1.116	1.060	1.010	0.963	1.200	1.219	1.175	1.129	1.116	1.060
151	1.219	1.219	1.355	1.355	0.973	0.973	1.180	1.180	1.202	1.153	1.160	1.106	1.045	1.004	1.237	1.259	1.202	1.153	1.160	1.106

Table E.2.A. Weight-loss of 4 x 11 in. (100 x 280 mm) moist-cured cylindrical specimens, stored in a controlled environment of 50% R.H. and 72 °F (Mix Nos. 100 to 119), pcf.

Days	Mix Numbers																			
Stored	100	101	102	103	104	105	106	107	108	109	110	111	112	113	114	115	116	117	118	119
172	1.283	1.283	1.440	1.440	1.034	1.034	1.247	1.247	1.242	1.194	1.215	1.158	1.072	1.029	1.264	1.287	1.242	1.194	1.215	1.158
193	1.333	1.333	1.498	1.498	1.072	1.072	1.285	1.285	1.270	1.219	1.253	1.197	1.094	1.053	1.259	1.287	1.270	1.219	1.253	1.197
214	1.370	1.370	1.549	1.549	1.087	1.087	1.293	1.293	1.310	1.256	1.276	1.217	1.092	1.053	1.291	1.318	1.310	1.256	1.276	1.217
235	1.396	1.396	1.561	1.561	1.100	1.100	1.318	1.318	1.320	1.267	1.309	1.250	1.123	1.084	1.296	1.322	1.320	1.267	1.309	1.250
256	1.427	1.427	1.608	1.608	1.146	1.146	1.338	1.338	1.344	1.291	1.328	1.268	1.135	1.095	1.311	1.338	1.344	1.291	1.328	1.268
284	1.448	1.448	1.631	1.631	1.148	1.148	1.353	1.353	1.346	1.286	1.348	1.287	1.145	1.105	1.310	1.337	1.346	1.286	1.348	1.287
312	1.465	1.465	1.646	1.646	1.166	1.166	1.346	1.346	1.324	1.258	1.326	1.264	1.113	1.069	1.279	1.295	1.324	1.258	1.326	1.264
340	1.414	1.414	1.591	1.591	1.115	1.115	1.299	1.299	1.353	1.286	1.325	1.258	1.136	1.098	1.300	1.316	1.353	1.286	1.325	1.258
368	1.438	1.438	1.602	1.602	1.135	1.135	1.314	1.314	1.375	1.308	1.364	1.287	1.155	1.115	1.317	1.330	1.375	1.308	1.364	1.287

Table E.2.B. Weight-loss of 4 x 11 in. (100 x 280 mm) moist-cured cylindrical specimens, stored in a controlled environment of 50% R.H. and 72 °F (Mix Nos. 120 to 139), pcf.

Days	Mix Numbers																			
Stored	120	121	122	123	124	125	126	127	128	129	130	131	132	133	134	135	136	137	138	139
0	0.000	0.000	0.000	0.000	0.000	0.000	0.000	0.000	0.000	0.000	0.000	0.000	0.000	0.000	0.000	0.000	0.000	0.000	0.000	0.000
2	0.052	0.045	0.128	0.127	0.163	0.186	0.180	0.219	0.071	0.047	0.098	0.103	0.036	0.059	0.134	0.038	0.062	0.068	0.065	0.068
4	0.160	0.142	0.231	0.245	0.215	0.241	0.322	0.388	0.161	0.166	0.216	0.199	0.072	0.181	0.254	0.075	0.124	0.138	0.145	0.172
6	0.206	0.181	0.324	0.316	0.269	0.297	0.450	0.526	0.190	0.284	0.260	0.294	0.105	0.303	0.373	0.113	0.183	0.187	0.191	0.230
9	0.264	0.231	0.447	0.438	0.372	0.405	0.561	0.640	0.252	0.404	0.344	0.406	0.212	0.425	0.481	0.217	0.225	0.230	0.225	0.276
12	0.322	0.284	0.519	0.511	0.403	0.436	0.649	0.761	0.313	0.482	0.428	0.471	0.262	0.492	0.553	0.280	0.279	0.279	0.291	0.346
15	0.388	0.349	0.581	0.572	0.448	0.483	0.735	0.885	0.367	0.537	0.491	0.504	0.330	0.551	0.582	0.349	0.309	0.311	0.360	0.417
18	0.443	0.401	0.609	0.600	0.494	0.521	0.798	0.916	0.407	0.566	0.536	0.574	0.365	0.569	0.656	0.384	0.357	0.347	0.376	0.434
21	0.492	0.449	0.650	0.642	0.541	0.568	0.848	0.932	0.416	0.619	0.557	0.635	0.418	0.620	0.719	0.444	0.372	0.362	0.400	0.459
26	0.525	0.479	0.685	0.678	0.620	0.588	0.915	0.996	0.475	0.678	0.625	0.673	0.455	0.677	0.749	0.478	0.423	0.408	0.462	0.520
31	0.560	0.513	0.728	0.723	0.651	0.675	0.985	1.066	0.515	0.724	0.676	0.737	0.517	0.721	0.804	0.541	0.468	0.452	0.520	0.582
36	0.611	0.535	0.768	0.764	0.732	0.742	1.005	1.092	0.553	0.772	0.723	0.796	0.576	0.762	0.855	0.663	0.565	0.529	0.595	0.652
41	0.621	0.572	0.800	0.794	0.746	0.757	1.063	1.146	0.586	0.882	0.769	0.883	0.703	0.861	0.957	0.680	0.604	0.564	0.638	0.695
46	0.647	0.608	0.838	0.823	0.787	0.795	1.133	1.210	0.664	0.911	0.854	0.933	0.706	0.888	0.993	0.730	0.634	0.590	0.680	0.730
53	0.681	0.630	0.857	0.858	0.849	0.855	1.224	1.297	0.711	0.967	0.910	0.983	0.760	0.932	1.045	0.783	0.680	0.623	0.742	0.780
60	0.706	0.658	0.896	0.898	0.902	0.921	1.291	1.357	0.760	1.010	0.964	1.041	0.803	0.976	1.100	0.828	0.732	0.669	0.794	0.825
67	0.739	0.693	0.980	0.981	0.982	0.967	1.344	1.418	0.802	1.060	1.012	1.090	0.855	1.026	1.149	0.881	0.766	0.697	0.813	0.837
74	0.811	0.764	1.008	1.011	1.023	1.001	1.410	1.465	0.838	1.092	1.062	1.108	0.874	1.051	1.163	0.897	0.792	0.719	0.845	0.861
81	0.829	0.782	1.032	1.038	1.081	1.053	1.426	1.476	0.862	1.133	1.087	1.164	0.919	1.086	1.220	0.943	0.821	0.741	0.878	0.887
95	0.889	0.844	1.097	1.108	1.141	1.104	1.501	1.539	0.906	1.173	1.143	1.220	0.965	1.123	1.277	0.990	0.883	0.787	0.960	0.954
109	0.927	0.884	1.140	1.154	1.200	1.158	1.557	1.588	0.979	1.227	1.223	1.259	1.008	1.170	1.319	1.030	0.928	0.816	1.013	0.989
123	0.957	0.913	1.183	1.200	1.243	1.192	1.660	1.683	1.033	1.278	1.285	1.304	1.039	1.214	1.368	1.056	0.956	0.834	1.024	0.995
137	1.010	0.963	1.200	1.219	1.276	1.221	1.650	1.665	1.047	1.286	1.304	1.340	1.077	1.223	1.406	1.096	1.003	0.862	1.050	1.005
151	1.045	1.004	1.237	1.259	1.323	1.261	1.696	1.705	1.071	1.294	1.339	1.344	1.086	1.230	1.407	1.101	1.011	0.852	1.062	1.010

Table E.2.B. Weight-loss of 4 x 11 in. (100 x 280 mm) moist-cured cylindrical specimens, stored in a controlled environment of 50% R.H. and 72 °F (Mix Nos. 120 to 139), pcf.

Days	Mix Numbers																			
Stored	120	121	122	123	124	125	126	127	128	129	130	131	132	133	134	135	136	137	138	139
172	1.072	1.029	1.264	1.287	1.314	1.266	1.698	1.698	1.087	1.318	1.354	1.346	1.088	1.248	1.410	1.105	1.022	0.858	1.065	0.995
193	1.094	1.053	1.259	1.287	1.332	1.262	1.743	1.738	1.118	1.345	1.393	1.380	1.119	1.272	1.449	1.135	1.059	0.881	1.103	1.022
214	1.092	1.053	1.291	1.318	1.360	1.295	1.751	1.739	1.134	1.365	1.414	1.381	1.112	1.289	1.444	1.130	1.080	0.892	1.111	1.019
235	1.123	1.084	1.296	1.322	1.385	1.316	1.774	1.754	1.156	1.371	1.436	1.395	1.131	1.294	1.458	1.148	1.094	0.900	1.119	1.017
256	1.135	1.095	1.311	1.338	1.386	1.322	1.776	1.754	1.164	1.379	1.448	1.400	1.129	1.296	1.459	1.150	1.098	0.901	1.112	1.005
284	1.145	1.105	1.310	1.337	1.340	1.286	1.722	1.699	1.131	1.350	1.409	1.379	1.092	1.270	1.425	1.125	1.076	0.885	1.101	1.000
312	1.113	1.069	1.279	1.295	1.365	1.318	1.755	1.734	1.159	1.392	1.443	1.407	1.122	1.311	1.450	1.159	1.125	0.921	1.141	1.028
340	1.136	1.098	1.300	1.316	1.385	1.344	1.768	1.750	1.185	1.403	1.476	1.428	1.135	1.321	1.472	1.177	1.166	0.952	1.181	1.056
368	1.155	1.115	1.317	1.330	1.392	1.353	1.784	1.762	1.201	1.439	1.499	1.459	1.176	1.361	1.507	1.216	1.210	0.979	1.221	1.084

APPENDIX F

WEIGHT-GAIN

Table F.1.A. Weight-gain of 4 x 8 in. (100 x 200 mm) heat-cured cylindrical specimens, stored submerged under water (Mix Nos. 100 to 119), pcf.

Days Stored	Mix Numbers																			
	100	101	102	103	104	105	106	107	108	109	110	111	112	113	114	115	116	117	118	119
0	0.000	0.000	0.000	0.000	0.000	0.000	0.000	0.000	0.000	0.000	0.000	0.000	0.000	0.000	0.000	0.000	0.000	0.000	0.000	0.000
7	1.910	2.243	2.164	2.304	1.008	0.978	1.110	1.266	1.417	1.527	1.944	2.020	0.815	0.781	1.209	1.307	1.334	1.110	1.819	1.978
21	1.971	2.493	2.482	2.531	1.091	1.088	1.224	1.395	1.580	1.773	2.152	2.315	0.898	0.856	1.349	1.467	1.501	1.334	1.993	2.168
42	2.334	2.603	2.615	2.675	1.194	1.186	1.326	1.493	1.713	1.971	2.277	2.512	1.004	0.978	1.417	1.516	1.618	1.493	2.080	2.251
70	2.395	2.691	2.763	2.785	1.277	1.296	1.413	1.573	1.864	2.152	2.406	2.694	1.065	1.091	1.531	1.645	1.751	1.660	2.160	2.421
105	2.569	2.770	2.891	2.941	1.406	1.432	1.542	1.709	1.971	2.327	2.497	2.766	1.201	1.224	1.694	1.804	1.834	1.736	2.304	2.554
147	2.649	2.857	2.990	3.024	1.467	1.504	1.611	1.792	2.092	2.456	2.581	2.880	1.277	1.288	1.713	1.853	1.910	1.834	2.365	2.687
196	2.679	2.910	3.054	3.096	1.520	1.565	1.667	1.853	2.084	2.437	2.645	2.960	1.296	1.364	1.758	1.921	1.948	1.880	2.425	2.747
252	2.717	2.956	3.153	3.176	1.550	1.603	1.717	1.925	2.168	2.497	2.721	3.035	1.311	1.372	1.777	1.936	2.012	1.921	2.486	2.797
315	2.759	2.963	3.168	3.221	1.576	1.652	1.739	1.933	2.221	2.554	2.728	3.051	1.387	1.459	1.815	1.993	2.054	1.982	2.528	2.865
385	2.781	2.986	3.206	3.225	1.618	1.660	1.762	1.978	2.240	2.573	2.785	3.073	1.406	1.493	1.823	2.008	2.084	1.986	2.577	2.891

Table F.1.B. Weight-gain of 4 x 8 in. (100 x 200 mm) heat-cured cylindrical specimens, stored submerged under water (Mix Nos. 120 to 139), pcf.

Days Stored	Mix Numbers																			
	120	121	122	123	124	125	126	127	128	129	130	131	132	133	134	135	136	137	138	139
0	0.000	0.000	0.000	0.000	0.000	0.000	0.000	0.000	0.000	0.000	0.000	0.000	0.000	0.000	0.000	0.000	0.000	0.000	0.000	0.000
7	0.868	0.803	1.019	1.137	1.629	0.913	2.433	1.467	1.190	0.959	1.789	0.875	1.413	0.978	1.811	1.103	1.880	0.947	1.845	1.448
21	0.902	0.887	1.141	1.228	1.899	0.993	2.641	1.573	1.364	1.088	1.959	0.970	1.580	1.080	1.952	1.213	2.027	1.061	1.948	1.482
42	1.016	0.963	1.216	1.296	2.103	1.080	2.838	1.713	1.516	1.182	2.069	1.156	1.773	1.201	2.096	1.296	2.183	1.179	1.955	1.508
70	1.114	1.072	1.296	1.421	2.312	1.209	2.982	1.804	1.694	1.349	2.205	1.194	2.008	1.330	2.236	1.448	2.380	1.349	2.069	1.614
105	1.175	1.163	1.395	1.531	2.493	1.341	3.176	1.940	1.880	1.432	2.376	1.357	2.103	1.467	2.410	1.497	2.421	1.368	2.198	1.709
147	1.235	1.216	1.448	1.595	2.581	1.383	3.289	1.986	1.936	1.520	2.459	1.425	2.194	1.523	2.539	1.554	2.463	1.444	2.266	1.796
196	1.277	1.277	1.489	1.645	2.656	1.459	3.407	2.031	2.005	1.573	2.554	1.482	2.274	1.546	2.637	1.576	2.550	1.539	2.319	1.838
252	1.330	1.341	1.512	1.667	2.766	1.504	3.483	2.080	2.046	1.626	2.596	1.527	2.338	1.599	2.698	1.618	2.592	1.614	2.365	1.861
315	1.357	1.360	1.539	1.717	2.797	1.508	3.539	2.118	2.099	1.652	2.672	1.561	2.403	1.629	2.766	1.629	2.611	1.675	2.406	1.861
385	1.379	1.391	1.565	1.739	2.850	1.565	3.592	2.152	2.118	1.743	2.694	1.599	2.433	1.675	2.838	1.664	2.660	1.728	2.463	1.906

Table F.2.A. Weight-gain of 4 x 8 in. (100 x 200 mm) moist-cured cylindrical specimens, stored submerged under water (Mix Nos. 100 to 119), pcf.

Days Stored	Mix Numbers																			
	100	101	102	103	104	105	106	107	108	109	110	111	112	113	114	115	116	117	118	119
0	0.000	0.000	0.000	0.000	0.000	0.000	0.000	0.000	0.000	0.000	0.000	0.000	0.000	0.000	0.000	0.000	0.000	0.000	0.000	0.000
7	0.870	0.870	0.961	0.961	0.640	0.640	0.801	0.801	0.726	0.684	0.820	0.853	0.584	0.585	0.775	0.820	0.726	0.684	0.820	0.853
21	0.955	0.955	1.089	1.089	0.659	0.659	0.824	0.824	0.796	0.771	0.911	0.945	0.637	0.686	0.832	0.875	0.796	0.771	0.911	0.945
42	1.048	1.048	1.177	1.177	0.707	0.707	0.872	0.872	0.875	0.839	0.993	1.055	0.709	0.743	0.873	0.923	0.875	0.839	0.993	1.055
70	1.089	1.089	1.292	1.292	0.760	0.760	0.934	0.934	0.955	0.951	1.089	1.161	0.777	0.817	0.959	1.004	0.955	0.951	1.089	1.161
105	1.184	1.184	1.436	1.436	0.811	0.811	1.016	1.016	1.023	1.010	1.180	1.254	0.837	0.898	1.072	1.122	1.023	1.010	1.180	1.254
147	1.283	1.283	1.510	1.510	0.866	0.866	1.078	1.078	1.086	1.067	1.256	1.351	0.862	0.936	1.089	1.146	1.086	1.067	1.256	1.351
196	1.324	1.324	1.542	1.542	0.885	0.885	1.101	1.101	1.093	1.103	1.292	1.404	0.873	0.944	1.110	1.167	1.093	1.103	1.292	1.404
252	1.370	1.370	1.614	1.614	0.908	0.908	1.146	1.146	1.129	1.124	1.334	1.448	0.894	0.966	1.116	1.171	1.129	1.124	1.334	1.448
315	1.389	1.389	1.618	1.618	0.909	0.909	1.127	1.127	1.182	1.163	1.353	1.472	0.911	0.968	1.161	1.196	1.182	1.163	1.353	1.472
385	1.415	1.415	1.629	1.629	0.915	0.915	1.154	1.154	1.165	1.188	1.387	1.501	0.921	0.985	1.133	1.188	1.165	1.188	1.387	1.501

Table F.2.B. Weight-gain of 4 x 8 in. (100 x 200 mm) moist-cured cylindrical specimens, stored submerged under water (Mix Nos. 120 to 139), pcf.

Days Stored	Mix Numbers																			
	120	121	122	123	124	125	126	127	128	129	130	131	132	133	134	135	136	137	138	139
0	0.000	0.000	0.000	0.000	0.000	0.000	0.000	0.000	0.000	0.000	0.000	0.000	0.000	0.000	0.000	0.000	0.000	0.000	0.000	0.000
7	0.584	0.585	0.775	0.820	0.815	0.754	1.307	1.197	0.614	0.837	0.792	0.784	0.963	0.875	1.000	0.944	0.894	0.720	0.909	0.822
21	0.637	0.686	0.832	0.875	0.902	0.792	1.372	1.228	0.686	0.883	0.883	0.864	0.997	0.902	1.095	1.004	0.921	0.758	1.016	0.868
42	0.709	0.743	0.873	0.923	0.955	0.822	1.520	1.341	0.762	0.936	0.970	0.944	1.061	0.959	1.160	1.080	1.016	0.800	1.046	0.879
70	0.777	0.817	0.959	1.004	1.110	0.909	1.648	1.413	0.856	1.016	1.061	0.985	1.239	1.031	1.288	1.163	1.175	0.932	1.156	0.993
105	0.837	0.898	1.072	1.122	1.243	0.993	1.770	1.523	0.966	1.110	1.182	1.099	1.269	1.122	1.436	1.228	1.201	0.917	1.285	1.088
147	0.862	0.936	1.089	1.146	1.273	0.989	1.853	1.550	0.978	1.103	1.232	1.163	1.345	1.133	1.512	1.269	1.190	0.925	1.353	1.141
196	0.873	0.944	1.110	1.167	1.353	1.031	1.929	1.599	1.027	1.125	1.273	1.171	1.391	1.156	1.569	1.296	1.258	0.955	1.364	1.175
252	0.894	0.966	1.116	1.171	1.429	1.057	1.993	1.611	1.038	1.141	1.292	1.194	1.440	1.167	1.611	1.315	1.273	0.978	1.391	1.186
315	0.911	0.968	1.161	1.196	1.444	1.050	2.058	1.637	1.076	1.137	1.330	1.197	1.493	1.163	1.660	1.341	1.288	0.997	1.406	1.179
385	0.921	0.985	1.133	1.188	1.493	1.076	2.099	1.671	1.095	1.163	1.326	1.209	1.520	1.216	1.713	1.357	1.304	0.981	1.448	1.216

APPENDIX G

BIBLIOGRAPHY

ON

HIGH STRENGTH CONCRETE

The initial compilation of this bibiliography was done as part of this research program. The list of references was subsequently modified to provide researchers and practitioners with an up-to-date list of references on high strength concrete pretaining particularly to precast and prestressed concrete. The list of the papers is given by author names in alphabetical order.

1. (1967), "Methods of Achieving High Strength Concrete," ACI Journal, 64(1), 45-48.
2. (1970), "High-Strength Concrete," Concrete, 83-84.
3. (1990), "Higher Strengths Tricky to Test," Engineering News-Record, 224(3), 56-58.
4. (1991), "Capping High Strength Cylinders with Sulphur," NRMCA Technical Information Letteer No. 484, National Ready Mixed Concrete Association, Silver Spring, MD, 5-7.
5. (1991), "High-Strength Concrete in High Seismic Zones?" Engineering News-Record, 226(18), C-76 to C-78.
6. (1991), "Report from CERF/NIST Strategy/Implementation Meeting on Research Programs for High Performance Concrete and Steel: Held in Washington, D.C., August 1991," Civil Engineering Research Foundation, Washington, D.C., 19 pp.
7. (1992), "A New Look at Quality Control Testing of High-Strength Concrete," CTL Review, 15(2).
8. (1992), "Meeting the Challenge of High-Strength Concrete," CTL Review, 15(2).
9. Abbasi, A. F.; Ahmad, Munir; and Wasim, Mohammad(1987), "Optimization of Concrete Mix Proportioning Using Reduced Factorial Experimental Technique," ACI Materials Journal, 84(1), 55-63.
10. Abe, Michihiko; Masuda, Yoshihiro; Shiomi, Itsuo; and Matsumoto, Masayuki(1993), "Experimental Study on Mix Design of High Strength Concrete," Proceedings of the Third International Symposium on Utilization of High-Strength Concrete, Lillehammer, Norway, Volume 2, 631-638.
11. ACI (1971), "Designing for Effects of Creep, Shrinkage, Temperature in Concrete Structures," ACI SP-27, 430 pp.
12. ACI 212.4R Committee Report (1993), "Guide for the Use of High-Range Water-Reducing Admixtures (superplasticizers) in Concrete," Concrete International, 15(4), 40-47.
13. ACI Committee 116 (1967), "Cement and Concrete Terminology," ACI SP-19.
14. ACI Committee 211 (1993), "Guide for Selecting Proportions for High-Strength Concrete with Portland Cement and Fly Ash," ACI Materials Journal, 90(3), 272-283. (see discussion January-February 1994)
15. ACI Committee 212 (1993), "Chemical Admixtures for Concrete," Concrete International, 15(10), 48-53.
16. ACI Committee 226 (1987), "Silica Fume in Concrete," ACI Materials Journal, 84(2), 158-166.
17. ACI Committee 363 (1987), "Research Needs for High-Strength Concrete," ACI Materials Journal, 84(6), 559-561.
18. ACI Committee 363 (1992), "State-of-the-Art Report on High-Strength Concrete," American Concrete Institute, Detroit, 55 pp.

19. Addis, B. J.; and Alexander, M. G. (1990), "A Method of Proportioning Trial Mixes for High-Strength Concrete," Proceedings of the Second International Symposium on Utilization of High-Strength Concrete, Berkeley, California, 287-308.

20. Adeline, R.; and Behloul, M. (1996), "High Ductile Beams without Passive Reinforcement," Proceedings of the Fourth International Symposium on the Utilization of High Strength/High Performance Concrete, Paris, France, Volume 3, 1383-1390.

21. Adelman, Douglas; and Cousins, Thomas E. (1990), "Evaluation of the Use of High Strength Concrete Bridge Girders in Louisiana," PCI Journal, 70-78.

22. Ahmad, S. H.; and Barker, R. (1991), "Flexural Behavior of Reinforced High-Strength Lightweight Concrete Beams," ACI Structural Journal, 88(1), 69-77.

23. Ahmad, S. H.; and Lue, D. M. (1987), "Flexure-Shear Interaction of Reinforced High-Strength Concrete Beams," ACI Structural Journal, 84(4), 330-341.

24. Ahmad, S.H.; and Shah, S. P. (1987), "High Strength Concrete-A New Material," Proceedings of ASCE Structures Congress, Orlando, FL, 421-434.

25. Ahmad, Shuaib H.; and Shah, S. P. (1985), "Structural Properties of High Strength Concrete and its Implications for Precast Prestressed Concrete," PCI Journal, 30(6), 92-119.

26. Ahmad, Shuaib H.; Khaloo, A. R.; and Poveda A. (1986), "Shear Capacity of Reinforced High-Strength Concrete Beams," ACI Journal, 83(2), 297-305.

27. Ahmad, Shuaib H.; Zia, Paul; Leming, Mike; and Hansen, M. R. (1992), "Mechanical Properties of High Performance Concretes," Proceedings of the 9th Conference on Engineering Mechanics, Published by ASCE, New York, NY., 864-867.

28. Aïtcin, P. C.; and Richard, P. (1996), "The Pedestrian-Bikeway Bridge of Sherbrooke," Proceedings of the Fourth International Symposium on the Utilization of High Strength/High Performance Concrete, Paris, France, Volume 3, 1399-1406.

29. Aïtcin, P. C.; Sarkar, S. L.; and Yaya, D. (1987) "Microstructural Study of Different Types of Very High-Strength Concrete," Proceedings, Material Research Society symposium, Material Research Society, Pittsburgh, Volume 85, 261-272.

30. Aïtcin, P.-C.; and Mehta, P. K. (1990), "Effect of Coarse-Aggregate Characteristics on Mechanical Properties of High-Strength Concrete," ACI Materials Journal, 87(2), 103-107.

31. Aïtcin, Pierre-Claude; and Laplante, P. (1990), "Long Term Compressive Strength of Silica-Fume Concrete," Journal of Materials in Civil Engineering, 2(3), 164-170.

32. Aïtcin, Pierre-Claude; and Lessard, Michel (1994), "Canadian Experience with Air-Entrained High-Performance Concrete," Concrete International, 16(10), 35-38.

33. Aïtcin, Pierre-Claude; and Neville, adam (1993), "High-Performance Concrete Demystified," Concrete International, 15(1), 21-26.

34. Aïtcin, Pierre-Claude; Jolicoeur, Carmel; and MacGregor, James G. (1994), "Superplasticizers: How They Work and Why They Occasionally Don't," Concrete International, 16(5), 45-52.

35. Aïtcin, Pierre-Claude; Laplante, Pierre; and Bedard, Claude (1985), "Development and Experimental Use of a 90 MPa(13,000 psi) Field Concrete," American Concrete Institute, SP-87, 51-70.

36. Aïtcin, Pierre-Claude; Miao, Buquan; Cook, William D.; and Mitchell, Denis (1994), "Effect of Size and Curing on Cylinder Compressive Strength of Normal and High-Strength Concretes," ACI Materials Journal, 91(4), 349-354.

37. Aïtcin, Pierre-Claude; Sarkar, Shondeep L; Ranc, Roger; and Levy, Christophe (1991), "A High Silica Modulus Cement for High-Performance Concrete," Ceramic Transactions, Volume 16, 795 pp.

38. Ajdukiewicz, A. B.; Kliszczewicz, A. T.; and Hulimka, J. S. (1996), "Test of Joints in Composite Slab-Column Structures with HSC/HPC Head-And-Column Precast Members," Proceedings of the Fourth International Symposium on the Utilization of High Strength/High Performance Concrete, Paris, France, Volume 3, 1009-1014.

39. Ajdukiewicz, Andrzej; and Kliszczewicz, Alina (1993), "Application of High-Strength Concrete in Composite Skeletal Structures," Proceedings of the Third International Symposium on Utilization of High-Strength Concrete, Lillehammer, Norway, Volume 1, 449-456.

40. Al-Hussaini, A.; Regan, P. E.; Xue, H-Y.; and Ramdane, K-E. (1993), "The Behaviour of HSC Columns Under Axial Load," Proceedings of the Third International Symposium on Utilization of High-Strength Concrete, Lillehammer, Norway, Volume 1, 83-90.

41. Al-Sugair, Faisal H.; and Almudaiheem, Jamal A. (1990), "Further Modification of the Ross Equation to Predict the Ultimate Drying Shrinkage of Concrete," ACI Materials Journal, 87(3), 237-240. (see discussion March-April 91)

42. Alameddine, Fadel; and Ehsani, Mohammad R. (1989), "Behavior of Ductile High-Strength Concrete Connections," Report No. CEEM-89-105, Department of Civil Engineering and Engineering Mechanics, The University of Arizona, Tucson, Arizona, 258pp.

43. Albinger, JOhn M. (1988), "High Strength Concrete in the United States," Presented on November 7, 1988 in Paris, France.

44. Alexander, K. M.; Bruere, G. M.; and Ivanusec, I. (1980), "The Creep and Related Properties of Very High-Strength Superplasticized Concrete," Cement and Concrete Research, 10(2), 131-137.

45. Aljassar, Ahmad; and Hass, Ralph (1994), "Towards Automating Size-Gradation Analysis of Mineral Afggregate," Papaer No. 940686, Transportation Research Board (TRB), 73rd Annual Meeting, 22 pp.

46. Almeida, I. R. (1990), "Cracking Resistance of High-Strength Concretes," Proceedings of the Second International Symposium on Utilization of High-Strength Concrete, Berkeley, California, 489-504.

47. Almeida, I. R. de; Cordeiro, T. J. R. B.; and Costa, J. P. M. (1993), "Structural Rehabilitation Using Shotcrete with Microsilica," Proceedings of the Third International Symposium on Utilization of High-Strength Concrete, Lillehammer, Norway, Volume 1, 457-467.

48. Almudaiheem, Jamal A.; and Hansen, Will (1987), "Effect of Specimen Size and Shape on Drying Shrinkage," ACI Materials Journal, 84(2), 130-135. (see discussion January-February 88)

49. Almudaiheem, Jamal A.; and Hansen, Will (1989), "Prediction of Concrete Drying Shrinkage from Short-Term Measurements," ACI Materials Journal, 86(4), 401-408.

50. Amor, C. Ben; Clement, J. -L. (1996), "Behaviour of HPC Under Thermal and Moisture Loads," Proceedings of the Fourth International Symposium on the Utilization of High Strength/High Performance Concrete, Paris, France, Volume 2, 433-438.

51. Anderson, F. David (1985), "Statistical Controls for High-Strength Concrete," American Concrete Institute, SP-87, 71-82.

52. Andrade, M. C.; Frías, M.; and Aarup, B. (1996), "Durability of Ultra-High Strength Concrete: Compact Reinforced Composite," Proceedings of the Fourth International Symposium on the Utilization of High Strength/High Performance Concrete, Paris, France, Volume 2, 529-534.

53. Aoyama, H.; Murota, T.; Hiraishi, H.; and Bessho, S. (1990), "Outline of the Japanease National Project on Advanced Reinforced Concrete Buildings with High-Strength and High-Quality Materials," Proceedings of the Second International Symposium on Utilization of High-Strength Concrete, Berkeley, California, 21-31.

54. Arioglu, Erdem; Arioglu, Basar; Arioglu, Ülkü; Arioglu, Ergin; and Alper, Hüsamettin (1993), "Experimental Investigations on Mechanical Properties of Very High-Strength Concrete," Proceedings of the Third International Symposium on Utilization of High-Strength Concrete, Lillehammer, Norway, Volume 2, 999-1006.

55. Armelin, Hugo S.; Lima, Maryangela G.; and Selmo, Silvia M. S. (1993), "High Strength LWA Concrete - The First Brazilizn Experience," Proceedings of the Third International Symposium on Utilization of High-Strength Concrete, Lillehammer, Norway, Volume 2, 639-645.

56. Asgeirsson, Haraldur (1992), "Intermilled Silica Fume in Icelandic Cement," Concrete International, 14(7), 56.

57. ASTM C 125-93 (1993), "Annual Book of ASTM Standards," American Society for Testing and Materials, Philadelphia, PA.

58. Aswad, Alex; and Hester, Weston T. (1985), "Impact of High-Strength Concrete on Design and Service Behavior of Prestressed Prercast Concrete Members," American Concrete Institute, SP-87, 9-20.

59. Atlassi, Elisabeth (1993), "Effect of Moisture Gradients on the Compressive Strength of High Performance Concrete," Proceedings of the Third International Symposium on Utilization of High-Strength Concrete, Lillehammer, Norway, Volume 2, 646-653.

60. Attard, M. M.; and Foster, S. J. (1996), "Static Ductility of High Strength Concrete Columns Under Eccentric Loading," Proceedings of the Fourth International Symposium on the Utilization of High Strength/High Performance Concrete, Paris, France, Volume 3, 863-872.

61. Australian Standard 1012.8 (1986), "Methods of Testing Concrete: Part 8- Method for Making and Curing Concrete Compression, Indirect Tensile and Flexure Test Specimens, in the Laboratory or in the Field," published by the Standards Association of Australia.

62. Azizinamini, A.; and Kebraei, M. (1996), "Flexural Capacity of High Strength Concrete Columns," Proceedings of the Fourth International Symposium on the Utilization of High Strength/High Performance Concrete, Paris, France, Volume 3, 873-882.

63. Azizinamini, Atorod; and Prakash, Bangalore A. (1993), "Application of High-Strength Concrete in High Rise Buildings," Proceedings of the Third International Symposium on Utilization of High-Strength Concrete, Lillehammer, Norway, Volume 1, 474-481.

64. Azizinamini, Atorod; and Russell, Henry G. (1993), "Design Criteria for Tension Splices in High-Strength Concrete," Proceedings of the Third International Symposium on Utilization of High-Strength Concrete, Lillehammer, Norway, Volume 1, 99-106.

65. Azizinzmini, Atorod; and Kuska, Sharon S. B. (1993), "Flexural Capacity and Ductility of High-Strength Concrete Columns," Proceedings of the Third International Symposium on Utilization of High-Strength Concrete, Lillehammer, Norway, Volume 1, 91-98.

66. Baalbaki, Moussa; Baalbaki, Walid; and Sarkar, Shondeep (1993), "A Comparative Study of Mechanical Properties and Microstructure of High Performance Concretes Containing Natural and Artificial Aggregates," Proceedings of the Third International Symposium on Utilization of High-Strength Concrete, Lillehammer, Norway, Volume 2, 654-670.

67. Baalbaki, W.; Benmokrane, B.; Chaallal, O.; and Aïtcin, P. -C. (1991), "Influence of Coarse Aggregate on Elastic Properties of High-Performance Concrete," ACI Materials Jopurnal, 88(5), 499-503.

68. Baalbaki, Walid; Aïtcin, Pierre-Claude; and Ballivy, Gerard (1992), "On Predicting Modulus of Elasticity in High-Strength Concrete," ACI Materials Journal, 89(5), 517-520. (see discussion July-August 93)

69. Baalbaki, Walid; Baalbaki, Moussa; Benmokrane, Brahim; and Aïtcin, Pierre-Claude (1992), "Influence of Specimen Size on Compressive Strength and Elastic Modulus of High-Performance Concrete," Cement, Concrete, and Aggregate, 14(2), 113-117.

70. Baalbaki, Walid; Benmokrane, Brahim; Chaallal, Omar; and Aïtcin, Pierre-Claude (1991), "Influence of Coarse Aggregate on Elastic Properties of High-Performance Concrete," ACI Materials Journal, 88(5), 499-503. (see discussion July-August 92)

71. Bakht, Baidar; Jaeger, Leslie G.; and Mufti, Aftab A. (1989), "Elastic Modulus of Concrete from Compression Tests," ACI Materials Journal, 86(3), 220-224.

72. Baroghel-Bouny, V.; Godin, J.; and Gawsewitch, J. (1996), "Microstructure and Moisture Properties of High Performance Concrete," Proceedings of the Fourth International Symposium on the Utilization of High Strength/High Performance Concrete, Paris, France, Volume 2, 451-462.

73. Barrow, Richard S.; and Carrasquillo, Ramon L. (1988), "The Effect of Fly Ash on the Temperature Rise in Concrete," Research Report 481-2, Center for Transportation Research, The University of Texas at Austin, 178 pp.

74. Bartlett, Michael F.; and MacGregor, James G. (1994), "Effect of Core Diameter on Concrete Core Strengths," ACI Materials Journal, 91(5), 460-470.

75. Bartlett, Michael F.; and MacGregor, James G. (1994), "Effect of Core Length-to-Diameter Ratio on Concrete Core Strengths," ACI Materials Journal, 91(4), 339-348.

76. Bartlett, Michael F.; and MacGregor, James G. (1994), "Effect of Moisture Condition on Concrete Core Strengths," ACI Materials Journal, 91(3), 227-236.

77. Barton, Robert B., "Water-Cement Ratio is Passe' (1989)," Concrete International, 11(11), 75-78.

78. Bayasi, Ziad (1992), "Effects of Fly Ash on the Properties of Silica-Fume Concrete," Concrete International, 14(4), 52-54.

79. Bayasi, Ziad; and Zhou, Jing (1993), "Properties of Silica Fume Concrete and Mortar," ACI Materials Journal, 90(4), 349-356. (see discussion anuary-February 1994)

80. Bazant, Z. P.; Kim, J. K.; Wittmann, F. H.; and Alou, F. (1987), "Statistical Extrapolation of Shrinkage Data-Part II: Bayesian Updating," ACI Materials Journal, 84(2), 83-91. (see discussion January-February 88)

81. Bazant, Z. P.; Wittmann, F. H.; Kim, J. K.; and Alou F. (1987), "Statistical Extrapolation of Shrinkage Data-Part I: Regression," ACI Materials Journal, 84(1), 20-34.

82. Bazant, Zdenek P.; and Schell, William F. (1993), "Fatigue Fracture of High-Strength Concrete and Size Effect," ACI Materials Journal, 90(5), 472-478.

83. Bazant, Zdenek P.; Kazemi, Mohammad Taghi; Hasegawa, Toshiaki; and Mazars Jacky (1991), "Size Effect in Brazilian Split-Cylinder Tests: Measurements and Fracture Analysis," ACI Materials Journal, 88(3), 325-332.

84. Behloul, M.; Bernier, G.; and Cheyrezy, M. (1996), "Tensile Behavior of Reactive Powder Concrete (RPC)," Proceedings of the Fourth International Symposium on the Utilization of High Strength/High Performance Concrete, Paris, France, Volume 3, 1375-1382.

85. Belanger, Paul R.; and Shirlaw, Michael R. (1993), "Temperature Control in High-Strength, Massive Concrete Girders," Concrete International, 15(11), 30-32.

86. Bentur, Arnon; and Goldman, Ariel (1989), "Curing Effects, Strength and Physical Properties of High Strength Silica Fume Concrete," Journal of Materials in Civil Engineering, 1(1), 46-58.

87. Bentz, Dale P.; and Garboczi, Edward J. (1991), "Simulation Studies of the Effects of Mineral Admixtures on the Cement Paste-Aggregate Interfacial Zone," ACI Materials Journal, 88(5), 518-529.

88. Berke, N. S.; Dallaire, M. P.; and Hicks, M. C. (1992), "Plastic, Mechanical, Corrosion, and Chemical Resistance Properties of Silica Fume(Microsilica) Concretes," Fly Ash, Silica Fume, Slag, and Natural Pozzolans in Concrete, Proceedings Fourth International Conference, Istanbul, Turkey, Volume 2, 1125-1149.

89. Berntsson, Leif; Chandra, Satish; and Kutti, Tomas (1990), "Principles and Factors Influencing High-Strength Concrete Production," Concrete International, 12(12), 59-62.

90. Berra, M.; and Ferrara, G. (1990), "Normal and Total-Lightweight High-Strength Concretes: A Comparative Experimental Study," Proceedings of the Second International Symposium on Utilization of High-Strength Concrete, Berkeley, California, 701-733.

91. Berra, M.; Melchiorri, G.; and Pastore, T. (1996), "Durability Tests on Normal and Total-Lightweight Reinforced Concretes in Marine Environment," Proceedings of the Fourth International Symposium on the Utilization of High Strength/High Performance Concrete, Paris, France, Volume 2, 499-508.

92. Berry, E. E.; and Malhotra, M. (1980), "Fly Ash for Use in Concrete-A Critical Review," ACI Journal, 77(2), 59-73.

93. Bickley, J. A. (1991), "The Canadian Network of Excellence on High-Performance Concrete," presentation at the National Institute of Standards and Technology's CBT Building Technology Symposium: "Properties, Performance and Application of High-Performance Concrete," Gaithersburg, MD.

94. Bickley, J. A.; Ryell, J.; Rogers, C.; and Hooton, R. D. (1991), "Some Characteristics of High-Strength Structural Concrete," Can. J. Ci Eng., 18, 885-889.

95. Bickley, John A. (1993), "Prequalification Requirements for the Supply and Testing of Very High Strength Concrete," Concrete International, 15(2), 62-64.

96. Bigaj, A. J.; Den Uijl, J. A.; and Walraven, J. C. (1996), "A Bond Model for Ribbed Bars in HSC and NSC - Experimental Study," Proceedings of the Fourth International Symposium on the Utilization of High Strength/High Performance Concrete, Paris, France, Volume 3, 1125-1134.

97. Bisaillon, André; Rivest, Michel; and Malhotra, M. (1994), "Performance of High-Volume Fly Ash Concrete in Large Experimental Monoliths," ACI Materials Journal, Vol. 91(2), 178-187.

98. Bjerkeli, L.; Tomaszewicz, A.; and Jensen, J. J. (1990), "Deformation Properties and Ductility of High-Strength Concrete," Proceedings of the Second International Symposium on Utilization of High-Strength Concrete, Berkeley, California, 215-238.

99. Blick, Ronald L. (1973), "Some Factors Influencing High-Strength Concrete," Modern Concrete, 36(12), 38-41.

100. Blick, Ronald L., Petersen, Charles F., and Winter, Michael E. (1985), "Proportioning and Controlling High Strength Concrete" Proportioning Concrete Mixes, ACI SP-46, 141-163.

101. Bloem, Delmar L.; and Gaynor, Richard D. (1964), "Effects of Aggregate Properties on Strength of Concrete," ACI Journal, 60(10), 1429-1454.

102. Bloom, R.; and Bentur, A. (1993), "Restrained Shrinkage of High Strength Concrete," Proceedings of the Third International Symposium on Utilization of High-Strength Concrete, Lillehammer, Norway, Volume 2, 1007-1014.

103. Bortolotti, Lionello (1988), "Double-Punch Test for Tensile and Compressive Strength in Concrete," ACI Materials Journal, 85(1), 26-32.

104. Bortolotti, Lionello (1990), "Interdependence of Concrete Strength Parameters," ACI Materials Journal, 87(1), 25-26.

105. Boulay, C. (1996), "Capping HPC Cylinders with the Sand Box: New Developments," Proceedings of the Fourth International Symposium on the Utilization of High Strength/High Performance Concrete, Paris, France, Volume 2, 197-202.

106. Boulay, C.; and de Larrard, F. (1993), "Capping High-Performance Concrete Cylinders with the 'Sand-Box'," Proceedings of the Third International Symposium on Utilization of High-Strength Concrete, Lillehammer, Norway, Volume 2, 1015-1023.

107. Boulay, Claude; and de Larrard, Francois (1993), "A New Capping System for Testing HPC Cylinders: The Sand-Box," Concrete International, 15(4), 63-66.

108. Brazillier, D.; Bar, P.; Milan, A. L.; de Larrard, F.; and Roi, S. (1996), "Innovative Design of Small Highway Bridges in HPC," Proceedings of the Fourth International Symposium on the Utilization of High Strength/High Performance Concrete, Paris, France, Volume 3, 1447-1456.

109. Breitenbücker, R. (1996), "High Strength Concrete C 105 with Increased Fire Resistance Due to Polypropylen Fibres," Proceedings of the Fourth International Symposium on the Utilization of High Strength/High Performance Concrete, Paris, France, Volume 2, 571-578.

110. Bresson, J. (1996), "Mixing and Compacting Techniques for the Production of Very High Performance Precast Concrete Products," Proceedings of the Fourth International Symposium on the Utilization of High Strength/High Performance Concrete, Paris, France, Volume 2, 269-272.

111. Brooks, J. J.; and Al-Kaisi, A. F. (1990), "Early Strength Development of Portland and Slag Cement Concretes Cured at Elevated Temperatures," ACI Materials Journal, 87(5), 503-507.

112. Brooks, Jeffery J. (1993), "The Influence of Steel Fiber Reinforcement on Compressive Strength and Deformation of Ultra High Strength Cement-Silica Fume Mortar Matrix," Proceedings of the Third International Symposium on Utilization of High-Strength Concrete, Lillehammer, Norway, Volume 2, 1024-1031.

113. Brooks, Jeffery J.; and Hynes, John P. (1993), "Flexural Creep and Shrinkage of Plain and Steel Fiber Reinforced Ultra High Strength Compact Matrix Composite," Proceedings of the Third International Symposium on Utilization of High-Strength Concrete, Lillehammer, Norway, Volume 2, 1032-1037.

114. Bruce, R. N.; Martin, B. T.; Russell, H. G.; and Roller, J. J. (1992), "Feasibility Evaluation of Utilizing High-Strength Concrete in Design and Construction of Highway Bridge Structures (Interim Report)," Publication No. FHWA/LA-92/264, Louisiana Transportation Research Center, Baton Rouge, LA, 227 pp.

115. Bryant, Anthony H.; and Vadhanavikkit, Chayatit (1987), "Creep, Shrinkage-Size, and Age at Loading Effects," ACI Materials Journal, 84(2), 117-123.

116. Burg, R. G.; and Ost, B. W. (1992), "Engineering Properties of Commercially Available High-Strength Concretes," PCA Research and Development Bulletin RD104T, 55 pp.

117. Burgess, A. James; Ryell, John; and Bunting, John (1970), "High Strength Concrete for the Willows Bridge," ACI Journal, 67(8), 611-619.

118. Burnett, Ian (1989), "High-Strength Concrete in Melbourne, Australia," Concrete International, 11(4), 17-25.

119. Burnett, Ian (1991), "Silica Fume Concrete in Melbourne, Australia," Concrete International, 13(8), 18-24.

120. Cai, S. -H.; and Gu, W. -P. (1996), "Behaviour and Ultimate Strength of Steel-Tube-Confined High Strength Concrete Columns," Proceedings of the Fourth International Symposium on the Utilization of High Strength/High Performance Concrete, Paris, France, Volume 3, 827-834.

121. Cai, S. -H.; and Xue, L. -H. (1996), "Bearing Strength of High Strength Concrete Blocks," Proceedings of the Fourth International Symposium on the Utilization of High Strength/High Performance Concrete, Paris, France, Volume 3, 1243-1250.

122. Campbell, Glen M.; and Detwiler, Rachel J. (1993), "Development of Mix Designs for Strength and Durability of Steam-Cured Concrete," Concrete International, 15(7), 37-39.

123. Cannon, Robert W., Tuthill, Lewis; Schrader, Ernest K; and Tatro, Stephen B. (1992), "Cement-When to Say When!," Concrete International, 14(1), 52-54.

124. Carette, G. G.; Malhotra, V. M.; and Aïtcin, P. C. (1987), "Preliminary data on long-term strength development on condensed silica-fume concrete," Proceedings, International Workshop on Condensed Silica Fume in Concrete.

125. Carette, George; Bilodeau, Alain; Chevrier, Raymond L.; and Malhotra, M. (1993), "Mechanical Properties of Concrete Incorporating High Volumes of Fly Ash from Sources in the U.S.," ACI Materials Journal, Vol. 90(6), 535-544.

126. Carino, N. J.; and Clifton, J. R. (1990), "Outline of a National Plan on High-Performance Concrete; Report on the NIST/ACI Workshop," Publication No. NISTIR 4465, National Institute of Standards and Technology, Washington, D.C., 50 pp.

127. Carino, Nicholas J.; and Clifton, James R. (1991), "High-Performance Concrete: Research Needs to Enhance its Use," Concrete International, 13(9), 70-76.

128. Carino, Nicholas J.; and Lew, H. S. (1982), "Re-examination of the Relation Between Splitting Tensile and Compressive Strength of Normal Weight Concrete," ACI Journal, 79(3), 214-219.

129. Carpenter, J. E. (1980), "Applications of High Strength Concrete for Highway Bridges," Public Roads, 44(2), 76-83.

130. Carrasquillo, P. M.; and Carrasquillo, R. L. (1986), "Guidelines for Use of High Strength Concrete in Texas Highways," Research Report 367-1F, Center for Transportation Research, The University of Texas at Austin, 227 pp.

131. Carrasquillo, P. M.; and Carrasquillo, R. L. (1988), "Effect of Using Unbonded Capping Systems on the Compressive Strength of Concrete Cylinders," ACI Materials Journal, 85(3), 141-147.

132. Carrasquillo, P. M.; and Carrasquillo, R. L. (1988), "Evaluation of the Use of Current Concrete Practice in Production of High-Strength Concrete," ACI Materials Journal, 85(1), 49-54.

133. Carrasquillo, P. M.; and Tikalsky, P. J.; and Carrasquillo, R. L. (1986), "Mix Proportioning of Concrete Containing Fly Ash for Highway Applications," Research Report 364-4F, center for Transportation Research, The University of Texas at Austin, 49 pp.

134. Carrasquillo, Ramon L.; Nilson, Arthur H.; and Slate, Floyd O. (1981), "Properties of High Strength Concrete Subject to Short-Term Loads," ACI Journal, 87(3), 171-178.

135. Carrasquillo, Ramon L.; Slate, Floyd O.; and Nilson, Arthur H. (1981), "Microcracking and Behavior of High Strength Concrete Subjected to Short-Term Loading," ACI Journal, 78(3), 179-186.

136. Casanova, P.; and Rossi, P. (1996), "HSC Beams Submitted to Shear: Steel Fibers vs Stirrups," Proceedings of the Fourth International Symposium on the Utilization of High Strength/High Performance Concrete, Paris, France, Volume 3, 993-1002.

137. Castrodale, Reid W.; Burns, Ned H.; and Kreger, Michael E. (1988), "A Study of Pretensioned High Strength Concrete Girders in Comosite Highway Bridges-Laboratory

Tests," Research Report 381-3, Center for Transportation Research, The University of Texas at Austin, 210 pp.

138. Castrodale, Reid W.; Kreger, M. E.; and Burns, Ned H. (1988), "A Study of Pretensioned High Strength Concrete Girders in Composite Highway Bridges-Design Considerations," Research Report 381-4F, Center for Transportation Research, The University of Texas at Austin, 281 pp.

139. Cederwall, K.; Engstrom, B.; and Grauers, M. (1990), "High-Strength Concrete Used in Composite Columns," Proceedings of the Second International Symposium on Utilization of High-Strength Concrete, Berkeley, California, 195-214.

140. CERF (1993), "High-Performance Construction Materials and Systems: An Essential National Program for America and Its Infrastructure," prepared by the Civil Engineering Research Foundation and the Planning Committee for the Nationally-Coordinated Program on High-Performance Concrete and Steel, Technical Report 93-5011.

141. Chen, H. J.; Yen, T.; Chiu, J. D. (1996), "Strength Development of High Performance Concrete at Early Ages," Proceedings of the Fourth International Symposium on the Utilization of High Strength/High Performance Concrete, Paris, France, Volume 2, 719-724.

142. Chen, Robert C.; Carrasquillo, Ramon L.; and Fowler, David W. (1985), "Behavior of High-Strength Concrete Under Uniaxial and Biaxial Compression," American Concrete Institute, SP-87, 251-273.

143. Chen, Z.; and Wang, D. (1996), "Utilization of High Strength Concrete in China," Proceedings of the Fourth International Symposium on the Utilization of High Strength/High Performance Concrete, Paris, France, Volume 3, 1571-1580.

144. Chen, Zhaoyuan; Wang, Zihao; and Zhao, Qinjin (1993), "Use of High-Strength Concrete in Blast-Resistant Structures," Proceedings of the Third International Symposium on Utilization of High-Strength Concrete, Lillehammer, Norway, Volume 1, 120-127.

145. Chew, Michael Y. L. (1993), "Utilisation of High Strength Concrete," Proceedings of the Third International Symposium on Utilization of High-Strength Concrete, Lillehammer, Norway, Volume 2, 678-690.

146. Chicago Committee on High-Rise Buildings (1977), "High Strength Concrete in Chicago High-Rise Buildings," Task Force Report No. 5, 63 pp.

147. Chorinsky, E. Gf. (1990), "Repair Systems for High-Strength Concrete," Proceedings of the Second International Symposium on Utilization of High-Strength Concrete, Berkeley, California, 735-740.

148. Chung, Hung W. (1993), "Control of Concrete Quality Through Statistics," Concrete International, 15(5), 38-43.

149. Claeson, C.; Gylltoft, K.; and Grauers, M. (1996), "Experiments and Numerical Analyses of Reinforced High Strength Concrete Columns," Proceedings of the Fourth International

Symposium on the Utilization of High Strength/High Performance Concrete, Paris, France, Volume 3, 797-806.

150. Cohen, Menashi D.; and Olek, Jan (1989), "Silica Fume in PCC: The Effects of Form on Engineering Performance," Concrete International, 11(11), 43-47.

151. Cohen, Menashi D.; Olek, Jan; and Mather, Bryant (1991), "Silica Fume Improves Expansive-Cement Concrete," Concrete International, 13(3), 31-37.

152. Cohen, Menashi D.; Zhou, Yixia; and Dolch, William L. (1992), "Non-Air-Entrained High-Strength Concrete-Is It Frost Resistant?," ACI Materials Journal, 89(4), 406-415. (see discussion May-June 93)

153. Colaco, Joseph P. (1985), "75-Story Texas Commerce Plaza, Houston-the Use of High-Strength Concrete," American Concrete Institute, SP-87, 1-8.

154. Collepardi, M. (1984), "Water Reducers/Retarders," Concrete Admixtures Handbook, V. S. Ramachandran ed., Noyes Publications, Park Ridge, New Jersey, 626 pp.

155. Collins, Michael P. (1993), "Shear Design of High-Strength Concrete Structures," Proceedings of the Third International Symposium on Utilization of High-Strength Concrete, Lillehammer, Norway, Volume 1, 128-135.

156. Collins, Michael P.; Mitchell, Denis; and MacGregor, James G. (1993), "Structural Design Considerations for High-Strength Concrete," Concrete International, 15(5), 27-34.

157. Collins, Therese M. (1989), "Proportioning High-Strength Concrete to Control Creep and Shrinkage," ACI Materials Journal, 86(6), 576-580. (see discussion September-October 90)

158. Cong, Xiaofeng; Gong, Shanglong, Darwin, David; and McCabe, Steven L. (1992), "Role of Silica Fume in Compressive Strength of Cement Paste, Mortar, and Concrete," ACI Materials Journal, 89(4), 375-387. (see discussion July-August 93)

159. Cook, W. D.; Miao, B.; Aïtcin, P. -C.; and Mitchell, D. (1992), "Thermal Stresses in Large High-Strength Concrete Columns," ACI Materials Journal, 89(1), 61-68.

160. Cordes, H.; and Burkhardt, J. (1996), "Bending and Shear Tests on Post- and Pretensioned High Strength Concrete Beams," Proceedings of the Fourth International Symposium on the Utilization of High Strength/High Performance Concrete, Paris, France, Volume 3, 845-852.

161. Cordon, William A.; and Gillespie, H. Aldridge (1963), "Variables in Concrete Aggregates and Portland Cement Paste which Influence the Strength of Concrete," ACI Journal, 60(8), 1029-1050.

162. Cordon, William A.; and Thorpe, J. Derle (1975), "Proportioning and Evaluation of Concrete Mixtures," ACI Journal, 72(2), 46-49.

163. Corley, W. G.; Sozen, M. A.; and Siess, C. P., "Time-Dependent Deflections of Prestressed Concrete Beams," 25 pp.

164. Cornelius, B. J.; and Hemmings, R. T. (1993), "Investigation of Koch Blast Furnace Slags for Improving the Sulphate Resistance of Concrete: Part 1. Physical Testing Program," Radian Report No. 14-034-A1, Radian Canada Inc., 35 pp.

165. Cornelius, B. J.; and Hemmings, R. T. (1993), "Investigation of Koch Blast Furnace Slags for Prevention of Alkali-Aggregate Reactivity in Concrete: Part 1. Physical Testing Program," Radian Report No. 14-035-01A, Radian Canada Inc., 50 pp.

166. Counto, Upendra J. (1964), "The Effect of Elastic Modulus of the Aggregate on the Elastic Modulus, Creep and Creep Recovery of Concrete," Cement and Concrete Association (London), 16(48), 129-138.

167. Creazza, G.; Di Marco, R.; Russo, S.; and Siviero, E. (1996), "Tension Stiffening in High Strength Concrete," Proceedings of the Fourth International Symposium on the Utilization of High Strength/High Performance Concrete, Paris, France, Volume 3, 1135-1144.

168. Csson, D.; de Larrard, F.; Boulay, C.; and Paultre, P. (1996), "Modelling of the Post-Peak Behaviour of Confined High Performance Concrete Columns - The Strain Localization Approach," Proceedings of the Fourth International Symposium on the Utilization of High Strength/High Performance Concrete, Paris, France, Volume 3, 807-816.

169. Cubaynes, J. -F.; and Pons, G. (1996), "Influence of the Type of Coarse Aggregate on Shrinkage and Creep of High Strength Concretes," Proceedings of the Fourth International Symposium on the Utilization of High Strength/High Performance Concrete, Paris, France, Volume 2, 397-404.

170. Cumming, N. A.; and Seabrook, P. T. (1988), "Quality Assurance Program for Volume-Batched High-Strength Concrete," Concrete International, 10(8), 28-32.

171. Cusson, Daniel; and Paultre, Patrick (1993), "Experimental Study of High-Strength Concrete Columns Confined by Rectangular Ties," Proceedings of the Third International Symposium on Utilization of High-Strength Concrete, Lillehammer, Norway, Volume 1, 136-145.

172. Daerga, Per Anders; Pettersson, Maria; and Pöntinen, David (1993), "Fracture Properties in Tension of a High Performance Concrete," Proceedings of the Third International Symposium on Utilization of High-Strength Concrete, Lillehammer, Norway, Volume 2, 1193-1200.

173. Dahl, K. K. B. (1990), "Bent Bars in High-Strength Concrete," Proceedings of the Second International Symposium on Utilization of High-Strength Concrete, Berkeley, California, 767-780.

174. Dahl, Per A.; Fluge, Finn; and Hansen, Einar Aa. (1993), "Influence of Specimen Geometry and Loading Rate on the Compressive Strength of High Strength Concrete," Proceedings of the Third International Symposium on Utilization of High-Strength Concrete, Lillehammer, Norway, Volume 2, 1038-1045.

175. Dalhuisen, D. H.; Stroeven, P.; Bui, D. D.; and Quy, N. T. (1996), "Replacement of Condensed Silica Fume by Rice Husk Ash for the Production of High Strength Concrete in

Developing Countries," Proceedings of the Fourth International Symposium on the Utilization of High Strength/High Performance Concrete, Paris, France, Volume 2, 235-244.

176. Day, K. W. (1990), "Automatic Adjustment of Concrete Mixtures," Concrete International, 12(6), 51-53.

177. Day, K. W. (1996), "Production of HS/HPC," Proceedings of the Fourth International Symposium on the Utilization of High Strength/High Performance Concrete, Paris, France, Volume 1, 21-28.

178. Day, R. L.; and Haque, M. N. (1993), "Correlation between Strength of Small and Standard Concrete Cylinders," ACI Materials Journal, 90(5), 452-462.

179. de Almeida, I. R. (1996), "Bond Between Reinforcing Steel and High Strength Concrete," Proceedings of the Fourth International Symposium on the Utilization of High Strength/High Performance Concrete, Paris, France, Volume 3, 1097-1104.

180. de Larrard, F. (1990), "Creep and Shrinkage of High-Strength Field Concretes," Proceedings of the Second International Symposium on Utilization of High-Strength Concrete, Berkeley, California, 577-598.

181. de Larrard, F. (1993), "A Survey of Recent Researches Performed in the French 'LPC' Network on High-Performance Concrete," Proceedings of the Third International Symposium on Utilization of High-Strength Concrete, Lillehammer, Norway, Volume 1, 57-67.

182. de Larrard, F. (1996), "Mechanical Material Properties," Proceedings of the Fourth International Symposium on the Utilization of High Strength/High Performance Concrete, Paris, France, Volume 1, 29-38.

183. de Larrard, F.; and Lacroix, R. (1996), "Utilization of High Strength/High Performance Concrete," Proceedings of The Fourth International Symposium on Utilization of High Strength/High Performance Concrete, Paris, France, Volumes I, II & III, 1593 pp.

184. de Larrard, F.; Gillet, G.; and Canitrot, B. (1996), "Preliminary HPC Mix-Design Study for the Grand Viaduct de Millau: An Example of LCPC's Approach," Proceedings of the Fourth International Symposium on the Utilization of High Strength/High Performance Concrete, Paris, France, Volume 3, 1323-1332.

185. de Larrard, F.; Ithurralde, G.; Acker, P.; and Chauvel, D., "High-Performance Concrete for a Nuclear Containment," Proceedings of the Second International Symposium on Utilization of High-Strength Concrete, Berkeley, California, 549-576.

186. de Larrard, Francois; and Aïtcin, Pierre-Claude (1993), "Apparent Strength Retrogression of Silica-Fume Concrete," ACI Materials Journal, 90(6), 581-585. (see discussion September-October 1994)

187. de Sitter, W. R.; and Fijneman, H. J. (1993), "The Fiber Pretensioned Concrete Bar; FPC-BAR," Proceedings of the Third International Symposium on Utilization of High-Strength Concrete, Lillehammer, Norway, Volume 1, 362-368.

188. De Vries, J.; Kaptijn, N.; and Ouwerkerk, H. (1996), "High Strength Concrete in Civil Bridge Engineering Practice in the Netherlands," Proceedings of the Fourth International Symposium on the Utilization of High Strength/High Performance Concrete, Paris, France, Volume 3, 1427-1436.

189. Delagrave, A.; Marchand, J.; and Pigeon, M. (1996), "Durability of High Performance Cement Pastes in Contact with Chloride Solutions," Proceedings of the Fourth International Symposium on the Utilization of High Strength/High Performance Concrete, Paris, France, Volume 2, 479-488.

190. Delgado, J. M.; Oteo, C. S.; and Hue, F. (1996), "The Guadalete River: The First Spanish Experience on High Strength Precast Concrete," Proceedings of the Fourth International Symposium on the Utilization of High Strength/High Performance Concrete, Paris, France, Volume 3, 1417-1426.

191. Den Uijl, J. A. (1996), "Bonds of Strands in High Performance Concrete," Proceedings of the Fourth International Symposium on the Utilization of High Strength/High Performance Concrete, Paris, France, Volume 3, 1175-1184.

192. Detwiler, Guy (1992), "High-Strength Silica Fume Concrete-Chicago Style," Concrete International, 14(10), 32-36.

193. Detwiler, Rachel J.; and Mehta P. Kumar (1989), "Chemical and Physical Effects of Silica Fume on the Mechanical Behavior of Concrete," ACI Materials Journal, 86(6), 609-614.

194. Detwiler, Rachel; Fapohunda, Chris A.; and Natale, Jennifer (1994), "Use of Supplementary Cementing Materials to Increase the Resistance to Chloride Ion Penetration of Concretes Cured at Elevated Temperatures," ACI Materials Journal, Vol. 91(1), 63-66.

195. Dezhen, Gu; Dayu, Xiong; and Zhang, LU (1982), "Model of Mechanism for Naphtalene Series Water-Reducing Agent," ACI Journal, 79(5), 378-386.

196. Diederichs, Ulrich; Spitzner, Joachim; Sandvik, Malvin; Kepp, Bernhard; and Gillen, Michael (1993), "The Behaviour of High-Strength Lightweight Aggregate Concrete at Elevated Temperatures," Proceedings of the Third International Symposium on Utilization of High-Strength Concrete, Lillehammer, Norway, Volume 2, 1046-1053.

197. Dilger, W. H.; Wang, C.; and Niitani, K. (1996), "Experimental Study on Shrinkage and Creep of High Performance Concrete," Proceedings of the Fourth International Symposium on the Utilization of High Strength/High Performance Concrete, Paris, France, Volume 2, 311-320.

198. Diniz, S. M. C. (1996), "Reliability Evaluation of High Strength Concrete Columns," Proceedings of the Fourth International Symposium on the Utilization of High Strength/High Performance Concrete, Paris, France, Volume 3, 925-934.

199. Djellouli, J.; Aïtcin, P. C.; and Chaallal, O. (1990), "Use of Ground Granulated Slag in High-Performance Concrete," Proceedings of the Second International Symposium on Utilization of High-Strength Concrete, Berkeley, California, 351-368.

200. Do, Minh-Tan; Schaller, Isabelle; de Larrard, François; and Aïtcin, Pierre-Claude (1993), "Fatigue of Plain and Reinforced High-Performance Concrete," Proceedings of the Third International Symposium on Utilization of High-Strength Concrete, Lillehammer, Norway, Volume 1, 146-154.

201. Dolan, Chales W.; and LaFraugh, Robert W. (1993), "High Strength Concrete in the Precast Concrete Industry," PCI Journal, 38(3), 16-19.

202. Dolan, Chales W.; Ballinger, Craig A.; and LaFraugh, Rober W. (1993), "High Strength Prestressed Concrete Bridge Girder Performance," PCI Journal, 38(3), 88-97.

203. Dolan, Charles W.. (1993), "Report of the PCI High Strength Concrete Committee," PCI Journal, 38(3), 14-15.

204. Dolan, Charles W.; Wade, S. W.; and LaFraugh, R. W. (1986), "Strength Design Age for Prestressed Bridge Girders," U.S. Department of Transportation, Federal Highway Administration Report No. FHWA/RD-86-036.

205. Domone, P. L. J.; and Soutsos, M. N. (1994), "An Approach to the Proportioning of High-Strength Concrete Mixes," Concrete International, 16(10), 26-31.

206. Donza, H. A.; and Cabrera, O. A. (1996), "The influence of Kinds of Fine Aggregate on Mechanical Properties of High Strength Concrete," Proceedings of the Fourth International Symposium on the Utilization of High Strength/High Performance Concrete, Paris, France, Volume 2, 153-160.

207. Dorner, H. W.; and Rüger, V. (1996), "Resistance of High Performance Concrete Against Acetic Acid," Proceedings of the Fourth International Symposium on the Utilization of High Strength/High Performance Concrete, Paris, France, Volume 2, 607-616.

208. Dotreppe, J. -C.; and Azizi, A. (1996), "Failure Mode of Prestressed Elements Made with High Performance Concrete and Simulation of Their Structural Behaviour," Proceedings of the Fourth International Symposium on the Utilization of High Strength/High Performance Concrete, Paris, France, Volume 3, 955-964.

209. Dowd, W. M.; and O' Neil, E. F. (1996), "Development of Reactive Powder Concrete (RPC) Precast Products for the USA Market," Proceedings of the Fourth International Symposium on the Utilization of High Strength/High Performance Concrete, Paris, France, Volume 3, 1391-1398.

210. Drake, Kingsley D. (1985), "High-Strength Concrete in Seattle," American Concrete Institute, SP-87, 21-34.

211. Duchesne, Josée; and Bérubé, Marc-André (1994), "Available Alkalies from Supplementary Cementing Materials," ACI Materials Journal, 91(3), 289-299.

212. Dugat, J.; Frouin, L.; and Clavaud, B. (1996), "Microstructure Analysis," Proceedings of the Fourth International Symposium on the Utilization of High Strength/High Performance Concrete, Paris, France, Volume 3, 1351-1358.

213. Dugat, J.; Verrier, R.; Valenchon, C.; and Rouillon, J. (1996), "The Nkossa Barge," Proceedings of the Fourth International Symposium on the Utilization of High Strength/High Performance Concrete, Paris, France, Volume 3, 1537-1546.

214. Durekovic, A. (1995), "Cement Pastes of Low Water to Solid Ratio: An Investigation of the Porosity Characteristics under the Influence of a Superplasticizer and Silica Fume," Cement and Concrete Research, 25(2), 365-375.

215. Düring, H. Sterud; Høyland, K.; Helland, K.; and Johnsrud, J. K. (1996), "Potentials in the Use of Low Density/High Performance Concrete," Proceedings of the Fourth International Symposium on the Utilization of High Strength/High Performance Concrete, Paris, France, Volume 3, 1261-1270.

216. Durning, Thomas A.; and Rear, Kenneth B., "Braker Lane Bridge: High Strength Concrete in Prestressed Bridge Girders," W. R. Grace & Co.-Conn.

217. Duwadi, S. Rimal; Lane, S. N.; and Berley, A. D. (1996), "High Performance Concrete Bridge Projects in the United States," Proceedings of the Fourth International Symposium on the Utilization of High Strength/High Performance Concrete, Paris, France, Volume 3, 1563-1570.

218. Ekerfors, Katarina; Jonasson, Jan-Erik; and Emborg, Mats (1993), "Behaviour of Young High Strength Concrete," Proceedings of the Third International Symposium on Utilization of High-Strength Concrete, Lillehammer, Norway, Volume 2, 691-697.

219. Ellis Jr., W. E. (1992), "For Durable Concrete, Fly Ash Does Not Replace Cement," Concrete International, 14(7), 47-51.

220. Ellis, C. (1996), "The Rheological and Mechanical Properties of Water Reduced Superplasticized High Strength Concretes," Proceedings of the Fourth International Symposium on the Utilization of High Strength/High Performance Concrete, Paris, France, Volume 2, 273-280.

221. Elzanaty, Ashraf H.; Nilson, Arthur H.; and Slate, Floyd O. (1986), "Shear Capacity of Prestressed Concrete Beams Using High-Strength Concrete," ACI Journal, 83(3), 359-368.

222. Elzanaty, Ashraf H.; Nilson, Arthur H.; and Slate, Floyd O. (1986), "Shear Capacity of Reinforced Concrete Beams Using High-Strength Concrete," ACI Journal, 83(2), 290-296.

223. Emborg, Mats; Westman, Gustaf; and Bernander, Stig (1993), "Assessment of the Risk of Thermal Cracking in Hardening High Strength Concrete," Proceedings of the Third International Symposium on Utilization of High-Strength Concrete, Lillehammer, Norway, Volume 2, 1054-1061.

224. Ernzen, James J.; and Carrasquillo, Ramon L. (1992), "Resistance of High Sttrength Concrete to Cold Weather Environments," Research Report 481-7, Center for Transportation Research, The University of Texas at Austin, 326 pp.

225. Ewertson, C.; and Petersson, P. E. (1993), "The Influence of Curing Conditions on the Permeability and Durability of Concrete: Results From a Field Exposure Test," Cement and Concrete Research, 23(3), 683-692.

226. Ezeldin, A. Samer; and Aïtcin, Pierre-Claude (1991), "Effect of Coarse Aggregate on the Behavior of Normal and High-Strength Concretes," Cement, Concrete and Aggregates, 13(2), 121-124.

227. Fang, I-K.; Jen, M. C.; and Liao, S. M. (1993), "Early Strength Development of High Strength Concrete," Proceedings of the Third International Symposium on Utilization of High-Strength Concrete, Lillehammer, Norway, Volume 2, 698-705.

228. Fang, I-K.; Wang, C. S.; Horn, K. L.; and Yen, S. T. (1993), "High Strength Concrete Short Beams for Seismic Regions," Proceedings of the Third International Symposium on Utilization of High-Strength Concrete, Lillehammer, Norway, Volume 1, 155-162.

229. Favre, R.; Charif, H.; and Jaccoud, J. -P. (1990), "Improved Serviceability of Reinforced Concrete Slabs with the Use of High-Strength Concrete," Proceedings of the Second International Symposium on Utilization of High-Strength Concrete, Berkeley, California, 89-108.

230. Felicetti, R.; Gambavora, P. G.; Rosati, G. P.; Corsi, F.; and Giannuzzi, G. (1996), "Residual Mechanical Properties of High Strength Concretes Subjected to High Temperature Cycles," Proceedings of the Fourth International Symposium on the Utilization of High Strength/High Performance Concrete, Paris, France, Volume 2, 579-588.

231. Fidjestol, Per (1993), "Applied Silica Fume Concrete," Concrete International, 15(11), 33-36.

232. Fiorato, A. E. (1989), "PCA Research on High-Strength Concrete," Concrete International, 11(4), 44-50.

233. Fiorato, A. E. (1991), "Current Research on High-Performance Concrete at the Portland Cement Association," Presentation at the Federal Executive Seminar, Arlington, VA.

234. Fiorato, A. E.; Person, A.; and Pfeifer, D. W. (1984), "The First Large Scale Use of High Strength Lightweight Concrete in the Arctic Environment," Second Arctic Offshore Symposium, Houston, Texas.

235. FIP Commission on Concrete (1988), "Condensed Silica Fume in Concrete," Thomas Telford Ltd, London, 37 pp.

236. FIP/CEB (1990), "High Strength Concrete - State of the Art Report," SR 90/1 Bulletin d'Information No. 197, 61 pp.

237. Forster, Stephen W. (1994), "High-Performance Concrete - Stretching the Paradigm," Concrete International, 16(10), 33-34.

238. Fouré, B. (1996), "Empirical Constitutive Law for Concrete in Compression and Extrapolation to Very High Strength Concrete," Proceedings of the Fourth International Symposium on the Utilization of High Strength/High Performance Concrete, Paris, France, Volume 2, 663-668.

239. François, R.; Konin, A.; and Arliguié, G. (1996), "Evolution of the Microstructure of Reinforced HPC in Relation to the Loading and the Influence on Durability," Proceedings of the Fourth International Symposium on the Utilization of High Strength/High Performance Concrete, Paris, France, Volume 2, 623-636.

240. Frantz, Gregory C.; and Stephens, Jack E. (1993), "Recycling Single-Use Cylinder Molds," Concrete International, 15(4), 67-68.

241. Freeman, Reed B.; and Carrasquillo, Ramon L. (1992), "Optimization of the Physical and Compositional Characteristics of Fly Ash Cement for the Production of Sulfate Resistant Concrete," Research Report 481-8F, Center for Transportation Research, The University of Texas at Austin, 530 pp.

242. French, C.; Shield, C.; Mokhtarzadeh, A.; Kriesel, R.; and Ahlborn, T. (1996), "Applications of High Performance Concrete to Long-Span Prestressed Bridge Girders," Proceedings of the US-Europe Workshop on Bridge Engineering, Barcelona, Spain, 613-637.

243. French, Catherine W.; and Mokhtarzadeh, Alireza (1993), "High Strength Concrete: Effects of Materials, Curing and Test Procedures on Short-Term Compressive Strength," PCI Journal, 38(3), 76-87.

244. French, P. J.; Montgomery, R. G.; and Robson, T. D. (1971), "High Concrete Strength within the Hour," Concrete, 5(8), 253-258.

245. Fukute, T.; Hamada, H.; Mashimo, M.; and Watanabe, Y. (1996), "Chloride Permeability of High Strength Concrete Containing Various Mineral Admixtures," Proceedings of the Fourth International Symposium on the Utilization of High Strength/High Performance Concrete, Paris, France, Volume 2, 489-498.

246. Gabrielsson, H.; and Elfgren, L. (1996), "Toughness in Prestressed High Performance Concret Structures - Hollow Core Slabs and Cylindrical Poles," Proceedings of the Fourth International Symposium on the Utilization of High Strength/High Performance Concrete, Paris, France, Volume 3, 1047-1056.

247. Gabrielsson, Henrik (1993), "High Performance Concrete Beams Tested in Shear. Comparison Between the Traditional Approach and the Modified Compression Field Theory," Proceedings of the Third International Symposium on Utilization of High-Strength Concrete, Lillehammer, Norway, Volume 1, 169-176.

248. Galeota, D.; Giammatteo, M. M.; and Marino, R. (1996), "High Strength RC Columns Subjected to Axial Load and Cyclic Flexure," Proceedings of the Fourth International Symposium on the Utilization of High Strength/High Performance Concrete, Paris, France, Volume 3, 905-914.

249. Galeota, Dante; Giammatteo, Matteo M.; and Marino, Roberto (1993), "Fracture Properties of High Strength Concrete," Proceedings of the Third International Symposium on Utilization of High-Strength Concrete, Lillehammer, Norway, Volume 2, 1062-1069.

250. Gardner, N. J. (1990), "Effect of Temperature on the Early-Age Properties of Type I, Type III, and Type I/Fly Ash Concretes," ACI Materials Journal, 87(1), 68-78.

251. Gardner, N. J.; and Zhao, J. W. (1993), "Creep and Shrinkage Revisited," ACI Materials Journal, 90(3), 236-246. (see discussion March-April 1994)

252. Gebler, S. H. (1982), "The Effects of High-Range Water Reducers on the Properties of Freshly Mixed and Hardened Flowing Concrete," PCA Research and Development Bulletin RD081.01T, 13 pp.

253. Gérard, B.; Marchand, J.; Breysse, D.; and Ammouche, A. (1996), "Constitutive Law of High Performance Concrete Under Tensile Strain," Proceedings of the Fourth International Symposium on the Utilization of High Strength/High Performance Concrete, Paris, France, Volume 2, 677-686.

254. Gettu, Ravindra; Aguado, Antonio; Oliveira, Marcel O. F.; and Carol, Ignacio (1993), "Damage in High-Strength Concrete Due to Monotonic and Cyclioc Compression," Proceedings of the Third International Symposium on Utilization of High-Strength Concrete, Lillehammer, Norway, Volume 2, 1070-1075.

255. Gettu, Ravindra; Bazant, Zdenek P.; and Karr, Martha E. (1990), "Fracture Properties and Brittleness of High-Strength Concrete," ACI Materials Journal, 87(6), 608-618.

256. Ghosh, S. K.; and Saatcioglu, Murat, "Ductility and Seismic Behavior," High Strength-Performance Concrete, Chapter 8, Edited by Ahmad and Shah, to be published by Edward Arnold & Kent, England.

257. Giaccio, G.; Rocco, C.; Violini, D.; Zappitelli, J.; and Zerbino, R. (1992), "High-Strength Concretes Incorporating Different Coarse Aggregtes," ACI Materials Journal, 89(3), 242-246.

258. Gjørv, Odd E.; and Martinsen, Jarle (1993), "Effect of Elevated Curing Temperature on High-Strength Lightweight Concrete," Proceedings of the Third International Symposium on Utilization of High-Strength Concrete, Lillehammer, Norway, Volume 2, 706-712.

259. Glucklich, Joseph; and Cohen, Leslie J. "Size as a Factor in the Brittle-Ductile Transition and the Strength of Some Materials," International Journal of Fracture Mechanics, 3(4), 278-288.

260. Glucklich, Joseph; and Cohen, Leslie J. "Strain-Energy and Size Effects in a Brittle Material," Materials Research and Standards (ASTM), 8(10), 17-22.

261. Godfrey Jr., K. A. (1987), "Concrete Strength Record Jumps 36%," Civil Engineering, 84-88.

262. Goldman, Ariel; and Bentur, Arnon (1989), "Bond Effects in High-Strength Silica-Fume Concretes," ACI Materials Journal, 86(5), 440-447.

263. Gomez, R. B.; and Andrade, M. A. S. (1996), "The Use of High Performance Concrete in Punching Failure of Reinforced Concrete Flat Slabs," Proceedings of the Fourth

International Symposium on the Utilization of High Strength/High Performance Concrete, Paris, France, Volume 3, 1027-1036.

264. Gonnerman, Harrison F. (1925), "Effect of Size and Shape of Test Specimen on Compressive Strength of Concrete," Proceedings, ASTM, 25, Part 2, 237-250.

265. Gopalan, M. K. (1993), "Mix Design and Microstructure Effects on High Strength Concrete," Proceedings of the Third International Symposium on Utilization of High-Strength Concrete, Lillehammer, Norway, Volume 2, 722-731.

266. Gopalan, M. K. (1993), "Nucleation and Pozzolanic Factors in Strength Development of Class F Fly Ash Concrete," ACI Materials Journal, 90(2), 117-121.

267. Gopalan, M. K.; and Haque, M. N. (1990), "Fly Ash in High-Strength Concrete," Proceedings of the Second International Symposium on Utilization of High-Strength Concrete, Berkeley, California, 331-349.

268. Goto, K.; Kuroha, K.; Namiki, H.; and Jinnai, H. (1996), "Experimental Study on High Strength Cast-In-Place Concrete with 100 MPa," Proceedings of the Fourth International Symposium on the Utilization of High Strength/High Performance Concrete, Paris, France, Volume 2, 125-134.

269. Gowripalan, N.; Cabrera, J. G.; Cusens, A. R.; and Wainwright, P. J. (1990), "Effect of Curing on Durability," Concrete International, 12(2), 47-54.

270. Granger, L.; and Acker, P. (1996), "What kind of Drying Creep for HSC/HPC?," Proceedings of the Fourth International Symposium on the Utilization of High Strength/High Performance Concrete, Paris, France, Volume 2, 357-366.

271. Groth, P.; and Noghabai, K. (1996), "Fracture Mechanics Properties of Steel Fiber-Reinforced High Performance Concrete," Proceedings of the Fourth International Symposium on the Utilization of High Strength/High Performance Concrete, Paris, France, Volume 2, 747-756.

272. Guimaraes, Gilson N.; Kreger, Michael E.; and Jirsa, James O. (1989), "Reinforced Concrete Frame Connections Copnstructed Using High-Strength Materials," PMFSEL Report No. 89-1, Department of Civil Engineering, The University of Texas at Austin, 158 pp.

273. Guo, Cheng-ju (1994), "Early-Age Behavior of Portland Cement Paste," ACI Materials Journal, 91(1), 13-25.

274. Gupta, Anshu; and Rangan, B. Vijaya (1993), "High-Strength Concrete Structural Walls Under Inplane Vertical and Horizontal Loads," Proceedings of the Third International Symposium on Utilization of High-Strength Concrete, Lillehammer, Norway, Volume 1, 177-183.

275. Gysel, A. Van; Taerwe, L. (1996), "Influence of High Carbon Steel Fibers on the Stress-Strain Curve for High Strength Concrete Under Compression," Proceedings of the Fourth International Symposium on the Utilization of High Strength/High Performance Concrete, Paris, France, Volume 2, 741-746.

276. Hadchiti, Karim M.; and Carrasquillo, Ramon L. (1988), "Abrasion Resistance and Scaling Resistance of Concrete Containing Fly Ash," Research Report 481-3, Center for Transportation Research, The University of Texas at Austin, 185 pp.

277. Hallgren, M.; and Kinnunen, S. (1996), "Increase of Punching Shear Capacity by Using High Strength Concrete," Proceedings of the Fourth International Symposium on the Utilization of High Strength/High Performance Concrete, Paris, France, Volume 3, 1037-1046.

278. Hallgren, Mikael; and Kinnunen, Sven (1993), "Punching Shear Tests on Circular High Strength Concrete Slabs," Proceedings of the Third International Symposium on Utilization of High-Strength Concrete, Lillehammer, Norway, Volume 1, 192-199.

279. Hammer, T. A.; and Sellevold, E. J. (1990), "Frost Resistance of High-Strength Concrete," Proceedings of the Second International Symposium on Utilization of High-Strength Concrete, Berkeley, California, 457-487.

280. Hammer, Tor Arne (1993), "The Maturation of Mechanical Properties of HIgh Strength Concrete Exposed to Different Moisture Condition," Proceedings of the Third International Symposium on Utilization of High-Strength Concrete, Lillehammer, Norway, Volume 2, 1084-1091.

281. Hammons, Michael I.; and Neeley, Billy D. (1993), "Triaxial Characterization of High-Strength Portland Cement Concrete," Paper No. 930126, Transportation Research Board (TRB), 72nd Annual Meeting, 22 pp.

282. Hamouda, M.; and Bourlon, D. (1996), "High Durability Concrete in UAE - A Case Study," Proceedings of the Fourth International Symposium on the Utilization of High Strength/High Performance Concrete, Paris, France, Volume 3, 1547-1556.

283. Han, N.; and Walraven, J. C. (1996), "Creep and Shrinkage of Young High Strength Concrete," Proceedings of the Fourth International Symposium on the Utilization of High Strength/High Performance Concrete, Paris, France, Volume 2, 339-348.

284. Han, Ningxu; and Walraven, J. C. (1993), "Sustained Loading Effects in High Strength Concrete," Proceedings of the Third International Symposium on Utilization of High-Strength Concrete, Lillehammer, Norway, Volume 2, 1076-1083.

285. Hansen, E. A.; and Thorenfeldt, E. (1996), "Bond Properties of Deformed Reinforcement Bars in High Strength Concrete," Proceedings of the Fourth International Symposium on the Utilization of High Strength/High Performance Concrete, Paris, France, Volume 3, 1105-1114.

286. Hansen, E. A.; Leivo, M.; Rodriguez, J.; and Cather, R. (1996), "Mechanical Properties of High Strength Concrete - Influence of Test Conditions, Specimens and Constituents," Proceedings of the Fourth International Symposium on the Utilization of High Strength/High Performance Concrete, Paris, France, Volume 2, 187-196.

287. Hansen, Einar Aa.; and Tomaszewicz, Andrzej (1993), "Effect of Confinement on the Ductility of Structural Members with High Strength Concrete," Proceedings of the Third

International Symposium on Utilization of High-Strength Concrete, Lillehammer, Norway, Volume 1, 184-191.

288. Hansen, Gro Kari; Rindal, Dag B.; and Horrigmoe, Geir (1993), "Diffusion of Chlorides in High-Strength Concrete," Proceedings of the Third International Symposium on Utilization of High-Strength Concrete, Lillehammer, Norway, Volume 2, 671-677.

289. Hansi, L.; Gallias, J. L.; nd Salomon, M. (1993), "The Effect of the Curing on the Durability of High Performance Concretes," Proceedings of the Third International Symposium on Utilization of High-Strength Concrete, Lillehammer, Norway, Volume 2, 732-743.

290. Haque, M. N., "Some Concretes Need 7 Day Curing (1990)," Concrete International, 12(2), 42-46.

291. Haque, M. N.; and Kayyali, O. A. (1996), "Blastfurnace Slag Aggregates Are Used to Produce High Strength Concretes," Proceedings of the Fourth International Symposium on the Utilization of High Strength/High Performance Concrete, Paris, France, Volume 2, 203-212.

292. Hartmann, David L.; Breen, J. E.; and Kreger, M. E. (1988), "Shear Capacity of High Strength Prestressed Concrete Girders," Research Report 381-2, Center for Transportation Research, The University of Texas at Austin, 249 pp.

293. Hashin, Zvi (1962), "The Elastic Moduli of Hetrogeneous Materials," Journal of Applied Mechanics, 143-150.

294. Hassanzadeh, Manouchehe; and Haghpassand, Akbar (1993), "Brittleness of Normal and High-Strength Concrete," Proceedings of the Third International Symposium on Utilization of High-Strength Concrete, Lillehammer, Norway, Volume 2, 1092-1099.

295. Hatfield, E.; Azizinamini, A.; and Pavel, R. (1996), "Minimum Stirrups Requirements for Tension Splices in High Strength Concrete," Proceedings of the Fourth International Symposium on the Utilization of High Strength/High Performance Concrete, Paris, France, Volume 3, 145-1154.

296. Haug, A. K.; and Jakobsen, B. (1990), "In Situ and Design Strength for Concrete in Offshore Platforms," Proceedings of the Second International Symposium on Utilization of High-Strength Concrete, Berkeley, California, 369-397.

297. Haug, Atle K.; and Fjeld, Svein (1993), "A Floating Concrete Platform Hull Made of Lightweight Aggregate Concrete," Proceedings of the Third International Symposium on Utilization of High-Strength Concrete, Lillehammer, Norway, Volume 1, 494-503.

298. Hegger, J.; and Burkhardt, J. (1996), "Structural Strength and Ductility of Reinforced Frame Structures from High Strength Concrete," Proceedings of the Fourth International Symposium on the Utilization of High Strength/High Performance Concrete, Paris, France, Volume 3, 1505-1514.

299. Hegger, Josef, "High Strength Concrete for a 186 m High Office Building in Frankfurt, Germany (1993)," Proceedings of the Third International Symposium on Utilization of High-Strength Concrete, Lillehammer, Norway, Volume 1, 504-511.

300. Held, Markus; König, Gert; and Simsch, Gerd (1993), "Ductility of Large High-Strength Concrete Columns in High-Rise Buildings," Proceedings of the Third International Symposium on Utilization of High-Strength Concrete, Lillehammer, Norway, Volume 1, 200-208.

301. Helland, S. (1990), "High-Strength Concrete Used in Highway Pavements," Proceedings of the Second International Symposium on Utilization of High-Strength Concrete, Berkeley, California, 757-766.

302. Helland, S. (1996), "Utilization of HS/HPC," Proceedings of the Fourth International Symposium on the Utilization of High Strength/High Performance Concrete, Paris, France, Volume 1, 67-74.

303. Helland, Steinar; and Maage, Magne (1993), "Strength Loss in Un-Remixed LWA-Concrete," Proceedings of the Third International Symposium on Utilization of High-Strength Concrete, Lillehammer, Norway, Volume 2, 744-751.

304. Hellesland, Jostein (1993), "Applicability of Normal Grade Selenderness Limits to HSC and LWA Columns," Proceedings of the Third International Symposium on Utilization of High-Strength Concrete, Lillehammer, Norway, Volume 1, 209-216.

305. Helmuth, Richard (1987), "Fly Ash in Cement and Concrete," Portland Cement Association, 203 pp.

306. Hester, Weston T. (1977), "High Strength Air-Entrained Concrete," Concrete Construction, 22(2), 77-82.

307. Hester, Weston T. (1980), "Field Testing High-Strength Concretes: A Critical Review of the State-of-the-Art," Concrete International, 27-38.

308. Hester, Weston T. (1990), "High-Strength Concrete," ACI SP-121, The Second International Symposium on Utilization of High-Strength Concrete, Berkely, California, 786 pp.

309. Hindy, Elie El.; Miao, Buquan; Chaallal, Omar; and Aïtcin, Pierre-Claude (1994), "Drying Shrinkage of Ready-Mixed High-Performance Concrete," ACI Materials Journal, 91(3), 300-305.

310. Hirsch, Teddy J. (1962), "Modulus of Elasticity of Concrete Affected by Elastic Moduli of Cement Paste Materix and Aggregate," Journal of the American Concrete Institute, 59, 427-451.

311. Hobbs, D. W. (1975), "Influence of Aggregate Restraint on the Shrinkage of Concrete," ACI Journal, 114-116.

312. Hoff, G. C. (1990), "High-Strength Lightweight Aggregate Concrete - Current Status and Future Needs," Proceedings of the Second International Symposium on Utilization of High-Strength Concrete, Berkeley, California, 619-644.

313. Hoff, George C. (1993), "Utilization of High Strength Concrete in North America," Proceedings of the Third International Symposium on Utilization of High-Strength Concrete, Lillehammer, Norway, Volume 1, 28-36.

314. Hoff, George C.; and Ramakrishnan, V. (1993), "Flexural Fatigue Performance Characteristics of High Strength Lightweight Concrete," Proceedings of the Third International Symposium on Utilization of High-Strength Concrete, Lillehammer, Norway, Volume 2, 1100-1113.

315. Hognestad, Eivind; Hanson, N. W.; and McHenry, Douglas (1955), "Concrete Stress Distribution in Ultimate Strength Design," ACI Journal, 52, 455-479.

316. Holand, I.; and Helland, S. (1996), "CEB/FIP Working Group on High Strength/High Performance Concrete," Proceedings of the Fourth International Symposium on the Utilization of High Strength/High Performance Concrete, Paris, France, Volume 3, 1251-1260.

317. Holand, Ivar (1987), "High-Strength Concrete," Proceedings of The First International Symposium on Utilization of High-Strength Concrete, Stavanger, Norway.

318. Holand, Ivar (1993), "High Strength Concrete in Norway. Utilization and Research," Proceedings of the Third International Symposium on Utilization of High-Strength Concrete, Lillehammer, Norway, Volume 1, 68-79.

319. Holand, Ivar; and Sellevold, Erik (1993), "High-Strength Concrete," Proceedings of the Third International Symposium on Utilization of High Strength Cocrete, Lillehammer, Norway, Volumes I & II, 1287 pp.

320. Holland, Terence C. (1987), "Testing High-Strength Concrete," Concrete Construction, 534-536.

321. Hollister, S. C. (1976), "Urgent Need for Research in High-Strength Concrete," ACI Journal, 136-137.

322. Holm T. A. (1980), "Physical Properties of High Strength Lightweight Aggregate Concretes," Proceedings of the Second International Congress on Lightweight Concrete, London U.K.

323. Holmberg, G.; and Cederwall, K. (1996), "Fatigue of Concrete Piles of High Strength Concrete Exposed to Impact Load," Proceedings of the Fourth International Symposium on the Utilization of High Strength/High Performance Concrete, Paris, France, Volume 2, 705-710.

324. Hooton, R. D. (1993), "Influence of Silica Fume Replacement of Cement on Physical Properties and Resistance to Sulfate Attack, Freezing and Thawing, and Alkali-Silica Reactivity," ACI Materials Journal, 90(2), 143-151.

325. Howard, Nathan L.; and Leatham, David M. (1989), "The Production and Delivery of High-Strength Concrete," Concrete International, 11(4), 26-30.

326. Hu, C.; de Larrard, F.; and Sedran, T. (1996), "A New Rheometer for High Performance Concrete," Proceedings of the Fourth International Symposium on the Utilization of High Strength/High Performance Concrete, Paris, France, Volume 2, 179-186.

327. Huang, Z.; Engström, B.; and Magnusson, J. (1996), "Experimental and Analytical Studies of the Bond Behavior of Deformed Bars in High Strength Concrete," Proceedings of the Fourth International Symposium on the Utilization of High Strength/High Performance Concrete, Paris, France, Volume 3, 1115-1124.

328. Hwang, Chao-Lung; and Shen, Der-Hsien (1991), "The Effects of Blast-Furnace Slag and Fly Ash on the Hydration of Portland Cement," Cement and Concrete Research, 21, 410-425.

329. Hwee, Yan Seng; and Rangan, B. Vijaya (1990), "Studies on Commercial High-Strength Concretes," ACI Materials Journal, 87(5), 440-445.

330. Ikeda, Shoji (1993), "Utilization of High Strength Concrete in Japan," Proceedings of the Third International Symposium on Utilization of High-Strength Concrete, Lillehammer, Norway, Volume 1, 37-44.

331. Imam, M.; and Vandewalle, L. (1996), "How Efficient Are Steel Fibres in High Strength Concrete Beams?," Proceedings of the Fourth International Symposium on the Utilization of High Strength/High Performance Concrete, Paris, France, Volume 3, 1067-1076.

332. Imam, M.; Vandewalle, L.; and Mortelmans, F. (1993), "Indirect Tensile Strength of Very High Strength Concrete, " Proceedings of the Third International Symposium on Utilization of High-Strength Concrete, Lillehammer, Norway, Volume 2, 1114-1121.

333. Ipatti, Ari (1993), "Evaluating the Feasibility of Test Specimen Grinding Using Factorial Experimental Technique," Proceedings of the Third International Symposium on Utilization of High-Strength Concrete, Lillehammer, Norway, Volume 2, 1122-1129.

334. Ismail, M. R. (1991), "Hydration Kinetics of Cement Paste Containing Concrete Admixture," Cement and Concrete Research, 21, 683-690.

335. Ithurralde, Gérard Jean-Baptiste; and Olivier, Joël (1993), "High Performance Concretes for French Nuclear Reactor Containment Vessels," Proceedings of the Third International Symposium on Utilization of High-Strength Concrete, Lillehammer, Norway, Volume 1, 217-224.

336. Iwai, N.; Masuda, Y.; Abe, M.; and Yasuda, M. (1996), "Mix Proportion and Fundamental Properties of High Fluidity Concrete," Proceedings of the Fourth International Symposium on the Utilization of High Strength/High Performance Concrete, Paris, France, Volume 3, 1305-1314.

337. Jaccoud, J. -P.; Farra, B.; and Leclercq, A. (1996), "Improvement of Existing Codes for Their Application to Crack Control of HSC/HPC Structures," Proceedings of the Fourth

International Symposium on the Utilization of High Strength/High Performance Concrete, Paris, France, Volume 3, 1155-1162.

338. Jaccoud, Jean-Paul; Charif, Hazem; and Farra, Bicher (1993), "Cracking Behaviour of HSC Structures and Practical Consequences for Design," Proceedings of the Third International Symposium on Utilization of High-Strength Concrete, Lillehammer, Norway, Volume 1, 225-232.

339. Jacobsen, S.; and Sellevold, E. J. (1996), "Frost Testing High Strength Concrete: Scaling and Cracking," Proceedings of the Fourth International Symposium on the Utilization of High Strength/High Performance Concrete, Paris, France, Volume 2, 597-606.

340. Jakobsen, Bernt; Gausel, Einar; Stemland, Hans; and Tomaszewicz, Andrzej (1993), "Large Scale Tests on Cell Wall Joints of a Concrete Gravity Base Structure," Proceedings of the Third International Symposium on Utilization of High-Strength Concrete, Lillehammer, Norway, Volume 1, 233-240.

341. Janak, Karl J. (1985), "Comparative Compressive Strength of 4x8 in. Versus 6x12 in. Concrete Cylinders along with the Investigation of Concrete Compressive Strength at 56 Days," Texas State Department of Highways and Public Transportation, Materials and Tests Division Report #3-I-4-116, 36 pp.

342. Jansen, Daniel C.; and Shah, Surendra P. (1993), "Stable Feedback Signals for Obtaining Full Stress Strain Curves of High Strength Concrete," Proceedings of the Third International Symposium on Utilization of High-Strength Concrete, Lillehammer, Norway, Volume 2, 1130-1137.

343. Jansze, W.; and Walraven, J. C. (1996), "Failure Behaviour of Joints Between HSC Members, Subjected to Shear- and Compressive Stresses," Proceedings of the Fourth International Symposium on the Utilization of High Strength/High Performance Concrete, Paris, France, Volume 3, 1085-1096.

344. Jensen, B. C.; Aarup, B. (1996), "Fire Resistance of Fibre Reinforced Silica Fume Based Concrete," Proceedings of the Fourth International Symposium on the Utilization of High Strength/High Performance Concrete, Paris, France, Volume 2, 551-560.

345. Jensen, J. J.; Opheim, E.; Aune, R. B. (1996), "Residual Strength of HSC Structural Elements Damaged by Hydrocarbon Fire or Impact Loading," Proceedings of the Fourth International Symposium on the Utilization of High Strength/High Performance Concrete, Paris, France, Volume 2, 589-596.

346. Jensen, Jens Jacob; Høiseth, Karl Vincent; and Hansen, Einar Assved (1993), "Ductility of High Strength Concrete at High Rate Loading," Proceedings of the Third International Symposium on Utilization of High-Strength Concrete, Lillehammer, Norway, Volume 1, 241-250.

347. Jiafen, Jiang (1993), "High-Strength Concrete in China," Concrete International, 15(1), 43-45.

348. Jobse, H. J. (1987), "Applications of High Strength Concrete for Highway Bridges, Executive Summary," Publication No. FHWA/RD-87/079, Federal Highway Administration, Washington, D.C., 27 pp.

349. Jobse, Harold J.; and Mustafa, Saad E. (1984), "Applications of High Strength Concrete for Highway Bridges," PCI Journal, 29(3), 44-73.

350. Johansen, K. I.; Lindgård, J.; and Smeplass, S. (1993), "Improving the Workability of High-Strength Concrete," Proceedings of the Third International Symposium on Utilization of High-Strength Concrete, Lillehammer, Norway, Volume 2, 801-809.

351. Johnson, M. K.; and Ramirez, J. A. (1989), "Minimum Shear Reinforcement in Beams With Higher Strength Concrete," ACI Structural Journal, 86(4), 376-382.

352. Jonasson, J. -E.; Ronin, V.; and Hedlund, H. (1996), "High Strength Concretes with Energetically Modified Cement and Modelling of Shrinkage Caused by Self-Desiccation," Proceedings of the Fourth International Symposium on the Utilization of High Strength/High Performance Concrete, Paris, France, Volume 2, 245-254.

353. Jonasson, Jan-Erik; and Ronin, Vladimir (1993), "Energetically Modified Cement(EMC)," Proceedings of the Third International Symposium on Utilization of High-Strength Concrete, Lillehammer, Norway, Volume 2, 752-759.

354. Joshi, R. C.; Lohtia, R. P.; and Salam, M. A. (1993), "High Strength Concrete with High Volumes of Canadian Sub-Bituminous Coal Fly Ash," Proceedings of the Third International Symposium on Utilization of High-Strength Concrete, Lillehammer, Norway, Volume 2, 760-768.

355. Kaar, P. H.; Hanson, N. W.; and Capell, H. T. (1977), "Stress-Strain Characteristics of High-Strength Concrete," PCA Research and Development Bulletin RD051.01D, 10 pp.

356. Kaar, Paul H.; LaFraugh, Robert W.; and Mass, Mark A. (1963), "Influence of Concrete Strength on Strand Transfer Length," PCI Journal, 8(5), 47-67.

357. Kaku, T.; Yamada, M.; Iizuka, S.; and Zhang, J., "A Proposal of Bond Strength Equation for R.C. Members Including High Strength Concrete Level," International Conference on Bond in Concrete: From Research to Practice, Proceedings, Volume 2, The CEB and Riga Technical University, Riga, Latvia, 4-1 to 4-10.

358. Kantro, D. L. (1980), "Influence of Water-Reducing Admixtures on Properties of Cement Paste-A Miniature Slump Test," Cement, Concrete and Aggregate, 2(2).

359. Kaplan, M. F. (1959), "Flexural and Compressive Strength of Concrete as Affected by the Properties of Coarse Aggregates," ACI Journal, 55(5), 1193-1208.

360. Kaufman, M. K.; and Ramirez, J. A. (1988), "Re-Evaluation of the Ultimate Shear Behavior of High-Strength Concrete Prestressed I-Beams," ACI Structural Journal, 85(3), 295-303.

361. Kaufman, M. K.; and Ramirez, Julio A. (1989), "Use of Higher Strength Concrete for Prestressed Beams in the State of Indiana," PCI Journal, 34(3), 78-93.

362. Keck, Roy; and Casey, Kevin (1991), "A Tower of Strength," Concrete International, 13(3), 23-25.

363. Khaloo, A. R.; and Ahmad, S. H. (1988), "Behavior of Normal and High-Strength Concrete Under Combined Compression-Shear Loading," ACI Materials Journal, 85(6), 551-559.

364. Khan, Shamim Mohammad; and Ayers, Michael E. (1992), "Interupted Concrete Curing," Concrete International, 14(12), 25-28.

365. Khatri, R. P.; and Sirivivatnanon, V. (1995), "Effect of Different Supplementary Cementitious Materials on Mechanical Properties of High Performance Concrete," Cement and Concrete Research, 25(1), 209-220.

366. Khayat, K. H.; and Lessard, M. (1994), "Influence of Early Heat Curing on Properties of 100-MPa Air-Entrained Concrete," Paper No. 940764, Transportation Research Board (TRB), 73rd Annual Meeting, 23 pp.

367. Kim, Jin-Keun; Park, Yon-Dong; and Lee, Soo-Gon (1993), "Shear Strength of Reinforced High Strength Concrete Beams," Proceedings of the Third International Symposium on Utilization of High-Strength Concrete, Lillehammer, Norway, Volume 1, 251-258.

368. Kimura, H.; Sugano, S.; and Nagashima, T. (1996), "Seismic Behaviour of Reinforced Concrete Columns Using Ultra-High Strength Concrete Under High Axial Load," Proceedings of the Fourth International Symposium on the Utilization of High Strength/High Performance Concrete, Paris, France, Volume 3, 893-904.

369. Kimura, Hideki; Sugano, Shunsuke; Nagashima, Toshio; and Ichikawa, Atsushi (1993), "Seismic Loading Tests of Reinforced Concrete Beams Using High Strength Concrete and High Strength Steel Bars," Proceedings of the Third International Symposium on Utilization of High-Strength Concrete, Lillehammer, Norway, Volume 1, 377-384.

370. Klieger, P. (1958), Proceedings of American Concrete Institute, 54, 1063.

371. Koenders, E. A. B.; Töllner, M.; Breugel, K. Van; and Obladen, B. (1996), "Evaluation of a Full-Scale Test of a U-Shaped Element in High Strength Concrete," Proceedings of the Fourth International Symposium on the Utilization of High Strength/High Performance Concrete, Paris, France, Volume 3, 973-984.

372. Koenders, E. A. B.; Töllner, M.; Breugel, K. Van; and Ouwerkerk, H. (1996), "Influence of Solar Radiation on Temperature Development in Thin High Strength Concrete Elements," Proceedings of the Fourth International Symposium on the Utilization of High Strength/High Performance Concrete, Paris, France, Volume 2, 423-432.

373. Kokusho, S.; Wada, A.; Kobayashi, K.; and Mitsugi, S. (1986), "Study on the Improvement in Bearing Capacity and Deformability of Prestressed High Strength Concrete Piles," Report of the Research Laboratory of Engineering Materials, Tokyo Institute of Technology, No. 11, 219-232.

374. Kompen, Reidar (1993), "Low Water-Binder Ratio Concrete for Bridges: Experience from Full Scale Construction," Proceedings of the Third International Symposium on Utilization of High-Strength Concrete, Lillehammer, Norway, Volume 1, 512-516.

375. König, G.; and Bergner, H. (1996), "Minimum Reinforcement of High Strength Concrete Members under Centrical Restraint," Proceedings of the Fourth International Symposium on the Utilization of High Strength/High Performance Concrete, Paris, France, Volume 3, 1225-1232.

376. Konig, G.; and Simsch, G. (1996), "Failure Mechanism and Load-Deformation Behaviour of High Strength Concrete Columns with Confining Reinforcement," Proceedings of the Fourth International Symposium on the Utilization of High Strength/High Performance Concrete, Paris, France, Volume 3, 777-786.

377. König, Gert; Bergner, Harald; Grimm, Rainer; and Simsch, Gerd (1993), "Utilization of High-Strength Concrete in Europe," Proceedings of the Third International Symposium on Utilization of High-Strength Concrete, Lillehammer, Norway, Volume 1, 45-56.

378. Korhonen, Charles J.; Cortez, Edel R.; and Charest, Brian A. (1992), "Strength Development of Concrete Cured at Low Temperature," Concrete International, 14(12), 34-39.

379. Kosmatka, Steven H. (1991), "In Defense of the Water-Cement Ratio," Concrete International, 13(9), 65-69.

380. Kudzys, Antanas; Kliukas, Romualdas; and Vadluga, Romualdas (1993), "Utilization of High-Strength Spun Concrete and Reinforced Steel in Compressive Structures," Proceedings of the Third International Symposium on Utilization of High-Strength Concrete, Lillehammer, Norway, Volume 1, 259-268.

381. Kukko, H.; and Matala, S. (1990), "Durability of High-Strength Concrete," Nordisk Betong 34, No. 2-3, 25-29.

382. Kumaat, Ellen; and Lorrain, Michel (1993), "Crack Resistance of Plain High Strength Concrete Slabs Under Bending," Proceedings of the Third International Symposium on Utilization of High-Strength Concrete, Lillehammer, Norway, Volume 2, 1138-1145.

383. Kwak, K. -W.; Ko, G. -S.; and Jang, K. -W. (1996), "Fatigue Strength and Durability of Ultra HighStrength Reinforced Concrete Beams," Proceedings of the Fourth International Symposium on the Utilization of High Strength/High Performance Concrete, Paris, France, Volume 3, 965-972.

384. Laamanen, Päivi-Helena (1993), "High Strength LWA Concrete for Bridge Construction - The New Sundbru Bridge in Eidsvoll, Norway," Proceedings of the Third International Symposium on Utilization of High-Strength Concrete, Lillehammer, Norway, Volume 1, 517-526.

385. Lacroix, R.; and Jaugey, P. (1985), "High-Strength Concrete: How to Use it Every Day," American Concrete Institute, SP-87, 35-50.

386. LaFraugh, Robert W. (1993), "Feasibility Study of 14,000 psi Prestressed Concrete for a Navigational Structure," PCI Journal, 38(3), 68-75.

387. Lajnef, Mona; Chaignon, Joël; Taïbi, Hamed; Tougne, Pierre; Hommel, Hubert; Legrand, Albert-Pierre; Bonnamy, Sylvie, Levitz, Pierre; Van Damme, Henri; Wenger, François; and

Galland, Jacques (1993), "Silica Fume Characterisation," Proceedings of the Third International Symposium on Utilization of High-Strength Concrete, Lillehammer, Norway, Volume 2, 769-776.

388. Lambotte, H.; and Taerwe, L. (1987), "Fatigue of Plain, High Strength Concrete Subjected to Flexural Tensile Stresses," Utilization of High Strength Concrete, Proceedings, Symposium in Stavanger, Norway, 331-342.

389. Lambotte, H.; and Taerwe, L. R. (1990), "Deflection and Cracking of High-Strength Concrete Beams and Slabs," Proceedings of the Second International Symposium on Utilization of High-Strength Concrete, Berkeley, California, 109-128.

390. Lambotte, H; and Taerwe, L. (1989), "The Use of High-Range Water-Reducers for High Strength Concrete," Book of Proceedings, ERMCO'89 The Norway to Concrete, 666-678.

391. Lane, Susan N.; and Podolny, Walter, Jr. (1993), "The Federal Outlook for High Strength Concrete Bridges," PCI Journal, 38(3), 20-33.

392. Lang, E.; and Geiseler, J. (1996), "Use of Blastfurnace Slag Cement with High Slag Content for High Performance Concrete," Proceedings of the Fourth International Symposium on the Utilization of High Strength/High Performance Concrete, Paris, France, Volume 2, 213-222.

393. Laplante, P.; and Aïtcin, P. -C. (1996), "Compressive Strength of Concrete: From Cylinders to the Structures," Proceedings of the Fourth International Symposium on the Utilization of High Strength/High Performance Concrete, Paris, France, Volume 2, 645-654.

394. Larbi, J. A.; and Bijen, J. M. J. (1991), "Orientation of Portlandite at the Paste-Aggregate Interface and Strength Development of the Paste-Aggregate Bond in Mortars in the Presence of Microsilica," Ceramic Transactions, Volume 16, 795 pp.

395. Larsen, Torbjorn J.; and McYay, Michael (1993), "Concrete Strength and Durability," Proceedings of the Third International Symposium on Utilization of High-Strength Concrete, Lillehammer, Norway, Volume 2, 777-784.

396. Lasse Toft, L. T. (1996), "Experiences From Data Collection and FE-Simulations on a High Strength Bridge," Proceedings of the Fourth International Symposium on the Utilization of High Strength/High Performance Concrete, Paris, France, Volume 3, 1457-1464.

397. Le Roy, R.; de Larrard, F.; and Pons, G. (1996), "The AFREM Code Type Model for Creep and Shrinkage of High Performance Concrete," Proceedings of the Fourth International Symposium on the Utilization of High Strength/High Performance Concrete, Paris, France, Volume 2, 387-396.

398. Légeron, F.; and Paultre, P. (1996), "Seismic Behaviour of High Strength Concrete Columns," Proceedings of the Fourth International Symposium on the Utilization of High Strength/High Performance Concrete, Paris, France, Volume 3, 883-892.

399. Leivo, Markku T.; and Penttala, Vesa E. (1993), "High Early Strength Concrete," Proceedings of the Third International Symposium on Utilization of High-Strength Concrete, Lillehammer, Norway, Volume 2, 785-792.

400. Leshchinsky, Alex; and Pattison, John (1994), "High-Performance Concrete for Australian Freeways," Concrete International, 16(10), 45-48.

401. Leshchinsky, M. Yu; and Velichko, A. (1991), "The Use of Fly Ash in Concretes Subject to Heat," Cement and Concrete Research, 21, 205-218.

402. Leslie, Keith E.; Rajagopalan, K. S.; and Everard, Noel J. (1976), "Flexural Behavior of High-Strength Concrete Beams," ACI Journal, 73(9), 517-521.

403. Lessard, M.; Sarkar, S. L.; Ksinsik, D. W.; and Aïtcin, P. C. (1992), "Long-Term Behavior of Silica Fume Concrete," Concrete International, 14(4), 25-30.

404. Lessard, Michel; Chaallal, Omar; and Aïtcin, Pierre-Claude (1993), "Testing High-Strength Concrete Compressive Strength," ACI Materials Journal, 90(4), 303-308.

405. Lessard, Michel; Gendreau, Martin; and Gagné, Richard (1993), "Statistical Analysis of the Production of a 75 MPa Air Entrained Concrete," Proceedings of the Third International Symposium on Utilization of High-Strength Concrete, Lillehammer, Norway, Volume 2, 793-800.

406. Leung, Christopher K. Y.; and Pheeraphan, Thanakorn (1995), "Very High Early Strength of Microwave Cured Concrete," Cement and Concrete Research, 25(1), 136-146.

407. Levi, Franco; and Marro, Piero (1993), "Shear Tests on HSC Prestressed Beams - Proposals of New Interpretative Models," Proceedings of the Third International Symposium on Utilization of High-Strength Concrete, Lillehammer, Norway, Volume 1, 293-305.

408. Li, Bing (1993), "Strength and Ductility of Reinforced Concrete Members and Frames Constructed Using High Strength Concrete," Ph.D. Thesis, University of Canterbury, Christchurch, New Zealand.

409. Limsuwan, Ekasit (1993), "Behaviour of Post-Tensioned High Strength Concrete Beams," Proceedings of the Third International Symposium on Utilization of High-Strength Concrete, Lillehammer, Norway, Volume 1, 285-292.

410. Limsuwan, Ekasit (1993), "Strengths of High Strength Concrete Columns," Proceedings of the Third International Symposium on Utilization of High-Strength Concrete, Lillehammer, Norway, Volume 1, 277-284.

411. Lin, Y.; Chang, M. -T.; and Changfan, H. (1996), "Nondestructive Evaluation of Strength Development of High Performance Concrete Using the P-Wave Velocity," Proceedings of the Fourth International Symposium on the Utilization of High Strength/High Performance Concrete, Paris, France, Volume 2, 735-740.

412. Lindgård, Jan; and Sellevold, Erik J. (1993), "Is High-Strength Concrete More Robust Against Elevated Curing Temperatures?," Proceedings of the Third International

Symposium on Utilization of High-Strength Concrete, Lillehammer, Norway, Volume 2, 810-821.

413. Lloyd, Natalie A.; and Rangan, Vijaya (1993), "High-Strength Concrete Columns Under Axial Load and Uniaxial Bending," Proceedings of the Third International Symposium on Utilization of High-Strength Concrete, Lillehammer, Norway, Volume 2, 1217-1224.

414. Lohtia, R. P.; Nautiyal, B. D.; and Jain, O. P. (1976), "Creep of Fly Ash Concrete," ACI Journal, 73(8), 469-472.

415. Lorrain, M.; and Hamouine, A. (1996), "Bond Performance of High Strength Concrete," Proceedings of the Fourth International Symposium on the Utilization of High Strength/High Performance Concrete, Paris, France, Volume 3, 1195-1200.

416. Loukili, A.; Roux, N.; Arlot, D.; and Feylessoufi, A. (1996), "Effects of a High Reduction in the Initial Water Content in Cement Based Matrices," Proceedings of the Fourth International Symposium on the Utilization of High Strength/High Performance Concrete, Paris, France, Volume 3, 1367-1374.

417. Lovewell, C. E.; and Washa, George W. (1958), "Proportioning Concrete Mixtures Using Fly Ash," ACI Journal, 54(12), 1093-1101.

418. Luciano, John J.; Nmai, Charles K.; and DelGado, James R. (1991), "A Novel Approach to Developing High-Strength Concrete," Concrete International, 13(5), 25-29.

419. Luther, Mark D. (1993), "Silica Fume(Microsilica) Concrete in Bridges," Concrete International, 15(4), 29-33.

420. Luther, Mark D. (1994), "Silica Fume," Chapter about silica fume, for Reeves, Clifford M., to be published in 1994(DRAFT).

421. Luther, Mark D.; and Bauer, Kenneth C. (1987), "Using High-Strength Concrete Simplifies Precast Column Design," Concrete Construction, 546-547.

422. Luther, Mark D.; and Mikola, Wayne J. (1993), "Effect of Ground Granulated Blast-Furnace Slag Fineness on High-Strength Concrete Properties," Proceedings of the Third International Symposium on Utilization of High-Strength Concrete, Lillehammer, Norway, Volume 2, 822-829.

423. Maage, M.; Heland, S.; and Carlsen, J. E. (1996), "Service Life Prediction of High Strength Concrete in the Shore Approach Structure," Proceedings of the Fourth International Symposium on the Utilization of High Strength/High Performance Concrete, Paris, France, Volume 2, 519-528.

424. Maage, M.; Smeplass, S.; and Johansen, R. (1990), "Long Term Strength of High-Strength Silica Fume Concrete," Proceedings of the Second International Symposium on Utilization of High-Strength Concrete, Berkeley, California, 399-408.

425. Maage, Magne; Helland, Steinar; and Carlsen, Jan Erik (1993), "Chloride Penetration in High Performance Concrete Exposed to Marine Environment," Proceedings of the Third

International Symposium on Utilization of High-Strength Concrete, Lillehammer, Norway, Volume 2, 838-846.

426. MacGregor, J. G. (1993), "Canadian Network of Centers of Excellence on High-Performance Concrete," Concrete International, 15(2), 60-61.

427. MacInnis, Cameron; and Kosteniuk, Paul W. (1979), "Effectiveness of Revibration and High-Speed Slurry Mixing for Producing High-Strength Concrete," ACI Journal, 76(12), 1255-1265.

428. MacInnis, Cameron; and Thomson, Donald V. (1970), "Special Techniques for Producing High Strength Concrete," ACI Journal, 67(12), 996-1002.

429. Mak, S. L.; and Sanjayan, G. (1990), "Mix Proportions for Very High Strength Concretes," National Conference Publication, Institution of Engineers, Austraulia, 90(10), 127-130.

430. Malhotra, M. (1975), "Development of Sulfur-Infiltrated High-Strength Concrete," ACI Journal, 72(9), 466-473.

431. Malhotra, M. (1976), "Are 4x8 Inch Concrete Cylinders as Good as 6x12 Inch Cylinders for Quality Control of Concrete?," ACI Journal, 73(1), 33-36.

432. Malhotra, M. (1990), "Properties of High-Strength Lightweight Concrete Incorporating Fly Ash and Silica Fume," Proceedings of the Second International Symposium on Utilization of High-Strength Concrete, Berkeley, California, 645-666.

433. Malhotra, M. (1993), "Fly Ash, Slag, Silica Fume, and Rice-Husk Ash in Concrete: A Review," Concrete International, 15(4), 23-28.

434. Malier, Y.; and de Larrard, F. (1993), "French Bridges in High-Performance Concrete," Proceedings of the Third International Symposium on Utilization of High-Strength Concrete, Lillehammer, Norway, Volume 1, 534-544.

435. Malier, Yves (1991), "The French Approach to Using HPC," Concrete International, 13(7), 28-32.

436. Markeset, G. (1996), "Eccentrically Loaded Prisms of Higgh Strength Concrete," Proceedings of the Fourth International Symposium on the Utilization of High Strength/High Performance Concrete, Paris, France, Volume 2, 669-676.

437. Markeset, Gro (1993), "Size Effect on Stress-Strain Relationship of Concrete in Compression," Proceedings of the Third International Symposium on Utilization of High-Strength Concrete, Lillehammer, Norway, Volume 2, 1146-1153.

438. Marro, P.; Taerwe, L.; Gysel, A. Van (1996), "Extension of Stress-Strain Curves for Design and Analysis to High Strength Concrete," Proceedings of the Fourth International Symposium on the Utilization of High Strength/High Performance Concrete, Paris, France, Volume 2, 655-662.

439. Marti, Peter (1989), "Size Effect in Double-Punch Tests on Concrete Cylinders," ACI Materials Journal, 86(6), 597-601.

440. Marushima, N.; Kuroha, K.; and Tomatsuri, K. (1990), "Application of Air-Entraining and Plasticizing Admixture to High-Strength Concrete," Proceedings of the Second International Symposium on Utilization of High-Strength Concrete, Berkeley, California, 599-617.

441. Marushima, Norio; Kuroha, Kenji; Tomatsuri, Kuniyuki; Kubota, Ken; Koibuchi, Kiyoshi; and Ishikawa, Youichi (1993), "Study on High Strength Concrete with Blast Furnace Slag Cement Incorporating Very Fine Slag," Proceedings of the Third International Symposium on Utilization of High-Strength Concrete, Lillehammer, Norway, Volume 2, 830-837.

442. Marzouk, H.; and Chen, Zhiwei (1993), "Tension Softening Behaviour of High-Strength Concrete Made with Silica Fume and Fly Ash," Proceedings of the Third International Symposium on Utilization of High-Strength Concrete, Lillehammer, Norway, Volume 2, 1154-1161.

443. Masuda, Yoshihiro; Abe, Michihoko; Matsumoto, Masayuki; and Shimizu, Akiyuki (1993), "Strength Development of High-Strength Concrete in Structure," Proceedings of the Third International Symposium on Utilization of High-Strength Concrete, Lillehammer, Norway, Volume 2, 847-854.

444. McDonald, David B.; and Roper, Harold (1993), "Accuracy of Prediction Models for Shrinkage of Concrete," ACI Materials Journal, 90(3), 265-271.

445. Mehta P. K. (1984), "Mineral Admixtures," Concrete Admixtures Handbook, V. S. Ramachandran ed., Noyes Publications, Park Ridge, New Jersey, 626 pp.

446. Mehta, P. K.; and Aïtcin, P. C. (1990), "Microstructural Basis of Selection of Materials and Mix Proportions for High-Strength Concrete," Proceedings of the Second International Symposium on Utilization of High-Strength Concrete, Berkeley, California, 265-286.

447. Mehta, P. Kumar (1986), "Concrete - Structure, Properties, and Materials," Prentice-Hall, Inc., Englewood Cliffs, New Jersey, 450 pp.

448. Melby, Karl; Jordet, Elljarn A.; and Hansvold, Carl (1993), "Long Span Bridges in Norway Constructed in High-Strength LWA-Concrete," Proceedings of the Third International Symposium on Utilization of High-Strength Concrete, Lillehammer, Norway, Volume 1, 545-553.

449. Mendis, P. A.; and Pendyala, R. S. (1996), "High Performance/Strength Concrete in Australia - Design and Applications," Proceedings of the Fourth International Symposium on the Utilization of High Strength/High Performance Concrete, Paris, France, Volume 3, 1581-1588.

450. Miao, Buquan; Chaallal, Omar; Perraton, Daniel; and Aïtcin, Pierre-Claude (1993), "On-Site Early-Age Monitoring of High-Performance Concrete Columns," ACI Materials Journal, 90(5), 415-420.

451. Mirambell, Enrique; Calmon, Joao Luiz; and Aguado, Antonio (1993), "Heat of Hydration in High-Strength Concrete: Case Study," Proceedings of the Third International

Symposium on Utilization of High-Strength Concrete, Lillehammer, Norway, Volume 1, 554-561.

452. Mitchell, Denis; Cook, William D.; Khan, Arshad A.; and Tham, Thomas (1993), "Influence of High Strength Concrete on Transfer and Development Length of Pretensioned Strand," PCI Journal, 38(3), 52-66.

453. Mitsui, K.; Yonezawa, T.; Kojima, M.; Tezuka, M.; and Kinoshita, M. (1996), "Design and Construction of Prestessed Concrete Bridge Using 100 Mpa High Strength Concrete," Proceedings of the Fourth International Symposium on the Utilization of High Strength/High Performance Concrete, Paris, France, Volume 3, 1493-1504.

454. Mitsui, Kenro; Li, zongjin; Lange, David A.; and Shah, Surendra P. (1994), "Relationship between Microstructure and Mechanical Properties of the Paste-Aggregate Interface," ACI Materials Journal, 91(1), 30-39.

455. Mittelacher, Martin (1992), "Compressive Strength and the Rising Temperature of Field Concrete," Concrete International, 14(12), 29-33.

456. Mittelacher, Martin (1992), "Re-Evaluating the Slump Test," Concrete International, 14(10), 53-56.

457. Mivelaz, P.; Jaccoud, J. -P.; and Favre, R. (1996), "Experimental Study of Air and Water Flow Through Cracked Reinforced Concrete Tension Members," Proceedings of the Fourth International Symposium on the Utilization of High Strength/High Performance Concrete, Paris, France, Volume 3, 1233-1242.

458. Miyauchi, Yasuyoshi; Higashibata, Yasuo; Nishimura, Yasushi; and Minami, Koichi (1993), "Design of Steel Reinforced Concrete Columns Using High Strength Concrete," Proceedings of the Third International Symposium on Utilization of High-Strength Concrete, Lillehammer, Norway, Volume 1, 306-313.

459. Mokhtarzadeh, A.; Ahlborn, T.; French, C.; and Leon R. (1992), "Applications of High Strength Concrete to Prestressed Industry," Proceedings of the Third Workshop on Bridge Engineering Research in Progress, National Science Foundation, La Jolla, CA, 23-26.

460. Mokhtarzadeh, A.; Ahlborn, T.; French, C.; and Leon R. (1993), "Applications of High Strength Concrete to Prestressed Industry," Proceedings of the Third International Symposium on Utilization of High-Strength Concrete, Lillehammer, Norway, Volume 1, 163-168.

461. Mokhtarzadeh, Alireza; Kriesel, Roxanne; French, Catherine; and Snyder, Mark (1995), "Mechanical Properties and Durability of High Strength Concrete for Prestressed Bridge Girders," Transportation Research Record No. 1478, Transportation Research Board, Washington, D.C., 20-29.

462. Monachon, P.; and Gaumy, A. (1996), "The Normandy Bridge and Société Générale Tower - HSC Grade 60," Proceedings of the Fourth International Symposium on the Utilization of High Strength/High Performance Concrete, Paris, France, Volume 3, 1525-1536.

463. Monteiro, Paulo J. M. (1991), "A Note on the Hirsch Model," Cement and Concrete Research, 21, 947-950.

464. Mor, A. (1992), "Steel-Concrete Bond in High-Strength Lightweight Concrete," ACI Materials Journal, 89(1), 76-82.

465. Mor, A.; Gerwick, B. C.; and Hester, W. T. (1992), "Fatigue of High-Strength Reinforced Concrete," ACI Materials Journal, 89(2), 197-207.

466. Moralez, Salvador Martinez (1982), "Short-Term Mechanical Properties of High-Strength Light-Weight Concrete," Departmental Report No. 82-9, Department of Structural Engineering, Cornell University, Ithaca, NY, 98 pp.

467. Moreno, Jaime (1990), "Ultra-High-Strength Concrete for 225 W. Wacker Project, Chicago," PCA Engineered Concrete Structures, 3(1).

468. Morgan, D. R. (1986), "Concrete in Transportation," ACI SP-93, International Conference on Concrete in Transportation, Vancouver, British Columbia, Canada, 929 pp.

469. Mørtsell, E.; Smeplass, S.; Hammer, T. A.; and Maage, M. (1996), "Flowcyl - How to Determine the Flow Properties of the Matrix Phase of High Performance Concrete," Proceedings of the Fourth International Symposium on the Utilization of High Strength/High Performance Concrete, Paris, France, Volume 2, 261-268.

470. Moussard, Michel M.; and Montens, Serge J. (1993), "Roize River Experimental Bridge," Proceedings of the Third International Symposium on Utilization of High-Strength Concrete, Lillehammer, Norway, Volume 1, 562-569.

471. Mphonde, Andrew G.; and Frantz, Gregory C. (1985), "Shear Tests of High- and Low-Strength Concrete Beams with Stirrups," Special Publication, SP-87, American Concrete Institute, Detroit, MI, 179-196.

472. Muguruma, H.; and Watanabe, F. (1990), "Ductility Improvement of High-Strength Concrete Columns with Lateral Confinement," Proceedings of the Second International Symposium on Utilization of High-Strength Concrete, Berkeley, California, 47-60.

473. Muguruma, Hiroshi; Matsunaga, Yoshihisa; Watanabe, Yoshiharu; and Sakai, Etsuo (1993), "Long Term Stability and Microstructure of Steam-Cured High Strength Concrete with Ettringite Based Additives," Proceedings of the Third International Symposium on Utilization of High-Strength Concrete, Lillehammer, Norway, Volume 2, 855-862.

474. Muguruma, Hiroshi; Nishiyama, Minehiro; and Watanabe, Fumio (1993), "Stress-Strain Curve for Concrete with a Wide-Range of Compressive Strength," Proceedings of the Third International Symposium on Utilization of High-Strength Concrete, Lillehammer, Norway, Volume 1, 314-321.

475. Müller, H. S.; and Küttner, C. H. (1996), "Creep of High Performance Concrete - Characteristics and Code-Type Prediction Model," Proceedings of the Fourth International Symposium on the Utilization of High Strength/High Performance Concrete, Paris, France, Volume 2, 377-386.

476. Naaman, A. E.; and Hamza, A. M. (1991), "Evaluation of Prestress Losses for Partially Prestressed High Strength Concrete Beams," Report No. UMCE 91-18, Department of Civil and environmental Engineering, University of Michigan, Ann Arbor, MI.

477. Naaman, Antoine E.; and Hamza, Ali M. (1993), "Prestress Losses in Partially Prestressed High Strength Concrete Beams," PCI Journal, 38(3), 98-114.

478. Naceer-Bey, M.; Zeghib, R.; and Baudeau, Ph. (1996), "Study of the Steel Fibers Behavior into a High Performance Concrete Matrix," Proceedings of the Fourth International Symposium on the Utilization of High Strength/High Performance Concrete, Paris, France, Volume 3, 1077-1084.

479. Nagaraj, T. S.; Shashiprakash, S. G.; and Prasad, B. K. (1993), "Reproportioning Concrete Mixes," ACI Materials Journal, 90(1), 50-58. (see discussion November-December 1993)

480. Naik, Tarun R.; and Ramme, Bruce W. (1990), "High Early Strength Fly Ash Concrete for Precast/Prestressed Products," PCI Journal, 35(6), 72-80.

481. Naik, Tarun R.; and Ramme, Bruce W. (1990), "Effects of High-Lime Fly Ash on Water Demand, Time of Set, and Compressive Strength of Concrete," ACI Materials Journal, 87(6), 619-626.

482. Naik, Tarun R.; Patel, Viral M.; and Brand, Larry E. (1991), "Performance of High-Strength Concrete Incorporating Mineral By-Products," Center for By-Products Utilization, Report No. REP-125, 33 pp.

483. Nasser, K. W.; and Al-Manaseer, A. A. (1986), "Creep of Concrete Containing Fly Ash and Superplasticizer at Different Stress/Strength Ratios," ACI Journal, 83(4), 668-673.

484. Nasser, K. w.; and Al-Manaseer, A. A. (1987), "It's Time for a Change from 6x12- to 3x6-in. Cylinders," ACI Materials Journal, 84(3), 213-216.

485. Nasser, K. W.; and Kenyon, J. C. (1984), "Why Not 3x6 Inch Cylinders for Testing Concrete Compressive Strength," ACI Journal, Proceedings, 81(1), 47-53.

486. Nelson, E. L.; Carrasquillo, R. L.; and Fowler, D. W. (1988), "Behavior and Failure of High-Strength Concrete Subjected to Biaxial-Cyclic Compression Loading," ACI Materials Journal, 85(4), 248-253.

487. Neville, Adam M. (1966), "A General Relation for Strengths of Concrete Specimens of Different Shapes and Sizes," ACI Journal, Proceedings, 63(10), 1095-1109.

488. Neville, Adam M. (1975), " Properties of Concrete," Pitman Publishing Ltd., London, Great Britain, 687 pp.

489. Neville, Adam, "Cementitious Materials - A Different Viewpoint (1994)," Concrete International, 16(7), 32-33.

490. Nielsen, C. V.; Olesen, J. F.; and Aarup, B. K. (1996), "Effect of Fibers on the Bond Strength of High Strength Concrete," Proceedings of the Fourth International Symposium on the Utilization of High Strength/High Performance Concrete, Paris, France, Volume 3, 1209-1218.

491. Nilsen, Arne Ulrik; and Gjørv, Odd E. (1993), "Elastic Properties of High-Strength Concrete," Proceedings of the Third International Symposium on Utilization of High-Strength Concrete, Lillehammer, Norway, Volume 2, 1162-1168.

492. Nilson, Arthur H. (1985), "Design Implications of Current Research on High-Strength Concrete," American Concrete Institute, SP-87, 85-118.

493. Nishiyama, Minehiro; Fukushima, Izuru; and Watanabe, Fumio (1993), "Axial Loading Tests on High-Strength Concrete Prisms Confined by Ordinary and High-Strength Steel," Proceedings of the Third International Symposium on Utilization of High-Strength Concrete, Lillehammer, Norway, Volume 1, 322-329.

494. Noghabai, Keivan; Ohlsson, Ulf; and Olofsson, Thomas (1993), "Bond Properties of High Strength Concrete," Proceedings of the Third International Symposium on Utilization of High-Strength Concrete, Lillehammer, Norway, Volume 2, 1169-1176.

495. Noguchi, T.; and Tomozawa, F. (1996), "Effect of Characteristics of Testing Machine on Measured Compressive Strength of High Strength Concrete," Proceedings of the Fourth International Symposium on the Utilization of High Strength/High Performance Concrete, Paris, France, Volume 2, 301-310.

496. Noumowe, A. N.; Clastres, P.; Debiki, G.; and Costaz J. -L. (1996), "Thermal Stresses and Water Vapour Pressure of High Performance Concrete at High Temperature," Proceedings of the Fourth International Symposium on the Utilization of High Strength/High Performance Concrete, Paris, France, Volume 2, 561-570.

497. Nour, D. S.; Pamfil, E.; and Barbuta, M. (1996), "Concrete with High Performance of Durability," Proceedings of the Fourth International Symposium on the Utilization of High Strength/High Performance Concrete, Paris, France, Volume 2, 535-538.

498. Novokshchenov, V.; and Whitcomb, W. (1990), "How to Obtain High-Strength Concrete Using Low Density Aggregate," Proceedings of the Second International Symposium on Utilization of High-Strength Concrete, Berkeley, California, 683-700.

499. Novokshchenov, Vladimir (1993), "Factors Controlling the Compressive Strength of Silica Fume Concrete in the Range 100 to 150 MPa," Proceedings of the Third International Symposium on Utilization of High-Strength Concrete, Lillehammer, Norway, Volume 2, 863-873.

500. Nykyri, Pekka; and Yli-Luukko, Elina (1993), "Tensile Strength of Concrete in Hollow Core Slab," Proceedings of the Third International Symposium on Utilization of High-Strength Concrete, Lillehammer, Norway, Volume 1, 330-337.

501. Okamoto, P. A.; and Whiting, D. (1994), "Use of Maturity and Pulse Velosity Techniques to Predict Strength Gain of Rapid Concrete Pavement Repairs During the Curing Period," Paper No. 940122, Transportation Research Board (TRB), 73rd Annual Meeting, 19 pp.

502. Olek, Jan; Cohen, Menashi D.; and Lobo, Colin (1990), "Determination of Surface Area of Portland Cement and Silica Fume by Mercury Intrusion Porosimetry," ACI Materials Journal, 87(5), 473-478.

503. Olsen, N. H. (1990), "Strength of Lapped Splices in High-Strength Concrete," Proceedings of the Second International Symposium on Utilization of High-Strength Concrete, Berkeley, California, 179-193.

504. Oluokun, Francis A. (1991), "Prediction of Concrete Tensile Strength from its Compressive Strength: Evaluation of Existing Relations for Normal Weight Concrete," ACI Materials Journal, 88(3), 302-309.

505. Oluokun, Francis A. (1994), "Fly Ash Concrete Mix Design and the Water-Cement Ratio Law," ACI Materials Journal, 91(4), 362-371.

506. Oluokun, Francis A.; Burdette, Edwin G.; and Deatherage, J. Harold (1991), "Elastic Modulus, Poisson's Ratio, and Compressive Strength Relationships at Early Ages," ACI Materials Journal, 88(1), 3-10.

507. Oluokun, Francis A.; Burdette, Edwin G.; and Deatherage, J. Harold (1991), "Splitting Tensile Strength and Compressive Strength Relationship at Early Ages," ACI Materials Journal, 88(2), 115-121. (see discussion January-February 92)

508. Owens, Philip L. (1989), "Water and its Role in Concrete, Part 1 of 2" Concrete International, 11(11), 68-74.

509. Owens, Philip L. (1989), "Water and its Role in Concrete, Part 2 of 2" Concrete International, 11(12), 68-71.

510. Ozyildirim, Celik (1985), "Neoprene Pads for Capping Concrete Cylinders," Cement, Concrete, and Aggregate, 7(1), 25-28.

511. Ozyildirim, Celik (1993), "High-Performance Concrete for Transportation Structures," Concrete International, 15(1), 33-38.

512. Ozyildirim, Celik (1994), "Laboratory Investigation of Low-Permeability Concretes Containing Slag and Silica Fume," ACI Materials Journal, 91(2), 197-202.

513. Papworth, Frank; and Burnett, Ian D. (1993), "High Performance Silica Fume Concrete Application," Proceedings of the Third International Symposium on Utilization of High-Strength Concrete, Lillehammer, Norway, Volume 1, 570-580.

514. Papworth, Frank; and Ratcliffe, Royce (1994), "High-Performance Concrete - The Concrete Future," Concrete International, 16(10), 39-44.

515. Parker, D. G. (1985), "Microsilica Concrete. Part I: the Material," Concrete International, 19(10), 21-22.

516. Parrott, L. J. (1969), "The Production and Properties of High-Strength Concrete," Concrete, 443-448.

517. Parrott, L. J. (1988), "A Literature Review of High Strength Concrete Properties," British Cement Association Report, 85 pp.

518. Paulson, Kent A.; Nilson, Arthur H.; and Hover, Kenneth C. (1989), "Immediate and Long-Term Deflection of High Strength Concrete Beams," Departmental Report No. 89-3, Department of Structural Engineering, Cornell University, Ithaca, NY, 230 pp.

519. Paultre, P.; Khayat, K. H.; Langlois, Y.; Trudel, A.; and Cusson, D. (1996), "Structural Performance of Some Special Concretes," Proceedings of the Fourth International Symposium on the Utilization of High Strength/High Performance Concrete, Paris, France, Volume 3, 787-796.

520. Pauw, Adrian (1960), "Static Modulus of Elasticity of Concrete as Affected by Density," ACI Journal, 32(6), 679-687.

521. Penttala, V.; and Komonen, J. (1996), "High Strength Concrete Produced by a Low Binder Amount," Proceedings of the Fourth International Symposium on the Utilization of High Strength/High Performance Concrete, Paris, France, Volume 2, 223-234.

522. Penttala, V.; and Rautanen, T. (1990), "Microporosity, Creep, and Shrinkage of High-Strength Concretes," Proceedings of the Second International Symposium on Utilization of High-Strength Concrete, Berkeley, California, 409-432.

523. Penttala, Vesa E. (1993), "Effects of Delayed Dosage of Superplasticizer on High Performance Concrete," Proceedings of the Third International Symposium on Utilization of High-Strength Concrete, Lillehammer, Norway, Volume 2, 874-881.

524. Perenchio, William F.; and Klieger, Paul (1978), "Some Physical Properties of High-Strength Concrete," PCA Research and Development Bulletin RD056.01T, 6 pp.

525. Persson, B. (1996), "(Early) Basic Creep of High Performance Concrete," Proceedings of the Fourth International Symposium on the Utilization of High Strength/High Performance Concrete, Paris, France, Volume 2, 405-414.

526. Persson, B. S. M. (1993), "Early Basic Creep of High-Strength Concrete," Proceedings of the Third International Symposium on Utilization of High-Strength Concrete, Lillehammer, Norway, Volume 2, 1185-1192.

527. Persson, B. S. M. (1993), "Self-Desiccating High-Strength Concrete Slabs," Proceedings of the Third International Symposium on Utilization of High-Strength Concrete, Lillehammer, Norway, Volume 2, 882-889.

528. Peterman, M. B.; and Carrasquillo, R. L. (1986), "Production of High Strength Concrete," Noyes Publications, Park Ridge, NJ, 286 pp.

529. Petkovic, G.; Lenschow, R.; Stemland, H.; and Rosseland, S. (1990), "Fatigue of High-Strength Concrete," Proceedings of the Second International Symposium on Utilization of High-Strength Concrete, Berkeley, California, 505-525.

530. Pettersson, K. (1996), "Criteria for Cracks in Connection with Corrosion in High Strength Concrete," Proceedings of the Fourth International Symposium on the Utilization of High Strength/High Performance Concrete, Paris, France, Volume 2, 509-518.

531. Pettersson, Karin H. (1993), "Corrosion of Steel in High Performance Concrete," Proceedings of the Third International Symposium on Utilization of High-Strength Concrete, Lillehammer, Norway, Volume 2, 890-897.

532. Pham, X. T.; and Rialland, Y. (1996), "An urban Bridge: The Viaduct Over the Rhone River, in Lyon, France," Proceedings of the Fourth International Symposium on the Utilization of High Strength/High Performance Concrete, Paris, France, Volume 3, 1437-1446.

533. Pigeon, M. (1996), "The Durability of HS/HPC," Proceedings of the Fourth International Symposium on the Utilization of High Strength/High Performance Concrete, Paris, France, Volume 1, 39-46.

534. Pigeon, Michel; Gagne, Richard; and Aïtcin, Pierre-Claude (1991), "Freezing and Thawing Tests of High-Strength Concretes," Cement and Concrete Research, 21, 844-852.

535. Ping, Xie; Beaudoin, J. J.; and Brousseau, R. (1991), "Effect of Aggregate Size on Transition Zone Properties at the Portland Cement Paste Interface," Cement and Concrete Reseach, 21, 999-1005.

536. Ping, Xie; Beaudoin, J. J.; and Brousseau, R. (1991), "Flat Aggregate-Portland Cement Paste Interfaces, I. Electrical Conductivity Models," Cement and Concrete Research, 21, 515-522.

537. Pinto, R. C. A.; and Hover, K. C. (1996), "Further Studies on the Utilization of Maturity Functions to a High Strength Concrete Mixture," Proceedings of the Fourth International Symposium on the Utilization of High Strength/High Performance Concrete, Paris, France, Volume 2, 711-718.

538. Pistilli, Michael F.; and Willems, Terry (1993), "Evaluation of Cylinder Size and Capping Method in Compression Strength Testing of Concrete," Cement, Concrete, and Aggregate, 15(1), 59-69.

539. Placas, Alexander; and Regan, Paul E. (1971), "Shear Failure of Reinforced Concrete Beams," ACI Journal, 68(10), 763-773.

540. Pleau, R.; Pigeon, M.; Lamontagne, A.; and Lessard, M. (1995), "Influence of Pumping on Characteristics of Air-Void System of High Performance Concrete," Transportation Research Record No. 1478, Transportation Research Board, Washington, D.C., 30-36.

541. Podmasova, S. A.; Babev, Sh. T.; and Volkov, Yu. S. (1993), "New Low Water Demand Binders for High-Strength Concretes," Proceedings of the Third International Symposium on Utilization of High-Strength Concrete, Lillehammer, Norway, Volume 2, 898-903.

542. Popovics, Sandor (1990), "Analysis of Concrete Strength versus Water-Cement Ratio Relationship," ACI Materials Journal, 87(5), 517-529. (see discussion July-August 91/September-October 91)

543. Popovics, Sandor (1994), "The Slump Test Is Useless - Or Is It?," Concrete International, 16(9), 30-33.

544. Potter, Robert J.; and Guirguis, Samia (1993), "High-Strength Concrete in Australia," Proceedings of the Third International Symposium on Utilization of High-Strength Concrete, Lillehammer, Norway, Volume 1, 581-589.

545. Price, W. F.; and Hynes, J. P. (1996), "Non-Destructive Testing of High Strength Concrete," Proceedings of the Fourth International Symposium on the Utilization of High Strength/High Performance Concrete, Paris, France, Volume 2, 637-644.

546. Price, Walter H. (1951), "Factors Influencing Concrete Strength," ACI Journal, 22(6), 417-432.

547. Punkki, J.; Gjørv, O. E.; and Monteiro, P. J. M. (1996), "Microstructure of High Strength Lightweight Aggregate Concrete," Proceedings of the Fourth International Symposium on the Utilization of High Strength/High Performance Concrete, Paris, France, Volume 3, 1281-1288.

548. Punkki, Jouni; and Gjørv, Odd E. (1993), "Water Absorption by High-Strength Lightweight Aggregate," Proceedings of the Third International Symposium on Utilization of High-Strength Concrete, Lillehammer, Norway, Volume 2, 713-721.

549. Radain, Talal A.; Samman, Tamim A.; and Wafa, Faisal F. (1993), "Mechanical Properties of High-Strength Concrete," Proceedings of the Third International Symposium on Utilization of High-Strength Concrete, Lillehammer, Norway, Volume 2, 1209-1216.

550. Ralls, M. L.; Carrasquillo, R. L.; and Burns, N. H. (1996), "Texas High Performance Concrete Bridges," Proceedings of the Fourth International Symposium on the Utilization of High Strength/High Performance Concrete, Paris, France, Volume 3, 1475-1482.

551. Ramachandran, V. S.; and Malhotra, V. M. (1984), "Superplasticizers," Concrete Admixtures Handbook, V. S. Ramachandran ed., Noyes Publications, Park Ridge, New Jersey, 626 pp.

552. Ramadier, C.; Rochefort, H.; Dugat, J.; and Verrier, R. (1996), "The Library of France," Proceedings of the Fourth International Symposium on the Utilization of High Strength/High Performance Concrete, Paris, France, Volume 3, 1515-1524.

553. Ramakrishnan, V.; and Akman, M. Suheyl (1992), "Fly Ash, Silica Fume, Slag and Natural Pozzolans in Concrete," Proceedings of the US-Turkey Workshop, Istanbul, Turkey, 201 pp.

554. Ramdane, K. -E. (1996), "Punching Shear of High Performance Concrete Slabs," Proceedings of the Fourth International Symposium on the Utilization of High Strength/High Performance Concrete, Paris, France, Volume 3, 1015-1026.

555. Ramezanianpour, A. A. (1993), "Selection of Materials and Mix Proportions for High Strength Concrete," Proceedings of the Third International Symposium on Utilization of High-Strength Concrete, Lillehammer, Norway, Volume 2, 904-912.

556. Randall, Vaughn; and Foot, Kenneth (1989), "High-Strength Concrete for Pacific First Center," Concrete International, 11(4), 14-16.

557. Rao, R. Prasada; and Olek, J. (1996), "Comparison of the Efects of belended Cementitious Binders on Selected Properties of High Performance Pastes and Concretes," Proceedings of the Fourth International Symposium on the Utilization of High Strength/High Performance Concrete, Paris, France, Volume 2, 143-152.

558. Ravindra, K. Dhir; and Byars, Ewan A.(1993), "Pulverized Fuel-Ash Concrete: Intrinsic Permeability," ACI Materials Journal, 90(6), 571-580.

559. Read, P.; Carette, G. G.; and Malhotra, M. (1990), "Strength Development Characteristics of High-Strength Concrete Incorporating Supplementary Cementing Materials," Proceedings of the Second International Symposium on Utilization of High-Strength Concrete, Berkeley, California, 527-547.

560. Reinhardt, H. W. (1996), "Structural Behavior of HS/HPC - Part I," Proceedings of the Fourth International Symposium on the Utilization of High Strength/High Performance Concrete, Paris, France, Volume 1, 47-56.

561. Reji, John; and Shah, Surendra P. (1989), "Fracture Mechanics Analysis of High-Strength Concrete," Journal of Materials in Civil Engineering, 1(4), 185-198.

562. Remmel, Gred; and König, Gert (1993), "The Tensile Behaviour of High-Strength Concrete(HSC) and its Effect on the Shear Strength of Longitudinally Reinforced Concrete Members," Proceedings of the Third International Symposium on Utilization of High-Strength Concrete, Lillehammer, Norway, Volume 1, 269-276.

563. Reza, M.; Spring, Gary; and Zhao, Shilong (1993), "Coarse-Aggregate Effect on Mechanical Properties of Plain Concrete," Paper No. 930268, Transportation Research Board (TRB), 72nd Annual Meeting, 17 pp.

564. Richard, P. (1996), "Reactive Powder Concrte: A New Ultra High Strength Cementitious Material," Proceedings of the Fourth International Symposium on the Utilization of High Strength/High Performance Concrete, Paris, France, Volume 3, 1343-1350.

565. Richard, P. (1996), "The Future of HS/HPC," Proceedings of the Fourth International Symposium on the Utilization of High Strength/High Performance Concrete, Paris, France, Volume 1, 101-106.

566. Richardson, David N. (1991), "Review of Variables that Influence Measured Concrete Compressive Strength," Journal of Materials in Civil Engineering, 3(2), 95-112.

567. Rindal, Dag B.; and Horrigmoe, Geir (1993), "High Quality Roller Compacted Concrete Pavements," Proceedings of the Third International Symposium on Utilization of High-Strength Concrete, Lillehammer, Norway, Volume 2, 913-920.

568. Rocole, Larry (1993), "Silica-Fume Concrete Proves to be an Economical Alternative," Concrete Construction, June Isuue, 441-442.

569. Roller, John J.; and Russell, Henry G. (1990), "Shear Strength of High-Strength Concrete Beams with Web Reinforcement," ACI Structural Journal, 87(2), 191-198.

570. Roller, John J.; Martin, Barney T.; Russell, Henry G.; and Bruce, Robert N., Jr. (1993), "Performance of Prestressed High Strength Concrete Bridge Girders," PCI Journal, 38(3), 34-45.

571. Rønneberg, Hanne; and Eeg, Inge R. (1993), "Production of High-Strength Concrete: The Views of a Readymix Concrete Company," Proceedings of the Third International Symposium on Utilization of High-Strength Concrete, Lillehammer, Norway, Volume 1, 482-494.

572. Rosenbaum, David (1991), "Concrete Was Never So Complicated," Engineering News-Record, January 21, 35-40.

573. Rosenberg, A. M.; and Gaidis, J. M. (1989), "A New Mineral Admixture for High-Strength Concrete," Concrete International, 11(4), 31-36.

574. Rossi, P.; and Renwez, S. (1996), "High Performance Multimodal Fiber Reinforced Cement Composites (HPMFRCC)," Proceedings of the Fourth International Symposium on the Utilization of High Strength/High Performance Concrete, Paris, France, Volume 2, 687-694.

575. Roy, Della M.; Silsbee, Michael R.; Sabol, Scott; and Scheetz, Barry E. (1995), "Superior Microstructure of High Performance Concrete for Long-Term Durability," Transportation Research Record No. 1478, Transportation Research Board, Washington, D.C., 11-19.

576. Rui-Wamba, Javier; Aguado, Antonio; Oliveria, Marcel O. F.; and Bellod, Juan Luis (1993), "A Non-Standard Structure on High-Strength Concrete," Proceedings of the Third International Symposium on Utilization of High-Strength Concrete, Lillehammer, Norway, Volume 1, 436-448.

577. Russell, Bruce W.; and Burns, Ned H. (1993), "Static and Fatigue Behavior of Pretensioned Composite Bridge Girders Made with High Strength Concrete," PCI Journal, 38(3), 116-128.

578. Russell, H. G. (1990), "Shortening of High-Strength Concrete members," Proceedings of the Second International Symposium on Utilization of High-Strength Concrete, Berkeley, California, 1-20.

579. Russell, H. G.; and Corley, W. G., "Time-Dependent Behavior of Columns in Water Tower Place," PCA Research and Development Bulletin RD052.01B, 10 pp.

580. Russell, H. G.; and Larson, S. C. (1989), "Thirteen Years of Deformations in Water Tower Place," ACI Structural Journal, 86(2), 182-191.

581. Russell, H. G.; Gebler, S. H.; and Whiting, D. (1989), "High Strength Concrete: Weighing The Benefits," Civil Engineering, 59(11), 59-61.

582. Russell, H. G.; Volz, J. S.; and Bruce, R. N. (1996), "Optimizing the Use of High Strength Concrete in Prestressed Concrete Bridge Girders," Proceedings of the Fourth International Symposium on the Utilization of High Strength/High Performance Concrete, Paris, France, Volume 3, 1465-1474.

583. Russell, Henry G. (1994), "Special Report No. 2- Long-Term Properties of High-Strength Concretes," Concrete International, 16(4), 57-58.

584. Russell, Henry G.; Roller, John J.; Bruce, Robert N.; and Martin, Barney T. (1993), "High-Strength Concrete for Highway Bridge Structures," Proceedings of the Third International Symposium on Utilization of High-Strength Concrete, Lillehammer, Norway, Volume 1, 107-114.

585. Sakaguchi, N.; Yamanobe, K.; Kitada, Y.; Kawachi, T.; and Koda, S. (1990), "Shear Strength of High-Strength Concrete Members," Proceedings of the Second International Symposium on Utilization of High-Strength Concrete, Berkeley, California, 155-178.

586. Sakata, K.; and Ayano, T. (1996), "Study on the Durability of Low Heat Highly Flowable Concrete Incorporating Urea," Proceedings of the Fourth International Symposium on the Utilization of High Strength/High Performance Concrete, Paris, France, Volume 3, 1333-1342.

587. Samman, T. A.; Radain, T. A.; and Al-Harbi, M. N. (1996), "Torsional Behavior of High Strength Concrete Deep Beams," Proceedings of the Fourth International Symposium on the Utilization of High Strength/High Performance Concrete, Paris, France, Volume 3, 1003-1008.

588. Samman, Tamim; Radain, Talal A.; and Mesawa, Adel A. (1993), "Torsion in High-Strength Plain Concrete Deep Beams," Proceedings of the Third International Symposium on Utilization of High-Strength Concrete, Lillehammer, Norway, Volume 1, 338-345.

589. Sanchez de Rojas, M. I.; Luxan, M. P.; Frias, M.; and Garcia, N. (1993), "The Influence of Different Additions on Portland Cement Hydration Heat," Cement and Concrete Research, 23, 46-54.

590. Sanchez, Alfonso; and Hester, Weston T. (1990), "Designer-Contractor Dialogue and High-Strength Concrete Construction," The Construction Specifier, 43(12), 56-59, 62.

591. Sandvik, M.; and Smeplass, S. (1996), "Modified Normal Density (MND) Concrete for the Toll GBS Platform," Proceedings of the Fourth International Symposium on the Utilization of High Strength/High Performance Concrete, Paris, France, Volume 3, 1271-1280.

592. Sandvik, Malvin (1993), "Utilization of High Strength LWA-Concrete in Norway," Proceedings of the Third International Symposium on Utilization of High-Strength Concrete, Lillehammer, Norway, Volume 1, 590-598.

593. Sandvik, Malvin; and Gjørv, Odd E. (1992), "High Curing Temperatures in Lightweight High-Strength Concrete," Concrete International, 14(12), 40-42.

594. Sarkar, S. L.; and Aïtcin, P. C. (1987), "Dissolution Rate of Silica Fume in Very High Strength Concrete," Cement and Concrete Research, Vol. 17, 591-601.

595. Sarkar, Shondeep L. (1993), "Performance of a High-Strength Field Concrete at 7 Years," Concrete International, 15(1), 39-42.

596. Sarkar, Shondeep L.; Baalbaki, Moussa; and Aïtcin, Pierre-Claude (1991), "Microstructural Development in a High-Strength Concrete Containing a Ternary Cementitious System," Cement, Concrete and Aggregates, 13(2), 81-87.

597. Sauzeat, E.; Feylessoufi, A.; Villiéras, F.; Yvon, J.; Cases, J. -M.; and Richard, P. (1996), "Textural Analysis of Reactive Powder Concretes," Proceedings of the Fourth International Symposium on the Utilization of High Strength/High Performance Concrete, Paris, France, Volume 3, 1359-1366.

598. Scali, Mauro J.; Chin, David; and Berke, Neal S. (1987), "Effect of Microsilica and Fly ash upon the Microstructure and Permeability of Concrete," Proceedings of the Ninth International Conference on Cement Microscopy, Reno, Nevada, 375-397.

599. Schmitt, James W. (1990), "Effects of Mica, Aggregate Coatings, and Water-Soluble Impurities on Concrete," Concrete International, 12(12), 54-58.

600. Schrage, I.; and Springenschmid, R. (1996), "Crep and Shrinkage Data of High Strength Concrete," Proceedings of the Fourth International Symposium on the Utilization of High Strength/High Performance Concrete, Paris, France, Volume 2, 331-338.

601. Schutter, G. (1996), "Influence of Retarding on the Early Age Thermal Cracking Behaviour of High Performance Concrete," Proceedings of the Fourth International Symposium on the Utilization of High Strength/High Performance Concrete, Paris, France, Volume 2, 439-450.

602. Sedran, T.; de Larrard, F. (1996), "RENE-LCPC: Software to Optimize the Mix Design of High Performance Concrete," Proceedings of the Fourth International Symposium on the Utilization of High Strength/High Performance Concrete, Paris, France, Volume 2, 169-178.

603. Sennour, Mohand L.; and Carrasquillo, Ramon L. (1989), "Creep and Shrinkage Properties in Concrete Containing Fly Ash," Reseach Report 481-6, Center for Transportation Research, The University of Texas at Austin, 112 pp.

604. Setunge, S.; and Darvall, P. LeP. (1990), "Engineering Properties of Very High Strength Concrete," National Conference Publication, Institution of Engineers, Austraulia, 90(10), 120-126.

605. Shah, S. P. (1996), "Special HPCs I: Fiber-Reinforced HPC, Ultra-High Strength Concrete," Proceedings of the Fourth International Symposium on the Utilization of High Strength/High Performance Concrete, Paris, France, Volume 1, 75-82.

606. Shah, S. P.; Li, Z.; and Lange, D. A. (1992), "Properties of Aggregate-Cement Interface for High Performance Concrete," Proceedings of the 9th Conference on Engineering Mechanics, Published by ASCE, New York, NY., 852-855.

607. Shah, Surendra P. (1990), "Fracture Toughness for High-Strength Concrete," ACI Materials Journal, 87(3), 260-265.

608. Shahawy, M. A. (1991), "Sttrength Evaluation and Load Testing of the Eau Gallie Bridge," Florida Department of Transportation, Tallahassee, FL.

609. Shehata, I. A. E. M.; and Shehata, L. C. D. (1996), "Ductility of High Strength Concrete Beams in Flexure," Proceedings of the Fourth International Symposium on the Utilization of High Strength/High Performance Concrete, Paris, France, Volume 3, 945-954.

610. Sheikh, Shamim A. (1993), "Deformability of High Strerngth Concrete Columns," Proceedings of the Third International Symposium on Utilization of High-Strength Concrete, Lillehammer, Norway, Volume 1, 346-353.

611. Shilstone Sr., James M. (1990), "Concrete Mixture Optimization," Concrete International, 12(6), 33-39.

612. Shilstone Sr., James M. (1991), "The Water-Cement Ratio-Which One and Where Do We Go?," Concrete International, 13(9), 66-69.

613. Shilstone Sr., James M.; and Shilstone Jr., James M. (1989), "Concrete Mixtures and Construction Needs," Concrete International, 11(12), 53-57.

614. Shin, S. -W.; Kamara, M.; and Ghosh, S. K. (1990), "Flexural Ductility, Strength Prediction, and Hysteretic Behavior of Ultra-High-Strength Concrete Members," Proceedings of the Second International Symposium on Utilization of High-Strength Concrete, Berkeley, California, 239-264.

615. Shin, S. W.; and Choi, J. S. (1996), "Bond Charcateristics of Reinforcing Bars Embeded in High Strength Concrete," Proceedings of the Fourth International Symposium on the Utilization of High Strength/High Performance Concrete, Paris, France, Volume 3, 1185-1194.

616. Shin, Sung-Woo (1990), "High-Strength Concrete in Korea," PCA Engineered Concrete Structures, 3(2).

617. Shin, Sung-Woo; Ahn, Jong-Moon; Lee, Kwang-Soo; and Ghosh, Satyendra K. (1993), "Behaviour of Beam-Column Joints with High and Low Strength Concrete," Proceedings of the Third International Symposium on Utilization of High-Strength Concrete, Lillehammer, Norway, Volume 1, 354-361.

618. Shiomi, Itsuo; Masuda, Yoshihiro; Yasuda, Masayuki; and Kodama, Kazumi (1993), "Influence of Various Factors on Drying Shrinkage of High-Strength Concrete," Proceedings of the Third International Symposium on Utilization of High-Strength Concrete, Lillehammer, Norway, Volume 2, 921-928.

619. SHRP (1993), "Mechanical Behavior of High Performance Concretes, Volume 1: Summary Report," SHRP-C-361, Strategic Highway Research Program, National Academy of Science, Washington, DC, 98 pp.

620. SHRP (1993), "Mechanical Behavior of High Performance Concretes, Volume 2: Production of High Performance Concrete," SHRP-C-362, Strategic Highway Research Program, National Academy of Science, Washington, DC, 92 pp.

621. SHRP (1993), "Mechanical Behavior of High Performance Concretes, Volume 3: Very Early Strength Concrete," SHRP-C-363, Strategic Highway Research Program, National Academy of Science, Washington, DC, 116 pp.

622. SHRP (1993), "Mechanical Behavior of High Performance Concretes, Volume 4: High Early Strength Concrete," SHRP-C-364, Strategic Highway Research Program, National Academy of Science, Washington, DC, 179 pp.

623. SHRP (1993), "Mechanical Behavior of High Performance Concretes, Volume 5: Very High Strength Concrete," SHRP-C-365, Strategic Highway Research Program, National Academy of Science, Washington, DC, 101 pp.

624. SHRP (1993), "Mechanical Behavior of High Performance Concretes, Volume 6: High Early Strength Fiber Reinforced Concrete," SHRP-C-366, Strategic Highway Research Program, National Academy of Science, Washington, DC, 297 pp.

625. Sicard, Vincent; and Pons, Gérard (1993), "About Creep and Shrinkage of Young High Strength Concrete," Proceedings of the Third International Symposium on Utilization of High-Strength Concrete, Lillehammer, Norway, Volume 2, 1201-1208.

626. Siedel, H.; Hempel, S; and Hempel, R. (1993), "Secondary Ettringite Formation in Heat Treated Portland Cement Concrete: Influence of Different W/C Ratios and Heat Treatment Temperatures," Cement and Concrete Research, 23(2), 453-461.

627. Simeonov, Peter; and Ahmad, Shuaib (1995), "Effect of Transition Zone on the Elastic Behavior of Cement-Based Composites," Cement and Concrete Research, 25(1), 165-176.

628. Sindre, Hallvard; and Larsen, Odd Georg (1993), "The New Varodd Bridge , Norway, A Large Concrete Bridge Currently Under Construction by the Balanced Cantilever Method," Proceedings of the Third International Symposium on Utilization of High-Strength Concrete, Lillehammer, Norway, Volume 1, 527-533.

629. Sivasundaram, Visanthy; Carette, George G.; and Malhotra, Mohan (1991), "Mechanical Properties, Creep, and Resistance to Diffusion of Chloride Ions of Concrete Incorporating High Volumes of ASTM Class F Fly Ashes from Seven Different Sources," ACI Materials Journal, 88(4), 407-416.

630. Slanicka, S. (1991), "The Influence of Fly Ash Fineness on the Strength of Concrete," Cement and Concrete Research, 21, 285-296.

631. Slanicka, Stefan (1991), "The Influence of Condensed Silica Fume on the Concrete Strength," Cement and Concrete Research, 21, 462-470.

632. Slate, Floyd O.; Nilson, Arthur H.; and Martinez, Salvador (1986), "Mechanical Properties of High-Strength Lightweight Concrete," ACI Journal, 83(4), 606-613.

633. Smadi, Mohammad M.; Slate, Floyd O.; and Nilson, Arthur H. (1987), "Shrinkage and Creep of High-, Medium-, and Low-Strength Concretes, Including Overloads," ACI Materials Journal, 84(3), 224-234.

634. Smadi, Mohammad Mahmoud (1982), "Time-Dependent Behavior of High-Strength Concrete Under High Sustained Compressive Stresses," Departmental Report No. 82-16, Department of Structural Engineering, Cornell University, Ithaca, NY, 264 pp.

635. Smeplass, S.; and Maage, M. (1990), "Heat of Hydration of High-Strength Concretes," Proceedings of the Second International Symposium on Utilization of High-Strength Concrete, Berkeley, California, 433-456.

636. Smeplass, Sverre; Barkenæs, Jan Erik; and Hansen, Einar Aasved (1993), "Effect of the Aggregate Type on Strength and Fracture of High Strength Concrete," Proceedings of the Third International Symposium on Utilization of High-Strength Concrete, Lillehammer, Norway, Volume 2, 1225-1238.

637. Smith, E. F., Tynes, W. O., and Saucier, K. L. (1964), "High Compressive Strength Concrete - Development of Concrete Mixtures," U.S. Army Waterways Experiment Station, (WES) TDR-63-3114.

638. Smith, Gregory J.; and Rad, Franz N. (1989), "Economic Advantages of High-Strength Concretes in Columns," Concrete International, 11(4), 37-43.

639. Smith, I. A. (1967), "The Design of Fly Ash Concretes," Proceedings, Institution of Civil Engineers, London, Vol. 36, 769-790.

640. Smith, J. L.; and Azimi, A. M. (1993), "Utilization of High-Strength Concrete in North Carolina," Proceedings of the Third International Symposium on Utilization of High-Strength Concrete, Lillehammer, Norway, Volume 1, 468-473.

641. Snell, Luke M.; Roekel, Jacob Van; and Wallace, Norval D. (1989), "Predicting Early Concrete Strength," Concrete International, 11(12), 43-47.

642. Soongswang, Prasit; Tia, Mang; and Bloomquist David (1991), "Factors Affecting the Strength and Permeability of Concrete Made with Porous Limestone," ACI Materials Journal, 88(4), 400-406.

643. Soroka, I. (1980), "Portland Cement Paste and Concrete," Chemical Publishing Co., New York, N. Y., 338 pp.

644. Soutsos, Marios N.; and Domone, Peter L. J. (1993), "Design of High Strength Concrete Mixes with Normal Weight Aggregates," Proceedings of the Third International Symposium on Utilization of High-Strength Concrete, Lillehammer, Norway, Volume 2, 937-944.

645. Soutsos, Marios N.; and Domone, Peter L. J. (1993), "Strength Development of Low Water-Binder Ratio Mixes Incorporating Mineral Admixtures," Proceedings of the Third International Symposium on Utilization of High-Strength Concrete, Lillehammer, Norway, Volume 2, 945-952.

646. Soutsos, Marios N.; and Domone, Peter L. J. (1993), "Workability of High Strength Concrete Mixes as Defined by Tattersall's Two Point Test," Proceedings of the Third International Symposium on Utilization of High-Strength Concrete, Lillehammer, Norway, Volume 2, 929-936.

647. Starr, Paul; and Wainwright, David (1993), "Design and Construction of a Concrete Floating Berth," Proceedings of the Third International Symposium on Utilization of High-Strength Concrete, Lillehammer, Norway, Volume 1, 607-614.

648. Strand, Glenn W. (1991), "High-Performance Concrete in All-Weather Deck Pours," Cold Regions Sixth International Specialty Conference, TCCP/ASCE, West Lebanon, 210-229.

649. Stroband, J.; Poot, S.; and Walraven, J. (1996), "The Effect of Mortar Joints Between Precast HSC Columns Loaded in Compression," Proceedings of the Fourth International Symposium on the Utilization of High Strength/High Performance Concrete, Paris, France, Volume 3, 817-826.

650. Sudo, Eiji; Masuda, Yoshihiro; Abe, Michihiko; and Yasuda, Masayuki (1993), "Mechanical Properties of Confined High-Strength Concrete," Proceedings of the Third International Symposium on Utilization of High-Strength Concrete, Lillehammer, Norway, Volume 1, 369-376.

651. Sugano, S.; Nagashima, T.; Kimura, H.; Tamura, A.; and Ichikawa, A. (1990), "Experimental Studies on Seismic Behaviour of Reinforced Concrete members of High-Strength Concrete," Proceedings of the Second International Symposium on Utilization of High-Strength Concrete, Berkeley, California, 61-87.

652. Sultanov, Fuad A. (1993), "Superplasticized Cement Applications in Azerbaijan and Other States of the Former USSR," Concrete International, 15(4).

653. Suraatmadja, D.; Munaf, D. R.; and Asnan, M. N. (1996), "Utilization of Glass for Fine Aggregate to Produce High Performance Concrete," Proceedings of the Fourth International Symposium on the Utilization of High Strength/High Performance Concrete, Paris, France, Volume 2, 255-260.

654. Suzuki, M.; Suzuki, K.; Abe, K.; and Ozaka, Y. (1996), "Mechanical Properties of Ultra High Strength Concrete Beams Subjected to Pure Bending Moment," Proceedings of the Fourth International Symposium on the Utilization of High Strength/High Performance Concrete, Paris, France, Volume 3, 835-844.

655. Sviridov, N. V. (1993), "Ultra High-Strength Concrete without Silica Fume," Proceedings of the Third International Symposium on Utilization of High-Strength Concrete, Lillehammer, Norway, Volume 2, 953-961.

656. Sviridov, N. V. (1996), "Ultra-High Strength Cement Concrete: The Properties and the Field of Effective Application," Proceedings of the Fourth International Symposium on the Utilization of High Strength/High Performance Concrete, Paris, France, Volume 2, 295-300.

657. Swamy, Narayan; Nakamura, Nobuyuki; and Sakai, Masami (1993), "High Strength with Durability The Twin Offsprings of Fine Slag Cements," Proceedings of the Third International Symposium on Utilization of High-Strength Concrete, Lillehammer, Norway, Volume 2, 962-971.

658. Swamy, R. N. (1985), "High-Strength Concrete-Material Properties and Structural Behavior," American Concrete Institute, SP-87, 119-146.

659. Swamy, R. N. (1986), "Cement Replacement Materials," Surrey University Press, London, 259 pp.

660. Swamy, R. N.; and Bouikni, Ammar (1990), "Some Engineering Properties of Slag Concrete as Influenced by Mix Proportioning and Curing," ACI Materials Journal, 87(3), 210-220. (see discussion March-April 91)

661. Swartz, S. E.; Nikaeen, A.; Narayan Babu, H. D.; Periyakaruppan, N; and Refai, T. M. E. (1985), "Structural Bending Properties of Higher Strength Concrete," American Concrete Institute, SP-87, 147-178.

662. Szalai, F.; and Farkas, G. (1996), "Results of High Performance Concrete Research at the Technical University of Budapest," Proceedings of the Fourth International Symposium on the Utilization of High Strength/High Performance Concrete, Paris, France, Volume 2, 617-622.

663. Tachibana, D.; Imai, M.; Yamazaki, N.; Kawai, T.; and Inada, Y. (1990), "High-Strength Concrete Incorporating Several Admixtures," Proceedings of the Second International Symposium on Utilization of High-Strength Concrete, Berkeley, California, 309-330.

664. Tachibana, Daisuke; Kishitani, Kouichi; Kimura, Kaoru; Shinozaki, Akio; and Omori, Yoshitaka (1993), "High-Strength Lightweight Concrete Using High-Performance Artificial Lightweight Aggregate," Proceedings of the Third International Symposium on Utilization of High-Strength Concrete, Lillehammer, Norway, Volume 2, 972-979.

665. Tachibana, Daisuke; Kumagai, Hitoshi; Yamazaki, Nobuyuki; and Suzuki, Tadahiko (1994), "High-Strength Concrete(f'c=600 kgf/cm^2) for Building Construction," ACI Materials Journal, 91(4), 390-400.

666. Taerwe, L. (1996), "Codes and Regulations," Proceedings of the Fourth International Symposium on the Utilization of High Strength/High Performance Concrete, Paris, France, Volume 1, 93-100.

667. Taerwe, L. (1996), "Structural Behavior of HS/HPC - Part II," Proceedings of the Fourth International Symposium on the Utilization of High Strength/High Performance Concrete, Paris, France, Volume 1, 57-66.

668. Taerwe, L. R. (1992), "Influence of Steel Fibers on Strain-Softening of High-Strength Concrete," ACI Materials Journal, 89(1), 54-60.

669. Taerwe, L.; Thomas, P.; and De Pauw, P. (1996), "Loading Tests on Two-Span Post-Tensioned HSC Beams," Proceedings of the Fourth International Symposium on the Utilization of High Strength/High Performance Concrete, Paris, France, Volume 3, 853-862.

670. Taerwe, Luc R., "Brittleness versus Ductility of High Strength Concrete,"

671. Taerwe, Luc R. (1993), "Bond Fracture and Crack Propagation in High Strength Concrete," Proceedings of the Third International Symposium on Utilization of High-Strength Concrete, Lillehammer, Norway, Volume 2, 1239-1246.

672. Taerwe, Luc R. (1993), "Partial Safety Factor for High Strength Concrete Under Compression," Proceedings of the Third International Symposium on Utilization of High-Strength Concrete, Lillehammer, Norway, Volume 1, 385-392.

673. Takagi, T.; Nakamura, Y.; Ueda, Y.; Yoshida, T.; Kinoshita, H.; and Kitaoka, Y. (1996), "A Quality Control Method for Self-Compactable HighPerformance Concrete at Precast Concrete Plants," Proceedings of the Fourth International Symposium on the Utilization of High Strength/High Performance Concrete, Paris, France, Volume 3, 1315-1322.

674. Takahata, A.; Iwashimizu, T.; and Ishibashi, U. (1990), "Construction of a High-Rise Reinforced Concrete Residence Using High-Strength Concrete," Proceedings of the Second International Symposium on Utilization of High-Strength Concrete, Berkeley, California, 741-755.

675. Tang, Tianxi (1992), "An Elastoviscoplastic Model for High Strengthh Concrete," Proceedings of the 9th Conference on Engineering Mechanics, Published by ASCE, New York, NY., 856-859.

676. Tavera, Ed A. (1993), "Behaviour of High-Strength Concrete Piling Under Driving Conditions," Proceedings of the Third International Symposium on Utilization of High-Strength Concrete, Lillehammer, Norway, Volume 1, 115-119.

677. Tazawa, E.; and Miyazawa, S. (1996), "Influence of Autogenous Shrinkage on Cracking in High Strength Concrete," Proceedings of the Fourth International Symposium on the Utilization of High Strength/High Performance Concrete, Paris, France, Volume 2, 321-330.

678. Tedesco, Joseph W.; Ross, C. Allen; and Kuennen, Steven T. (1993), "Experimental and Numerical Analysis of High Strain Rate Splitting Tensile Tests," ACI Materials Journal, 90(2), 162-169.

679. Thomas, Michael D. A.; and Matthews, John D. (1993), "Performance of Fly Ash Concrete in U.K. Structures," ACI Materials Journal, 90(6), 586-593.

680. Thorenfeldt, E.; and Drangsholt, G. (1990), "Shear Capacity of Reinforced High-Strength Concrete Beams," Proceedings of the Second International Symposium on Utilization of High-Strength Concrete, Berkeley, California, 129-154.

681. Tikalsky, P. J.; and Carrasquillo, R. L. (1988), "Effect of Fly Ash on the Sulfate Resistance of Concrete Containing Fly Ash," Research Report 481-1, Center for Transportation Research, The University of Texas at Austin, 92 pp.

682. Tikalsky, P. J.; and Carrasquillo, R. L. (1993), "Fly Ash Evaluation and Selection for Use in Sulfate-Resistant Concrete," ACI Materials Journal, 90(6), 545-551. (see discussion September-October 1994)

683. Tikalsky, P. J; and Carrasquillo, R. L. (1989), "The Effect of Fly Ash on the Sulfate Resistance of Concrete," Research Report 481-5, Center for Transportation Research, The University of Texas at Austin, 317pp.

684. Tognon, Giampietro; and Cangiano, Stefano (1980), "Air Contained in Superplasticized Concretes," ACI Journal, 79(5), 350-354.

685. Töllner, M.; Koenders, E. A. B.; Breugel, K. Van; and Ouwerkerk, H. (1996), "The Efect of Restraint on Risk of Cracking on in-situ Cast Slab in HighStrength Concret," Proceedings

of the Fourth International Symposium on the Utilization of High Strength/High Performance Concrete, Paris, France, Volume 3, 1057-1066.

686. Tomaszewicz, A. J. (1996), "Crep of High Strength LWA Concrete," Proceedings of the Fourth International Symposium on the Utilization of High Strength/High Performance Concrete, Paris, France, Volume 3, 1289-1294.

687. Tomaszewicz, Andrzej (1993), "Punching Shear Capacity of Reinforced Concrete Slabs," Proceedings of the Third International Symposium on Utilization of High-Strength Concrete, Lillehammer, Norway, Volume 1, 393-401.

688. Tomosawa, F. (1996), "Special HPCs II: Lightweight Aggregate HPC, Self-Compacting HPC," Proceedings of the Fourth International Symposium on the Utilization of High Strength/High Performance Concrete, Paris, France, Volume 1, 83-92.

689. Tomosawa, F.; Masuda, Y.; Abe, M.; Shimizu, A.; and Nakane, S. (1990), "High-Strength Concretes for High-Rise Buildings in Japan," Proceedings of the Second International Symposium on Utilization of High-Strength Concrete, Berkeley, California, 33-45.

690. Tomosawa, F.; Noguchi, T.; and Omura N. (1996), "Development of High Strength Concrete Using Wide-Graded Cement," Proceedings of the Fourth International Symposium on the Utilization of High Strength/High Performance Concrete, Paris, France, Volume 2, 135-142.

691. Tomosawa, Fuminori; and Noguchi, Takafumi (1993), "Relationship Between Compressive Strength and Modulus of Elasticity of High-Strength Concrete," Proceedings of the Third International Symposium on Utilization of High-Strength Concrete, Lillehammer, Norway, Volume 2, 1247-1254.

692. Tomosawa, Fuminori; Kawase, Kiyotaka; Masuda, Yoshihiro; Watanabe, Yoshiharu; and Sakai, Etsuo (1993), "Properties of Cast-In-Site High Strengh Concrete with Ettringite Based Additives Containing Fine Particles," Proceedings of the Third International Symposium on Utilization of High-Strength Concrete, Lillehammer, Norway, Volume 2, 980-987.

693. Tomosawa, Fuminori; Noguchi, Takafumi; and Onoyama, Kanzo (1993), "Test Method for Compressive Strength of High-Strength Concrete," Proceedings of the Third International Symposium on Utilization of High-Strength Concrete, Lillehammer, Norway, Volume 2, 1255-1262.

694. Toralles-Carbonari, B.; Gettu, R.; Agullo, L.; Aguado, A.; and Acena, V. (1996), "A Synthetical Approach for the Mix Design of High Strength Concrete," Proceedings of the Fourth International Symposium on the Utilization of High Strength/High Performance Concrete, Paris, France, Volume 2, 161-168.

695. Torrenti, J. -M.; Matte, V.; Maret, V.; and Richet, C. (1996), "High Integrity Containers for Interim Storage of Nuclear Wastes Using Reactive Powder Concrete," Proceedings of the Fourth International Symposium on the Utilization of High Strength/High Performance Concrete, Paris, France, Volume 3, 1407-1416.

696. Toutlemonde, F.; and Rossi, P. (1996), "Are High Performance Concretes Suitable in Case of High Rate Dynamic Loading?," Proceedings of the Fourth International Symposium on the Utilization of High Strength/High Performance Concrete, Paris, France, Volume 2, 695-704.

697. Towles, T. T. (1932), "Advantages in the Use of High Strength Concretes," ACI Journal, 28(9), 607-612.

698. Trinh, J. -L.; Menezes, N. C.; and Foure, B. (1996), "Time-Dependent Behavior of High Strength Concrete, Dimension Effect," Proceedings of the Fourth International Symposium on the Utilization of High Strength/High Performance Concrete, Paris, France, Volume 2, 349-356.

699. Tsivilis, S.; and Parissakis, G. (1995), "A MathematicalModel for the Prediction of Cement Strength," Cement and Concrete Research, 25(1), 9-14.

700. Tucker, John, Jr. (1941), "Statistical Theory of the Effect of Dimensions and of Method of Loading upon the Modulus of Rupture of Beams," Proceedings, ASTM, 41, 1072-1094.

701. Tucker, John, Jr. (1945), "Effect of Dimensions of Specimen Upon the Precision of Strength Data," Proceedings, ASTM, 45, 952-960.

702. Tucker, John, Jr. (1945), "Effect of Length on the Strength of Compression Test Specimens," Proceedings, ASTM, 45, 976-984.

703. Tucker, John, Jr. (1945), "The Maximum Stresses Present at Failure of Brittle Materials," Proceedings, ASTM, 45, 961-973.

704. Tuthill, L. H. (1991), "Long Service Life of Concrete," Concrete International, 13(7), 15-17.

705. U.S. Department of Transportation (1987), "Applications of High Strength Concrete for Highway Bridges," Publication No. FHWA/RD-87/079, 28 pp.

706. Uchizaki, I. (1996), "Finishing High Strength Concrete Using Ultrasonic Vibration," Proceedings of the Fourth International Symposium on the Utilization of High Strength/High Performance Concrete, Paris, France, Volume 2, 287-294.

707. Ulm, F. -J.; Schaller, I.; Chauvel, D.; Rossi, P.; and de Larrard, F. (1996), "Minimum Reinforcement in Nuclear Cooling Towers: FE-Durability Analysis of Concrete Cracking due to Drying," Proceedings of the Fourth International Symposium on the Utilization of High Strength/High Performance Concrete, Paris, France, Volume 3, 163-1174.

708. Vandewalle, L. (1996), "Influence of the Curing Temperature on the Strength Development of High Strength Concrete," Proceedings of the Fourth International Symposium on the Utilization of High Strength/High Performance Concrete, Paris, France, Volume 2, 725-734.

709. Vanhala, Jorma K.; and Nykyri, Pekka O. (1993), "Development of the Mechanical Properties of Lightweight Aggregate Concrete with the Aid of a Strength Model,"

Proceedings of the Third International Symposium on Utilization of High-Strength Concrete, Lillehammer, Norway, Volume 2, 1177-1184.

710. Vanikar, S. N.; and Goodspeed, C. H. (1996), "U.S. Approach to Technology Transfer on Using HPC in Bridge Construction," Proceedings of the Fourth International Symposium on the Utilization of High Strength/High Performance Concrete, Paris, France, Volume 3, 1557-1562.

711. Verdier, A.; and Varcin, M. (1996), "Concrete Containers for Radioactive Waste," Proceedings of the Fourth International Symposium on the Utilization of High Strength/High Performance Concrete, Paris, France, Volume 2, 539-550.

712. Vinches, Marc; Leguet, Jean Louis; and Dugat, Jérome (1993), "The Amphitheatre of Ales School of Mines: An Experimental Building for High Performance Concretes," Proceedings of the Third International Symposium on Utilization of High-Strength Concrete, Lillehammer, Norway, Volume 1, 599-606.

713. Virlogeux, M.; and Deroubaix, B. (1991), "Design and Construction of the Normandie Bridge," IABSE Symposium, Leningrad/St. Petersburg, 235-254.

714. Walker, Stanton; and Bloem Delmar L. (1960), "Effects of Aggregate Size on Properties of Concrete," ACI Journal, 57(9), 283-299.

715. Waller, V.; de Larrard, F.; and Roussel, P. (1996), "Modelling the Temperature Rise in Massive HPC Structures," Proceedings of the Fourth International Symposium on the Utilization of High Strength/High Performance Concrete, Paris, France, Volume 2, 415-422.

716. Wallevik, O. H.; and Kjellsen, K. O. (1996), "A Microstructural and Microanalytical Study of High Strength Concretes with Porous Aggregates," Proceedings of the Fourth International Symposium on the Utilization of High Strength/High Performance Concrete, Paris, France, Volume 2, 471-478.

717. Walraven, J. C.; and StroBand, J. (1996), "Behavior of Biaxially Loaded Reinforced Panels in High Strength Concrete," Proceedings of the Fourth International Symposium on the Utilization of High Strength/High Performance Concrete, Paris, France, Volume 3, 985-992.

718. Walraven, Joost (1993), "High Strength Concrete: A Material For the Future?", Proceedings of the Third International Symposium on Utilization of High-Strength Concrete, Lillehammer, Norway, Volume 1, 17-27.

719. Walter, Erich; and Ammann, Walter (1993), "Effects of High Strength Concrete on the Pull-Out Behaviour of Fastening Elements," Proceedings of the Third International Symposium on Utilization of High-Strength Concrete, Lillehammer, Norway, Volume 1, 402-411.

720. Wanatabe, Fumio; Nishiyama, Minehiro; and Muguruma, Hiroshi (1993), "Strength and Ductility of High Strength Concrete Beams Subjected to Combined Bending and Shear,"

Proceedings of the Third International Symposium on Utilization of High-Strength Concrete, Lillehammer, Norway, Volume 1, 412-419.

721. Wang, Chu-Kia, and Salmon, Chales G. (1992), "Reinforced Concrete Design," 5th ed., HarperCollins Publishers Inc.

722. Washa, G. W.; and Withey, N. H. (1953), "Strength and Durability of Concrete Containing Chicago Fly Ash," ACI Journal, 49(8), 701-713.

723. Washa, George W.; and Wendt, Kurt F. (1975), "Fifty Year Properties of Concrete," ACI Journal, 72(1), 20-28.

724. Watanabe, H.; Kawano, H.; and Nomura, S. (1996), "Study on the Bending Capacity and Shear Crack Strength of PC beams using HSC," Proceedings of the Fourth International Symposium on the Utilization of High Strength/High Performance Concrete, Paris, France, Volume 3, 935-944.

725. Webb, John (1993), "High-Strength Concrete: Economies, Design and Ductility," Concrete International, 15(1), 27-32.

726. Weber, S.; and Reinhardt, H. W. (1996), "Various Curing Methods Applied to High Performance Concrete with Natural and Blended Aggregates," Proceedings of the Fourth International Symposium on the Utilization of High Strength/High Performance Concrete, Paris, France, Volume 3, 1295-1304.

727. Westman, G. (1996), "Creep and Relaxation of High Performance Young Concrete," Proceedings of the Fourth International Symposium on the Utilization of High Strength/High Performance Concrete, Paris, France, Volume 2, 367-376.

728. Whiting, D., "Concrete Materials, Mix Design, Construction Practice, and Their Effects on the Corrosion of Reinforcing Steel," Compilation of Papers on Rebar Corrosion: 1976-1982, National Association of Corrosion Engineers, Houston, TX, 55-71.

729. Whiting, David (1979), "Effects of High-Range Water Reducers on Some Properties of Fresh and Hardened Concretes," PCA Research and Development Bulletin RD061.01T, 15 pp.

730. Wollmann, Gregor P.; and Wernli, Markus (1993), "Detailing for Post-Tensioning in High Strength Concrete," Proceedings of the Third International Symposium on Utilization of High-Strength Concrete, Lillehammer, Norway, Volume 1, 420-427.

731. Wolsiefer, John Sr.; and Morgan, Dudley R. (1993),"Silica Fume in Shotcrete," Concrete International, 15(4), 34-39.

732. Wood, Sharon L. (1991), "Evaluation of the Long-Term Properties of Concrete," ACI Materials Journal, 88(6), 630-643.

733. Yanagita, Katsumi; and Wami, Hiroki (1993), "Evaluating the Flow Properties of High-Strength Concrete," Proceedings of the Third International Symposium on Utilization of High-Strength Concrete, Lillehammer, Norway, Volume 2, 988-995.

734. Yen, T.; Chen, H. J.; Tang, J. W.; and Wu, W. H. (1996), "The Rheolgical Behavior of Fresh High Performance Concrete," Proceedings of the Fourth International Symposium on the Utilization of High Strength/High Performance Concrete, Paris, France, Volume 2, 281-286.

735. Yerlici, V.; Ersoy, U.; Özturan, T.; Türk, M.; and Özden, S. (1996), "An Investigation on Bond Performance of High Strength Concrete," Proceedings of the Fourth International Symposium on the Utilization of High Strength/High Performance Concrete, Paris, France, Volume 3, 1201-1208.

736. Yogendran, V.; Langan, B. W.; Haque, M. N.; and Ward, M. A. (1987), "Silica Fume in High-Strength Concrete," ACI Materials Journal, 84(2), 124-129.

737. Yong, Y. K.; McCloskey, Douglas H.; and Nawy, Edward G. (1985), "Reinforced Corbels of High-Strength Concrete," Special Publication, SP-87, American Concrete Institute, Detroit, MI, 197-212.

738. Yong, Yook-Kong; and Sethi, Manoj (1988), "Shear Strength of Plain High-Strength Concrete Beams with Silica Fume under Axial Compression," ACI Materials Journal, 85(2), 75-81.

739. Yssorche, M. -P.; and Ollivier, J. -P. (1996), "Relationship Between Air Permeability and Compressive Strength of Concrete," Proceedings of the Fourth International Symposium on the Utilization of High Strength/High Performance Concrete, Paris, France, Volume 2, 463-470.

740. Yuan, R. L.; Ragab, M.; Hill, R. E.; and Cook, J. E. (1991), "Evaluation of Core Strength in High-Strength Concrete," Concrete International, 13(5), 30-34.

741. Yue, Lingling; and Taerwe, Luc R. (1993), "Empirical Investigation of Creep and Shrinkage of High Strength Concrete," Proceedings of the Third International Symposium on Utilization of High-Strength Concrete, Lillehammer, Norway, Volume 2, 1263-1270.

742. Zachar, John A.; and Naik, Tarun R. (1993), "Analysis of the Flexural Interaction Between High-Strength Concrete and High-Strength Reinforcement," Proceedings of the Third International Symposium on Utilization of High-Strength Concrete, Lillehammer, Norway, Volume 1, 428-434.

743. Zeitler, R. (1996), "Experimental and Numerical Analysis of Pull-Out Tests with Anchors n High Strength Concrete," Proceedings of the Fourth International Symposium on the Utilization of High Strength/High Performance Concrete, Paris, France, Volume 3, 1219-1224.

744. Zhang, M. -H.; and Gjørv, O. E. (1990), "Development of High-Strength Lightweight Concrete," Proceedings of the Second International Symposium on Utilization of High-Strength Concrete, Berkeley, California, 667-681.

745. Zhang, Min-Hong; and Gjørv, Odd E. (1991), "Mechanical Properties of High-Strength Lightweigh Concrete," ACI Materials Journal, 88(3), 240-247.

746. Zhang, Min-Hong; Rønning, Terje F.; and Gjørv, Odd E. (1993), "Mechanical Properties of High-Strength Concrete," Proceedings of the Third International Symposium on Utilization of High-Strength Concrete, Lillehammer, Norway, Volume 2, 1271-1279.

747. Zhao, G. -Y.; Wu, P. -G.; and Bai, L. -M. (1996), "Research on Fatigue Behaviour of High Strength Concrete Under Compressive Cyclic Loading," Proceedings of the Fourth International Symposium on the Utilization of High Strength/High Performance Concrete, Paris, France, Volume 2, 757-764.

748. Zhao, Guang-Yi; Wu, Pei-Gang; and Zhan, Wei-Wei (1993), "Experimental Research on Fatigue Behaviour of High-Strength Concrete Under Constant Amplitude Tensile Cyclic Loading," Proceedings of the Third International Symposium on Utilization of High-Strength Concrete, Lillehammer, Norway, Volume 2, 1280-1287.

749. Zhou, F. P.; Lydon, F. D.; and Barr, B. I. G. (1995), "Effect of Coarse Aggregate on Elastic Modulus and Compressive Strength of High Performance Concrete," Cement and Concrete Research, 25(1), 177-186.

750. Zhu, J.; Wang, L.; and Chen, Z. (1996), "Experimental Study on Confined HSC Columns Under Cyclic Loading," Proceedings of the Fourth International Symposium on the Utilization of High Strength/High Performance Concrete, Paris, France, Volume 3, 915-924.

751. Zia, P.; Leming, M. L.; and Ahmad, S. H. (1991), "High Performance Concretes, A State-of-the-Art Report," SHRP-C/FR-91-103, Strategic Highway Research Program, National Research Council, Washington, D.C.

752. Zia, P.; Schemmel, J. J.; and Tallman, T. E. (1989), "Structural Applications of High Strength Concrete," Publication No. FHWA/NC/89-006, Federal Highway Administration, Washington, D.C., 330 pp.

753. Zihua, Y. (1996), "The Application of High Strength Concrete in the Design of Wanxian Yangtze River Highway Bridge," Proceedings of the Fourth International Symposium on the Utilization of High Strength/High Performance Concrete, Paris, France, Volume 3, 1483-1492.

754. Zsutty, Theodore C. (1968), "Beam Shear Strength Prediction by Analysis of Existing Data," ACI Journal, 65(11), 943-951.